U.S. DEPARTMENT OF COMMERCE
National Technical Information Service

AD-A031 031

Tanker Structural Analysis for Minor Collisions

M. Rosenblatt and Son, Inc, New York

Prepared for

Coast Guard, Washington, D C

Dec 75

300.20

Report No. CG-D-72-76

AD A031031

TANKER STRUCTURAL ANALYSIS FOR MINOR COLLISIONS

FINAL REPORT

DECEMBER 1975

DDC
OCT 21 1976
D

Document is available to the U. S. public through the
National Technical Information Service,
Springfield, Virginia 22161

Prepared for

DEPARTMENT OF TRANSPORTATION
UNITED STATES COAST GUARD
Office of Research and Development
Washington, D.C. 20590

REPRODUCED BY
NATIONAL TECHNICAL
INFORMATION SERVICE
U. S. DEPARTMENT OF COMMERCE
SPRINGFIELD, VA. 22161

252 76 C 2535

Technical Report Documentation Page

1. Report No.	2 Government Accession N	3. Recipient's Catalog No
CG-D-72-76		

4. Title and Subtitle	5. Report Date
Tanker Structural Analysis for Minor Collisions	December 1975
	6. Performing Organization Code
7. Author's	8. Performing Organization Report No.
9. Performing Organization Name and Address M. Rosenblatt & Son, Inc. 350 Broadway New York, N.Y. 10013	10 Work Unit No (TRAIS)
	11 Contract or Grant No CG-10,605-A
12. Sponsoring Agency Name and Address U. S. Coast Guard (G-DST-2/TRPT) 400 7th Street, S. W. Washington, D. C. 20590	13. Type of Report and Period Covered Final Report
	14 Sponsoring Agency Code G-DST-2

15. Supplementary Notes

The U. S. Coast Guard's research and development technical representative for the work performed herein was LTJG James R. DWYER.

16. Abstract

This report describes the work accomplished during the course of the project on the Evaluation of Tanker Structure in Collision. The intent of the report is to present the investigations performed in evaluating the phenomena that contribute to the ability of a longitudinally framed ship, particularly a tanker, to withstand a minor collision. A minor collision is one in which the cargo tanks remain intact. The ability to withstand a minor collision is quantized by the total energy that can be absorbed during the collision.

DDC
RECEIVED
OCT 21 1976
D

17. Key Words	18. Distribution Statement
Collision Energy Absorption	The document is available to the U. S. public through the National Technical Information Service, Springfield, Virginia 22161.

19. Security Classif. (of this report)	20. Security Classif. (of this page)	21. No. of Pages	22. Price
Unclassified	Unclassified	642	16.25

Form DOT F 1700.7 (8-72) Reproduction of completed page authorized

NOTICE

This document is disseminated under the sponsorship of the U. S. Department of Transportation in the interest of information exchange. The United States Government assumes no liability for the contents or use thereof.

The United States Government does not endorse products or manufacturers. Trade or manufacturers' names appear herein solely because they are considered essential to the object of this report.

The contents of this report reflect the views of M. Rosenblatt & Son, which is responsible for the facts and accuracy of data presented. This report does not constitute a standard, specification or regulation.

Project Summary

This volume is a final report on the subject of collision energy absorption done by M. Rosenblatt and Sons for the U. S. Coast Guard Office of Research and Development. It consists of the following five parts:

Part I - Tanker Structural Analysis for Minor Collisions
Part II - Tanker Structural Analysis Procedure Primer
Part III - Tanker Structural Analysis Collision Inspection Reports
Part IV - Evaluation of an LNG Ship Structure in Collision
Part V - Non-Standard Structural Schemes for Increased Collision Resistance of Tankers

Parts I through III represent a final report on the entire project. Parts IV and V are interim reports on two subtasks that were completed in November 1973. They are included because they did not form part of the main report. It is to be also noted that the U. S. Coast Guard does not endorse or approve of any of the concepts or procedures reported on anywhere herein.

PART I

TANKER STRUCTURAL ANALYSIS FOR MINOR COLLISIONS

Preceding page blank

SUMMARY

This report describes the work accomplished during the course of the project on the Evaluation of Tanker Structure in Collision. The intent of the report is to present the investigations performed in evaluating the phenomena that contribute to the ability of a longitudinally framed ship, particularly a tanker, to withstand a minor collision. A minor collision is one in which the cargo tanks remain intact. The ability to withstand a minor collision is quantized by the total energy that can be absorbed during the collision.

Although the project was specifically related to structural considerations, brief order of magnitude studies were conducted to evaluate the role of rigid body motion of colliding ships. These studies indicated that this form of energy absorption could be significant although only a fraction of the overall energy absorption.

The structural energy absorption phenomena were divided into elastic and plastic. The elastic include hull girder vibratory response during collision, elastic bending of the whole hull girder, and local elastic deformation in the vicinity of the strike. It was determined that these were negligible when compared to the plastic.

The final output of the project has consequently been an analytical procedure and its numerical application, for estimating the plastic energy absorbed by longitudinally framed ships, particularly tankers, when involved in either right angle or oblique collisions, providing the collision is not a "glancing blow." This procedure employs a static analysis, which is an obvious simplification of the dynamic phenomena of collisions; the striking bow is assumed rigid, although means of analyzing striking ships with non-rigid bows were explored; and the possibility of dynamic tearing

or puncturing of the shell prior to rupture is neglected. A step-by-step calculation form of the procedure and numerical examples are contained in a primer published as a separate report. That report and the calculations therein are intended to be an aid in understanding the material presented herein.

The plastic energy analysis has indicated that the most significant energy-absorbing phenomena are membrane tension in the sideshell, membrane tension in the deck, shearing of web frames, and plastic bending of the sideshell. The most important of these is the membrane tension in the sideshell.

In the course of developing the analysis procedure, component structures tests and investigations of actual collisions were performed in order to determine the validity of many assumptions which were made. A total of ten component structure tests were conducted with stiffened and unstiffened flat-plate specimens that were one-fifth scale models of a representative portion of the side of a typical tanker. The actual collision inspections involved six different collisions. Valuable information was gained regarding structural failure mechanisms and extent of damage.

Parametric analyses are also presented which consist of the numerical application of the plastic energy collision analysis procedure to six collision incidents in which a 120,000 DWT tanker (and its variants) is struck by a 20,000-ton displacement ship. The results of this limited evaluation show that (1) the membrane-tension energy is by far the greatest energy-absorbing mechanism, and (2) the total energy absorbed by the struck ship varies drastically with the location of the strike with respect to webs and bulkheads.

Another objective of the project was to perform an investigation of non-rigid bows to propose methods of evaluating their significance. The most important effect was shown to arise from dynamic loading, and was the increased buckling strength of deck structure in both colliding ships and the bow sideshell plating of the striking ship. These areas may then act as hard points that can "knife" through other structure.

It was concluded that with additional effort it may be possible to develop the present procedure for use in ranking the ability of the structure of longitudinally framed ships, particularly tankers, to withstand minor collisions, and thereby assist in increasing the safety of these ships The procedure is sufficiently general that with judicious modifications it can be made suitable for the analysis of other ship types.

Limitations of the procedure to be recognized are: (1) the procedure employs a static analysis, (2) the striking bows are assumed infinitely rigid, (3) damage to the structure does not extend into the bilge area, and (4) the possibility of the striking bow immediately cutting or punch-shearing the shell of the struck ship has not been considered. Additional effort is required and recommended to minimize the limitations of the procedure in order to simulate collisions more precisely.

TABLE OF CONTENTS

	Page
SUMMARY	ii
NOMENCLATURE	ix
1. INTRODUCTION	1-1
1.1 Background	1-1
1.2 Scope	1-2
1.3 Organization of the Report	1-3
2. COLLISION ANALYSIS THEORY	2-1
2.1 General	2-1
2.2 Elastic Energy Analysis	2-3
2.2.1 Background	2-3
2.2.2 Analytical Approach	2-7
2.2.3 Calculation Results	2-8
2.2.4 Conclusions	2-9
2.3 Rigid Body Motion Energy Analysis	2-9
2.3.1 General	2-9
2.3.2 Approach and Calculation Results	2-10
2.3.3 Conclusions	2-11
2.4 Basic Theories of Inelastic Phenomena	2-14
2.4.1 General	2-14
2.4.2 Theory for Plastic Bending	2-14
2.4.3 Theory for Plastic Membrane Straining	2-19
2.4.4 Theories for Inelastic Shearing	2-22

	Page
3. COLLISION ANALYSIS PROCEDURE	3-1
3.1 General	3-1
3.2 Assumptions	3-1
3.2.1 Overall Behavior of Colliding Ships	3-2
3.2.2 Basic Assumptions	3-5
3.3 Collision Phenomena	3-11
3.3.1 General	3-11
3.3.2 Sequence of Phenomena	3-11
3.3.3 Strike by a Raked Bow	3-14
3.3.4 Strike by a Vertical Bow	3-15
3.4 Plastic Analysis	3-15
3.4.1 General	3-15
3.4.2 Longitudinal Plastic Bending	3-16
3.4.3 Hull Sideshell Membrane Tension	3-19
3.4.4 Web-Frame Analysis	3-34
3.4.5 Deck Analyses	3-41
3.4.6 Additional Considerations for Double-Shell Ships	3-42
4. COLLISION ANALYSIS PARAMETRIC STUDY RESULTS	4-1
4.1 General	4-1
4.2 Input Information	4-2
4.2.1 Struck Ship	4-8
4.2.2 Striking Ship	4-8
4.3 Results of the Parametric Study	4-8
4.4 Membrane Tension Energy for Arbitrary Strike Locations	4-11

	Page
5. COLLISION INSPECTIONS	5-1
5.1 General	5-1
5.2 Observations	5-2
5.2.1 Overall Extent of Damage	5-2
5.2.2 Longitudinally Stiffened Hull Plates	5-3
5.2.3 Deck or Bilge Areas	5-4
5.2.4 Transverse Structure	5-4
5.2.5 Oblique Collisions	5-5
5.2.6 Striking Bows	5-5
5.3 Conclusions	5-5
6. COMPONENT STRUCTURES TESTS	6-1
6.1 Purpose of the Tests	6-1
6.2 Test Programs and Apparatus	6-1
6.3 Experimental Results of Lateral Load Tests	6-12
6.3.1 General Behavior	6-12
6.3.2 Prediction of Deflections	6-17
6.3.3 Stresses, Strains, and Energies within Straight-Line Portions of the Specimen at Rupture	6-18
6.3.4 Apparent Maximum Strain Under Sharp Bearing	6-22
6.4 Experimental Results of Longitudinal Resistance to a Traveling Yield Zone	6-28

		Page
7.	NON-RIGID BOW INVESTIGATION	7-1
	7.1 Background	7-1
	7.2 Purpose	7-3
	7.3 Approach	7-3
	7.4 Model Collision Tests	7-5
	7.5 Analytical Methods	7-7
	7.5.1 Estimation of Dynamic Load Regime	7-7
	7.5.2 Buckling Strength Amplification	7-8
	7.5.3 Local Strength of Stem and Gunnel	7-10
	7.5.4 Beam Strength of Stem and Gunnel	7-14
	7.5.5 Effective Plating	7-16
	7.5.6 Tearing Energy	7-19
	7.6 Conclusions and Recommendations	7-20
8.	CONCLUSIONS	8-1
	8.1 Results	8-1
	8.2 Recommendations	8-4
APPENDIX A	BIBLIOGRAPHY	
APPENDIX B	ELASTIC ENERGY ANALYSIS	

NOMENCLATURE

a = stiffener spacing, or the actual width between two specific reference lines

b = effective design width of a plate, except for the flange of a stiffener, for which 0.5b is the width of the outstanding leg, measured from the center of the web

c = speed of sound in material

d = depth of the web of a stiffener flange or clear depth of web plate

d' = depth of the hull plate cross section that is assumed to be uniformly stressed in compression at σ_u.

d_1 = distance traveled by striking ship during collision

d_2 = distance traveled by struck ship during collision

e = membrane-tension elongation

e_t = total membrane-tension elongation of a stiffened-plate T-beam

h = E/E_t

k_f = foundation modulus

m_1 = effective mass of striking ship (including added mass of water)

m_2 = effective mass of struck ship

p = penetration (relative movement of ship's centers of gravity during collision process)

r = radius

r_m = minimum radius of gyration

s = ratio of ε_{sh} to the yield strain, σ_y/E

t = time

t_f or t = thickness of a stiffener flange

t_w or w = thickness of web of a stiffener

v = velocity

v_1 = velocity of striking ship at beginning of collision process

v_2 = 0 = initial velocity of struck ship

v_f = final velocity of both ships

x = longitudinal distance toward the load from a point of tangency where a straight-line portion meets the curved portion of the hull plate, in the vicinity of the load

y = lateral deflection relative to a horizontal line through a point of tangency where the two straight-line portions meet the curved portion

x_m, y_m = maximum value of x and y, respectively, in the hull plate at the centerline of the load

A, B and k = material property constant relating to when buckling or rupture will occur during plastic bending

A_f = area of stiffener flange

A_s = cross sectional area of T-beam

A_w = area of stiffener web

C = spring constant for lateral restraint, expressed as a force per inch for member per inch of lateral movement of the member

C' = a constant greater than zero, reflecting lateral restraint to axial buckling

D = tension-test ductility in a 2-inch gage length

E = modulus of elasticity

E_{bc} = maximum value of bending plastic energy in stiffened-plate T-beam unit, occurring when a longitudinal stiffener flange buckles or ruptures

E_d = membrane-tension plastic energy in deck

E_{mt} = membrane-tension plastic energy in ship side

E_{ps} = in-plane shearing plastic energy in web frame

E_t = tangent modulus

F = force

F_R = force required to propagate longitudinally the yield line at the strike

I = moment of inertia about the axis of bending

K = constant

K_a = $\varepsilon/\varepsilon_r$

K_e = ratio of strain in the web frame spaces adjacent to the undistorted web frames or bulkheads bounding the damaged length to ε_r

KE_i = initial kinetic energy

KE_f = final kinetic energy

KE_a = absorbed kinetic energy = $KE_i - KE_f$

L = length or distance along a T-beam

L' = distance from load to nearest support for a right-angle collision, or distance from load to support behind the load (in direction opposite to longitudinal direction of strike) for an oblique collision

L'' = $L_t - L'$

L_c = length of an axially loaded member between points of inflection

L_d = length of damage between undistorted web frames or bulkheads, measured in longitudinal direction

L_{eq} = equivalent length of plating compressed by the collision force

L_s = space between two consecutive web frames

L_t = value of L_d when the length of damage is only one or two spaces between web frames

L_y = yielded length of flange at beginning of local buckling of a stiffener flange

M = $m_1 + m_2$

M_o = maximum moment

M_p = plastic bending moment in a stiffened-plate T-beam

N = normal force

P = maximum penetration or concentrated lateral load

P_b = load on a stiffened-plate T-beam that will occur during plastic bending

P_c = crushing load

P_m = axial load capacity

P_{tm} = a maximum value of the load on a stiffened-plate T-beam that will occur during membrane tension

P_{wf} = load exerted by the most highly strained stiffened-plate T-beam on a web frame at the instant that the web frame yields or buckles

P_y = concentrated radial load

P_E = static Euler load

R (with number subscript) = radius or ratio of force (shear, moment, or thrust) within a web frame, subjected to a given lateral load, to the ultimate force required to fail the frame

R_m = maximum value of R (with number subscript)

T = average membrane tension throughout the damaged length

τ = duration of collision process

V = shear in a stiffened-plate T-beam

V_p = ultimate shear in web frame

δ = a specified lateral deflection; also, the deflection of the centroid of a stiffened-plate T-beam

δ_{bc} = maximum value of δ during the bending phase for only one or two web-frame spaces damaged

δ_m = maximum value of δ during the membrane-tension phase for only one or two web-frame spaces damaged

δ_n = maximum normal-to-plane deflection of a web plate

δ_{tc} = value of δ at the instant of rupture, during the membrane-tension phase, when only one or two web-frame spaces are damaged

ε = average longitudinal strain in hull throughout the damaged length

ε_c = longitudinal compression strain that results from elastic bending of the entire ship cross-section

ε_ℓ = average strain over $L^{\sim}$

ε_m = maximum bending-plus-membrane-tension strain at hull rupture

$\varepsilon_r = 0.10 \left(\frac{D}{32\text{ft}} \right)$

ε_s = theoretical bending strain in the flange of a longitudinal stiffener when it buckles near a web frame support

ε_{sh} = strain at onset of strain hardening

ε_E = Euler strain

θ = portion of the bend angle between a straight-line portion of the hull and the location of maximum curvature at the midpoint of a sharp bend

θ_p = angle change in stiffened-plate T-beam at end of L_t that corresponds to buckling or rupture of a longitudinal stiffener flange

λ = length of a flange buckle wave

$\bar{\lambda} = \sqrt[4]{\frac{k_f}{4EI}}$

σ_{ty} = tension-field tensile stress at tension-field yielding

σ_u = tensile strength

σ_y = yield strength

$\sigma' = 0.5(\sigma_y + \sigma_u)$ = average plastic stress

$\sigma'_E = \frac{1}{2}\sigma'$ = average elastic stress

σ_E = Euler buckling stress

α = angle of collision measured from the struck ship undeformed side shell behind the strike point to the centerline of the striking ship

γ = shearing strain

γ_e = total shearing strain up to tension-field yielding

γ_e' = portion of γ_e due to straining up to elastic shear buckling

γ_e'' = portion of γ_e due to straining between elastic shear buckling and tension-field yielding

γ_m = maximum shearing strain before unloading

τ_{cr} = elastic shear buckling stress

τ_y = shear yield strength

Ω = dynamic similarity number

ω = fundamental frequency of the plate

μ = mass density of the material

1. INTRODUCTION

1.1 Background

Bulk-liquid marine transportation has proved to be a source of pollution due to spillage of cargo when vessels are damaged in collisions and groundings. In view of this, the governments of the world's maritime nations have committed themselves individually and collectively to take all reasonable measures to minimize such pollution. The government agency in the United States delegated to deal with such matters is the Coast Guard.

In order to minimize cargo spillage due to collisions, studies have been proposed and implemented simultaneously in several areas, such as for cargo and ballast tank arrangements, navigational aids, and traffic control.

Another consideration for minimizing spillage is to modify the cargo containment structure to withstand collision damage. In keeping with this objective, the Coast Guard sponsored the research study presented in this report to develop an analytical procedure to evaluate the structure of a tanker from the viewpoint of the actual protection it affords the cargo during a minor collision. A minor collision is defined as one in which the cargo tank remains intact, irrespective of whether the vessels in question have single or double shell.

Previous work in the area of structural protection from collision damage has been done both in the United States and abroad, starting late in the 1950's. This work has mainly been concerned with protection of the nuclear reactors in nuclear-powered vessels; therefore the collisions studied have characteristically involved high ship speed, and large incursions into the ship's structure with resulting catastrophic structural failure and flooding by the sea of compartments adjacent to the area of penetration. This type of collision cannot be classed as a minor collision.

The well-known works by Minorsky [1]* and Gibbs & Cox, Inc. [2] account for the energy absorption characteristics of the ship structure by assuming that the energy absorbed is essentially proportional to the volume of steel damaged in the striking ship and the struck ship. The technique is easy to use and is based on the detailed analytical examination of many collisions. However, it applies to the energy associated with damage occurring after initial rupture of the hull and therefore does not apply to a minor collision.

1.2 Scope

As previously discussed, the research presented in this report is concerned with the development of an analytical procedure to evaluate the protection afforded to bulk-liquid cargo by the ship structure during a minor collision. A measure of the protection is the amount of energy absorbed by the structure during the collision. The various topics considered naturally include elastic structural energy absorption and plastic structural energy absorption. In addition, the possibility of significant energy absorption due to rigid body motion of the ships' hulls initiated by the collision impulse is considered.

The approaches to identify the elastic and rigid body motion energies are quite simplified, but are adequate to conclude that these energies are small compared with the potential plastic energy available, and can be neglected when estimating the energy absorbed in minor collisions.

Other phases of the present research have included developing a plastic structural analysis procedure for longitudinally framed tankers, applying the procedure to the parametric analyses of typical ship designs,

*Numbers in brackets designate references in the Bibliography. Appendix A.

inspecting and evaluating damage that resulted from actual ship collisions, conducting component-structure model tests, and developing overall judgments and conclusions based on these studies.

1.3 Organization of the Report

This report describes all aspects of the project, but emphasizes the plastic analysis procedure and the insight it provides toward understanding structural design for collision resistance.

Section 2 describes the theories underlying the elastic energy, rigid body motion energy, and plastic energy analyses. In addition, the elastic and rigid body motion analyses and results are presented since the energy associated with these phenomena is shown to be small and need not be considered elsewhere.

Section 3 describes the collision plastic analysis procedure and Section 4 the results of case studies using the analysis procedure.

Sections 5 and 6 describe two areas of investigation that greatly aided in comparing theory with actuality. Section 5 presents the results of the inspections of actual collisions. Section 6 presents the results of a limited series of structural tests on tanker structural components.

The plastic analysis procedure described in Section 3 considers striking ships with infinitely stiff bows only. Section 7 consideres the implications of striking bows which are not infinitely stiff and therefore may deform.

Finally, the results , recommendations and the impact of this study on the shipbuilding industry are discussed in Section 8.

2. COLLISION ANALYSIS THEORY

2.1 General

The analytical theories of this study were developed to form the basis of an analysis procedure for the determination of energy absorption during a minor tanker collision. The theories presented below have been developed from a literature survey, inspections of actual collisions, model tests of ship structural components, and experience. Different approaches are applied to identify the elastic and plastic structural deformation energy absorption, and ship rigid body motion energy absorption of a tanker collision.

The assumed ship collision consists of four simultaneous phenomena as illustrated in Figure 2-1: (1) Local elastic deformation of the struck ship, (2) Rigid body motion of the struck ship, (3) Plastic deformation of the struck ship, and (4) Overall elastic deformation of the struck ship. Although these phenomena occur concurrently, it is of interest to note their cause and relation to the overall collision. The local elastic deformation of the struck ship (1. in Figure 2-1) occurs immediately on contact of the struck and striking ships. This will consist of elastic distortions in the struck ship structure in the vicinity of the bow of the striking ship. Also immediately upon contact and throughout the rest of the collision, the striking ship applies a force (the striking force) to the struck ship. Besides causing local structural failure, this force can induce rigid body motion (2.), vibration (4.), and an elastic bending of the entire hull girder (4.) of the struck ship. After the local elastic deformation of the struck ship ends, local plastic deformation (3.) will start and end with rupture of a cargo tank.

Preceding page blank

1.

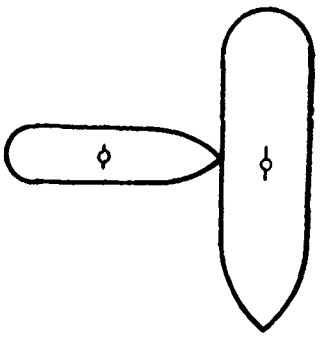

LOCAL ELASTIC ENERGY ABSORPTION DUE TO LOCAL ELASTIC STRUCTURAL DEFORMATION OF THE STRUCK SHIP.

2.

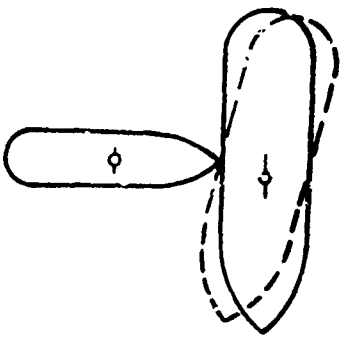

SHIP DYNAMIC ENERGY ABSORPTION DUE TO TRANSLATION AND/OR ROTATION OF THE STRUCK SHIP.

3.

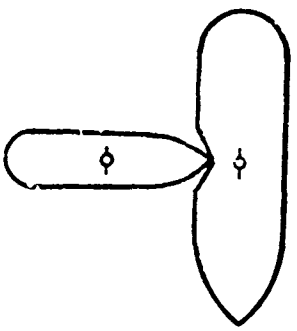

LOCAL PLASTIC ENERGY ABSORPTION DUE TO PLASTIC STRUCTURAL DEFORMATION OF THE STRUCK SHIP.

4.

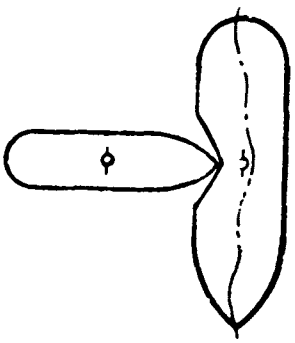

OVERALL ELASTIC ENERGY ABSORPTION DUE TO OVERALL ELASTIC STRUCTURAL DEFORMATION OF THE STRUCK SHIP.

FIGURE 2-1
COLLISION PHENOMENA INVOLVING
ENERGY ABSORPTION

These four phenomena each have associated energy absorption which may be summarized as follows:

(1) Energy absorbed by local elastic deformation of the struck ship. This energy absorption corresponds to 1. of the ship collision shown in Figure 2-1. The hull material will be stressed in its elastic range as shown in Figure 2-2, which is a typical stress-strain curve for structural steel.

(2) Energy absorbed in rigid body motion of the struck ship. This energy absorption corresponds to 2. of the ship collision shown in Figure 2-1.

(3) Plastic energy absorbed by local plastic deformation as shown in 3. of Figure 2-1. The local structure will be stressed in the inelastic range as shown in Figure 2-2.

(4) Energy absorbed by overall elastic deformation of the ship. The deformation includes that due to vibratory response. This energy absorption corresponds to 4. of Figure 2-1.

The theories used to analyze the absorption of elastic energy, plastic energy, and rigid body motion energy are developed separately below.

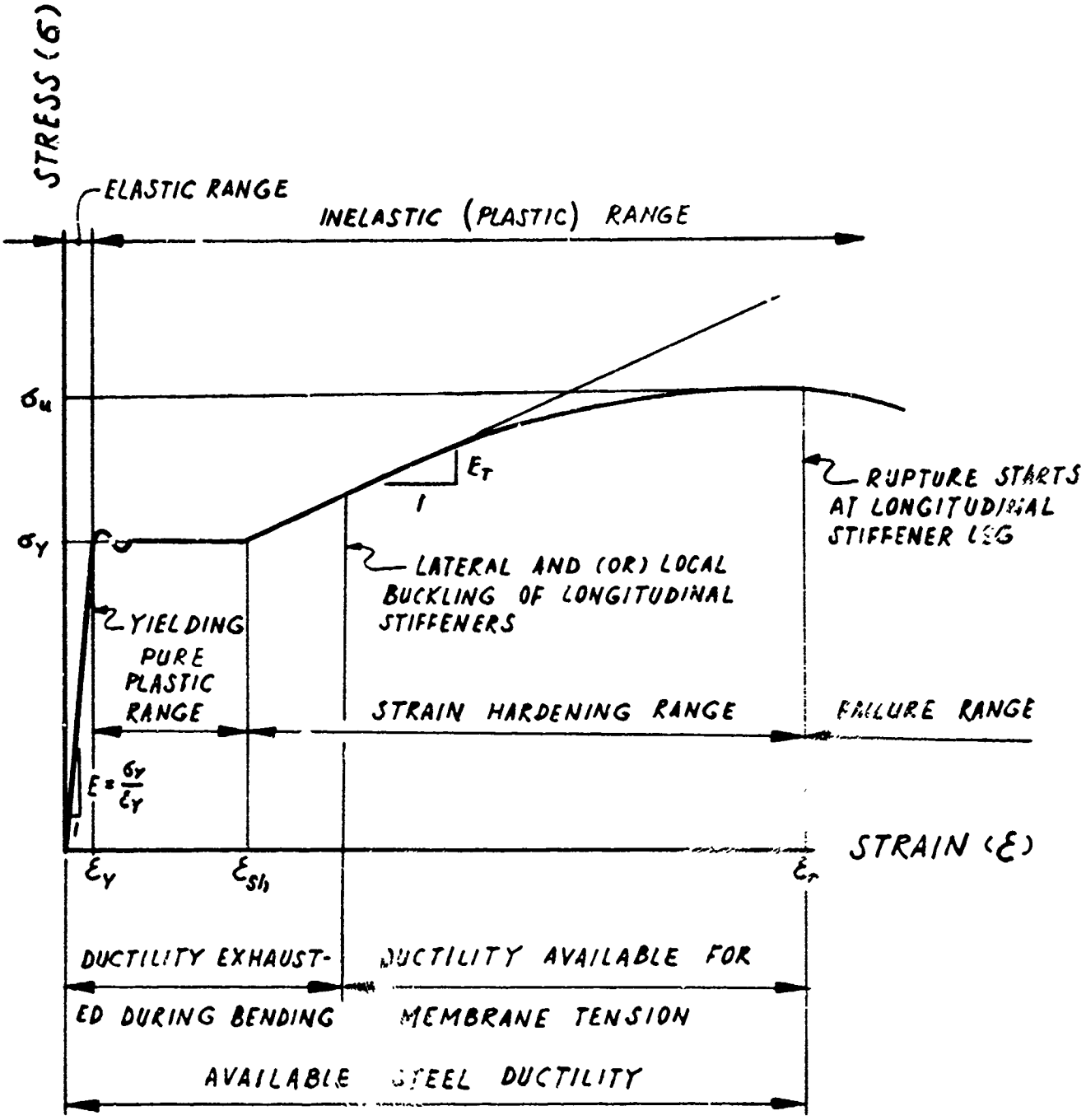

FIGURE 2-2

TYPICAL STRESS-STRAIN CURVE FOR STRUCTURAL STEELS

2.2 Elastic Energy Analysis

2.2.1 Background

Most past analyses of the energy absorbed in ship collisions[1,3-7] have been conducted for the purpose of studying the protection of nuclear reactors on nuclear-powered ships. These have been concerned with high speed collisions resulting in large incursions and catastrophic structural failure, and can be classified as moderate to severe.

In the collision analysis considered in this report, it is necessary to concentrate on relatively minor collisions in which the amount of structural deformation of local structure does not exceed the capacity of the structure to stretch or deform without rupture. Therefore, it is reasonable to assume that elastic deformations could result in a relatively significant amount of energy absorption.

Guida and Haywood [8,9] have investigated the importance of elastic energy absorption in ship collisions. Haywood concluded that for a significant portion of the collision energy to be absorbed elastically as potential or kinetic energy of overall ship vibration, the collision duration should be as short as, or shorter than, the fundamental period of horizontal ship vibration. The generation of a large collision force lasting only a short period of time requires that the strength and stiffness of the struck ship's side structure be extremely large. The analysis that was used to formulate these conclusions treated the struck ship as an elastic uniform beam subjected to two simple types of collision impulse and did not include a treatment of local structural behavior in the vicinity of the impact.

In the work by Kline and Clough [10] on dynamic response of ship structures to hydrodynamic loading, the ship is treated as an idealized symmetrical structure supported on a series of buoyancy springs. The force-time history and structural behavior of local and overall structures are predicted for slamming type impacts by the use of a slam analysis computer program. The dynamic response of the ship structure to slamming indicates that the response of local structure at the impact location can strongly influence the elastic response of the overall structure by modifying the magnitude and time-history of the applied forces as they are transmitted through the local structure to the overall structure.

In light of the latter findings and because the present minor collision analysis involves the study of various local structural configurations in the vicinity of the collision damage, the importance of modeling local structural strength was identified as an important consideration in this study.

Since the slam analysis computer program of reference [10] was available and offered the advantages of being able to specify complex force-time histories of impact and also of obtaining both local and overall displacement, velocity, and bending moment histories throughout the duration of the collision, it was modified to be used in the collision analyses.

2.2.2 Analytical Approach

In a collision the relative movement between the two ships and the penetration into the struck ship depend on the initial momentum of both ships, the structural resistance to penetration, the inertia forces generated in the immediately affected structure (i.e. local structure) and the relative heading of both ships. The latter effect has not been considered for this "relative magnitude" study. The remaining considerations will result in a force-time history at the location of the strike once the collision process has commenced (following initial contact). This force-time history will result in the collision impulse to the struck ship.

The problem then reduces to that of determining a suitable force-time history or collision impulse. Once this is accomplished, the modified slam analysis computer program discussed above can be used to determine the elastic response of the hull.

In the present study various total collision impulses are assumed and input to the modified slam analysis computer program. Then by comparing results, the most suitable impulse is determined as described in Appendix B. The various impulses are constructed by separating each into structural resistance forces and local inertia forces. The structural resistance forces are derived from the plastic energy absorption calculations and are assumed to vary linearly with time. Various local inertia force-time histories are assumed and added to the structural resistance forces, yielding the various collision impulses.

The details of the analytical approach can be found in Appendix B.

2.2.3 Calculation Results

Two basic groups of parametric analyses were conducted in an effort to determine the importance of elastic energy absorption.

The first group of calculations used an assumed deceleration of about one-tenth the acceleration of gravity to obtain short duration collisions of less than 1.0-second duration. This series of calculations indicated that elastic energy absorption could be significant; however, after the completion of the first set of plastic energy absorption calculations, it became evident that the assumed decelerations were too great and that realistic structural resistance forces would provide only a fraction of the deceleration that was originally assumed.

In the second group of elastic energy absorption calculations, the energy absorption was calculated for three assumed collision situations representative of a T-2 tanker colliding with a 120,000 DWT tanker. The three collision situations that were investigated are as follows: (1) 1" mild steel single shell, strike at web frame, 15° bow rake on striking ship; (2) 1" mild steel single shell, strike between web frames, 15° bow rake on striking ship; (3) 1-3/8" mild steel single shell, strike between webs, 15° bow rake. The energy absorption attributed to elastic deformation of the overall ship was found to be negligible.

2.2.4 Conclusions

The conclusions to be drawn from the elastic energy absorption analyses described herein are limited by the assumptions made with regard to the separate calculation of plastic and elastic energies, by the simplifications incorporated in the dynamic analysis computer program, and by the structural characteristics of the tanker that was chosen to represent the struck ship. Nevertheless, the evidence seems very substantial that the collision energy absorbed in elastic deformations of overall ship structure will be negligible compared to plastic energy absorption for all practical collision situations. It should be noted, however, that the plastic energies used in the elastic energy analyses corresponded to those determined by a preliminary form of the plastic analysis. The plastic analysis presented in this report predicts much greater plastic energies and therefore larger structural resistance forces. It is felt, however, that the ratio of elastic to plastic energy will remain approximately the same or decrease if the present plastic analysis is incorporated. Therefore elastic energy absorption should still be negligible.

2.3 Rigid Body Motion Energy Analysis

2.3.1 General

The energy absorption occurring in rigid body motion of the struck ship (Figure 2-1) includes: (1) the energy absorbed by the resistance of the struck ship's inertia to motion, (2) and the energy absorbed by the hydrodynamic resistance to motion of the struck ship. An objective of this investigation was to determine the significance of the rigid body motion in a minor collision analysis process.

2.3.2 Approach and Calculation Results

Two separate sets of calculations were made in determining the effect of rigid body motion in a tanker collision. Both calculations were performed with the application of the slam analysis computer program.

The first calculations determined the energy absorption due to overcoming the struck ship's inertia and hydrodynamic resistance for a T-2 tanker colliding with a 120,000 DWT tanker (1-3/8" MS single shell, struck between webs, 15^{o} bow rake). The force-time history used was representative of a linear force-penetration relationship with a maximum force of 900 tons and a penetration of 3 feet. A summary of the calculation is included in Table B-1 of Appendix B, which shows that the energy absorbed in overcoming the struck ship's inertia and hydrodynamic resistance can be significant (approximately 10% in the case shown in Table B-1) when compared with the overall energy absorption in a minor ship collision.

The second set of calculations were made for evaluating the yaw tendency of the struck ship during a minor collision. The rigid body motions, for both a 150,000-tons-displacement and a 20,000-tons-displacement ship were determined when the ships were subjected to three separate impacts at three locations along their length. The force-time history used was representative of a linear force-penetration relationship (see Figure 2-3) with a maximum force of 1000 tons and durations of 2, 3, and 4 seconds. The points of application were midships, the forward quarter point and the bow. The results of the calculations are summarized in Table 2-2 in terms of the velocities and lateral movement of various points along the length of the struck ship. The bow and stern displacements were used to

calculate the yaw angles of the struck ship. The amount of rotation (yawing) resulting from a minor collision at the forward portion of a ship's hull, for ships between 20,000-tons and 150,000-tons-displacement, is relatively small at the time the collision force is terminated. When the four-second collision force is applied to the bow of the 20,000-ton ship, the resulting yaw angle is about 4 degrees. The same force and location produce a yaw angle of less than ½ degree for the 150,000-ton ship.

2.3.3 Conclusions

Based on the calculation results described, it is concluded that rigid body motion energy absorption during a minor collision can be significant. This energy is not considered elsewhere in this report because it should not affect the structural energy absorption. Also, the yaw motions appear to be small.

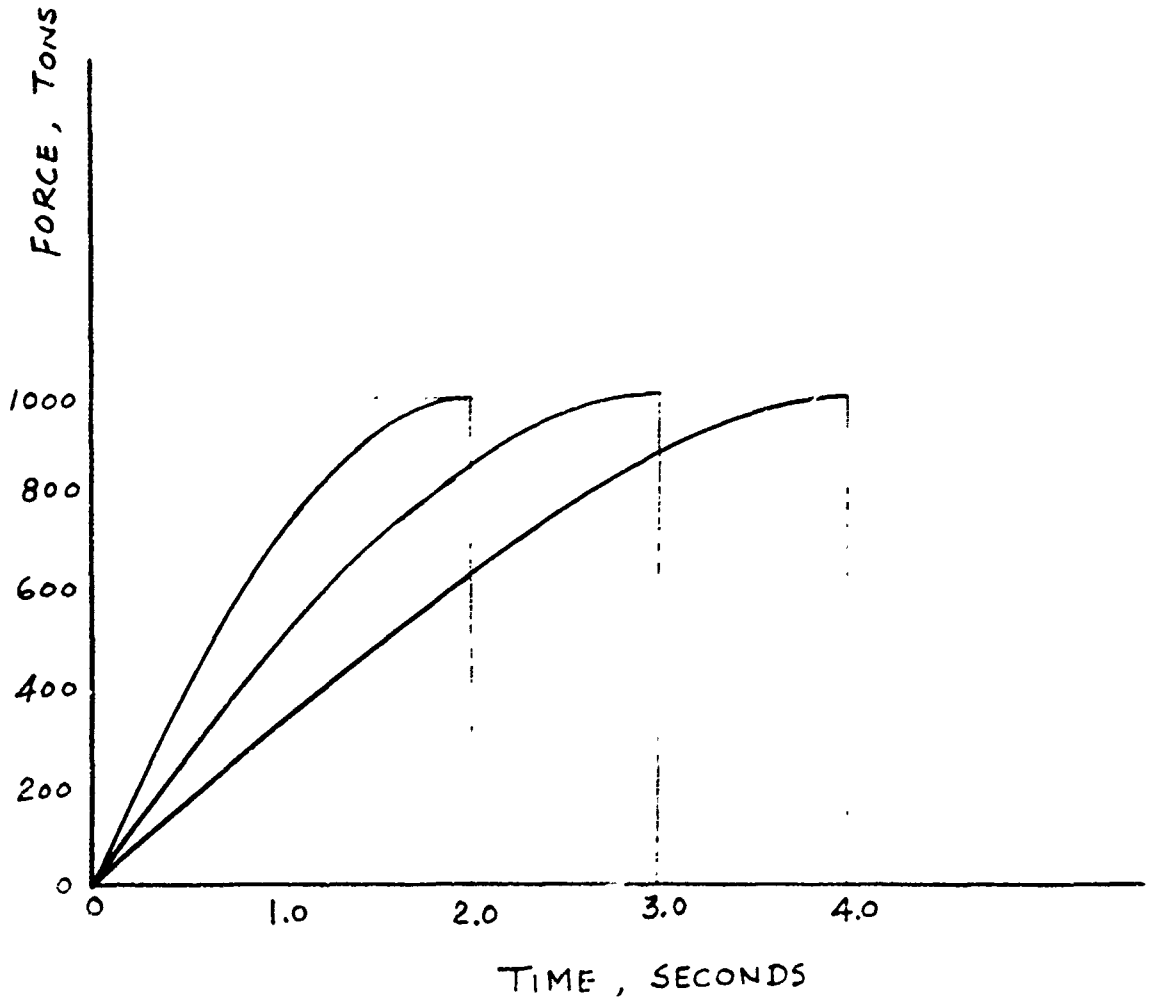

FIGURE 2-3

COLLISION FORCE - TIME HISTORIES

TABLE 2-2

YAW TENDENCY CALCULATION

20,000-TON DISPLACEMENT SHIP

Collision Location		Collision Duration 2 Sec.	3 Sec.	4 Sec.
Midship, $\frac{L}{2}$	$v(\frac{L}{2})$* $\left(\frac{ft.}{sec.}\right)$	1.23	1.81	2.35
	$d(\frac{L}{2})$** (ft.)	1.24	2.78	4.88
$\frac{L}{4}$	$v(\frac{L}{4})$	2.26	3.33	4.32
	d(bow) - d(stern)	4.61	10.30	18.00
	$d(\frac{L}{4})$	2.28	5.09	8.95
Bow	v(bow)	5.43	7.96	10.30
	d(bow) - d(stern)	9.62	20.60	36.10
	d(bow)	5.48	12.20	21.40
	YAW ANGLE (DEGREE)	1.04	2.33	4.12

150,000-TON DISPLACEMENT SHIP

Midship, $\frac{L}{2}$	$v(\frac{L}{2})$	0.206	0.303	0.386
	$d(\frac{L}{2})$	0.208	0.464	0.815
$\frac{L}{4}$	$v(\frac{L}{4})$	0.378	0.556	0.722
	d(bow) - d(stern)	0.770	1.710	2.000
	$d(\frac{L}{4})$	0.381	0.850	1.490
Bow	v(bow)	0.792	1.260	1.680
	d(bow) - d(stern)	1.550	3.440	6.030
	d(bow)	0.920	2.040	3.580
	YAW ANGLE (DEGREE)	0.10	0.20	0.35

* v = velocity at termination of collision

** d = distance traveled at termination of collision

2.4 Basic Theories of Inelastic Phenomena

2.4.1 General

The theoretical background for the plastic energy analysis of the ship-side-collision consists of a suitable arrangement of established principles and equations of structural engineering. The plastic theories involved in this analysis are described below.

2.4.2 Theories for Plastic Bending

2.4.2.1 Rotation at Stationary Plastic Hinges

The rotation capacity at a plastic hinge, that is, a location of plastic bending in a beam, is a measure of the ability of a member to sustain plastic hinge rotation without local buckling or rupture. Based on strain-hardening limitations only (i.e. no buckling or rupture) and neglecting any membrane forces, the expression [10,11] for the rotation capacity at a plastic hinge is

$$\theta_p = k \frac{M_p}{EI} L \qquad (2\text{-}1)$$

where $$k = \left(1 - \frac{M_p}{M_o}\right) \left[s + \frac{h}{2} \left(\frac{M_o}{M_p} - 1 \right) \right] \qquad (2\text{-}2)$$

and where E = modulus of elasticity; I = moment of inertia; L = distance between the locations of zero bending moment on the two sides of a plastic hinge or distance between the location of zero bending moment and a fixed support at which a plastic hinge occurs; M_p = plastic bending moment; M_o = maximum moment; s = ratio of the strain at onset of strain hardening, ϵ_{sh}, to the yield strain, σ_y/E; σ_y = yield stress; $h = E/E_t$; and E_t = tangent modulus. For calculating θ_p at the load point at the center of a span, L is the span length if the span ends are simply supported or L is one-half the span length if the span ends are fixed. For calculating θ_p at the end of a centrally loaded end span, L is one-fourth the span length.

If the steel ruptures before buckling, $M_p/M_o = \frac{\sigma_y}{\sigma_u}$,

where σ_u is the tensile stress. Then, equation (2-2) becomes

$$k = A\left[\left(\frac{\varepsilon_{sh}}{\sigma_y/E}\right) + B\left(\frac{E}{2E_T}\right)\right] \qquad (2\text{-}3)$$

where the constants $A = (1 - \sigma_y/\sigma_u)$ and $B = (\sigma_u/\sigma_y - 1)$. This is not common for tank ship stiffeners.

For angle stiffeners of tank ships, buckling will generally occur before strain-hardening relative to rotation capacity. Based on some tests, it was hypothesized [11] that a "compact" (as defined by AISC) [13] flange in compression will form a plastic local buckle in a region of moment gradient when the yielded length L_y equals or exceeds the theoretical plastic-local-buckle wave length λ, which is

$$1.42\left(\frac{bt}{w}\right)\left(\frac{A_w}{A_f}\right)^{\frac{1}{4}}$$

where b is the total width of flange (two times one flange projection, measured from the center of the stiffener web), t is the flange thickness, A_f is b times t, w is the web thickness, and A_w is the web area. For the analysis to be generally applicable to "compact," "non-compact," and "extra-compact" sections, an examination of some test data [12,14] indicated that it would be reasonable to multiply each of the values

$$1 - \frac{M_p}{M_o} = \frac{VL_y}{VL_y + M_p} \qquad (2\text{-}4)$$

and

$$\frac{M_o}{M_p} - 1 = \frac{VL_y}{M_p} \qquad (2\text{-}5)$$

by a compactness factor

$$\frac{52.2\ t}{0.5b\sqrt{\sigma_y}}$$

where V is the shear in the region between M_p and M_o and σ_y is the yield strength. For a distance $L'/2$ (see Section 3.4.2) from a point of zero moment to a plastic hinge, the approximation may be made that $M_p = VL'/2$. Then, the expressions for A and B in equation (2-3) become

$$A = \left(\frac{2L_y}{2L_y + L'}\right)\left(\frac{52.2\ t}{0.5b\sqrt{\sigma_y}}\right) \leq \left(1 - \frac{\sigma_y}{\sigma_u}\right) \qquad (2\text{-}6)$$

$$B = \left(\frac{2L_y}{L'}\right)\left(\frac{52.2\ t}{0.5b\sqrt{\sigma_y}}\right) \leq \left(\frac{\sigma_u}{\sigma_y} - 1\right) \qquad (2\text{-}7)$$

For exactly compact sections, the compactness factor is 1.0.

2.4.2.2 Energy Absorbed in a Traveling Yielded Zone during an Oblique Collision

The two longitudinal force components occurring at the location of the strike during an oblique collision are the friction force between the ships and the resistance to the traveling plastic hinge (yielded zone) (see Figure 3-5) that is associated with the plastic energy absorbed in forming a bend angle in the struck hull. Thus, the latter force adds to the plastic energy. A theoretical evaluation of the longitudinal resistant force of the stiffened plates due to the occurrence of the traveling plastic hinge can be made by equating (1) the plastic energy consumed in bending and then straightening a given length, L, of the stiffened plates to (2) the product of L times the unknown longitudinal resistance force.

Within a square inch of a plate with a thickness t, yield stress σ_y, and yield strain ε_y (Figure 2-4), the plastic energy consumed in cylindrical bending to a maximum strain $\varepsilon_m > \varepsilon_y$ is, neglecting strain hardening.

$$\frac{\sigma_y \varepsilon_m t}{2} \left(1 - \frac{\varepsilon_y}{\varepsilon_m}\right)^2$$

Multiplying this expression by 2 to include the plastic energy consumed in straightening, and substituting $\varepsilon_y = \sigma_y / E$ and $\varepsilon_m = 0.5t/R$, where E is the modulus of elasticity and R is the maximum midplane radius of bending, results in a total plastic energy which is equal to the longitudinal resisting force, F_R, per inch of plate width. That is,

$$F_R = \frac{\sigma_y t^2}{2R} \left(1 - \frac{\sigma_y R}{0.5Et}\right)^2 \qquad (2\text{-}3)$$

where the subscript R (for F) corresponds to radius R. Thus, the resisting force is a function of the plate thickness, yield strength and the maximum radius of bend.

For a plate acting monolithically with a longitudinal angle or tee-shaped stiffener, the evaluation of F_R is more complex, although the basic theory is the same. The unknown depth, d′, from the neutral axis of pure bending to the outer fiber of the stiffener which is strained at $\varepsilon_m = \frac{d'}{R}$, can be determined from equating to zero the forces on the cross-section; σ_y occurs where $\varepsilon_y \geq \varepsilon_m$, but the stress is proportional to the strain where $\varepsilon_y < \varepsilon_m$. Plastic straining will occur only within a depth (from the outer fiber of the stiffener) of

$$d'\left(1 - \frac{\varepsilon_y}{\varepsilon_m}\right)$$

Consequently, the portion of F_R due to plastic straining of the stiffener web (thickness t_w) is obtained by substituting $d' = 0.5t$ and multiplying Equation (2-8) by $t_w/2$, giving

$$\frac{\sigma_y (d')^2 t_w}{R} \left(1 - \frac{\sigma_y R}{d' E}\right)^2$$

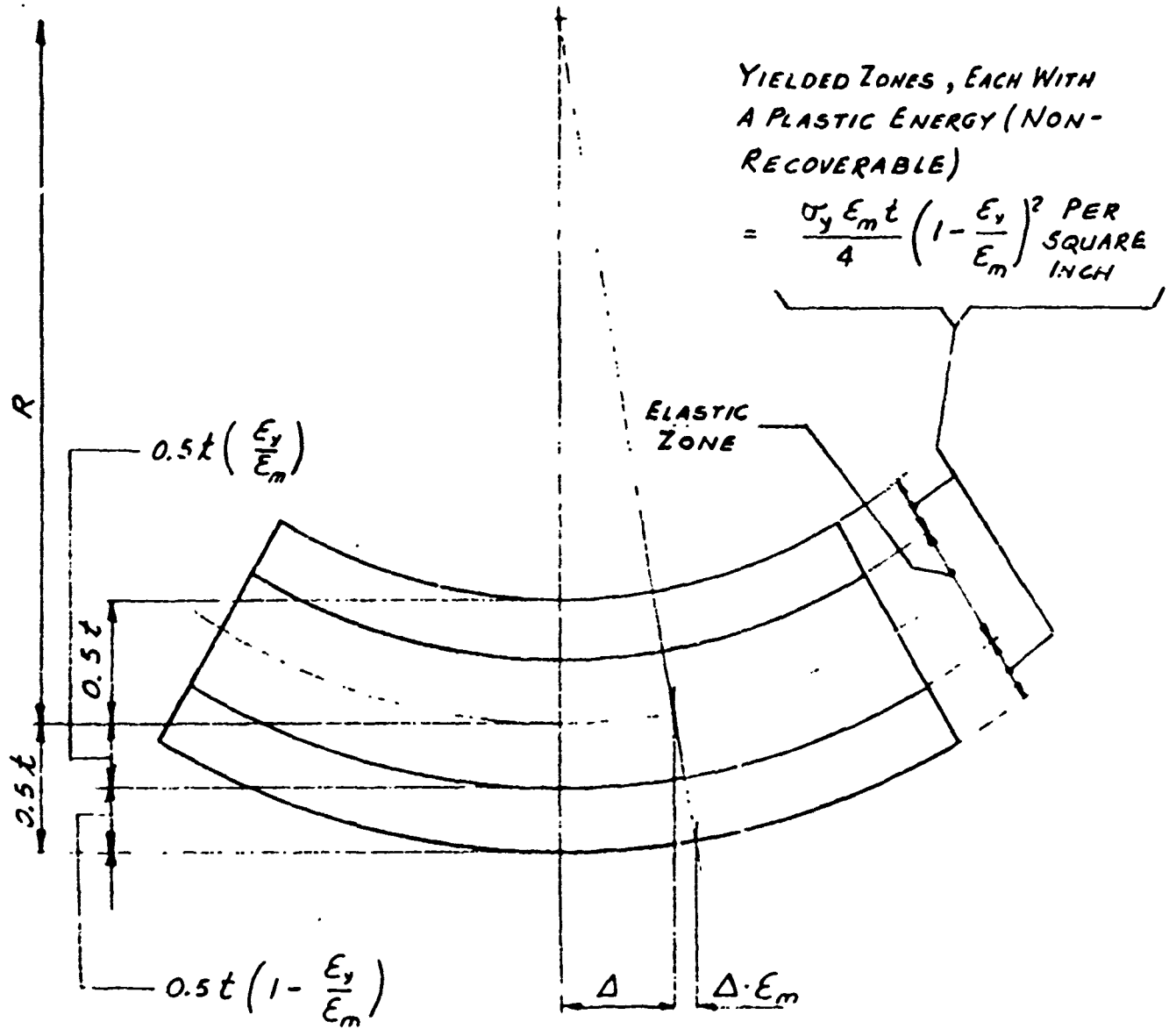

FIGURE 2-4

PLASTIC CYLINDRICAL BENDING OF A PLATE

The portion of F_R due to plastic straining of the remaining portion (width $b - t_w$, thickness of the stiffener flange is

$$\sigma_y t_f (b - t_w) \left(\frac{d' - 0.5t_f}{R} - \frac{\sigma_y}{E} \right)$$

Thus, corresponding to one longitudinal stiffener, the theoretical longitudinal resisting force is

$$F_R = \frac{\sigma_y d'}{R} \left[d' t_w \left(1 - \frac{\sigma_y R}{d' E}\right)^2 + t_f (b - t_w) \left(\frac{d' - 0.5t_f}{d'} - \frac{\sigma_y R}{d' E} \right) \right] \quad (2\text{-}9)$$

For an approximate evaluation of F_R, d' may be assumed to be equal to the depth of the stiffener.

Finally, the plastic energy associated with F_R is F_R times the longitudinal length of the portion of the hull that is traversed by the strike.

2.4.3 Theory for Plastic Membrane Tension

2.4.3.1 Apparent Ductility for Membrane Straining

Although it has been observed for ABS steels that the elongation, at rupture, within a 2-inch gage length is typically as much as 32 percent, the high point of the stress-strain curve, after which the steel starts to unload, is typically only about 10 percent, see Fig. 2-2. Thus, when a large portion of the steel is strained at about 10 percent, some critical portion is likely to be unloading, perhaps rapidly. Therefore, it is realistic to assume that the useful ductility for membrane straining is only

$$\varepsilon_r = 0.10 \frac{D}{32\%} \quad (2\text{-}10)$$

where D is the tension-test ductility.

2.4.3.2 Relation Between Bend Angle and Apparent Maximum Strain

As developed in relation to the component structures tests, Section 6, an equation relating the maximum combined bending plus membrane-tension strain at hull rupture, ε_m, to the bend angle, is

$$\varepsilon_m = \frac{4}{3} \frac{\sigma'}{\sigma_u - \sigma' \cos \theta_n} \sin \theta_n \tan \theta_n \qquad (2\text{-}11)$$

where $\sigma' = 0.5(\sigma_u + \sigma_y)$ and θ_n is one half the critical bend angle (see Figure 2-5) at which rupture will occur.

The results of the component structure tests, Section 6, indicate that (1) the limitations implied by this equation need only to be considered for bend angles in the hull at web frames or transverse bulkheads away from the strike (the limitations would apply at the strike only for a strike by a very sharp object, sharper than a conventional bow), and (2) it is reasonable in this equation to assume $\varepsilon_m = 1.5\ D$, where D is the tensile-test ductility. The value of ε_r does not apply to ε_m.

2.4.3.3 Membrane Stretching

When a straight-line portion of a plate (or stiffened plate) of original length L stretches so that one end of the straight-line portion moves laterally a distance δ without a shortening of projected distance L, the new length of the plate is $(L^2 + \delta^2)^{\frac{1}{2}}$. Using the first two terms of the binomial series, the difference between the new length and the original length can be expressed as

$$e = (L^2 + \delta^2)^{\frac{1}{2}} - L \approx \frac{\delta^2}{2L} \qquad (2\text{-}12)$$

However, if the projected distance L shortens, by moving longitudinally, e also shortens by approximately the same amount.

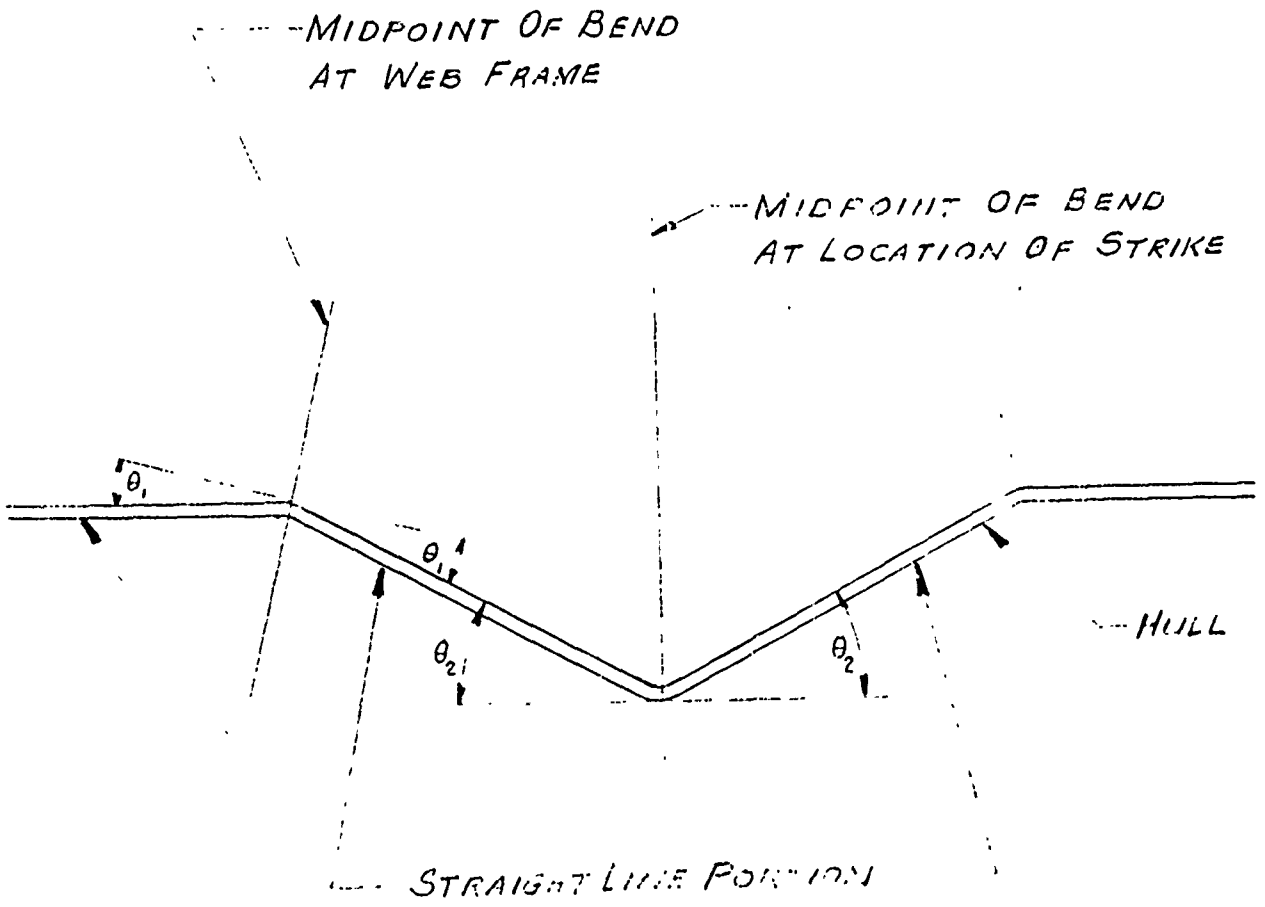

NOTE: THE BEND ANGLE AT THE LOCATION OF THE STRIKE IS NOT CONSIDERED CRITICAL IF THE RADIUS OF THE STRIKING OBJECT IS 6" OR GREATER

Figure 2-5 Bend Angles in Stiffened Hull During Membrane-Tension Phase

2.4.4 Theories for Inelastic Shearing

2.4.4.1 Energy of In-Plane Shearing

A summary is given in a Column Research Council publication [15] of a theory for tension-field action resisting shear in thin webs of stiffened plate girders, following elastic shear buckling. The governing assumption is that the flanges are so flexible that all of the tension is "anchored" at the transverse stiffeners and none is anchored at the flanges. The extension of this theory to obtain general expressions for the plastic energy of in-plane shearing is shown in Section 3.

2.4.4.2 Energy of Normal-to-Plane Shearing

A series of tests [16] indicated that the force required to shear a hot-rolled steel plate is the area sheared times an average stress equal to 73.5 percent of the maximum shearing strength. The work expended in shearing the plate is 35 percent of this force times the plate thickness (see Section 3).

3. COLLISION ANALYSIS PROCEDURE

3.1 General

The Collision Analysis Procedure described below generally relates to plastic deformation of structure only. As discussed in Section 2, the energy absorption involved in local elastic deformations and in the overall elastic vibratory response to the collision "impact" is negligible compared with the plastic energy. Also, it was confirmed that the rigid body motion of the struck and striking ship together is small during the minor collision process (as also observed in actual collisions) regardless of where the ship is struck, with the result that the associated energy absorption is negligible.

The general assumptions of the Collision Analysis Procedure will be given in Section 3.2. These assumptions and the plastic energy analyses theories of Section 2 form the foundation of the Procedure.

The Collision Analysis Procedure is summarized in Sections 3.3 and 3.4. A step-by-step calculation-oriented version of the Procedure is contained in a primer[17] published as a separate report.

3.2 Assumptions

Because the dynamics of ship collisions are quite complex, a few reasonable simplifying assumptions must be made to keep the analysis tractable and to isolate the most important parameters that determine to what extent a ship can successfully resist hull rupture during a minor collision. However, this does not mean that each is completely proven.

In fact, some of the assumptions stated herein have changed considerably from those made at the beginning of the study in light of collision inspections, testing and sample calculations. In consideration of this, the recommendations given at the end of the report outline further analyses and testing to more fully evaluate the assumptions.

Some assumptions regarding membrane tension analyses have been included in the section describing these, Section 3.4.3, instead of below, for convenience.

3.2.1 Overall Behavior of Colliding Ships

1. The most significant measure of incursion resistance without hull rupture is the capacity for absorbing plastic energy as indicated in Section 2. The collision is conceived as any inelastic (or plastic) impact -- that is, one in which the striking and struck bodies remain together after the impact. The energy "lost" during the collision, which is the plastic energy absorbed by the struck ship distortion, is therefore a function of the ship masses (including virtual masses of the water), the initial bearings, and velocities.

2. Throughout the analysis, the bow of the striking ship is considered infinitely stiff. This was accepted as a conservative assumption, based on the belief that a non-rigid bow structure can increase the total energy absorption in a minor ship collision due to energy absorption in the striking ship. However, it is realized that the non-rigid bow of a striking ship may distort in such a way as to provide a sharper profile for puncturing the struck ship. This can result in a severe decrease in the total energy absorption. The effect of such a distortion is discussed

further in Section 7. Inspections of actual collisions described in Section 5 indicate that striking bows may remain undistorted except where they encounter stiff horizontal resistance at a deck or bilge area of the struck ship.

3. The case of rigid sharp bow structure with the capability of immediately cutting or punch-shearing the shell of the struck ship is a special case and does not fit within the scope of this investigation.

4. The collision angle is assumed to remain constant throughout the collision process, implying that the inertia of each ship is so great that neither ship rotates during the collision. This assumption has been theoretically validated as described in Section 2 and is also consistent with observed damaged profiles of actual ships as discussed in Section 5.

5. The bottom of the ship, the bilge strake, and the transverse bulkheads do not buckle, yield, or rupture. The distortions occur in a portion of the struck ship between two consecutive transverse bulkheads and above the bilge strake. The damaged area may be equal to or less than the area thus bounded (See Figure 3-1). This assumption therefore limits the types of the collisions that can be analyzed with the Collision Analysis Procedure presented below.

6. Dynamic structural effects are ignored, so that the analysis corresponds to a static analysis. It is realized, however, that even in a slow collision dynamic response of the structure to the striking force may have a significant effect on the overall plastic deformation. This aspect is discussed further in the recommendations outlined in Section 8.

7. Failure occurs when the plating of a cargo tank is ruptured.

8. The length of damage is the same for the deck, hull plate, and all damaged longitudinals (Figure 3-1).

9. Glancing blow collisions are not considered.

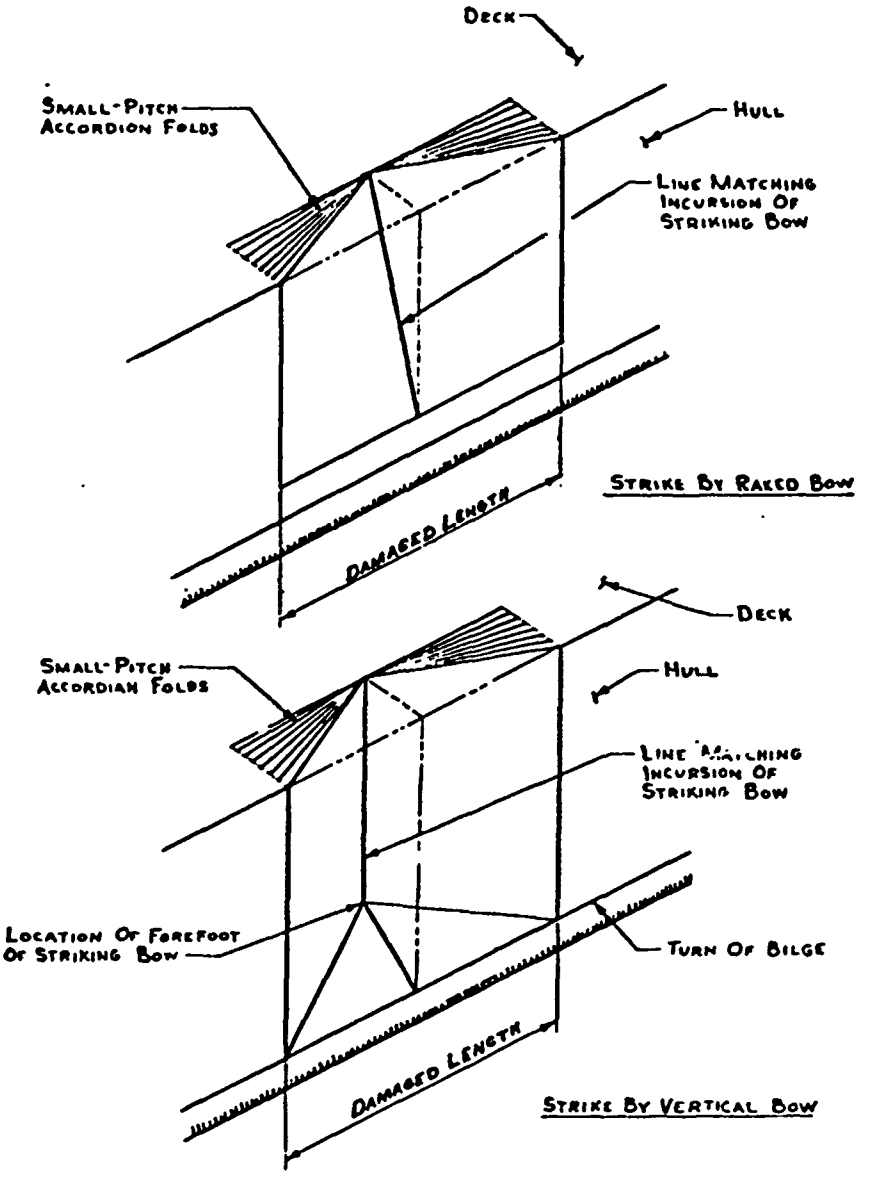

FIGURE 3-1 Assumptions for Collision Imprint in Struck Ship

3.2.2. Basic Assumptions

On the basis of the observations and analyses of actual collision damage and the component-structure model tests, the basic assumptions given below were applied to the analysis procedure.

3.2.2.1 Modes of Failure

1. Plastic-bending and membrane-tension phases of the structural behavior of the longitudinally stiffened plates are considered separately, as illustrated in the force-deflection diagram, Figure 3-2. Membrane tension is not considered prior to stiffener buckling (tripping) or rupture. If the stiffener flange ruptures, either during the plastic-bending phase or at the end of the membrane-tension phase, the rupture is assumed to continue through the stiffener and attached plate. After stiffener buckling (tripping) only, the stiffened plates are assumed to immediately unload in bending but reload in membrane tension. Evidence of this mode of behavior has been observed in the inspection of several actual collisions.

2. Once a rupture is initiated, it will propagate throughout the stiffened hull plating to the extent determined by the incursion of the striking ship, regardless of whether the fracture is brittle or ductile. The only difference assumed between ductile and brittle fractures in a single-shell ship is that a relatively minor energy is absorbed in the propagation of a ductile failure but none in the propagation of a brittle failure. In a double-shell ship, it is presumed that details of the ship construction will arrest the progress of the cracking so that a ductile rupture will not spread from the outer hull to the inner hull; the striking bow must engage the inner hull before it can rupture.

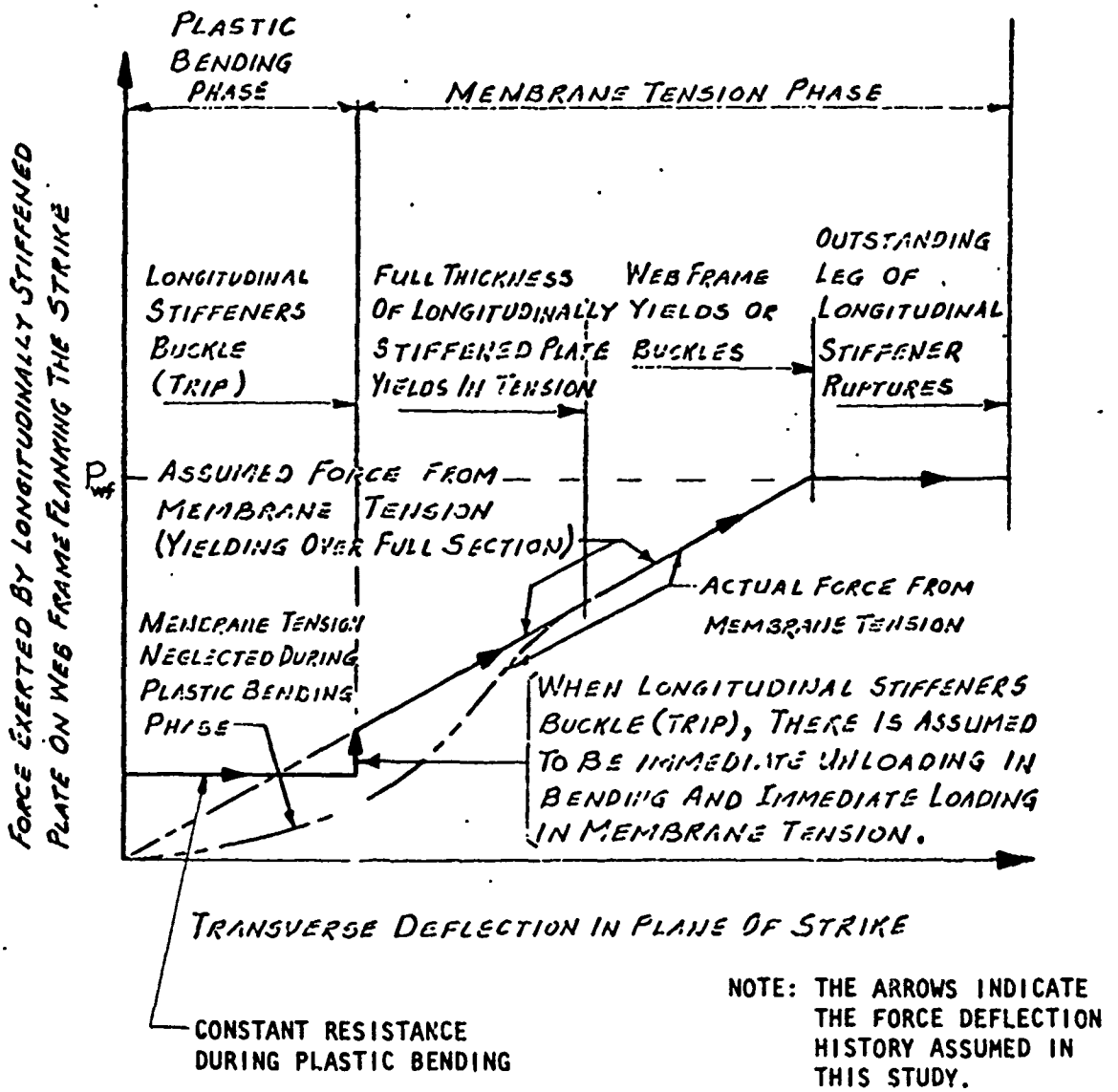

FIGURE 3-2

VARIATION OF TRANSVERSE FORCES WITH INCURSIONS

3. It is assumed that the deck may easily rip away from the web frames, so that the deformed portion of the deck may always be assumed to appear as an inverted V in the deck plan. Ductile-tearing energy is neglected in the ripping of the stiffened deck plate from the web frames.

4. A combination of membrane-tension straining and bending, which results in the limitation of the bend angle as discussed in Section 2.4.3.2, needs to be considered during the membrane-tension phase only at bend angles in the stiffened hull at web frames or transverse bulkheads away from the strike. Although the total bend angle at the strike is greater, it generally is not critical because the curvature there is moderate, corresponding to the horizontal curvature of the stem of the striking bow. Equation 2-11, Section 2.4.3.2, relates the critical bend angle to the material strength and ductility parameters.

3.2.2.2 Models of Hull Structure

1. Behavior and rupturing of the outer shell, inner shell, and deck are each considered separately, and it is assumed that rupture in one is not automatically propagated to another.

2. It is assumed that the transverse bulkheads act as longitudinally fixed restraints for the longitudinally stiffened plates loaded in membrane tension. This behavior has been observed during inspections of actual collisions. The short distances transverse bulkheads move toward the transverse plane of the strike are equal to the distance to the plane of the strike times the longitudinal compressions strain ε_c that results from elastic bending of the entire ship cross-section. These movements are neglected since this compression

straining is always much less than the plastic elongation.

3. Where web frames are yielded, buckled, or otherwise permanently distorted in the transverse direction, they do not act as longitudinally fixed restraints, and longitudinal forces and strains on either side of a distorted web frame tend to be nearly equal (see Section 3.4.3.2). This behavior has been observed during the component structures test described in Section 6. Conversely, where web frames are not distorted transversely, they are assumed to be longitudinally fixed restraints, and they (and/or one or two transverse bulkheads) bound the damaged length (the length over which the hull is distorted transversely).

4. If the top of the striking bow is above the deck of the struck ship, the struck deck forms a series of low-pitch longitudinal folds, Figure 3-1, "gathered" at the location of maximum incursion and extending over a length equal to the damaged length of the hull; any deck failure is by transverse rupturing resulting from longitudinal membrane tension. This behavior has been observed during actual collision inspections.

5. Both the longitudinally stiffened side plates and deck plates are considered to be assemblies of independently acting "T-beams," with each T-beam consisting of one longitudinal stiffener and the portion of the side plate with which it may be assumed to act in structural unison. Generally, the dividing line between two adjoining T-beams is halfway between the stiffeners.

6. With a vertical striking bow, a vertical incursion is assumed. The transverse deflections of the stiffened hull may be assumed to vary linearly from the elevation of the forefoot of the striking bow down to zero at the bilge strake of the struck ship (see Figure 3-1).

7. With a raked striking bow, a sloping incursion identical to the outline of the striking bow is assumed (see Figure 3-1). In addition, the imprint of the damaged area will appear rectangular in side elevation regardless of the number of web frame spaces damaged. It should be noted that even though it is assumed the least stressed T-beam deflects along the whole damaged length, the absolute value of the deflection will be small enough to result in a small amount of energy absorption when compared to the most highly strained T-beam.

8. If the top of the striking bow is below the deck of the struck ship, the deck does not deform; then, the transverse distortion of the struck hull varies linearly from zero at the deck elevation of the struck ship to a maximum value at the elevation of the striking bow.

9. The transverse resisting force offered by a web frame is assumed to be equal to the shearing capacity of the web plate for a strike in the plane of that web frame, or constant and equal to the set of forces from the T-beams initially causing yielding or buckling of the web frame for the web frames flanking the strike.

10. After a web frame starts to yield or buckle, the resisting force, P_{wf}, offered by the web frame against the most highly strained T-beam of the stiffened hull remains constant while the web frame distorts transversely. The distorted configuration of the web frame should correspond to the vertical incursions of the vertical and raked striking bows discussed in assumptions 6. and 7. above.

11. Plastic tensile strains equal to one half the strains at the ends of the damaged length occur in the stiffened hull within the web-frame space just beyond the damaged length, as discussed in Section 6.

12. For oblique collisions, plastic membrane-tension strains occur in the stiffened hull only behind the strike (on the acute-angle side of the strike) and not ahead of the strike (on the obtuse-angle side of the strike). Over the longitudinal distance traversed by the strike, the striking bow propagates in bending a yielded zone longitudinally through the stiffened hull of the struck ship.

13. The collision angle differentiates between a right-angle and an oblique collision and it determines the longitudinal distance over which the bending yielded zone is propagated through the hull.

3.2.2.3 Material Properties

1. As discussed in Section 2.4.3.1, the steel ductility, ε_r, available before unloading during either the bending or the membrane-tension phase is 0.10 in./in. strain for ABS steels (with a tension-test ductility in a 2-in. gage length of about 32 percent) or, Equation 2-10,

$$\varepsilon_r = 0.10 \frac{D}{32\%}$$

for another steel with a tension-test ductility of D in a 2-in. gage length. This limitation applies to either maximum bending strains during the bending phase only or to overall stretching during the membrane-tension phase (see Section 6).

2. During either the bending phase or the membrane-tension phase, the value of longitudinal stress, tension or compression in the bending phase or tension in the membrane phase, in plastically deformed portions of the stiffened hull plate is assumed to be (see Section 6)

$$\sigma' = \frac{\sigma_u + \sigma_y}{2} \qquad (3\text{-}1)$$

For an oblique strike, the damaged portion of the side-shell ahead of the strike is assumed to be stressed elastically to a value of one-half the stress in the plastically deformed areas or:

$$\sigma'_E = \frac{\sigma_u + \sigma_y}{4} \qquad (3\text{-}2)$$

This is based on the judgement that in an oblique collision the extent of the damaged length ahead of the strike may typically be only roughly one-half of the extent of the damaged length behind the strike. (The procedure outlined in Section 3.4.3.2 would lead to an observation that the extent of damage on each side of a strike would be roughly proportional to the membrane tension thrust on that side.)

3. The ductile-tearing energy is assumed to be 1000 foot-pounds-per-square-inch, which is roughly the "shelf" (top portion of transition curve) energy for A36 and ABS-C steels[18]. No ductile-tearing energy is assigned for components at a temperature below the transition temperature for the steel.

3.3 Collision Phenomena

3.3.1 General

The lading will escape from a single-shell ship when the hull ruptures. For a double-shell ship the inner shell must also rupture before the lading escapes. The analyses presented in this Section relate to the forces, distortions, and plastic energy absorbed in the structure up to the incidence of hull rupture that results in the escape of the lading.

The mathematical model assumed for analyzing the structural behavior of a struck ship primarily involves three phenomena producing plastic distortions: (1) longitudinal plastic bending of the stiffened hull plating, (2) plastic membrane tension in the stiffened hull and deck plating, and (3) yielding or buckling of the web frames.

As stated above it is convenient to analyze the stiffened hull of the struck ship as a series of independent longitudinal T-beams, each consisting of one longitudinal stiffener and the portion of hull plating that may be assumed to act monolithically with that stiffener. Furthermore, it is convenient to perform a stress-and-strain analysis for only the most highly strained T-beam and to assume that the ratio of the transverse deflection, plastic energy, or interacting force (on a web frame) of any particular T-beam to that of the most highly strained T-beam is equal to some proportion determined by the incursion. The deck is also conveniently considered to be divided into longitudinally extending T-beams for the analysis of membrane stretching of the damaged deck.

3.3.2 Sequence of Phenomena

The sequence of the possible phenomena, up to rupture of the struck ship sideshell, is outlined in the flow diagram of Figure 3-3 for a single shell ship. For a double shell ship the phenomena are similar and presented later.

Initially, the stiffened hull plating will distort in a plastic bending phase, with plastic "hinges" forming in the vicinities of the strike and the web frames flanking the strike. During this phase, insignificant membrane tension will be developed. For a typical tanker with longitudinal angles stiffening the hull plating, the longitudinal angle-shaped stiffeners will then buckle in the vicinity of the flanking

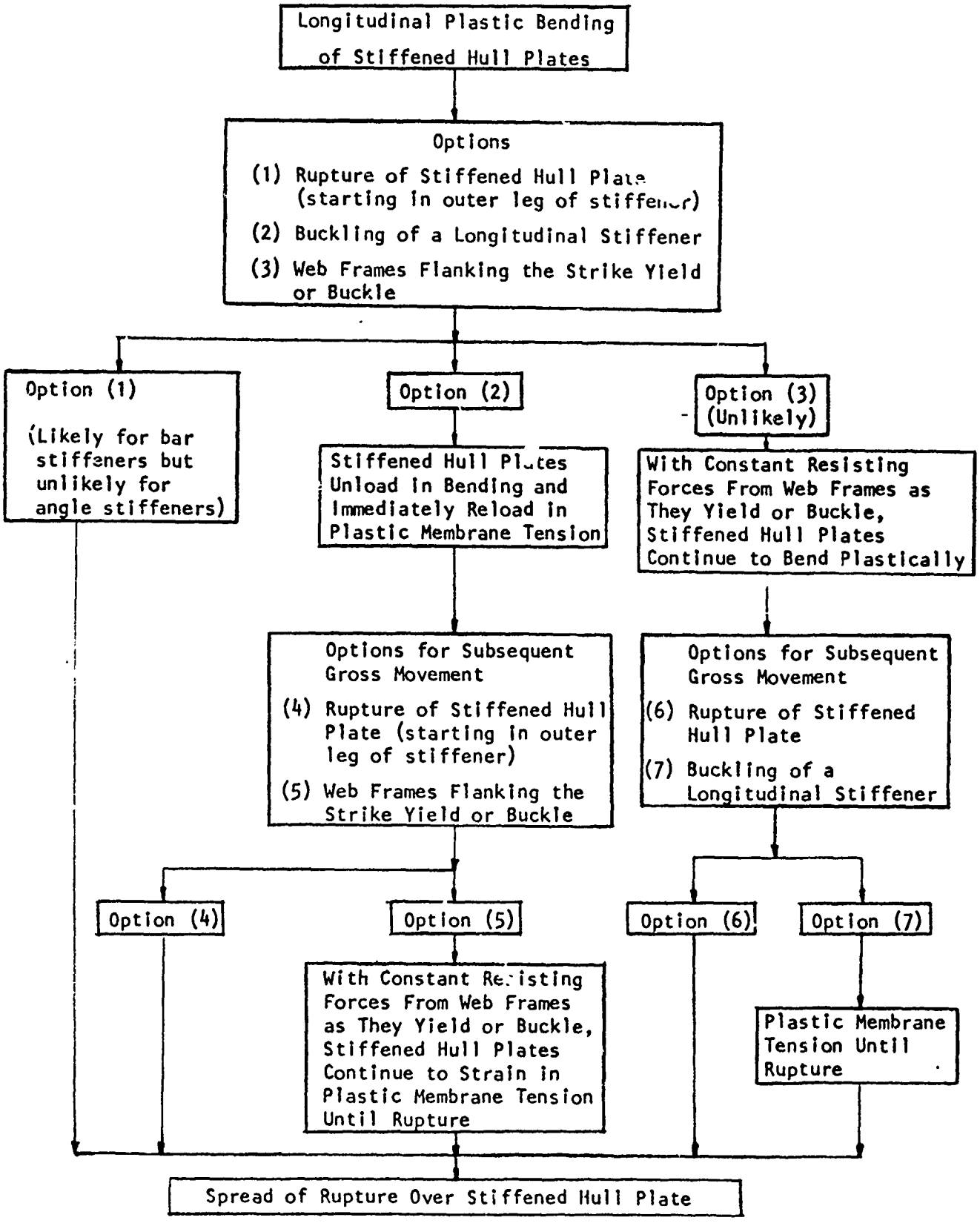

FIGURE 3-3 Macro Flow Diagram for Side-Collision Plastic-Energy Analysis for a Single Shell Ship

web frames, and possibly "trip" in the vicinity of the strike. Subsequently, the stiffened hull will unload momentarily as the strike continues, but will reload in a membrane-tension phase. The hull will rupture at the end of this phase, with possibly the flanking web frames yielding or buckling before the hull ruptures. In such cases, the membrane-tension phase is divided into two subphases respectively: (1) there is no transverse movement of the web frames flanking the strike and (2) the web frames flanking the strike move inward toward the ship's centerline and the damage extends into the adjacent web frame spaces. During these phases, the deck is also distorting in membrane tension. However, as discussed in Section 3.2.2.2, the deck behavior is presumed not to affect the sequences of the options listed in Figure 3-3.

As indicated in Figure 3-3, other sequences of phenomena are possible. A hull with longitudinal stiffeners such as rectangular bars that are not apt to buckle or trip, will tend to rupture before significant membrane tension has a chance to develop. Alternatively, with any type of hull stiffeners, very weak web frames could conceivably yield or buckle before rupture or buckling of the longitudinal stiffeners, in which case the damaged length would increase during the bending phase. These phenomena would be unlikely, however, for typical ships.

3.3.3 Strike by a Raked Bow

For a strike by a raked bow, the most highly strained T-beam in the struck stiffened hull is the one nearest to the elevation of the top of the striking bow, Figure 3-1. The transverse deflections of the T-beams and any web frames that are deformed transversely are assumed to vary linearly from the elevation of the most highly strained T-beam down to zero at the elevation of the lower limit of the incursion by the striking bow as discussed

in Section 3.2.2.2. This means that (1) the elevation view of the "imprint" evidencing the transverse distortion of the stiffened hull will be rectangular, as indicated in Figure 3-1 (rather than triangular); and (2) as an incursion by a raked bow increases, the vertical dimension of the imprint becomes greater, with proportionately more T-beams being distorted transversely.

3.3.4 Strike by a Vertical Bow

All T-beams struck by the vertical portion of a vertical bow will tend to be equally strained. The one T-beam that by inspection is deemed most highly stressed is analyzed, and the other T-beams are assumed to deflect transversely by the same amount. Transverse deflections of the stiffened hull may be assumed to vary linearly from the elevation of the forefoot of the striking bow down to zero at the bilge strake of the struck ship, Figure 3-1, as discussed in Section 3.2.2.2.

3.4 Plastic Analysis

3.4.1 General

The procedures for analyzing the most highly strained T-beam will be presented below. As discussed in Section 3.3.1 for other T-beams, the ratio of incursions at each can be used to determine forces and plastic energy absorptions pertaining to those T-beams.

Also, as discussed in Section 3.3.1, the plastic analysis consists of three phenomena, namely longitudinal plastic bending of the stiffened hull plating, plastic membrane tension in the stiffened hull plating and deck, and yielding or buckling of the web frames. These three phenomena will be discussed separately below.

3.4.2 Longitudinal Plastic Bending

The basic analysis for the bending phase, assuming no lateral movement of the web frames flanking the strike, is summarized in Figure 3-4. As in conventional plastic bending analysis, the T-beam shown in the sketch in Figure 3-4 is assumed to deflect as straight-line segments extending between plastic hinges. In the analyses herein the location of the maximum incursion during the bending phase is assumed to be the same as at the end of the membrane-tension phase -- even for oblique collisions, for simplicity.

As described in Section 2.4.2.1, the rotation capacity of a continuous beam subjected to a concentrated lateral load is, Equation 2-1,

$$\theta_p = k\frac{M_p}{EI} L$$

As applied to the collision analysis, Figure 3-4, L is one-half the span length between two consecutive web frames if θ_p is the total rotation at the plane of the strike; or,at the location of a supporting web frame,L is considered to be $L'/2$ since there is a point of zero bending moment at the center of the length L', where L' extends from the load to the nearest support. Assuming $L=L'/2$ is a lower-bound assumption for computing θ_p at a supporting web frame because it corresponds to a fixed end of the loaded span, as would only be provided by a web frame resisting rotation of the stiffened hull plating. However, using that

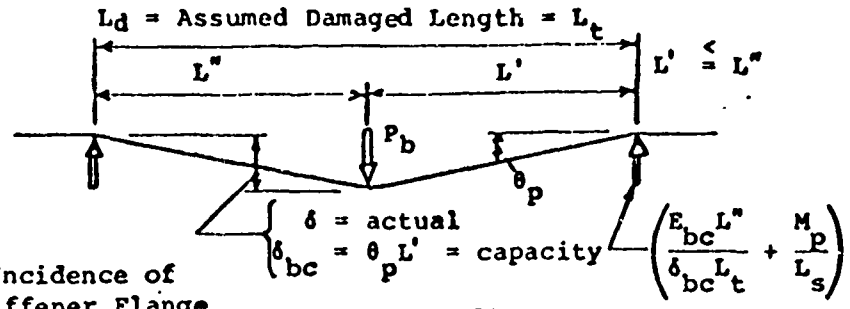

Distortion at Incidence of Buckling of Stiffener Flange

$$\theta_p = k\left(\frac{M_p}{EI}\right)\left(\frac{L'}{2}\right)$$

where

$$k = A\left[\left(\frac{\varepsilon_{sh}}{\sigma_y/E}\right) + B\left(\frac{E}{2E_t}\right)\right]$$

$$A = \left(\frac{2L_y}{2L_y + L'}\right)\left(\frac{52.2t}{0.5b\sqrt{\sigma_y}}\right) \leq \left(1 - \frac{\sigma_y}{\sigma_u}\right)$$

$$B = \left(\frac{2L_y}{L'}\right)\left(\frac{52.2t}{0.5b\sqrt{\sigma_y}}\right) \leq \left(\frac{\sigma_u}{\sigma_y} - 1\right)$$

M_p = plastic moment of one tee-beam unit.
I = moment of inertia of one tee-beam unit.
E = modulus of elasticity
E_t = tangent modulus
ε_{sh} = strain at onset of strain hardening.
L_y = yielded length of stiffener flange.
λ = length of a flange buckle wave.
$0.5b$ = width of outstanding leg of stiffener flange, measured from center of web.
t = thickness of stiffener flange.
w = thickness of stiffener web.
$A_f = bt$
A_w = area of stiffener web.

Yielded Length = Length of Buckle

$$L_y = \lambda = 1.42\left(\frac{bt}{w}\right)\left(\frac{A_w}{A_f}\right)^{1/4}$$

Plastic Bending Energy

$$E_{bc} = 2M_p\left(1 + \frac{L'}{L''}\right)\left(\frac{\sigma_y + \sigma_u}{2\sigma_y}\right)\theta_p = \text{capacity}$$

$$E_b = E_{bc}\frac{\delta}{\delta_{bc}} = \text{energy corresponding to } \delta$$

Force From Strike

$$P_b = \frac{E_{bc}}{\delta_{bc}} + \left[\begin{array}{c}\text{resistance of web frame directly} \\ \text{at strike (if present)}\end{array}\right]$$

FIGURE 3-4 RIGHT-ANGLE OR OBLIQUE COLLISION -- BENDING ANALYSIS OF LONGITUDINALLY STIFFENED HULL PLATE FOR NO LATERAL MOVEMENT OF WEB FRAMES FLANKING THE STRIKE

assumption resulted in a fair correlation with the results of the component structures tests. Furthermore, with that assumption, it is generally not necessary to compute θ_p at the plane of the strike. Although the hull stiffeners tend to trip at the plane of the strike, the stiffener flanges, which are in tension at that location may rupture but will not buckle.

As shown in Figure 3-4, k becomes a formulation with two parameters, A and B. If the plate ruptures before buckling, the right-side expressions for A and B in Figure 3-4 govern. If the stiffener buckles plastically without rupturing, A and B are represented by the other (left-side) expressions in Figure 3-4, each being the product of a factor employing the yielded length, L_y, and a "compactness" factor.

The expressions for plastic bending energy in Figure 3-4 include the plastic energy of the three plastic hinges. The external force necessary to cause the plastic bending is a constant value, equal to the plastic bending energy divided by the lateral deflection at the strike.

3.4.3 Hull Sideshell Membrane Tension

3.4.3.1 General

The analyses of the membrane tension phase are summarized in the figures of this Section.

Rupture of the plate is assumed to occur when the available steel ductility, ε_r, as defined by Equation 2-10 of Section 2.4.3.1, is exhausted or the critical bend angle is exceeded as defined by Equation 2-11 of Section 2.4.3.2. Multiplying ε_r by the length of the portion of the damaged length of the stiffened hull plate that stretches plastically (the entire damaged length for a right angle collision, but only the portion of the damaged length behind the strike for an oblique collision) gives the approximate limitation on the amount of total longitudinal stretching within the damaged length that the steel can endure without rupturing.

The membrane-tension analyses described herein are derived based on certain assumptions in addition to those given in Section 3.2.2. These assumptions are as follows:

1. The stiffened hull is assumed to deflect in straight-line segments between web frames.

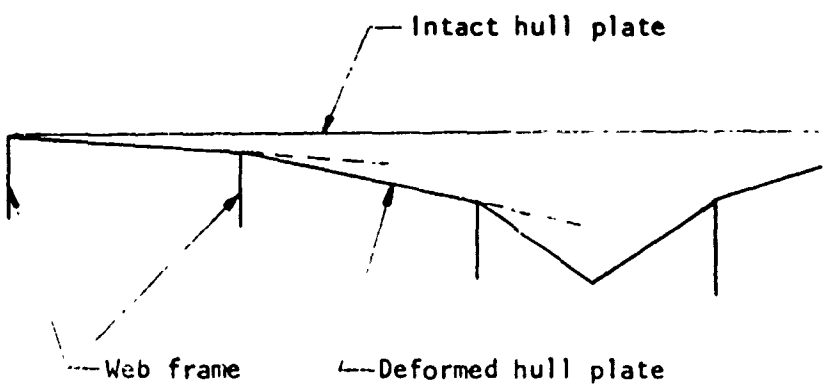

2. Small deflections are assumed so that $\tan \theta_n \approx \sin \theta \approx \theta_n$. This allows the deflection of the hull plate δ to be expressed in terms of the distance between webs L, membrane tension T and strength of the web frame P_{wf}.

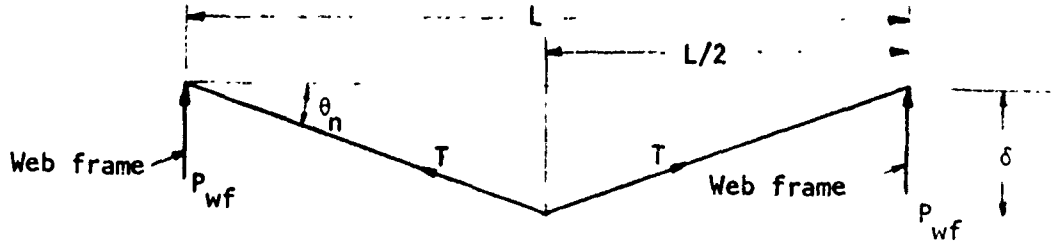

$$P_{wf} = T \sin \theta_n \cong T \frac{\delta}{\frac{1}{2}L} \qquad (3\text{-}3)$$

$$\therefore \delta = \frac{P_{wf} L}{2T} \qquad (3\text{-}4)$$

$$\text{and} \quad \theta = \frac{P_{wf}}{T} \qquad (3\text{-}4a)$$

3. Referring to Section 2.4.3.3, Equation 2-12 expressed as

$$e = \frac{\delta^2}{2L} \qquad (3\text{-}5)$$

is used the compute a hypothetical elongation of each straight-line segment (of length L) of the deformation profile over the damaged length of the stiffened hull, based on the hypothetical assumption that the distances between web frames do not change; δ is the transverse offset corresponding to a length L. The web frames within the damaged length do actually move longitudinally, but those at the ends of the damaged length do not move. Although such longitudinal movements of web frames within the damaged length affect the distortion geometry within each web frame space, the total elongation of the sideshell over the damaged length is ciosely approximated by summing, for all straight-line segments of the damaged sideshell, values of e computed by Equation 3-5 as discussed above.

4. Structural components of the hull can yield in only one mode at a time. For example, in the case of a double shell hull, the web frames between hulls cannot fail due to buckling and bending or shear simultaneously when a force is applied to the outer hulls.

5. The membrane tension T in the sideshell varies as a second degree parabola with the strain ε as shown below. The vertex of the parabola is at $\varepsilon_{max.}$. This simplifying approximation, as derived from typical stress-strain curves, is the basis for development of Figure 3-11.

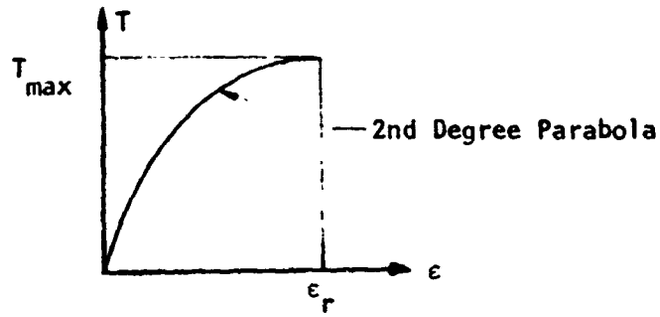

Assumed Variation of T with ε

However, in Section 3.2.2.3 it was noted that the value of longitudinal stress in the plastically deformed structure, σ', is assumed to be constant so that the membrane tension should be likewise unlike above. The reasons for this treatment of T are several. First, typical stress-strain curves of structural steels indicate the variation of strain in the inelastic range is proportionally much greater than that of stress. In fact, the possibility of large variation in strain was the reason for developing the analysis in Figure 3-11. Second, the inelastic stress range of the steel may vary significantly from ship to ship. Last, the average membrane stress assumed should account for some of the variation in thrust. Thus it was determined that the described treatment of the membrane tension would not result in significant error and would aid in simplifying the analysis.

6. In an oblique strike the forces acting at the strike are described by the force polygon of Figure 3-5. The force required to propagate a yielded zone, F_R, is discussed in detail in Section 2.4.2.2.

3.4.3.2 Procedure

Figure 3-6 shows an overall view of the possible collision conditions and damaged configurations that may occur.

Figure 3-7 gives the equations (based on Equations 3-1 and 3-5) necessary for the membrane-tension analysis of a most highly strained T-beam when only one web frame space is damaged. The solution considers the deflection at the termination of the bending phase.

Figures 3-8, 3-9, and 3-10 indicate in greater detail the analysis steps that should in general be followed when more than one web frame space is damaged and/or when the ship has a double hull.

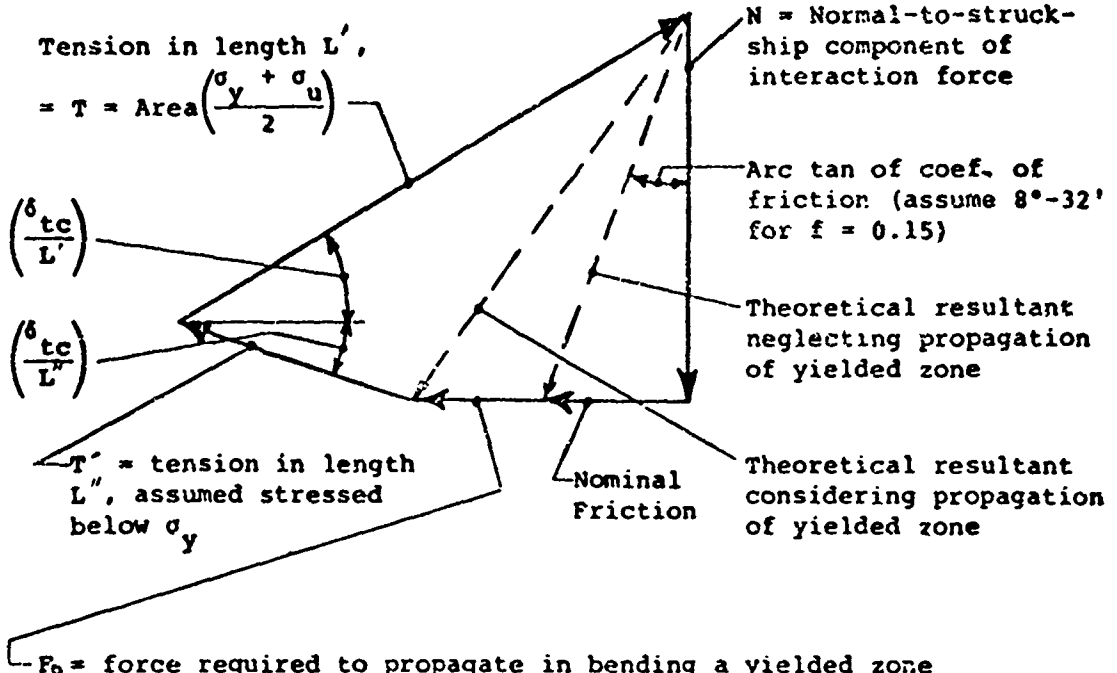

$$F_R = \frac{\sigma_y d'}{R}\left[d' t_w \left(1 - \frac{\sigma_y R}{d' E}\right)^2 + t_f (b - t_w)\left(\frac{d' - 0.5 t_f}{d'} - \frac{\sigma_y R}{d' E}\right)\right]$$

for one stiffened plate T-beam

- σ_y = yield strength
- d' = distance from neutral axis of inelastic bending to outer fiber of stiffener, conveniently approximated as the depth of stiffener
- R = radius of bend at neutral axis of inelastic bending
- t_w = thickness of web of stiffener
- t_f = thickness of flange of stiffener
- b = width of flange of stiffener
- E = modulus of elasticity

FIGURE 3-5 POLYGON OF HORIZONTAL FORCES AT STRIKE POINT IN OBLIQUE COLLISIONS

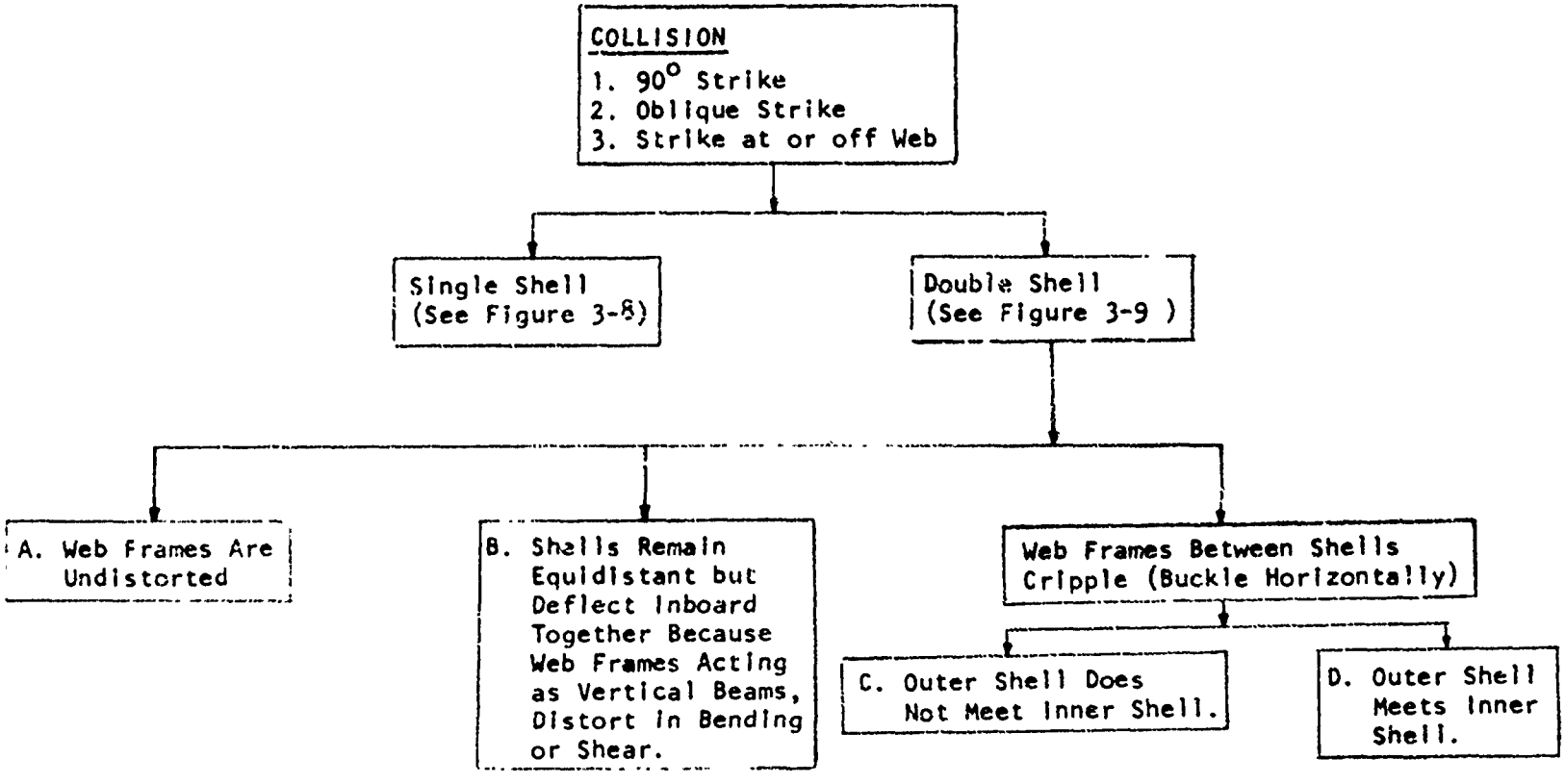

FIGURE 3-6 POSSIBLE COLLISION CONDITIONS AND DAMAGE CONFIGURATIONS

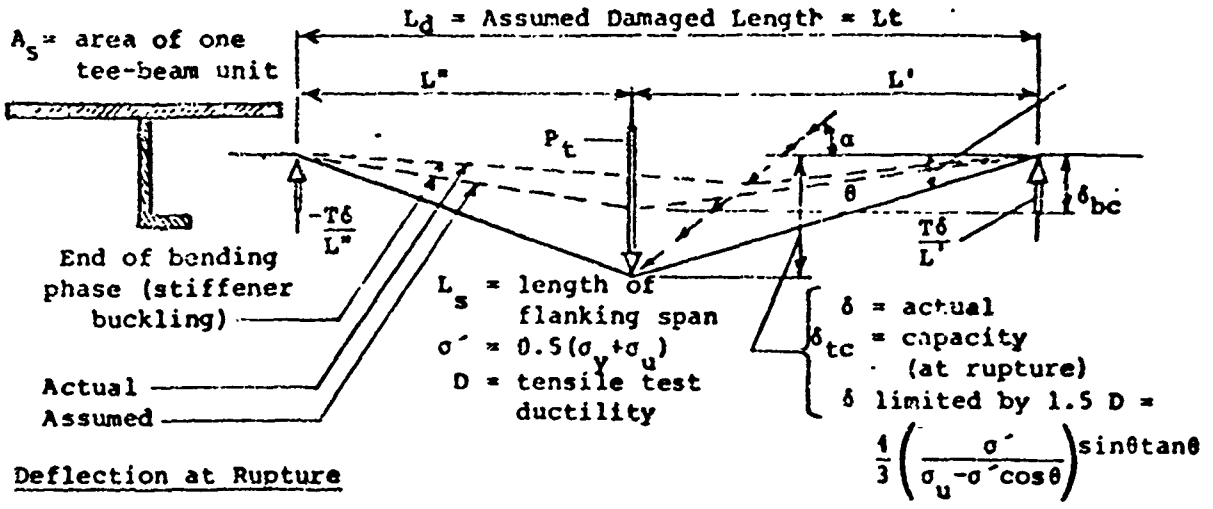

Deflection at Rupture

For lateral deflection limited by overall stretching in membrane tension,

$$\delta_{tc}=\sqrt{\frac{2L'L"}{L_t}(L'\epsilon_r + L"\epsilon_\ell + L_t\epsilon_c) + \delta_{bc}^2}$$

where

$$\epsilon_r = 0.10\left(\frac{D}{32\ell}\right)$$

ϵ_ℓ = ϵ_r for a right-angle collision with L' = L", zero for an oblique collision, or a value determined from a statics-and-compatibility analysis for a right-angle collision with L' ≠ L".

Average Membrane Tension Force Within the Yielded Portion of the Damaged Length of One Tee-Beam

$$T = A_s\left(\frac{\sigma_y + \sigma_u}{2}\right)$$ where σ_y = yield strength and σ_u = tensile strength

Membrane Tension Elongation

$$\epsilon_t = \left[\frac{L_t}{2L'L"}\left(\delta^2 - \delta_{bc}^2\right) - L_t\epsilon_c\right] \leq L_t\epsilon_r$$

Membrane Tension Plastic Energy (including energy in flanking spans)

$E_{mt} = Te_t(1 + L_s/L_t)$ for right angle collision or $E_{mt} = Te_t(1 + 0.5L_s/L')$ + $F_p\frac{\delta}{\tan\theta}$ for oblique collision

(For F_p see force polygon, Figure 3-5)

Right-Angle Strike With L' = L"

$$\delta_{tc} = \sqrt{\frac{L_t^2}{2}(\epsilon_r + \epsilon_c) + \delta_{bc}^2} \qquad \epsilon_t = \frac{2}{L_t}\left(\delta^2 - \delta_{bc}^2\right) - \epsilon_c L_t \leq L_t\epsilon_r$$

FIGURE 3-7 RIGHT-ANGLE OR OBLIQUE COLLISION MEMBRANE-TENSION ANALYSIS OF STIFFENED HULL PLATE FOR NO LATERAL MOVEMENT OF WEB FRAMES FLANKING THE STRIKE

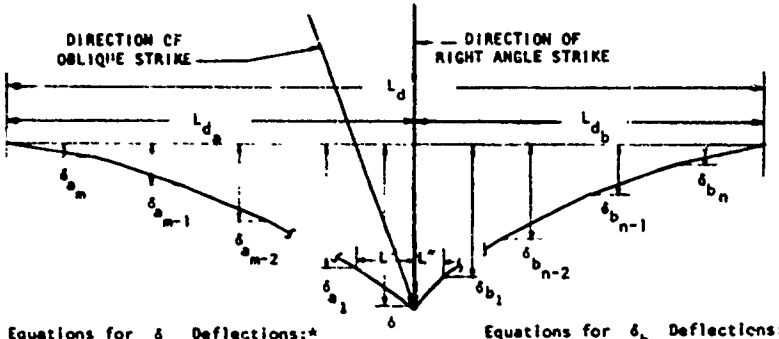

FIGURE 3-8 MEMBRANE TENSION - SINGLE SHELL

Equations for δ_{a_m} Deflections:*

$$\delta_{a_m} = \frac{L_s}{L_{d_a}}\left\{\delta - \frac{P_{wf}}{T_a}\left(m L' + \sum_{q=1}^{m-1} q L_s\right)\right\}$$

$$\delta_{a_{m-1}} = 2\delta_{a_m} + \frac{P_{wf} L_s}{T_a}$$

$$\delta_{a_{m-2}} = 3\delta_{a_m} + 3\frac{P_{wf} L_s}{T_a}$$

$$\delta_{a_1} = m\delta_{a_m} + \sum_{q=1}^{m-1} q \frac{P_{wf} L_s}{T_a}$$

Equations for δ_{b_n} Deflections:*

$$\delta_{b_n} = \frac{L_s}{L_{d_b}}\left\{\delta - \frac{P_{wf}}{T_b}\left(n L'' + \sum_{q=1}^{n-1} q L_s\right)\right\}$$

$$\delta_{b_{n-1}} = 2\delta_{b_n} + \frac{P_{wf}}{T_b} L_s$$

$$\delta_{b_{n-2}} = 3\delta_{b_n} + 3\frac{P_{wf}}{T_b} L_s$$

$$\delta_{b_1} = n\delta_{b_n} + \sum_{q=1}^{n-1} q \frac{P_{wf}}{T_b} L_s$$

Equation for Membrane Tension Elongation:

$$e_t = \frac{\delta_{a_m}^2}{2L_s} + \frac{\left(\delta_{m-1} - \delta_{a_m}\right)^2}{2L_s} + \ldots + \frac{\left(\delta_{a_1} - \delta_{a_2}\right)^2}{2L_s} + \frac{\left(\delta - \delta_{a_2}\right)^2}{2L'} + \frac{\delta_{b_n}^2}{2L_s} + \frac{\left(\delta_{b_{n-1}} - \delta_{b_n}\right)^2}{2L_s} + \ldots + \frac{\left(\delta_{b_1} - \delta_{b_2}\right)^2}{2L_s} + \frac{\left(\delta - \delta_{b_1}\right)^2}{2L''} \leq (L_{d_a} + L_{d_b})\,\epsilon_r .$$

For a first trial calculation assume:

$$e_t = (L_{d_a} + L_{d_b})\,\epsilon_r$$

*NOTE: For oblique collisions the following assumptions should be made:

1) $L_{d_b} = 0$ 2) $T_a = 2T_b$

Membrane Tension Plastic Energy (Including Energy in Flanking Span):

For Right Angle Strike: $E_{mt} = T(K_a e_t + K_e L_s \epsilon_r)$

For Oblique Strike: $E_{mt} = T_a(K_a e_t + 0.5\, K_e L_s \epsilon_r) + F_R \frac{\delta}{\tan\alpha}$ [Energy due to elastic deformation ahead of strike is neglected]

DEFINITIONS

A_s = cross-sectional area of T-beam

L_d = length of damage between undistorted web frames or bulkheads, measured in the longitudinal direction

L_{d_a} = length of damage to left of strike or behind strike in oblique collision

L_{d_b} = length of damage to right of strike or ahead of strike in oblique collision

L' = distance from strike to nearest web frame or bulkhead to left of strike

L'' = distance from strike to nearest web frame or bulkhead to right of strike

L_s = web frame spacing

δ = total lateral deflection at strike point

δ_{a_m} = lateral deflection of m^{th} web frame from strike to the left

δ_{b_n} = lateral deflection of n^{th} web frame from strike to the left

P_{wf} = load exerted by the most highly strained stiffened-plate T-beam unit on a web frame at the instant that the web frame yields or buckles

T = average membrane tension throughout the damaged length = $A_s\sigma'$

T_a = membrane tension to left of strike or behind strike in oblique collision ($T_a = T$ for right angle or oblique strike)

T_b = membrane tension to right of strike or ahead of strike in oblique collision ($T_b = T$ for right angle strike, $T_b = \frac{1}{2}T$ for oblique strike)

e_t = total strain in damaged length

$\epsilon_r = .10\left(\frac{D}{32\frac{1}{2}}\right)$

ϵ = average longitudinal strain in hull throughout the damaged length

$K_a = \epsilon/\epsilon_r$

K_e = ratio of (1) strain in the web frame spaces adjacent to the undistorted web frames or bulkheads bounding the damaged length to (2) ϵ_r.

F_R = force required to propagate longitudinally the yield line at the strike

α = angle of collision measured from the struck ship undeformed side shell behind the strike point to the centerline of the striking ship

n = number of damaged web frames to the right of the strike

m = number of damaged web frames to the left of the strike

$\sigma' = 0.5\,(\sigma_y + \sigma_u)$ = average plastic stress

FIGURE 3-9 DERIVATION OF DEFLECTION AND ENERGY ABSORPTION EQUATIONS FOR A SINGLE-SHELL SHIP

DEFLECTION EQUATIONS:

The geometry given below of the profile of the damaged sideshell is based on the approximation that the angle change at each damaged web frame is P_{wf}/T (Equation 3-4a). The stiffened sideshell is assumed to deflect in straight-line segments between any two web frames.

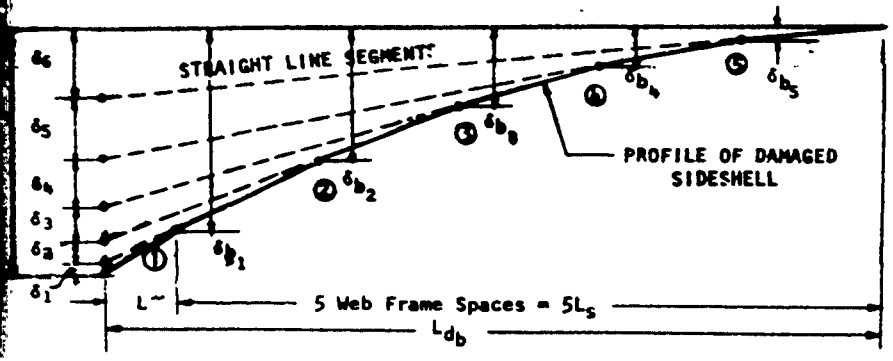

As an example, δ_{b_5} can be determined as follows:

$$\delta_1 = \frac{P_{wf}}{T} L^{\sim}$$

$$\delta_2 = \frac{P_{wf}}{T} (L_s + L^{\sim})$$

$$\delta_3 = \frac{P_{wf}}{T} (2L_s + L^{\sim})$$

$$\delta_4 = \frac{P_{wf}}{T} (3L_s + L^{\sim})$$

$$\delta_5 = \frac{P_{wf}}{T} (4L_s + L^{\sim})$$

$$\delta_6 = \delta_{b_5} (5 + \frac{L^{\sim}}{L_s}) = \delta_{b_5} (\frac{5L_s + L^{\sim}}{L_s}) = \delta_{b_5} \frac{L_{d_b}}{L_s}$$

From the above profile:

$$\delta = \delta_1 + \delta_2 + \delta_3 + \delta_4 + \delta_5 + \delta_6$$

$$= \delta_{b_5} (\frac{L_{d_b}}{L_s}) + \frac{P_{wf}}{T} (\sum_{q=0}^{4} qL_s + 5L^{\sim})$$

Therefore:

$$\delta_{b_5} = \frac{L_s}{L_{d_b}} \left[\delta - \frac{P_{wf}}{T} (\sum_{q=0}^{q=4} qL_s + 5L^{\sim})\right]$$

or, in general terms with n = 5,

$$\delta_{b_n} = \frac{L_s}{L_{d_b}} \left[\delta - \frac{P_{wf}}{T} (nL^{\sim} + \sum_{q=1}^{n-1} qL_s)\right]$$

The last equation is as given in Figure 3-8. The other equations for $\delta_{b_{n-1}}$ ...., and δ_{b_1} follow from the geometry of the damaged profile, considering each angle change is P_{wf}/T.

MEMBRANE TENSION ELONGATION:

Equation 3-5 gives the elongation of a straight line segment:

$$e = \frac{\delta^2}{2L}$$

By applying this equation to all the straight-line portions of the damaged length, the overall membrane-tension elongation can be determined. Specifically for the profile of damaged sideshell considered above the elongation is:

$$e_t = \frac{\delta_{b_5}^2}{2L_s} + \frac{(\delta_{b_4} - \delta_{b_5})^2}{2L_s} + \frac{(\delta_{b_3} - \delta_{b_4})^2}{2L_s} \frac{(\delta_{b_2} - \delta_{b_3})^2}{2L_s}$$

$$+ \frac{(\delta_{b_1} - \delta_{b_2})^2}{2L_s} + \frac{(\delta - \delta_{b_1})^2}{2L^{\sim}}$$

Combining the effects on both the left and right side of the strike gives the equation for e_t shown in Figure 3-8.

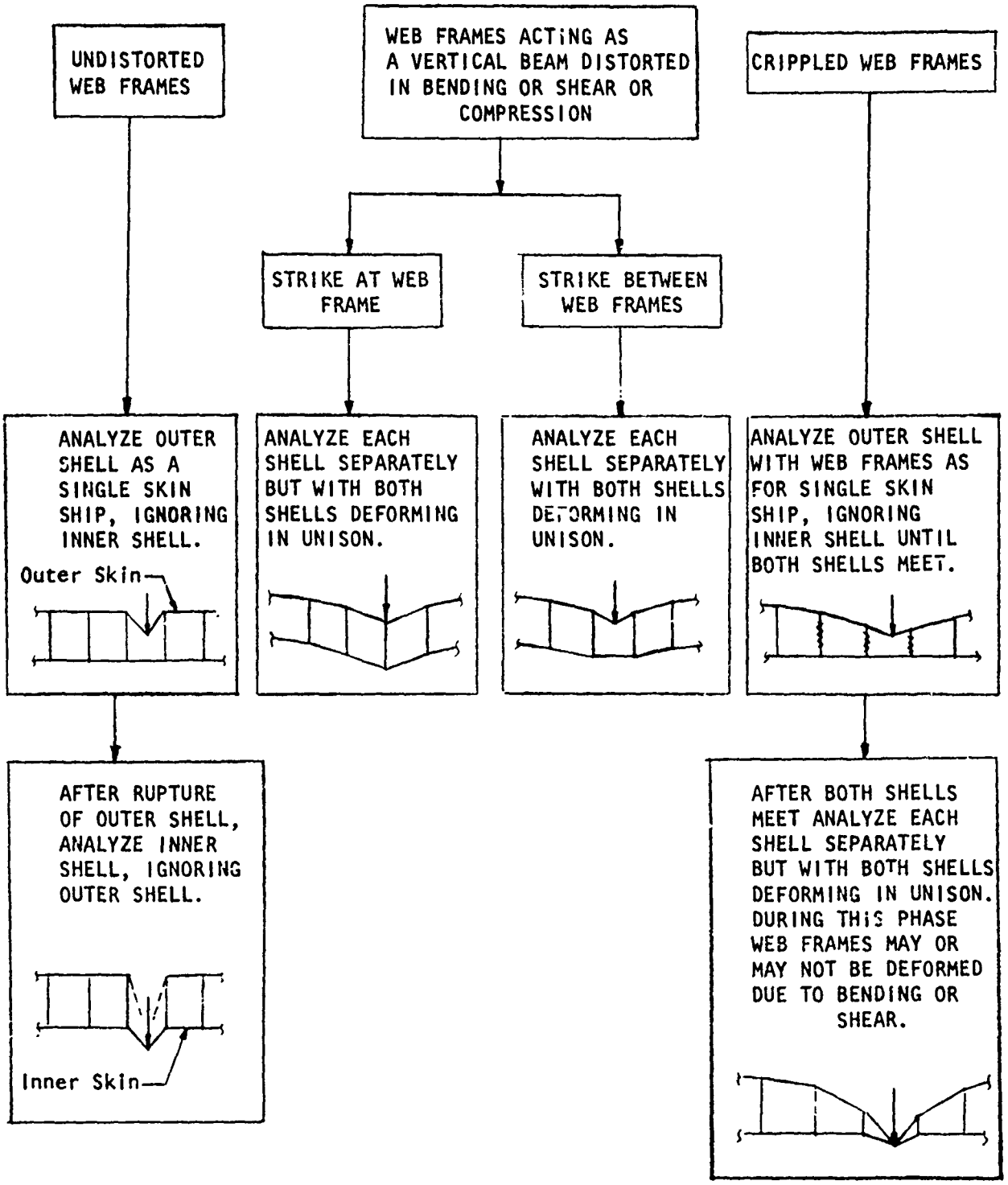

FIGURE 3-10 MACRO FLOW DIAGRAM FOR SIDE COLLISION PLASTIC ANALYSIS FOR A DOUBLE-SHELL SHIP

Figure 3-8 gives the equations necessary for the membrane-tension analysis of a most highly strained T-beam of a single shell ship for varying number of web frame spaces damaged. The solution ignores the bending phase as being relatively insignificant. The derivations for the equations in Figure 3-8 are given in Figure 3-9.

An inspection of Figure 3-8 will indicate that in order to evaluate the web deflections, side elongation and energy absorption, the total incursion, δ, the damaged length, L_d, and the average longitudinal strain, ε, throughout the damaged length must be determined first. Specific methods for evaluating these quantities are not given in the figure, as there may be several ways to do so. However, the total incursion, δ, may be determined as shown, for example, in Figure 3-9 in terms of P_{wf}, T, L', L'' and L_s. The damaged length, L_d, can be determined by first assuming that only one web frame space is damaged. Using the equations shown in Figure 3-6, but ignoring ε_c and δ_{bc} (for convenience since these effects will be small), determine the value of the striking force, P_{tm}, that would just result in rupture. If the resulting P_{tm} causes reactions at either or both of the frames that are equal to or larger than P_{wf}, the web frames will yield, and determining the number of web frames damaged on either side of the strike will give the damaged length. More specifically, for a right angle strike, a static analysis of the one web frame space will give:

$$P_{tm} = \left(\frac{T_a \delta}{L'} + \frac{T_b \delta}{L''}\right) = T\left(\frac{\delta}{L'} + \frac{\delta}{L''}\right) \qquad (3\text{-}6)$$

The reaction forces at the flanking webs are then $T\frac{\delta}{L'}$ left of the strike and $T\frac{\delta}{L''}$ right of the strike in accordance with Figure 3-8. The web frames can only resist a certain force before yielding, therefore by dividing the lateral force to the left and to the right by the force required to fail a web frame, P_{wf}, will give the number of web frames damaged to the left and right respectively, when rounded downward to the nearest integer. As a check, the damaged length must be such that the least web frame deflection, Figure 3-8, is:

$$\delta_{a_m} \text{ or } \delta_{b_n} \leq \frac{P_w L_s}{T}$$

In the case of an oblique collision, only the damaged length behind the strike is yielded. Then, as discussed in Section 3.2.2.3.2, the membrane tension ahead of the strike, from Equation 3-2, is one-half that behind the strike, from Equation 3-1. Therefore, for one web frame space:

$$P_{tm} = \left(\frac{T_a\delta}{L'} + \frac{T_b\delta}{L''}\right) = T\left(\frac{\delta}{L'} + \frac{\delta}{2L''}\right) \qquad (3\text{-}7)$$

corresponding to reaction forces $T\frac{\delta}{L'}$ and $T\frac{\delta}{2L''}$.

The average longitudinal strain, ε, throughout the damaged length can be determined by assuming, as a first approximation, that over the entire damaged length the tensile strain in the critical T-beam is a uniform value, ε_r, as indicated in Figure 3-8. Actually this value of the strain occurs in the struck web frame space only. When more than one web frame space is damaged, the membrane tension in the web frame space at the strike is greater than in the web frame spaces beyond, and the membrane tensions are least at the ends of the damaged length. This results in some variation of strains in the stiffened hull over the damaged length.

Such a difference in membrane tension results from considering the static equilibrium of components of forces in the longitudinal direction at angle changes in the stiffened hull occurring at the web frames within the damaged length, as shown in Figure 3-11. After a membrane tension solution is obtained with assumed strain ε_r over all web frame spaces, revised values of the hull strains within the individual spaces between web frames can be determined by the general procedure suggested in Figure 3-11. The average of the strains so determined in each damaged web frame space is the average longitudinal strain, ε, throughout the damaged length. Then a more accurate solution would consist of recalculating the lateral deflections based on revised values of the strain to account for the strains being different in the different web frame spaces. However, with the revised values of the strains within the individual spaces, the first approximation (assuming ε_r in all spaces) can be corrected by applying the factors "K" indicated in the expressions for plastic energy, Figure 3-8. Specifically, K_a is the ratio of (1) the average value of tensile strain, ε, over the yielded portion of the damaged length to (2) ε_r. K_e is the ratio of (1) the strain in the spaces adjacent to the undistorted web frames or bulkheads bounding the damaged length to (2) ε_r. In computing the strain just beyond the damaged length, the cosine in the denominator of the expression in Figure 3-11 is 1.0.

As shown in Figure 3-11, membrane tensions vary inversely with the cosine of the deformation angle, ϕ, because longitudinal components of the hull membrane tension forces must balance at each web frame (Note

the assumption that web frames do not offer any resistar in the longitudinal direction is utilized here). The relationships between strains and deformation angles result from that relationship and the assumed parabolic variation of membrane tension with respect to strain, discussed in Section 3.4.3.1.

Figure 3-10 indicates the analysis steps that should be followed for the double shell damage configurations listed in Figure 3-6.

If a structural configuration presents an unusual case not covered by the figures, the principles of Section 3.4.3.1 should be utilized to evaluate the case in question.

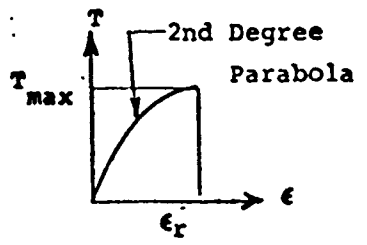

Assumed Variation of T with ϵ

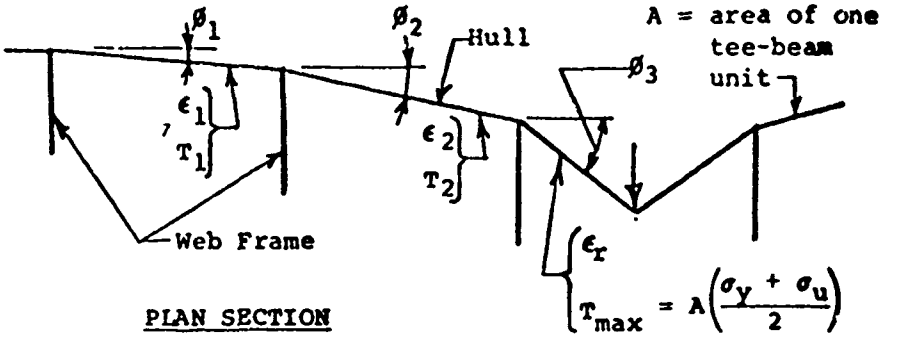

PLAN SECTION

Basic Assumptions

1. A solution based on an assumed variation of strain, ϵ, in the various web frame spaces has been obtained, so that values of ϕ_1, ϕ_2, and ϕ_3 are known.

2. The web frames within the damaged length offer no resistance to longitudinal forces. Consequently,

$$T_1 \cos \phi_1 = T_2 \cos \phi_2 = T_{max} \cos \phi_3$$

from which

$$T_1 = T_{max} \left(\frac{\cos \phi_3}{\cos \phi_1}\right) \quad \text{and} \quad T_2 = T_{max} \left(\frac{\cos \phi_3}{\cos \phi_2}\right)$$

3. T varies with ϵ as a second degree parabola centered at ϵ_{max}, as indicated above. (This approximation is derived from typical stress-strain curves.) Consequently,

$$\epsilon = \epsilon_{max} \left[1 - \left(\frac{T_{max} - T}{T_{max}}\right)^{1/2}\right]$$

Resulting Equations for Strain

$$\epsilon_1 = \epsilon_r \left[1 - \left(1 - \frac{\cos \phi_3}{\cos \phi_1}\right)^{1/2}\right]$$

$$\epsilon_2 = \epsilon_r \left[1 - \left(1 - \frac{\cos \phi_3}{\cos \phi_2}\right)^{1/2}\right]$$

FIGURE 3-11 PROCEDURE FOR CHECKING THE HULL MEMBRANE-TENSION STRAINS IN WEB-FRAME SPACES BEYOND THE WEB-FRAME SPACE(S) AT THE STRIKE

3.4.4 Web-Frame Analysis

The analysis of a web frame flanking the strike is concerned with evaluating the transverse forces from the deformed T-beams that result in the incidence of yielding or buckling of the web frame and the plastic energy absorbed by the web frame at the incidence of hull rupture.

3.4.4.1 Transverse Forces from T-Beams

Before the analyses in Figures 3-8 or 3-10 can be performed, the transverse force which causes the web frame to fail must be evaluated. The portion of the force which is exerted by the most highly strained T-beam is just one of the transverse forces exerted on the web frame by the deformed T-beam units. Therefore, a closed form solution for P_{wf} is not practical, and an iterative solution relating to assumptions 9 and 10 of Section 3.2.2.2 is suggested, consisting of the following steps:

1. Assume some incursion, preferably an incursion corresponding to the most highly strained T-beam about to rupture. A second solution based on the actual final incursion will likely be required for failure of web frames during a strike by a raked bow, since the number of T-beams deformed will change when the incursion changes, as discussed below.

2. Determine the corresponding transverse forces that each deformed T-beam would exert on the two web frames flanking the strike.

3. Perform a strength analysis of the web frame as acted upon by the transverse forces from all the deformed T-beams. If the analysis does not indicate failure due to bending, shearing, or buckling, the web frame does not fail for the given incursion.

4. If the strength analysis does indicate failure due to bending, shearing, or buckling, determine a single constant, R_m, by which each of the applied transverse forces would have to be divided for the web frame just not to fail.

5. For a strike by a vertical bow or for horizontal crushing failure in the vicinity of the top of the incursion during a strike by a raked bow, assume that P_{wf} is the original transverse force from the most highly strained T-beam divided by R_m.

6. For bending or shearing failure during a strike by a raked bow, divide the total of the original transverse forces from all the T-beams by R_m to give a diminished total force. Then, determine a revised (lesser) incursion, corresponding to a diminished height of collision imprint, Figure 3-1, and a proportionately lesser number of hull T-beams damaged, that will result in values of transverse forces giving the same diminished total force. In this last set of transverse forces, the force exerted by the most highly strained hull T-beam is P_{wf}. Approximately, P_{wf} may be calculated as the original transverse force from the most highly strained T-beam divided by $R_m^{\frac{1}{2}}$ because, for the sloping incursion offered by a raked bow, both the value of the transverse forces and the number of hull T-beam units exerting transverse forces will tend to vary in proportion to the incursion.

3.4.4.2 Details of Strength Analysis

The analyses of the web frames for strength include evaluations of bending, shearing, and column strengths and resistances to buckling. Conventional elastic frame analyses, with "effective widths" [19-22] of the hull plates assumed to act as "flanges" are sufficient for computing shearing and bending stresses, which are subsequently compared with the limiting stresses that are equal to yield strengths or computed local buckling stresses. One exception is that elastic web buckling in shear is not considered to be a failure in a stiffened web but instead implies merely a transition in shear resistance from pure shearing action to "tension field" action. [15]

Because of the stocky proportions typical of web frames, initial web-frame failure may be merely the incidence of vertically extending folds in the outer vertical web of the web frame, particularly if the web is not well reinforced with horizontal stiffeners. In analyzing such folding, the web may effectively be considered to be several horizontal "columns," each consisting of a portion of the web plating and any attached horizontal stiffeners, with "effective widths" of the web plating determined by references [19-22].

3.4.4.3 Plastic Energy

3.4.4.3.1 General

The energy absorbed by any web frame during a collision depends on whether the web frame maintains in-plane distortions, as is likely when the web is well reinforced with horizontal stiffeners, or suffers vertically extending folds after the incidence of yielding or buckling, as is likely when the web is not reinforced with horizontal stiffeners.

For in-plane distortions of web frames with typical stocky proportions, the energy of in-plane shearing is by far the most significant, and the only bending energy is that absorbed in the "kinking" of the flanges of the web frame, computed as the flange-plate plastic bending moment multiplied by the angle change at the kink line.

The energy absorbed in column buckling of horizontal struts or in forming vertically extending folds in the webs is essentially energy of plastic bending (rather than energy of axial distortion). For any given element, this energy of plastic bending is approximately equal to the plastic bending moment of the element times the angle change through which the element is bent. This energy is small and may be neglected.

A strength analysis of a web frame in the line of strike in a right-angle collision is not required in the analysis of the most highly strained T-beam. If the struck web frame is well reinforced with horizontal stiffeners, it is logical to assume that the web frame suffers only in-plane (in the plane of the web) displacements, and the total of the forces exerted on the web frame can be approximated as the shearing force in the web corresponding to the maximum shearing distortion of the web as determined from the geometry of the incursion. If the struck web frame is not well reinforced with horizontal stiffeners, the incidence of vertically extending folds may be anticipated, and an analysis of the folding portion as a series of horizontal "columns" as discussed above would give a more realistic evaluation of the resisting forces.

3.4.4.3.2 In-Plane Shearing Analysis of Each Panel

For a panel which is bounded by flanges and a pair of transverse stiffeners and is subjected to a given in-plane shear distortion γ ($\gamma \leq \gamma_m$ where γ_m is the maximum capacity of shearing strain of the panel), the critical elastic shear buckling stress τ_{cr} is

$$\tau_{cr} = \left[5.35 + 4\left(\frac{d}{a}\right)^2\right]\frac{\pi^2 Et^2}{12(1-\nu^2)d^2} \qquad \text{for } d/a \leq 1.0$$

$$\tau_{cr} = \left[5.35 + 4\left(\frac{a}{d}\right)^2\right]\frac{\pi^2 Et^2}{12(1-\nu^2)a^2} \qquad \text{for } d/a \geq 1.0$$

where a, d, and t are, respectively, the panel length, depth, and thickness.

The plastic in-plane shearing energy is calculated as follows:

(1) if $\tau_{cr} < \tau_y$ (where τ_y is the shear yield stress):

The plastic shearing energy absorbed in the panel (see Figures 3-12 and 3-13 for typical locations) is

$$E_{ps} = R_s\,(adt)\,(\gamma-\gamma_e)\left(\tau_{cr} + \sigma_{ty}\sin\frac{\theta}{2}\cos\frac{\theta}{2}\right)$$

where $\theta = \tan^{-1} d/2$

$R_s = 1 - \dfrac{\tan\frac{\theta}{2}}{d/a}$ (plastic-range stress-to-yield ratio = 1.0)

$\gamma_e = \gamma_e' + \gamma_e''$ (total elastic shearing strain

$\gamma_e' = \dfrac{\tau_{cr}}{11{,}150}$ (Straining up to elastic shear buckling)

$\gamma_e'' = \dfrac{\sigma_{ty}}{29{,}000\,(\sin\frac{\theta}{2})(\cos\frac{\theta}{2})}$ (the additional elastic straining up to tension-field yielding)

σ_{ty} = maximum tension-field tensile stress

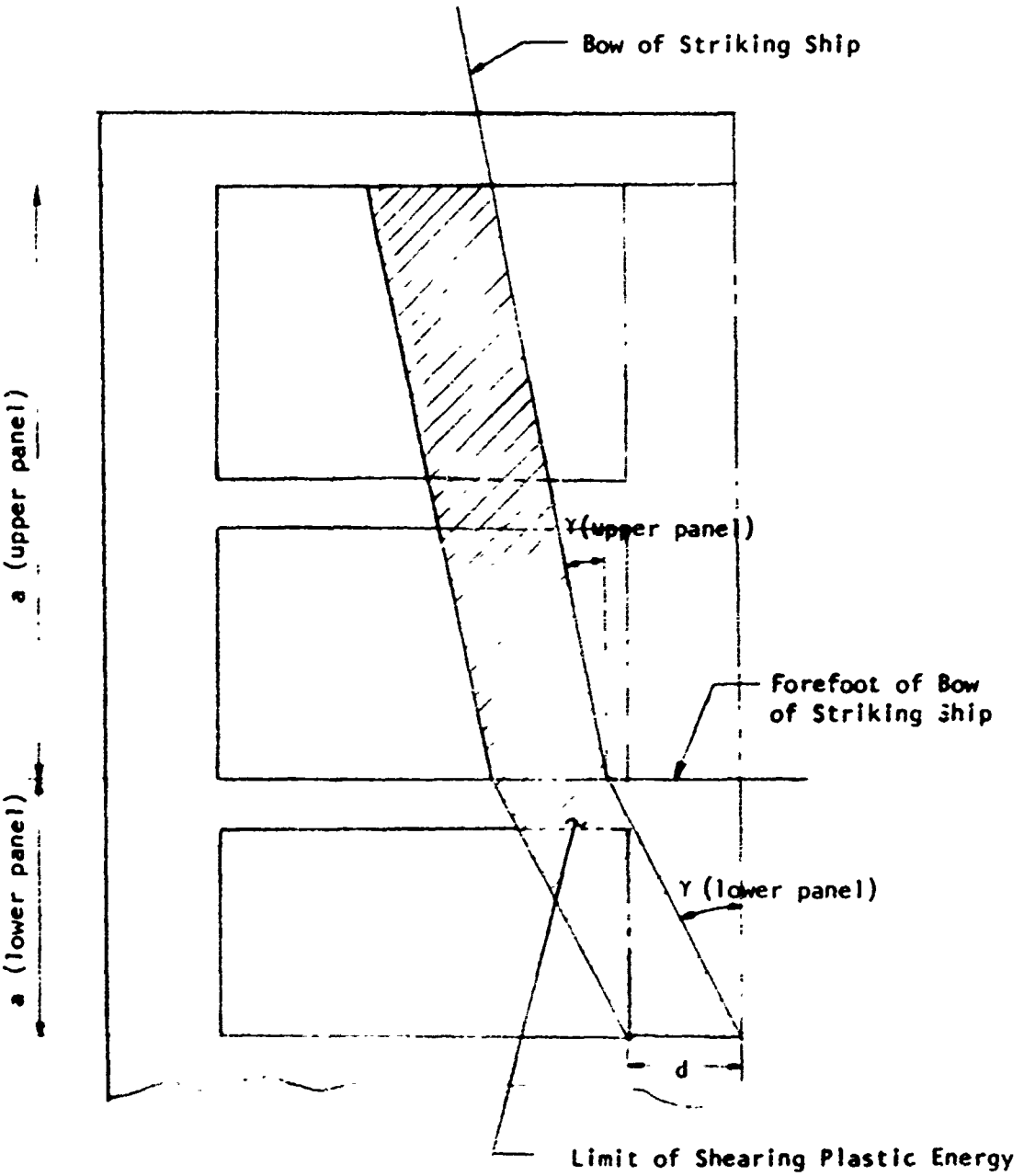

TRANSVERSE SECTION AT WEB FRAME

Figure 3-12 PLASTIC ENERGIES ASSOCIATED WITH GIVEN WEB FRAME DISTORTIONS FOR RAKED STRIKING BOW

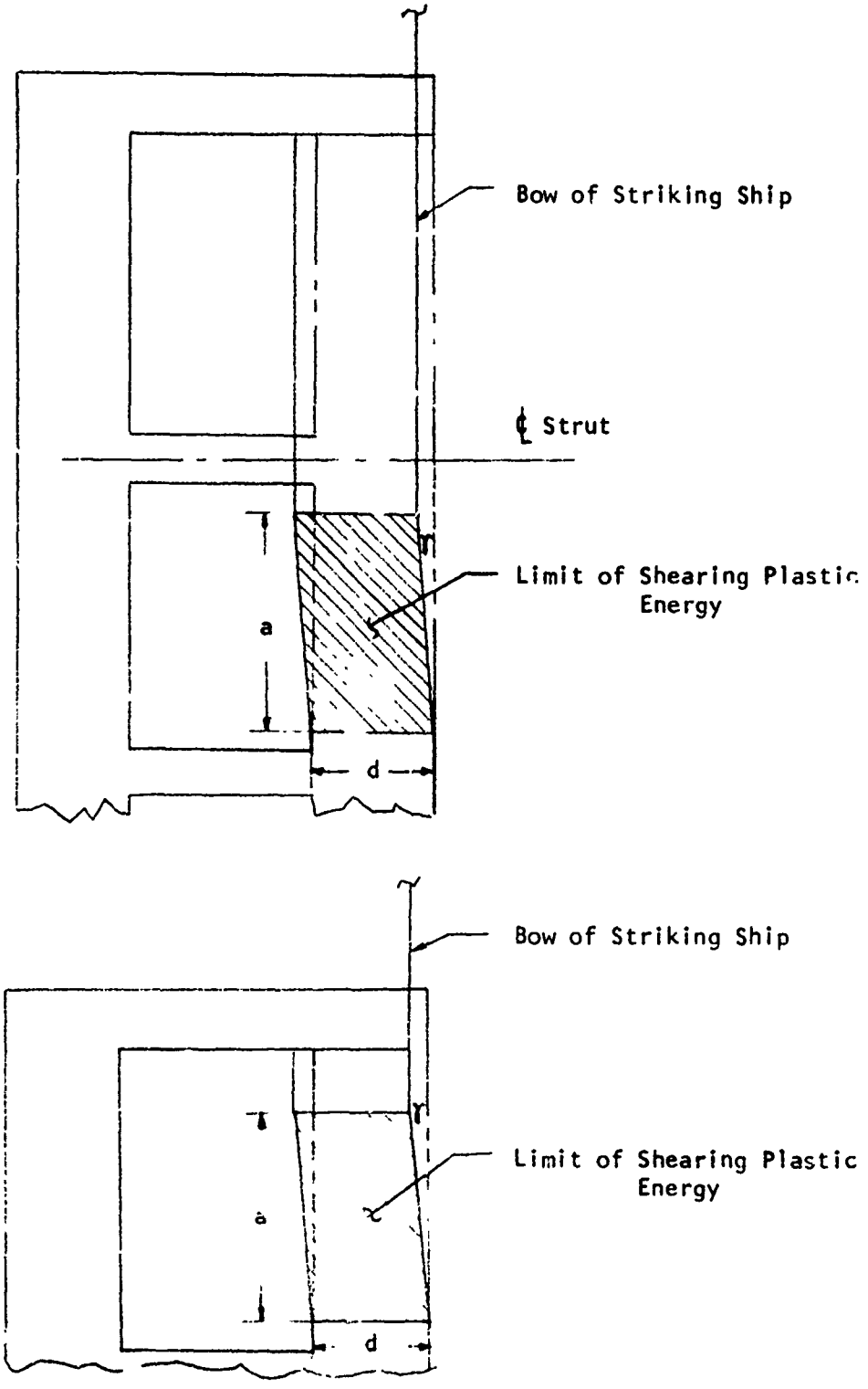

TRANSVERSE SECTIONS AT WEB FRAME

FIGURE 3-13 PLASTIC ENERGIES ASSOCIATED WITH GIVEN WEB FRAME DISTORTIONS FOR VERTICAL STRIKING BOW

The total transverse shearing force in the panel at onset of yielding is

$$V_p = \tau_{cr}\, dt + \sigma_{ty} \sin\frac{\theta}{2} \cos\frac{\theta}{2}(t)(d - a \tan\frac{\theta}{2})$$

This value of V_p may be used in evaluating the web-frame shearing capacity.

(2) If $\tau_{cr} > \tau_y$:

The plastic shearing energy absorbed in the panel is

$$E_{ps} = (adt)\ (\gamma - \frac{\tau_y}{11,150})\ (\tau_y)$$

The total transverse shearing force in the panel at onset of yielding is

$$V_p = \tau_y\, dt$$

This value of V_p may be used in evaluating the web-frame shearing capacity.

3.4.5 Deck Analyses

Since the bow of the striking ship is assumed to be infinitely stiff, the deck of the struck ship must distort radically if there is appreciable incursion during the collision.

Inspections of actual collisions have shown that generally, during a tanker collision, the deck of the struck ship forms a series of small-pitch accordion folds extending in the longitudinal direction, Figure 3-1, if the deck of the struck ship is below the top of the bow of the striking ship. Also, it has been observed that the damaged deck is stretched horizontally in membrane tension over a length about equal to the damaged length of the stiffened hull, with tensile ruptures of the deck plating extending perpendicular to the ship side.

It is logical to assume that the deck is divided into elements originally longitudinal (each may conveniently be considered a deck stiffened-plate T-beam), which stretch horizontally in membrane tension over a length equal to the damaged length of the stiffened hull. Equation 3-5 may be used to evaluate the elongation of each longitudinal element. The plastic energy of each element is its total elongation times $\sigma_{mt}A_s$, where A_s is its cross-sectional area.

3.4.6 Additional Considerations for Double-Shell Ships

The plastic energy absorbed in a double-shell ship includes the plastic energy of each shell at the time of its rupture, the plastic energy of the deck when the second shell ruptures, any plastic energy absorbed by the web frames up to the instant that the second shell ruptures, and the ductile tearing energy associated with tensile rupture of the outer hull plating if its temperature is above the transition temperature for the steel. To assess the relative importance of such ductile tearing of the outer hull, a nominal 1 kip-ft per square inch of fracture may be assumed for the ductile tearing energy (it has been found to be relatively insignificant compared with the other components of plastic energy).

4. Collision Analysis Parametric Study Results

4.1 General

The collision analysis parametric study consisted of the numerical application of the plastic energy evaluation procedure described in Section 3 to collision incidents in which a 120,000 DWT tanker was struck by a 20,000 tons displacement ship. The collision cases studied were:

Case #1 1" Single Shell Ship - struck at right-angle by a vertical stem ship, strike midspan between bulkheads and webs

Case #2 1" Single Shell Ship -struck at right-angle by a 15° raked bow ship, strike midspan between bulkheads and webs

Case #3 1-3/4" Single Shell Ship -struck at right-angle by a vertical stem ship, strike midspan between bulkheads and webs

Case #4 1-3/4" Single Shell Ship-struck at right-angle by a 15° raked bow ship, strike midspan between bulkheads and webs

Case #5 1-3/4" Single Shell Ship -struck at oblique angle by a vertical stem ship, strike midspan between bulkheads and webs

Case #6 1" + 3/4" Double Shell Ship - struck at right-angle by a vertical stem ship, strike midspan between bulkheads and webs

The plastic energy absorption varies greatly depending on the location of strike with respect to the location of the webs and bulkheads. Therefore, a very approximate estimation (as described in Section 4.4) was made for the energy absorbed in strikes at different points along the length of the ship between bulkheads. This estimation was made by using the value of the energy absorbed in a midspan strike as a reference.

The parent hull of the struck ship was the Newport News Shipbuilding & Dry Dock Company 120,000 DWT CMX tanker design. This ship has longitudinal framing. Figure 4-1 shows the Midship Section of the parent hull, and Figures 4-2 and 4-3 show the modified single and double shell hulls used in the calculations. The hulls were modified in order to simplify the calculations.

The hull was assumed to be of mild steel with the properties given in Table 4-1. In comparison with mild steel, a high-strength steel has a greater yield strength but generally a lesser ductility. Since energy absorption is approximately proportional to the product of mass, strength, and ductility, a ship with mild steel plating would be expected to have somewhat more energy absorption capacity than a comparable ship with thinner high strength steel plating.

Two bow shapes of the striking ship were assumed in the case studies: (1) a T-2 tanker bow with a rake of 15^{o} and (2) a similar bow with a vertical stem. A sketch of these two bow shapes is shown in Figure 4-4.

4.2 Input Information

The information described below was required for the calculation of plastic energy absorption for the case studies and was determined before beginning the calculation procedure.

FIGURE 4-1 MIDSHIP SECTION OF 120,000 DWT CMX TANKER DESIGN

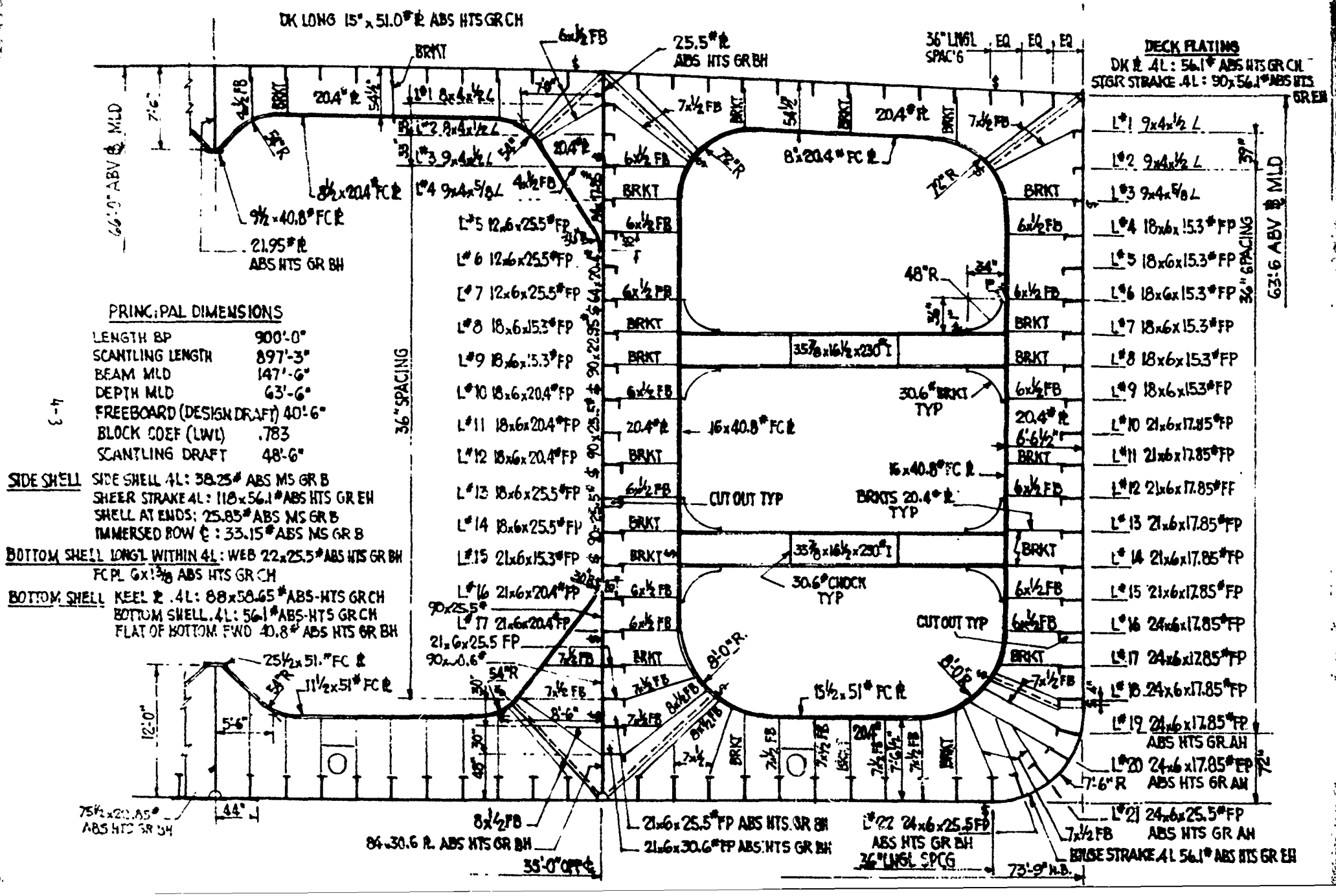

PRINCIPAL DIMENSIONS

LENGTH BP	900'-0"
SCANTLING LENGTH	897'-3"
BEAM MLD	147'-6"
DEPTH MLD	63'-6"
FREEBOARD (DESIGN DRAFT)	40'-6"
BLOCK COEF (LWL)	.783
SCANTLING DRAFT	48'-6"

SIDE SHELL: SIDE SHELL 4L: 38.25# ABS MS GR B
SHEER STRAKE 4L: 118x56.1# ABS HTS GR EH
SHELL AT ENDS: 25.85# ABS MS GR B
IMMERSED BOW ℄: 33.15# ABS MS GR B

BOTTOM SHELL LONGL WITHIN 4L: WEB 22x25.5# ABS HTS GR BH
FC PL 6x1⅜ ABS HTS GR CH

BOTTOM SHELL: KEEL ℓ 4L: 88x58.65# ABS-HTS GR CH
BOTTOM SHELL 4L: 56.1# ABS-HTS GR CH
FLAT OF BOTTOM FWD 40.8# ABS HTS GR BH

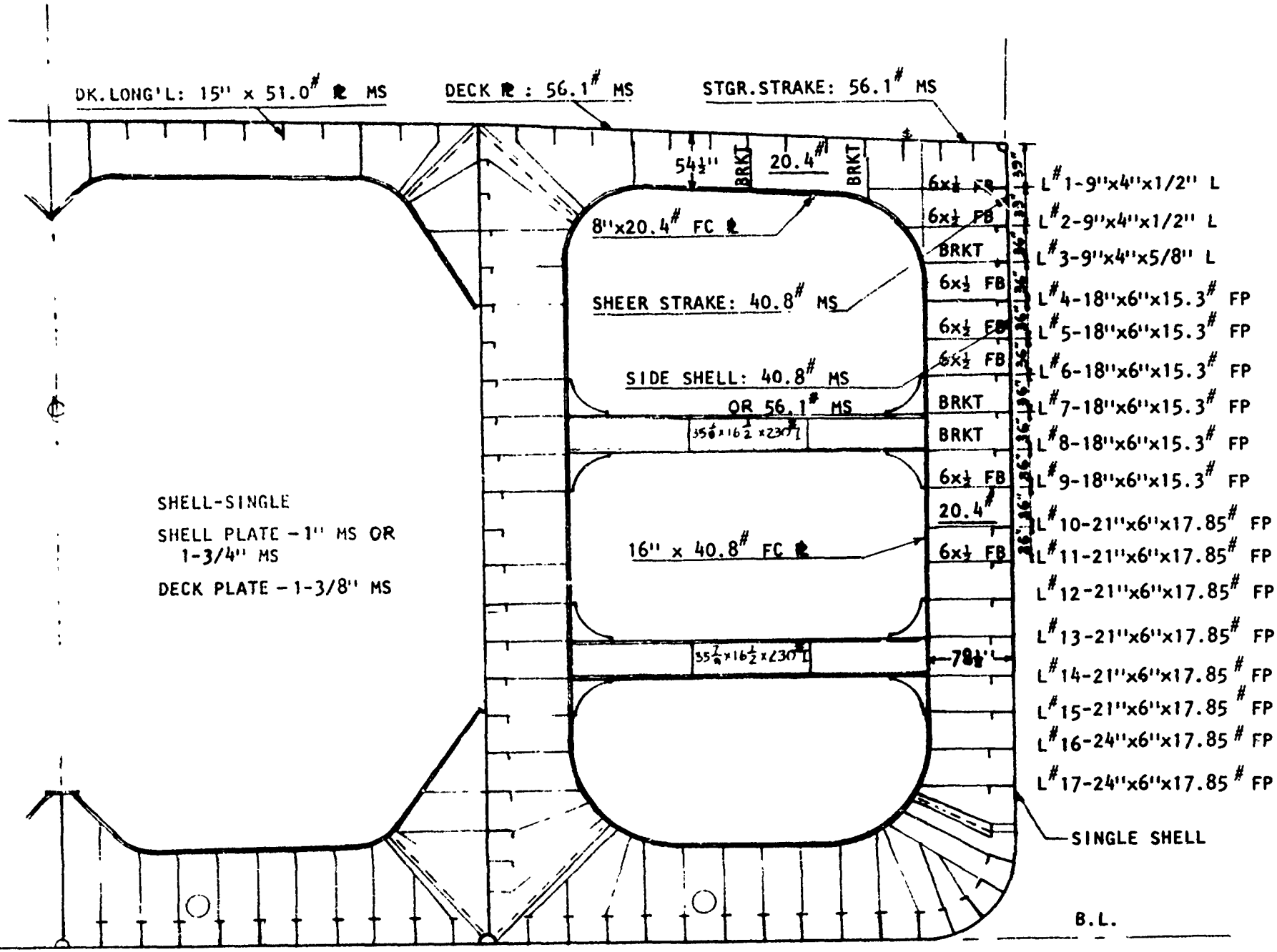

FIGURE 4-2 MODIFIED CMX DESIGN - SINGLE SHELL

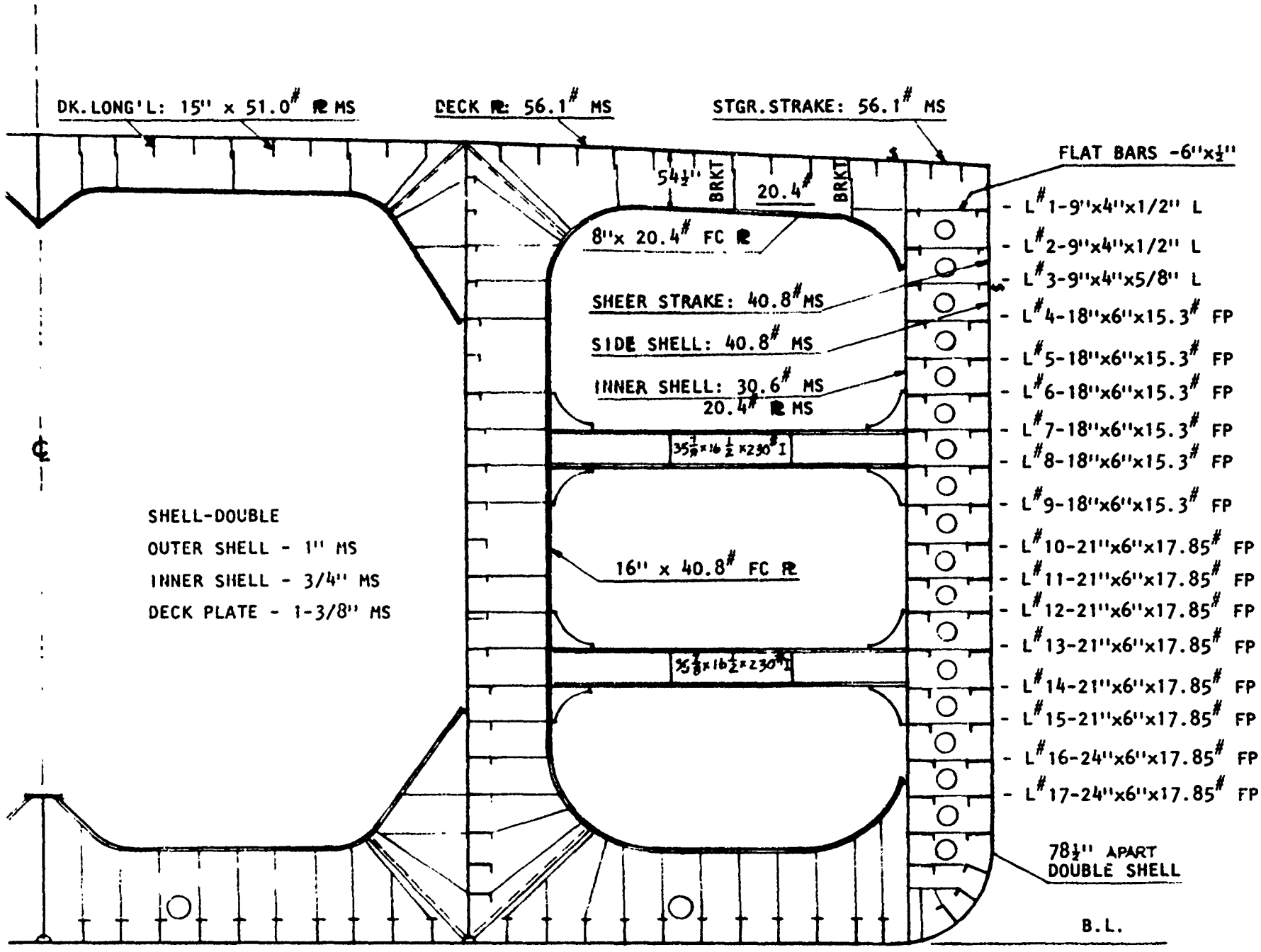

FIGURE 4-3 MODIFIED CMX DESIGN - DOUBLE SHELL

Table 4-1

MATERIAL PROPERTIES TYPICAL OF STEELS WITH YIELD POINT OF 35 KSI (MILD STEEL)

Description	Item	Yield Strength σ_y = 35 ksi
Tensile Strength	σ_u	65 ksi
Strain-Hardening Strain	ε_{sh}	0.014 in./in.
Modulus of Elasticity	E	29,000 ksi
Tangent Modulus	E_t	900 ksi
Factors in Equation for k	$\varepsilon_{sh}/\sigma_y/E$	11.6
	$E/2E_t$	16.1
Average Plastic-Range Stress	$(\sigma_y + \sigma_u)/2$	50.0 ksi
Plastic-Range Stress-to-Yield Ratio	$(\sigma_y + \sigma_u)/2\sigma_y$	1.43
Shear Yield Strength	τ_y	20.2 ksi
Maximum Shear Distortion for Plastic Energy	$\gamma_m = 2\left(\varepsilon_{sh} + \frac{\sigma_u - \sigma_y}{E_t}\right)$	0.0947 rad

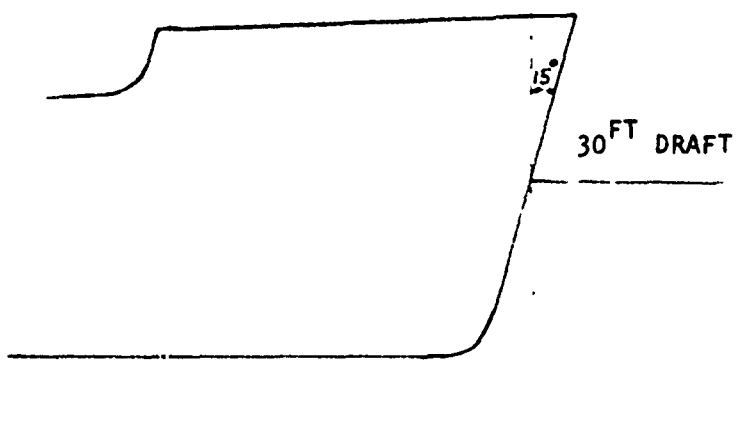

(a) T-2 Tanker Bow with a rake of 15°

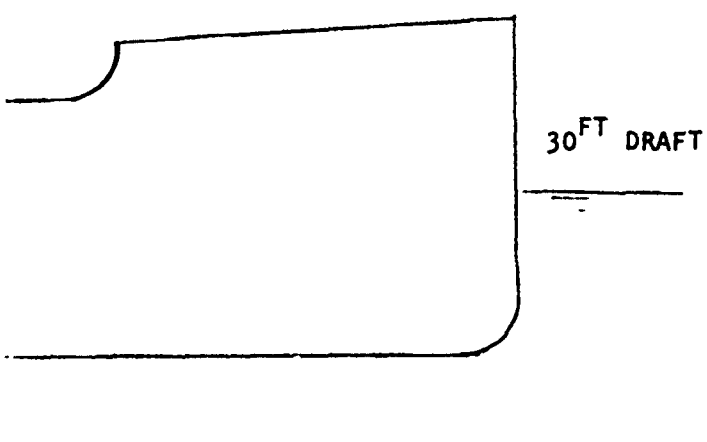

(b) T-2 Tanker Bow with vertical stem

FIGURE 4-4 BOW CONFIGURATION OF STRIKING VESSEL

4.2.1 Struck Ship

4.2.1.1 Configuration

1. The principal dimensions and draft of the struck tanker.

2. The web frame spacing and the number of web frame spaces between two consecutive transverse bulkheads.

3. The midship section (either Figure 4-2 or 4-3).

4. Material Properties.

4.2.1.2 Collision Condition

The energy absorption of the struck ship depends on the collision condition which is described by the following factors:

1. Angle of strike.

2. Location of strike - the location of strike may be midspan between the web frames and/or bulkheads, off-midspan, or at a web frame or bulkhead.

4.2.2 Striking Ship

Only the bow configuration and the draft are needed in the calculation.

4.3 Results of the Parametric Study

Calculations of plastic energy absorption were made for strikes at midspan between webs and bulkheads. The detailed calculations of the different collision cases are presented in another report[17]. The values of the calculated energy absorption due to bending of the sideshell, membrane tension in the sideshell, shearing of the web frames, and membrane tension in the deck, are summarized in Table 4-2.

Case No.	1	2	3	4	5	6
Hull	Single	Single	Single	Single	Single	Double
Shell Plate	1" M.S.	1" M.S.	1-3/4" M.S.	1-3/4" M.S.	1-3/4" M.S.	Outer 1" M.S. Inner 3/4" M.S.
Deck Plate	1-3/8" M.S.	1-3/8" M.S.	1-3/8" M.S.	1-3/8" M.S.	1-3/8" M.S.	1-3/8" M.S.
Collision Condition	Right Angle w/Vertical Bow	Right Angle w/15° Raked Bow	Right Angle w/Vertical Bow	Right Angle w/15° Raked Bow	Oblique Collision w/Vertical Bow	Right Angle w/Vertical Bow
1. Bending Energy in Long'l Side (E_{bc})	6,517	6,613	8,642	8,642	8,642	6,517 6,264
2. Membrane Tension Energy in Long'l Side (E_t)	2,975,298	824,256	5,033,042	2,422,717	3,448,217	5,746,419
3. Shearing Energy in Web Frame (E_{ps})	79,031	137,325	79,031	233,779	65,860	65,860
4. Deck Membrane Energy (E_d)	472,890	249,987	530,360	514,195	174,748	542,997
5. Ductile Tearing Energy	——	——	——	——	——	Outer Shell 7,848 Deck 4,658
Total Energy In-Kips	3,533,736	1,218,181	5,651,075	3,179,333	3,697,467	6,380,563
Total Energy Ft-Tons	131,500	45,300	210,200	118,300	137,600	237,400

TABLE 4-2 SUMMARY OF PLASTIC ENERGY ABSORBED BEFORE SHELL PLATE RUPTURE

A review of Table 4-2 reveals the following results:

1. In all six cases, the most significant contribution to the total plastic energy absorption comes from the membrane tension energy developed by the sideshell and the deck. It varies as a percentage of total energy from about 88 to 98. Second to the membrane tension in importance is the energy absorbed in shearing of the web frames.

2. The configuration of the bow of the striking ship has a significant effect on energy absorption. By comparing the total energy absorbed in case #1 with #2, and that in case #3 with #4, it can be seen that the struck ship energy absorption when struck by a vertical bow is twice that when struck by a raked bow. This significant difference in energy absorption results from the difference in the vertical extent of damage involved in the total deformation. A vertical bow can deform a greater number of T-beams than can a raked bow even if the maximum incursion is identical.

3. The total plastic energy absorption is approximately proportional to shell thickness. This is deduced from comparing the energy absorbed in cases #1 and #3, and the fact that the greatest energy-absorbing mechanism, membrane tension in the sideshell, is directly proportional to plate thickness.

4. A comparison of energy absorbed between cases #3 and #5 shows that the total energy absorption in an oblique collision is about 35% less than that in a right-angle collision. The difference can be attributed to the fact that membrane tension is not developed ahead of the striking bow in an oblique collision.

5. In most of the collision cases considered, the damaged length was equal to the bulkhead spacing. Had the bulkheads been further apart, greater damage and energy absorption would have occurred.

6. A comparison of the energy absorption in cases #3 and #6, for a single shell and double shell hull respectively (with identical overall side thicknesses), shows that the energy absorption capability of the two ships is approximately equal and directly proportional to their T-beam cross-sectional areas. It should be noted that the double shell hull web frames distorted due to bending so that both shells deformed in membrane tension in unison. If the web frames deform by crippling, with the result that the outer shell deflects while the inner does not unless the outer actually touches the inner, the energy absorption may be less for the double shell hull when compared to the single shell. In the case of punching or tearing action, where little energy absorption is involved, the double shell is superior to the single shell since the inner shell may remain intact and prevent leakage of the cargo after rupture of the outer shell.

4.4 Membrane Tension Energy for Arbitrary Strike Locations

The results described in Section 4.3 are all for strikes midspan between webs and bulkheads.

Figure 4-5 displays the results of the energy absorptions in the component structures tests described in Section 6. In these tests strikes were made at different locations along a span supported by "webs" that simulated the resistances of transverse bulkheads. The figure indicates the large changes in energy absorbed as the distance of the strike from a test web frame is varied.

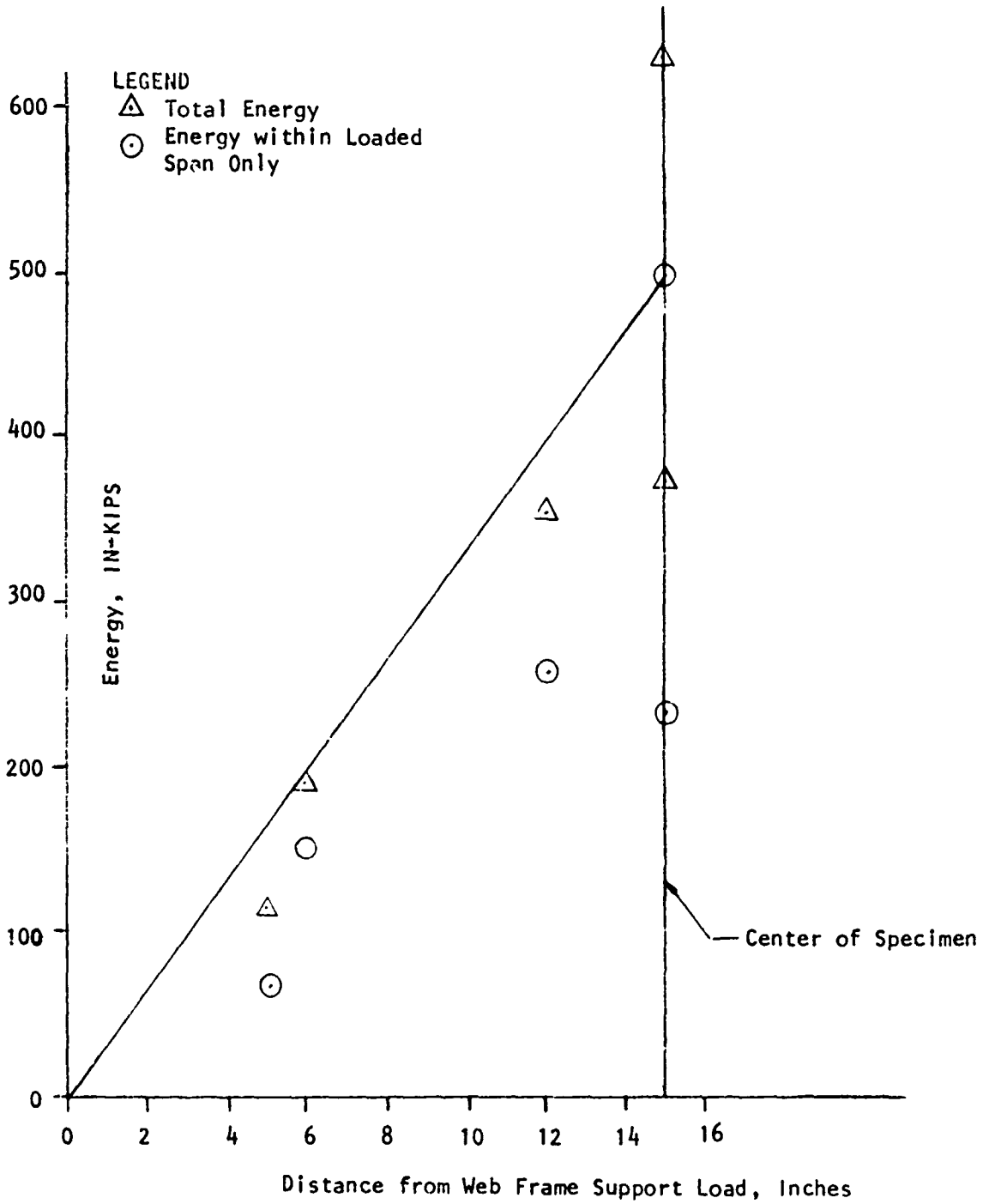

FIGURE 4-5 PLASTIC ENERGIES EXHIBITED AT RUPTURE IN COMPONENT STRUCTURES TESTS

In trying to extend these results to a collision case, it is pertinent to (1) examine Figure 4-5 and (2) consider an approximate hypothetical case of a damaged length extending over seven web frame spaces, Figures 4-6 and 4-7. Comparison of Figure 4-5 to Figure 4-7 indicates that assuming a triangular variation of energy absorption with strikes at different points along the length of the ship between bulkheads, is a reasonable assumption for a collision.

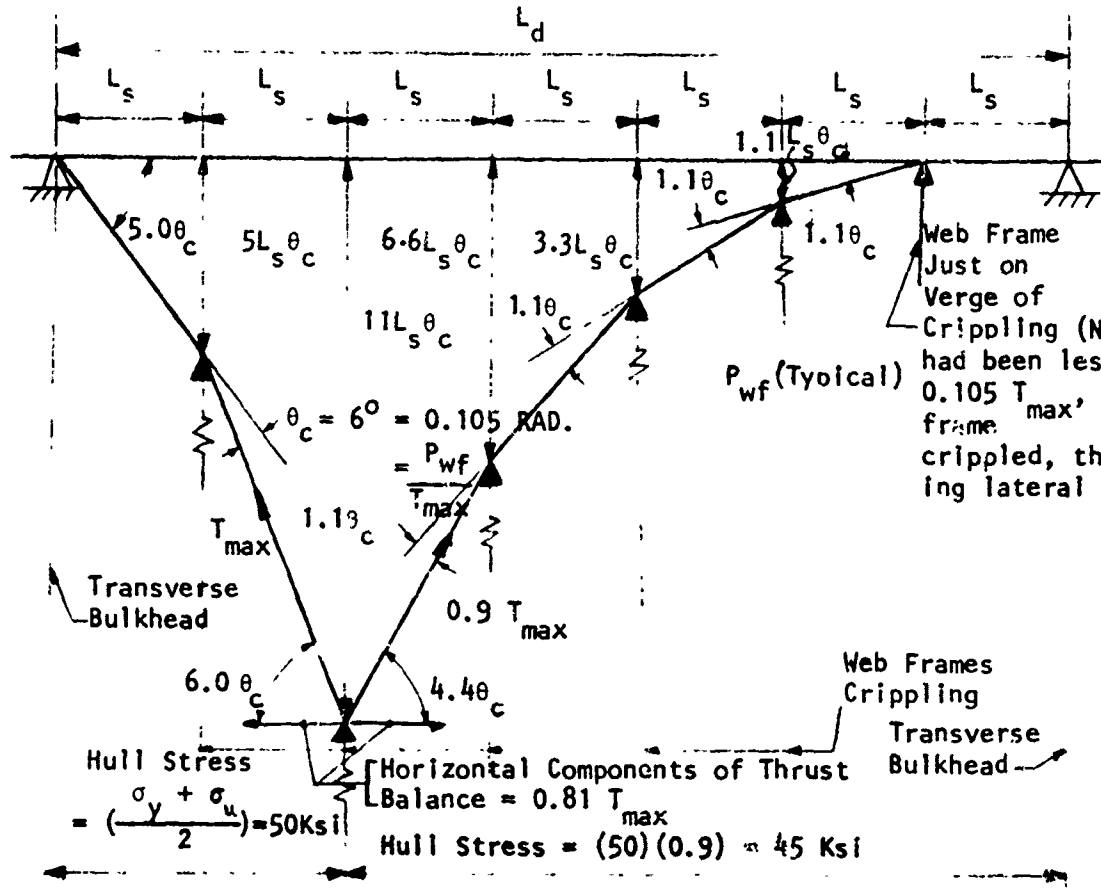

PLAN SECTION OF DISTORTED HULL BASED ON ARBITRARY RATIO OF WEB FRAME RESISTANCE TO MAXIMUM THRUST IN HULL

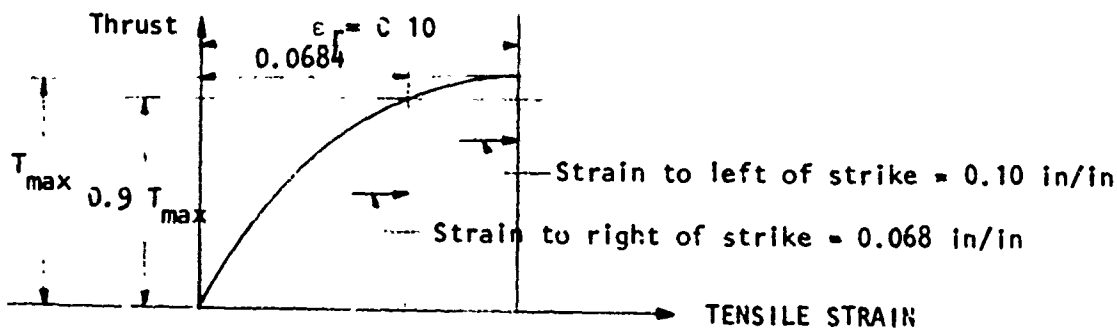

ASSUMED VARIATION OF THRUST WITH STRAIN (Section 3.4.3.1, Item 4)

TOTAL ELONGATION

$$e_t = \frac{L_s}{2}\theta_c^2\left[(5)^2 + (6)^2 + (4.4)^2 + (3.3)^2 + (2.2)^2 + (1.1)^2\right] = 0.54L_s$$

To left of strike, $\Sigma e = (0.10 \text{ in/in})(2L_s) = 0.20L_s$

To right of strike, $\Sigma e = (0.068 \text{ in/in})(5L_s) = 0.34L_s$

Total $= 0.54L_s$ (checks)

MEMBRANE TENSION ENERGY

$$E_{mt} = (T_{max})(0.20L_s) + (0.9\ T_{max})(0.34L_s) = 0.506\ T_{max}\ L_s$$

$$E_{mt} = 5.06\ T_{max}\ L_s\ \varepsilon_r$$

FIGURE 4-6 OFF-CENTER LOADING ON A DAMAGED LENGTH EXTENDING OVER SEVEN WEB FRAME SPACES

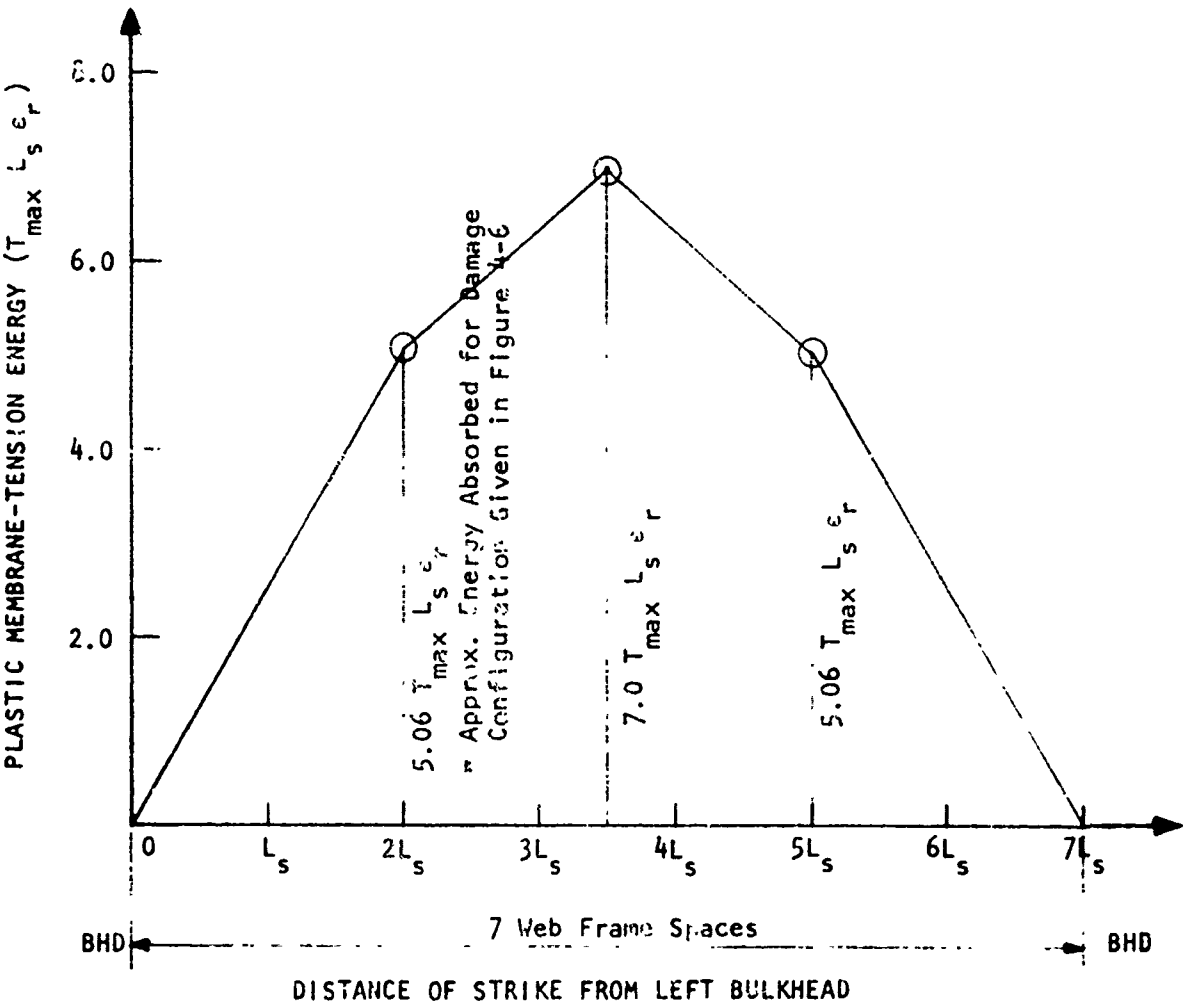

FIGURE 4-7 VARIATION OF MEMBRANE-TENSION PLASTIC ENERGY WITH LOCATION OF STRIKE

5. COLLISION INSPECTIONS

5.1 General

The objectives of the inspections were to obtain first-hand knowledge of the collision condition, the structural failure mechanisms, and extent of damage. The knowledge gained from the actual collisions was to be incorporated in the plastic energy evaluation procedure as judged desirable.

Although only six cases of collision damage were available for inspection, the information gained was considerable. None of the cases involved an ocean tanker with minor or moderate damage, and none included damage to horizontally stiffened web frames, which were of particular interest for the formulation of the analysis procedure. The six collision cases inspected (the reports for which are published as a separate report[23]) were as follows:

1. Collision of a longitudinally stiffened single-hull barge with concrete dolphin adjacent to railroad bridge pier in the Mississippi River at Burlington, Iowa. Inspected on October 30, 1971, in Hartford, Illinois.

2. Collision of a longitudinally framed double-hull barge for compressed chlorine gas with piers on a dam on the Ohio River. Inspected on May 17, 1972, in Louisville, Kentucky.

3. Collision between two transversely framed cargo ships, the Aegean Sea and the C.E. Dant. The ships were inspected September 8, 1972, in Victoria, British Columbia, and Seattle, Washington, respectively.

4. Collision between a tugboat and a longitudinally framed sulphuric acid barge. Inspected October 24, 1972, in Edgemore, Delaware.

Preceding page blank

5. Collision of a longitudinally framed double-hull chemical barge with a bridge pier inspected May 30, 1973, in Port Allen, Louisiana.

6. Collision between a longitudinally framed tanker, the Esso Brussels, and a transversely framed containership, the C.V. Sea Witch. The ships were inspected June 28, 1973, in Hoboken, New Jersey, and New York, New York, respectively.

5.2 Observations

5.2.1 Overall Extent of Damage

The longitudinal extent of damage appeared to be somewhat limited in two collisions (Nos. 4 and 6), but to be of the general magnitude expected of longitudinally framed ships in three other collisions (Nos. 1, 2, and 5), although theoretical calculations were not made for direct comparison. Collision No. 3 was between two transversely framed ships; the apparent "brittleness" of that particular collision in comparison with Collision Nos. 1, 2, and 5 suggests that the damaged length and the extent of incursion before hull rupture will tend to be greater for a longitudinally framed ship than for a comparable transversely framed ship. The limited extent of the damage to the longitudinally-stiffened shell and outboard structure of the struck ship (tanker) in collision No. 6 may possibly be explained by the fact that it was an oblique collision, and the portion of the hull behind the strike, where plastic membrane tension strains may be expected to occur in oblique collisions, was rigidly supported during the initial stages of the collision by a transverse bulkhead. The longitudinal bulkhead was also ruptured and seemed to have developed membrane tension prior to rupture.

"Hard points," such as the transverse bulkheads and/or strong web frames that define the ends of the overall length of damage have a significant effect on limiting the plastic deformation of a struck ship. In most collisions, there appears to be more of a tendency for ruptures to occur at hard points before occurring at the imprint of the striking bow.

Considerably more plastic distortion is exhibited in a stiffened hull that is struck about midway between transverse bulkheads than one that is struck near to a transverse bulkhead.

The deck and the ship bottom seem to act as "hard lines" in resisting side incursions, and ruptures generally occur in the hull at the deck and bilge elevations. This suggests that the strength of the deck and the ship bottom in resisting side incursions may have a very significant effect on collision phenomena.

5.2.2 Longitudinally Stiffened Hull Plates

At the location of greatest incursion by the striking ship, the hull longitudinal stiffeners of the struck ship tend to trip and in many cases, there are ruptures of the welds connecting the stiffeners to the hull plate. As a result, the bending strains in the stiffeners are not as great as they would be if the stiffeners remained in their normal geometric position. Consequently, large incursions are resisted primarily by membrane tension in the side plate and longitudinal stiffeners and not by bending.

5.2.3 Deck or Bilge Areas

When the striking bow does not directly bear against a deck or the bilge area of the struck ship, the deck or bilge area is likely to survive (without extensive damage) a significant incursion of the hull. If the deck or bilge area is struck directly or if the struck hull is extensively damaged, the deck or bilge area will tend to fail by first forming a series of longitudinal folds (each typically only one or two feet deep) and eventually forming transverse ruptures across the folds. Such transverse ruptures indicate that ultimately the primary strains in a distorted deck or bilge area are longitudinal membrane tension strains.

5.2.4 Transverse Structure

The transverse structure of a longitudinally framed tanker generally consists of transverse bulkheads and intermediate transverse web frames. Generally, the transverse bulkheads do not suffer any significant damage unless the striking ship has actually "plowed" through them. Conversely, the transverse web systems are generally quite vulnerable to collisions. Web trusses as opposed to web plates buckle under relatively minor side distortions, without much overall straining. Web trusses between the outer and inner plating of double-skin ships appear to be particularly ineffective in causing the two platings to distort in unison (or parallel) during a collision; web plates appear to be more effective for causing the two hulls to distort in unison.

In single-skin tank barges vertical web plates without attached horizontal stiffeners tend to fail in a crushing mode by developing vertical folds. In larger single-skin ships vertical web frames with attached horizontal stiffeners offer significant in-plane resistance to inward movement of the hull and eventually will fail by rupturing and/or overall twisting rather than by crushing.

5.2.5 Oblique Collisions

In oblique collisions the struck hull back of the strike (shell area transversed by the striking bow) tends to be in nearly a single flat plane. This indicates that the collision angle (the acute angle between the centerlines of the colliding ships) tends to remain practically constant during a collision. Whereas the hull in back of the strike generally appears to be stretched fairly straight in membrane tension, the hull ahead of the location of greatest incursion tends to develop vertical folds. This indicates that in an oblique collision it is most reasonable to assume plastic longitudinal strains in the hull in back of but not ahead of the location of maximum incursion.

5.2.6 Striking Bows

The striking bows generally are relatively undistorted except where they encounter stiff horizontal resistance at a deck or bilge area of the struck ship. At such elevations, the horizontal structure of the struck ship tends to "knife through" the striking bow.

5.3 Conclusions

Analyses of the results of the six ships' collision inspection cases have brought forth the following generalized conclusions:

(1) The bow of the striking ship distorts significantly only if it encounters relatively stiff horizontal resistance at a deck or bilge.

(2) The longitudinal extent of damage is the same for the deck, shell plate, and all damaged longitudinals.

(3) The energy absorption capacity of a longitudinally framed ship is generally greater than that of a comparable transversely framed ship.

(4) The longitudinal extent of damage is likely to be restricted between the transverse bulkheads and/or strong web frames.

(5) The deck and bilge area are "hard points" in resisting side incursion unless the striking bow directly bears against them.

(6) The relative location of strike to the transverse bulkhead has a significant effect on energy absorption.

(7) For a longitudinally stiffened hull, the collision energy is primarily absorbed by membrane tension in the side shell plate and longitudinal stiffeners.

(8) For a double-skin struck ship, web plates are more effective than web trusses for causing the two skins to distort in unison.

(9) In an oblique collision, the angle of collision remains constant throughout the collision.

(10) For oblique collisions, plastic membrane-tension strains occur in the portion of hull behind the strike.

(11) The damaged deck forms a series of small-pitch accordion folds extending in the longitudinal direction.

The above findings have provided useful information about the phenomena of ship collisions that has aided in development of the collision analysis theory as described in Section 2, and the procedure described in Section 3.

6. COMPONENT STRUCTURES TESTS

6.1 Purpose of the Tests

The purpose of the test program[24] was (1) to investigate the validity of various assumptions used in predicting loads, stresses, deflections, and strains prior to rupture in the sides of tankers, (2) to evaluate the large-distortion behavior of flat-plate and stiffened-plate structures which are typical of the side construction of tankers, and (3) to verify the theoretical equations which were developed to evaluate the force required to propagate a yielded zone through a stiffened-plate.

6.2 Test Programs and Apparatus

Two sets of test programs were conducted at the U.S. Steel Laboratory:

(1) Lateral Load Tests:

The first tests were conducted to simulate a concentrated static lateral load on reduced scale (approximately 1:5 scale) models (Figure 6-1) of representative portions of the side of a typical longitudinally framed tanker.

The setups for this test included plate specimens that were end-bolted to a horizontal 10-ft by 2-ft box-shaped frame (Figures 6-2, 6-3, and 6-4) and supported laterally by the frame at the ends and also at intermediate locations which would correspond to web frames in a ship. Six specimens each represented a model of a single stiffened-plate T-beam unit -- that is, a single angle-shaped longitudinal stiffener and the portion of hull plate which is considered to act compositely with the stiffener (Figure 6-1). Four specimens

each represented the same portion of the hull plate but without a stiffener attached. An external vertical box-shaped frame (Figure 6-4) served as (1) the downward restraint on the jacking system applying load to the specimen and (2) the upward restraint to the horizontal supporting frame shown in Figure 6-2. Through the bolted connections to the structural tees that were welded to the ends of each test specimen, the horizontal test frame anchored the specimens so that membrane tension could be realistically developed. Intermediate lateral supports for each specimen consisted of two transverse 3-in-dia round bars, 30 in. on center, that were, in turn, supported by the central portion of the box frame. Consequently, when positioned in

Stiffened-Plate Specimen	Flat-Plate Specimen	
	Plates	Stiffeners
Yield Strength, σ_y, ksi	43.8	37.3
Tensile Strength, σ_u, ksi	67.2	51.5
Elongation in 2 inches	32.5	37.0

* Corresponds to spacing of longitudinal stiffeners.

FIGURE 6-1 Cross-Section of Test Specimens

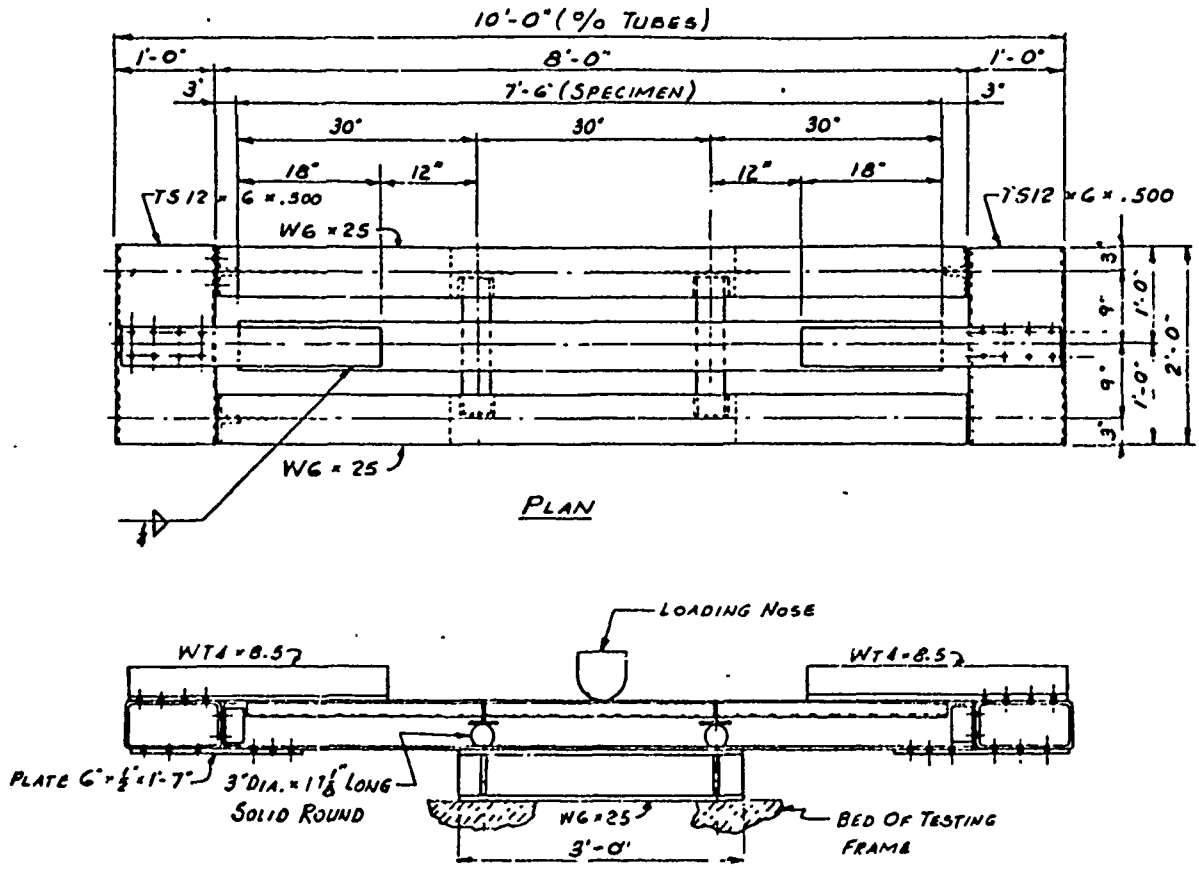

FIGURE 6-2 Details of a Stiffened Specimen and the Horizontal Restraining Frame

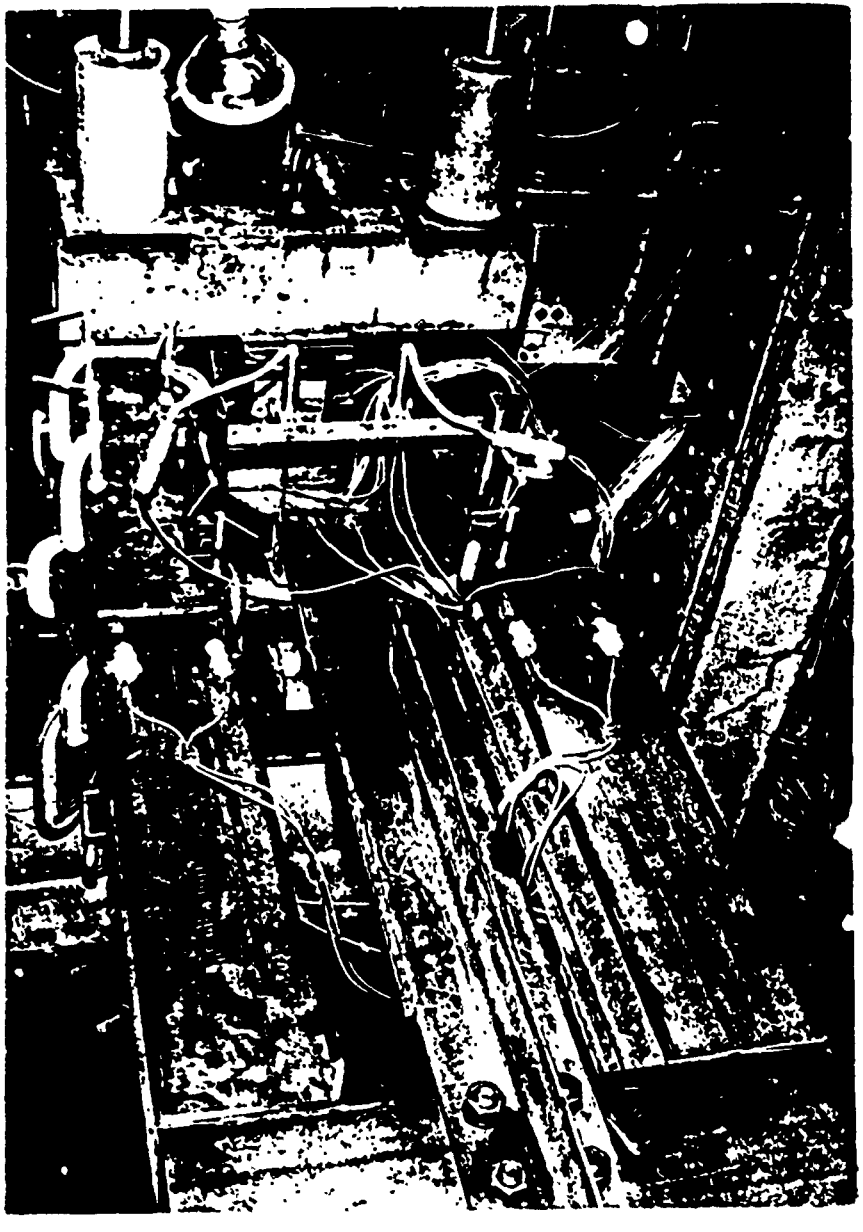

FIG.6-3 Test Setup Showing Specimen and Horizontal Test Frame

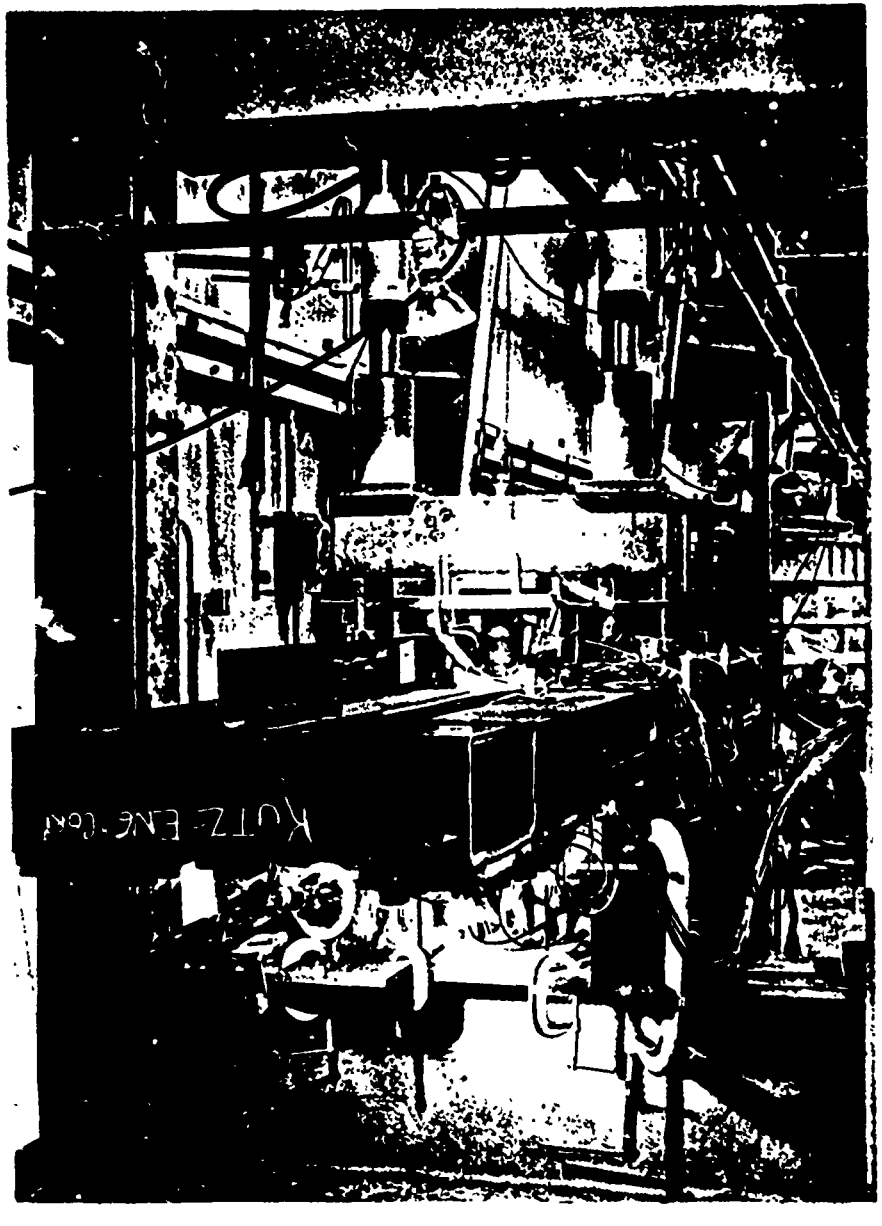

FIG.6-4 Test Setup Showing Jacking Against Vertical Test Frame

the test frame, a specimen simulated a portion of hull extending over three web-frame spaces. Additionally, short pieces of tees, which were notched to accommodate the hull stiffener, separated each of the six stiffened-plate specimens and one flat-plate specimen from each roller bearing (Figure 6-2). These simulated the support of transverse web frames. The other three flat-plate specimens were supported directly by the roller bearings.

The specimen material, with the dimensions and material properties given in Figure 6-1, was intended to represent an ABS steel with a yield strength of about 35 ksi, a tensile strength of about 65 ksi, and a ductility of 32 percent elongation in an 8-in. gage length. In tensions tests, the specimen material exhibited approximately this ductility and somewhat greater strengths, except for the tensile strength of the stiffener steel, which was considerably less.

Instrumentation for the tests consisted of longitudinally oriented electric-resistance strain gages on the test specimens and on the longitudinal beams of the horizontal supporting frame, direct-current differential transformers (DCDT's) to measure lateral deflections, and load cells to measure the applied jack loads (Figure 6-5). The number within each circle in Figure 6-5 indicates the number of strain gages at a particular location. Where possible, a pair of strain gages was placed on the top and bottom of the specimen plates, and on the bottom of the stiffener flange, if present.

the test frame, a specimen simulated a portion of hull extending over three web-frame spaces. Additionally, short pieces of tee:, which were notched to accommodate the hull stiffener, separated each of the six stiffened-plate specimens and one flat-plate specimen from each roller bearing (Figure 6-2). These simulated the support of transverse web frames. The other three flat-plate specimens were supported directly by the roller bearings.

The specimen material, with the dimensions and material properties given in Figure 6-1, was intended to represent an ABS steel with a yield strength of about 35 ksi, a tensile strength of about 65 ksi, and a ductility of 32 percent elongation in an 8-in. gage length. In tensions tests, the specimen material exhibited approximately this ductility and somewhat greater strengths, except for the tensile strength of the stiffener steel, which was considerably less.

Instrumentation for the tests consisted of longitudinally oriented electric-resistance strain gages on the test specimens and on the longitudinal beams of the norizontal supporting frame, direct-current differential transformers (DCDT's) to measure lateral deflections, and load cells to measure the applied jack loads (Figure 6-5). The number within each circle in Figure 6-5 indicates the number of strain gages at a particular location. Where possible, a pair of strain gages was placed on the top and bottom of the specimen plates, and on the bottom of the stiffener flange, if present.

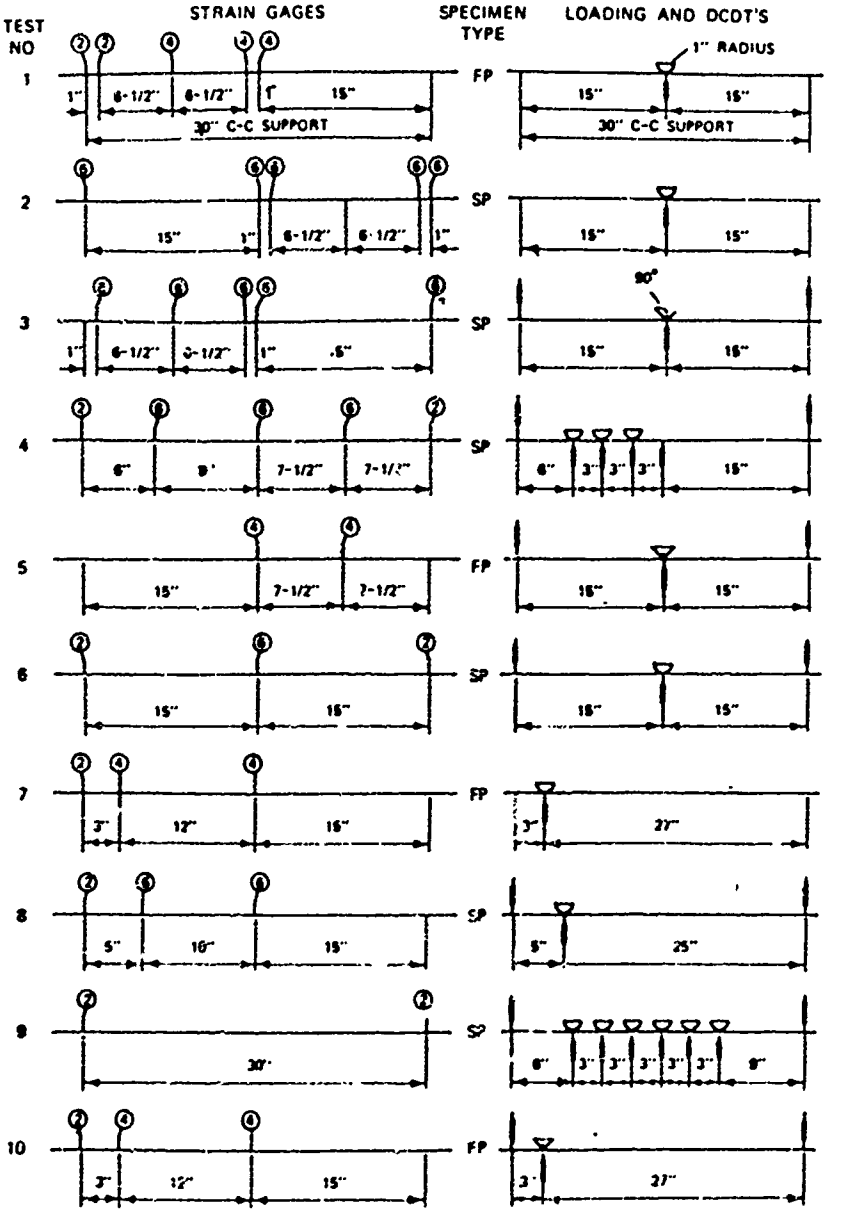

FIGURE 6-5 Test Instrumentations and Loadings

In each test the load was applied in increments, varying generally from about 0.5 to 6 kips, by the hydraulic jacking system through a nose of the configuration indicated by a symbol in Figure 6-5, bearing transversely on the specimen plate. A 1-in-radius nose, corresponding to a 5-in-radius bow of a full-size ship, was applied in seven tests, represented in Figure 6-5 as a semicircle. In three tests, a sharper, 90-deg-angle nose with a blunted (about 1/16-in) flat surface, represented in Figure 6-5 as a triangle, was fitted between the specimen and the rounded nose.

As indicated in Figure 6-5, in all tests except tests Nos. 4 and 9, the loading was increased monotonically at one station until specimen failure or until the test was terminated. In tests Nos. 4 and 9 a stiffened-plate specimen was deflected increasing amounts along the specimen at a succession of locations 3 in. apart to simulate the progressive inward and longitudinal movement of a striking ship bow in an oblique collision; there was no attempt to simulate the longitudinal forces applied by a striking bow during a collision.

(2) Longitudinal Resistance to Traveling Yield Zone Tests:

The second test was conducted to simulate the longitudinal resistance of stiffened plates to the occurrence of a traveling yield zone.

This second test was accomplished with a strip friction tester, Figure 6-6. When a thin sheet is pulled through a set of lubricated flat dies, Figure 6-7, the tensile machine records a net pull equal to F_l, the sum of the friction forces on two surfaces, and the pressure gage measures the normal force, N_l. From this, the "lubricated" coefficient of friction is:

$$\alpha = \frac{F_1}{2N_1}$$

When a thin sheet is pulled through a set of lubricated male-female dies, Figure 6-8, the tensile machine records a net pull equal to F_2, which is the sum of the friction forces and the longitudinal resistance force F_R to the traveling yield zone, and the pressure gage measures the normal force, N_2. Thence:

$$\Sigma F_R = F_2 - 2N_2\alpha$$

where $\Sigma F_R = F_{R_1} + F_{R_2} + F_{R_3}$, in which R_1, R_2, R_3 correspond to each of the three bend radii indicated in Figure 6-8.

Tests were made on five 24-gage (0.0239 inch thick) steel strips with a 33.4-ksi yield point and five 28-gage (0.0151 inch thick) steel strips with a 34.8-ksi yield point. All strips were 1½ inches wide. For each thickness, two different strips were tested with flat dies and three strips were tested with male-female dies. The normal force (measured by the pressure gage) was varied in increments between 200 and 1200 pounds, and the corresponding vertical pull was recorded.

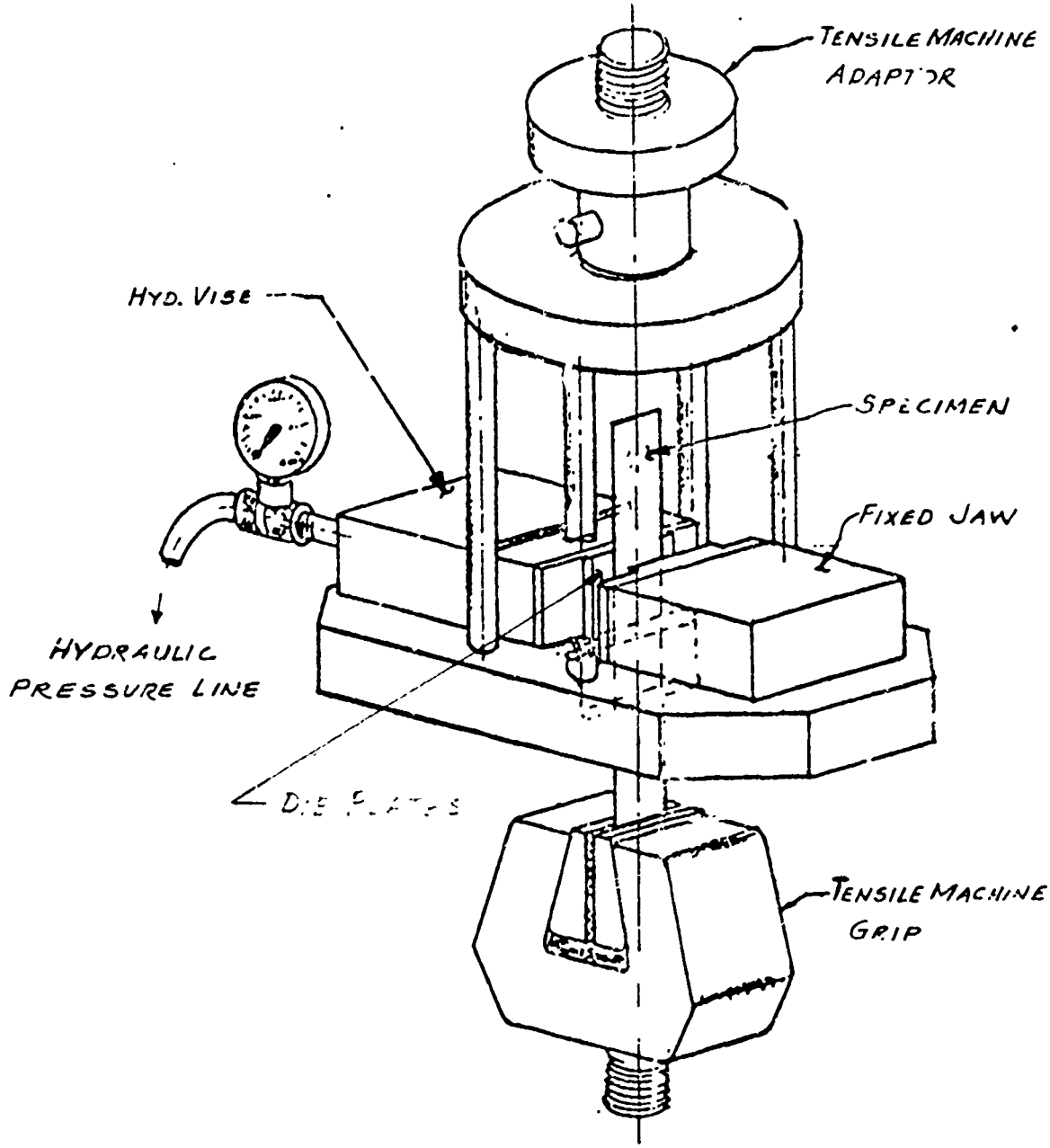

FIGURE 6-6

DIAGRAM OF THE STRIP FRICTION TESTER

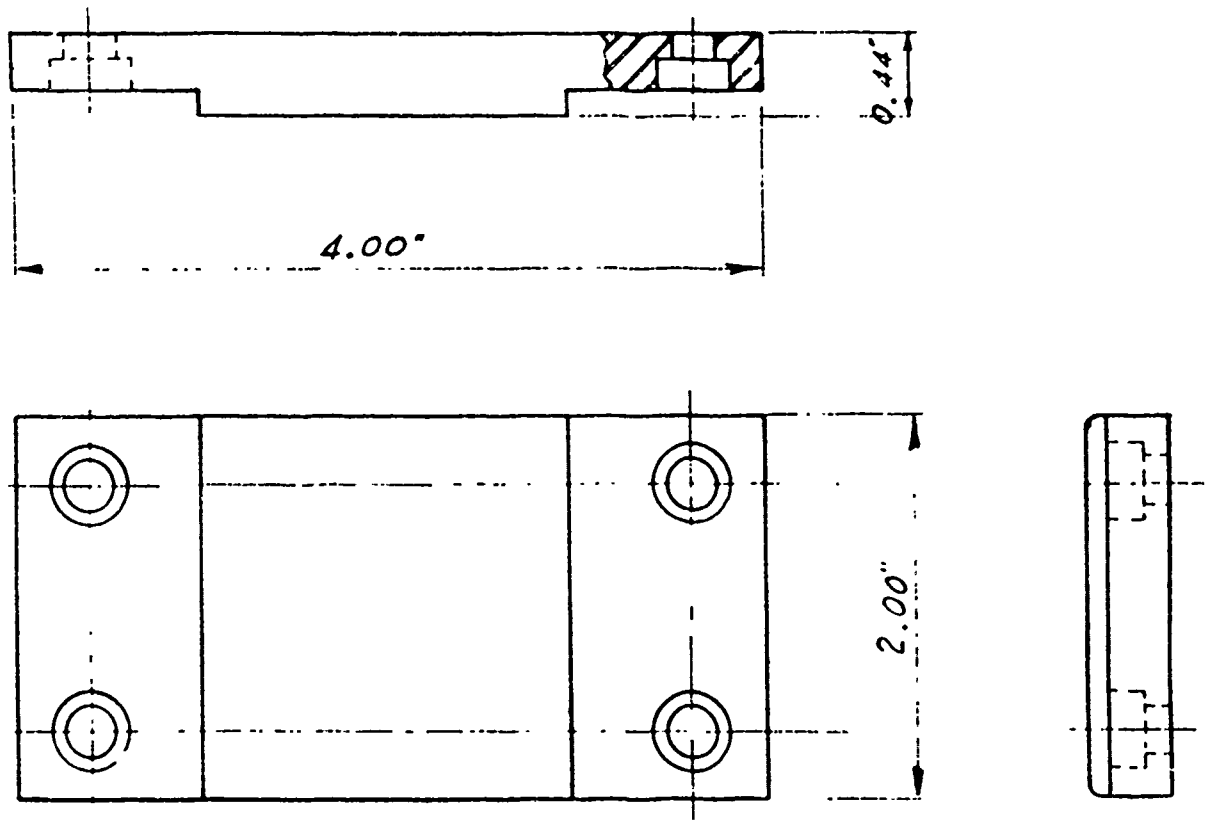

SPECIMEN GRIP

FIGURE 6-7

DIAGRAM OF DIE PLATES WITH FLAT SURFACES

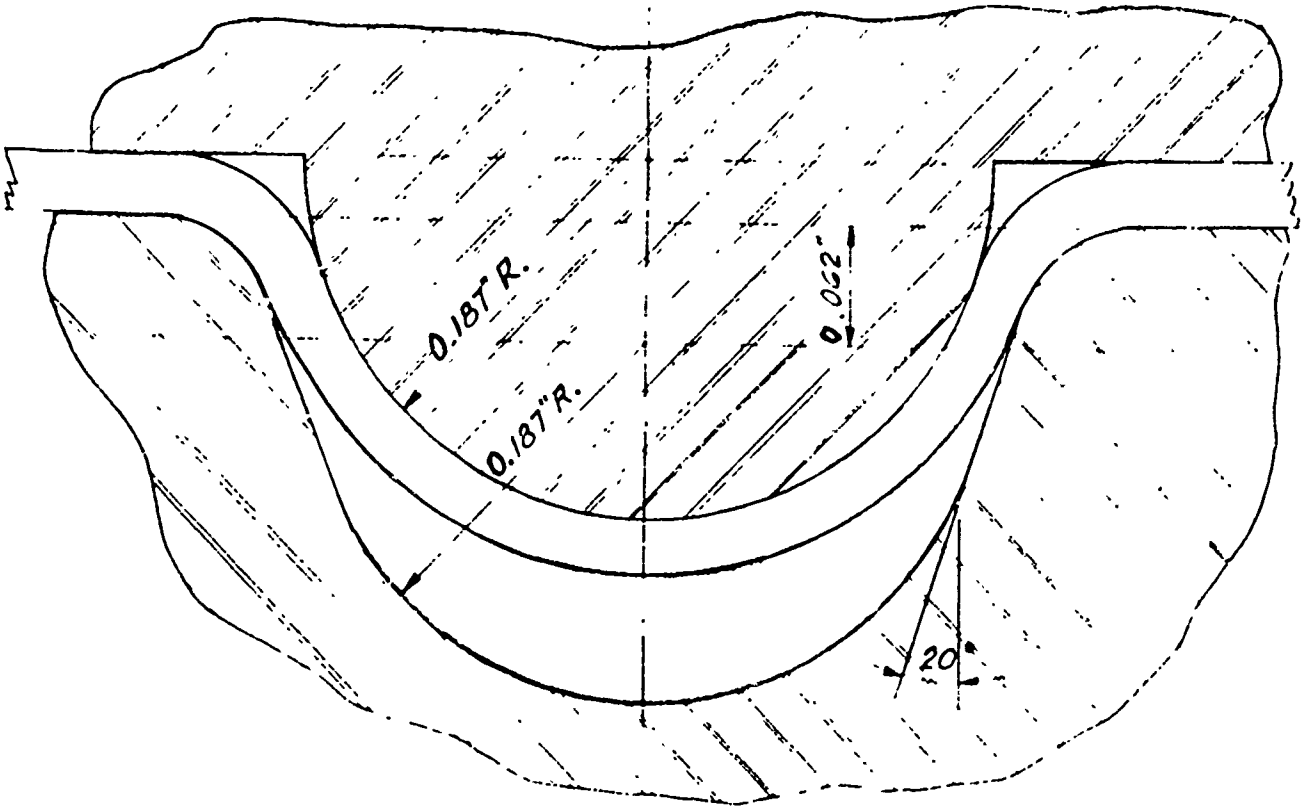

DETAIL OF MATING PIECES

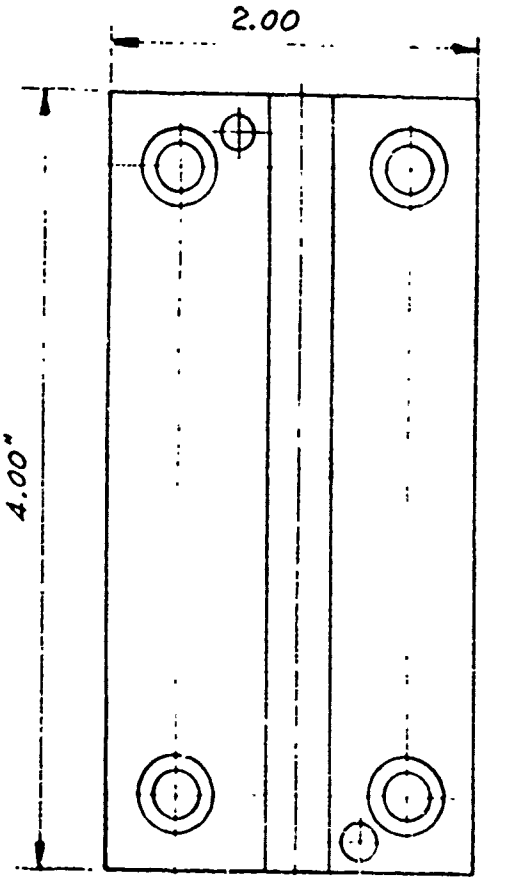

PLAN VIEW OF DIES

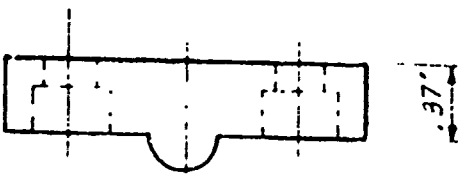

END VIEW OF MALE DIE

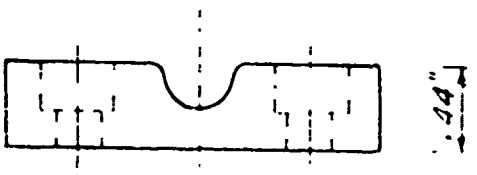

END VIEW OF FEMALE DIE

FIGURE 6-8

DIAGRAM OF DIE PLATES WITH MALE AND FEMALE GROOVED SURFACES

Additionally, one 24-gage strip and one 28-gage strip were deformed statically under normal forces varying from about 200 to about 400 pounds, and the resulting permanent curvatures were recorded photographically (10X). At each deformation, three radii of the curvature as shown in Figure 6-8 were determined from the photographic records.

6.3 Experimental Results of Lateral Load Tests

6.3.1 General Behavior

The general behavior of the test specimens is illustrated by the load-deflection curves of Figure 6-9 (for a stiffened-plate specimen) and Figure 6-10 (for a flat-plate specimen). During the first one to three loading increments, the specimens all exhibited yielding early, as predicted by the bending theory. The bending phase terminated at a relatively small load, as indicated by the significant increase in the slope of the load-deflection curve after the relatively flat portion of the curve. However, much greater loads, deflections, and rotation occurred during the subsequent membrane-tension phase before rupture. (Only test No. 7 was terminated before specimen rupture). Maximum deflections, loads, and, for some tests, rotations are listed in Table 6-1. During the membrane-tension phase, the profile of the loaded span was V-shaped, Figure 6-3, even under the moving load, Figure 6-11, but somewhat rounded at the supports and the load line. The stiffeners tripped at midspan during the membrane-tension phase but at loads greater than the loads causing buckling at the supports.

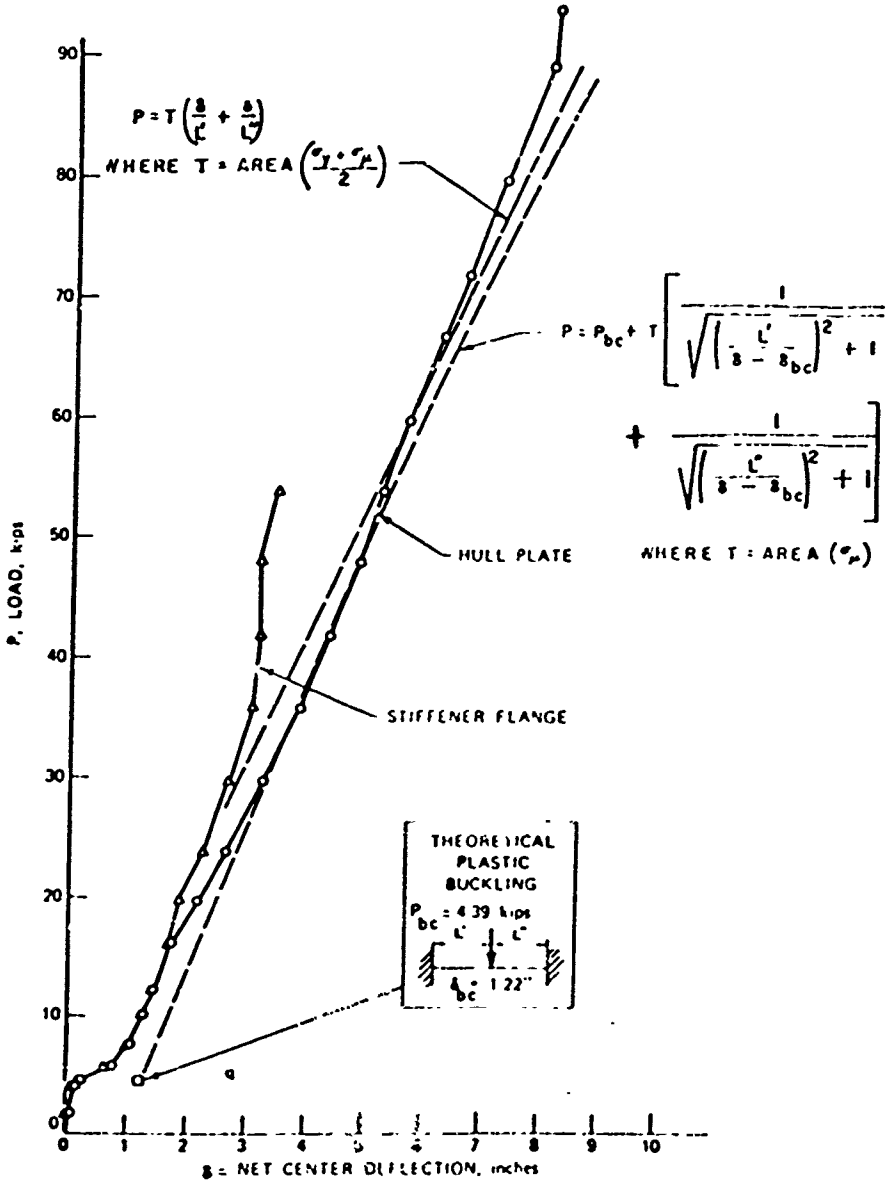

FIGURE 6-9 Deflection in Test No. 6, Stiffened-Plate Specimen

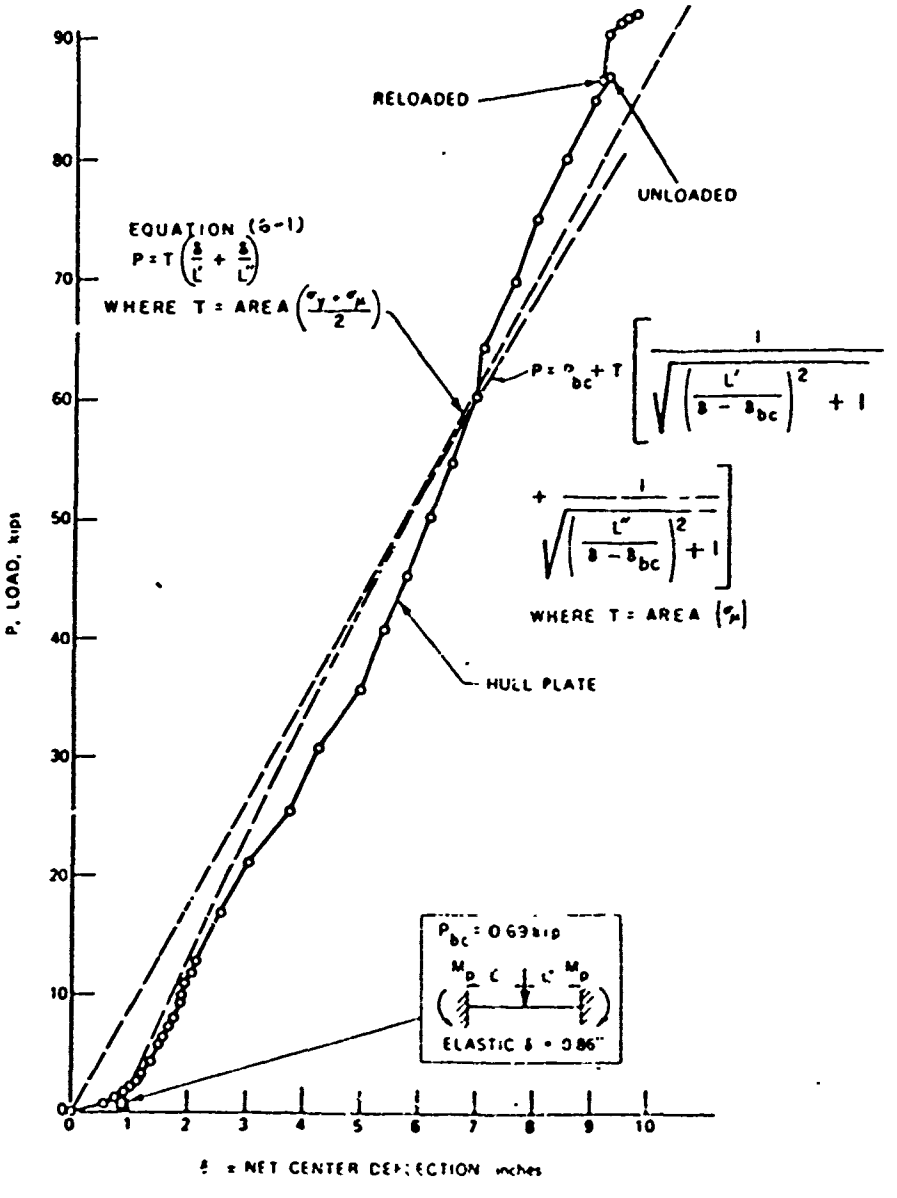

FIGURE 6-10 Deflection in Test No. 1, Flat-Plate Specimen

TABLE 6-1

SPECIMEN DATA AT TERMINATION OF TESTS

Test No.	Specimen	Nose	Station of Applied Loading at Termination of Test	Maximum Net Deflection Recorded at Station, in	Maximum Recorded Angle With Horizontal, deg	Maximum Load For Which Data Were Recorded, kips	Approximate Loading At Rupture, kips	Location Of Rupture	Maximum Angle At Location Of Rupture, deg.
1	Flat plate	1 in. radius	midspan	9.70	...	92.1	94	between load and support	...
2	Stiffened plate	1 in. radius	midspan	10.23	...	101.3	104	At web frame	...
3	Stiffened plate	90-deg	midspan	4.47	18[a]	48.3	52	under load	36
4	Stiffened plate	1 in. radius	3 in. from midspan	7.73	...	92.9	94	at web frame	...
5	Flat Plate	90-deg	midspan	4.81	19[a]	39.5	44	under load	38
6	Stiffened plate	1 in. radius	midspan	8.11	...	93.8	97	at web frame	...
7	Flat plate	1 in. radius	3 in. from support	...	...	60.1	...	(no rupture)	...
8	Stiffened plate	1 in. radius	5 in. from support	3.69	44	72.9	73	at web frame	44
9	Stiffened plate	1 in. radius	6 in. from midspan	6.32	35	71.9	74	at web frame	35
10	Flat plate	90-deg	3 in. from support	1.88	41[b]	51.8	53	under load	46

[a]Same on each side of the load

[b]41 deg within the 3-in. length, 5 deg within the remaining 27-in. length of the span.

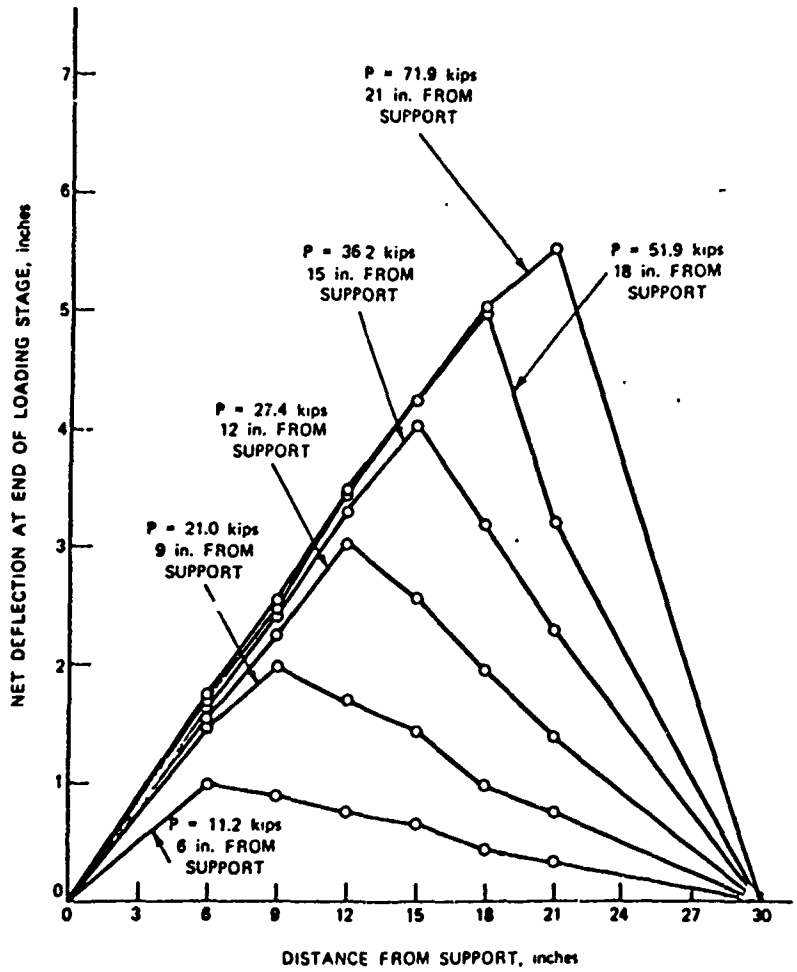

FIGURE 6-11 Deflection Profiles of Hull Plate at Ends of Loading Stages in Test No. 9

As listed in Table 6-1, all the stiffened-plate specimens that were subjected to the 1-in-radius loading nose, ruptured adjacent to the weld at a supporting web frame. These ruptures apparently initiated in the hull plate. Of the two flat-plate specimens that were subjected to the 1-in-radius loading, one specimen ruptured midway between the load and a bearing, and test on the other specimen was terminated before any rupture. The three specimens that were subjected to the sharp right-angle bearing all ruptured under the load.

6.3.2 Prediction of Deflections

As indicated in Figures 6-9 and 6-10, two different equations, both assuming a V-shaped deflection profile, were examined for predicting, approximately, the load-deflection curve. In the derivation of the more simple equation (6-1), the tension stress is assumed constant and equal to the average of the yield (σ_y) and ultimate tensile (σ_u) stresses, the geometry of small-deflection theory is utilized, and the bending phase is completely neglected. In the derivation of the more complex equation, a constant tension stress is assumed equal to σ_u, the geometry of large-deflection theory is utilized, and the theoretical curve begins at the theoretical end of the bending phase (load P_{bc}, deflection δ_{bc}). Neither equation considers any longitudinal shortening of the loaded span.

Considering the approximate extent to which either equation fits the test data, the more simple equation seems appropriate for approximate prediction of deflections, as follows:

$$P = T \left(\frac{\delta}{L^2} + \frac{\delta}{L''} \right) \qquad (6\text{-}1)$$

where : $T = (\text{area}) \cdot \frac{\sigma_y + \sigma_u}{2}$

δ = maximum deflection, at load

L' = horizontal distance from load to nearest support

L'' = horizontal distance from load to other support

This equation may be used for predicting the deflection at a load applied at midspan, away from midspan, or even moving across the span. As shown in Figure 6-11, each successive application of a load at different locations in the span resulted in the formation of a new V-shaped profile.

6.3.3 Stresses, Strains, and Energies within Straight-Line Portions of the Specimen at Rupture

By assuming that the deflection profile is a triangle and using small-deflection geometry, the deflection at rupture, δ_{tc}, is approximated by the equation (6-2).

$$\delta_{tc} = \sqrt{\frac{2L'L''}{L_t}(L'\varepsilon_r + L''\varepsilon_\ell + \Delta_s) + \delta_{bc}^2} \qquad (6\text{-}2)$$

where L_t = loaded span = $L' + L''$

ε_r = reserve ductility available within L' during membrane-tension phase

ε_ℓ = strain within L'' when strain within L' is ε_r

Δ_s = amount by which span length shortens during loading (due to straining of horizontal resisting frame during the test, or in a ship, due to longitudinal elastic strain, ε_c, that is caused by overall horizontal bending of the ship)

δ_{bc} = deflection at the instant when bending phase is assumed to terminate and membrane-tension phase to begin

Equation (6-2) was used to analyze the data of the present test series; values of ε_r and ε_ℓ were determined from the corresponding maximum deflections, δ_{tc}, given in Table 6-1. For loads applied at midspan, $\varepsilon_\ell = \varepsilon_r$ and equation (6-2) was used directly, with Δ_s determined from experimental measurements. However, for loads applied at locations other than midspan, $\varepsilon_\ell < \varepsilon_r$; then ε_ℓ was related to ε_r by a statics-and-compatibility analysis, based on equating the longitudinal components of the tensile force in the two straight-line portions of the deflected specimens on either side of the load, and by using the stress-strain curves for the two specimen materials to relate the tensile forces to ε_r and ε_ℓ.

The resulting values of ε_r and ε_ℓ are listed in Table 6-2. In all tests except No. 3, it was apparent that tensile rupture initiated in the hull plate, which was not significantly strained during the bending phase because the neutral axis of bending was located within the cross-section of the hull plate, even for the stiffened-plate specimens. Therefore, for those tests, ε_r and ε_ℓ were each the apparent maximum gross strain, ε_a, within the straight-line portions of the loaded span. For test No. 3, the apparent maximum strain listed also includes a theoretical bending-phase strain of 0.077 in./in., because of the stiffened plate specimens, only the specimen of test No. 3 ruptured at the load, where maximum tensile strains theoretically are greater in the stiffener than in the hull plate. Also listed in Table 6-2 are end-span plastic strains, which were obtained based on the assumption that the measured end-span elongations each occurred only within the length between the structural tee and the support for the loaded span.

TABLE 6-2

Summary of strains and plastic energy at rupture

Loading nose	Specimen type	Test no.	Location of applied load at rupture	Maximum angle at location of rupture,[a] deg	ϵ_a = Apparent maximum gross strain, in./in., in straight-line portion				Range of ratios of stress $\div \left(\frac{\sigma_y + \sigma_u}{2}\right)$ within loaded span	Total plastic energy, in loaded span and end spans kip-in., from strain analysis	Plastic energy, kip-in., up to δ_u on the P-δ plot	
					Loaded span ϵ_r	Loaded span ϵ_l	End span nearest to sta. of load at rupture	End span farthest from sta. of load at rupture			Area under experimental curve	Area under line for equation (6 - 1)
1-in radius	flat plate	1	midspan	...	0.195	0.195	0.048	0.048	1.21	514	391	414
	stiffened plate	2	midspan	..	0.176	0.176	0.065	0.065	1.15–1.21	630	not available	548
	"	6	midspan	...	0.086	0.086	0.069	0.069	1.07–1.15	372	346	344
	"	4	3 in. from midspan	..	0.137	0.066	0.053	0.047	1.01–1.20	352	360[b]	326
	"	9	6 in. from midspan	35	0 090	0.045	0 031	0.018	0.92–1.16	188	not obtained	191
	"	8	10 in. from midspan	44	0.060	0.025	0.039	0 016	0.84–1.08	116	128	128
"	"	5	midspan	38	0.039	0.039	0.020	0.020	0.99	98	79	102
90-deg	flat plate	10	12 in. from midspan	46	<0.030	<0.020	0.018	...	0.79–0.93	<45	42	43
"	stiffened plate	3	midspan	36	0.102[c]	0.102[c]	0 018	0.018	1.09–1.17	94	95	105

[a] From Table 6-4.
[b] The sum of 37, 110, and 213 kip-in. for loadings 9, 6, and 3 in., respectively, from midspan.
[c] For test No. 3 only, $\epsilon_r = \epsilon_l = 0.025$ in./in., but the apparent maximum strain also includes a theoretical bending-phase strain of 0.077 in./in.

Examination of the data in Table 6-2 suggests that it would be reasonable in future collision analyses to limit the apparent maximum strain, ε_r, to a value

$$\varepsilon_r = 0.10 \left(\frac{\text{tensile-strength ductility}}{32\%} \right)$$

based on a limit of $\varepsilon_r = 0.10$ in./in. in the present tests for ruptures associated with bend angles not exceeding 35 deg (0.61 radian). (The significance of ruptures associated with recorded bend angles of 35 deg or more is discussed in the following section.) Such a criterion would have only slightly overestimated ε_r in test No. 6, with $\varepsilon_r = 0.086$ in./in., and in test No. 9, with $\varepsilon_r = 0.090$ in./in., and underestimated the values of ε_r in tests Nos. 1, 2, and 4. The criterion even fits test No. 3, with $\varepsilon_r = 0.102$ in./in. Examination of the data in Table 6-2 also suggests that it would be reasonable to consider the strain in each end span to be about one half the strain within the nearest straight-line portion of the loaded span.

The strain-analysis calculations for ε_r and ε_ℓ involved determination of corresponding plastic-range maximum stresses in the hull plate and stiffener, if present. The ranges of these computed stresses are divided by $(\sigma_y + \sigma_u)/2$ to give the ratios listed in Table 6-2. From these ratios, it is apparent that the assumption of a stress in the straight-line portion at rupture equal to $(\sigma_y + \sigma_u)/2$ (as assumed in equation (6-1)), would not be grossly inaccurate. This assumption would underestimate the stress for specimens subjected to a rounded loading nose at or near midspan and would overestimate the stress for specimens, subjected to a sharp loading nose at or near midspan or to a load with either nose near a support.

Table 6-2 compares the plastic energy from the strain analysis with the plastic energies computed as the area under the experimental load-deflection curve, such as given in Figures 6-9 and 6-10, or the area under the theoretical curve using equation 6-1 . For the strain analysis, the plastic energy within each straight-line portion is the volume of strained steel times the maximum membrane-tension strain times the stress corresponding to the maximum gross strain. This should be an upper-bound estimate of the energy because the stress is generally less at lesser strains. There appears to be reasonable agreement between the three different ways of computing the plastic energy, a further indication that the assumption of a constant tensile stress of $(\sigma_y + \sigma_u)/2$ is reasonable.

6.3.4 Apparent Maximum Strain Under Sharp Bearing

Table 6-3 presents a simplified mathematical model of the hull plate, without stiffeners, for relating apparent ductility to the angle of rotation, 2θ, under a midspan sharp load bearing, such as was applied by the 90-deg nose (θ is the angle subtended by the plate between the straight-line portion and the location of maximum curvature within the bend as shown in Figure 3-3 of Section 3). The purpose of developing the mathematical model was primarily to establish what variables interrelate relative to sharp bending in the hull plate.

Certain arbitrary assumptions were made to simplify this very complex problem: (1) It was assumed that each straight-line portion of the hull plate that extends most of the distance between the loading nose and a support is stressed uniformly over the plate thickness, t, in tension at a stress, σ', corresponding to ε_r or ε_ℓ, Table 6-2. (2) At the centerline of the sharp loading nose, where rupture is anticipated, a depth d' of the cross-section is arbitrarily assumed to be uniformly stressed in compression at a stress σ_c, and the remainder of the cross-section is assumed to be uniformly stressed in tension at a stress σ_t as indicated in the diagram at the top of Table 6-3. Rupture occurs when $\sigma_t = \sigma_u$. These assumptions for stress correspond to the usual assumption of "pure plastic" analysis, and neglect the fact that the stress is somewhat less near the neutral axis.

Under the load, a very short portion of the span is curved, between the two straight-line portions of the deflected hull. Despite the curvature being "sharp", the geometry of small-deflection theory is assumed in the present analysis. The equation for the deflection within this curved region is not readily attained in a closed-form solution. For the derivation in Table 6-3, an equation that would define the deflection of a simple beam is assumed, namely

$$y = k(3x_m^2 x - x^3) \qquad (6\text{-}3)$$

where

y = lateral deflection relative to a line through the points of tangency where the two straight-line portions meet the curved portion

x = longitudinal distance from one point of tangency

x_m = longitudinal distance from load to one point of tangency

k = a constant

TABLE 6-3 Mathematical model for relating bend angle to apparent maximum strain in centrally loaded hull plate under sharp load bearing

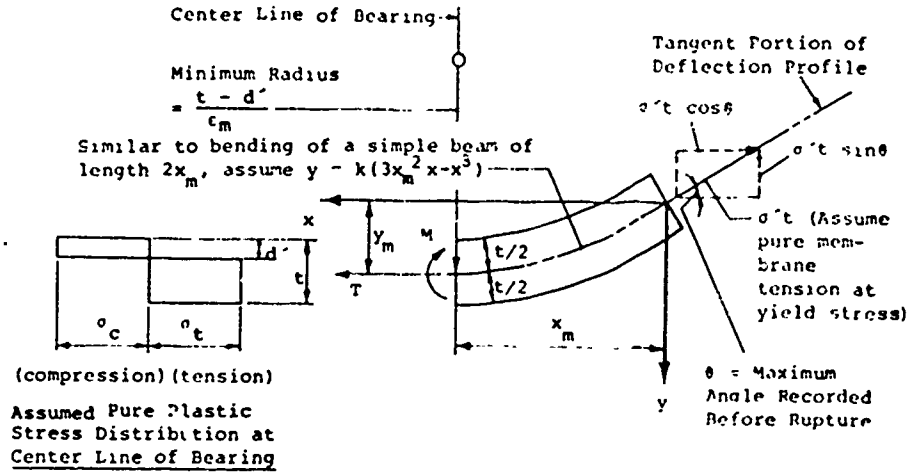

1. Given δ_{tc} and σ' (the stress corresponding to hull-plate strains),

$$\theta = \tan^{-1}\left(\frac{\delta_{tc}}{0.5L_t}\right)$$

2. Stresses σ_t and σ_c are unknown values corresponding, respectively, to strains ϵ_m and $\epsilon_m d'/(t-d')$.

3. The horizontal component of membrane tension, centered at the midplane of the plate, is

$$T = \sigma' t \cos\theta = \sigma_t(t - d') - \sigma_c d' \text{ from which } d' = \left(\frac{\sigma_t - \sigma' \cos\theta}{\sigma_t + \sigma_c}\right) t$$

4. Relative to the midplane of the plate, the bending moment under the load, which is superimposed on T, is

$$M = \sigma' t\,(x_m \sin\theta - y_m \cos\theta) = \left(\frac{\sigma_c + \sigma_t}{2}\right) d'(t - d')$$

from which, utilizing Step 3,

$$(x_m \sin\theta - y_m \cos\theta) = \left(\frac{\sigma_t - \sigma' \cos\theta}{2\sigma'}\right)(t - d')$$

5. For small-deflection theory, the maximum curvature under the load is

$$\frac{\epsilon_m}{t - d'} = -\left(\frac{d^2y}{dx^2}\right)_{x_m}$$

6. Combining Steps 4 and 5 gives

$$\epsilon_m = -\left(\frac{d^2y}{dx^2}\right)_{x_m}\left(\frac{2\sigma'}{\sigma_t - \sigma' \cos\theta}\right)(x_m \sin\theta - y_m \cos\theta)$$

7. Using $y = k\,(3x_m^2\, x - x^3)$ and $\left(\frac{dy}{dx}\right)_{x=0} = \tan\theta$,

$$k = \frac{\tan\theta}{3x_m^2} \quad \text{and} \quad \left(\frac{d^2y}{dx^2}\right)_{x_m} = -6kx_m = -\frac{2\tan\theta}{x_m}$$

8. Combining Steps 6 and 7 gives

$$\epsilon_m = \left(\frac{2\tan\theta}{x_m}\right)\left(\frac{2\sigma'}{\sigma_t - \sigma' \cos\theta}\right)\left(x_m \sin\theta - \frac{2x_m \tan\theta \cos\theta}{3}\right)$$

$$= \frac{4}{3}\left(\frac{\sigma'}{\sigma_t - \sigma' \cos\theta}\right) \sin\theta \tan\theta$$

Equation (6-3) applies only in the interval $0 \leq x \leq x_m$ and would apply to pure bending in the strain-hardening range of behavior. Thus, it is presumed that k includes the reciprocal of the strain-hardening stiffness term, $E_t I$, where E_t is the tangent modulus and I is the moment of inertia. Although equation (6-3) does not reflect the effect of membrane tension, it does give a reasonable and simple approximation of the way in which the curvature increases from zero at a point of tangency to a maximum value at the load.

As indicated in Step 3 of Table 6-3, an expression for d' is obtained by equating the horizontal component of the tensile force in the straight-line portion of the hull plate to the net tensile force in the hull plate at the centerline of the load. At each section, the net tensile force is centered at the mid-depth of the plate. In Step 4, the "external" bending moment at the centerline of the load, resulting from $\sigma' t$, is equated to the "internal" bending moment about the mid-depth of the plate at that section, expressed in terms of the stresses. In Step 5, the geometric definition for the curvature of the plate at the centerline of the load is equated to the "small deflection" definition for curvature. Step 7 utilizes the fact that the slope of the plate at the point of curvature is equal to the tangent of the angle between the straight-line portion and the horizontal. The result of the various combinations of these expressions is an equation (given in Step 8) for the apparent maximum strain (before rupture) in the plate under the load:

$$\varepsilon_m = \frac{4}{3} \left(\frac{\sigma'}{\sigma_t - \sigma' \cos \theta} \right) \sin \theta \tan \theta \qquad (6\text{-}4)$$

ε_m is apparently related only to θ and the plate strength, but not to the plate thickness.

Equation 6-4 can be applied to the test data in Table 6-1 for the tests for which final bend angles were recorded. In addition to relating the bend angle to the tensile strain under a centrally applied load, it is useful to apply the equation to relating the bend angle to (1) the tensile strain of the plate at a web-frame support, with θ = one half the total bend angle at that location, and (2) to the tensile strain under a load that is not centrally applied, with θ = one half the total bend angle and σ' arbitrarily assumed to be the average of the stresses in the straight-line portions of the plate on either side of the load. With these assumptions, Table 6-4 gives values of ε_m computed from equation 6-4 , using values of θ derived from the angles listed in Table 6-1. The values of ε_m ranged from 1.05 to 2.4 times the tension-test ductility, 0.325 in./in., in a 2-in. gage length. Apparently, the bending ductility was greater than the tension-test ductility because the bending measures, more closely, the "local ductility." As discussed in two recent papers (25, 26), "local ductility," which is defined as the maximum strain exhibited in a $\frac{1}{2}$ in. length spanning the location of the rupture, is considerably greater than (for some steels may be almost three or four times as great as the percent elongation within the 2-in. gage length.

For collision analyses using equation 6-4 , it is useful to set a practical limit on the ratio of ε_m to the tension-test ductility so that the equation can be used to indicate at what value of θ rupture can be expected. By using the smallest angle listed in Table 6-4 and assuming that $\sigma' = (\sigma_y + \sigma_u)/2$ (as used in equation 6-1) rather than the values listed in Table 6-4, equation 6-4 gives $\varepsilon_m = 0.49$ in./in.,

TABLE 6-4

APPARENT MAXIMUM TENSILE STRAINS AT

LOCATIONS OF RUPTURE

Test No.	θ = 1/2 Bend Angle at Location of Rupture,* deg	σ' = Average Of Stresses In Straight-Line Portions of Plate, ksi	ε_m = Apparent Maximum Tensile Strain Computed From Equation (6-4) With $\sigma_t = \sigma_u$ in./in.
3	18	50.0	0.34
5	19	55.0	0.54
8	22	54.6	0.66
9	17.5	60.4	0.79
10	23	47.7	0.45

*θ is the angle subtended by the plate between the straight-line portion and the location of maximum curvature within the bend.

which is 1.5 times the tension-test ductility in a 2-in. gage length. Without a more elaborate analysis, it seems reasonable to assume that this ratio is always 1.5 when equation 6-4 is used to establish approximate limitations on bend angles resulting in rupture. For an ABS steel with σ_y = 35 ksi, σ_u = 65 ksi, and tension-test ductility = 0.32 in./in., the total bend angle resulting in rupture (2θ) would then be 41 deg (0.72 radians).

6.4 Experimental Results of Longitudinal Resistance to a Traveling Yield Zone

From the flat-die tests, an average coefficient of friction for the lubricated surfaces was determined to be α = 0.136. The results of the male-female-die tests, using this value of α, are compared, in Table 6-5, to theoretical values using equation 6-5 with each recorded radius of curvature to give a total net tension that is the sum of three different calculations of F_R.

$$F_R = \frac{\sigma_y t^2}{2R}\left(1 - \frac{\sigma_y R}{0.5Et}\right)^2 \qquad (6\text{-}5)$$

where

F_R = Longitudinal resisting force per inch of plate width

R = Maximum midplane radius of curvature

t = Sheet thickness

TABLE 6-5

COMPARISON OF THEORETICAL AND EXPERIMENTAL RESULTS

Gage of 1-1/2-Inch-Wide Sheet Specimen	Normal Force, N_2' Pounds	Longitudinal Resistance of Sheets to Traveling Yield Zone = Tensile Force Minus Friction			
		Theoretical (Equation (6-5)) $= F_{R_1} + F_{R_2} - F_{R_3}$ Pounds	Experimental (Equation (6-5) With $\alpha = 0.136$) Pounds		
			First Specimen	Second Specimen	Third Specimen
24	199	41	6	-	2
	239	87	35	40	35
	278	126	44	37	41
	318	156	106	90	78
	358	167	145	134	137
	398	196	172	170	176
	437		201	191	200
	477		228	216	222
	517		247	239	245
	557		276	264	274
	596		306	294	306
	795		504	494	488
	994		557	573	602
	1193		647	628	666
28	199	72	56	51	36
	239	82	80	70	71
	278	128	106	103	96
	318	143	132	125	121
	358	149	158	159	150
	398	155	185	179	177
	437		208	206	205
	477		226	224	226
	517		243	240	240
	557		253	246	253
	596		250	243	257
	795		253	245	273
	994		264	266	292
	1193		272	286	310

It is seen that the general magnitude of the theoretical and experimental values agree. Contrary to theory, there was an increase in net tension after the dies were closely clamped to prevent the radius from changing appreciably, i.e., for $N_2 > 400$ pounds. This was probably due to the oil being progressively squeezed out, resulting in a greater coefficient of friction as the normal force was progressively increased during each test.

7. NONRIGID-BOW INVESTIGATION

7.1 Background

The analysis procedures for plastic energy absorption in tanker side structure were based on the assumptions:

(1) The striking ship bow is sufficiently strong that the stem profile remains unchanged throughout the collision process.

(2) The stem along with its associated backup structure, does not deform plastically and absorb collision energy.

(3) The collision circumstances are such that the side of the struck ship deforms by progressive plastic deformation of backup structure, together with plastic membrane stretching of side shell structure, until the ductility of the side shell is exhausted, rather than by an initial cutting of the struck ship's side and subsequent tearing and/or shearing of shell and bow plating.

Because of these assumptions, the plastic analysis procedure estimates the near maximum energy absorbing capabilities of the struck ship but ignores any energy-absorbing capabilities of the striking ship's bow structure.

If the bow structure of the striking ship is not sufficiently strong for the above assumptions to hold, or if it has a tendency to cut rather than stretch the shell plating of the struck ship, several alternative modes of structural failure may conceivably take place:

(1) If the stem remains rigid but the backup bow structure is not sufficiently strong, the striking ship bow will progressively collapse and absorb collision energy in addition to that absorbed by the struck ship; and by providing a more blunt profile, may even enable the struck ship to absorb more collision energy before rupturing.

(2) if the backup bow structure is weak over a sufficiently large portion of its length, it may absorb all of the collision energy without causing significant damage to the struck ship.

(3) If the stem lacks sufficient local strength, it may buckle or be cut by the deck of the struck ship, thus providing a sharper profile for puncturing the struck ship.

(4) If the stem is locally weak and the backup bow structure is also weak, the cutting of the stem may be followed by collapse of the stem and bow structure below the deck of the struck ship.

(5) If the stem and backup structure are relatively strong and the stem is sharp in cross section, the side of the struck ship may be cut or rupture with an almost negligible absorption of collision energy.

Thus, a weak bow structure can increase the total energy absorption in a collision by absorbing a significant portion of the collision energy itself or by becoming uniformly more blunt and thus allowing the side structure to absorb more energy due to an increased area of plastically deformed side structure. Or it can decrease total energy absorption by deforming in such a way that the side shell of the struck ship is punctured prematurely. In either case, it is necessary to analyze two aspects of striking ship bow strength:

(1) the strength of the stem or leading edge of the bow, and

(2) the strength of the backup bow structure.

The case of the sharp bow structure with the capability of immediately cutting the shell of the struck ship is a special case within the realm of rigid bows and does not fit within the scope of this investigation. In addition, it is believed to be pertinent only to severe collisions. The almost identical problem of having the gunnel of the struck ship cut the stem

of the striking ship will be discussed; however, the discussion will necessarily be of a general nature.

7.2 Purpose

The purpose of this nonrigid-bow investigation was to propose methods of evaluating the local and overall strength of the striking bow in relation to the gunnel and side structure of the struck ship. These evaluation procedures are intended to complement the plastic analysis procedures for the side structure, but the two procedures are not intended to be interdependent.

The intended use for these evaluation procedures is primarily to determine the circumstances under which the plastic analysis procedure for side structure is valid rather than to calculate the energy absorption capabilities of bow structure.

7.3 Approach

There are a large number of possible variations in collision circumstances dependent on such parameters as: relative size of struck and striking ship, relative drafts and freeboards, collision angles and relative velocities, and the large number of possible configurations for the striking bow. As a simplifying assumption and to be consistent with the scope of the plastic-energy-analysis procedure, only those collision circumstances will be considered in which the stem of the striking ship, below its uppermost deck, contacts the gunnel of the struck ship. The colliding ship stem is assumed to be raked or plumb with no protruding bulbous portion.

As mentioned before, the purpose of this investigation is to provide the tools for determining the applicability of the rigid bow assumption used in the plastic analysis procedure, given the configuration and scantlings of the striking ship's bow and the struck ship's side structure. These tools or methods of analysis will be based on the assumption that the structural

behavior of the bow and side structure in a collision can be separated into a preliminary phase in which dynamic effects predominate and a concluding phase in which quasi-static behavior can be assumed to predominate. In addition, the bow and side structure will be analyzed for both the local strength of the stem or gunnel and also for the backup strength of the stiffened plate structure that is contiguous to the stem or gunnel.

First, the ability of the stem or gunnel to support a concentrated load without sustaining gross local deformations should be evaluated. The strength of the stem or gunnel, acting as a beam supported by the adjoining deck and/or side shell plating, should also be evaluated. Finally, the crushing strength of the backup structure under dynamic or static loading (whichever is applicable) should be determined.

Generally speaking, if the local stength of the gunnel is stronger than the stem, the stem will deform locally and shortly thereafter be cut by the main deck of the struck ship as described in failure mode 3 or 4 under Section 7.1. Which of these two modes of failure will actually take place is strongly dependent on the location of local stiffening in the stem, local reversed inertia forces, and other details not analyzed here. The importance of some of these factors can probably only be determined by dynamic structural tests.

If the local strength of the stem is stronger than the gunnel, then the dynamic strength of the struck ship deck should be checked to determine if it will buckle under the stem loading. If it is determined that the deck will buckle, then the static strength of the bow should be determined and compared with the force needed to cause final rupture of the struck ship's side. If it possesses sufficient strength, it will satisfy the rigid bow assumption.

If it is determined that the deck of the struck ship will not buckle when subjected to the maximum possible stem loading for local stem failure, then the beam strength of the stem (as supported by the backup bow structure) should be checked.

The sequence of failure events from this point on is difficult to hypothesize; however, if enough local deformations occur (timewise) the loadings quickly get out of the dynamic load regime and buckling strengths decrease. The overall buckling or crushing strength of the bow structure will then determine if the rigid bow assumption is valid.

7.4 Model Collision Tests

Model collision tests have been conducted primarily in Japan and Italy[3, 27, 28], and have included both dynamic and static loading conditions. For the dynamic loading conditions, the tests reported by Spinelli attempted to duplicate the hydrodynamic damping of struck ship motion, while the Japanese tests restrained lateral movement of the side model completely. With respect to the models themselves, the model of the struck ship, in each case, was of limited length and depth (in the direction of the strike) so that the boundary conditions on the side model are very unrealistic.

In view of the above limitations on the modeling, it is doubtful if any valid conclusions, with respect to dynamic behavior, can be drawn from the results of these tests; and the lack of inplane restraint on the side-shell plating of the struck-ship model, has probably allowed for greater incursions than would otherwise have been possible. Nevertheless, some valuable information can be derived from these tests concerning the structural behavior of various components of the bow and side structure.

Other limitations on the model tests conducted in Japan are the simplified bow structure and the limited number of encounter situations investigated. Most bow models had a plumb stem and encountered the side model at mid height. These tests did indicate, however, that a rather complete range of bow strength from soft to rigid can be achieved and be representative of standard construction.

The model tests did indicate that transversely or longitudinally framed, wedge-shaped structure will uniformly collapse at a static load reasonably close to the predicted one. However, bow decks and the forefoot structure do tend to deform in such a way that they will puncture the side shell plating. This puncturing action is very difficult to handle analytically.

The model test reported by Spinelli was the only one in which information on the stem-gunnel interaction could be obtained, and that information is questionable because of the lack of side-shell restraint. It did indicate, however, that both bow and side structure could absorb significant plastic deformation energy, and the only rupture appeared to be at the point where a buckled forefoot structure punctured the side shell.

7.5 Analytical Methods

The analytical methods presented herein are, for the most part, based on static analysis procedures for elastic structures. Some of the procedures, however, have an empirical basis, and others pertain to plastic analysis and to dynamic response of structure.

7.5.1 Estimation of Dynamic Load Regime

To determine the significance of dynamic effects on certain aspects of the structural behavior in the early stages of the collision process, estimates must be made of velocities, strain rates, force durations, natural frequencies, etc. For structures subjected to impulsive loading, dynamic amplification factors are important if the force duration is approximately the same as the natural period of vibration of the structure. For load applications of longer duration, the dynamic load factor is dependent, primarily, on the rate of build-up of the load.

For steels with strength properties that are strain-rate sensitive such as the structural carbon steels used in most ships, the fracture characteristics are also strain rate sensitive[29]; however, the strain rate at which these effects become apparent are quite high and probably only attainable at the tip of a rapidly opening crack.

Data presented by McGoldrick[30] indicates that the vibratory frequencies of ship decks fall in the range: 20 to 300 cycles per second. Thus, on the most flexible of these deck panels, a dynamic load would be one with a duration of approximately 1/20 of a second. Presumably, side shell natural frequencies would fall into approximately the same range. If a striking vessel's speed is assumed to be between 5 and 10 feet per second (3 to 6 knots), the incursion at the end of the 1/20 second would be about 3 to 6 inches. Since the speed of sound in steel is about 16,850 feet per second, the entire structure affected by the collision would "feel" the collision forces before the incursion had progressed much beyond the 3 to 6 inches mentioned above.

On the basis of the above reasoning, it is assumed that rolled gunnels and stems that are fabricated from plates that have been formed to a radius that is 10 to 20 times their thickness, will not exhibit a behavior that is strongly influenced by the dynamics of the collision. However, bar stems and square-intersection gunnel connections may be strongly influenced by collision dynamics particularly if the plating forming these hard points is in a plane parallel to motion of the striking ship.

7.5.2 Buckling Strength Amplification

The increased buckling strength of a panel of deck or side-shell plating lying in a plane parallel to the line of the collision force is the result of the inertia of the plate material as the struck edge is accelerated toward the inboard edge of the panel and the central portion is accelerated out of the plane of the plate. The factor by which the buckling strength is increased over the buckling strength of the static loading

is a function of the flatness of the plate and its "dynamic similarity number," Ω. Ω for columns may be defined in the following ways [3.1]:

$$\Omega = \pi^2 \varepsilon_E^3 \left(\frac{\dot{\varepsilon}}{\mu v^2}\right) \qquad (7\text{-}1.a)$$

$$= \pi^2 \varepsilon_E \left(\frac{\omega\rho}{v}\right)^2 \qquad (7\text{-}1.b)$$

$$= \pi^4 \left(\frac{\rho}{L}\right)^2 \left(\frac{\omega\rho}{v}\right)^2 \qquad (7\text{-}1.c)$$

of the symbols used, ε_E is the Euler strain $\left(\varepsilon_E = \pi^2 \frac{\rho^2}{L^2}\right)$, E is Young's Modulus, μ is the mass density of the material, v is the loading velocity, c is the speed of sound in the material, ρ is the radius of gyration, and ω is the natural frequency of the column in bending.

A comparable dynamic similarity number can be calculated for plates if it is assumed that for wide plates a unit-width strip of plating can be used to determine a $\frac{\rho}{L}$ value, or alternatively, ε_E may be calculated from the plate buckling stress. The fundamental frequency of the plate, ω, may be calculated from the equation

$$\omega = 6.09 \times 10^5 \, t \left(\frac{1}{a^2} + \frac{1}{b^2}\right) \qquad (7\text{-}2)$$

where t is the plate thickness, a is the length of the short side, and b is the length of the long side [30].

Using Equation (7-2) in conjunction with Equation (7-1.c), values of Ω were calculated for a 30-inch by 90-inch plate at thicknesses of 0.75-inch, 1.00-inch, and 1.50-inch and for collision velocities of 5 and 10 feet per second. These values are shown in Table 7-1.

Table 7-1

Ω Values for 30-Inch x 90-Inch Plate

Plate Thickness, inches	$\frac{L}{\rho}$	ω	Ω @ 5.0 fps	Ω @ 10.0 fps
0.75	133	565.5	0.020	0.005
1.00	99	754.0	0.112	0.028
1.50	66	1131.0	1.276	0.319

The buckling strength augmentation factor [31] for wide plates, $\frac{P}{P_E}$, which is the ratio of the dynamic buckling load to the static Euler load, for various plate eccentricities, e, where e is the ratio of initial deflection of the plate to the plate thickness (See Figure 7-1).

The relationship between Ω and the augmentation factor, $\frac{P}{P_E}$, as a function of e, is not straightforward; and the information presented in Figure 7-1 was developed through the use of trial and error approximate calculation procedures. Unfortunately the plot does not cover the entire parameter range of interest.

Nevertheless, it is obvious from an examination of Figure 7-1 in conjunction with Table 7-1 that high values of the augmentation factor will apply to moderate collision circumstances.

7.5.3 Local Strength of Stem and Gunnel

The analysis of the local strength of the stem or gunnel is difficult for several reasons. Because the local strength is pertinent to the initial phase of the collision process, it is highly dependent on dynamic effects, such as local reversed inertia forces, dynamic buckling, cutting

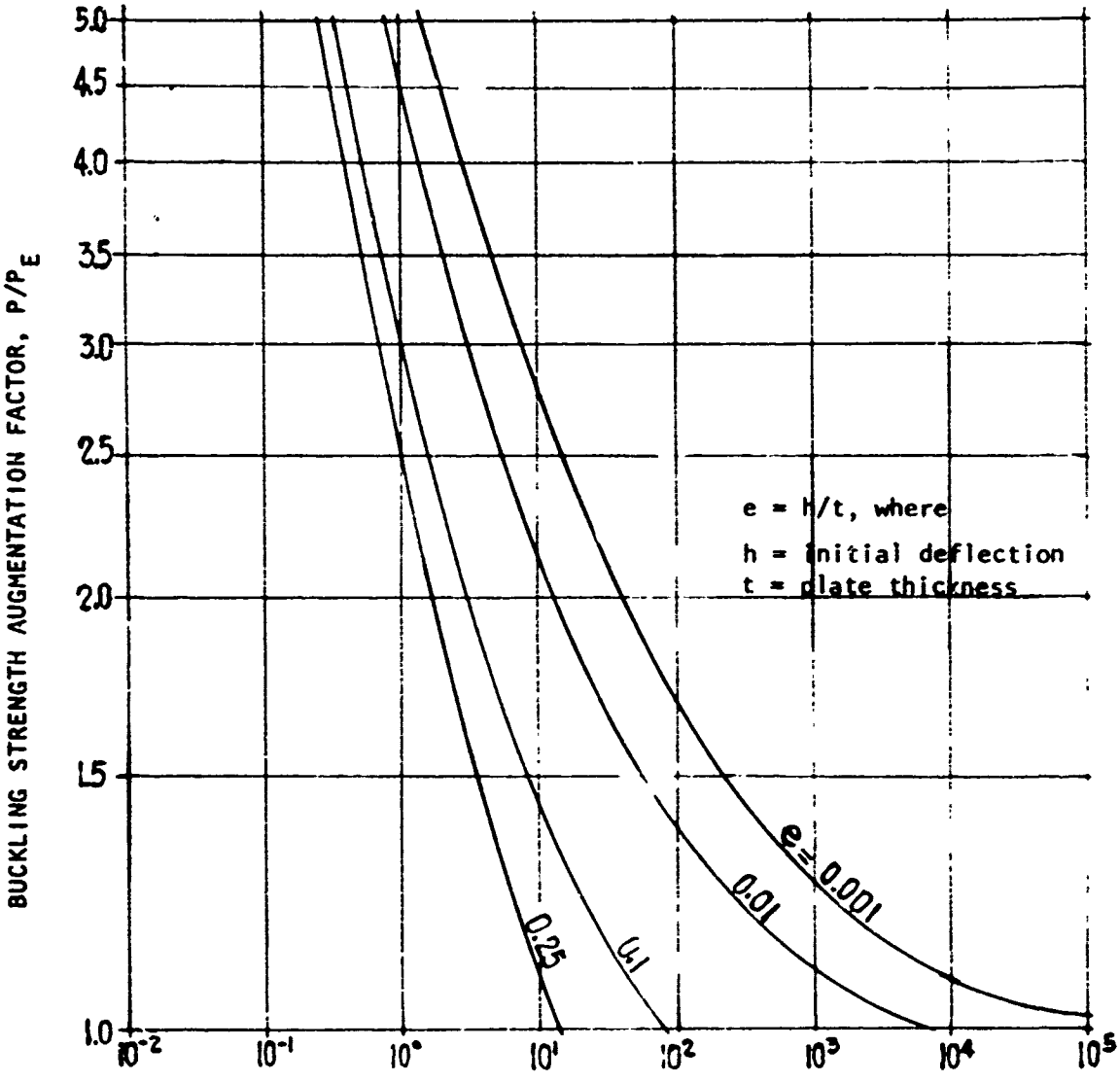

FIGURE 7-1 Buckling Strength Augmentation - Dynamic Load

and tearing, etc. In addition, there are various configurations of stem and gunnel construction in use, few of which really lend themselves to structural analysis. Also, the loads tend to be highly localized and difficult to define.

Although the details of stem and gunnel configuration can be quite varied, most tend to be either cylindrical in cross section or made up of interesecting flat plates. See Figure 7-2(a). For the ones that are cylindrical in cross section, it will be assumed that because the portion of the stem or gunnel first contacted lies in a plane normal to the direction of motion, the reversed inertia forces will be relatively small. Thus, an elastic stress analysis based on static loading will be used to obtain a relative measure of the local strength of cylindrical or rolled stems and gunnels.

For bar stems and gunnels — those made up of intersecting deck- and side-plating or bow-side plating reinforced with structurals or flat bars — it is proposed that a more simplified evaluation procedure be adopted. It is suggested that the strength of this type of stem or gunnel connection is a function of the sharpness and mass or density of the loading edge and the rigidity of the back-up structure. The comparable strength of a rolled stem versus a bar gunnel or vice versa is not possible with the tools presently available.

The local strength of rolled stems and gunnels will be based on an empirical equation[32] that may be used to predict the magnitude of the concentrated radial load, P_y, that will cause yielding in a cylindrical member of radius, R, when the contact area has a radius, r. This equation can be expressed as follows:

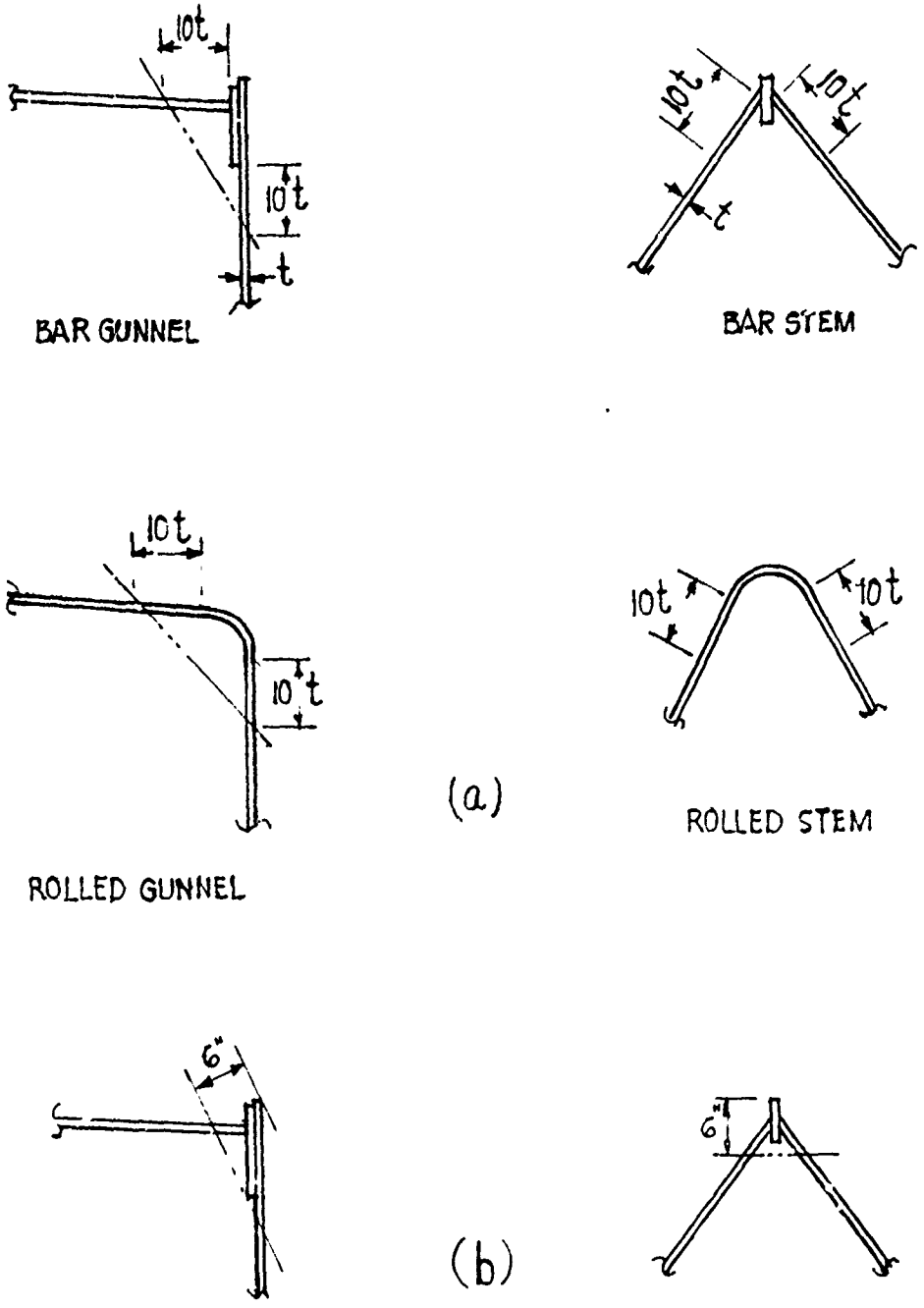

FIGURE 7-2 Beam and Local Strength of Stem and Gunnel

$$P_y = K \sigma_y t^2$$

Where $K = \dfrac{1}{0.42 \text{ Ln } 0.215 \dfrac{R}{r} + \dfrac{6}{4\pi}}$

σ_y = yield stress of material, and

t = thickness of cylindrical member.

For values of $\frac{R}{r}$ ranging from 5 to 100, the value of K varies from about 2.0 to 0.566.

For bar stems and gunnels, it is suggested that the relative strength be judged on the basis of the cross-sectional area of steel within the first 6 inches of incursion as indicated in Figure 7-2(b). This evaluation is intended to reflect the strength of density of the local edge construction. The sharpness can best be judged by visual comparison or possibly by the concentration of steel cross-sectional area near the loading edge.

It is suggested that the relative strength of bar versus rolled gunnel or stem can best be evaluated through a series of dynamic structural tests.

7.5.4 Beam Strength of Stem and Gunnel

It is the beam strength of stem or gunnel that tends to soften and distribute the localized loading at first contact from the point of contact into the backup structure. The strength of the stem or gunnel can only be evaluated if it is separated from the rest of the ship and the beam strength and stiffness properties calculated.

The limits of the stem or gunnel are not distinct and it is necessary to assume an effective width of deck or side plating to be acting as part of the stem structure. For this purpose, it is suggested that for

rolled stems and gunnels, the edge structure be assumed to consist of the cylindrical portion plus a width of plating equal to ten times the plate thickness. For bar stems and gunnels, it is suggested that the edge structure be assumed to consist of the reinforcement structure plus ten thicknesses of plating beyond the boundaries of the reinforcement structure, as drawn in Figure 7-2(a). This figure indicates the portion of the structure to be treated as a beam. The strength and stiffness properties should be calculated with respect to the direction of application of the collision force. When both the moment of inertia and the section modulus of the stem or gunnel have been calculated, they may be used in evaluating the beam strength of the stem or gunnel by application of the theory of beams on elastic foundations [33].

The first step in evaluating the strength of a beam on an elastic foundation is to estimate the foundation modulus, k_f. The foundation modulus is a measure of the force required to deform the foundation per unit length of beam. For stem and gunnel structure, the elastic foundation supporting the beam will be linearly elastic only as long as the backup plating does not buckle, and its foundation modulus, k_f, will be

$$k_f = \frac{Et}{L_{eq}} \cos \alpha \qquad (7\text{-}4)$$

for each stiffened plate field supporting the edge structure, where E is Young's Modulus, t is the plating thickness, L_{eq} is an equivalent length of plating compressed by the collision force, and α is the angle between the collision force and the plane of the plate.

It is suggested that for rolled stems and gunnels, the modulus be calculated for static loading conditions and for bar stems and gunnels that it be augmented by the "buckling augmentation factor" to reflect the effective increase in stiffness of the plate material.

Once the foundation modulus has been estimated, the bending moment in the stem or gunnel may be estimated by the equation,

$$M = \frac{P}{4\bar{\lambda}} \qquad (7\text{-}5)$$

where $\bar{\lambda} = \sqrt[4]{\frac{k_f}{4EI}}$ and

I = the moment of inertial of the beam structure.

The local buckling strength of the backup plating may be estimated by assuming a distributed length of compressive load equal to $\frac{1}{\bar{\lambda}}$. This is an estimation based on the length of foundation loaded in compression by the deflected beam [33].

The buckling strength of plates subjected to localized edge loading [34] and the buckling load as a fraction of the Euler load varies from about 35 to 75 percent, depending on the fraction of edge length subjected to the load, the boundary conditions on the plate, and the plate aspect ratio. Again the local buckling strength of backup plating should be augmented for dynamic loading in accordance with the existing edge configuration.

7.5.5 Effective Plating

In the secondary phase of the collision process, when quasi-static structural performance predominates, the failure mode will consist primarily of uniform crushing of longitudinally or transversely framed bow structure in accordance with the relative bow and side-shell strength and the portion of the bow structure that is being affected by the collision force. Generally speaking, the cross-sectional area of plating is high compared to that of the supporting beams and girders -- particularly for trans-

versely framed structure. Thus, it is suggested that the crushing strength of bow structure be evaluated on the basis of the total cross-sectional area of structure at the longitudinal location in question, along with the plating effectiveness as discussed below.

In estimating the compressive strength of stiffened plating, it is necessary to take into account the reduced load-carrying capacity of those portions of the plate that have either buckled or distorted out of their original plane due to fabrication distortions or normal pressure loadings. For longitudinally stiffened plates, the effects of plating unfairness and lateral load are not as important as in transversely stiffened plating.

It is proposed that for longitudinally stiffened plates the effective width ratio, $\frac{b_e}{b}$, be calculated by an equation of the form

$$\frac{b_e}{b} = \frac{1.90}{B} - \frac{0.90}{B} \qquad (7\text{-}6)$$

where $B = \frac{b}{t}\sqrt{\frac{\sigma_y}{E}}$

This equation has been plotted on Figure 7-3 along with similar information on transversely stiffened plates. As noted before, the effective width of longitudinally stiffened plates has been assumed to be independent of initial curvature of the plating between stiffeners. The crushing load is calculated by the equation

$$P_c = \frac{b_e}{b} A_s \sigma_y \qquad (7\text{-}7)$$

where P_c is the crushing load, A_s is the cross-sectional area of the stem, and $\frac{b_e}{b}$ is the applicable effective width ratio.

For transversely stiffened plates, the post buckling strength has been derived by Schade [35] with both plating unfairness and boundary

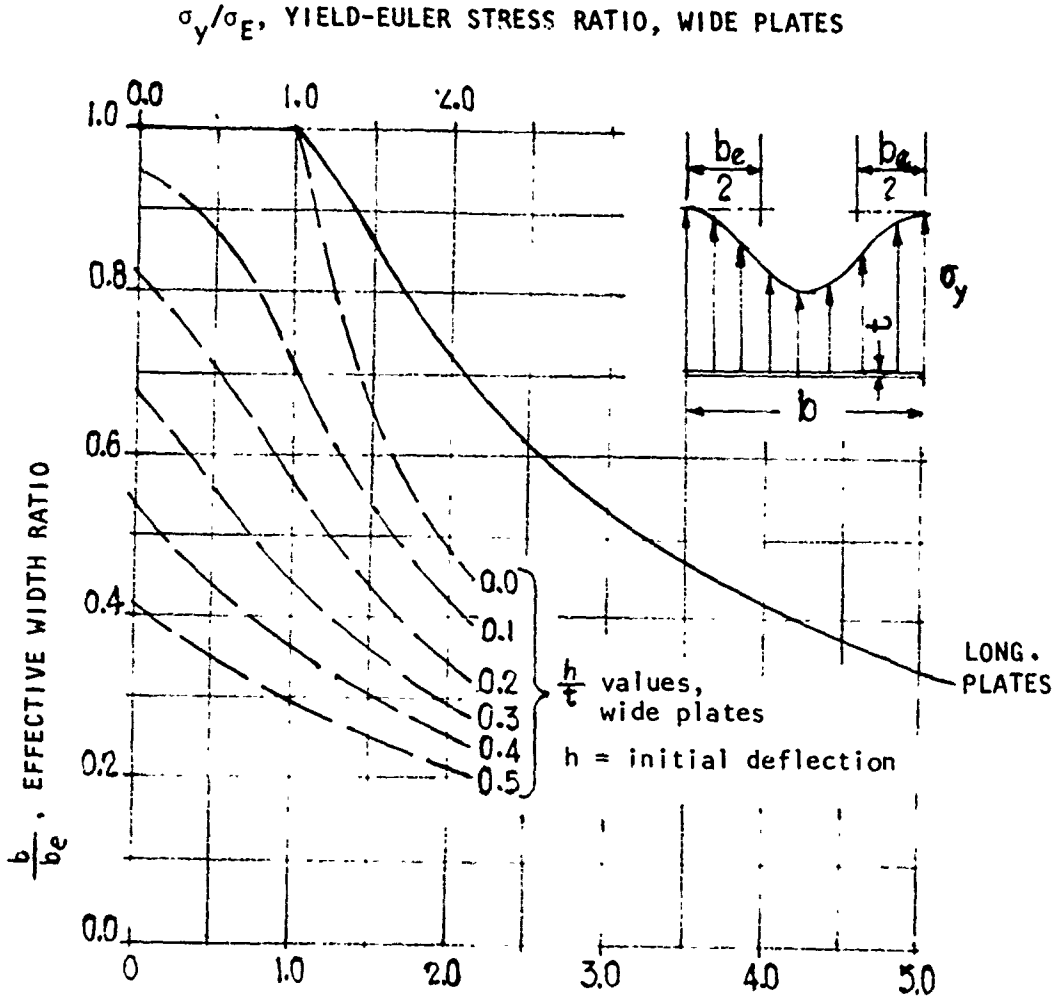

B, NON-DIMENSIONAL BUCKLING PARAMETER, LONG. PLATES

$$B = \frac{b}{t}\sqrt{\sigma_y/E}$$

FIGURE 7-3 Effective Width of Stiffened Plates

fixity being taken into account. The information derived by Schade is also presented on Figure 7-3 (for simply supported plating) in terms of the effective width ratio, $\frac{b_e}{b}$, the ratio of material yield stress to the Euler buckling stress, $\frac{\sigma_y}{\sigma_E}$, for the wide plate in question, and the ratio of initial unfairness (assumed to be of sine wave form), $e = \frac{h}{t}$, where h is the maximum amplitude of unfairness.

For raked bows, where there may be some question of where the collapse strength should be calculated, it should be noted that the resistance force of the side structure will generally increased at a faster rate than the incursion. thus, if the bow is stronger than the side structure at maximum incursion, it will be stronger for the entire incursion and may be assumed to constitute a rigid bow.

7.5.6 Tearing Energy

Unfortunately, there is relatively little information available on tearing energy of steel plates that is directly applicable to the collision situation in question. Information on the mechanical shearing of steel plates indicates that energies in the range of 1000 ft.lbs./in.^{2} are involved. For dynamic loads comparable to those experience in the Charpy V-Notch test, the upper shelf energies indicate tearing energies in the order of 200 to 800 ft.lbs./in.^{2}, depending on the notch toughness of the steel.

Complicating the problem still further is the uncertainty associated with the load magnitude, rate of application, and degree of load concentration needed to initiate a tear. A review of collision photographs and the collisions that were inspected, strongly suggests that minor collisions do not involve plate tearing or shearing in the early stages of the

collision process, while for more severe collisions, either the bow is sliced at each deck level encountered in the struck ship, or the gunnel, deck, and side plating of the struck ship are cut and/or torn.

Fracture tests on steels indicate that for steels with strain-rate-sensitive strength properties, the tearing energies decrease at high strain rates [29]. Yet there is little data available on the magnitude of this decrease that can be directly applied to this problem. It is suggested that a large amount of valuable information could be obtained from a few well controlled structural tests of this phenomenon.

7.6 Conclusions and Recommendations

Because of the nature of the nonrigid-bow investigation, some of the conclusions and recommendations pertain to the analysis procedures, themselves, as well as to the results of their application. A great deal of developmental and analytical work remains to be done in this area, and the recommendations in the following list are intended to enumerate them.

(1) Two important dynamic loading effects related to nonrigid-bow structural behavior are the increased buckling strength of deck structure and bow-side-shell plating as collision velocity is increased and the decrease in the energy absorbed in shearing and tearing of stem or gunnel structure with increased strain rates.

(2) The dynamic effects related to structural behavior in moderate collisions are generally confined to the very early stages of the collision process, probably within the first foot of incursion.

(3) The rounded portion of a stem or of a rolled gunnel is beneficial in preventing the backup plating from being dynamically strengthened and forming a cutting edge that would result in puncturing of either ship in the initial stages of the collision.

(4) Because of its resistance to the cutting action of the main deck, a strong stem structure may be more desirable than a weak one with regard to the maximum absorption of collision energy before side-shell rupture.

(5) Sharp, square gunnel connections should be accompanied by a heavy, strong sheer strake to guard against the puncturing action of a cut stem and, in addition, to soften the cutting action of the main deck.

(6) Experimental work should be conducted to obtain data on the resistance of various stem configurations to the cutting action of the struck ship gunnel, and on the resistance of the sheer strake to the subsequent puncturing by the cut stem.

(7) Similar experimental work should be conducted on gunnel configurations with regard to their resistance to the cutting action of a sharp bar stem.

8. CONCLUSIONS

8.1 Results

This report has presented an evaluation of tanker minor collisions in an effort to develop an analytical proced e to evaluate the structure of a tanker from the viewpoint of the actual pro.ection it affords the cargo during the collision. The degree of protection is determined by the amount of energy absorbed during the collision, since this can be converted to striking ship mass and velocity. In addition to structural considerations, the energy absorption due to rigid body motions of the colliding ships was investigated. The analyses indicated that this energy could be significant although only a fraction of the plastic structural energy absorption, but further investigation was curtailed because this phenomenon should not have any effect on the structural energy absorption.

The evaluation of the structural energy-absorbing capabilities of tankers was divided into elastic energy and plastic energy and the results have shown the elastic energy absorption is relatively insignificant when compared to the plastic energy absorption.

The principal results of the study are then twofold. Firstly, the mechanics of minor collisions and their importance with respect to energy absorption have been identified and investigated. This results in giving the shipbuilding industry a better understanding of the minor collision phenomena. Secondly, an analytical procedure and its numerical applications for estimating the plastic energy absorbed by longitudinally frames ships, particularly tankers, during a minor collision has been developed for the first time. With additional effort it may be possible to develop this procedure for use in ranking the ability of the structure of longitudinally framed tankers to withstand side collisions without shell rupture, and

Preceding page blank

thereby assist in increasing the safety of these ships. The procedure is sufficiently general that with judicious modifications it can be made suitable for the analysis of other ship types. This procedure is not intended to be used as a design procedure but may be of value for the comparison of various candidates.

Although assumptions and limitations are noted throughout the report, it is of value to note a few of the more significant here. First, the plastic analysis procedure employs a static analysis, which is an obvious simplification of the dynamic phenomena of collision; second, although means of analyzing striking ships with non-rigid bows were explored, the procedure still assumes rigid bows; third, the possibility of dynamic tearing or puncturing of the shell prior to rupture is neglected.

The numerical calculations show that in the idealized collision considered, typically between 2/3 and 9/10 of the plastic energy absorbed could potentially be that of membrane tension in the stiffened hull. The other areas of significant energy absorption potential are membrane tension in the stiffened decks and in-plane shearing of the web frames. Therefore, an efficient minor collision-resistant design is one which insures that the membrane energy reasonably available in the steel structure is utilized in a collision situation. This inherently indicates that web frames should be weak, and the most efficient way to increase the ability to absorb collision energy (provided the web frames are weak) is to increase the thickness of shell plating. Of course, developing a structural design from a collision standpoint may be difficult when considering other design requirements.

The numerical solutions employing the plastic analysis procedure presented in the report indicate that when the web frames of a double shell hull distort due to bending, so that both hulls deform in membrane tension in unison, the energy absorbed is approximately equal to that absorbed by a single shell hull of thickness equal to the combined thicknesses of the double shells. If the web frames deform by crippling, with the result that the outer shell deflects while the inner does not (unless the outer actually touches the inner), the energy absorption may be less for the double shell hull when compared to the single shell. In the case of punching or tearing action, where little energy absorption is involved, the double shell is superior to the single shell since the inner shell may remain intact and prevent leakage of the cargo after rupture of the outer shell.

The plastic energy absorbed in the struck ship by the mechanisms just described was found to be greatly dependent on the location of the strike with respect to the locations of webs and bulkheads. This implies that the assessment of the cargo containment protection afforded by a particular ship should be made after collisions with strikes at different points along the length of cargo spaces are evaluated.

It has also been shown that the shape of the bow of the striking ship has a significant influence on the energy absorbed. The greater the vertical extent of side shell which can be engaged, the greater the plastic energy absorbed.

The material properties of the steel also play a significant role. Since the most important mode of energy absorption is in the plastic deformation, the steel must be ductile. Also, the effect of ambient temperature on rupture is significant since no plastic energy can be absorbed where the temperature is below the transition temperature.

With respect to non-rigid bow structural behavior, the most important effect arises from dynamic loading and is the increased buckling strength of deck structure in both the struck and striking ships and the striking ship bow side shell plating. These areas may then act as hard points that can "knife" through other structure. This phenomenon has been observed in actual collision inspections with respect to horizontal structure of the struck ship cutting the striking bow.

8.2 Recommendations

It has been shown that the procedure for the evaluation of tanker structure in collision presented in this report will serve as a step to assist in increasing the safety of ships. It is recommended that the project be continued to refine the procedure with the tasks described below. In addition it is urged that all organizations involved and interested in preventing spillage of liquid cargo in ship collisions make an effort to gather collision data with as much detail as possible to aid in the development of studies such as presented herein.

1. Perform detailed investigations of the different dynamic aspects of collision. Further, develop methods of analysis which can be incorporated into the principal procedure as it now exists for those aspects which could influence ranking of ships with respect to their ability to withstand collisions.

2. Perform dynamic tests of component structures for those dynamic aspects which do not lend themselves to analytical investigations.

3. Develop a more accurate analytical model of the struck ship decks and extend the existing procedure to include damage to bilge area and bulkheads.

4. Perform component tests with high-strength steels and multiple web frames.

5. Continue to inspect actual collisions. Collision inspections have been the only means of comparing theoretical predictions to full-scale occurrences and in this light have been invaluable. Observations made during inspections have led to significant changes to or confirmation of the analyses throughout the course of the project.

6. Investigate the feasibility of full-scale or large-model tests.

7. Consider the oblique collision in greater detail since most collisions are of this type. Specifically investigate membrane tensions ahead of the strike, and strikes at webs and bulkheads.

8. Investigate the role and failure mechanisms of web frames and bulkheads in more detail.

9. Consider the case of the striking bow immediately cutting or punch-shearing the shell of the struck ship. If possible suggest methods for limiting this occurrence.

APPENDIX A

BIBLIOGRAPHY

Preceding page blank

BIBLIOGRAPHY

1. Minorsky, V.U., "An Analysis of Ship Collisions with Reference to Protection of Nuclear Power Plants," Journal of Ship Research, Volume 3, No. 2, October 1959.

2. Gibbs & Cox, Inc., "Criteria for Guidance in the Design of Nuclear Powered Merchant Ships."

3. Spinelli, F., "Protection of Nuclear Reactors in Ships Against Collision," Schiff und Hafen (Ship and Port), 16(2): 148-154, 1964.

4. Spinelli, Franco, "Considerations of Anticollision Protection for Nuclear-Powered Vessels," Review of Engineering and Sciences, No. 8, Trieste, November 1961.

5. Spinelli, Franco, "Outline of Nuclear Marine Engineering Specialization Course in University of Naples," Tecnica Italiana (Italian Technology), No. 8, October 1961.

6. "Provisional Guide for the Classification of Nuclear Ships," Nippon Kaiji Kyokai, 1964.

7. Spinelli, Franco, "The Safety of the Nuclear Reactor on Merchant Ships," Tecnica Italiana, pp 797-812 1963, Technica Naval

8. Guida, Aurelio, "Analysis of the Similarity of Comparability of Results from Collision Experiments," Tecnica Italiana (Italian Technology), Trieste, 1964.

9. Haywood, J.H., "A Theoretical Note on Ship Collisions," NCRE Report #R445, February 1961.

10. Kline, R.G., and Clough, R.W., "The Dynamic Response of Ships' Hull as Influenced by Proportions, Arrangement, Loading and Structural Stiffness," Presented at the Spring Meeting SNAME, July 1967.

11. Lay, M.G., and Galambos, T.V., "Inelastic Beams Under Moment Gradient," Paper No. 5110, Journal of the Structural Division, Proceedings ASCE, February 1967.

12. McDermott, J.F., "Plastic Bending of A514 Steel Beams," Paper No. 6762, Journal of the Structural Division, Proceedings ASCE, September 1969.

13. "Specification for the Design, Fabrication, and Erection of Structural Steel for Buildings," American Institute of Steel Construction, February 12, 1969.

Preceding page blank

14. Lukey, A.F., and Adams, P.E., "Rotation Capacity of Beams Under Moment Gradient," Paper No. 6599, Journal of the Structural Division, Proceedings ASCE, June 1969.

15. Column Research Council, Guide to Design Criteria for Metal Compression Members. Second Edition, edited by B.J. Johnston, John Wiley and Sons, inc., New York, 1967.

16. Flynn, F.E., and MacArthur, D.A., "Shearing Flat-Rolled Steel," Iron and Steel Engineer, December 1944. (Later reference giving the same information: Metals Handbook, 8th edition, American Society for Metals, 1969).

17. U.S. Department of Transportation - U.S.C.G., "Tanker Structural Analysis Procedure Primer," prepared by M. Rosenblatt & Son, Inc. and U.S. Steel Corp., MR&S Report No. 2087-19, December, 1975.

18. H. Yajima, M. Nakajima, T. Okabe, and R. Nagamoto, "Study of Welded-Type Crack Arrestor -- First Report," Technical Review, Volume 8, No. 2, Ser. No. 21, June 1971, Mitsubishi Heavy Industries, Ltd.

19. Specification for the Design of Cold-Formed Steel Structural Members, 1968 edition, American Iron and Steel Institute, Section 2.3.1.1.

20. Timoshenko, S.P., and Gere, J.M., Theory of Elastic Stability, McGraw-Hill, New York, 1961, Equations (9-22), p. 402.

21. Shade, H.A., "The Effective Breadth Concept in Ship-Structure Design," Trans. SNAME, Vol. 61, 1953, pp. 410-430.

22. Shade, H.A., "The Effective Breadth of Stiffened Plating Under Bending Loads," Trans. SNAME, Vol. 59, 1951, pp. 403-420, 429, and 430.

23. U.S. Department of Transportation - U.S.C.G., "Tanker Structural Analysis for Minor Collisions - Collision Inspection Reports," prepared by M. Rosenblatt & Son, Inc. and U.S. Steel Corp., MR&S Report No. 2087-20, December 1975.

24. McDermott, J.F., "Tests to Verify the Plastic Behavior of Stiffened Hulls of Struck Tank Ships," Report 46.019-200(1), U.S. Steel Applied Research Laboratory, June 13, 1973.

25. Dhalla, A.K., and Winter, G., "Steel Ductility Measurements," Paper No. 10365, Journal of the Structural Division, Proceedings ASCE, February 1974.

26. Dhalla, A.K., and Winter, G., "Suggested Steel Ductility Requirements," Paper No. 10366, Journal of the Structural Division, Proceedings ASCE, February 1974.

27. Y. Akita, K. Kitamura, "A Study on Collision by an Elastic Stem to a Side Structure of Ships," Journal of the Society of Naval Architects of Japan, Vol. 131, June 1972.

28. "Research Concerning Atomic-Powered Ship Hull Construction," Japan Atomic-Powered Ship Research Association, Development Section, Hull Branch, June 1963.

29. A.S. Tetelman, A.J. McEvily, Jr., "Fracture of Structural Materials," John Wiley & Sons, Inc., 1967.

30. R.T. McGoldrick, "Ship Vibration," David Taylor Model Basin Report 1451, December 1960.

31. N.J. Hoff, S.V. Nardo, B. Ericson, The Maximum Load Supported by an Elastic Column in a Rapid Compression Test. Proceedings of the First U.S. National Congress of Applied Mechanics Published by American Society of Mechanical Engineers, New York 1952.

32. R.J. Roark, "Formulas for Stress and Strain," McGraw-Hill Book Company, Inc., 1954.

33. M. Hetenyi, "Beams on an Elastic Foundation," The University of Michigan Press, Ann Arbor, Michigan, 1946.

34. M.Z. Khan, A.C. Walker, Buckling of Plates Subjected to Localized Edge Loading, The Structural Engineer, Vol. 50, No. 6, 1972.

35. A.M. D'Arcangelo, "Ship Design and Construction," SNAME, 1969, Chapter 3.

APPENDIX B
ELASTIC ENERGY ANALYSIS

Preceding page blank

B-1. BACKGROUND

Most past analyses of the energy absorbed in ship collisions have been conducted for the purpose of studying the protection of nuclear reactors on nuclear-powered ships[1,3-7]*. These past anslyses have considered a full range of collision severity; however, the data upon which these analyses have been based were, for the most part, derived from moderate to severe collisio situations. The reason for this is that the more severe collisions have been of greater interest and importance than the minor collisions and have been more carefully documented.

In a tanker collision analysis designed to determine the amount of collision energy that can be absorbed prior to the rupture of cargo oil tanks, it is necessary to concentrate on relatively minor collisions in which the amount of plastic deformation of local structure does not exceed the capacity of the structure to stretch or deform without rupture. If this plastic deformation is not greater than a couple of feet in the direction of penetration, then it would appear to be possible for the elastic deformations to be significant by comparison.

In many past analyses of moderate to severe ship collisions, elastic energy absorption has been ignored or has been assumed to be negligible[1]. This was justified intuitively on the basis that the relative magnitude of elastic and plastic energy absorption is directly related to the relative magnitude of elastic and plastic deformations. In a severe collision, the plastic deformations are obviously much greater than any elastic deformations that the struck ship could sustain.

*Numbers in brackets designate references in the Bibliography, Appendix A

Preceding page blank

Guida and Haywood[8,9] do investigate the importance of elastic energy absorption in ship collisions; and Haywood, in his NCRE report, concluded that for a significant portion of the collision energy to be absorbed elastically as potential or kinetic energy of overall ship vibration, the collision duration should be as short as, or shorter than, the fundamental period of horizontal ship vibration. The generation of a large collision force lasting only a short period of time requires that the strength and stiffness of the struck ship's side structure be extremely large. The analysis that was used to formulate these conclusions treated the struck ship as an elastic uniform beam subjected to two simple types of collision impulse and did not include a treatment of local structural behavior in the vicinity of the impact.

Studies of the dynamic response of ship structures to slamming type impacts[10] indicated that the response of local structure at the impact location can strongly influence the elastic response of the overall structure by modifying the magnitude and time-history of the applied forces as they are transmitted through the local structure to the overall structure. Because the present collision analysis involved the study of various local structure configurations in the vicinity of the collision damage, the importance of modeling local structural strength was identified as an important consideration in this study.

The slam analysis computer program[10] was available to the investigators. It offered the additional advantages over the NCRE investigation of being able to specify more complex force-time histories of impact, and the advantage of obtaining both local and overall displacement, velocity, and bending moment histories throughout the duration of the collision.

B-2. METHOD OF ANALYSIS

B-2.1 Computer Program

The computer program that was used in the study of elastic energy absorption was originally developed to calculate the local and overall dynamic response of ships of the dry-cargo type to impacts on the flexible bottom structure. The program utilizes a lumped mass idealization of the structure in which flexible-bottom-structure degrees of freedom are considered in addition to main hull girder motions. The dynamic response is obtained by a mode superposition method in which the response of each mode is obtained through the use of a step-by-step integration procedure. The degrees of freedom are confined to the vertical centerline plane of the ship, and the double elastic axis hull idelaization is supported on a series of buoyancy springs as shown in Figure B-1.

As indicated in Figure B-1, two types of couplings are assumed between the main hull and double bottom girders: (1) bulkheads provide rigid connections which require the two girders to displace equally at these locations, and (2) the transverse stiffness of the bottom structure permits relative movement of the two girders, but provides an elastic restraint between them.

In applying the slam analysis program to the tanker collision problem, it was necessary to use an idealization intended to represent vertically symmetrical structure to solve for the response of a structure that was unsymmetrical in the direction of vibration. For this analysis to be valid, the predominant mode of vibratory response of the struck ship must be the horizontal flexural vibration of the main hull. The assumption that the torsional response is negligible was primarily one of convenience

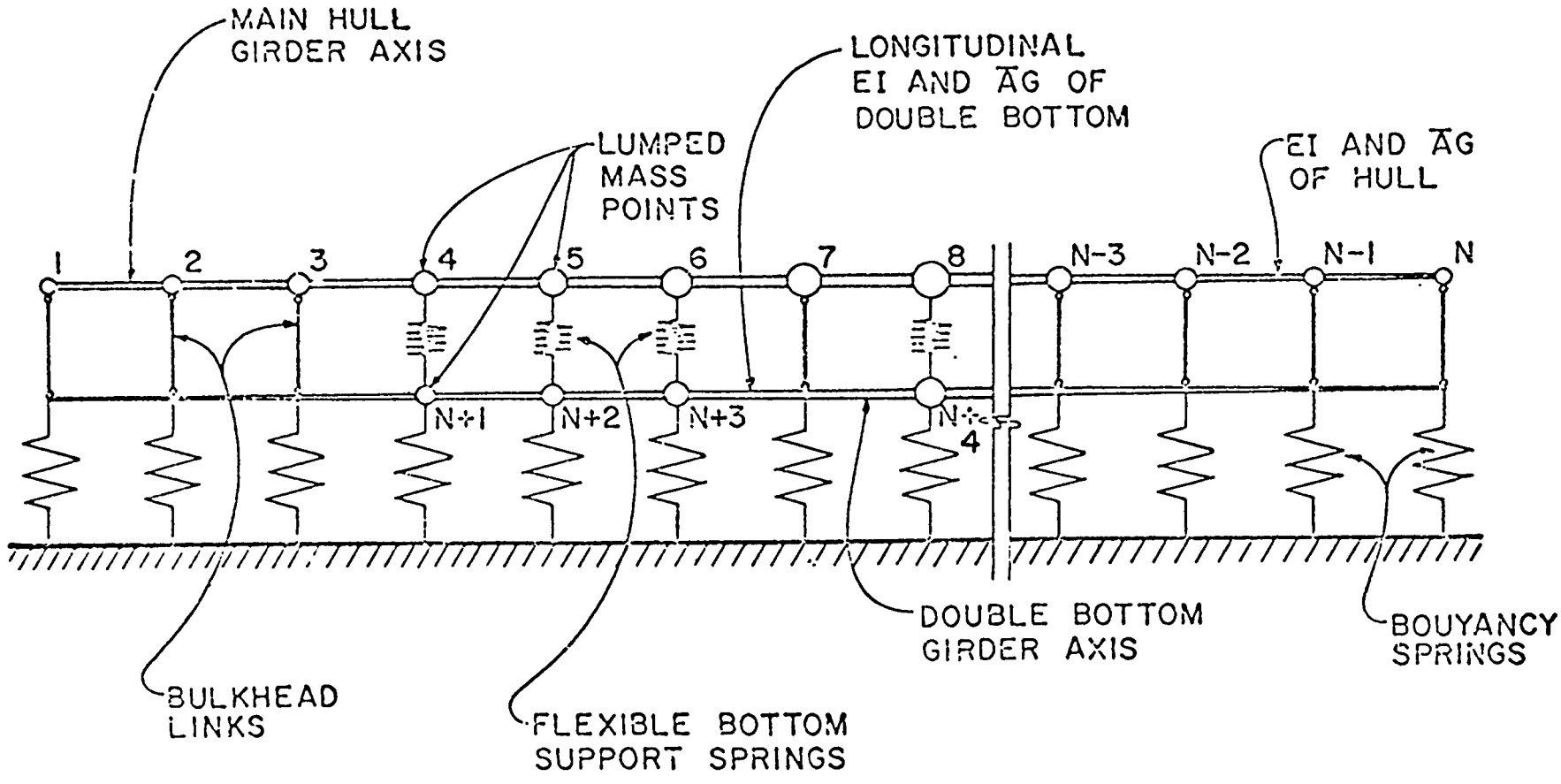

FIGURE B-1 SHIP IDEALIZATION USED IN SLAM ANALYSIS PROGRAM

and can only be justified if the direction of the resultant collision force passes close to the shear center, center of twist, and center of gravity of the tanker, and if the coupling between horizontal and torsional vibration is small. These qualifications could be partially satisfied if the striking ship's bow were properly raked and if the tanker cross-section were close to being doubly symmetrical with regard to section properties. The tanker hull certainly comes much closer to meeting these qualifications than does a dry-cargo ship. In addition, the single or double side shell construction was assumed to behave in a manner similar to double bottom structure, and appropriate values of added mass for cargo and sea water for horizontal motion had to be assumed.

In addition to the above simplifying assumptions with regard to the structural idealization, the transformation from vertical response to horizontal response required a different interpretation for the springs used to represent buoyancy forces. It was decided that by suitable manipulations a spring constant could be chosen so that the springs previously used to represent buoyancy could represent the hydrodynamic resistance of the ship to transverse motion. This choice was accomplished by arbitrarily assigning a spring constant to the buoyancy springs (resistance springs for transverse motion) and determining the resulting velocity- and displacement-time histories of the struck ship's center of gravity in transverse motion. Using incremental values of velocity from the velocity-time history, a series of resistance-to-lateral-motion calculations were made for various displaced positions of the ship. A simple drag-coefficient approach was employed. From these calculations, a plot of ship-resistance versus lateral-movement was made and then linearized to obtain an approximate spring constant. This new spring constant was then substituted for the arbitrarily chosen one, and a new collision calculation was performed. From the new calculation, a corrected velocity-time history and displacement-time were obtained for the struck ship's center of gravity.

In the above-mentioned calculations, the corrected "resistance spring" was about twice the value of the arbitrarily chosen spring constant; however, the new velocity- and displacement-time histories were approximately the same as the original. Thus, it was concluded that the major resistance to transverse motion was the struck ship's inertia and that the energy lost to hydrodynamic resistance could be ignored in most cases. Nevertheless, an approximation to this resistance, and hence to the energy absorbed by it, is contained in the revised slam-analysis computer program.

In addition to the alterations in the ship idealization, a modification was made to the computer program to provide for calculating the work done by the collision force on the struck ship during the time of its application. This included not only the work done in moving the ship laterally through the water but also in elastically deforming the local and overall structure. The work was calculated for each mode of dynamic response and provisions were made so that it could be summed over any specified number of response modes. This provision was necessary so that work of elastic deformation could be separated from the work done in overcoming inertia and hydrodynamic resistance.

As mentioned previously, a mode-superposition method was used in solving for the dynamic response of the struck ship. In this mode-superposition method, the first two modes of response are rigid-body modes representing a rigid body translation and rotation of the entire ship, and the remaining modes represent the various modes of flexural response of the ship structure. Thus, if the work done by the collision force was summed over the first two modes of response, that work would be representative of the work expended in overcoming the struck ship's inertia or in transferring some initial kinetic energy of the striking ship into final kinetic energy

of the struck ship. If the work was summed over the first 25 modes of response, it would include the energy absorbed by the elastic deformations of the struck ship. This assumes that energy absorbed by the modes higher than the 25th are negligible and this fact was verified by trial calculations. The difference of these two summations gives the energy absorbed by elastic deformations of the ship. It is important to keep in mind that this method of analysis assumes elastic behavior of the entire ship and includes both local and overall deformations.

The elastic response of a struck ship is a direct function of the impulse or force-time history that it experiences. The force-time history, in turn, results from the relative movement between the two ships that takes place once the collision process has commenced (following initial contact). This relative movement or penetration depends on the initial momentum of both ships as well as on the structural resistance to penetration and the inertia forces generated in the immediately affected structure of the struck ship. Thus, in deriving suitable force-time histories or collision impulses to be used in the present study, it was assumed that the total impulse could be separated into structural resistance forces and local inertia forces. The structural resistance forces were derived from the plastic energy absorption calculations and the local inertia forces were estimated by trial and error solutions of the dynamic response of the local structure. The relationships between these various factors can best be studied by applying the principles of conservation of energy and momentum to a simplified collision process.

B-2.2 Collision Dynamics

The term "simple ship collision" as used in the following development refers to a collision situation in which the struck ship is originally stationary in the water and is hit at its coinciding centers of gravity and lateral resistance at an angle of 90 degrees to its longitudinal centerline. The striking ship is rigid and unpowered at the instant of collision; and the resulting collision force drops to zero at the time of maximum penetration, after which the two ships continue their motion as a single mass. The situation is described graphically in Figure B-2.

In addition to the assumptions regarding the "simple ship collision," it is also assumed that the effective mass of both ships remains constant during the collision, i.e., the added mass of entrained water is assumed constant. An effective total mass for the struck ship was chosen that corresponded to an added mass coefficient of 0.65. The added mass for the striking ship was ignored.

With the previously mentioned assumptions and ignoring the effects of ship resistance, the final common velocity of the two ships can be expressed as follows:

$$v_f = v_i \frac{m_1}{M} \qquad \text{(B-1)}$$

From this expression and the fact that $v_2 = 0$, the initial, the final, and the absorbed kinetic energies can be written in terms of the ship masses and the initial velocity of the striking ship:

$$KE_i = \frac{m_1}{2} v_i^2 \qquad \text{(B-2)}$$

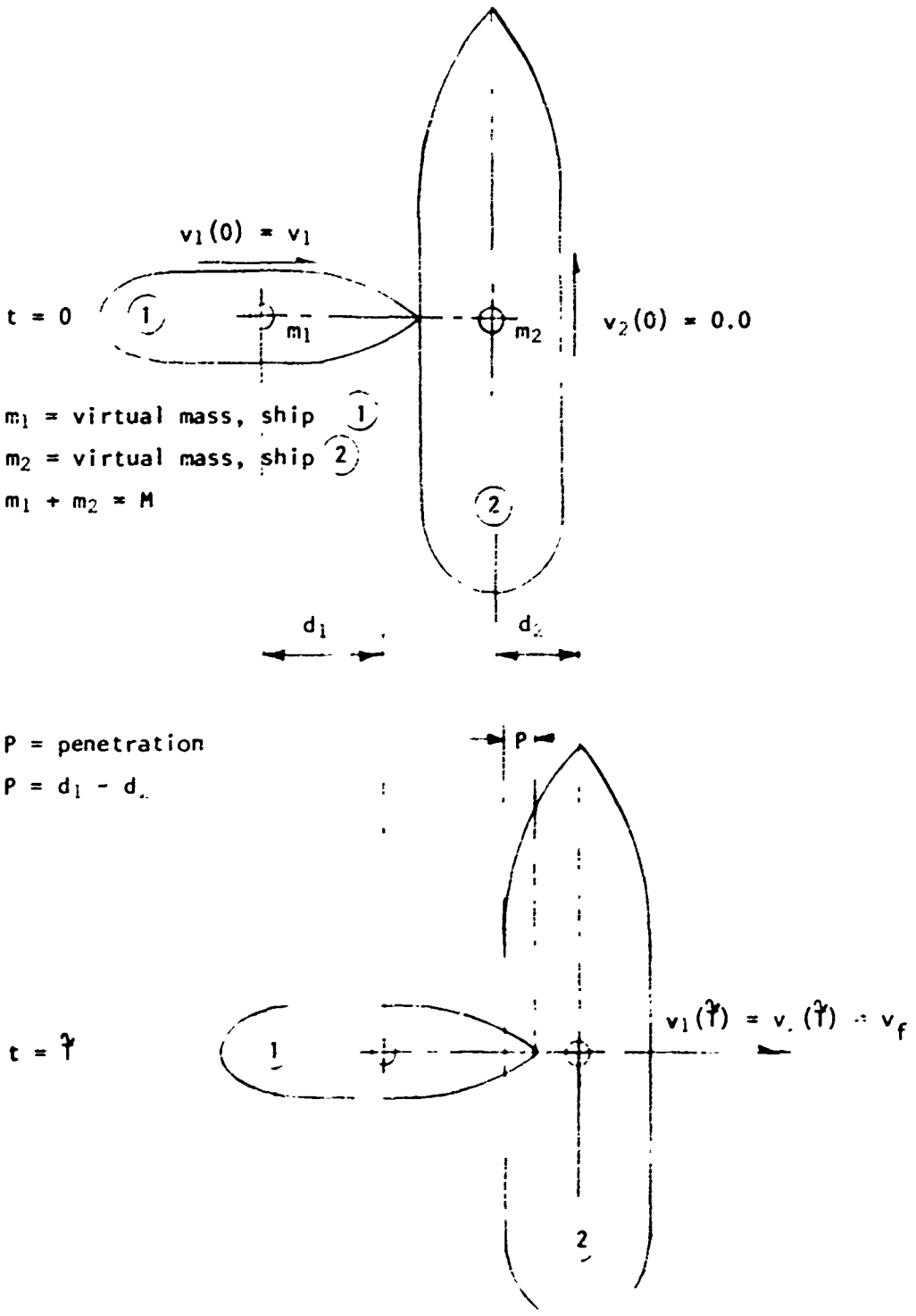

FIGURE B-2 Simple Ship Collision

$$KE_f = \frac{M}{2} v_f^2 \qquad \text{(B-3)}$$

$$= \frac{M}{2} \left(v_1 \frac{m_1}{M}\right)^2$$

$$= \frac{m_1}{2} v_1^2 \frac{m_1}{M}$$

$$= KE_i \frac{m_1}{M} \qquad \text{(B-4)}$$

$$KE_a = KE_i - KE_f$$

$$= KE_i \left(1 - \frac{m_1}{M}\right)$$

$$= KE_i \frac{m_2}{M} \qquad \text{(B-5)}$$

In the computer runs that were carried out to determine elastic energy absorption, the ship resistance was not ignored, and the final velocities varied slightly from the value indicated by equation B-1. For this reason, final and absorbed kinetic energies are different from those calculated by equations B-4 and B-5 by the amount of energy lost to ship resistance.

The total kinetic energy absorbed in a ship collision can also be expressed as the integral of the collision force (as a function of penetration) and the collision penetration:

$$KE_a = \int_0^P F(p)dp \qquad \text{(B-6)}$$

where the collision penetration, P, is made up of both elastic and plastic deformations; and if the striking ship is assumed rigid (as in the present analysis), these deformations all occur in the struck ship. This definition of penetration is illustrated in Figure B-3, in which the distance (a) is

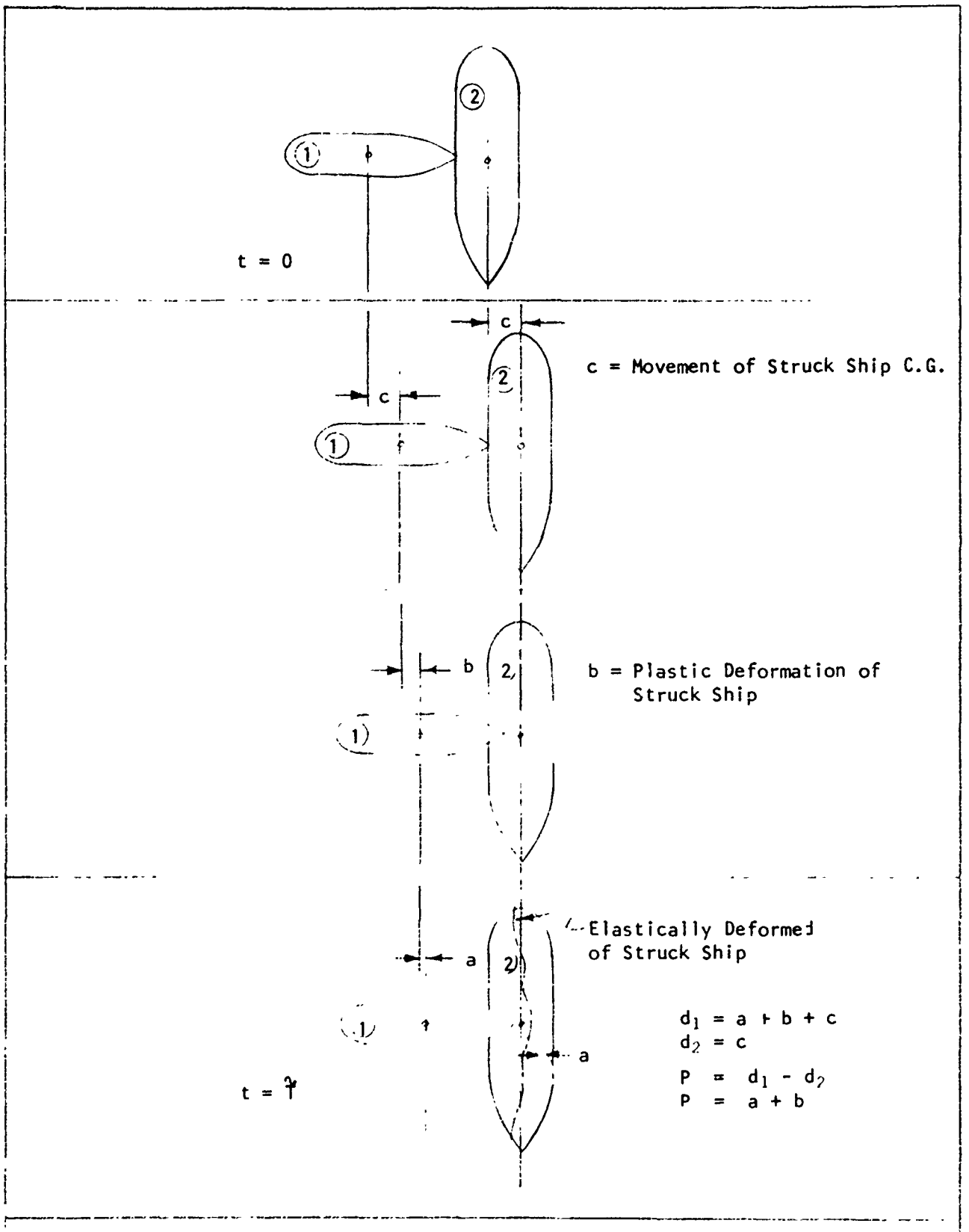

FIGURE B-3 Components of Total Penetration

the elastic deformation of the struck ship with respect to its own center of gravity, the distance (b) is the depth of penetration caused by plastic deformation of the struck ship, and distance (c) is the distance through which the struck ship's center of gravity is moved —— d_2. The elastic deformation is calculated by the slam-analysis computer program and the plastic deformation by the "plastic energy analysis." The assumptions made in order to justify the separate calculation of these two types of deformation are explained in Section 2.3 of this appendix.

The penetration, P, may also be defined in terms of the difference in distances traveled by the centers of gravity of both ships,

$$P = d_1 - d_2 \ , \qquad \text{(B-7)}$$

which in turn can be expressed as a function of the initial ship velocities and the time history of the collision force.

With the collision penetration expressible in terms of elastic and plastic deformations (or work done by the striking ship's bow) as well as in terms of movement of the two ships' centers of gravity, it is then possible to relate the force-deflection history of the collision to the force-time history of the collision.

A very simple relationship exists between the force-penetration history and force-time history of a so-called "constant force collision" -- one of the collision situations examined in Reference 9. Obviously, if the force remains constant from zero penetration to the maximum penetration, it is also constant for the time duration of the collision process. As shown in Figure B-4, a constant force collision results in a linear velocity-time curve for both the struck and striking ship. The constant force results in a constant acceleration of each ship and, therefore, a linear velocity.

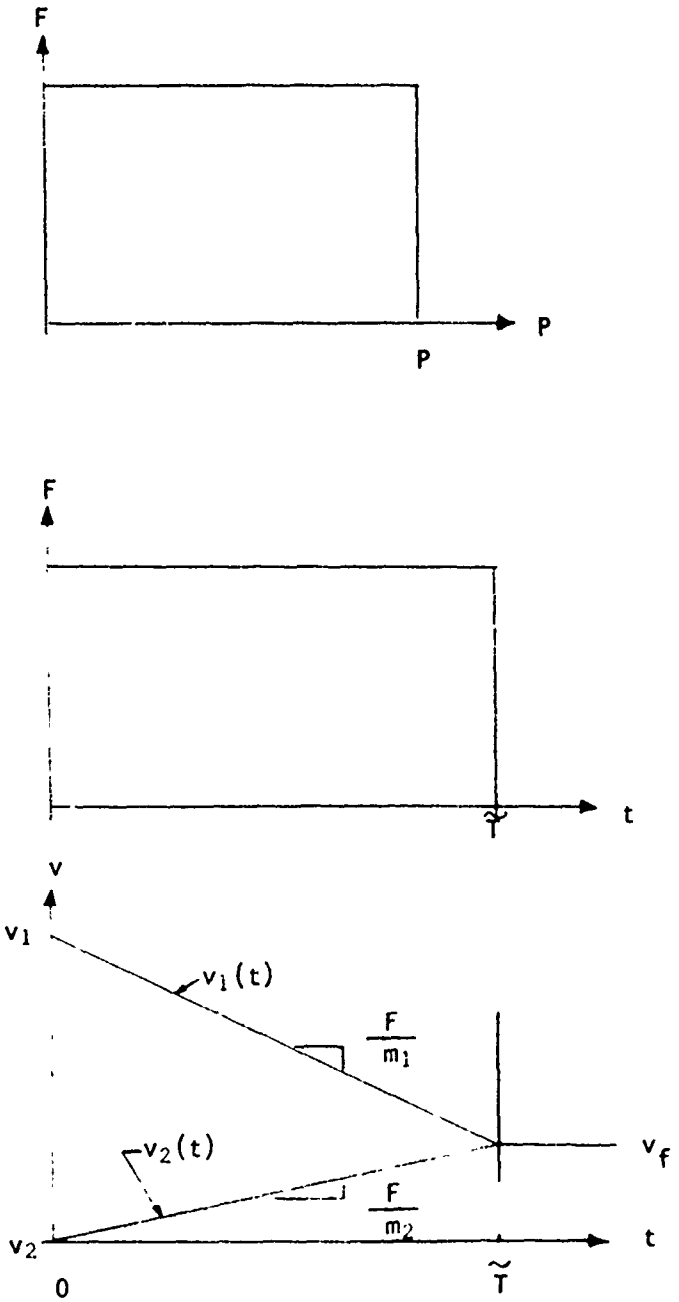

FIGURE B-4 Constant Force Collision Diagram

As indicated in Figure B-5, the distance traveled by each ship may be simply calculated from the areas under their respective velocity-time curves as follows:

$$d_1 = \frac{v_1 + v_f}{2} \hat{\tau}$$

$$d_2 = \frac{v_f}{2} \hat{\tau}$$

and hence,

$$P = d_1 - d_2 = \frac{v_1 \hat{\tau}}{2} \qquad \text{(B-8)}$$

regardless of the value of v_f; i.e., regardless of the relative magnitude of m_1 and m_2, as long as v_1 and $\hat{\tau}$ are given.

For other than constant-force collisions, the slopes of the velocity curves for the struck and striking ships at a given time are inversely proportional to the ship masses and directly proportional to the collision force at that time. Thus, as indicated in Figure B-6, the distance traveled by the struck ship, area (a), is related to the distance traveled by the striking ship in the following manner:

$$d_1 = \text{area (c)} + \text{area (a)}$$

$$d_2 = \text{area (a)}$$

$$\text{area (c)} = v_1 \hat{\tau} - \text{area (a)} - \text{area (b)}$$

$$\text{area (b)} = \text{area (a)} \times \frac{(v_1 - v_f)}{v_f}$$

$$= \text{area (a)} \times \frac{m_2}{m_1}$$

Let area (a) $= d_2 = v_f \hat{\tau} \times f_1(F) = v_1 \frac{m_1}{M} \hat{\tau} f_1(F)$

where $f_1(F)$ is a shape function determined by $F(t)$.

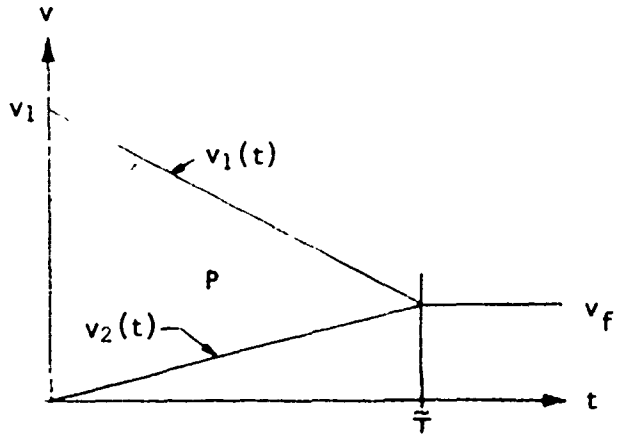

$$P = d_1 - d_2$$

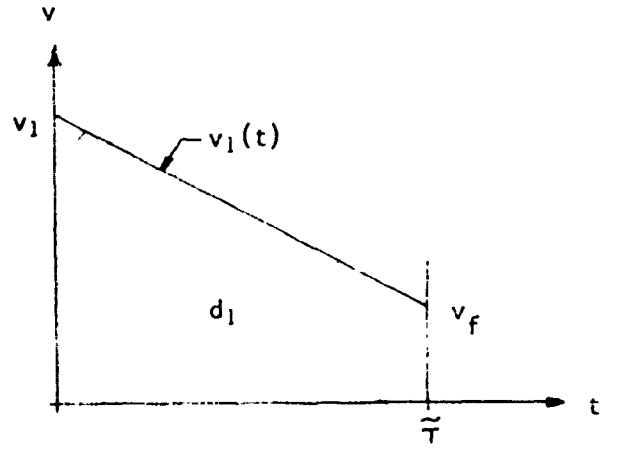

$$d_1 = \int v_1(t)dt$$

$$d_1 = \frac{v_1 + v_f}{2} \times \tilde{T}$$

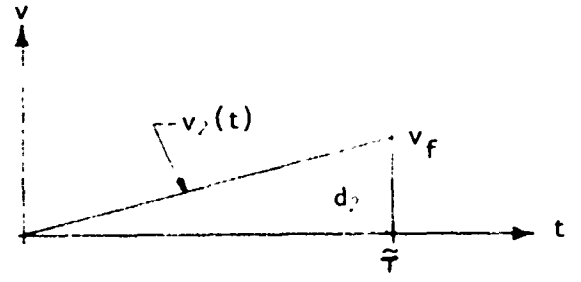

$$d_2 = \int v_2(t)dt$$

$$d_2 = \frac{v_f}{2} \times \tilde{T}$$

FIGURE B-5 Distance Calculation for Constant-Force Collision

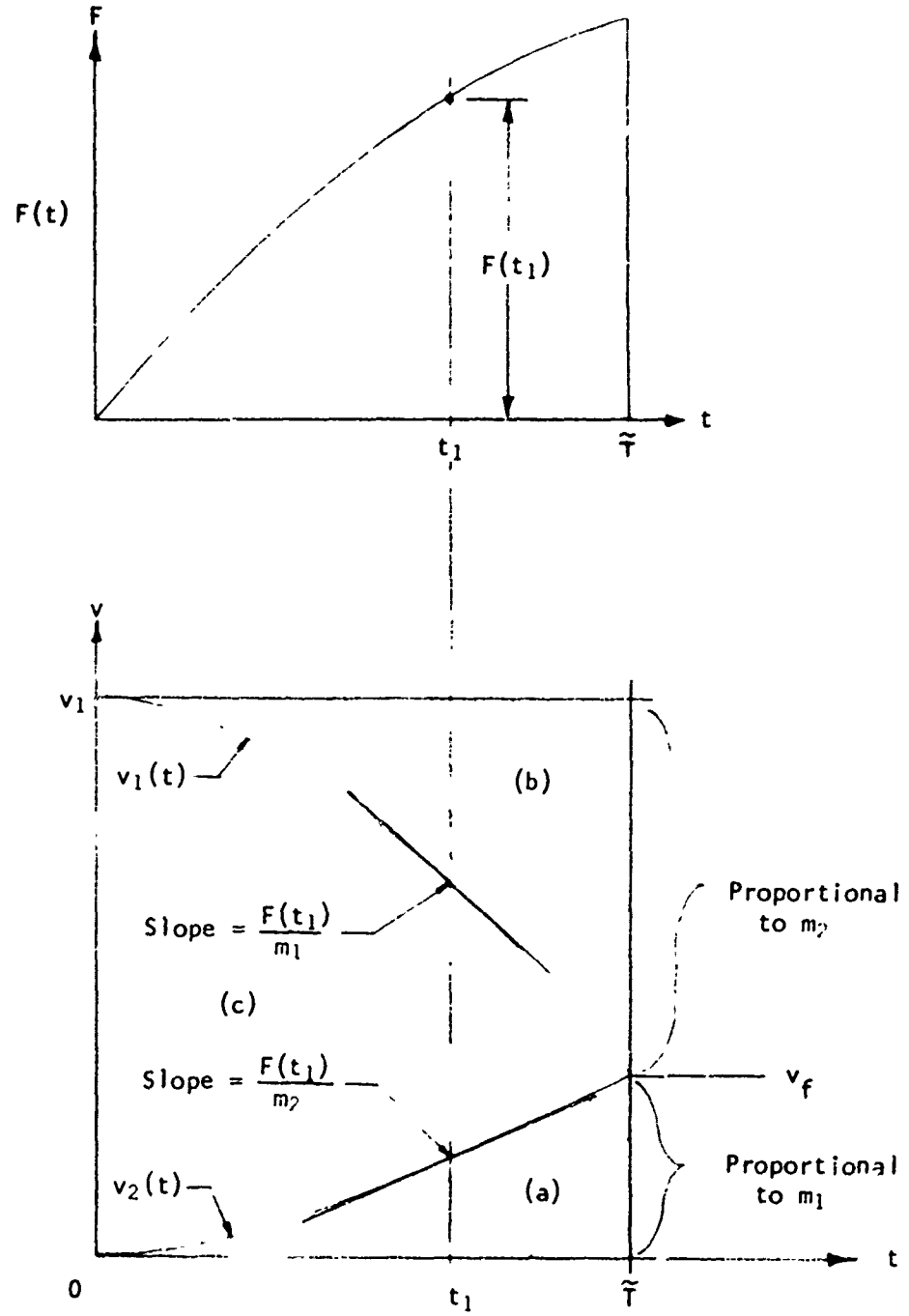

FIGURE B-6 General Force-Time History Collision Diagram

Since

$$P = d_1 - d_2$$

$$P = \text{area (c)}$$

$$= v_1 \hat{\tau} - \text{area (e)} \left[1 + \frac{m_2}{m_1} \right]$$

$$= v_1 \hat{\tau} - d_2 \frac{M}{m_1}$$

$$= v_1 \hat{\tau} - v_1 \hat{\tau} \frac{m_1}{M} \frac{M}{m_1} f_1(F)$$

$$P = v_1 \hat{\tau} \left[1 - f_1(F) \right]$$

or $$P = v_1 \hat{\tau} f_2(F) \qquad \text{(B-9)}$$

where $$f_2(F) = 1 - f_1(F)$$

It can be shown that $f_2(F)$, or simply f_2, is a unique function of $F(t)$ and is independent of the ratio of ship masses; and thus, as was true for the constant force collision, the penetration is equal to the product of initial velocity, v_1, and collision duration, $\hat{\tau}$, times a factor that is a function of the collision force-time history, only. Further, it can be shown that it is only a function of the shape of the force-time history and not its magnitude.

For example, the second type of collision studied in the NCRE report[9] was a linear force-penetration relationship in which the collision force varied from zero to a maximum value as a direct function of penetration. This force-penetration relationship results in a sinusoidal force-time relationship as shown in Figure B-7, and in a velocity-time relationship similar to that shown in Figure B-5. For this type of collision:

$$P = \frac{2}{\pi} v_1 \hat{\tau} \qquad \text{(B-10)}$$

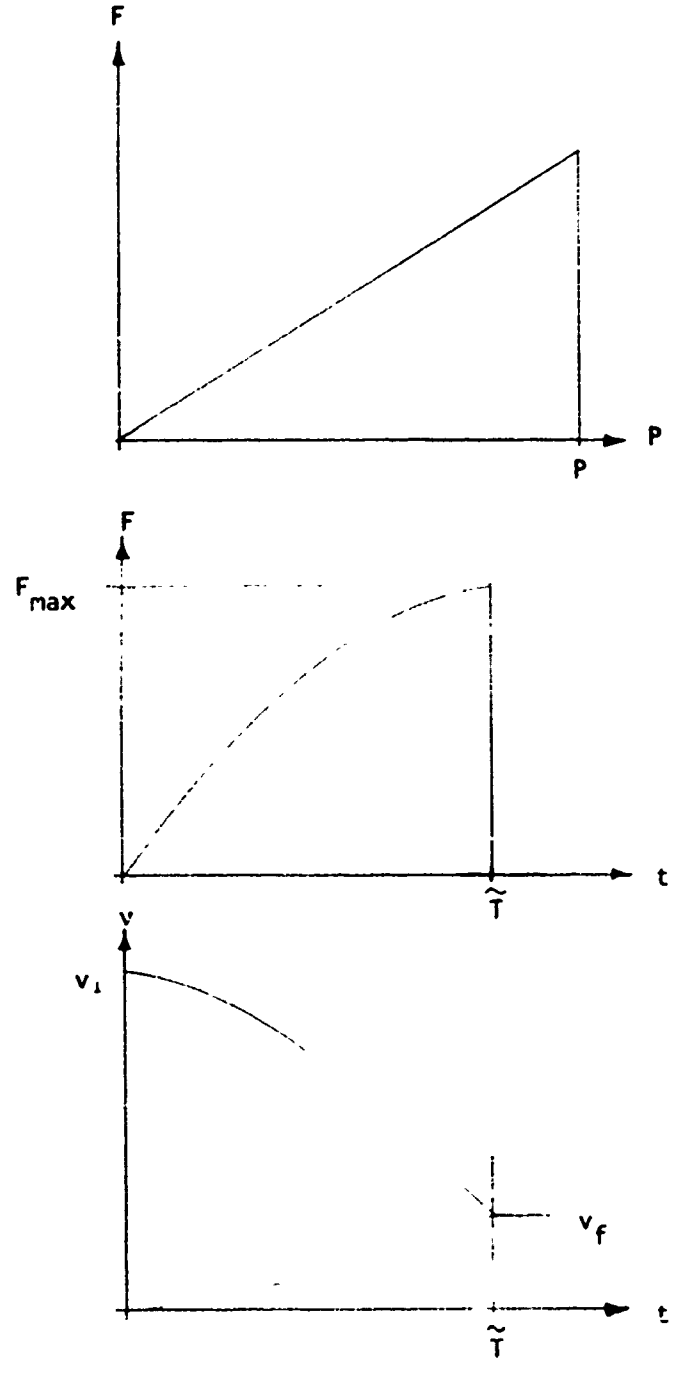

FIGURE B-7 Linear-Force Collision Diagram

Similarly simple expressions for penetration in terms of the initial velocity of the striking ship, the duration of the collision, and the shape of the collision impulse (force-time history of the collision) can be determined for other shapes of collision impulse. The important conclusion, however, is that it is possible to relate the total penetration, as made up of plastic deformations from the plastic energy absorption analysis and elastic deformations from the dynamic analysis, to the shape of the collision impulse -- which in turn can be related to the structural resistance forces and the local inertia forces.

B-2.3 Combining Plastic and Elastic Collision Energies

The assumption that forms the basis for calculating separately the plastic and elastic energy absorption for minor collisions is that the plastic work done on the ship structure is confined to a small region in the immediate vicinity of the penetration and that this plastic distortion does not significantly change the elastic properties of the overall ship. In addition, it is assumed that the elastic ship feels only the forces acting on the boundary of this region; i.e., the structural resistance forces of the penetration and the inertia of the plastically deformed structure and its entrained sea water and cargo oil. The dynamic response of elastic local structure is ignored because its natural frequency is relatively high compared to the collision duration; and its response, therefore, should be quasi-static and directly related to deformations.

As mentioned previously, the total movement (during the collision process) of the stem of an infinitely rigid striking ship contains the following components:

1. Local elastic deformations of the struck ship.

2. Overall elastic deformation of the struck ship.

3. Movement of the struck ship's center of gravity as resisted by the struck ship's inertia and by hydrodynamic forces.

4. Local plastic deformations -- penetration of the striking ship bow as calculated by the plastic-energy absorption procedure.

It is assumed that the movement consisting of components 1, 2, and 3, and hence the work done by these components, can be treated separately from the 4th component. This assumes that a force-time history can be chosen for estimating components 1, 2, and 3, that is representative of the force-time history produced by the force-penetration history of the 4th component, in conjunction with the inertia forces of local structure.

Thus, once a plastic energy absorption calculation has been completed -- giving values for plastic energy absorbed, plastic penetration, and the maximum structural resistance force -- estimates can be made for the total penetration and the total force-time history of the collision that includes the local-mass inertia forces. The local-mass inertia forces depend on the acceleration imparted to the plastically deformed structure (and its entrained cargo and sea water) by the striking ship bow. From a series of these estimates, elastic energy absorption calculations can be made that yield a range of elastic energy absorbed, elastic penetration, local velocities, and other information on struck-ship response, which can then be compared to determine which estimate gave the most consistent results for the entire collision process. Primarily, this comparison consists of checking to see if the assumed collision impulse for local inertia forces produces local velocities on the struck ship that correspond to the velocity of the striking bow.

This trial and error process generally progresses as follows:

1. From a specific plastic energy absorption calculation, values for plastic energy absorbed, plastic deformation or penetration, and maximum structural resistance force are obtained.

2. A mass is assumed for the striking ship: m_1.

3. The calculated values of plastic deformation and energy absorption are slightly modified to be consistent with a linear-force collision, i.e.,

$$KE_a \text{ (plastic)} = \tfrac{1}{2} \bar{p} F \qquad \text{(B-11)}$$

where KE_a = calculated plastic energy absorbed

F = calculated maximum structural resistance force

and $\bar{p}$ = calculated plastic deformation.

4. A force-time history is assumed for the local-structure inertia forces and is added to the linear-force-collision force-time history. Some typical combined force-time histories are shown in Figure B-8. Values of f_1 and f_2 can then be determined.

5. Several estimates of p', the elastic deformation, are made, thus yielding a series of values for P, the total penetration. $P = p' + \bar{p}$

6. For each value of P and using the assumed total collision impulse, a collision duration can be determined in the following manner:

From momentum considerations,

$$F\hat{\gamma} f_1 = m_2 v_f = \frac{m_1 m_2}{M} v_1$$

Thus,

$$v_1 = \frac{FM\hat{\gamma}}{m_1 m_2} f_1 \qquad \text{(B-12)}$$

Also,

$$P = v_1 \hat{\gamma} f_2$$

or

$$v_1 = \frac{P}{\hat{\gamma} f_2} \qquad \text{(B-13)}$$

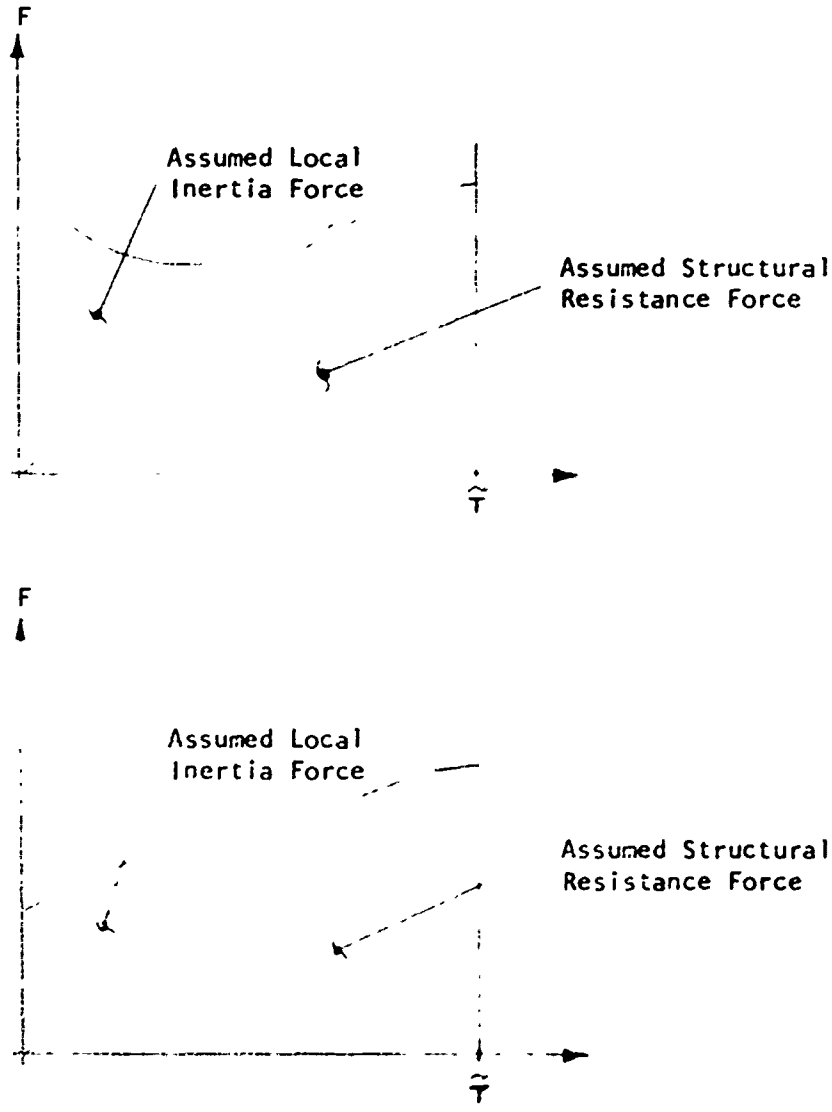

FIGURE B-8 Typical Collision Impulses for Elastic Energy Absorption Calculations

From (a) and (b)

$$\tau = \left[\frac{P m_1 m_2}{FM f_1 f_2} \right]^{\frac{1}{2}} \qquad \text{(B-14)}$$

where f_1 and f_2 are computable functions of the assumed pulse shape.

7. For each value of τ, a corresponding value of v_1 can be determined from the above equation (B-13).

8. For each v_1 and the assumed m_1 value, the various energies -- KE_i, KE_f, and KE_a -- can be determined.

9. Using the assumed collision-impulse shapes and the corresponding duration, τ, elastic energy absorption and penetration, p', can be determined with the slam-analysis computer program.

10. For each trial, the computed elastic energy absorbed was added to the previously calculated plastic energy and compared to KE_a from step 8. The calculated elastic deformation, p', was checked against the assumed value, and the velocity of the locally deformed structure was compared to the velocity of the striking bow at a time shortly after the initial contact.

11. The combination of original estimates of p' and the local-inertia force-time history that gave the best agreement in all three categories was assumed to be a correct solution.

B-3. SUMMARY OF INVESTIGATIONS

Several groups of parametric analyses were conducted in an effort to determine the importance of elastic energy absorption in relatively minor collisions. Prior to formulating the first series of parametric studies for the slam-analysis computer program, the equations developed above were used in an attempt to define the relevant range for such parameters as collision force, penetration, striking-ship size and speed, and the various components of energy absorption. This was also prior to having completed the first plastic energy absorption calculations.

This first series of calculations used ship sizes of from 30,000 to 120,000 tons displacement, penetration values of from 1.0 to 10.0 feet, and an assumed deceleration of about one-tenth the acceleration of gravity (a value suggested by some model collision tests conducted by Spinelli -- see References 3-5). To obtain short duration collisions of 0.2, 0.6, and 1.0 seconds, a collision force of 12,000 long tons was required. Figure B-9 shows the relationship between collision force, collision duration, and penetration for a 30,000 ton striking ship and a 120,000 ton struck ship. Also shown in Figure B-9 is the force and range of collision durations used in the preliminary analysis. The relationship between initial velocity, collision duration, and penetration for constant force collisions is shown in Figure B-10 and is independent of ship size. This series of calculations indicated that elastic energy absorption could be significant; however, after the completion of the first set of plastic energy absorption calculations, it became evident that the assumed decelerations were too great and that realistic structural resistance forces would provide only a fraction of the deceleration that was originally assumed. Since a much smaller collision force implies a much longer duration of the collision to obtain the same magnitude of hull penetration, the next series of computer calculations covered a significantly different range of collision parameters than did the first.

The second group of elastic energy absorption calculations were based on information gained from the first plastic energy absorption calculation. This plastic energy absorption calculation, which provided the collision force and penetration representative of a T-2 tanker colliding with a 120,000 DWT tanker (operating at an assumed displacement of 120,000 tons)

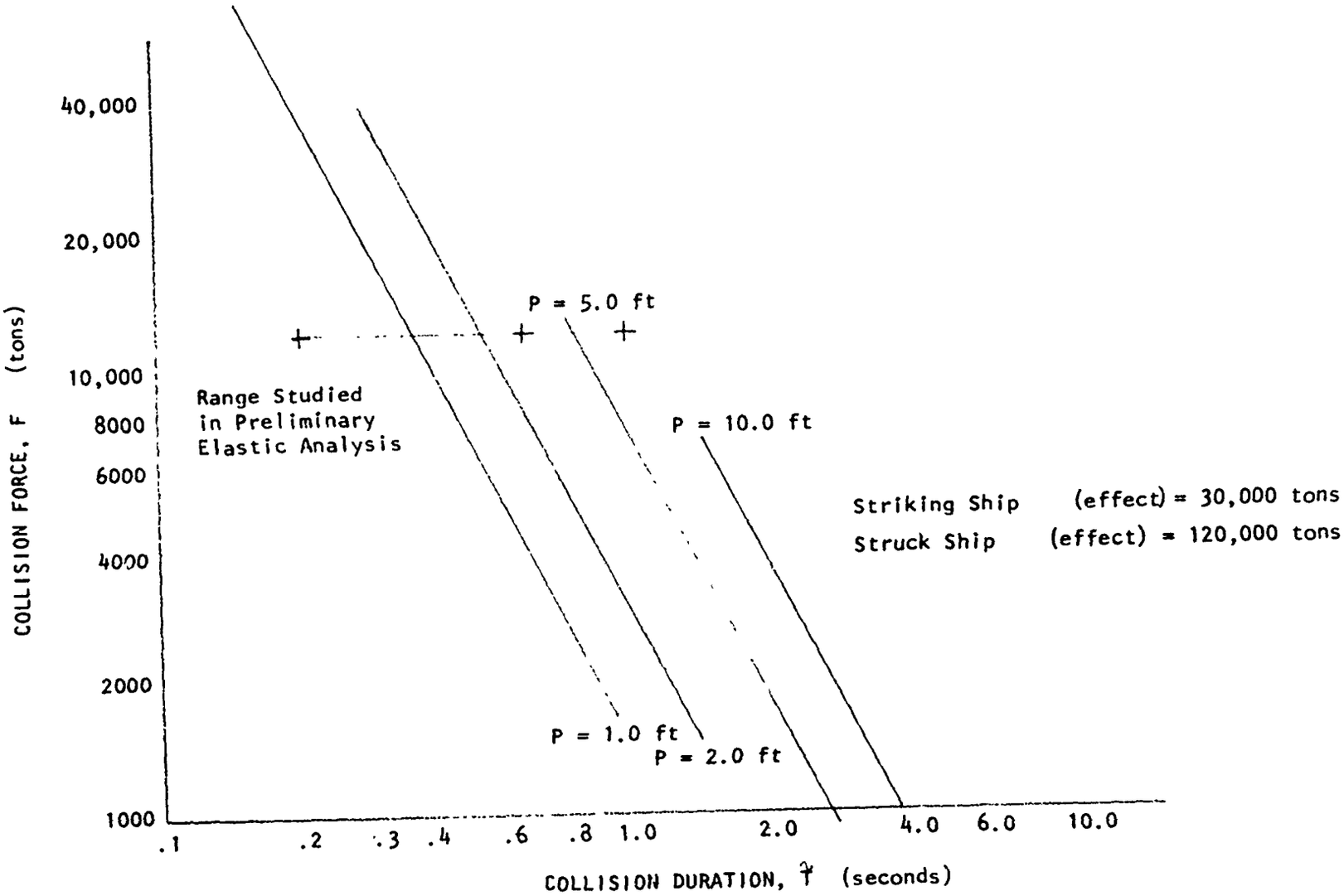

FIGURE B-9 Penetration as a Function of Force and Duration

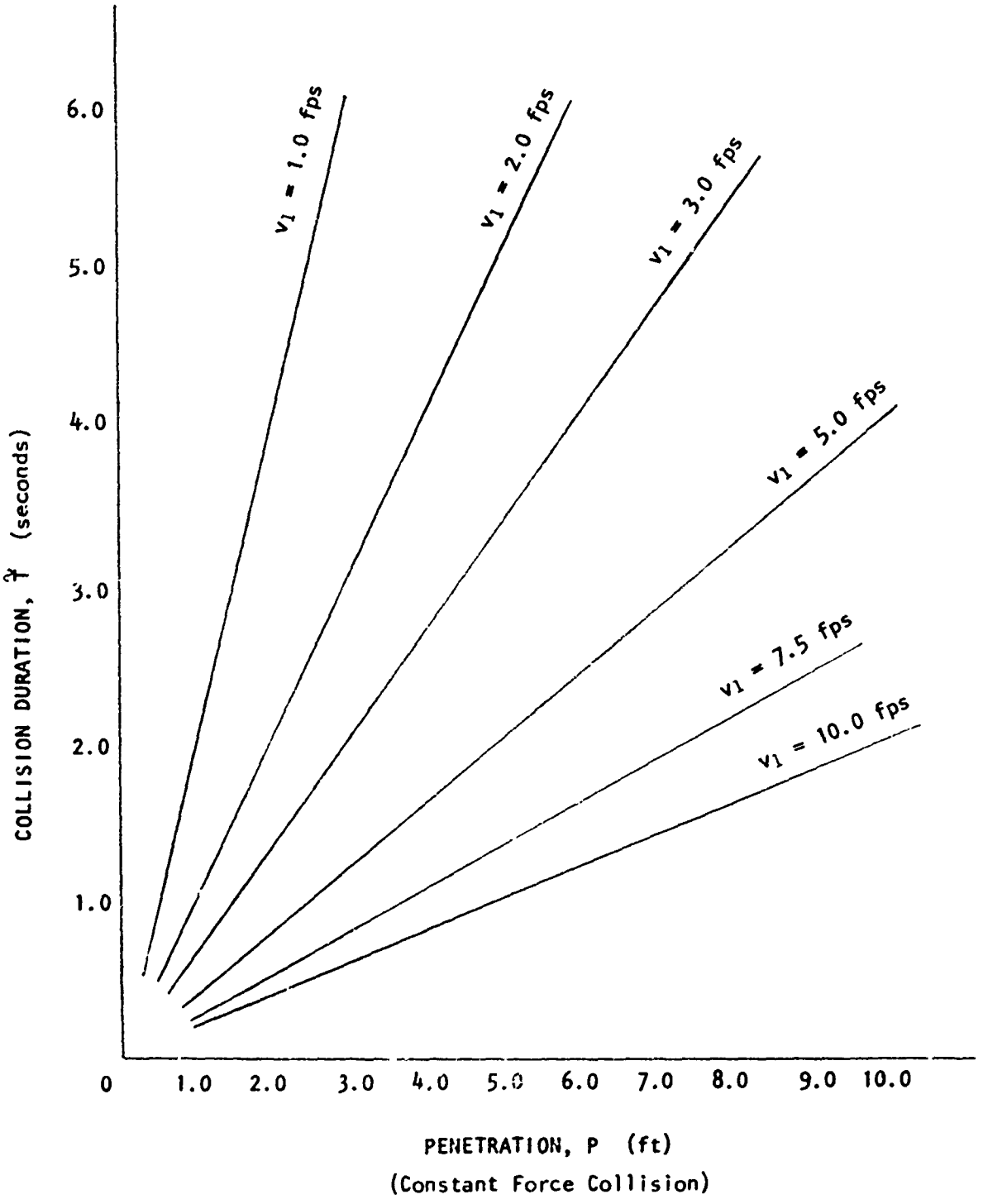

FIGURE 8-10 Penetration as a Function of Collision Time & Velocity

in a simple collision situation, indicated that the maximum structural resistance force generated prior to rupture of the side shell was approximately 1500 tons and resulted in a plastic energy absorption of approximately 2400 ft-tons. This energy absorption corresponds to a plastic deformation of structure of over 3.0 ft, if a linear force-penetration relationship is assumed.

For this series of elastic energy absorption calculations, the major variable was the magnitude and variation of the inertia force contributed by the acceleration of the plastically deformed structure and its entrained mass of cargo oil and sea water. The total impulses used are shown in Figure I-11. In addition, the local stiffness of the struck ship was modified in the computer idealization to approximate more closely the stiffness of the plastically deformed structure. If the structure remained elastic, the maximum force developed at penetration of 3.0 ft would greatly exceed 1500 tons. To model the actual transfer of force from the striking bow, through local structure, and into the overall ship then required that the structural stiffness at the collision point be reduced to represent the resistance to penetration (over the collision time interval) of the plastically deformed structure. These modifications were made so that a comparison could be made between the initial velocity of the striking bow and the velocity of the local structure near the start of the collision process. The purpose of the comparison was to determine which inertia force augmentation gave a realistic shape for the collision impulse, and thus identify which elastic energy absorption calculation was the most valid.

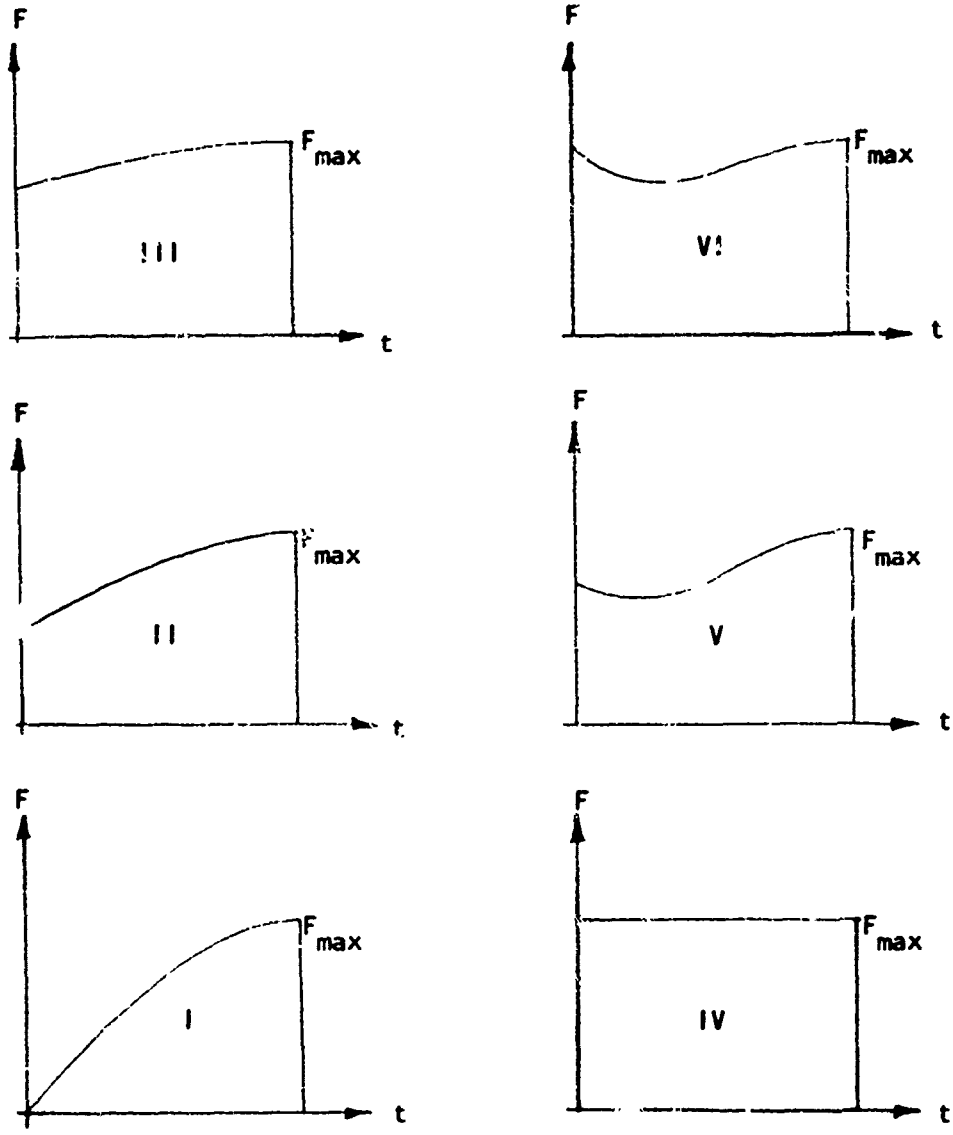

FIGURE B-11 Collision Impulse Variations Used in Elastic Energy Absorption Calculations

As in previous calculations, the elastic energy absorption calculated in this series of analyses contained energy due to local elastic deformations as well as that due to the overall elastic deformations. In view of the fact that the local elastic properties now had been radically changed to simulate the stiffness of plastically deformed structure, the need for subtracting the elastic energy absorbed in local deformations from the total calculated elastic energy absorption became obvious.

A procedure was developed for calculating the elastic energy absorption in the overall structure that did not include energy absorbed in local deformations. This procedure utilized information from the computer-derived displacement time history of the total response.

For certain total force-time histories, the energy absorbed in local deformations could be calculated directly from the local displacements at the collision location and subsequently subtracted from the total elastic energy absorptions. This was true for cases in which the total force-time history approximated a constant force collision. For cases in which the force-time history differed substantially from the constant-force impulse, the force-time history corresponding to a linear force-penetration relationship unaugmented by local inertia forces was applied directly to the main hull structure of the struck ship and the elastic energy absorption was determined. This procedure ignores the effects of local structure in transmitting the applied force-time history to the overall structure and assumes that the main effect is the difference caused by local inertia forces.

When the local energy absorption was removed from the total energy absorption in the above manner, the remaining energy absorption which could be attributed to elastic deformations of the overall ship was found to be negligible.

These calculations were performed for three assumed collision situations representative of a T-2 tanker colliding with a much larger tanker operating at a displacement of 120,000 tons. The three collision situations correspond to (1) 1" MS single skin, struck at web, 15° bow rake, (2) 1" MS single skin, struck between webs, 15° bow rake, (3) 1-3/8" MS single skin, struck between webs, 15° bow rake; however, the values used were from preliminary calculations of plastic energy absorption.

The force-penetration histories as calculated in the plastic energy absorption analysis for these three collision situations are summarized in Figures B-12, B-13, and B-14, and were derived before finalization of the plastic energy absorption analysis procedure.

A summary of results for the calculations* performed on the last of the above collision situations is presented in Table B-1. The plastic energy absorbed in this collision was approximately 1350 ft-tons; and, within

*These calculations were based on the force-penetration history from a calculation based on a preliminary plastic energy analysis.

Long. No.	δ_{bc} = Maximum Bending Defl. before Stiff. Buckling (inches)	Bending Resistance, Constant Up to δ_{bc} $(P_b-P_{wf}) = \frac{E_{bc}}{\delta_{bc}}$ (Kips)	Mem. Tens. Thrust, T (Kips)	2 Web Frame Spa. Damaged: Damaged Lgth, L_t (inches)	2 Web Frame Spa. Damaged: δ_1 = Defl. When Web Frames Flanking The Strike Yield (inches)	2 Web Frame Spa. Damaged: Max * Resist. $(P_{tm}-P_{wt}) = \frac{4T\delta_1}{L_t}$ (kips)	Rupture Conditions 4 Web Frame Spa. Dam.: δ = Max. Defl. of Long. (inch)	Rupture Conditions 4 Web Frame Spa. Dam.: δ_2 = Corr. Defl. of Web Frame (inch)	Rupture Conditions 4 Web Frame Spa. Dam.: Max. Resistance $(P_{tm}-P_{wf}) = \frac{4T}{L_t}(\delta-\delta_2)$ (kips)
1	6.03	65	2265	288	30.1	947	36.7	3.3	1051
2	6.03	64	2190	288	19.6	596	26.2	2.4	724
3	5.32	108	2185	288	10.0	303	16.6	1 4	461
4	1.36	232	2245	288	0.4	-	7.0	0.5	203
Struck Web Frame	**								787
Total									3226

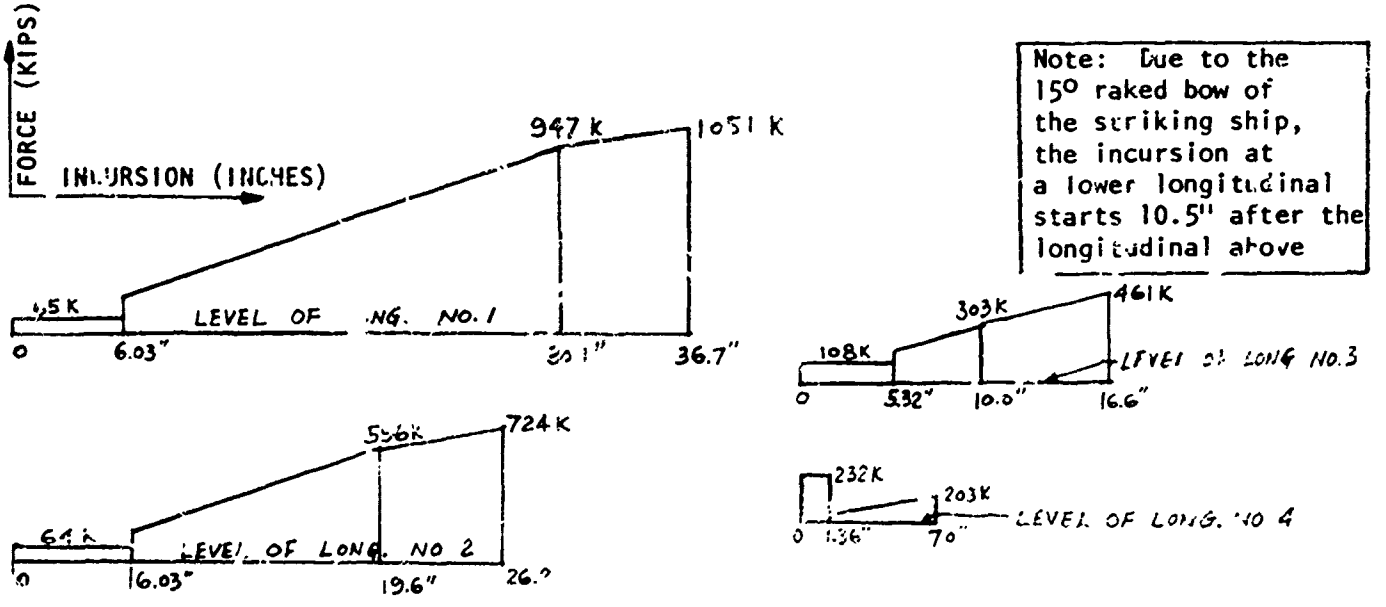

Note: Due to the 15° raked bow of the striking ship, the incursion at a lower longitudinal starts 10.5" after the longitudinal above

* This resistance, which is from the membrane tension in the longitudinally stiffened plate, is assumed to increase linearly with deflection, but all membrane tension resistance for $\delta > \delta_{bc}$ is discounted.

**Shear capacity of the web frame in the plane of the strike.

FIGURE B-12 COLLISION FORCE ON 1.0" MS HULL HIT AT WEB FRAME

Long. No.	δ_{bc} Max. Bending Defl. before Stiff. Buckling (inches)	Bending Resistance, Constant up to δ_{bc}, $P_b = \frac{E_{bc}}{\delta_{bc}}$ (Kips)	Mem. Tens. Thrust, T (Kips)	1 Web Frame Spa. Damaged		
				Damaged Lgth L_t (inches)	δ_m = Defl. at First Rupture (inches)	Max. Resistance* $P_{tm} = \frac{4T\,\delta_m}{L_t}$ (Kips)
1	2.74	129	2265	144	14.6	919
2	2.74	128	2190	144	4.1	249
Total						1168

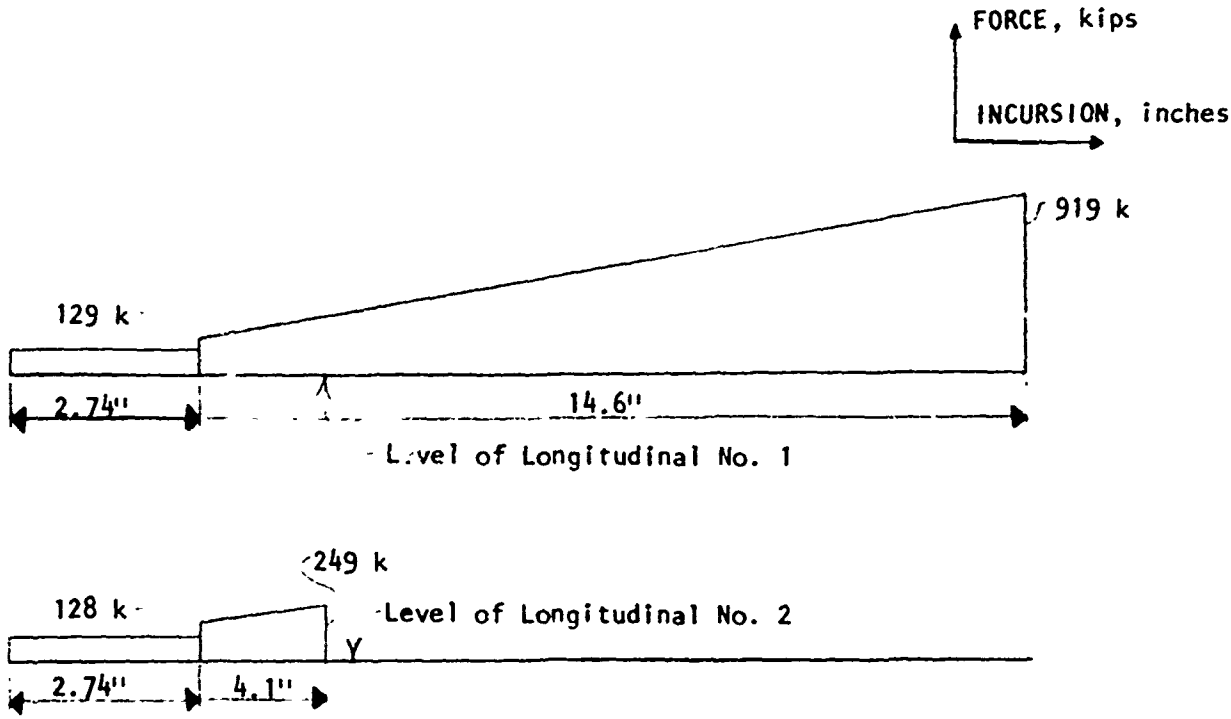

* This resistance, which is from the membrane tension in the longitudinally stiffened plate, is assumed to increase linearly with deflection, but all membrane tension resistance for $\delta < \delta_{bc}$ is discounted.

Note: Due to the 15° raked bow of the striking ship, the incursion at the level of long. No. 2 starts 10.5" after the incursion at the level of long. No. 1.

FIRGURE B-13 COLLISION FORCE ON 1.0" MS HULL HIT BETWEEN WEB FRAMES

Long. No.	δ_{bc} Max. Bending Defl. before Stiff. Buckling (inches)	Bending Resistance, Constant up to δ_{bc} $P_b = \frac{E_{bc}}{\delta_{bc}}$ (kips)	Membrane Tension Thrust, T (kips)	1 Web Frame Spa. Damaged: Damaged Length $L_t = L_s$	δ_1 Defl. When Web Frames Flanking the Static Yield (inches)	Max. Resistance* $= P_{tm} = \frac{4T\delta_1}{L_t}$ (kips)	Rupture Condition, 3 Web Frame Spa. Damaged: Max. Defl. of Long. (inches)	Corr. Defl. of Web Frame (inches)	Max. Resistance P_{tm} $\frac{4T(\delta-\delta_2)}{L_t}$ (Kips)
1	3.00	155	2998	144	11.3	941	21.8	7.0	1233
2	2.98	154	2898	144	0.8	64	11.3	3.6	620
3	3.95	176	2868	144	-	-	1.7	0.3	use 176
Total									2029

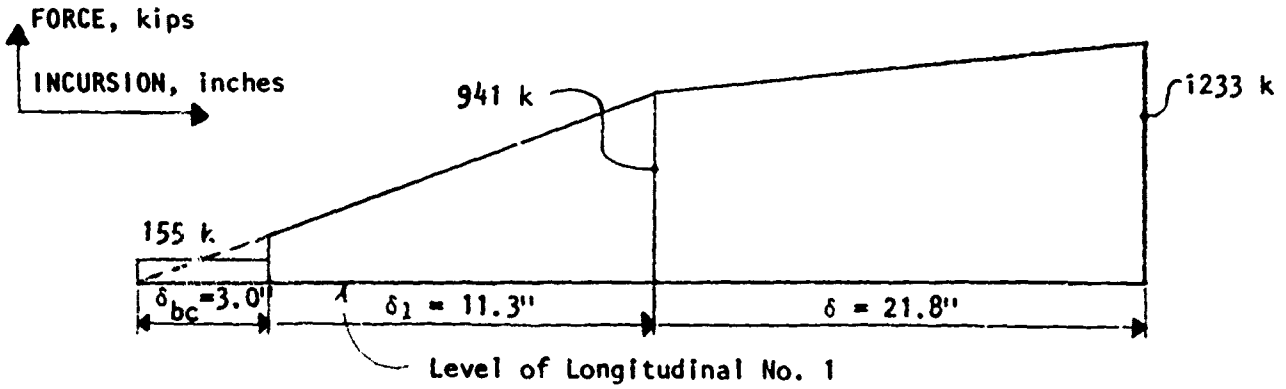

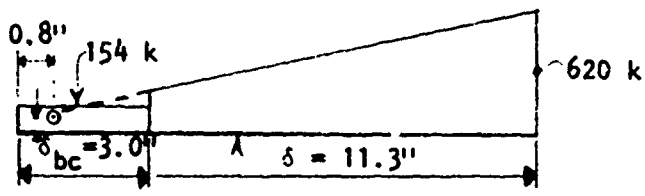

Level of Longitudinal No. 2

* This resistance, which is from the membrane tension in the longitudinally stiffened plate, is assumed to increase linearly with deflection, but all membrane tension resistance for $\delta < \delta_{bc}$ is discounted.

Note: Due to 15° raked bow of the striking ship, the incursion at a lower diagonal starts 10.5" after the longitudinal above it.

FIGURE B-14 COLLISION FORCE ON 1 3/8" MS HULL HIT BETWEEN WEB FRAMES

TABLE B-1

ELASTIC ENERGY ABSORPTION CALCULATION, 1-3/8" MS HULL HIT BETWEEN WEB FRAMES, 15° RAKED BOW

Given: $m_1 = 683.8 \frac{\text{Ton-Sec}^2}{\text{Ft}}$ $\quad F_{max} = 900$ Ton

$m_2 = 6154.0 \frac{\text{Ton-Sec}^2}{\text{Ft}}$ $\quad P = 3.0$ Ft.

$M = 6838 \frac{\text{Ton-Sec}^2}{\text{Ft}}$ $\quad P'$ assumed $\tilde{=} 0$

	COLLISION IMPULSE*	UNITS	I	II	III	IV	V	VI
	F_{max}	Tons	900	900	900	900	900	900
	Impulse, Total (Assumed)	Ton-Sec	1289	1568	1698	1823	1675	1666
	$\hat{T}$, Duration (Eq.B-14)	Sec	2.250	2.129	2.075	2.026	2.070	2.145
	v_1 (Equation B-12)	Ft/Sec	2.095	2.548	2.759	2.962	2.560	2.703
(a)	Total Work Done By Striking Ship (From Computer Output 25 modes)	Ft-Ton	135.8	290.9	450.3	634.1	335.0	514.0
(b)	Work Done On Inertia + Resistance (From Computer Output - First 2 Modes)	Ft-Ton	137.1	203.3	238.7	275.3	205.6	230.6
(c)	KE_a (Elast.), Total ((a) - (b))	Ft-Ton	-1.3	87.6	211.6	358.8	129.4	283.4
(d)	Work Absorbed in Local Deformation (From Computer Output)	Ft-Ton	NIL.	86.6	212.0	358.0	136.9	298.5
	KE_a (Elast.) Main Hull ((c) - (d))		-	+1.0	-0.4	+0.8	-7.5	-15.2
	KE_i (Equation B-2)		1500	2219	2503	3000	2240	2507
(e)	KE_a (TOTAL) (Eq. B-5)		1350.9	1998	2342	2700	2016	2256
(f)	KE_a (PLAST.) (Eq.B-11)		1350	1350	1350	1350	1350	1350
(g)	KE_a (INERTIA & RESISTANCE) (b)		137.1	203.3	238.7	275.3	205.6	230.6
(h)	KE_a (TOTAL) (COMPUTER - (f)+(c)+(g))		1485.8	1640.9	1800.3	1984.1	1685	1864
	(h) - (e)		134.9	-357.1	-541.7	-715.9	-331.0	-392.0

CONCLUSIONS: The correct impulse lies somewhere between shapes I and II for the following reasons:

1. The computer calculated main hull elastic energy (KE_a (Elast.)) is so small for all impulses that P' can be assumed $\tilde{=}$ 0.0. This corresponds to the initial assumption of $P' \tilde{=} 0.0$. All impulses pass this criterion.

2. The response velocities of the local structure were close to the striking ship velocity, v_1, for all pulse shapes. All impulses pass this criterion.

3. The computer calculated total energy (h), when compared to the previously calculated total energy (e), indicates that a pulse shape somewhere between I and II should yield identical values for both.

* Roman numerals refer to impulse shapes shown in Figure B-11.

the accuracy of the calculation procedure, all of the elastic energy absorption occurred as deformation of local structure. The elastic deformation of the overall ship (with respect to its own center of gravity) at the collision location was negligible.

Considering that the stiffness of the local side structure, as represented in the computer idealization of the struck ship, was modified to be representative of the stiffness of the plastically deformed structure, it can be assumed that the energy absorbed in local deformations is a partial duplication of the separately calculated plastic energy absorption. The plastic energy absorption calculation does include a small amount of local elastic deformation.

The results of the elastic energy absorption calculations for all three of the above collision situations indicate that either the collision force is too minor to excite significant elastic response or that the collision durations are too long with regard to the fundamental frequency of the ship, or both. Compared to the plastic energy absorbed in penetrating to the verge of rupture, significant elastic energy absorption can only occur if a much higher collision force can be generated by the resisting side structure of the struck ship.

B-4. CONCLUSIONS

The conclusions to be drawn from the elastic energy absorption analyses described herein, are limited by the assumptions made with regard to the separate calculation of plastic and elastic energies, by the simplifications incorporated in the dynamic analysis computer program, and by the structural characteristics of the tanker that was chosen to represent the struck ship. Nevertheless, the evidence seems very substantial that the collision energy absorbed in elastic deformations of overall ship structure will be negligible for all practical collision situations.

For the elastic energy absorption to become significant, the struck ship must have exceptionally strong local side structure, so that high collision forces are generated and so that the striking ship is brought to rest in a period of time that is substantially shorter than the fundamental period of transverse vibration of the struck ship. The side structure of tanker investigated in this study did not come close to providing the necessary resistance to collision.

PART II

TANKER STRUCTURAL ANALYSIS PROCEDURE PRIMER

TABLE OF CONTENTS

	Nomenclature	iii
1.	INTRODUCTION	1-1
2.	COLLISION ANALYSIS PROCEDURE	2-1
	2.1 Input Information	2-1
	2.2 Flow Diagram	2-1
	2.3 Step-by-Step Calculation Procedure	2-4
3.	COLLISION ANALYSIS EXAMPLES	3-1
	3.1 Case #1 1" MS Sincle Shell Ship, Struck at Right-Angle by a 15° Raked Bow Ship	3-1
	3.2 Case #2 1" MS Single Shell Ship, Struck at Right-Angle by a 15° Raked Bow Ship	3-14
	3.3 Case #3 1-3/4" MS Single Shell Ship, Struck at Right-Angle by a Vertical Stem Ship	3-31
	3.4 Case #4 1-3/4" MS Single Shell Ship, Struck at Right-Angle by a 15° Raked Bow Ship	3-44
	3.5 Case #5 1-3/4" MS Single Shell Ship, Struck at Obilique Angle by a Vertical Stem Ship	3-61
	3.6 Case #6 1" MS + 3/4" MS Double Shell Ship, Struck at Right-Angle by a Vertical Stem Ship	3-75
	3.7 Miscellaneous Calculations	3-92

NOMENCLATURE

a = stiffener spacing, or the actual width between two specific reference lines

b = effective design width of a plate, except for the flange of a stiffener, for which 0.5b is the width of the outstanding leg, measured from the center of the web

c = speed of sound in material

d = depth of the web of a stiffener flange or clear depth of web plate

d' = depth of the hull plate cross section that is assumed to be uniformly stressed in compression at σ_u.

d_1 = distance traveled by striking ship during collision

d_2 = distance traveled by struck ship during collision

e = membrane-tension elongation

e_t = total membrane-tension elongation of a stiffened-plate T-beam

h = E/E_t

k_f = foundation modulus

m_1 = effective mass of striking ship (including added mass of water)

m_2 = effective mass of struck ship

p = penetration (relative movement of ship's centers of gravity during collision process)

r = radius

r_m = minimum radius of gyration

s = ratio of ε_{sh} to the yield strain, σ_y/E

t = time

t_f or t = thickness of a stiffener flange

t_w or w = thickness of web of a stiffener

v = velocity

v_1 = velocity of striking ship at beginning of collision process

$v_2 = 0$ = initial velocity of struck ship

v_f = final velocity of both ships

Preceding page blank

x = longitudinal distance toward the load from a point of tangency where a straight-line portion meets the curved portion of the hull plate, in the vicinity of the load

y = lateral deflection relative to a horizontal line through a point of tangency where the two straight-line portions meet the curved portion

x_m, y_m = maximum value of x and y, respectively, in the hull plate at the centerline of the load

A, B and k = material property constant relating to when buckling or rupture will occur during plastic bending

A_f = area of stiffener flange

A_s = cross-sectional area of T-beam

A_w = area of stiffener web

C = spring constant for lateral restraint, expressed as a force per inch for member per inch of lateral movement of the member

C' = a constant greater than zero, reflecting lateral restraint to axial buckling

D = tension-test ductility in a 2-inch gage length

E = modulus of elasticity

E_{bc} = maximum value of bending plastic energy in stiffened-plate T-beam unit, occurring when a longitudinal stiffener flange buckles or ruptures

E_d = membrane-tension plastic energy in deck

E_{int} = membrane-tension plastic energy in ship side

E_{ps} = in-plane shearing plastic energy in web frame

E_t = tangent modulus

F = force

F_R = force required to propagate longitudinally the yield line at the strike

I = moment of inertia about the axis of bending

K = constant

K_a = $\varepsilon / \varepsilon_r$

K_e = ratio of strain in the web frame spaces adjacent to the undistorted web frames or bulkheads bounding the damaged length to ε_r

KE_i = initial kinetic energy

KE_f = final kinetic energy

KE_a = absorbed kinetic energy = $KE_i - KE_f$

L = length or distance along a T-beam

L' = distance from load to nearest support for a right-angle collision, or distance from load to support behind the load (in direction opposite to longitudinal direction of strike) for an oblique collision

L'' = $L_t - L'$

L_c = length of an axially loaded member between points of inflection

L_d = length of damage between undistorted web frames or bulkheads, measured in longitudinal direction

L_{eq} = equivalent length of plating compressed by the collision force

L_s = space between two consecutive web frames

L_t = value of L_d when the length of damage is only one or two spaces between web frames

L_y = yielded length of flange at beginning of local buckling of a stiffener flange

M = $m_1 + m_2$

M_o = maximum moment

M_p = plastic bending moment in a stiffened-plate T-beam

N = normal force

P = maximum penetration or concentrated lateral load

P_b = load on a stiffened-plate T-beam that will occur during plastic bending

P_c = crushing load

P_m = axial load capacity

P_{tm} = a maximum value of the load on a stiffened-plate T-beam that will occur during membrane tension

P_{wf} = load exerted by the most highly strained stiffened-plate T-beam on a web frame at the instant that the web frame yields or buckles

P_y = concentrated radial load

P_E = static Euler load

R (with number subscript) = radius or ratio of force (shear, moment, or thrust) within a web frame, subjected to a given lateral load, to the ultimate force required to fail the web frame.

R_m = maximum value of R (with number subscript)

T = total membrane-tension thrust in a stiffened-plate T-beam after yielding

τ = duration of collision process

V = shear in a stiffened-plate T-beam

V_p = ultimate shear in web frame

δ = a specified lateral deflection; also, the deflection of the centroid of a stiffened-plate T-beam

δ_{bc} = maximum value of δ during the bending phase for only one or two web-frame spaces damaged

δ_m = maximum value of δ during the membrane-tension phase for only one or two web-frame spaces damaged

δ_n = maximum normal-to-plane deflection of a web plate

δ_{tc} = value of δ at the instant of rupture, during the membrane-tension phase, when only one or two web-frame spaces are damaged

ε = average longitudinal strain in hull throughout the damaged length

ε_c = longitudinal compression strain that results from elastic bending of the entire ship cross-section

ε_ℓ = average strain over $L^{\sim}$

ε_m = maximum bending-plus-membrane-tension strain at hull rupture

$\varepsilon_r = 0.10 \left(\frac{D}{32\%} \right)$

ε_s = theoretical bending strain in the flange of a longitudinal stiffener when it buckles near a web frame support

ε_{sh} = strain at onset of strain hardening

ε_E = Euler strain

θ = portion of the bend angle between a straight-line portion of the hull and the location of maximum curvature at the midpoint of a sharp bend

θ_p = angle change in stiffened-plate T-beam at end of L_t that corresponds to buckling or rupture of a longitudinal stiffener flange

λ = length of a flange buckle wave

$\bar{\lambda} = \sqrt[4]{\frac{k_f}{4EI}}$

σ_{ty} = tension-field tensile stress at tension-field yielding

σ_u = tensile strength

σ_y = yield strength

$\sigma' = 0.5(\sigma_y + \sigma_u)$ = Average Plastic Stress

$\sigma'_E = \frac{1}{2}\sigma'$ = Average Elastic Stress

σ_E = Euler buckling stress

α = angle of collision measured from the struck ship undeformed side shell behind the strike point to the centerline of the striking ship

γ = shearing strain

γ_e = total shearing strain up to tension-field yielding

γ_e' = portion of γ_e due to straining up to elastic shear buckling

γ_e'' = portion of γ_e due to straining between elastic shear buckling and tension-field yielding

γ_m = maximum shearing strain before unloading

τ_{cr} = elastic shear buckling stress

τ_y = shear yield strength

Ω = dynamic similarity number

ω = fundamental frequency of the plate

μ = mass density of the material

1. INTRODUCTION

The purpose of this report is to provide an aid in understanding the Collision Analysis Procedure presented in the report, "Tanker Structural Analysis for Minor Collisions" (U.S. Department of Transportation - U.S.C.G. report, prepared by M. Rosenblatt & Son, Inc. and U.S. Steel Corp., MR&S Report No. 20[illegible]18, December 1975). Herein is presented a step-by-step calculation procedure form of the Collision Analysis Procedure that can be easily followed.

The assumptions and limitations of the Collision Analysis Procedure are noted in the above referenced report. It is of value to note a few of the more important here. First, the plastic analysis procedure employs a static analysis, which is an obvious simplification of the dynamic phenomena of collision; second, although means of analyzing striking ships with non-rigid bows were explored, the procedure still assumes rigid bows; third, the possibility of dynamic tearing or puncturing of the shell prior to rupture is neglected.

The actual use of the procedure is illustrated herein by application to the following six different collision cases:

Case #1 1" MS Single Shell Ship, Struck at Right-Angle by a 15° Raked Bow Ship

Case #2 1" MS Single Shell Ship, Struck at Right-Angle by a 15° Raked Bow Ship

Case #3 1-3/4" MS Single Shell Ship, Struck at Right-Angle by a Vertical Stem Ship

Preceding page blank

Case #4 1-3/4" MS Single Shell Ship, Struck at Right-Angle by a 15° Raked Bow Ship

Case #5 1-3/4" MS Single Shell Ship, Struck at Oblique Angle by a Vertical Stem Ship

Case #6 1" MS + 3/4" MS Double Shell Ship, Struck at Right-Angle by a Vertical Stem Ship

It should be noted that the calculation procedure is not intended for use in the design or evaluation of a tanker to withstand collision.

2. COLLISION ANALYSIS PROCEDURE

2.1 Input Information

The following information is required for the calculation of plastic energy absorption of a minor collision.

2.1.1 Data Pertaining to the Struck Ship

2.1.1.1 Configuration

(1) The principal dimensions and draft of the struck tanker

(2) The web frame spacing and the number of web frame spaces between two consecutive transverse bulkheads

(3) The midship section

2.1.1.2 Collision Condition

(1) Angle of strike - right-angle or oblique collision

(2) Location of strike - the location of strike as related to web frames and bulkheads

2.1.2 Striking Ship

Only the bow configuration and draft of the striking ship are needed for the calculation.

2.2 Flow Diagram

The flow diagrams shown in Figures 2-1 and 2-2 indicate the sequence of the Step-by-Step Calculation Procedure.

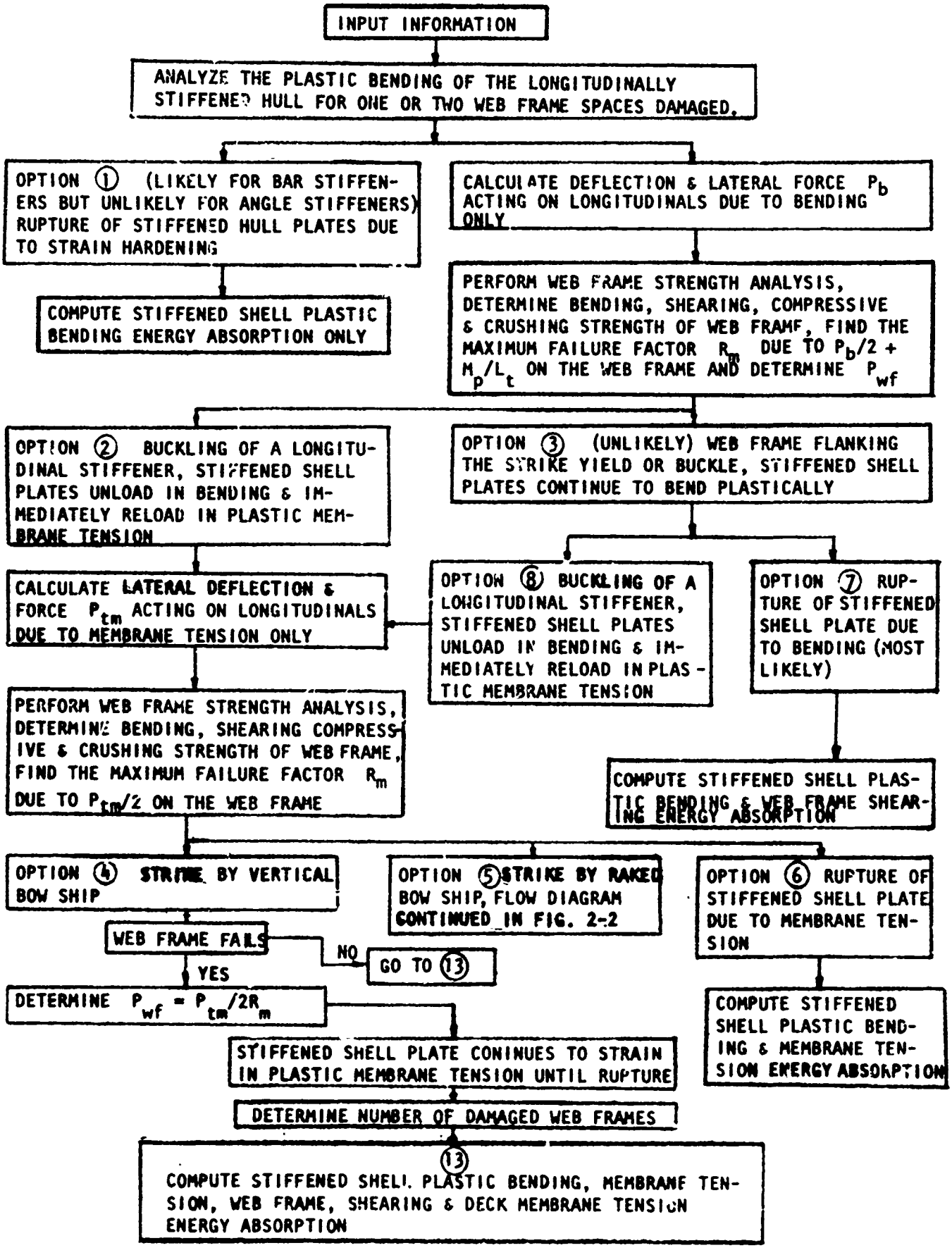

FIGURE 2-1 COLLISION ANALYSIS PROCEDURE, FLOW DIAGRAM

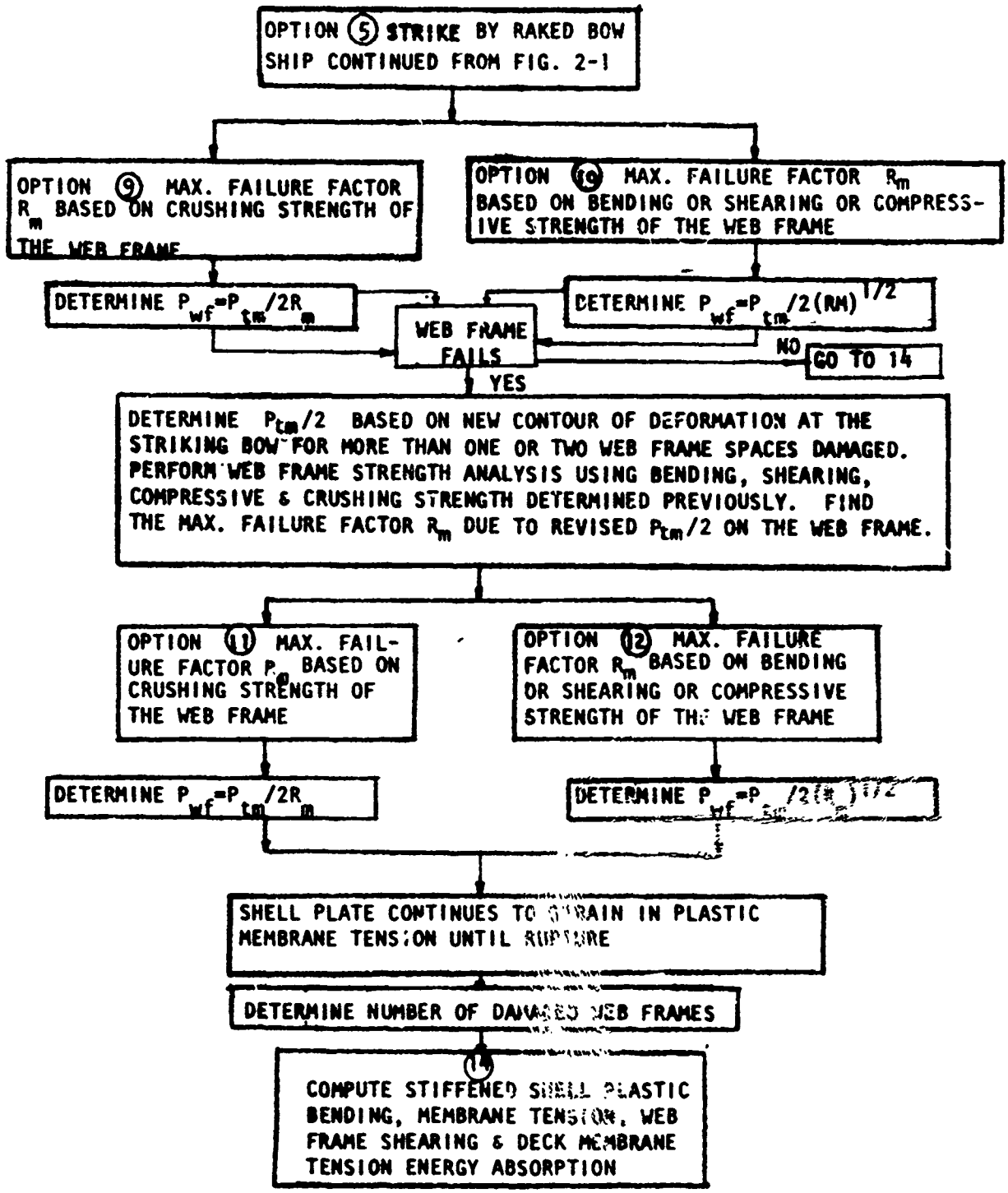

FIGURE 2-2 COLLISION ANALYSIS PROCEDURE FLOW DIAGRAM FOR SHIP STRUCK BY RAKED BOW SHIP

2.3 Step-by-Step Calculation Procedure

(1) Make a sketch which shows the principal characteristics pertaining to the struck ship and the striking ship (see page 3-2 for example).

(2) Show the geometry of the collision and scantlings of the struck ship section (see page 3-3).

(3) Provide the physical characteristics and properties of the shell longitudinals (page 3-4) which include:

(a) Basic dimensions of the shell longitudinals.

(b) Sectional area of longitudinals with portion of shell plate - A_s (in^2). Use Figure 2-3 to determine effective width of stiffened plate. However, the effective width is generally equal to the longitudinal stiffener spacing.

(c) Moment of intertia of longitudinals with portion of shell plate - I (in^4).

(d) Breadth of flange of T-beam or two times flanges of angle beam - b (in).

(e) Thickness of flange - t_f (in).

(f) Breadth - thickness ratio - b/t_f.

(g) Depth of web of longitudinal - d (in).

(h) Breadth-depth ratio - b/d.

(4) Assume only one or two (only with strike at a web) web frame spaces damaged. Analyze the plastic bending of the longitudinally stiffened shell plate (see page 3-5) as follows:

(a) Determine the yielded length of flange at beginning of local buckling from Figure 2-4 - L_y (in).

(b) Determine the distance from the load to the nearest support for a right-angle collision, or distance from the load to the support behind the load (in the direction opposite to the longitudinal direction of the strike) for an oblique collision - L' (in).

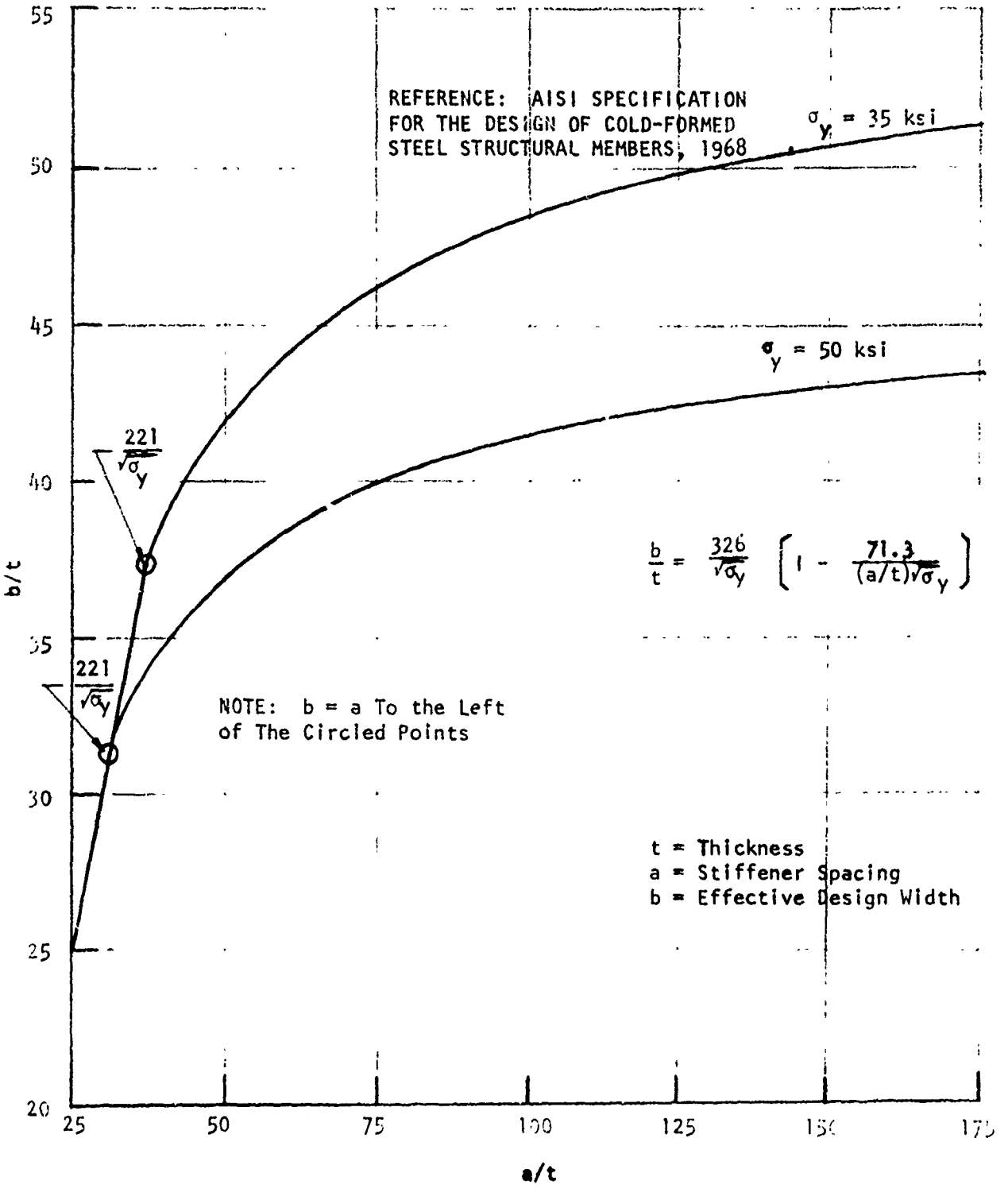

FIGURE 2-3 Chart for Determining Effective Width of Stiffened Plate in Axial Compression

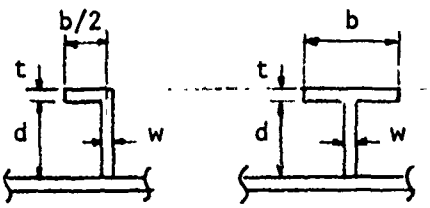

L_y = Yielded Length of Flange
At Beginning of Flange Local Buckling.

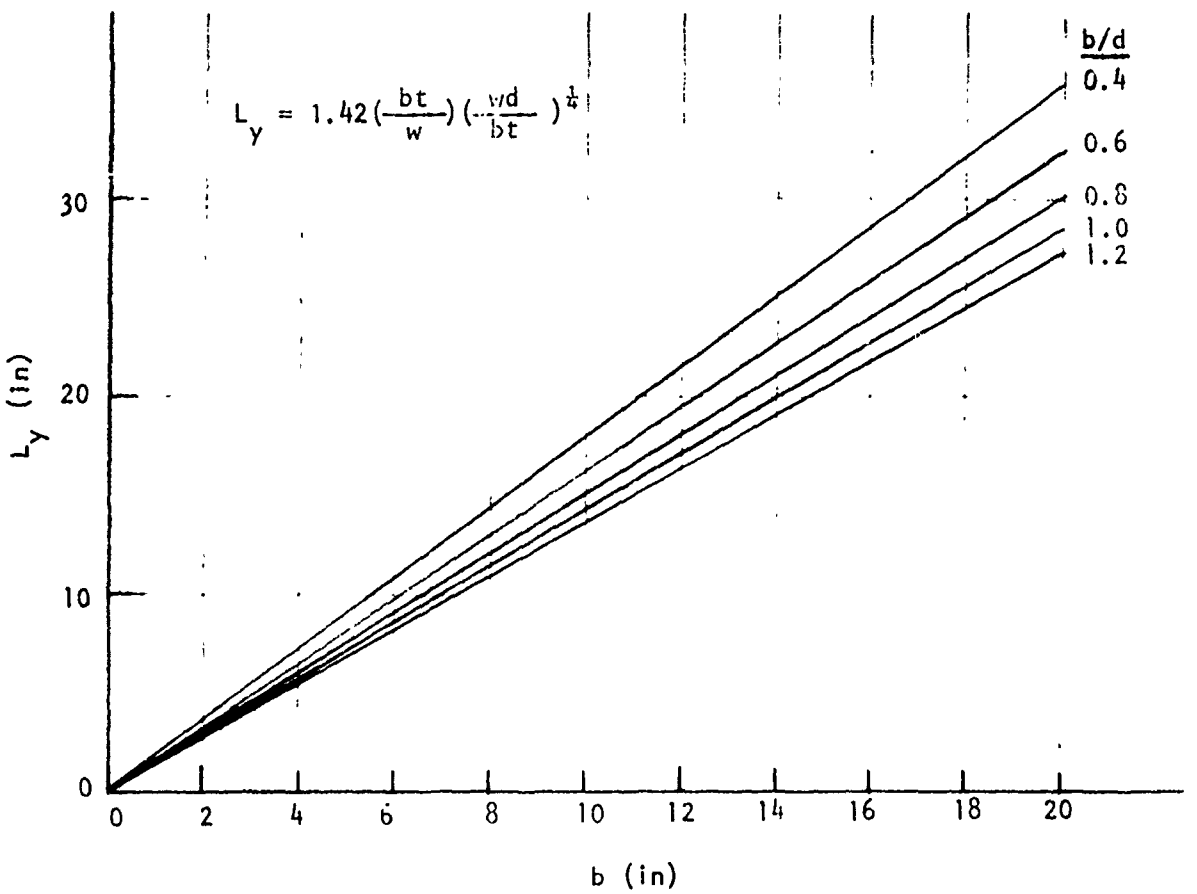

FIGURE 2-4 Charts to Determine Yielded Length of Flange at Beginning of Local Buckling

(c) Calculate the values of $\frac{2L_y}{L'}$ and $\frac{2L_y}{2L_y + L'}$.

(d) Calculate the values of constant A and constant B:

$$A = \left(\frac{2L_y}{2L_y + L'} \right) \left(\frac{52.2t}{0.5b\sqrt{\sigma_y}} \right) \leq \left(1 - \frac{\sigma_y}{\sigma_u}\right)$$

$$B = \left(\frac{2L_y}{L'}\right) \left(\frac{52.2t}{0.5b\sqrt{\sigma_y}}\right) \leq \left(\frac{\sigma_u}{\sigma_y} - 1\right)$$

(e) Calculate the rotation capacity constant k with

$$k = A \left(\frac{\varepsilon_{sh}}{\sigma_y/E} \right) + B \left(\frac{E}{2E_t} \right) .$$

The values of $\frac{\varepsilon_{sh}}{\sigma_y}$ and $\frac{E}{2E_t}$ may be obtained from Table 2-1.

(f) Calculate or obtain the plastic curvature M_p/EI from Figure 2-5 by entering the overall depth of the longitudinal.

(g) Calculate the capacity of plastic rotation angle θ_p:

$$\theta_p = k \left(\frac{M_p}{EI}\right)\left(\frac{L'}{2}\right) .$$

(h) Calculate the bending deflection capacity δ_{bc} :

$$\delta_{bc} = \theta_p \times L' .$$

(i) Calculate the plastic bending moment M_p :

$$M_p = \left(\frac{M_p}{EI} \right) EI .$$

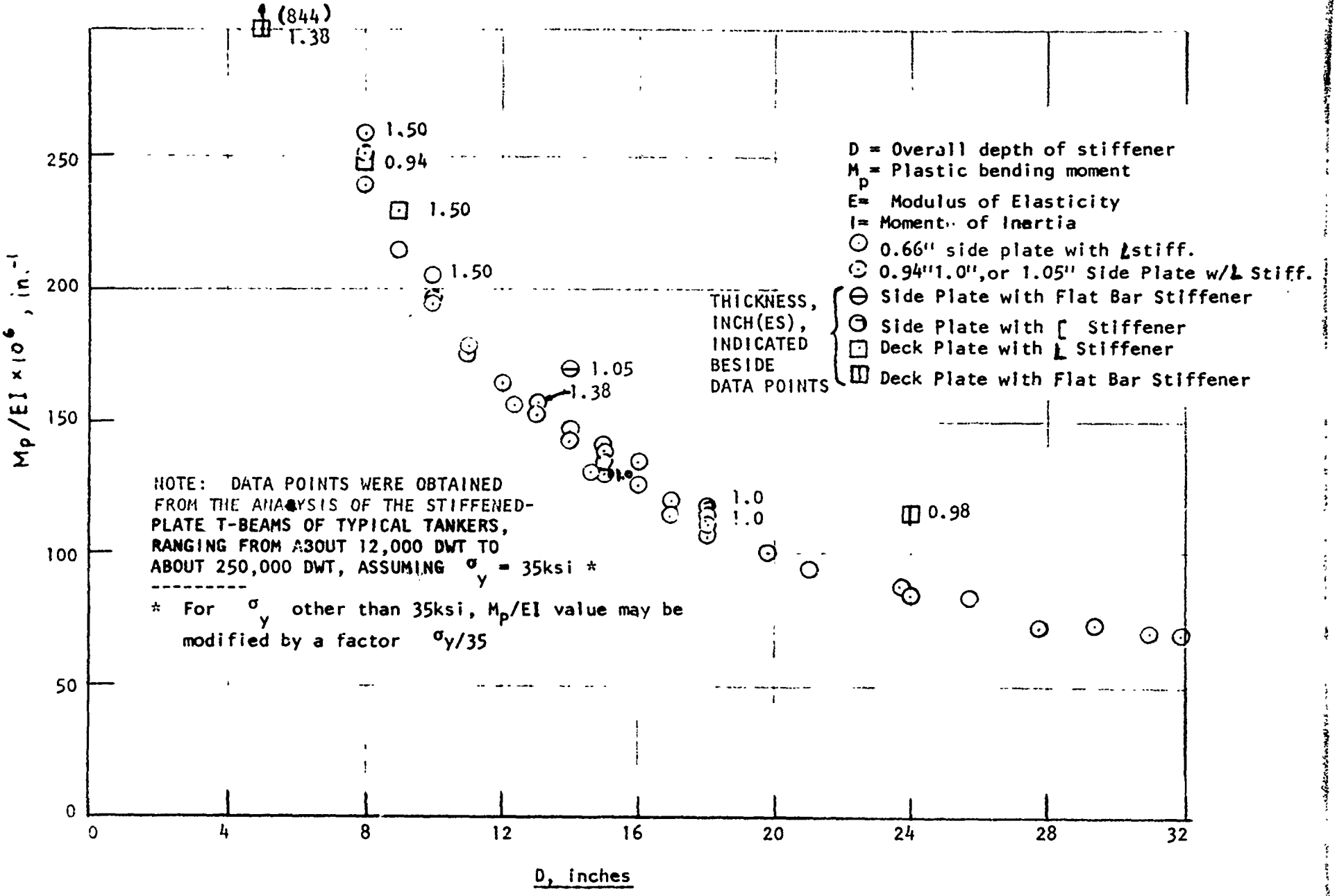

Figure 2-3 Chart to determine Approximate Value of Plastic Curvature

Table 2-1

MATERIAL PROPERTIES TYPICAL OF STEELS
WITH YIELD STRENGTHS OF 35 AND 50 KSI

Description	Item	Yield Strength σ_y = 35 ksi	Yield Strength σ_y = 50 ksi
Tensile Strength	σ_u	65 ksi	75 ksi
Strain-Hardening Strain	ε_{sh}	0.014 in./in.	0.021 in./in.
Modulus of Elasticity	E	29,000 ksi	29,000 ksi
Tangent Modulus	E_t	900 ksi	700 ksi
Factors in Equation for K	$\frac{\varepsilon_{sh}}{\sigma_y/E}$	11.6	12.2
	$E/2E_t$	16.1	20.7
Average Plastic-Range Stress	$(\sigma_y + \sigma_u)/2$	50.0 ksi	62.5 ksi
Plastic-Range Stress-to-Yield Ratio	$(\sigma_y + \sigma_u)/2\sigma_y$	1.43	1.25
Shear Yield Strength	τ_y	20.2 ksi	28.9 ksi
Maximum Shear Distortion for Plastic Energy	$\gamma_m = 2(\varepsilon_{sh} + \frac{\sigma_u - \sigma_y}{E_t})$	0.0947 rad	0.1134 rad

(j) Calculate the plastic bending energy capacity E_{bc} :

$$E_{bc} = 2M_p \left(1 + \frac{L'}{L''}\right) \left(\frac{\sigma_y + \sigma_u}{2\sigma_y}\right) \theta_p$$

The value of $\left(\frac{\sigma_y + \sigma_u}{2\sigma_y}\right)$ may be obtained from Table 2-1.

The total plastic bending energy in the longitudinally stiffened side structure is then determined by summing of these values for each longitudinal. If the deformation of the longitudinal, δ, is less than δ_{bc}, the plastic bending energy is

$$E_{bc} = E_{bc} \left(\frac{\delta}{\delta_{bc}}\right)$$

(k) Calculate the lateral force required for bending only:

$$P_b = \frac{E_{bc}}{\delta_{bc}} + \left(\begin{array}{l}\text{resistance of web frame}\\ \text{directly at strike if any}\end{array}\right) .$$

The forces on the webs at each end of L_t are:

$$\frac{P_b L'' + M_p}{L_t} \quad \text{and} \quad \frac{P_b L' + M_p}{L_t}$$

to the nearest and farthest flanking the strike respectively.

It is unlikely for actual ship structures that the forces on the web frames at the ends of L due to bending are large enough to cause failure of the web frames, as indicated in Figure 2-1. For this reason the analysis to follow if they do fail is not described in detail here. If it is suspected that the forces developed are large enough to cause failure of the web frames, the procedure

for web frame strength determination presented in step (7) should be followed using the forces on the webs determined above. Then the sequence of steps given in Figure 2-1 should be completed (longitudinal bending over a length greater than L_t).

(5) Assume only one or two web frame spaces damaged. Analyze the plastic membrane-tension action of the longitudinally stiffened side plates as follows (see page 3-6):

(a) Enter $\varepsilon_r = 0.10 \frac{D}{32\%}$ for strain limit within the longitudinal length L_t.

(b) Calculate the membrane-tension deflection capacity for the longitudinally stiffened side within the length L_t for the purpose of determining the maximum deflection of the most highly strained T-beam (assume $\varepsilon_c = 0$):

$$\delta_{tc} = \sqrt{\frac{2L'L''}{L_t}(L'\varepsilon_r + L''\varepsilon_\ell + L_t\varepsilon_c) + \delta_{bc}^2}$$

ε_ℓ = average strain over L''

(c) Calculate the average membrane tension force:

$$T = A_s\sigma_y\left(\frac{\sigma_y + \sigma_u}{2\sigma_y}\right)$$

(d) Choose the values of δ_m to match the striking bow configuration. The values of δ_m are limited to δ_{tc}.

(e) Calculate the lateral force due to membrane-tension only:

$$P_{tm} = \frac{T \cdot L_t \cdot \delta_m}{L'L''} .$$

(6) Analyze the bending, shearing, compressive and crushing loads due to membrane tension forces acting on the web frame (see page 3-7), assuming only 1 or 2 web frame spaces damaged.

(a) Make a sketch which shows the imposed lateral loads

$$\frac{T\delta_m}{L^2} \text{ or } \frac{T\delta_m}{L^2}$$

acting on nearest and farthest web frame from strike respectively, within L_t.

(b) Calculate the bending moment, shearing, compressive and crushing force at each shell longitudinal (see pages 3-8 through 3-10).

(7) Analyze the strength of web frame as follows:

(a) Bending strength calculation (see pages 3-95 through 3-97)

(i) Determine the effective breadth of shell plate, b, from Figure 2-3 by entering with a/t and σ_y .

(ii) Calculate the section modulus of the longitudinal with an effective breadth of shell plate.

(iii) Calculate the bending strength, $M_{P_{wf}}$ (in kips):

$M_{P_{wf}}$ = S.M. x σ_y x factor for plastic bending

(factor for plastic bending = 1.12 for I Section).

(b) Shear strength calculation (see page 3-98)

(i) Obtain the critical elastic shear buckling stress τ_{cr} of web frame from Figure 2-6 by entering with d/t and d/a

(ii) Calculate $\tau_y = 0.58\sigma_y$

(iii) Determine the tensile stress σ_{ty} at tension field yielding from Figure 2-7 by entering with τ_{cr} and σ_y (for $\tau_{cr} < \tau_y$ only).

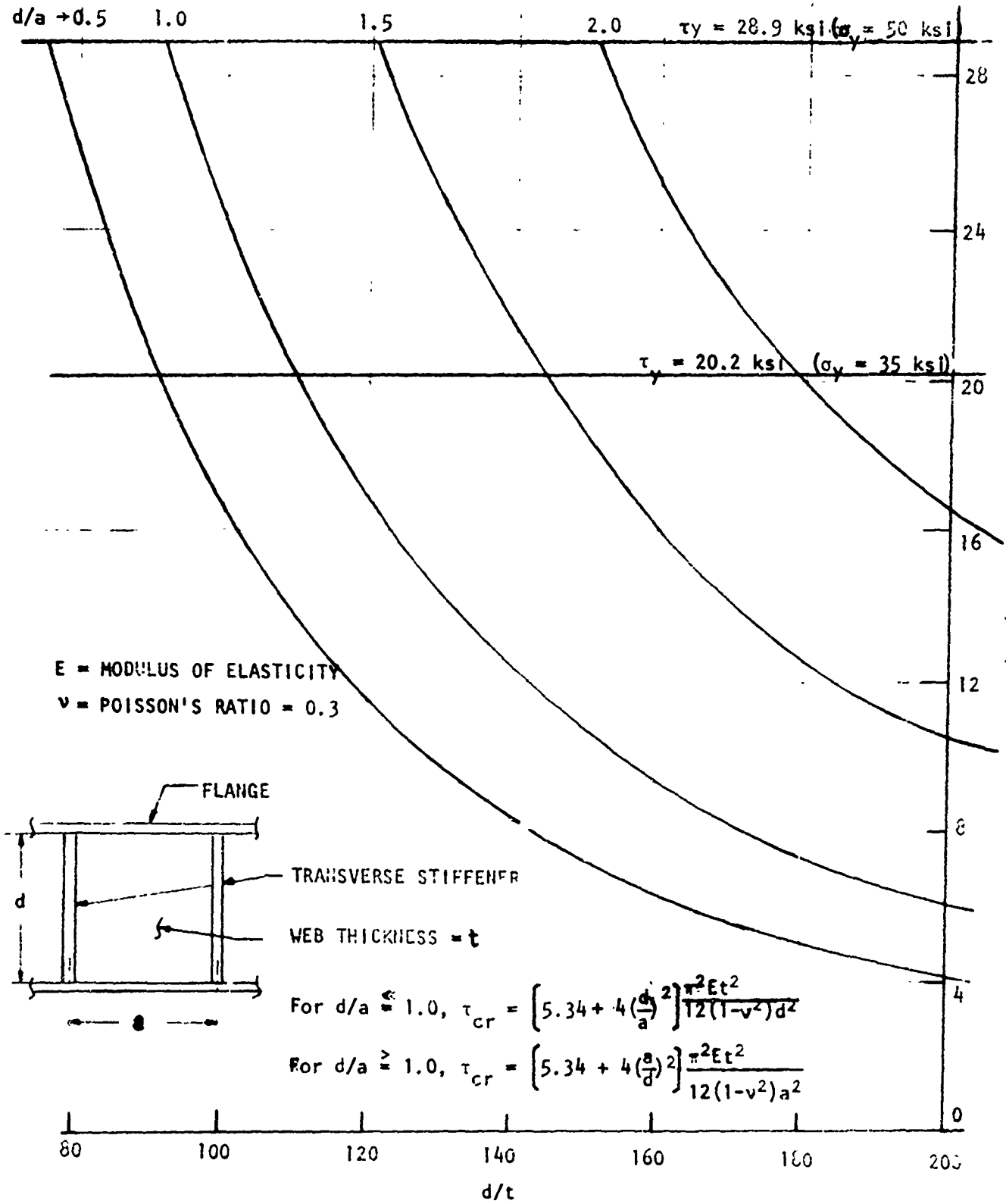

FIGURE 2-6 Chart to Determine Web Frame Critical Elastic Shear Buckling Stress

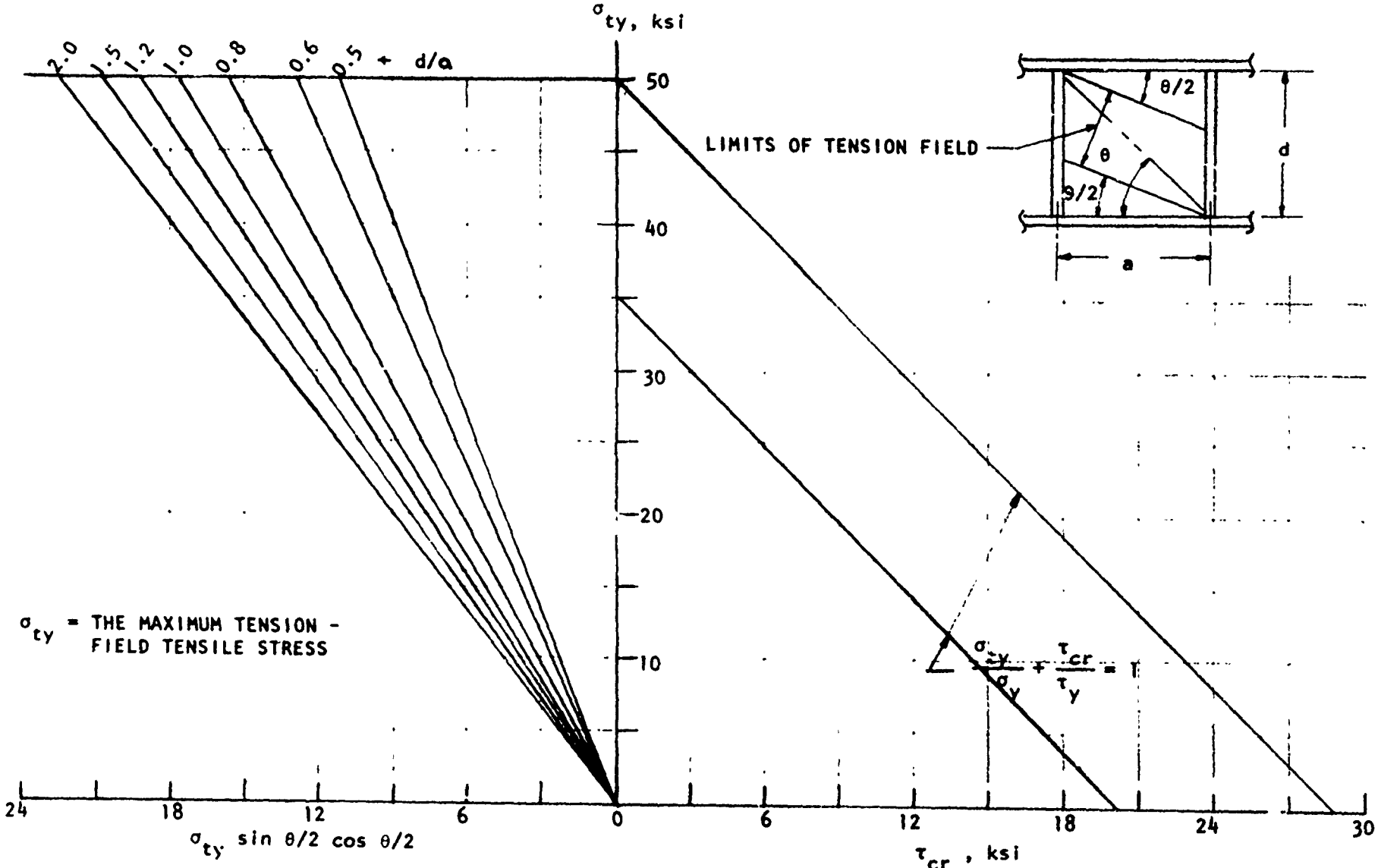

Figure 2-7 Chart to Determine ($\tau_{cr} + \sigma_{ty} \sin \theta/2 \cos \theta/2$) in the Web Frame Shearing Energy Equation

(iv) Calculate the shear strength V_p.

For $\tau_{cr} < \tau_y$:

$$V_p = \tau_{cr} \cdot d \cdot t + (\sigma_{ty} \sin \frac{\theta}{2} \cos \frac{\theta}{2}) \cdot t \cdot (d - a \tan \frac{\theta}{2})$$

The value of $\sigma_{ty} \sin \frac{\theta}{2} \cos \frac{\theta}{2}$ can be obtained from Figure 2-7, and $\theta = \tan^{-1} \frac{d}{a}$.

For $\tau_{cr} > \tau_y$:

$$V_p = \tau_y dt$$

(c) Compression strength at strut of web frame (see page 3-99)

(i) Calculate the slenderness ratio L_c/r_m of the strut.

(ii) Determine the thrust-area ratio P_m/A_c from Figure 2-8.

(iii) Compute the compression strength P_m of the strut.

(d) Crushing strength at web frame stiffener (see page 3-100)

(i) Determine the effective breadth b from Figure 2-3 by entering $\frac{a}{t}$ and σ_y where a is stiffener spacing.

(ii) Calculate the slenderness ratio of the stiffener L_c/r_m.

(iii) Obtain P_m/A_c from Figure 2-8 by entering L_c/r_m and σ_y.

(iv) Calculate crushing strength P_m of the web frame stiffener:

$$P_m = (P_m/A_c) \cdot A_c$$

(8) Based on only one or two web frame spaces damaged, compute the factors R (imposed lateral load of step 6 divided by web frame capacity for resisting the force) given in Figure 2-9 (also see page 3-11). R_m is the maximum value of R.

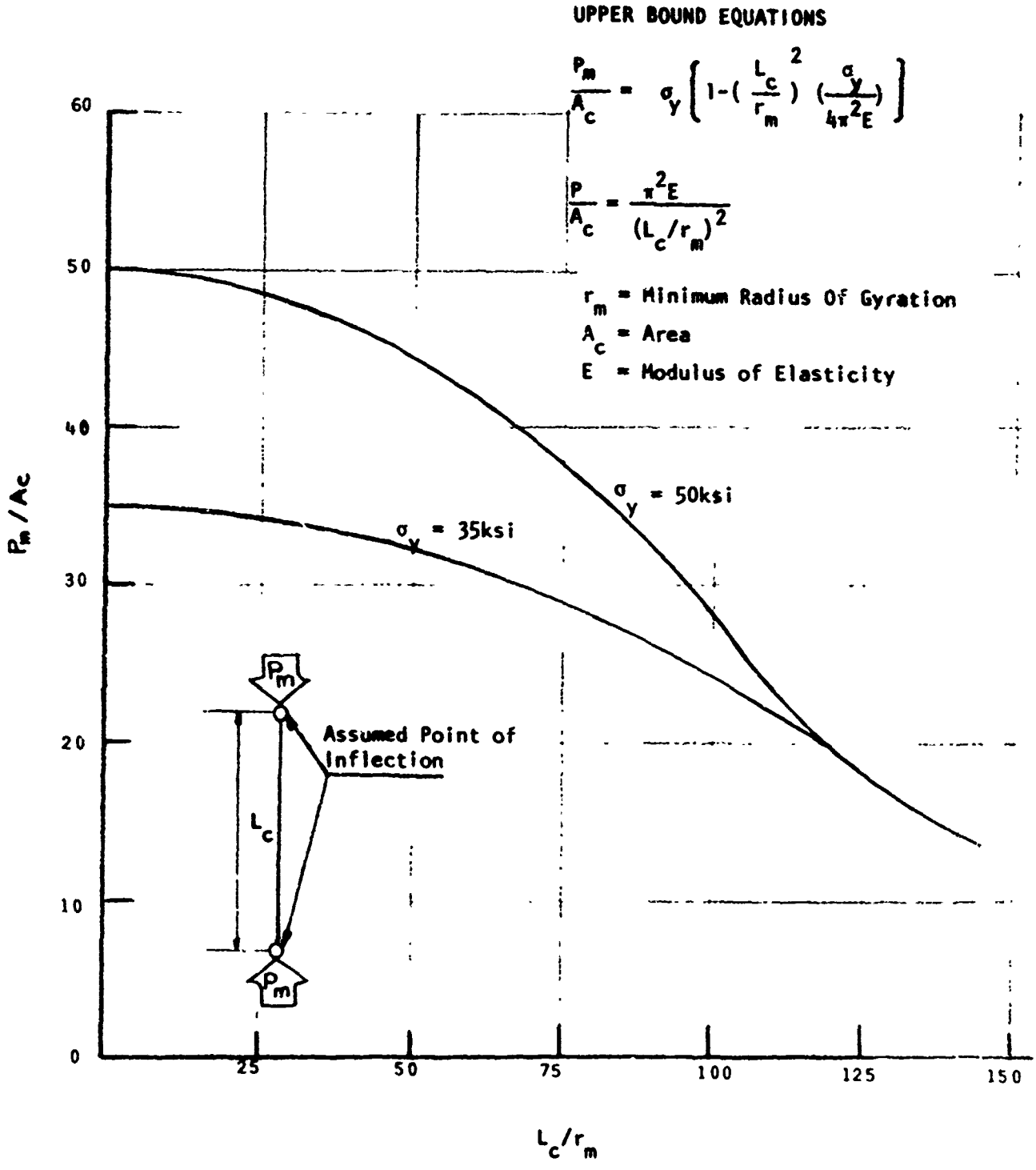

Figure 2-8 Chart for Determining Thrust in Web-Frame Intermediate Strut during Shortening of Distance between Ends

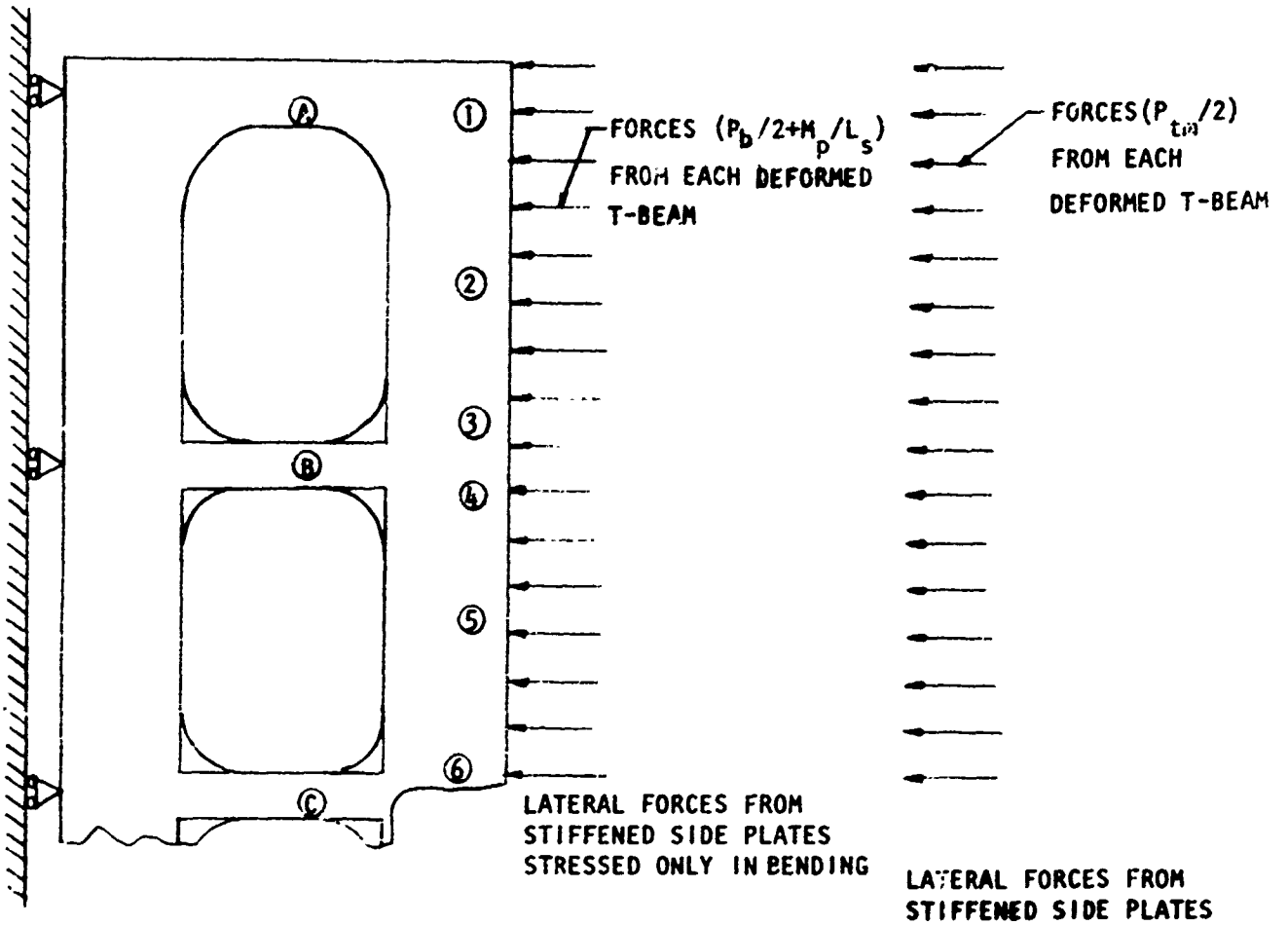

STEPS IN DETERMINING FORCES P_{wf} FROM EACH STIFFENED SIDE PLATE T-BEAM, STRESSED EITHER ONLY IN BENDING OR ONLY IN MEMBRANE TENSION, SUFFICIENT TO INITIATE WEB FRAME FAILURE :

I. DETERMINE:

R_1 = THRUST IN STRUT Ⓐ/P_m R_2 = THRUST IN STRUT Ⓑ/P_m R_3 = THRUST IN STRUT Ⓒ/P_m

R_4 = MOMENT AT ① /M_{pwf} R_5 = MOMENT AT ② /M_{pwf} R_6 = MOMENT AT ③ /M_{pwf}

R_7 = MOMENT AT ④ /M_{pwf} R_8 = MOMENT AT ⑤ /M_{pwf} R_9 = MOMENT AT ⑥ /M_{pwf}

R_{10} = TRANSVERSE SHEAR AT ① /V_p AT ① R_{11} = TRANSVERSE SHEAR AT ③ /V_p AT ③

R_{12} = TRANSVERSE SHEAR AT ④ /V_p AT ④ R_{13} = TRANSVERSE SHEAR AT ⑤ /V_p AT ⑥

NOTE: M_{pwf} = PLASTIC MOMENT CAPACITY OF WEB FRAME AND SIDE PLATE

P_m = COLUMN ACTION STRUT CAPACITY

II. SELECT R_m THE MAXIMUM VALUE OF R. FOR EACH T-BEAM P_{wf} IS COMPUTED:

FOR STIFFENED SIDE PLATES STRESSED ONLY IN BENDING, $P_{wf}=(P_b/2+M_p/L_s)/R_m$

FOR STIFFENED SIDE PLATES STRESSED ONLY IN MEMBRANE TENSION,

$$P_{wf}=(P_{tm}/2)/R_m$$

FIGURE 2-9 Analysis of Lateral Forces Sufficient to Initiate Web Frame Failure

(9) Compute the actual damaged length

(a) If $R_m < 1.0$ the web frames flanking the strike do not distort, and the damaged ler does not exceed one or two web frame spaces.

(b) Otherwise, calculate P_{wf} from the value of $\frac{T\delta_m}{L''}$ or $\frac{T\delta_m}{L'}$ and the corresponding R_m from (8).

$$P_{wf} = \frac{T\delta_m}{L'R_{m'}} \text{ or } \frac{T\delta_m}{L''R_{m''}} .$$

(c) Compute the number of web frames damaged

$= n + m$ where: n = integer $> (R_{m'} - 1)$

m = integer $> (R_{m''} - 1)$

(d) Select the actual number of web frames damaged in accordance to the location of strike relative to adjacent bulkheads.

(10) Based on the actual damaged length, analyze the plastic membrane tension action in accordance with Figure 2-10

(a) Develop an equation for δ in terms of P_{wf}, L', L'', ε_r, L_{d_a}, L_{d_b}, T_a, T_b and L_t in accordance with Figure 2-10. Note that in the example calculation the equation for δ is in terms of δ_1, defined as:

$$\delta_1 = \frac{P_{wf}L_t}{2T} .$$

(This intermediate variable δ_1 was omitted from Figure 2-10 by suitable algebraic substitutions.)

(b) Compute δ, average strain ε, maximum bend angle and ε_1 (see pages 3-101 through 3-104).

(c) Calculate e_t and plastic membrane tension energy E_{mt} according to Figure 2-10.

(11) For collision analysis with a raked bow striking ship, the flow diagram of Figure 2-2 is to be followed (see pages 3-19 and 3-20).

(12) For an oblique collision calculate the energy absorbed in a traveling plastic hinge (see page 3-67).

(a) Calculate the longitudinal resisting force

$$F_R = \frac{\sigma_y d}{R}\left[dt_w\left(1 - \frac{\sigma_y R}{dE}\right)^2 + t_f(b - t_w)\left(\frac{d - 0.5t_f}{d} - \frac{\sigma_y R}{dE}\right)\right] \text{ (kips)}$$

where R is the radius of the striking bow.

(b) Calculate the energy absorption due to F_R as:

$F_R \cdot \delta/\tan\alpha$ (in-kips)

where α is the collision angle.

(13) Calculate the shear energy absorbed by distorted web frames (see page 3-12)

$$E_{ps} = R_s(adt)\ (\gamma - \gamma_e)\left(\tau_{cr} + \sigma_{ty} \sin\frac{\theta}{2}\cos\frac{\theta}{2}\right) \quad (\text{for } \tau_{cr} < \tau_y)$$

$$E_{ps} = (adt)\left(\gamma - \frac{\tau_y}{11{,}150}\right)(\tau_y) \quad (\text{for } \tau_{cr} > \tau_y)$$

where a, d, and t are, respectively, the panel length, depth, and thickness, as shown in Figures 2-11 and 2-12, and R_s is proportion of web plate that is plastically deformed during in-plane shearing failure.

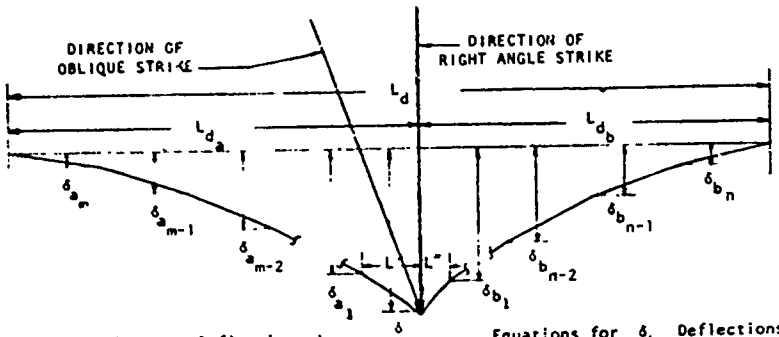

FIGURE 2-10 MEMBRANE TENSION - SINGLE SHELL

Equations for δ_{a_m} Deflections:*

$$\delta_{a_m} = \frac{L_s}{L_{d_a}}\left\{\delta - \frac{P_{wf}}{T_a}\left[m L' + \sum_{q=1}^{m-1} q L_s\right]\right\}$$

$$\delta_{a_{m-1}} = 2\delta_{a_m} + \frac{P_{wf} L_s}{T_a}$$

$$\delta_{a_{m-2}} = 3\delta_{a_m} + \frac{3 P_{wf} L_s}{T_a}$$

$$\delta_{a_1} = m\delta_{a_m} + \sum_{q=1}^{m-1} q \frac{P_{wf} L_s}{T_a}$$

Equations for δ_{b_n} Deflections:*

$$\delta_{b_n} = \frac{L_s}{L_{d_b}}\left\{\delta - \frac{P_{wf}}{T_b}\left[n L'' + \sum_{q=1}^{n-1} q L_s\right]\right\}$$

$$\delta_{b_{n-1}} = 2\delta_{b_n} + \frac{P_{wf}}{T_b} L_s$$

$$\delta_{b_{n-2}} = 3\delta_{b_n} + 3\frac{P_{wf}}{T_b} L_s$$

$$\delta_{b_1} = n\delta_{b_n} + \sum_{q=1}^{n-1} q \frac{P_{wf}}{T_b} L_s$$

Equation for Membrane Tension Elongation.

$$e_t = \frac{\delta_{a_m}^2}{2L_s} + \frac{\left(\delta_{a_{m-1}} - \delta_{a_m}\right)^2}{2L_s} + \cdots + \frac{\left(\delta_{a_1} - \delta_{a_2}\right)^2}{2L_s} + \frac{\left(\delta - \delta_{a_1}\right)^2}{2L'} + \frac{\delta_{b_n}^2}{2L_s} + \frac{\left(\delta_{b_{n-1}} - \delta_{b_n}\right)^2}{2L_s} + \cdots + \frac{\left(\delta_{b_1} - \delta_{b_2}\right)^2}{2L_s} + \frac{\left(\delta - \delta_{b_1}\right)^2}{2L''} \leq (L_{d_a} + L_{d_b})\,\epsilon_r .$$

For a first trial calculation assume:

$$e_t = (L_{d_a} + L_{d_b})\,\epsilon_r$$

*NOTE: For oblique collisions the following assumptions should be made:

1) $L_{d_b} = 0$ 2) $T_a = 2T_b$

Membrane Tension Plastic Energy (Including Energy in Flanking Span):

For Right Angle Strike: $E_{mt} = T(K_a e_t + K_e L_s \epsilon_r)$

For Oblique Strike. $E_{mt} = T_a(K_a e_t + 0.5\, K_e L_s \epsilon_r) + F_R \frac{\delta}{\tan\alpha}$ [Energy due to elastic deformation ahead of strike is neglected]

DEFINITIONS

A_s = cross-sectional area of T-beam

L_d = length of damage between undistorted web frames or bulkheads, measured in the longitudinal direction

L_{d_a} = length of damage to left of strike or behind strike in oblique collision

L_{d_b} = length of damage to right of strike or ahead of strike in oblique collision

L' = distance from strike to nearest web frame or bulkhead to left of strike

L'' = distance from strike to nearest web frame or bulkhead to right of strike

L_s = web frame spacing

δ = total lateral deflection at strike point

δ_{a_m} = lateral deflection of m^{th} web frame from strike to the left

δ_{b_n} = lateral deflection of n^{th} web frame from strike to the left

P_{wf} = load exerted by the most highly strained stiffened-plate T-beam unit on a web frame at the instant that the web frame yields or buckles

T = average membrane tension throughout the damaged length = $A_s\sigma'$

T_a = membrane tension to left of strike or behind strike in oblique collision ($T_a = T$ for right angle or oblique strike)

T_b = membrane tension to right of strike or ahead of strike in oblique collision ($T_b = T$ for right angle strike, $T_b = \frac{1}{2}T$ for oblique strike)

e_t = total strain in damaged length

$\epsilon_r = .10(\frac{D}{32t})$

ϵ = average longitudinal strain in hull throughout the damaged length

$K_a = \epsilon/\epsilon_r$

K_e = ratio of (1) strain in the web frame spaces adjacent to the undistorted web frames or bulkheads bounding the damaged length to (2) ϵ_r.

F_R = force required to propagate longitudinally the yield line at the strike

α = angle of collision measured from the struck ship undeformed side shell behind the strike point to the centerline of the striking ship

n = number of damaged web frames to the right of the strike

m = number of damaged web frames to the left of the strike

σ' = $0.5\,(\sigma_y + \sigma_u)$ = average plastic stress

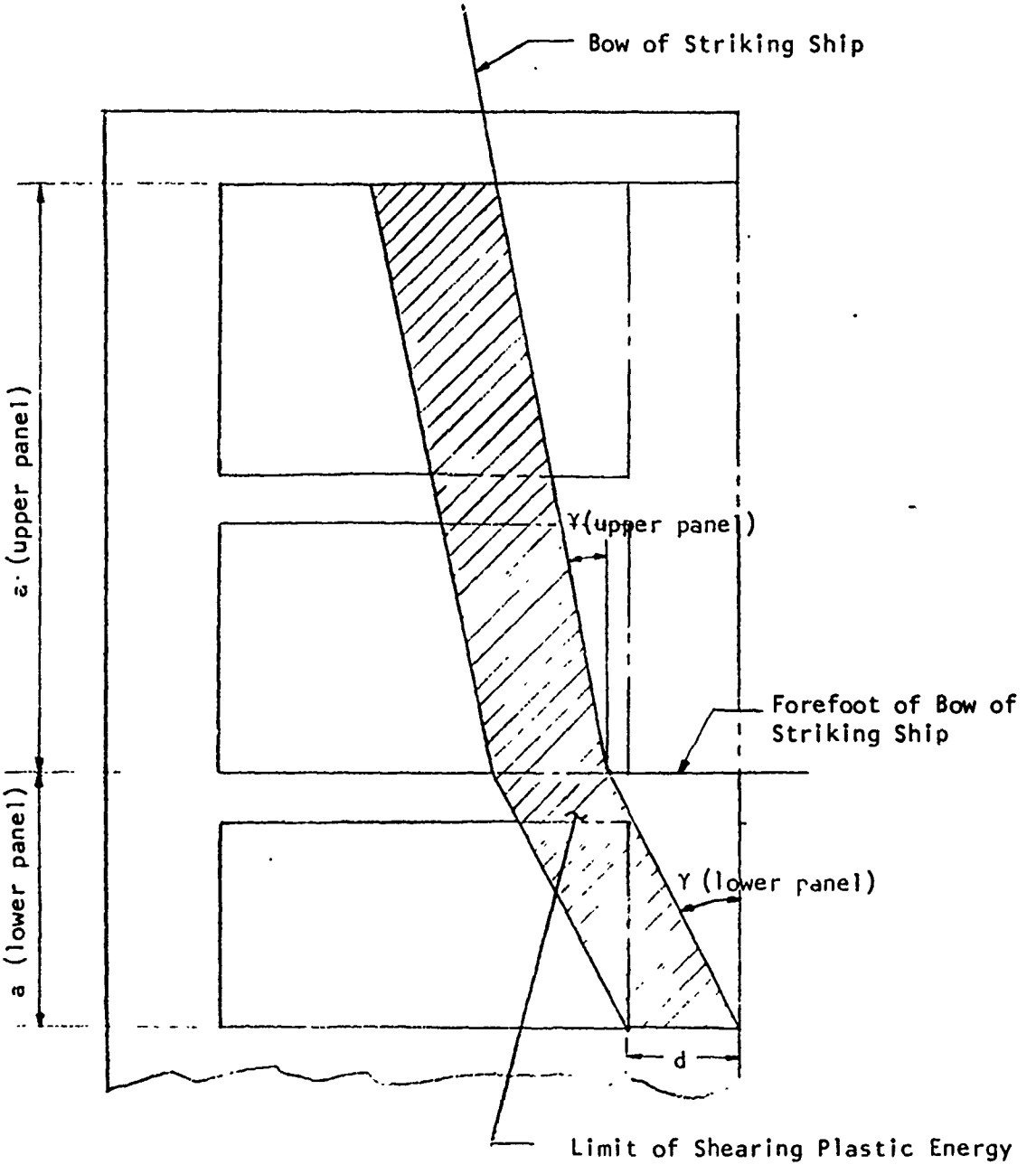

TRANSVERSE SECTION AT WEB FRAME

Figure 2-11 Plastic Energies Associated with Given Web Frame Distortions for Raked Striking Bow

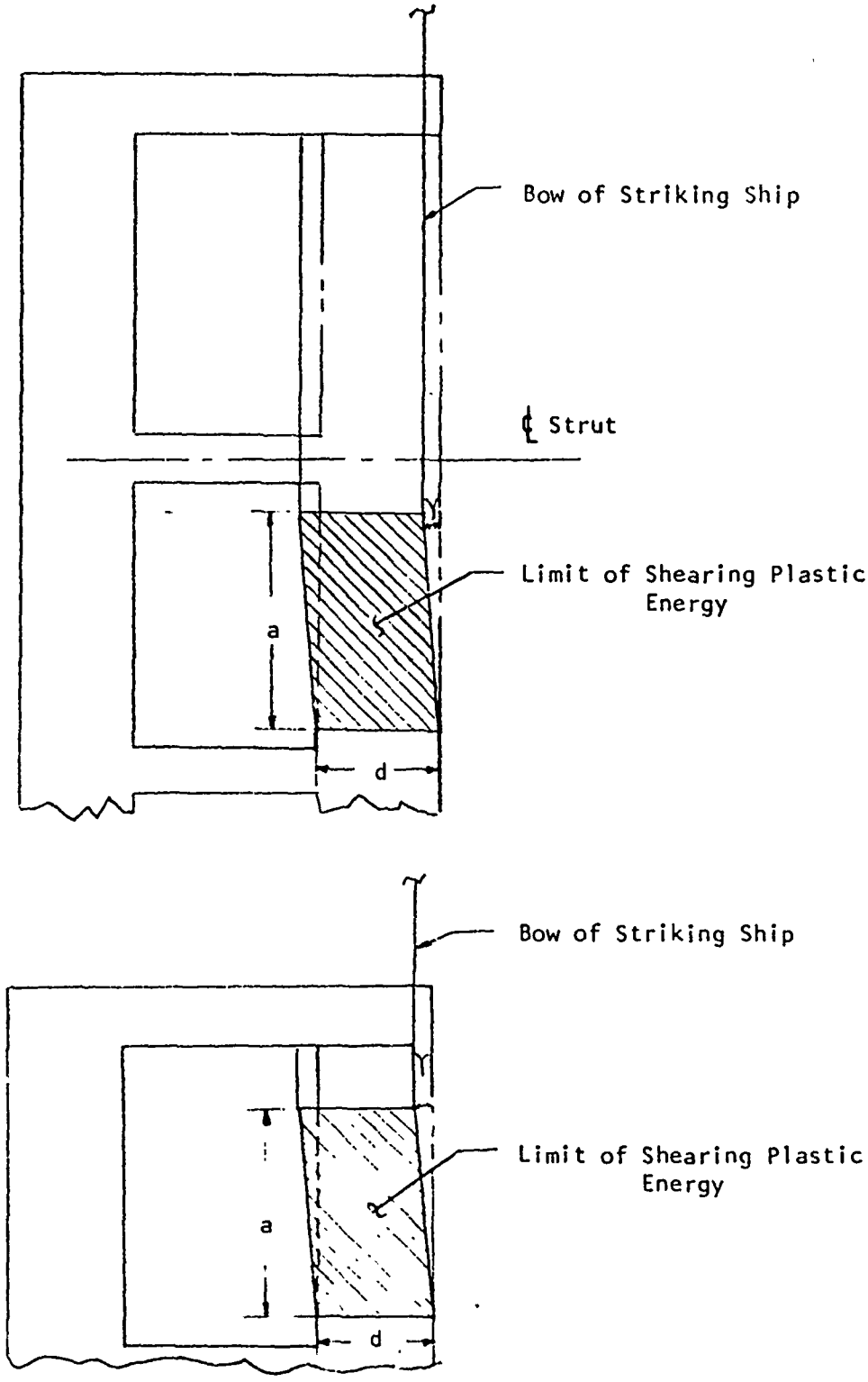

TRANSVERSE SECTIONS AT WEB FRAME

FIGURE 2-12 Plastic Energies Associated with Given Web Frame Distortions for Vertical Striking Bow

(14) Calculate the plastic membrane tension energy due to deck deformation (see page 3-13).

(a) Using the maximum deformation computed in 9(f) above, determine the number of deck longitudinals damaged:

$$\frac{\delta}{\text{Spacing of deck longitudinals}}$$

(b) Compute the average strain and energy absorption for each deck longitudinal together without the effective breadth of the deck plate. The average strain is assumed equal to that in the sideshell longitudinal adjacent to the deck as calculated in 9(f) reduced by the square of the ratio of the deck longitudinal overall deflection (i.e., its maximum inboard deflection) to the overall sideshell longitudinal deflection.

(c) Summarize total deck energy absorption.

(15) The ductile tearing energy absorbed by the outer shell of a double shell struck ship.

(a) Calculate the outer shell ductile tearing energy as: vertical side shell length x side shell thickness x 12 (in-kips)

(b) Calculate the deck ductile tearing energy as: (maximum lateral deflection at deck + distance between outer and inner shell) x deck thickness x 12 (in-kips) (This assumes that when the outer shell tears, the deck will do likewise up to the inner hull.)

3. COLLISION ANALYSIS EXAMPLES

3.1 CASE I - RIGHT ANGLE COLLISION - STRUCK BY VERTICAL BOW

SUMMARY OF PLASTIC ENERGY ABSORBED BEFORE SHELL PLATE RUPTURE — STRUCK MIDSPAN BETWEEN WEB FRAMES & BULKHEADS BY VERTICAL BOW, 7 WEB FRAME SPACES BETWEEN BULKHEADS.

	ENERGY (IN-KIPS)
E_{bc} = PLASTIC BENDING ENERGY IN LONG'L. STIFFENED SIDE	= 6,517
E_{mt} = MEMBRANE TENSION PLASTIC ENERGY IN LONG'L. STIFFENED SIDE	= 2,979,298
E_{ps} = SHEARING PLASTIC ENERGY IN WEB FRAMES	= 79,031
E_d = DECK MEMBRANE TENSION PLASTIC ENERGY	= 472,890
TOTAL ENERGY ABSORBED	= 3,533,736 IN-KIPS

SHELL — SINGLE

SIDE SHELL PLATE = 1" M.S
DECK PLATE = 1⅜" M S

Preceding page blank

CASE I — RIGHT ANGLE COLLISION - STRUCK BY VERTICAL BOW

CONFIGURATION OF THE STRIKING & THE STRUCK SHIP

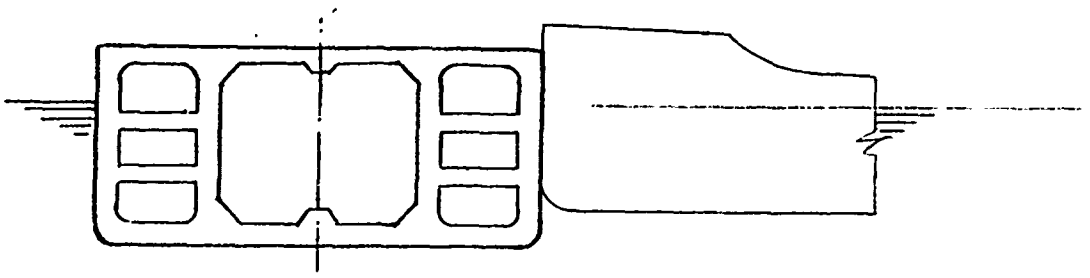

	STRUCK SHIP	STRIKING SHIP
TYPE	TANKER	TANKER
DWT	120,000 TONS	15,000 TONS
L	900.0 FT	500 FT
B	147.5 FT	68 FT
D	63.5 FT	39 FT
d	48.5 FT	30 FT

NOTE:

1. STRUCK SHIP'S WEB SPACING (L_s) EQUALS 12 FEET; SINGLE SHELL 1" M.S
2. STRIKING SHIP HAS VERTICAL BOW
3. THE TANKER IS STRUCK MIDSPAN BETWEEN WEB FRAMES & BULKHEADS AT RIGHT ANGLE, DISTANCE BETWEEN ADJACENT BULKHEADS IS 7 WEB FRAME SPACES.
4. DECK PLATE = 1 3/8 M.S

CASE I - RIGHT ANGLE COLLISION - STRUCK BY VERTICAL BOW

SCANTLINGS IN WAY OF WEB FRAME

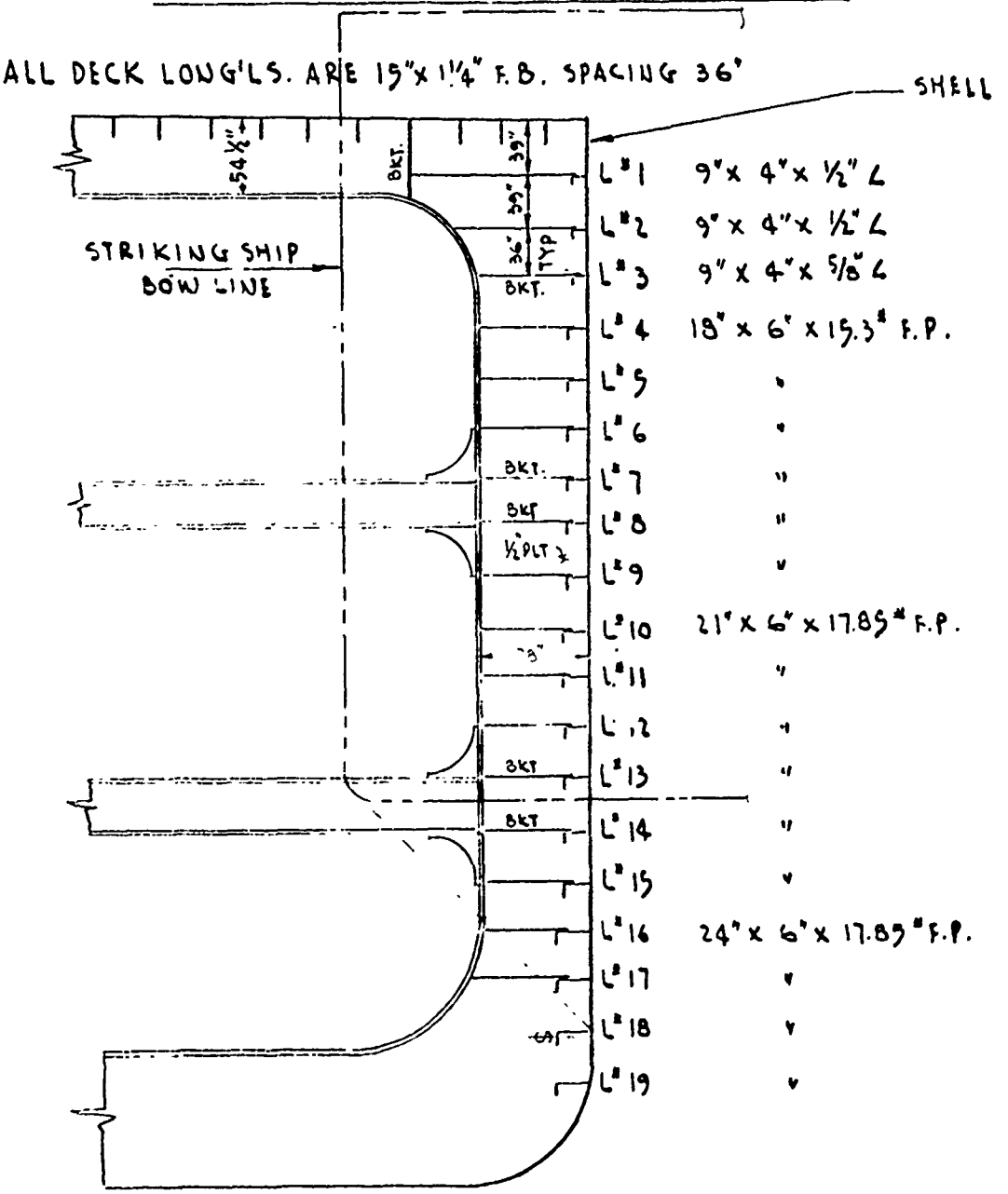

SIDE LONGITUDINAL SPACING = 36"
EXCEPT AS NOTED.

CASE I – RIGHT ANGLE COLLISION - STRUCK BY VERTICAL BOW.

SHELL LONGITUDINAL NO.	1	2	3	4	5	6	7	8	9	10	11	12	13	14	15	16	17	REMARK
BASIC DIMENSIONS	9"x6"x½" ∠	9"x6"x½" ∠	9"x6"x⅜" ∠	18"x6"x 19.5°F.P	18"x6"x 19.5°F.P	18"x6"x 19.5°F.P	18"x6"x 19.5°F.P	18"x6"x 19.5°F.P	18"x6"x 19.5°F.P	21"x6"x 17.85°F.P	21"x6"x 17.85°F.P	21"x6"x 17.85°F.P	21"x6"x 17.85°F.P	21"x6"x 17.85°F.P	21"x6"x 17.85°F.P	24"x6"x 17.85°F.P	24"x6"x 17.85°F.P	
A_s = SECTIONAL AREA OF LONG'L WITH PORTION OF SHELL PLT (in²)	4.45	4.30	4.37	4.49	4.49	4.49	4.49	4.49	4.49	4.76	4.76	4.76	4.76	4.76	4.76	4.90	4.90	
I = MOMENT OF INERTIA OF LONG'L WITH PORTION OF SHELL PLT (in⁴)	274	261	307	1,263	1,263	1,263	1,263	1,263	1,263	2,060	2,060	2,060	2,060	2,060	2,060	2,836	2,836	
b = BREADTH OF FLANGE (in) = 2 × FLANGE OF T.P. OR ANGLE	8	8	8	12	12	12	12	12	12	12	12	12	12	12	12	12	12	
t_f = THICKNESS OF FLANGE (in)	0.300	0.300	0.315	0.375	0.375	0.375	0.375	0.375	0.375	0.438	0.438	0.438	0.438	0.438	0.438	0.438	0.438	
b/t_f = BREADTH - THICKNESS RATIO	16.0	16.0	12.8	32.0	32.0	32.0	32.0	32.0	32.0	27.4	27.4	27.4	27.4	27.4	27.4	27.4	27.4	
d = DEPTH OF WEB OF LONGITUDINAL (in)	9	9	9	18	18	18	18	18	18	21	21	21	21	21	21	24	24	
b/d = BREADTH - DEPTH RATIO	0.89	0.89	0.89	0.67	0.67	0.67	0.67	0.67	0.67	0.57	0.57	0.57	0.57	0.57	0.57	0.50	0.50	

CASE I - RIGHT ANGLE COLLISION - STRUCK BY VERTICAL BOW

SHELL LONGITUDINAL NO.	1	2	3	4	5	6	7	8	9	10	11	12	13	14	15	16	17	REMARK
L_y = YIELD LENGTH FIG. 2-5	12.0"	12.0"	12.0"	18.9"	18.9"	18.9"	18.9"	18.9"	18.9"	19.6"	19.6"	19.6"	19.6"	19.6"	19.6"	20.5"	20.5"	
L'	72.0"																	
$\frac{2L_y}{L'}$	0.33	0.33	0.33	0.53						0.54						0.57	0.57	
$\frac{2-y}{2-y+L'}$	0.25	0.25	0.25	0.34						0.35						0.36	0.36	
CONSTANT A $\left(\frac{2L_y}{L'}\right)\left(\frac{52.2\,\xi}{0.9\,\sigma_y}\right)\leq\left(1-\frac{\sigma_y}{\sigma_u}\right)$	0.28	0.28	0.34	0.19						0.23						0.24	0.24	
CONSTANT B $\left(\frac{2L_y}{L'}\right)\left(\frac{52.2\,\xi}{0.9\,\sigma_y}\right)\leq\left(\frac{\sigma_u}{\sigma_y}-1\right)$	0.36	0.36	0.65	0.29						0.35						0.37	0.37	
ROTATION CAPACITY CONST. $K = A(11.6 + 15.1B)$	4.87	4.87	6.81	3.09						3.96						4.21	4.21	
PLASTIC CURVATURE M_p/EI	221 $\times 10^{-6}$	221 $\times 10^{-6}$	220 $\times 10^{-6}$	106 $\times 10^{-6}$						94 $\times 10^{-6}$						85 $\times 10^{-6}$	85 $\times 10^{-6}$	THESE ARE CALCULATED VALUES, FIG 2-4 MAY BE USED.
PLASTIC ANGLE CHANGE CAP. $\theta_p = K\left(M_p/EI\right)\left(L'/2\right)$	0.0387	0.0387	0.0508	0.0118						0.0134						0.0129	0.0129	
BENDING DEFLECTION CAP. $\delta_{BC} = \theta_p \cdot L'$	2.79	2.79	3.66	0.85						0.96						0.93	0.93	
PLASTIC BENDING MOMENT M_p (IN-KIPS)	1,756	1,673	1,959	1,892						5,616						6,991	6,991	E = 29,000 KSI
PLASTIC BENDING ENERGY $E_{BC} = .572\, M_p \theta_p$	388	370	569	643						430						516	516	ΣE_{BC} = 917 IN-K CORRECTED $E_{BC} = \frac{P}{P_{BC}} \cdot E_{BC}$ IF $P_{BC} < P$
LATERAL FORCE, (KIPS) (BENDING ONLY) $P_{BC} = E_{BC} / \delta_{BC}$	1391	1326	1555	3096						4479						554.8	994.8	
FORCE ON WEB AT ENDS OF L_E (KIPS) $(P_{BC}/2 + M_p/L_E)$	817	779	914	1817						2630						325.9	325.9	

CASE I - RIGHT ANGLE COLLISION - STRUCK BY VERTICAL BOW

SHELL LONGITUDINAL NO.	1	2	3	4	5	6	7	8	9	10	11	12	13	14	15	16	17	REMARK
ε_r (WITHIN L_t)	0.10	----	----	----	----	----	----	----	----	----	----	----	----	----	----	0.10	0.10	
MEMBRANE TENSION DEFL $\delta_{tc} = \sqrt{\frac{L_t}{2}(\varepsilon_r + \varepsilon_c) + \delta_{bc}^2}$	32.37	32.37	32.46	32.26	----	----	----	----	----	----	----	----	----	----	----	32.26	32.26	
AVERAGE MEMBRANE TENSION FORCE $T = A_s \sigma_y \left(\frac{\sigma_{cr} + \sigma_u}{2\sigma_y}\right)$	1,128	2,167	2,187	2,247	----	----	----	----	----	2,382	----	----	----	----	----	2,496	2,496	
δ_m (DEFORMATIONS TO MATCH STRIKING BOW CONFIGURATION ARE LIMITED TO δ_{bc})	32.26	----	----	----	----	----	----	----	----	----	----	----	----	25.81	19.38	12.96	6.45	
NET LATERAL FORCE ON LONGL DUE TO MEMBRANE TENSION ONLY $P_{rm} = 4T\,\delta_m / L_t$	2,592	1,962	1,960	2,013	----	----	----	----	----	2,134	----	----	----	1,704	1,283	880	440	
$P_{wf} = P_{rm}/2 \div R_m$	309	208	209	215	----	----	----	----	----	228	----	----	----	182	137	94	47	$R_m = 4.681$ SEE SHEET NO. 3-11
NO OF WEB FRAME SPACES DAMAGED $n = \left[\frac{0.5\,P_{rm}}{P_{wf}}\right] 2 - 1$	9	9	9	9	9	9	9	9	9	9	9	9	9	9	9	9	9	ROUNDED OF TO NEXT HIGHER ODD INTEGER
ACTUAL 7 WEB FRAME SPACES DAMAGED $L_d = 7 L_s$	1.008	----	----	----	----	----	----	----	----	----	----	----	----	----	----	----	----	
$\delta_1 = \frac{P_{wf} L_t}{2T}$	6.91	----	----	----	----	----	----	----	----	----	----	----	----	5.49	4.14	2.66	1.32	
RESIDUAL δ (DEFORMATION AT LONGL'S WHERE WEB FRAMES FOLLOWS BOW CONFIGURATION TO LONGL'S)	193.08	----	----	----	----	----	----	----	----	----	----	----	----	194.46	115.85	77.23	38.62	MAX. DEVD. ANGLE = 14°-22' SEE SHT NO. 3-11
$\varepsilon = \frac{\delta' + 92\,\delta'_1}{3.54 \times L_d}$	0.07817	----	----	----	----	----	----	----	----	----	----	----	----	0.05006	0.02817	0.01269	0.00511	
$e_T = L_d \cdot \varepsilon$	78.90	----	----	----	----	----	----	----	----	----	----	----	----	50.46	28.60	12.55	5.15	
$E_{mt} = T e_t \left(1 + \frac{0.06 \times 69\,L_t}{0.07817\,L_d}\right)$	187,035	192,690	196,669	199,804	199,806	199,806	199,804	199,806	199,806	211,808	211,808	211,808	211,808	139,607	76,240	36,757	8,664	$\Sigma E_{mt} = 2,975,298$ KIPS/FT

S-6

CASE I – RIGHT ANGLE COLLISION - STRUCK BY VERTICAL BOW

ANALYSIS OF WEB FRAMES

(LATERAL LOAD = ½ Ptm)

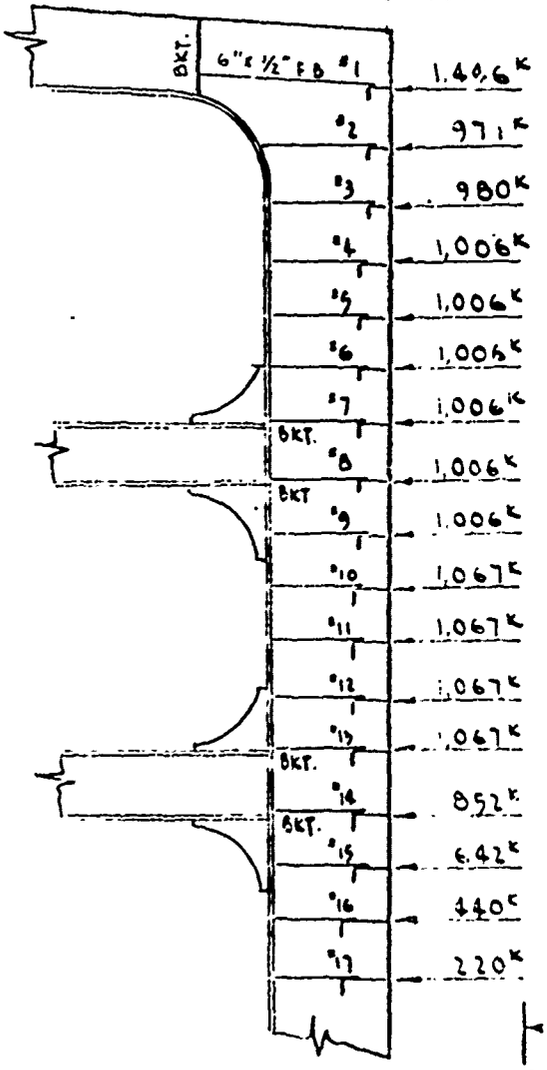

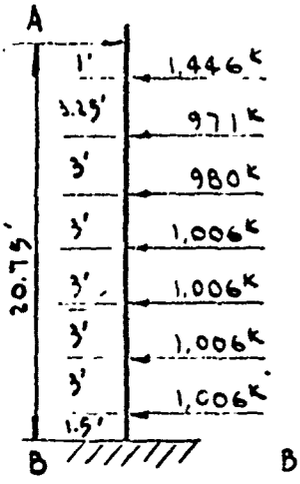

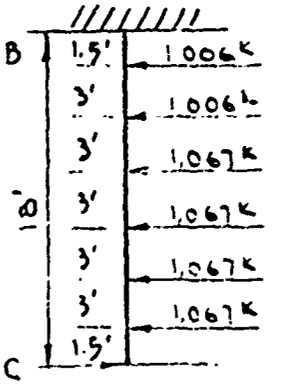

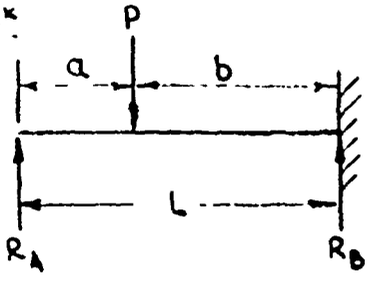

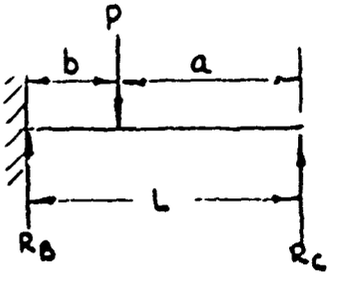

$$R_A = \frac{Pb^2}{2L^3}(a+2L), \qquad R_C = \frac{Pb^2}{2L^3}(a+2L)$$

$$R_B = \frac{Pa}{2L^3}(3L^2 - a^2)$$

CASE I – RIGHT ANGLE COLLISION - STRUCK BY VERTICAL BOW

ANALYSIS OF WEB FRAMES
DETERMINATION OF R_A, R_B & R_C

LONGLS	L	P/2	a	b	2L+a	L^3	$3L^2-a^2$	R_A	R_B	R_C
A	—	—	—	—	—	—	—	—	—	—
1	20.75	723	1.00	19.75	42.50	8,934.16	1,291	1,342	104	
2	″	486	4.25	16.50	45.75	″	1,274	678	295	
3	″	490	7.25	13.50	48.75	″	1,239	487	493	
4	″	503	10.25	10.50	51.75	″	1,187	321	685	
5	″	″	13.25	7.50	54.75	″	1,116	173	833	
6	″	″	16.25	4.50	57.75	″	1,028	66	940	
7	↓	↓	19.25	1.50	60.75	↓	921	7	998	
B		—	—	—	—				4,348	—
8	18.00	503	16.50	1.50	52.50	5,832.00	700		996	10
9	″	503	13.50	4.50	49.50	″	790		919	86
10	″	534	10.50	7.50	46.50	″	862		829	240
11	″	″	7.50	10.50	43.50	″	916		629	439
12	″	″	4.50	13.50	40.50	″	952		392	676
13	↓	↓	1.50	16.50	37.50	↓	970		133	935
C		—	—	—	—				3,897	
TOTAL								3,074	8,245	2,386

CASE I – RIGHT ANGLE COLLISION-STRUCK BY VERTICAL BOW

SHEAR & BENDING MOMENT FOR THE UPPER PART OF THE WEB FRAME

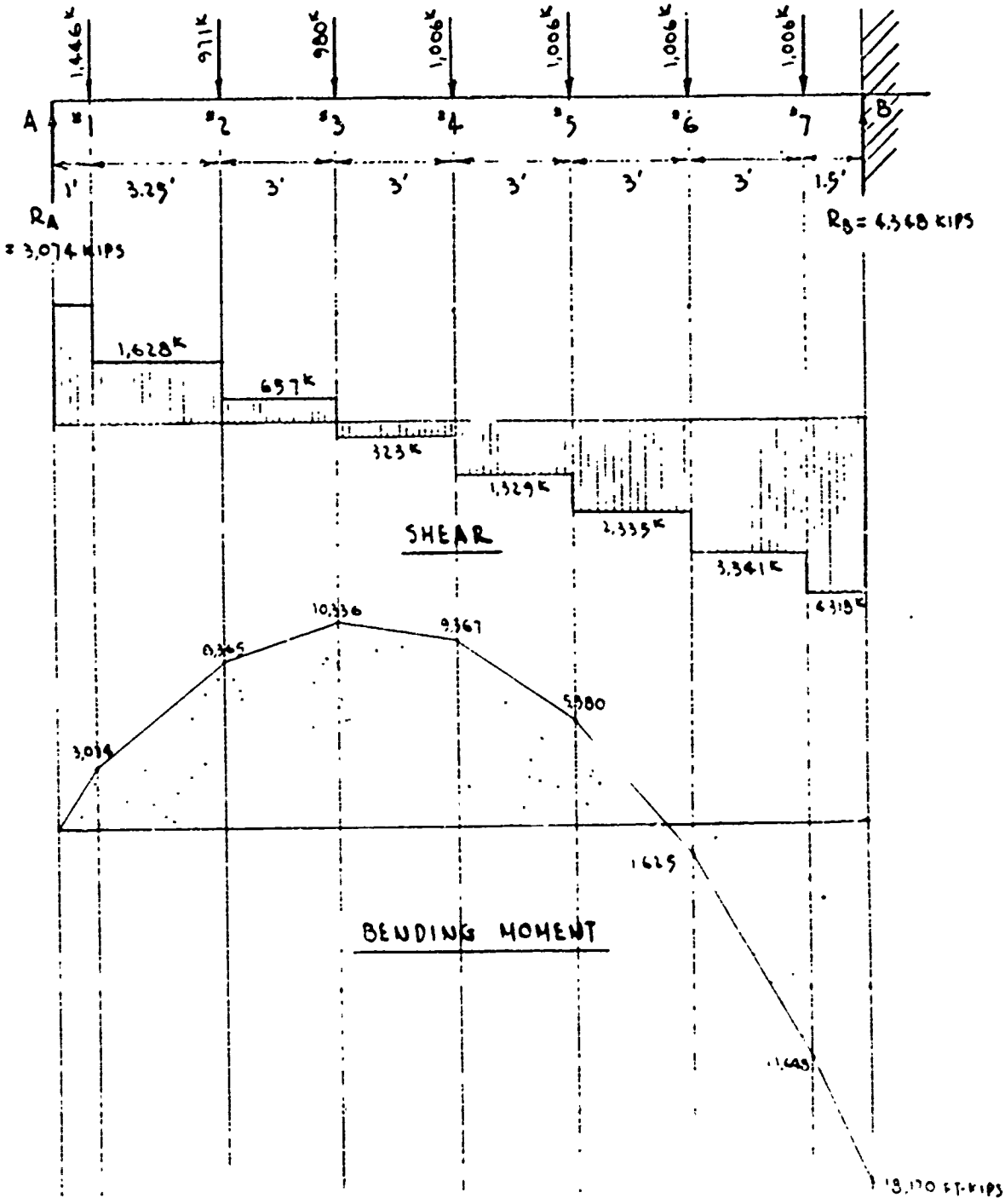

CASE I RIGHT ANGLE COLLISION - STRUCK BY VERTICAL BOW

SHEAR & BENDING MOMENT FOR THE LOWER PART OF THE WEB FRAME

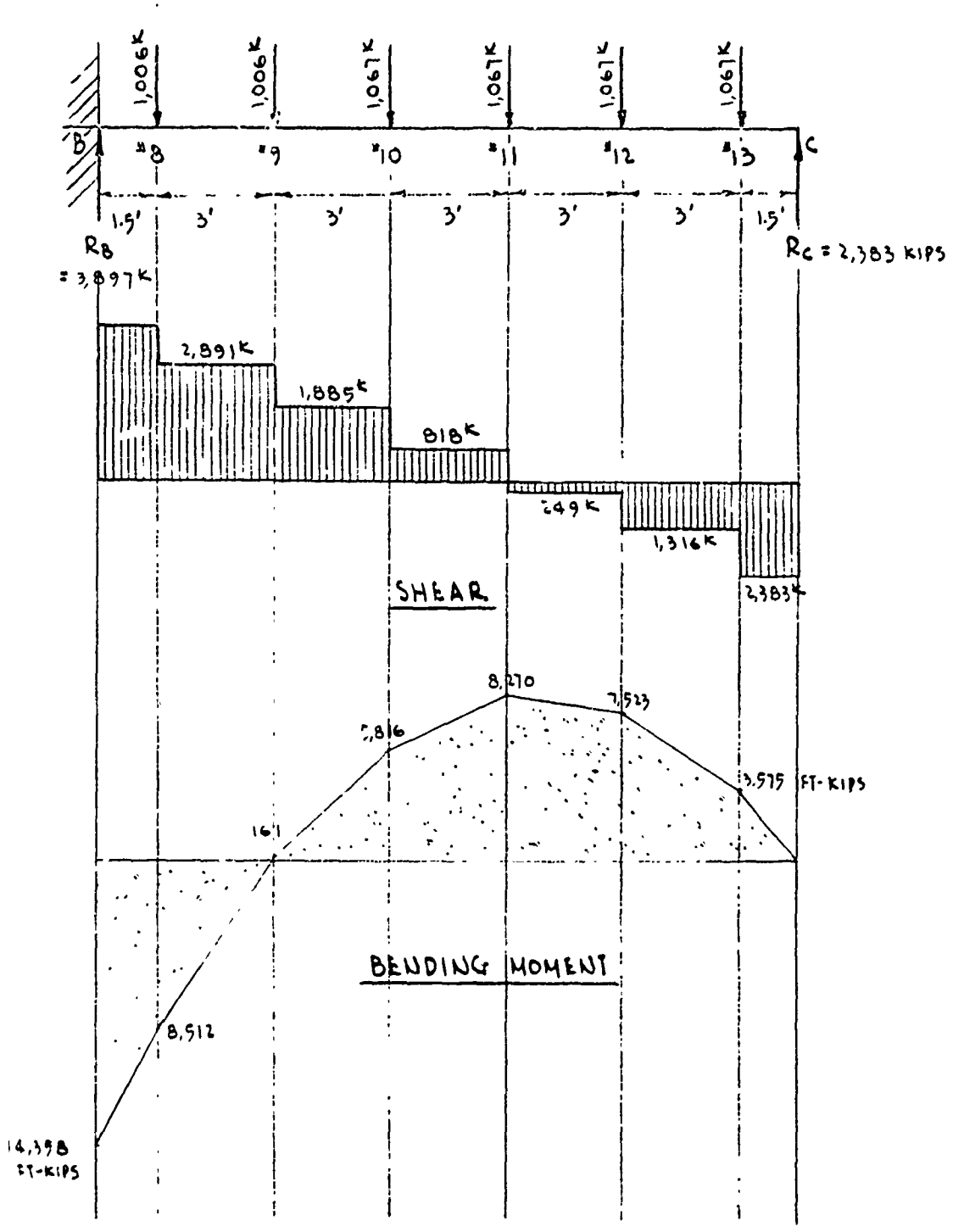

CASE I – RIGHT ANGLE COLLISION - STRUCK BY VERTICAL BOW

SUMMARY OF "R"

(LATERAL LOADS / STRENGTH OF WEB FRAME)

LOCATION \ TYPE OF LOAD	.R BENDING	R SHEAR	R CRUSHING	R COMPR.
A	—	—	—	—
1	—	—	2.987	—
2	1.280	2.065	2.006	—
3	1581	0.833	—	—
4	1.433	1686	2.078	—
5	0.823	2.963	2.078	—
6	0.249	4.239	2078	—
7	—	—	—	—
B	—	—	—	4681
8	—	—	—	—
9	0025	3668	2.078	—
10	0.890	2392	2.195	—
11	1.265	1.038	2195	—
12	1.151	1.670	2195	—
13	—	—	—	—
C				1.353
MAX. R = 4.681				

FOR SUMMARY OF WEB FRAME STRENGTH SEE SHT NO. 3-92

CASE 1 - RIGHT ANGLE COLLISION - STRUCK BY VERTICAL BOW

SHEARING PLASTIC ENERGY (E_{ps})

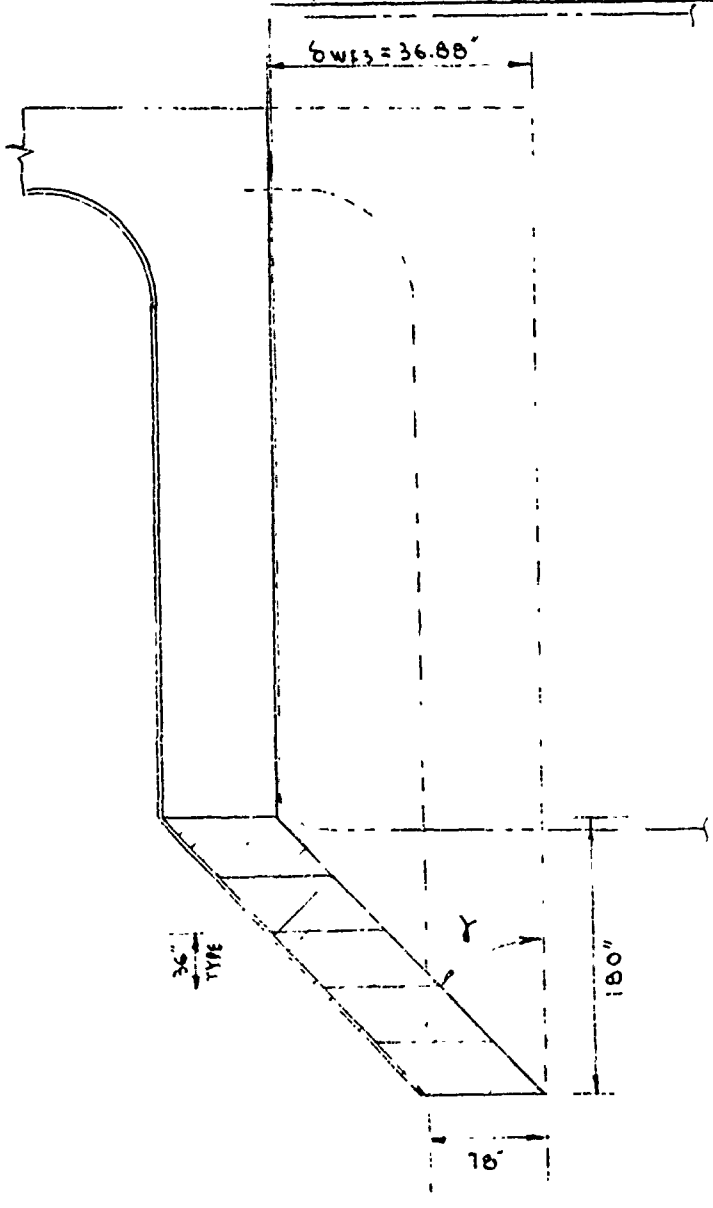

$$\gamma = \tan^{-1}\frac{36.88}{180} = 0.2049$$

$$\gamma = 11.58^\circ = 0.2021 \text{ RADIAN}$$

$$\gamma_m = 0.0947 \text{ RADIAN}$$

$$\gamma > \gamma_m$$

WEB PANEL :

$a = 36"$

$d = 78"$

$t = 0.5"$

$d/a = 2.17$

$d/t = 156$

FROM FIG 2-6, $\tau_{cr} = 27.0$, $\tau_y = 20.2$

SINCE $\tau_{cr} > \tau_y$

$$E_{ps} = (a,d\,t)\left(\gamma - \frac{\tau_y}{11{,}150}\right)(\tau_y)\times 6$$

$$= 180"\times 78"\times 0.5"\left(0.0947 - \frac{20.2}{11{,}150}\right)20.2\times 6$$

$$= 79{,}031 \text{ IN-KIPS}$$

CASE I - RIGHT ANGLE COLLISION - STRUCK BY VERTICAL BOW

PLASTIC ENERGY DUE TO DECK DEFORMATION (Ed)

DEFORMATION AT LONG'L. NO.1 = 193.08", $\varepsilon = 0.07827$
= 16.09'.

NO. OF DECK LONG'LS DAMAGED = $\frac{193.08}{36} = 5.36$

$$Ed_x = T \cdot e_t = A_s \times \frac{\sigma_y + \sigma_u}{2} \times L_d \times \varepsilon$$

$Ed_1 = 93.00 \times 50 \times 1{,}008 \times 0.07827 \times \left(\frac{13.09'}{16.09'}\right)^2 = 242{,}815$ IN-KIPS

$Ed_2 = 68.25 \times 50 \times 1{,}008 \times 0.07827 \times \left(\frac{10.09'}{16.09'}\right)^2 = 105{,}876$ IN-KIPS

$Ed_3 = 68.25 \times 50 \times 1{,}008 \times 0.07827 \times \left(\frac{7.09'}{16.09'}\right)^2 = 52{,}277$ IN-KIPS

$Ed_4 = 68.25 \times 50 \times 1{,}008 \times 0.07827 \times \left(\frac{4.09'}{16.09'}\right)^2 = 17{,}397$ IN-KIPS

$Ed_5 = 68.25 \times 50 \times 1{,}008 \times 0.07827 \times \left(\frac{1.09'}{16.09'}\right)^2 = 1{,}236$ IN-KIPS

$\Sigma Ed_x = 419{,}601$ IN-KIPS

DECK MEMBRANE TENSION ENERGY

$$Ed = \Sigma Ed_x \left(1 + \frac{0.06949}{0.07827} \frac{}{L_d}\right)$$

$= 419{,}601 \times 1.127 = 472{,}890$ IN-KIPS

3.2 CASE 2 - RIGHT ANGLE COLLISION - STRUCK BY 15° RAKED BOW

SUMMARY OF PLASTIC ENERGY ABSORBED BEFORE SHELL PLATE RUPTURE — STRUCK MIDSPAN BETWEEN WEB FRAMES & BULKHEADS BY 15° RAKED BOW, 7 WEB FRAME SPACES BETWEEN BULKHEADS.

		ENERGY (IN-KIPS)
E_{bc} = PLASTIC BENDING ENERGY IN LONG'L. STIFFENED SIDE	=	6,613
E_{mt} = MEMBRANE TENSION PLASTIC ENERGY IN LONG'L. STIFFENED SIDE	=	824,256
E_{ps} = SHEARING PLASTIC ENERGY IN WEB FRAMES	=	137,325
E_d = DECK MEMBRANE TENSION PLASTIC ENERGY	=	249,987
TOTAL ENERGY ABSORBED	=	1,218,181 IN-KIPS

SHELL — SINGLE

SIDE SHELL PLATE = 1" M S
DECK PLATE = 1⅛" M.S

CASE 2 - RIGHT ANGLE COLLISION - STRUCK BY 15° RAKED BOW

CONFIGURATION OF THE STRIKING & THE STRUCK SHIP

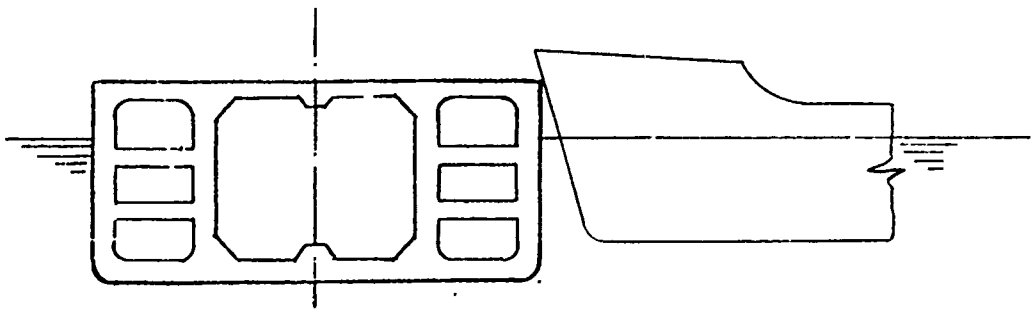

	STRUCK SHIP	STRIKING SHIP
TYPE	TANKER	TANKER
DWT	120,000 TONS	19,000 TONS
L	900.0 FT	500 FT
B	147.5 FT	68 FT
D	63.5 FT	39 FT
d	48.5 FT	30 FT

NOTE:

1. STRUCK SHIP'S WEB SPACING (L_S) EQUALS 12 FEET; SINGLE SHELL 1" M S
2. STRIKING SHIP HAS 15° RAKED BOW
3. THE TANKER IS STRUCK MIDSPAN BETWEEN WEB FRAMES & BULKHEA AT RIGHT ANGLE, DISTANCE BETWEEN ADJACENT BULKHEADS IS 7 WEB FRAME SPACES.
4. DECK PLATE = 1 3/8" M S

CASE 2 - RIGHT ANGLE COLLISION - STRUCK BY 15° RAKED BOW

SCANTLINGS IN WAY OF WEB. FRAME

ALL DECK LONG'LS. ARE 15"x 1¼" F.B. SPACING 36"

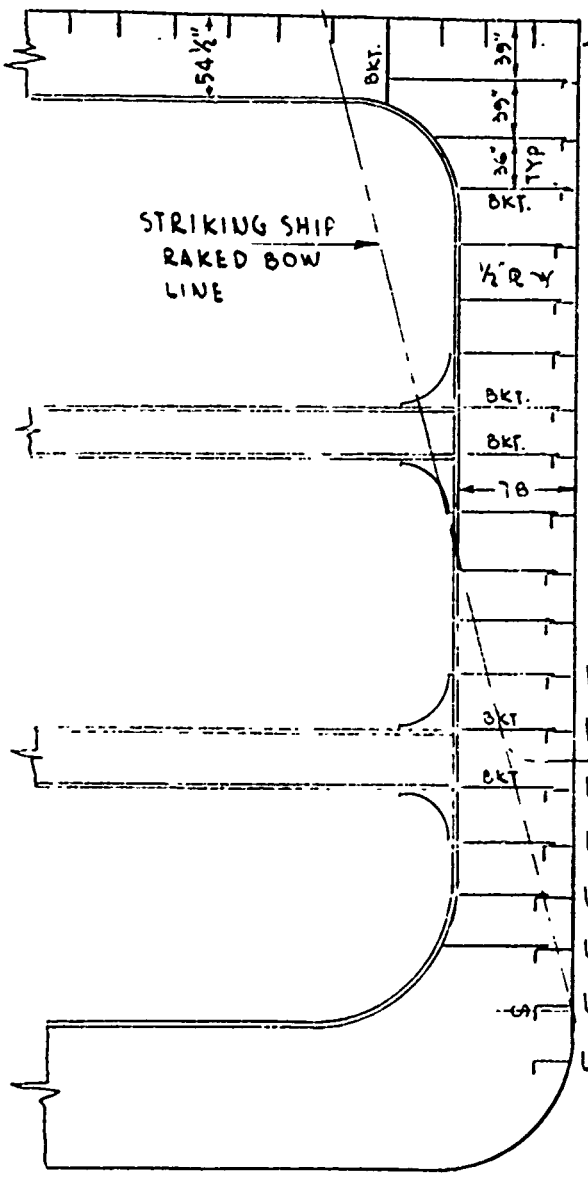

SIDE LONGITUDINAL SPACING = 36"
EXCEPT AS NOTED.

CASE 2 - RIGHT ANGLE COLLISION - STRUCK BY 15° RAKED BOW

SHELL LONGITUDINAL NO.	1	2	3	4	5	6	7	8	9	10	11	12	13	14	15	16	17	REMARK
BASIC DIMENSIONS	9"x6"x½" ∠	9"x6"x½" ∠	9"x6"x⅜" ∠	18"x6"x 19.5°FF	18"x6"x 19.5°FF	18"x6"x 19.5°FF	18"x6"x 19.5°FF	18"x6"x 19.5°FF	18"x6"x 19.5°FF	21"x6"x 17.85°FF	21"x6"x 17.85°FF	21"x6"x 17.85°FF	21"x6"x 17.85°FF	21"x6"x 17.85°FF	21"x6"x 17.85°FF	24"x6"x 17.85°FF	24"x6"x 17.85°FF	
A_S = SECTIONAL AREA OF LONGL WITH PORTION OF SHELL PLT (IN²)	4.43	4.38	4.37	4.49	4.49	4.49	4.49	4.49	4.49	4.76	4.76	4.76	4.76	4.76	4.76	4.90	4.90	
I = MOMENT OF INERTIA OF LONGL WITH PORTION OF SHELL PLT (IN⁴)	2.74	2.61	3.07	1.265	1.265	1.265	1.265	1.265	1.265	2.060	2.060	2.060	2.060	2.060	2.060	2.836	2.836	
b = BREADTH OF FLANGE (IN) = 2 × FLANGE OF T.P. OR ANGLE	8	8	8	12	12	12	12	12	12	12	12	12	12	12	12	12	12	
t_f = THICKNESS OF FLANGE (IN)	0.500	0.500	0.625	0.375	0.375	0.375	0.375	0.375	0.375	0.438	0.438	0.438	0.438	0.438	0.438	0.438	0.438	
b/t_f = BREADTH - THICKNESS RATIO	16.0	16.0	12.8	32.0	32.0	32.0	32.0	32.0	32.0	27.4	27.4	27.4	27.4	27.4	27.4	27.4	27.4	
d = DEPTH OF WEB OF LONGITUDINAL (IN)	9	9	9	18	18	18	18	18	18	21	21	21	21	21	21	24	24	
b/d = BREADTH - DEPTH RATIO	0.89	0.89	0.89	0.67	0.67	0.67	0.67	0.67	0.67	0.57	0.57	0.57	0.57	0.57	0.57	0.50	0.50	

CASE 2 - RIGHT ANGLE COLLISION - STRUCK BY 15° RAKED BOW

SHELL LONGITUDINAL NO.	1	2	3	4	5	6	7	8	9	10	11	12	13	14	15	16	17	REMARK
L_y = YIELD LENGTH FIG 2-3	12.0'	12.0'	12.0'	18.9'	18.9'	18.9'	18.9'	18.9'	18.9'	19.6'	19.6'	19.6'	19.6'	19.6'	19.6'	20.5'	20.5'	
L'	72.0'	—	—	—	—	—	—	—	—	—	—	—	—	—	—	—	—	
$\frac{2L_y}{L'}$	0.33	0.33	0.33	0.53	—	—	—	—	→	0.54	—	—	—	—	→	0.57	0.57	
$\frac{2L_y}{2L_y+L}$	0.25	0.25	0.25	0.36	—	—	—	—	→	0.35	—	—	—	—	→	0.36	0.36	
CONSTANT A $\left(\frac{2L_y}{L'}\right)\left(\frac{32.2P}{0.5\rho C\sigma_y}\right) \leq \left(1-\frac{\sigma_y}{\sigma_u}\right)$	0.28	0.28	0.36	0.19	—	—	—	—	→	0.23	—	—	—	—	→	0.24	0.24	
CONSTANT B $\left(\frac{2L_y}{L'}\right)\left(\frac{32.2P}{0.5\rho C\sigma_y}\right) \leq \left(\frac{\sigma_u}{\sigma_y}-1\right)$	0.36	0.36	0.45	0.29	—	—	—	—	→	0.35	—	—	—	—	→	0.37	0.37	
ROTATION CAPACITY CONST $K = A(11.6 - 6.18)$	6.87	6.87	6.41	3.09	—	—	—	—	→	3.96	—	—	—	—	→	4.21	4.21	
PLASTIC CURVATURE M_p/EI	221 $\times 10^{-6}$	221 $\times 10^{-6}$	220 $\times 10^{-6}$	106 $\times 10^{-6}$	—	—	—	—	→	94 $\times 10^{-6}$	—	—	—	—	→	85 $\times 10^{-6}$	85 $\times 10^{-6}$	THESE ARE CALCULATED VALUES, FIG. 1-6 MAY BE USED.
PLASTIC ANGLE CHANGE CAP $\theta_p = K\left(\frac{M_p}{EI}\right)\left(\frac{L'}{2}\right)$	0.0387	0.0387	0.0508	0.0118	—	—	—	—	→	0.0134	—	—	—	—	→	0.0129	0.0129	
BENDING DEFLECTION CAP $\delta_{BC} = \theta_p \times L'$	2.79	2.79	3.66	0.85	—	—	—	—	→	0.96	—	—	—	—	→	0.93	0.93	
PLASTIC BENDING MOMENT M_p (IN-KIPS)	1,693	1,673	1,960	3,892	—	—	—	—	→	5,639	—	—	—	—	→	7,647	7,647	E = 29,000 KSI
PLASTIC BENDING ENERGY $E_{BC} = .572\, M_p \theta_p$	375	370	570	163					→	432	—	—	—	—	→	564	564	$\Sigma E_{BC} = 6,613$ IN-K CORRECTED $E_{BC} = \frac{\Sigma}{E_{BC}} \cdot E_{BC}$ IF $E_{BC} > \Sigma$
LATERAL FORCE (KIPS) (BENDING ONLY) $P_B = E_{BC}/\delta_{BC}$	1364	1326	1557	3084														
FORCE ON WEB AT ENDS OF L_E (KIPS) $(P_B/2 + M_p/L_E)$	790	779	915	1817														

CASE 2 - RIGHT ANGLE COLLISION - STRUCK BY 15° RAKED BOW

SMALL LONGITUDINAL NO.	1	2	3	4	5	6	7	8	9	10	11	12	13	14	15	16	17	REMARK
ε_r (WITHIN L_s)	0.10	—	—	—	—	—	—	—	—	—	—	—	—	—	—	0.10	0.10	
MEMBRANE TENSION DEFL $\delta_{EC} = \frac{L_s^2}{2}(\varepsilon_r + \varepsilon_c) + \delta_{BC}'$	32.57	32.57	32.46	32.26	—	—	—	—	—	—	—	—	—	—	—	32.26	32.26	
AVERAGE MEMBRANE TENSION FORCE $T = A_s\sigma_y\left(\frac{\sigma_x + \sigma_u}{2\sigma_y}\right)$	3,228	3,077	2,187	2,247	—	—	—	—	—	2,382	—	—	—	—	—	2,456	2,456	
THE FOLLOWING EIGHT LINES ARE INTIAL CALCULATIONS FOR δ_i																		
δ_m (DEFORMATIONS TO MATCH STRIKING BOW CONFIGURATION ARE LIMITED TO δ_{EC})	32.57	21.92	12.27	2.62														
NET LATERAL FORCE ON LONG'L DUE TO MEMBRANE TENSION ONLY $P_{rm} = 4T\ \delta_m/L_s^2$	2,905	1,265	745	164														
$P_{wf} = P_{rm_{1/2}} - R_m$	483	210	124	27														$R_m = 3,000$ SEE SHT. NO. 5-13
NO. OF WEB FRAME SPACES DAMAGED $n = \left[\frac{0.5\,r_{rm}}{P_{wf}}\right]_{2-1}$	5	5	5	5														
ACTUAL NO. OF WEB FRAME SPACES DAMAGED	5	5	5	5														
$L_d = 5\,L_s$	720	720	720	720														
$\delta_i = \frac{P_{wf}\,L_s}{2T}$	1077	7.28	4.08	0.86														
δ_i (DEFORMATION AT LONG'L°1 SEE SHT 5-105, FOLLOWS 15° RAKE CONTOUR TO LONG'L°13)	116.34	129.89	116.24	106.60	96.95	87.31	77.66	68.01	58.37	48.72	39.08	29.43	19.78	15.82	11.87	7.91	3.96	MAX. DEAD ANGLE 14°-24' SEE SHT NO 5-106
δ_m	32.57	29.89	27.60	25.31	23.02	20.73	18.44	16.15	13.86	11.57	9.28	6.99	4.70	3.76	2.82	1.88	0.94	δ_m AT LONG'L°2 TO 13 PROPORTIONAL TO δ_i, δ_m @ LONG'L°1 = 32.57
NET LATERAL FORCE ON LONG'L DUE TO MEMBRANE TENSION ONLY $P_{rm} = 4T\ \delta_m/L_s^2$	2,905	1,724	1,677	1,582	1,457	1,294	1,151	1,008	869	766	614	465	311	249	187	128	64	

CASE 2 - RIGHT ANGLE COLLISION - STRUCK BY 15° RAKED BOW

SHELL LONGITUDINAL NO.	1	2	3	4	5	6	7	8	9	10	11	12	13	14	15	16	17	REMARK
$P_{wi} = P_{im}/L \div R_m$	483	257	279	264	259	216	192	168	144	128	102	77	52	42	31	21	11	
NO OF WEB FRAME SPACES DAMAGED $\eta = \left[\frac{0.5 P_{cm}}{P_{wi}}\right] \geq 1$	5	5	5	5	5	5	5	5	5	5	5	5	5	5	5	5	5	
ACTUAL 5 WEB FRAME SPACES DAMAGED $L_d = 5 L_s$	720	—		—													—	
$b_i = \frac{P_{wi} \cdot L_c}{2T}$	10.77	9.95	9.19	8.45	7.66	6.92	6.15	5.38	4.61	3.87	3.08	2.33	1.57	1.27	0.94	0.62	0.32	
*FINAL b (DEFORMATION AT KNUCKLE NO 1 SEE SHT NO. FOLLOWS 15° RAKE CONTOUR TO KNUCKLE NO 13)	136.34	125.89	116.21	106.60	96.95	87.31	77.66	68.01	58.37	48.72	39.08	29.45	19.78	15.82	11.87	7.91	3.96	MAX. BEND ANGLE = 14°-26' SEE SHT NO 2-108
$\varepsilon = \frac{b^2 + 14 b_i^2}{2.5 L_c^2 \cdot L_d}$	0.01798	0.00649	0.03669	0.04770	0.03963	0.03200	0.01531	0.01961	0.01429	0.00997	0.00660	0.00367	0.00164	0.00105	0.00059	0.00026	0.00008	
$e_t = L_d \cdot \varepsilon$	56.15	47.87	40.82	34.34	28.59	23.04	18.22	13.98	10.29	7.18	4.61	2.64	1.18	0.76	0.42	0.19	0.06	
$E_{mt} = T e_t \left(1 + \frac{0.06873 L_s}{0.01798 L_d}\right)$	213,878	182,323	155,343	130,851	108,945	88,090	68,310	49,067	37,184	20,181	12,958	7,420	3,517	1,883	1,181	551	174	$\Sigma E_{mt} = 814,256$

* SINCE $R_m = 5000$ IN BOTH INITIAL AND FINAL CALCULATIONS, $\therefore b = b_i$

CASE 2 - RIGHT ANGLE COLLISION - STRUCK BY 15° RAKED BOW

INITIAL ANALYSIS OF WEB FRAMES

(LATERAL LOAD = ½ P_{tm})

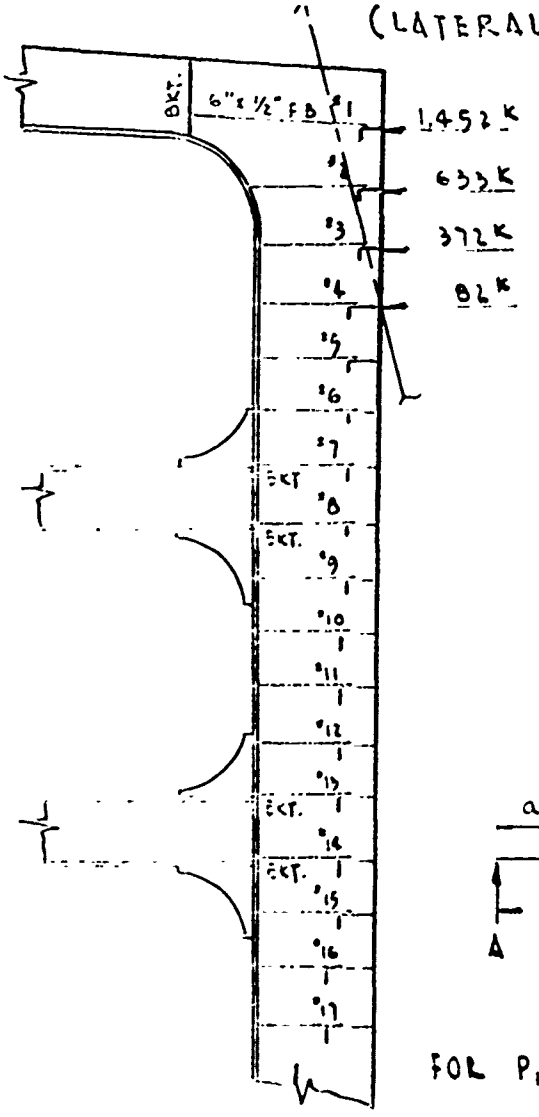

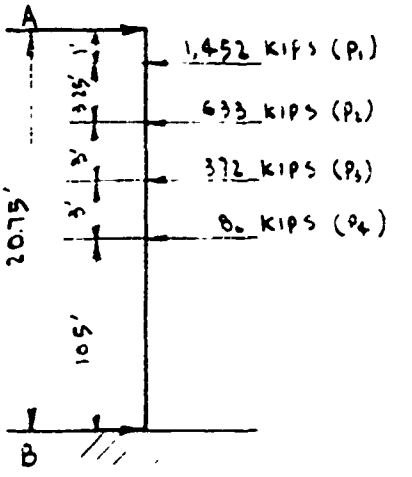

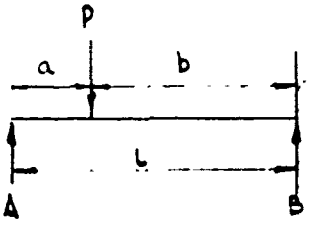

$$R_B = \frac{Pa}{2L^3}(3L^2 - a)$$

		KIPS
FOR P_1	$\frac{1,452 \times 1}{2(2075)^3}[3(20.75)^2 - (100)^2]$ =	04 48
FOR P_2	$\frac{633 \times 425}{2(2075)^3}[3(2075)^2 - (425)^2]$ =	191 75
FOR P_3	$\frac{372 \times 725}{2(2075)^3}[3(2075)^2 - (725)^2]$ =	186 36
FOR P_4	$\frac{82 \times 1025}{2(2075)^3}[3(2075)^2 - (1025)^2]$ =	55 50

R_B = 540 00 KIPS

R_A = 1999 00 KIPS

CASE 2 - RIGHT ANGLE COLLISION - STRUCK BY 15° RAKED BOW

INITIAL ANALYSIS OF WEB FRAMES

SHEAR & BENDING MOMENT FOR THE UPPER PART OF THE WEB FRAME

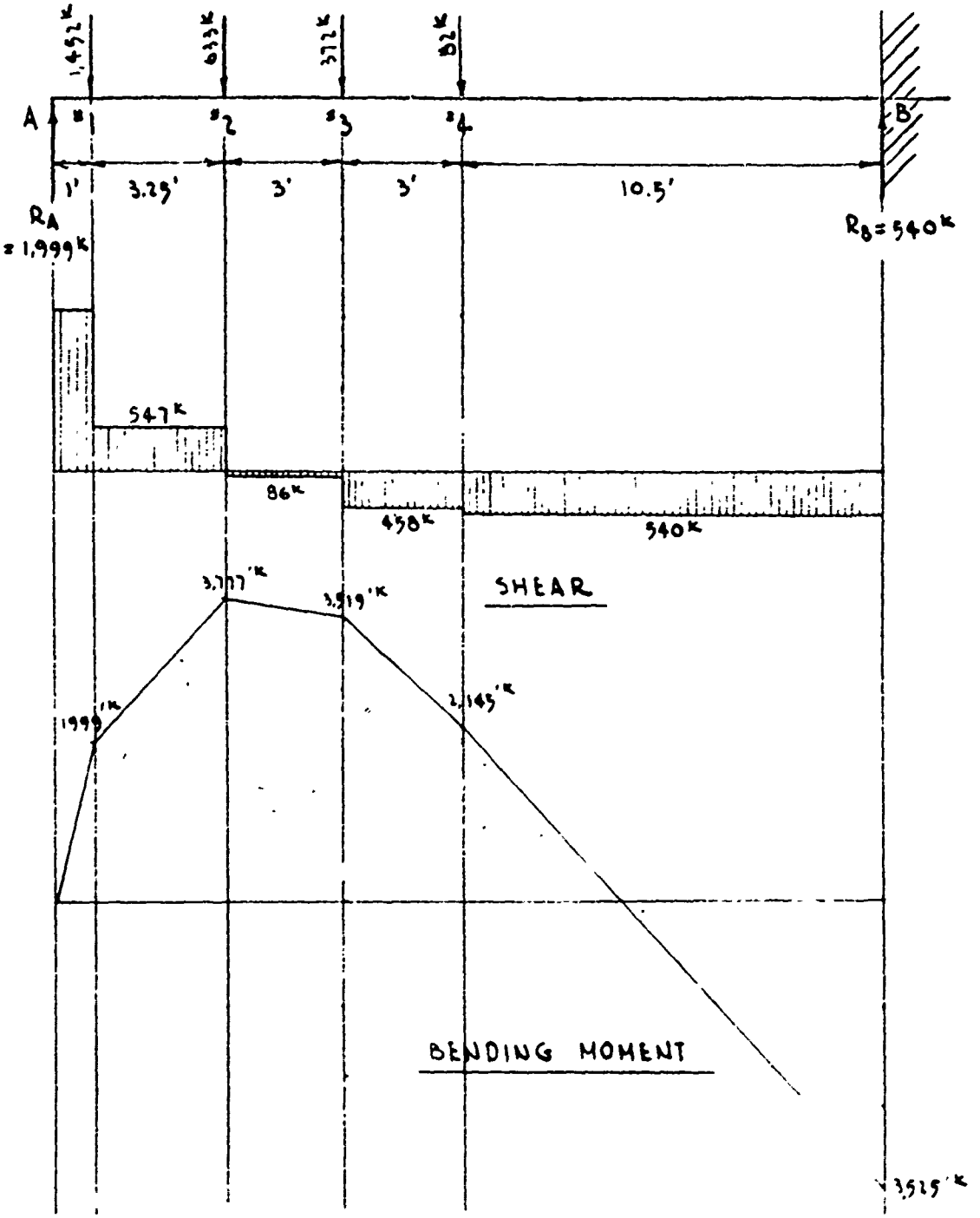

CASE 2 - RIGHT ANGLE COLLISION - STRUCK BY 15° RAKED BOW

INITIAL ANALYSIS OF WEB FRAMES
SUMMARY OF "R"

(LATERAL LOADS / STRENGTH OF WEB FRAME)

LOCATION \ TYPE OF LOAD	R BENDING	R SHEAR	R CRUSHING	R COMPR.
A	—	—	—	—
1	—	—	3.000	—
2	0.626	0.694	1 307	—
3	0583	0 581	—	—
4	0355	0 685	0.169	—
5	—	—	—	—
6	—	—	—	—
7	—	—	—	—
8	—	—	—	0 306
8	—	—	—	—
9	—	—	—	—
10	—	—	—	—
11	—	—	—	—
12	—	—	—	—
13	—	—	—	—
C	—	—	—	—

MAX. R = 3 000

FOR SUMMARY OF WEB FRAME STRENGTH SEE SHT NO 3-9

CASE 2 - RIGHT ANGLE COLLISION - STRUCK BY 15° RAKED BOW

FINAL CHECK OF WEB FRAME ANALYSIS

(LATERAL LOAD = ½ P_{tm})

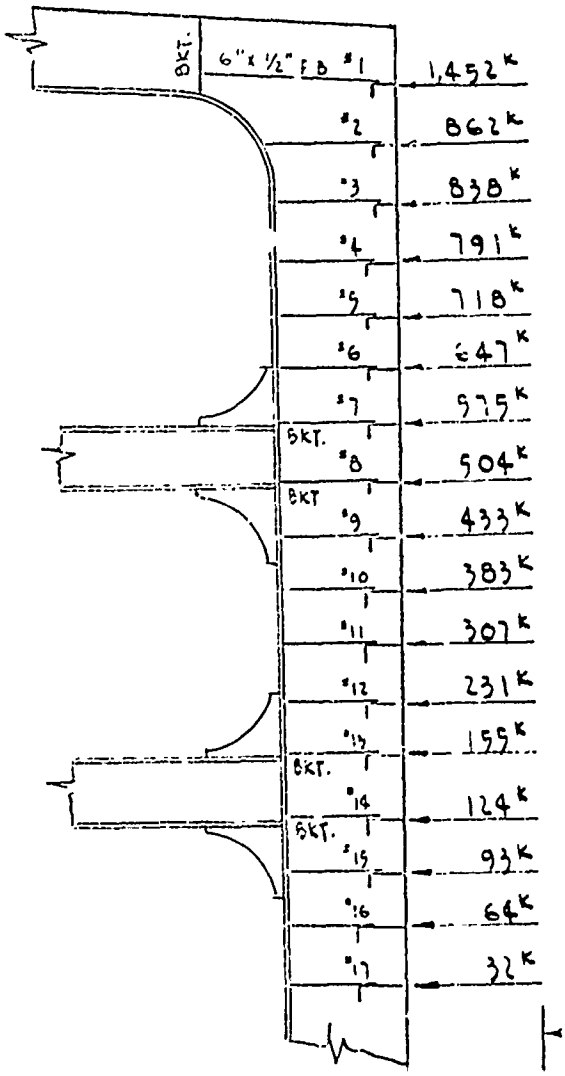

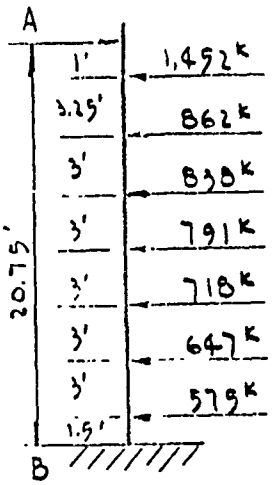

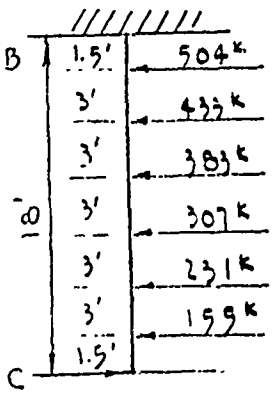

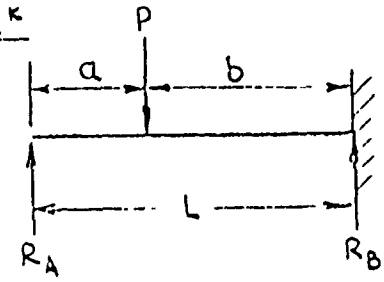

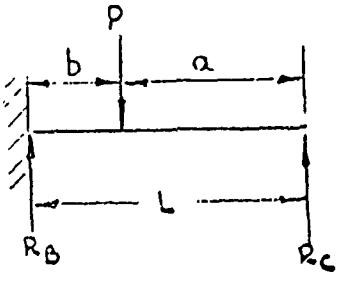

$$R_A = \frac{Pb^2}{2L^3}(a+2L), \qquad R_C = \frac{Pb^2}{2L^3}(a+2L)$$

$$R_B = \frac{Pa}{2L^3}(3L^2 - a^2)$$

CASE 2 - RIGHT ANGLE COLLISION - STRUCK BY 15° RAKED BOW

FINAL CHECK OF FRAME ANALYSIS

DETERMINATION OF R_A, R_B & R_C

LONG'LS	L	P/2	a	b	2L+a	L^3	$3L^2-a^2$	R_A	R_B	R_C
A	—	—	—	—	—	—	—	—	—	—
1	20.75	726.0	1.00	19.75	42.50	8,934.16	1,291	1,347	105	
2		431.0	4.25	16.50	45.75		1,274	601	261	
3		419.0	7.25	13.50	48.75		1,239	417	421	
4		395.5	10.25	10.50	51.75		1,187	253	538	
5		359.0	13.25	7.50	54.75		1,116	124	594	
6		323.5	16.25	4.50	57.75		1,028	42	605	
7		287.5	19.25	1.50	60.75		921	4	571	
B		—	—	—	—				3.095	—
8	18.00	252.0	16.50	1.50	52.50	5,832.00	700		499	5
9		216.5	13.50	4.50	49.50		790		396	37
10		191.5	10.50	7.50	46.50		662		297	86
11		153.5	7.50	10.50	43.50		916		181	126
12		115.5	4.50	13.50	40.50		952		85	146
13		77.5	1.50	16.50	37.50		970		19	136
C		—	—	—	—				1,477	—
TOTAL								2,788	5,108	536

CASE 2 - RIGHT ANGLE COLLISION - STRUCK BY 15° RAKED BOW

FINAL CHECK OF WEB FRAME ANALYSIS

SHEAR & BENDING MOMENT FOR THE UPPER PART OF THE WEB FRAME

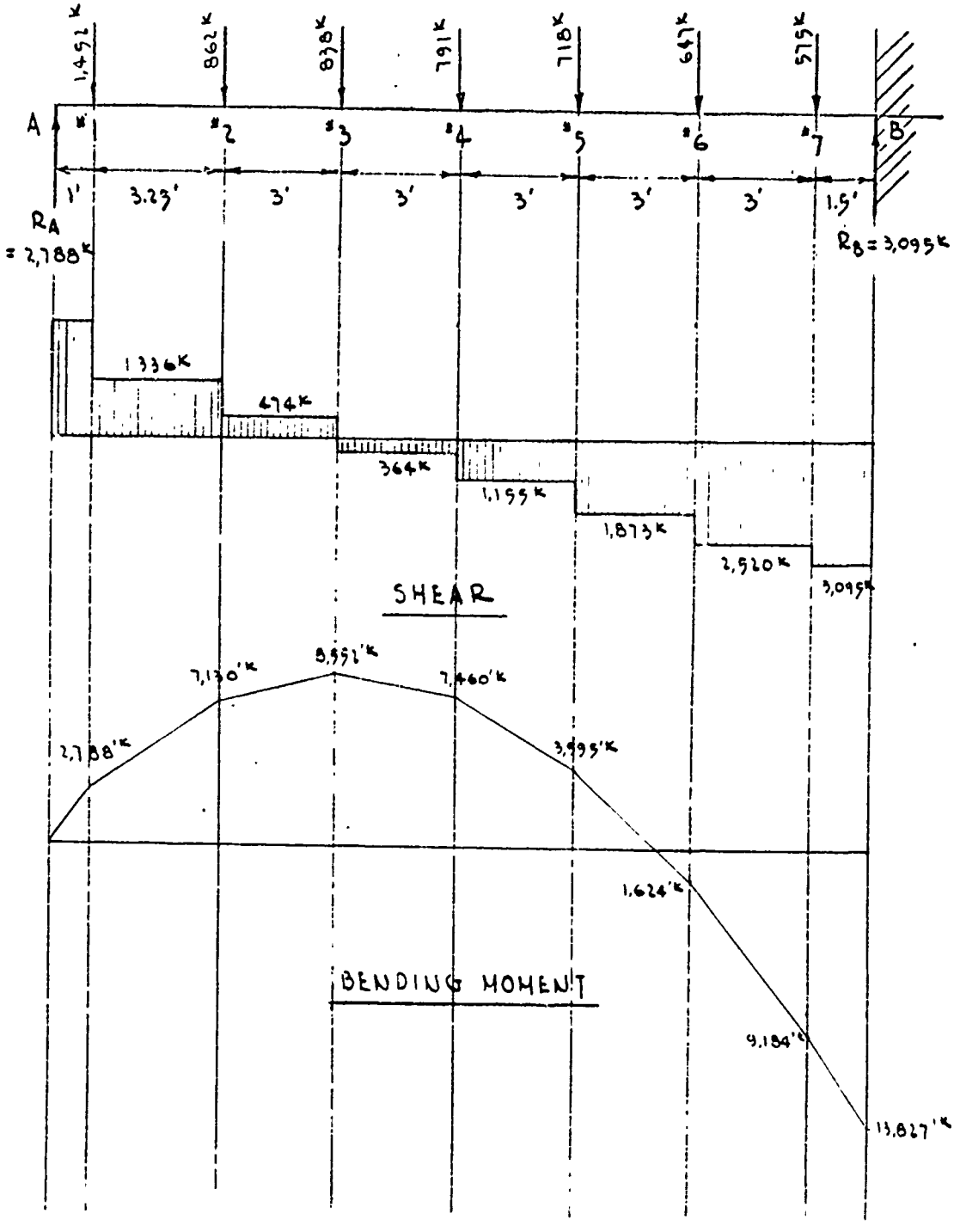

CASE 2 - RIGHT ANGLE COLLISION - STRUCK BY 15° RAKED BOW

FINAL CHECK OF WEB FRAME ANALYSIS

SHEAR & BENDING MOMENT FOR THE LOWER PART OF THE WEB FRAME

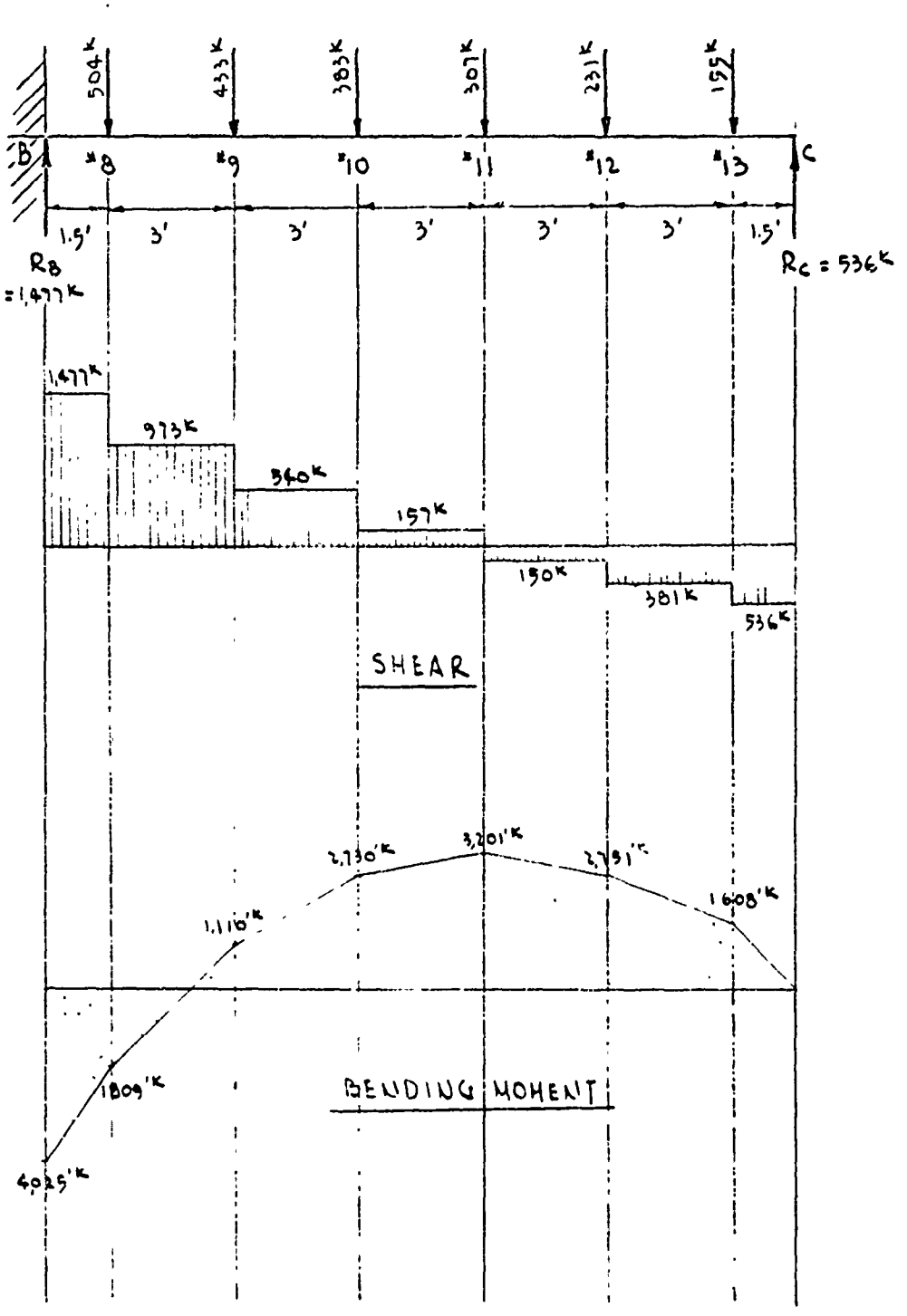

CASE 2 - RIGHT ANGLE COLLISION - STRUCK BY 15° RAKED BOW

FINAL CHECK OF WEB FRAME ANALYSIS

SUMMARY OF "R"

(LATERAL LOAD / STRENGTH OF WEB FRAME)

LOCATION \ TYPE OF LOAD	R BENDING	R SHEAR	R CRUSHING	R COMPR.
A	—	—	—	—
1	—	—	3.000	—
2	1.091	1695	1.781	—
3	1.308	0.602	—	—
4	1.141	1.466	1.634	—
5	0.611	2.377	1.483	—
6	0.248	3.198	1337	—
7	—	—	—	—
B	—	—	—	2.901
8	—	—	—	—
9	0.170	1.235	0.895	—
10	0.418	0.685	0791	—
11	0.490	0.199	0.634	—
12	0.421	0.484	0.477	—
13	—	—	—	—
C	—	—	—	0.306

MAX. R = 3.198 FOR BENDING, SHEAR & COMPR
MAX R = 3.000 FOR CRUSHING

FOR $(Rm)^{1/2} = (3198)^{1/2} = 1788$ WHICH IS LESS THAN $Rm = 3000$ FOR CRUSHING.
THEREFORE $Rm = 3000$ IS USED IN THE FINAL ABSORBED ENERGY CALCULATION

FOR SUMMARY OF WEB FRAME STRENGTH SEE SHT NO. 3-92

CASE 2 - RIGHT ANGLE COLLISION - STRUCK BY 15° RAKED BOW

SHEARING PLASTIC ENERGY (Eps)

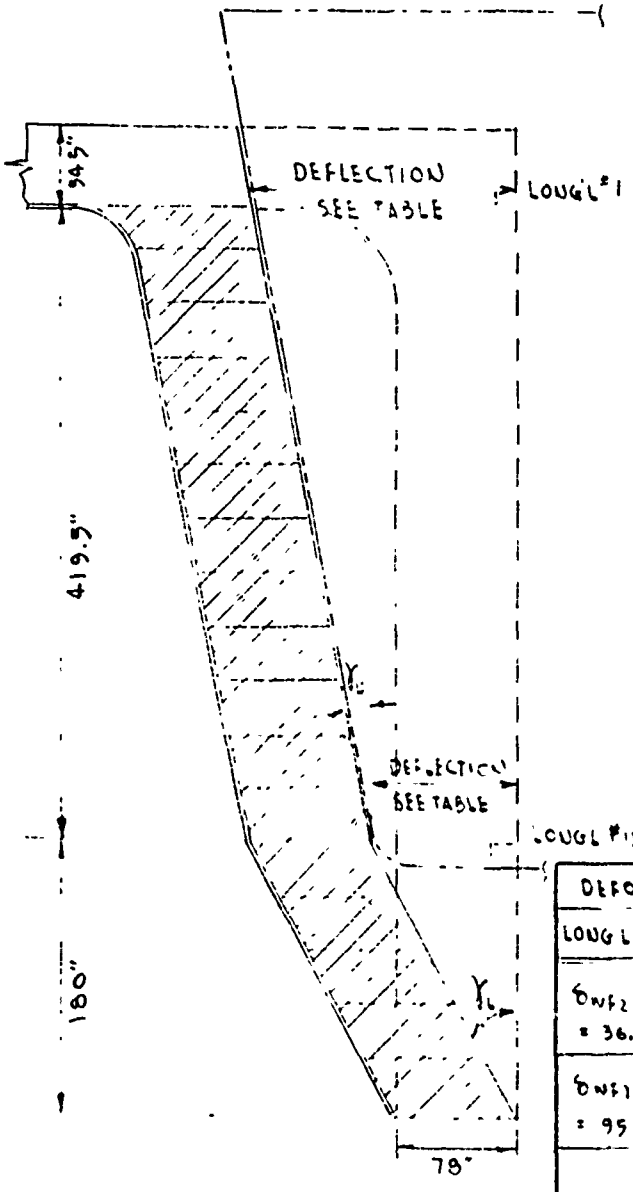

IF $\gamma > 0.0947$ RADIAN

USE $\gamma_m = 0.0947$

WEB PANEL

$a = 36"$, $d = 78"$ & $t = 0.5"$

$d/a = 2.17$, $d/t = 156$

FROM FIG 2-6, $J_{cr} = 27.0$, $J_y = 20.2$

SINCE $J_{cr} > J_y$

USE SHEAR PLASTIC ENERGY FORMULA

FOR THE FOLLOWING TABLE

$$E_{ps} = (a_1 d t)\left(\gamma - \frac{J_x}{1150}\right)\left(J_y\right)$$

$$= a_1 \cdot 39 \times 0 \times \left(\gamma - \frac{20.2}{1150}\right) 20.2$$

DEFORMATION LOUGL #1	DEFORMATION LOUGL #3	a_1 IN	d IN	t IN	γ RADIAN	SHEAR ENERGY IN-KIPS
δ_{WEB} = 36.98"	5.37"	419.5	78	0.5	0.0725	UPPER WEB: E_{PS1U} = 46,722
		180.0			0.0298	LOWER WEB: E_{PS1L} = 7,938
δ_{WEB} = 95.50"	13.85"	419.5			0.0947	UPPER WEB: E_{PS3U} = 61,397
		180.0	1	1	0.0768	LOWER WEB: E_{PS3L} = 21,268
						ΣE_{PS} = 137,325

CASE 2 - RIGHT ANGLE COLLISION - STRUCK BY 15° RAKED BOW

PLASTIC ENERGY DUE TO DECK DEFORMATION (E_d)

DEFORMATION AT LONG'L. NO.1 = 136.34", $\varepsilon = 0.07798$

DEFORMATION AT DECK = 136.34" + 39 × TAN 15° = 146.79" = 12.23'

NO. OF DECK LONG'LS DAMAGED = $\frac{146.79"}{36} = 4.08$

$$E_{dx} = T \cdot e_t = A_s \times \frac{\sigma_y + \sigma_u}{2} \times L_d \times \varepsilon$$

$E_{d_1} = 93.00 \times 50 \times 720 \times 0.07798 \times \left(\frac{9.23'}{12.23'}\right)^2 = 148,703$ IN-KIPS

$E_{d_2} = 68.25 \times 50 \times 720 \times 0.07798 \times \left(\frac{6.23'}{12.23'}\right)^2 = 49,718$ IN-KIPS

$E_{d_3} = 68.25 \times 50 \times 720 \times 0.07798 \times \left(\frac{3.23'}{12.23'}\right)^2 = 13,364$ IN-KIPS

$E_{d_4} = 68.25 \times 50 \times 720 \times 0.07798 \times \left(\frac{0.23'}{12.23'}\right)^2 = 68$ IN-KIPS

$\Sigma E_{dx} = 211,853$ IN-KIPS

DECK MEMBRANE TENSION ENERGY

$$E_d = \Sigma E_{dx} \left(1 + \frac{.00687\,5}{.00798}\frac{L_s}{L_d}\right)$$

$= 211,853 \times 1.18 = 249,987$ IN-KIPS

3.3 CASE 3 - RIGHT ANGLE COLLISION - STRUCK BY VERTICAL BOW

SUMMARY OF PLASTIC ENERGY ABSORBED BEFORE SHELL PLATE RUPTURE — STRUCK MIDSPAN BETWEEN WEB FRAMES & BULKHEADS BY VERTICAL BOW, 7 WEB FRAMES SPACES BETWEEN BULKHEADS.

		ENERGY (IN-KIPS)
E_{bc} = PLASTIC BENDING ENERGY IN LONG'L. STIFFENED SIDE	=	8,642
E_{mt} = MEMBRANE TENSION PLASTIC ENERGY IN LONG'L. STIFFENED SIDE	=	5,033,042
E_{ps} = SHEARING PLASTIC ENERGY IN WEB FRAMES	=	79,031
E_d = DECK MEMBRANE TENSION PLASTIC ENERGY	=	530,360
TOTAL ENERGY ABSORBED	=	5,651,075 IN-KIPS

SHELL - SINGLE

SIDE SHELL PLATE = 1 3/4" M.S
DECK PLATE = 1 3/8" M.S.

CASE 3 - RIGHT ANGLE COLLISION STRUCK BY VERTICAL BOW

CONFIGURATION OF THE STRIKING & THE STRUCK SHIP

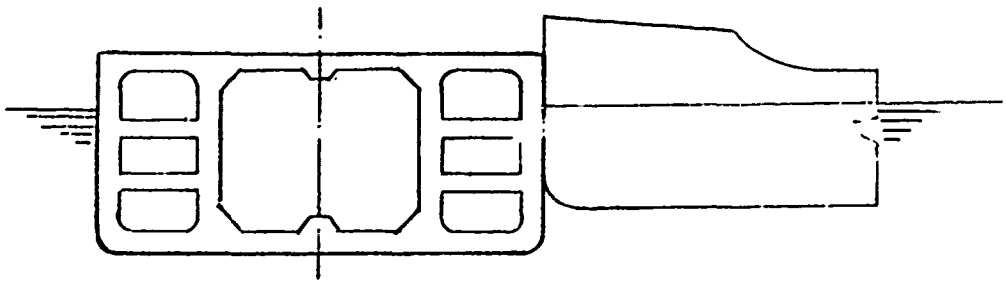

	STRUCK SHIP	STRIKING SHIP
TYPE	TANKER	TANKER
DWT	120,000 TONS	15,000 TONS
L	900.0 FT	500 FT
B	147.5 FT	68 FT
D	63.5 FT	39 FT
d	48.5 FT	30 FT

NOTE:

1. STRUCK SHIP'S WEB SPACING (L_S) EQUALS 12 FEET; SINGLE SHELL 1¾" M S
2. STRIKING SHIP HAS VERTICAL BOW.
3. THE TANKER IS STRUCK MIDSPAN BETWEEN WEB FRAMES & BULKHEAD AT RIGHT ANGLE, DISTANCE BETWEEN ADJACENT BULKHEADS IS 7 WEB FRAME SPACES.
4. DECK PLATE = 1⅜" M.S

CASE 3 - RIGHT ANGLE COLLISION STRUCK BY VERTICAL BOW

SCANTLINGS IN WAY OF WEB FRAME

ALL DECK LONG'LS. ARE 15"x 1¼" F.B. SPACING 36"

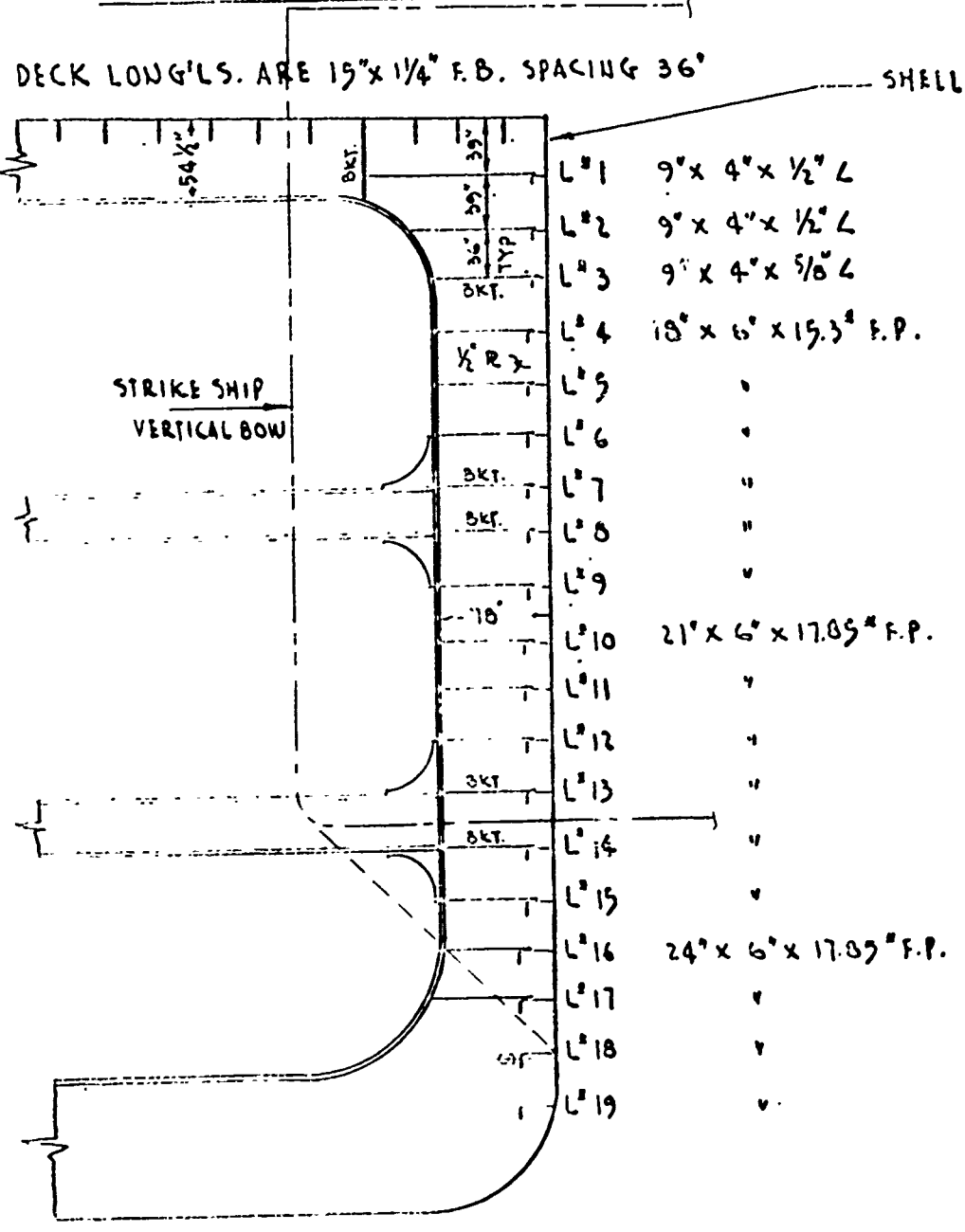

SIDE LONGITUDINAL SPACING = 36"
EXCEPT AS NOTED.

CASE 5 - RIGHT ANGLE COLLISION STRUCK BY VERTICAL POW

SHELL LONGITUDINAL NO	1	2	3	4	5	6	7	8	9	10	11	12	13	14	15	16	17	REMARK
BASIC DIMENSIONS	8"x6"x ½" ∠	8"x6"x ½" ∠	8"x6"x ½" ∠	18"x6"x 19.5°FP	18"x6"x 19.5°FP	18"x6"x 19.5°FP	18"x6"x 19.5°FP	18"x6"x 19.5°FP	18"x6"x 19.5°FP	21"x6"x 17.85°FP	21"x6"x 17.85°FP	21"x6"x 17.85°FP	21"x6"x 17.85°FP	21"x6"x 17.85°FP	21"x6"x 17.85°FP	24"x6"x 17.85°FP	24"x6"x 17.85°FP	
A_s = SECTIONAL AREA OF LONG. WITH PORTION OF SHELL PLT (in²)	0065	0929	7081	7186	—	—	—	—	—	7662	—	—	—	—	—	7595	7595	
I = MOMENT OF INERTIA OF LONG. WITH PORTION OF SHELL PLT (in⁴)	550 31	517 65	581 40	14558.00	—	—	—	—	—	21,379 00	—	—	—	—	—	31,149 00	31,149 00	
b = BREADTH OF FLANGE (in) = 2 x FLANGE OF I.P. OR ANGLE	8	8	8	12	12	12	12	12	12	12	12	12	12	12	12	12	12	
t_f = THICKNESS OF FLANGE (in)	0 500	0 500	0 625	0 375	0.375	0 375	0 375	0 375	0 375	0 438	0.438	0 438	0 438	0 438	0.438	0 438	0.438	
b/t_f = BREADTH - THICKNESS RATIO	16	16	12 8	32	32	32	32	32	32	27.4	27.4	27.4	27.4	27.4	27.4	27.4	27.4	
d = DEPTH OF WEB OF LONGITUDINAL (in)	9	9	9	18	18	18	18	18	18	21	21	21	21	21	21	24	24	
b/d = BREADTH - DEPTH RATIO	0 89	0 89	0 89	0 67	0 67	0 67	0.67	0 67	0.67	0.57	0.57	0.57	0 57	0.57	0.57	0.50	0.50	

CASE 3 - RIGHT ANGLE COLLISION STRUCK BY VERTICAL BOW

SHELL LONGITUDINAL NO.	1	2	3	4	5	6	7	8	9	10	11	12	13	14	15	16	17	REMARK
L_y = YIELD LENGTH FIG 2-5	12.0"	12.0"	12.0"	18.9"	18.9"	18.9"	18.9"	18.9"	18.9"	19.6"	19.6"	19.6"	19.6"	19.6"	19.6"	20.5"	20.5"	
L	12.0"	—															—	
$\frac{2L_y}{L}$	2.33	0.33	0.33	0.53	—	—	—	—	—	0.54	—	—	—	—	—	0.57	0.57	
$\frac{2L_y}{2L_y + L}$	0.25	0.25	0.25	0.34	—	—	—	—	—	0.35	—	—	—	—	—	0.36	0.36	
CONSTANT A $\left(\frac{2L_y}{L}\right)\left(\frac{3.3 \times 10^7}{0.29 \cdot \sigma_y}\right)^2\left(1 - \frac{\sigma_y}{\sigma_u}\right)$	0.28	0.28	0.34	0.19	—	—	—	—	—	0.23	—	—	—	—	—	0.24	0.24	
CONSTANT B $\left(\frac{2L_y}{L}\right)\left(\frac{3.3 \times 10^7}{0.29 \cdot \sigma_y}\right)^2\left(\frac{\sigma_u}{\sigma_y} - 1\right)$	0.36	0.36	0.45	0.29	—	—	—	—	—	0.35	—	—	—	—	—	0.37	0.37	
ROTATION CAPACITY CONST $K = A(11.6 - 6.18)$	4.87	4.87	6.41	3.09	—	—	—	—	—	3.96	—	—	—	—	—	4.21	4.21	
PLASTIC CURVATURE M_p/EI	311.0×10^{-6}	254.0×10^{-6}	249.9×10^{-6}	109.0×10^{-6}	—	—	—	—	—	96.9×10^{-6}	—	—	—	—	—	85.0×10^{-6}	85.0×10^{-6}	THESE ARE CALCULATED VALUES, FIG. 1 MAY BE USED.
PLASTIC ANGLE CHANGE CAP $\theta_p = K\left(\frac{M_p}{EI}\right)\left(\frac{L}{2}\right)$	0.0547	0.0465	0.0567	0.0121	—	—	—	—	—	0.0135	—	—	—	—	—	0.0129	0.0129	
BENDING DEFLECTION CAP $\delta_{BC} = \theta_p \cdot L$	3.96	3.20	4.08	0.87	—	—	—	—	—	0.97	—	—	—	—	—	0.93	0.93	
PLASTIC BENDING MOMENT M_p (IN-KIPS)	2,989	2,388	2,779	4,108	—	—	—	—	—	6,676	—	—	—	—	—	7,762	7,762	E = 29,000 KSI
PLASTIC BENDING ENERGY $E_{BC} = .572\, M_p \theta_p$	935	608	901	326	—	—	—	—	—	516	—	—	—	—	—	573	573	$\Sigma E_{BC} = 6663$ IN-K CONSIDERED $E_{BC} = \frac{2}{3} E_{BC}$ IS $E_{BC} =$
LATERAL FORCE, (KIPS) (BENDING ONLY) $P_{BC} = E_{BC}/\delta_{BC}$	257	190	221	315	—	—	—	—	—	551	—	—	—	—	—	616	616	
FORCE ON WEB AT ENDS OF L_y (KIPS) $\left(\frac{P_{BC}}{2} + \frac{M_p}{L_y}\right)$	139	112	130	188	—	—	—	—	—	312	—	—	—	—	—	474	474	

CASE 5 - RIGHT ANGLE COLLISION STRUCK BY VERTICAL BOW

SHELL LONGITUDINAL NO.	1	2	3	4	5	6	7	8	9	10	11	12	13	14	15	16	17	REMARK
ε_r (CRITICAL VALUE)	0.10	—	—	—	—	—	—	—	—	—	—	—	—	—	—	0.10	0.10	
MEMBRANE TENSION DEFL $\delta_{tc} = \frac{L}{2}(\varepsilon_r + \varepsilon_c) + \delta_{mc}$	32.49	32.41	32.91	32.26	—	—	—	—	—	—	—	—	—	—	—	32.26	32.26	
AVERAGE MEMBRANE TENSION FORCE $T = A_s\sigma_y(\frac{\sigma_y}{2E_s} + \varepsilon_r)$	3,457	3,466	3,545	3,597	—	—	—	—	—	3,735	—	—	—	—	—	3,798	3,798	
δ_m (DEFORMATIONS TO MATCH STRIKING BOW CONFIGURATION ARE ASSUMED TO BE)	32.26				—	—	—	—	—	—	—	—	—	25.81	19.36	12.90	6.45	
NET LATERAL FORCE ON LONGL DUE TO MEMBRANE TENSION SUM $= \Sigma T \delta_m/L$	6,872	3,106	3,177	3,223	—	—	—	—	—	3,367	—	—	—	2,678	2,009	1,361	680	
$P_{WF} = P_{TM}/2 \div R_m$	327	208	213	216	—	—	—	—	—	224	—	—	—	179	134	91	45	$R_m = 7.685$ SEE SHEET NO. 3-41
NO OF WEB FRAME SPACES DAMAGED $n = \left[\frac{0.9 P_{TM}}{P_{WF}}\right] 2 - 1$	15	15	15	15	15	15	15	15	15	15	15	15	15	15	15	15	15	ROUNDED OFF TO NEXT HIGHER ODD INTEGER
ACTUAL 7 WEB FRAME SPACES DAMAGED $L_1 = 7L_s$	1.008	—	—	—	—	—	—	—	—	—	—	—	—	—	—	1.008	1.008	
$\delta_{1m} = \frac{P_{WF} L_1^3}{2T}$	4.55													3.45	2.58	1.75	0.85	
FINAL δ (DEFORMATION AT LONGL #1 SEE SH #3-41 FOLLOWS BOW CONTOUR TO LONGL NO. 13	.0252													162.02	121.51	81.08	40.50	MAX. BEND ANGLE = 17°-55' SEE SHT NO 3-106
$\varepsilon = \frac{\delta^2 + 92\delta_1^2}{19 L_1 L_d}$	0.08265	—			—	—								0.05289	0.02970	0.01325	0.00330	
$e_L = L_d \cdot \varepsilon$	83.51													53.51	29.96	13.36	3.33	
$E_{mT} = T e_L \left(1 + \frac{0.07619 L_1}{0.08265 L_d}\right)$	511,861	126,290	333,727	338,623	338,623	338,623	338,623	338,623	338,623	351,614	351,614	351,614	351,614	224,998	126,565	51,338	14,291	$\Sigma E_{mL} = 3,033,062$

CASE 3 - RIGHT ANGLE COLLISION STRUCK BY VERTICAL BOW

ANALYSIS OF WEB FRAMES

(LATERAL LOAD = ½ P_{tm})

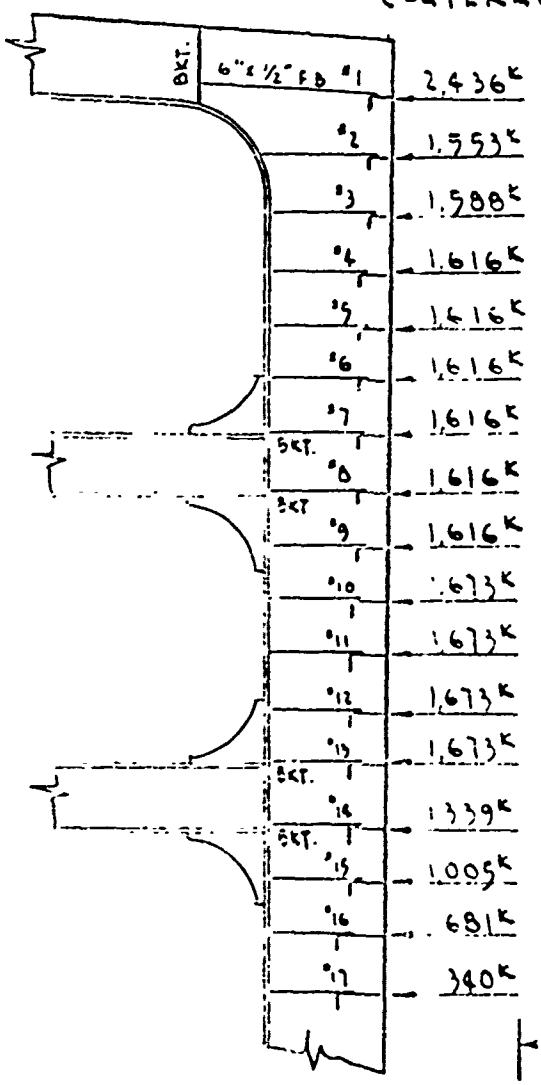

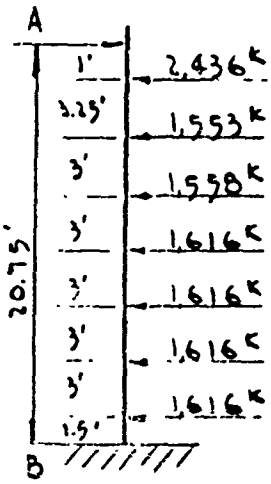

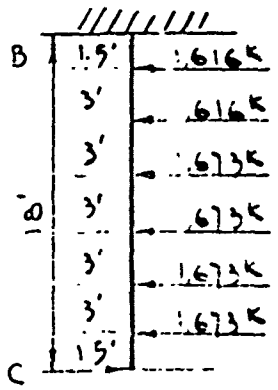

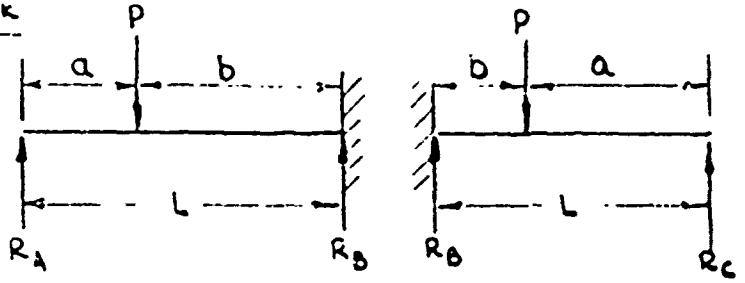

$$R_A = \frac{Pb^2}{2L^3}(a+2L), \qquad R_C = \frac{Pb^2}{2L^3}(a+2L)$$

$$R_B = \frac{Pa}{2L^3}(3L^2 - a^2)$$

CASE 3 - RIGHT ANGLE COLLISION STRUCK BY VERTICAL BOW

ANALYSIS OF WEB FRAMES
DETERMINATION OF R_A, R_B & R_C

LONG'LS	L	P/2	a	b	2L+a	L^3	$3L^2-a^2$	R_A	R_B	R_C
A	—	—	—	—	—	—	—	—	—	—
1	20.75	1,218	1.00	19.75	42.50	8,934.16	1,291	2,260	176	
2		777	4.25	16.50	45.75		1,274	1,083	471	
3		794	7.25	13.50	48.75		1,239	790	798	
4		808	10.25	10.50	51.75		1,187	516	1,100	
5		808	13.25	7.50	54.75		1,116	278	1,337	
6		808	16.25	4.50	57.75		1,028	106	1,510	
7		808	19.25	1.50	60.75		921	12	1,604	
B		—	—	—	—				6996	—
8	18.00	808	16.50	1.50	52.50	5,832.00	700		1,600	16
9		808	13.50	4.50	49.50		790		1,477	139
10		836	10.50	7.50	46.50		862		1,297	375
11		836	7.50	10.50	43.50		916		985	687
12		836	4.50	13.50	40.50		952		614	1,058
13		836	1.50	16.50	37.50		970		209	1,464
C		—	—	—	—				6,182	
TOTAL								5,045	13,178	3,739

CASE 3 - RIGHT ANGLE COLLISION STRUCK BY VERTICAL BOW

SHEAR & BENDING MOMENT FOR THE UPPER PART OF THE WEB FRAME

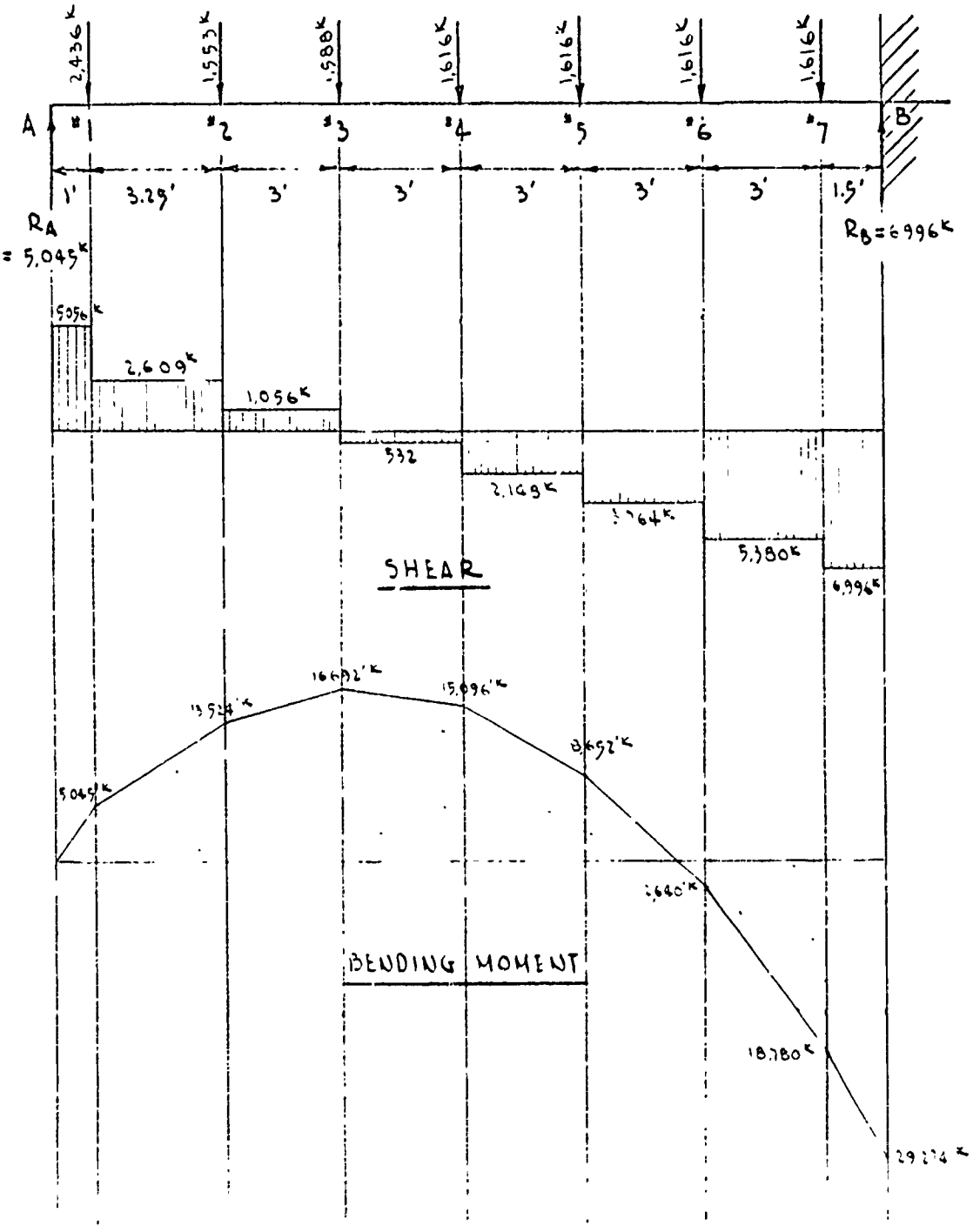

CASE 3 - RIGHT ANGLE COLLISION STRUCK BY VERTICAL BOW

SHEAR & BENDING MOMENT FOR THE LOWER PART OF THE WEB FRAME

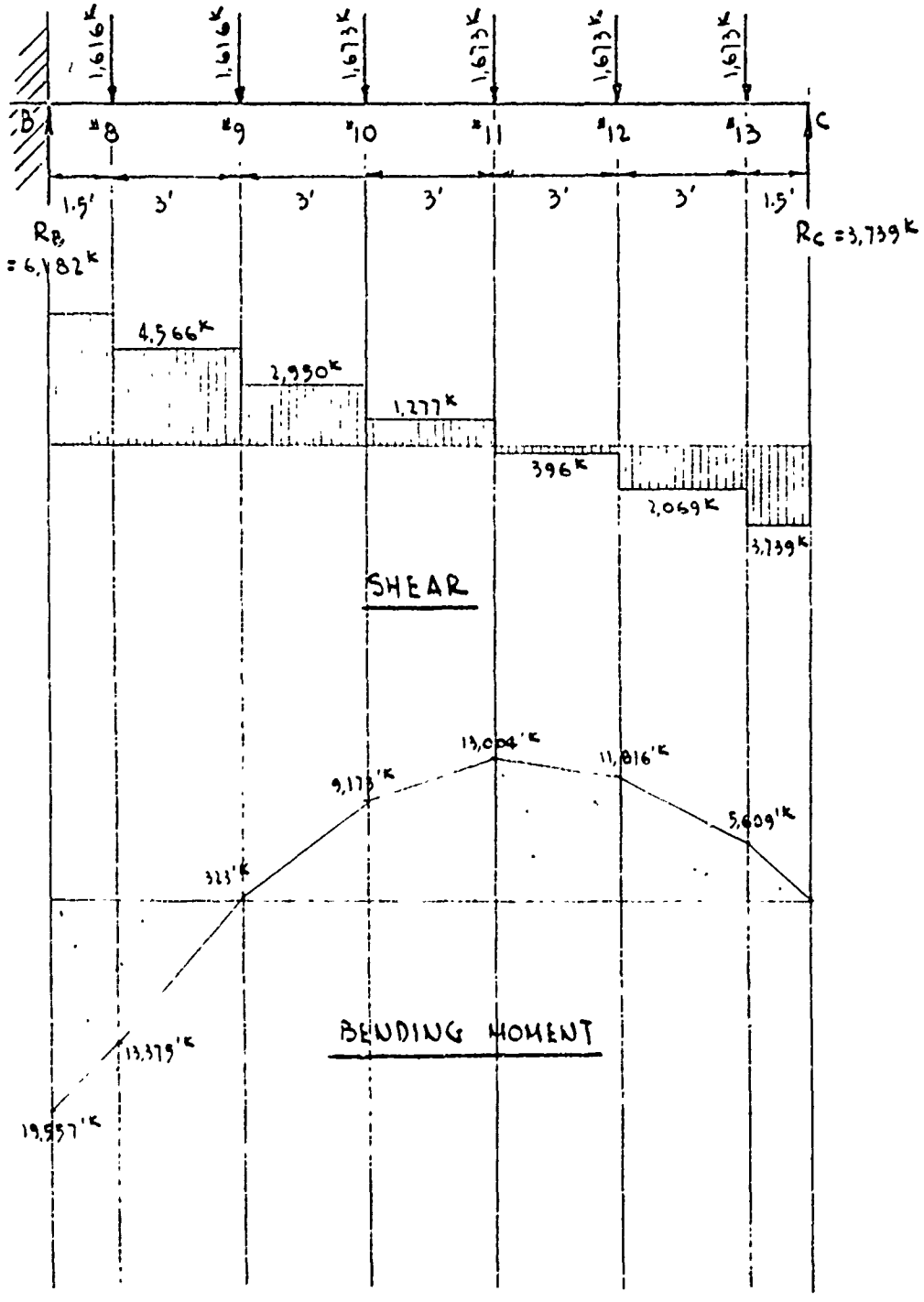

CASE 5 - RIGHT ANGLE COLLISION STRUCK BY VERTICAL BOW

SUMMARY OF "R"

(LATERAL LOADS / STRENGTH OF WEB FRAME)

LOCATION \ TYPE OF LOAD	R BENDING	R SHEAR	R CRUSHING	R COMPR.
A	—	—	—	—
1	—	—	5 033	—
2	1.906	3 311	3.208	—
3	2 393	1.340	—	—
4	2.128	2 726	3 338	—
5	1 219	4 776	3 338	—
6	0 372	6 827	3.338	—
7	—	—	—	—
8	—	—	—	7 483
9	0 046	5.794	3 338	—
10	1 293	3 743	3 338	—
11	1 833	1 621	3 456	—
12	1 665	2 625	3 456	—
13	0 795	—	3 456	—
C	—	—	—	2 123

MAX R = 7483

SUMMARY OF WEB FRAME STRENGTH SEE SHT NO 3-03

CASE 3 · RIGHT ANGLE COLLISION STRUCK BY VERTICAL BOW

SHEARING PLASTIC ENERGY (E_{ps})

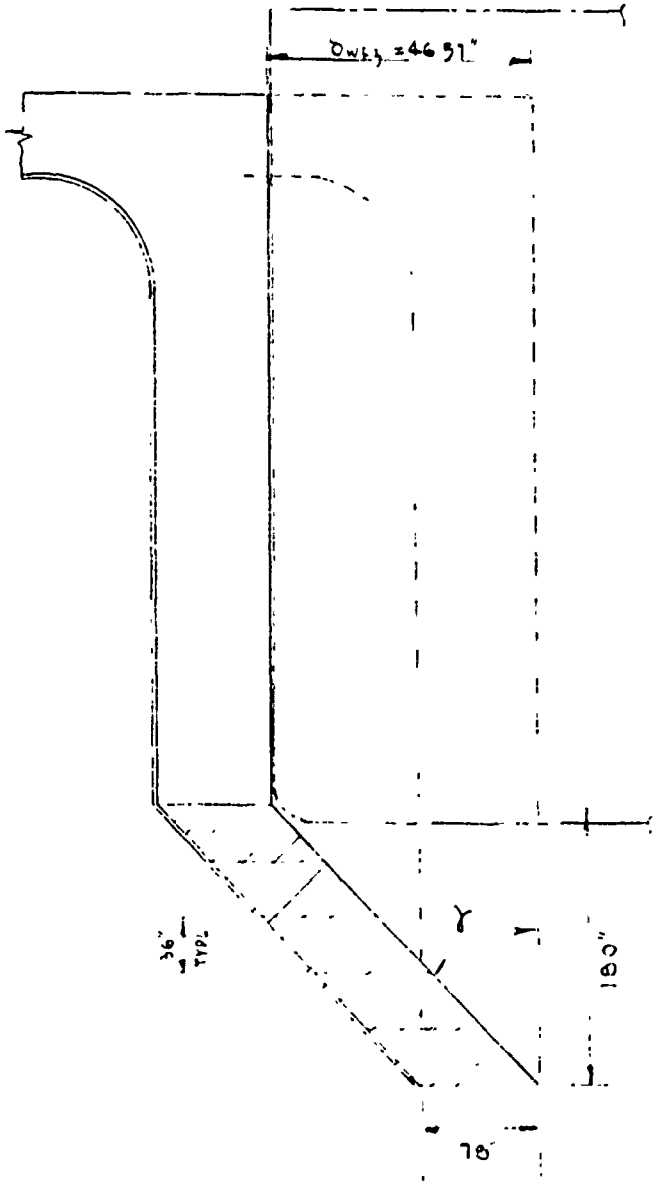

$$\gamma = \text{TAN}^{-1}\frac{46.51}{180} = 0.2587$$

$$\gamma = 14.51^\circ = 0.2531 \text{ RADIAN}$$

$$\gamma_m = 0.0947 \text{ RADIAN}$$

$$\gamma > \gamma_m$$

WEB PANEL :

$a = 36"$

$d = 78"$

$t = 0.5"$

$d/a = 2.17$

$d/t = 156$

FROM FIG 2-6, $\tau_{cr} = 27.0$, $\tau_y = 20.2$

SINCE $\tau_{cr} > \tau_y$

$$E_{ps} = (a,a\,t)\left(\gamma - \frac{\tau_y}{11150}\right)(\tau_y) \times 6$$

$$= 180" \times 78" \times 0.5" \left(0.0347 - \frac{20.2}{11,150}\right) 202 \times 6$$

$$= 79,031 \text{ IN-KIPS}$$

CASE 3 - RIGHT ANGLE COLLISION STRUCK BY VERTICAL BOW

PLASTIC ENERGY DUE TO DECK DEFORMATION (E_d)

DEFORMATION AT LONG'L. NO.1 = 202.52", ε = 0.08266
= 16.88'

NO. OF DECK LONG'LS DAMAGED = $\frac{202.52}{36}$ = 5.63

$$E_{dx} = T \cdot e_t = A_s \times \frac{\sigma_y + \sigma_u}{2} \times L_d \times \varepsilon$$

$$E_{d_1} = 93.00 \times 50 \times 1.008 \times 0.08266 \times \left(\frac{13.88'}{16.88'}\right)^2 = 261.965 \text{ IN-KIPS}$$

$$E_{d_2} = 68.25 \times 50 \times 1.008 \times 0.08266 \times \left(\frac{10.88'}{16.88'}\right)^2 = 118.129 \text{ IN-KIPS}$$

$$E_{d_3} = 68.25 \times 50 \times 1.008 \times 0.08266 \times \left(\frac{7.88'}{16.88'}\right)^2 = 61.964 \text{ IN-KIPS}$$

$$E_{d_4} = 68.25 \times 50 \times 1.008 \times 0.08266 \times \left(\frac{4.88'}{16.88'}\right)^2 = 23.764 \text{ IN-KIPS}$$

$$E_{d_5} = 68.25 \times 50 \times 1.008 \times 0.08266 \times \left(\frac{1.88'}{16.88'}\right)^2 = 3.527 \text{ IN-KIPS}$$

$$\Sigma E_{dx} = 469.345 \text{ IN-KIPS}$$

DECK MEMBRANE TENSION ENERGY

$$E_d = \Sigma E_{dx} \left(1 + \frac{0.07525}{0.08266} \frac{L_s}{L_d}\right)$$

$$= 469.345 \times 1.13 = 530.360 \text{ IN-KIPS}.$$

3.4 CASE 4 - RIGHT ANGLE COLLISION - STRUCK BY 15° RAKED BOW

SUMMARY OF PLASTIC ENERGY ABSORBED BEFORE SHELL PLATE RUPTURE — STRUCK MIDSPAN BETWEEN WEB FRAMES & BULKHEADS BY 15° RAKED BOW, 7 WEB FRAMES SPACES BETWEEN BULKHEADS.

	ENERGY (IN-KIPS)
E_{bc} = PLASTIC BENDING ENERGY IN LONG'L. STIFFENED SIDE	= 8,642
E_{mt} = MEMBRANE TENSION PLASTIC ENERGY IN LONG'L. STIFFENED SIDE	= 2,422,717
E_{ps} = SHEARING PLASTIC ENERGY IN WEB FRAMES	= 233,779
E_d = DECK MEMBRANE TENSION PLASTIC ENERGY	= 514,195
TOTAL ENERGY ABSORBED	= 3,179,333 IN-KIPS

SHELL - SINGLE

SIDE SHELL PLATE = 13/4" M.S
DECK PLATE = 1 3/8" M.S

CASE 4 - RIGHT ANGLE COLLISION - STRUCK BY 15° RAKED BOW

CONFIGURATION OF THE STRIKING & THE STRUCK SHIP

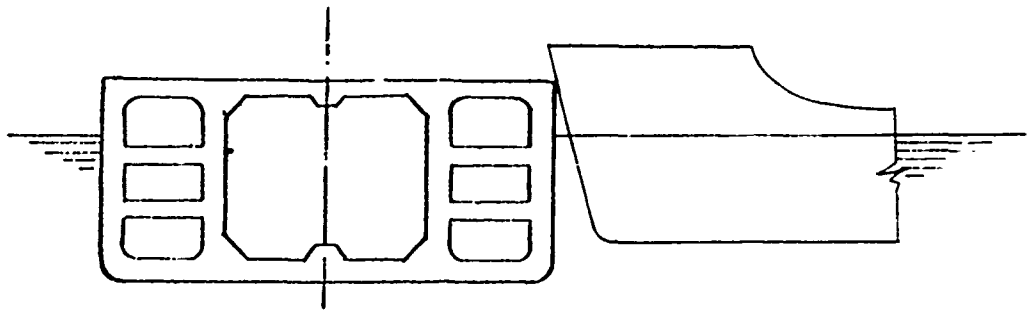

	STRUCK SHIP	STRIKING SHIP
TYPE	TANKER	TANKER
DWT	120,000 TONS	15,000 TONS
L	900.0 FT	500 FT
B	147.5 FT	68 FT
D	63.5 FT	39 FT
d	48.5 FT	30 FT

NOTE:

1. STRUCK SHIP'S WEB SPACING (L_S) EQUALS 12 FEET; SINGLE SHELL 1¾" M.S.
2. STRIKING SHIP HAS 15° RAKE BOW
3. THE TANKER IS STRUCK MIDSPAN BETWEEN WEB FRAMES & BULKHEADS AT RIGHT ANGLE, DISTANCE BETWEEN ADJACENT BULKHEADS IS 7 WEB FRAME SPACES.
4. DECK PLATE = 1¾" M.S.

CASE 4 - RIGHT ANGLE COLLISION - STRUCK BY 15° RAKED BOW

SCANTLINGS IN WAY OF WEB FRAME

ALL DECK LONG'LS. ARE 15"x 1¼" F.B. SPACING 36"

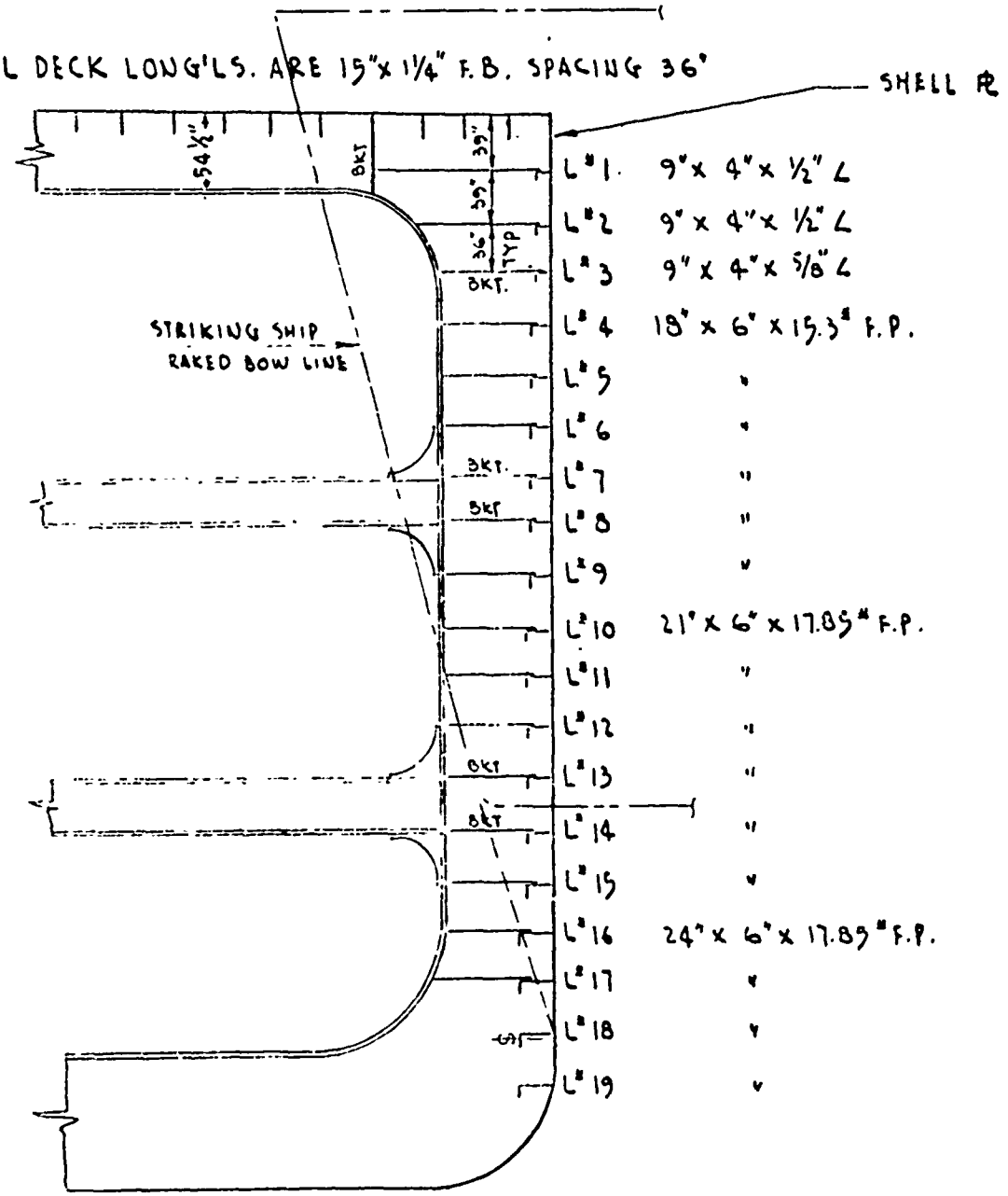

SIDE LONGITUDINAL SPACING = 36"
EXCEPT AS NOTED.

CASE 4 - RIGHT ANGLE COLLISION - STRUCK BY 15° RAKED BOW

SHELL LONGITUDINAL NO.	1	2	3	4	5	6	7	8	9	10	11	12	13	14	15	16	17	REMARK
BASIC DIMENSIONS	9"x6"x½" L	9"x6"x½" L	9"x6"x½" L	8"x6"x 19.33°F	15"x6"x 19.33°F	15"x6"x 19.33°F	15"x6"x 19.33°F	15"x6"x 19.33°F	15"x6"x 19.33°F	21"x6"x 17.85°F	21"x6"x 17.85°F	21"x6"x 17.85°F	21"x6"x 17.85°F	21"x6"x 17.85°F	21"x6"x 17.85°F	24"x6"x 17.85°F	24"x6"x 17.85°F	
A_s = SECTIONAL AREA OF LONG. WITH PORTION OF SHELL PLT. (IN²)	10.86	6.93	7.081	7.186	—	—	—	—	—	7.462	—	—	—	—	—	7.595	7.595	
I = MOMENT OF INERTIA OF LONG. WITH PORTION OF SHELL PLT. (IN⁴)	330.51	317.43	302.40	1,695.00	—	—	—	—	—	2,375.00	—	—	—	—	—	3,149.00	3,149.00	
b = BREADTH OF FLANGE (IN) = 2 x FLANGE OF L, T, OR ANGLE	9	9	9	12	12	12	12	12	12	12	12	12	12	12	12	12	12	
t_f = THICKNESS OF FLANGE (IN)	0.500	0.500	0.615	0.375	0.375	0.375	0.375	0.375	0.375	0.438	0.438	0.438	0.438	0.438	0.438	0.438	0.438	
b/t_f = BREADTH-THICKNESS RATIO	18.0	18.0	12.5	32.0	32.0	32.0	32.0	32.0	32.0	27.4	27.4	27.4	27.4	27.4	27.4	27.4	27.4	
d = DEPTH OF WEB OF LONGITUDINAL (IN)	9	9	9	18	18	18	18	18	18	21	21	21	21	21	21	24	24	
D/d = BREADTH - DEPTH RATIO	0.89	0.89	0.89	0.67	0.67	0.67	0.67	0.67	0.67	0.57	0.57	0.57	0.57	0.57	0.57	0.50	0.50	

CASE 4 - RIGHT ANGLE COLLISION - STRUCK BY 15° RAKED BOW

SHELL LONGITUDINAL NO.	1	2	3	4	5	6	7	8	9	10	11	12	13	14	15	16	17	REMARK
L_y = YIELD LENGTH FIG 3-5	12.0'	12.0'	12.0'	18.9'	18.9'	18.9'	18.9'	18.9'	18.9'	19.6'	19.6'	19.6'	19.6'	19.6'	19.6'	20.5'	20.5'	
L	72.0'	—																
$\frac{2L_y}{L}$	0.33	0.33	0.33	0.53	—	—	—	—	→	0.54	—	—	—	—	→	0.57	0.57	
$\frac{2L_y}{2L_y+L}$	0.25	0.25	0.25	0.34	—	—	—	—	→	0.35	—	—	—	—	→	0.36	0.36	
CONSTANT A $\left(\frac{2L_y}{L}\right)\left(\frac{33}{0.9D_x}\right)=\left(1-\frac{\nabla_y}{\nabla_u}\right)$	0.28	0.25	0.36	0.19	—	—	—	—	→	0.23	—	—	—	—	→	0.24	0.24	
CONSTANT B $\left(\frac{2L_y}{L}\right)\left(\frac{33}{0.9D_x}\right)=\left(\frac{\nabla_u}{\nabla_y}-1\right)$	0.36	0.36	0.65	0.29	—	—	—	—	→	0.35	—	—	—	—	→	0.57	0.57	
ROTATION CAPACITY CONST $K=A(11.6-16.8)$	6.87	4.87	0.41	3.09	—	—	—	—	→	3.96	—	—	—	—	→	4.21	4.21	
PLASTIC CURVATURE M_p/EI	312.0 $\times 10^{-6}$	2540 $\times 10^{-6}$	1695 $\times 10^{-6}$	1090 $\times 10^{-6}$	—	—	—	—	→	94.9 $\times 10^{-6}$	—	—	—	—	→	89.0 $\times 10^{-6}$	89.0 $\times 10^{-6}$	THESE ARE CALCULATED VALUES. FIG. 3-6 MAY BE USED
PLASTIC ANGLE CHANGE CAP $\theta_p=K\left(\frac{M_p}{EI}\right)\left(\frac{L}{2}\right)$	0.0547	0.0445	0.0367	0.0121	—	—	—	—	→	0.0135	—	—	—	—	→	0.0129	0.0129	
BENDING DEFLECTION CAP $\delta_{BC}=\theta_p\times L'$	3.94	3.20	4.08	0.87	—	—	—	—	→	0.97	—	—	—	—	→	0.93	0.93	
PLASTIC BENDING MOMENT M_p (IN-KIPS)	2,989	2,380	2779	4,108	—	—	—	—	→	6,676	—	—	—	—	→	7,762	7,762	E = 29,000 KSI
PLASTIC BENDING ENERGY $E_{BC}=.5\,M_p\theta_p$	955	605	901	326	—	—	—	—	→	516	—	—	—	—	→	573	573	$\Sigma E_{BC}=8,642$ IN-K CORRECTED $E_{BC}=\frac{\delta}{\delta_{BC}}E_{BC}$ IF $\delta_{BC}>\delta$.
LATERAL FORCE, (KIPS) (BENDING ONLY) $P_{BC}=E_{BC}/\delta_{BC}$	257	190	221	373														
FORCE ON WEB AT ENDS OF L_y (KIPS) $(P_{BC}/2+M_p/L_y)$	159	112	130	188														

CASE 4 - RIGHT ANGLE COLLISION - STRUCK BY 15° RAKED BOW

SHELL LONGITUDINAL NO.	1	2	3	4	5	6	7	8	9	10	11	12	13	14	15	16	17	REMARK
ε_1 (WITHIN LE)	0.10	—	—	—	—	—	—	—	—	—	—	—	—	—	—	0.10	0.10	
MEMBRANE TENSION DEFL $b_{ec} = \frac{1}{2}(\varepsilon_r + \varepsilon_{r_1}) + b_{wc}$	32.49	32.41	32.51	32.26	—	—	—	—	—	—	—	—	—	—	—	32.26	32.26	
AVERAGE MEMBRANE TENSION FORCE $T = A_s \sigma_y \left(\frac{\sigma_y + \sigma_u}{2\sigma_y}\right)$	3,437	3,466	3,545	3,597	—	—	—	—	—	3,735	—	—	—	—	—	3,798	3,798	
THE FOLLOWING EIGHT LINES ARE INITIAL CALCULATIONS FOR b_i																		
b_m (DEFORMATIONS TO MATCH STRIKING BOW CONFIGURATION ARE LIMITED TO DEC	32.49	22.04	12.39	2.76														
NET LATERAL FORCE ON LONG'L DUE TO MEMBRANE TENSION ONLY $P_{em} = 4T\, b_m / L_0$	6,907	2,122	1,220	274														
$P_{wi} = P_{em}/2 - R_m$	404	209	120	27														$R_m = 5,070$ SEE SHT. NO 3-93
NO OF WEB FRAME SPACES DAMAGED $n = \left[\frac{L_0}{L_{WB}}\right] 2 - 1$	11	11	11	11														
ACTUAL NO OF WEB FRAME SPACES DAMAGED	7	7	7	7														
$L_d = 7 \cdot L_s$	1,008	1,008	1,008	1,008														
$b_i = \frac{P_{wi} \cdot L_s}{2T}$	641	636	244	056														
b_i (DEFORMATION AT LONG'L SEE SHT NO 3-105 FOLLOWS 15° RAKE CONTOUR TO LONG'L 15)	94.97	184.52	174.87	165.13	159.58	149.94	136.29	122.64	111.00	101.35	91.71	88.06	78.41	62.75	47.05	31.37	15.68	MAX. BEND ANGLE 19°-9' SEE SHT NO 3-104
b_m	32.49	30.75	29.14	27.93	25.92	24.51	22.70	21.09	19.49	17.89	16.28	14.67	13.06	10.45	7.84	5.13	0.65	b_m AT LONG'L 2 (0.15 PROPORTIONAL TO b_i b_m @ LONG'L 1 = 32.49
NET LATERAL FORCE ON LONG'L DUE TO MEMBRANE TENSION ONLY $P_{em} = 4T\, b_m / L_0$	6,907	6,961	6,869	2,791	2,990	2,619	2,268	2,107	1,967	1,856	1,689	1,522	1,355	1,084	813	550	66	

CASE 6 - RIGHT ANGLE COLLISION - STRUCK BY 15° RAKED BOW

SHELL LONGITUDINAL NO.	1	2	3	4	5	6	7	8	9	10	11	12	13	14	15	16	17	REMARK
$P_{wt} = P_m/L \div R_m$	696	.92	283	231	255	240	224	208	192	183	167	150	134	107	80	53	7	
NO. OF WEB FRAME SPACES DAMAGED $\eta = \left[\frac{0.95 P_m}{R_m L}\right] 2-1$	11	11	11	11	11	11	11	11	11	11	11	11	11	11	11	11	11	ROUNDED OFF TO NEXT HIGHER ODD INTEGER
ACTUAL 7 WEB FRAME SPACE DAMAGED $L_d = 7 L_s$	7	7	7	7	7	7	7	7	7	7	7	7	7	7	7	7	7	
$b_1 = \frac{P_{wt} \cdot L_E}{2T}$	4.1	4.07	5.39	5.42	5.10	4.80	4.48	4.16	3.84	3.53	3.22	2.89	2.58	2.06	1.54	0.63	0.13	
* FINAL b (DEFORMATION AT LOWER NO 1 SEE SHT NO 1 FOLLOWING 5° RAKE CONTAINS TO LOWER NO 15)	194.91	84.52	174.87	165.23	155.50	145.94	136.29	126.64	117.00	107.35	97.71	88.06	78.41	62.73	47.05	31.37	15.68	MAX. BEND ANGLE = 15°-5° SEE SHT NO. 5-154
$\varepsilon = \frac{b' + 57 b_1'}{57 L_E + L_d}$	.01305	.001079	.006558	.005615	.005031	.004374	.003862	.003333	.002845	.002396	.001985	.001611	.001278	.000818	.000460	.000198	.000049	
$e_t = L_d \cdot \varepsilon$	.9144	.1356	.4594	.1120	.5071	.4409	.3893	.3360	.2868	.2419	.2000	.1624	.1288	.0825	.0464	.0200	.0049	
$E_{mt} = T e_t \left(1 + \frac{0.01 \cos 4\phi}{0.01 + L_d}\right)$	648,117	178,145	156,053	251,818	205,569	178,733	151,315	136,208	116,264	101,696	84,187	68,360	54,216	34,127	19,331	8,561	2,097	$\Sigma E_{mt} = 2,422,717$ IN-K

* SINCE $\Sigma m = 5010$ IN BOTH INITIAL AND FINAL CALCULATIONS, $b = b_1$

CASE 4 - RIGHT ANGLE COLLISION - STRUCK BY 15° RAKED BOW

INITIAL ANALYSIS OF WEB FRAMES

(LATERAL LOAD = ½ P_{tm})

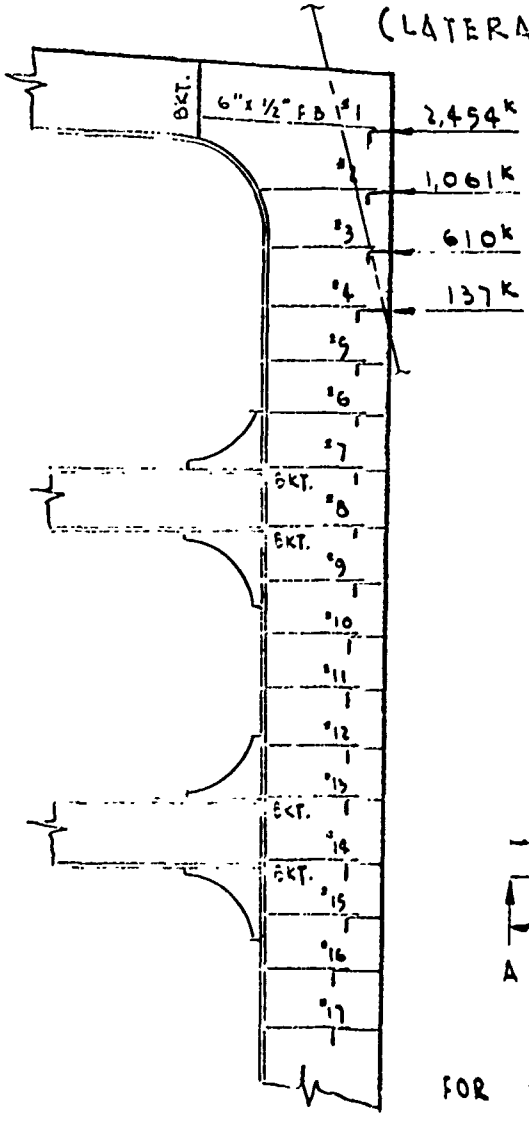

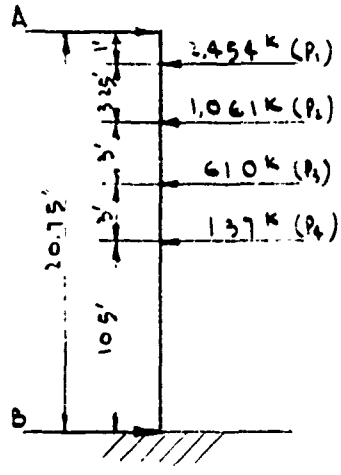

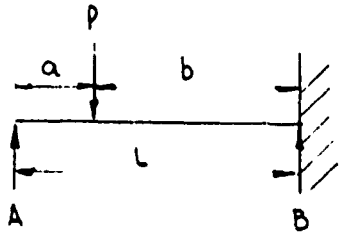

$$R_B = \frac{Pa}{2L^3}(3L^2 - a)$$

FOR P_1 $\quad \frac{2.454 \times 1}{2(20.75)^3}\left[3(20.75)^2 - (1.00)^2\right] = 177.25$

FOR P_2 $\quad \frac{1.061 \times 4.25}{2(20.75)^3}\left[3(20.75)^2 - (4.25)^2\right] = 321.37$

FOR P_3 $\quad \frac{.610 \times 7.25^2}{2(20.75)^3}\left[3(20.75)^2 - (7.25)^2\right] = 306.26$

FOR P_4 $\quad \frac{.137 \times 10.25^2}{2(20.75)^3}\left[3(20.75)^2 - (10.25)^2\right] = 93.19$

$R_B = 898$ KIPS

$R_A = 3,364$ KIPS

CASE 4 - RIGHT ANGLE COLLISION - STRUCK BY 15° RAKED BOW

INITIAL ANALYSIS OF WEB FRAME

SHEAR & BENDING MOMENT FOR THE UPPER PART OF THE WEB FRAME

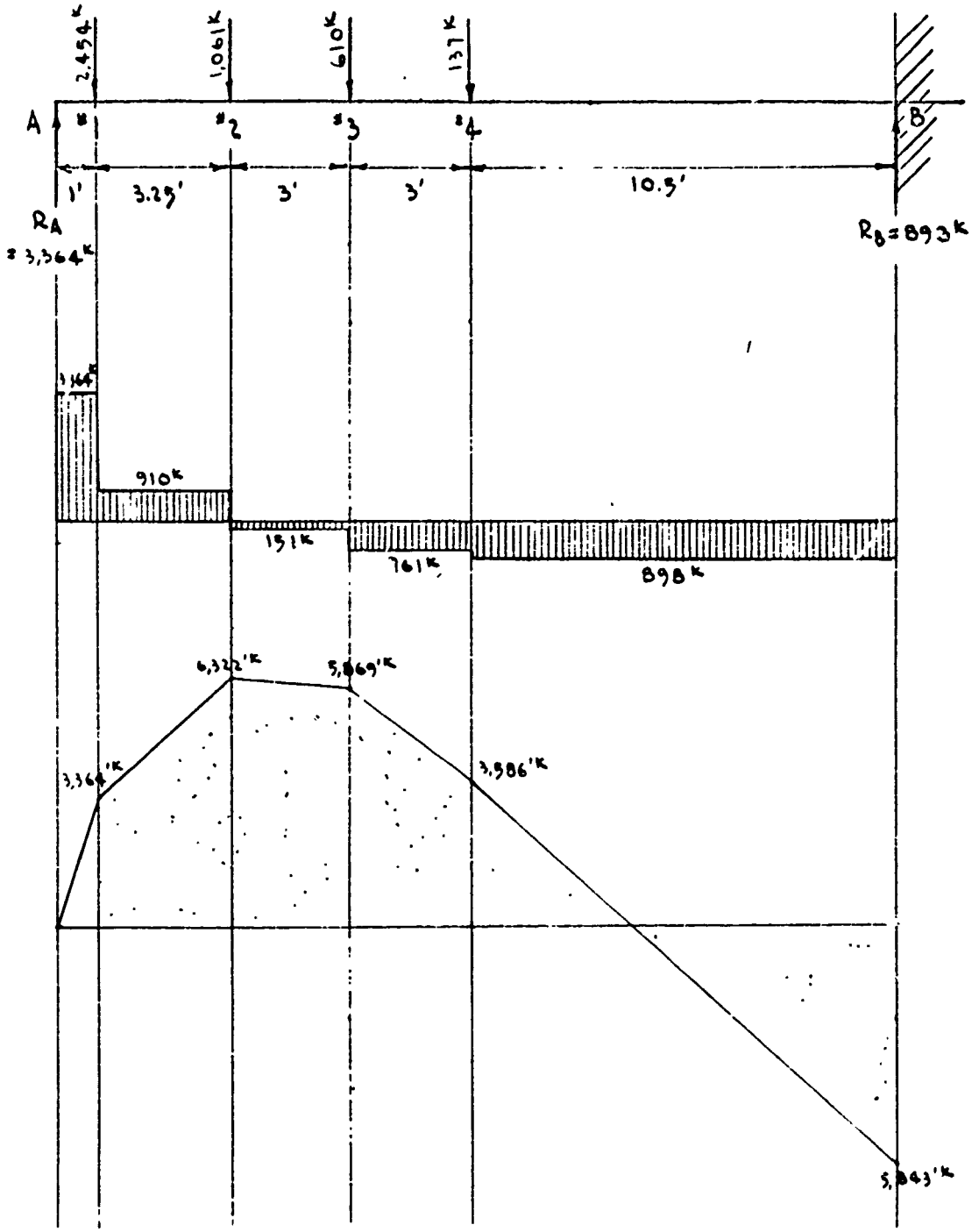

CASE 4 - RIGHT ANGLE COLLISION - STRUCK BY 15° RAKED BOW

INITIAL ANALYSIS OF WEB FRAME
SUMMARY OF "R"
(LATERAL LOADS / STRENGTH OF WEB FRAME)

LOCATION \ TYPE OF LOAD	R BENDING	R SHEAR	R CRUSHING	R COMPR.
A	—	—	—	—
1	—	—	5.070	—
2	0.891	1.154	2.192	—
3	0.827	0.965	—	—
4	0.505	1.163	0.283	—
5	—	—	—	—
6	—	—	—	—
7	—	—	—	—
8	—	—	—	0.509
8	—	—	—	—
9	—	—	—	—
10	—	—	—	—
11	—	—	—	—
12	—	—	—	—
13	—	—	—	—
C	—	—	—	—
MAX. R = 5.070				

FOR SUMMARY OF WEB FRAME STRENGTH SEE SHT. NO 3-93

CASE 4 - RIGHT ANGLE COLLISION - STRUCK BY 15° RAKED BOW

FINAL CHECK OF WEB FRAME ANALYSIS

(LATERAL LOAD = ½ Ptm)

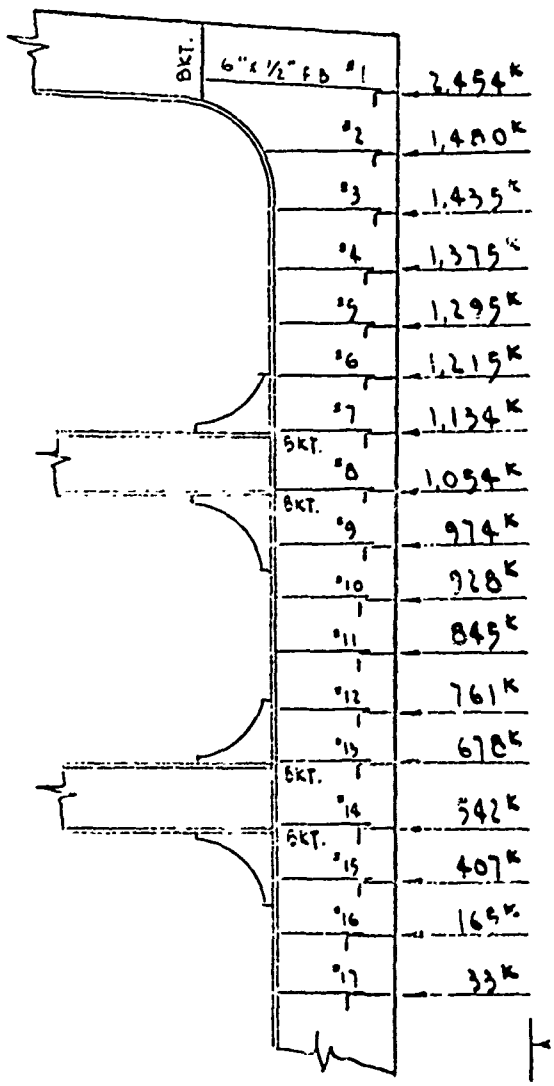

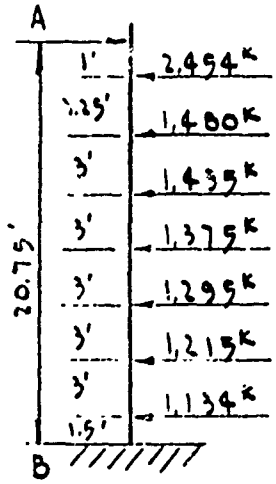

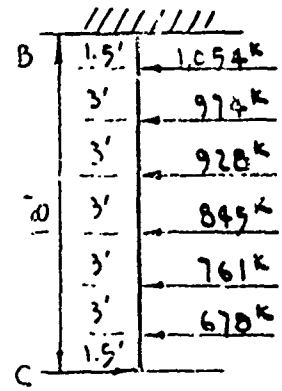

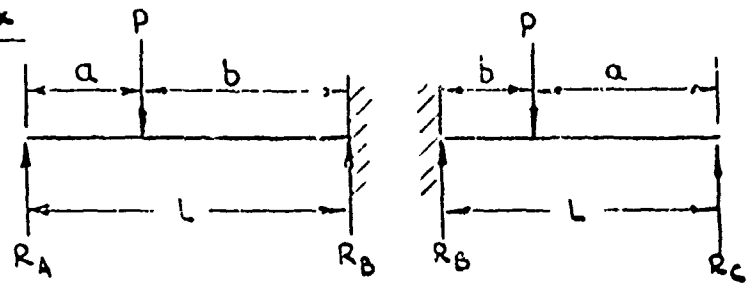

$$R_A = \frac{Pb^2}{2L^3}(a+2L), \qquad R_C = \frac{Pb^2}{2L^3}(a+2L)$$

$$R_B = \frac{Pa}{2L^3}(3L^2 - a^2)$$

CASE 4 - RIGHT ANGLE COLLISION - STRUCK BY 15° RAKED BOW

FINAL CHECK OF FRAME ANALYSIS

DETERMINATION OF R_A, R_B & R_C

LONG'LS	L	P/2	a	b	2L+a	L^3	$3L^2-a^2$	R_A	R_B	R_C
A	—	—	—	—	—	—	—	—	—	—
1	20.75	1,227.0	1.00	19.75	42.50	8,934.16	1,291	2,277	177	
2		740.0	4.25	16.50	45.75		1,274	1,032	488	
3		711.5	7.25	13.50	48.75		1,239	714	721	
4		687.5	10.25	10.50	51.75		1,187	439	936	
5		647.5	13.25	7.50	54.75		1,116	223	1,072	
6		607.5	16.25	4.50	57.75		1028	79	1,136	
7		567.0	19.25	1.50	60.75		921	9	1,125	
B		—	—	—	—				5,615	—
8	18.00	527.0	16.50	1.50	52.50	5,832.00	700		1,044	10
9		487.0	13.50	4.50	49.50		790		891	83
10		446.0	10.50	7.50	46.50		862		720	208
11		422.5	7.50	10.50	43.50		916		498	347
12		380.5	4.50	13.50	40.50		952		280	481
13		339.0	1.50	16.50	37.50		970		85	593
C		—	—	—	—				3,618	
TOTAL								4,773	9,133	1,722

CASE 4 - RIGHT ANGLE COLLISION - STRUCK BY 15° RAKED BOW

FINAL CHECK OF WEB FRAME ANALYSIS

SHEAR & BENDING MOMENT FOR THE LOWER PART OF THE WEB FRAME

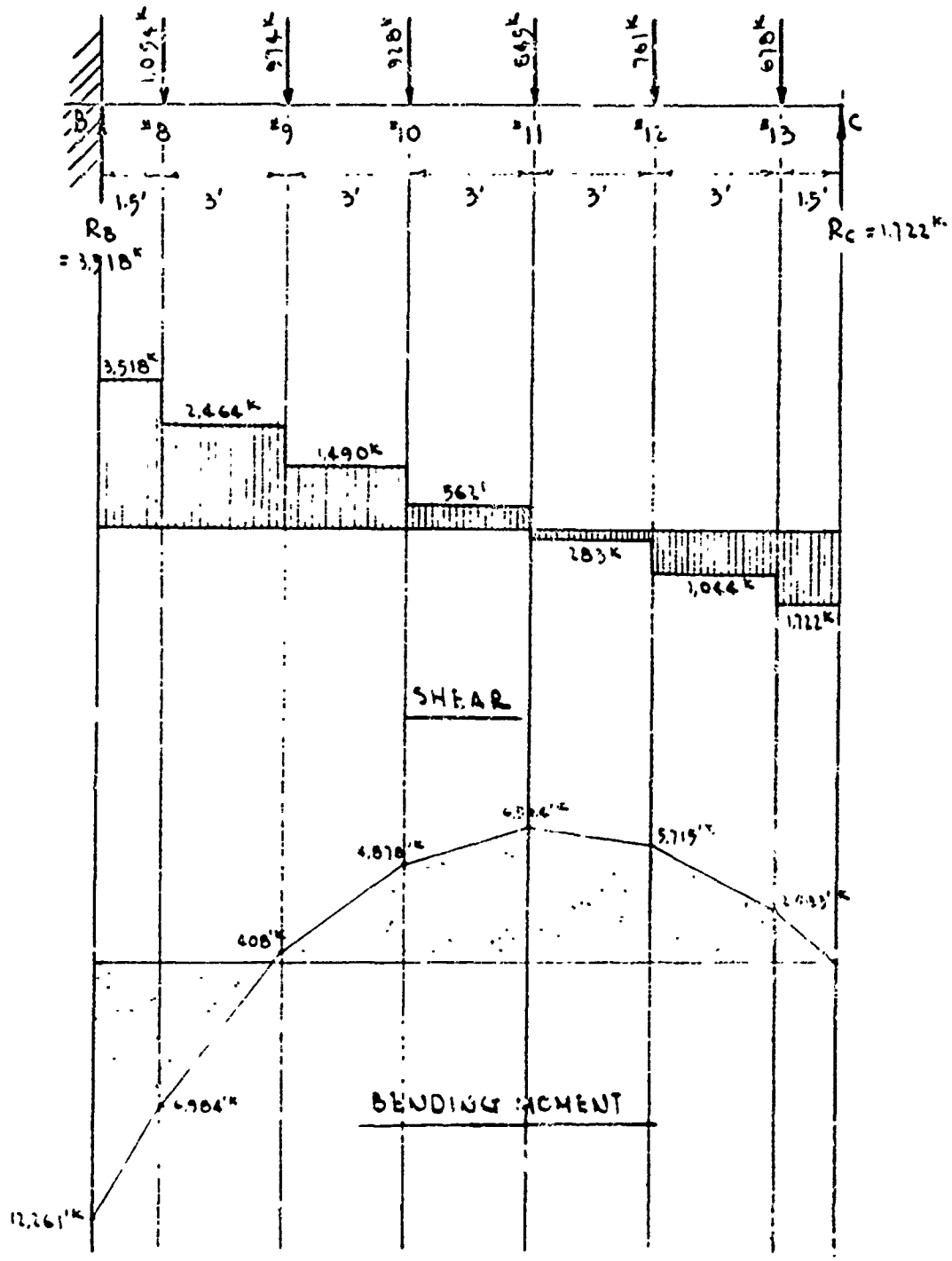

CASE 4 - RIGHT ANGLE COLLISION - STRUCK BY 15° RAKED BOW

FINAL CHECK OF WEB FRAME ANALYSIS

SHEAR & BENDING MOMENT FOR THE UPPER PART OF THE WEB FRAME

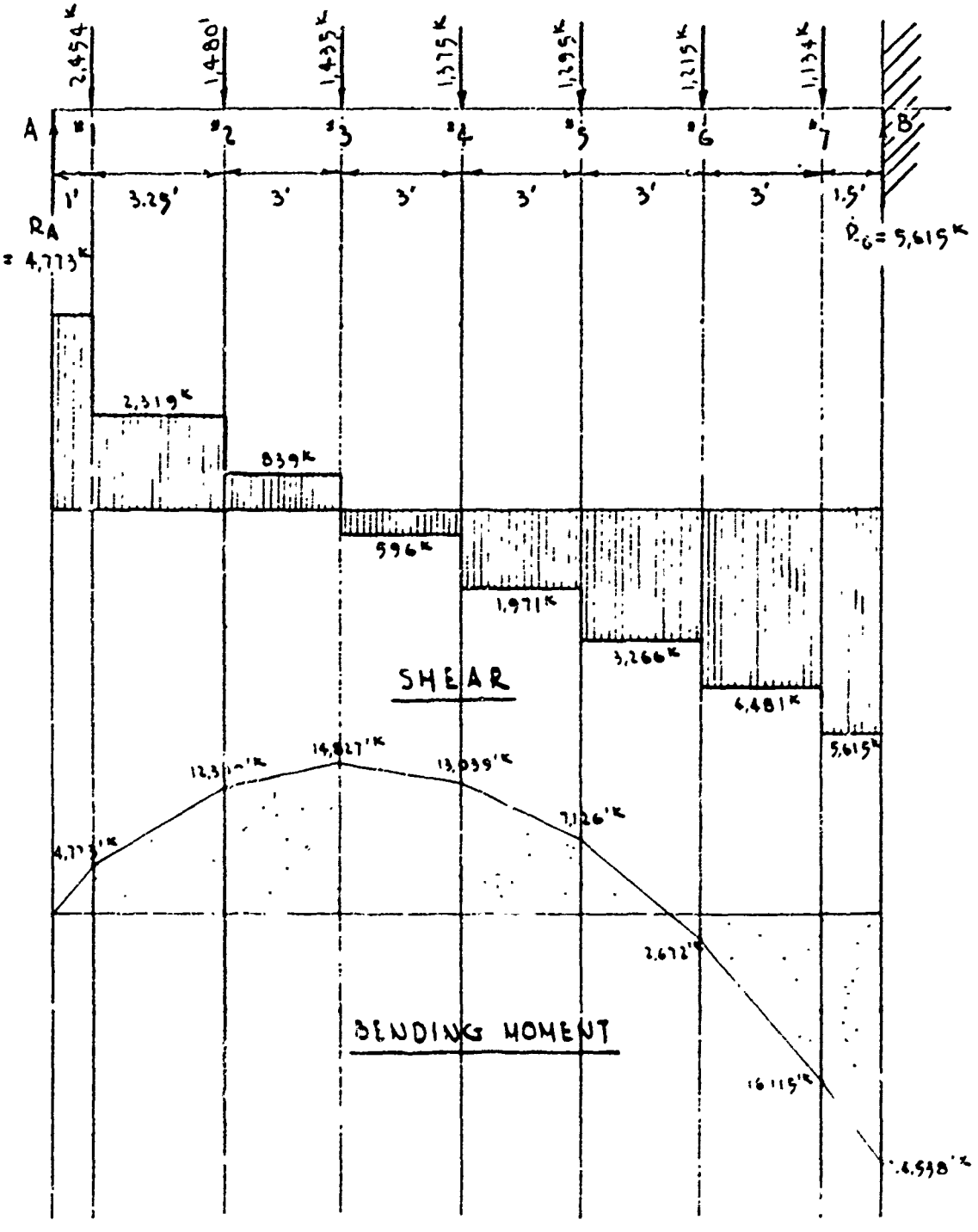

CASE 4 - RIGHT ANGLE COLLISION - STRUCK BY 15° RAKED BOW

FINAL CHECK OF WEB FRAME ANALYSIS

SUMMARY OF "R"

(LATERAL LOAD / STRENGTH OF WEB FRAME)

LOCATION \ TYPE OF LOAD	R BENDING	R SHEAR	R CRUSHING	R COMPR.
A	—	—	—	—
1	—	—	5070	—
2	1.735	6943	3058	—
3	2090	1065	—	—
4	1838	2501	2841	—
5	1.004	1145	2674	—
6	0.377	5687	2510	—
7	—	—	—	—
8	—	—	—	5186
	—	—	—	—
9	0058	3127	2012	—
10	0688	1891	1917	—
11	0.925	0713	1746	—
12	0905	1329	1572	—
13	—	—	—	—
C.	—	—	—	0978

MAX R = 5687 FOR BENDING, SHEAR & COMPR
MAX R = 5070 FOR CRUSHING

FOR $(Rm)^{1/2} = (5687)^{1/2} = 2385$ WHICH IS LESS THAN Rm = 5070 FOR CRUSHING. THEREFORE Rm = 5070 IS USED IN THE FINAL ABSORBED ENERGY CALCULATION FOR SUMMARY OF WEB FRAME STRENGTH SEE SHT NO 3-93

CASE 4 · RIGHT ANGLE COLLISION - STRUCK BY 15° RAKED BOW

SHEARING PLASTIC ENERGY (E_{ps})

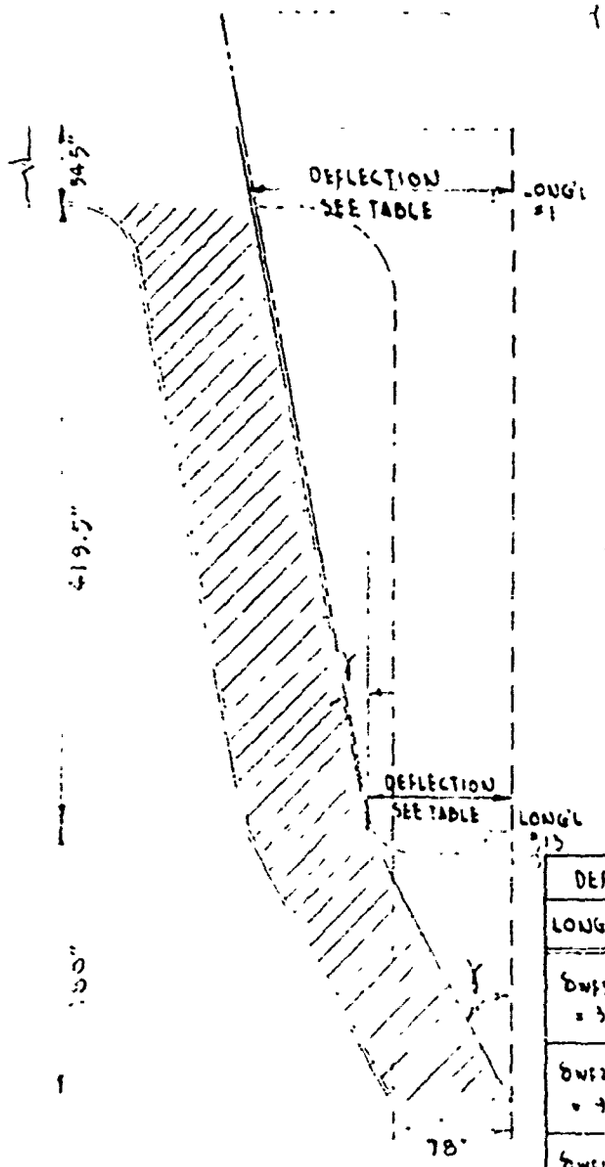

IF γ = 0.0947 RADIAN

USE γ_m = 0.0947

WEB PANEL:

$a = 36"$, $d = 78"$ & $t = 0.5"$

$d/a = 2.17$, $d/t = 156$

FROM FIG 2-6, $\tau_{cr} = 27.0$, $\tau_y = 20.2$

SINCE $\tau_{cr} > \tau_y$

USE SHEAR PLASTIC ENERGY FORMULA

FOR THE FOLLOWING TABLE

$$E_{ps} = (a_1 d t)\left(\gamma - \frac{\tau_y}{11{,}150}\right)(\tau_y)$$

$$= a_1 \times 78 \times 0.5 \left(\gamma - \frac{20.2}{11{,}150}\right) 20.2$$

DEFORMATION LONG'L #1	DEFORMATION LONG'L #15	a_1 IN	d IN	t IN	γ RADIAN	SHEAR ENERGY IN-KIPS
δ_{WEB1} = 38.97"	15.68"	419.5	78.0	0.5	0.0595	UPPER WEB $2 \times E_{ps1U}$ = 34.165
		180.0			0.0869	LOWER WEB $2 \times E_{ps1L}$ = 24.132
δ_{WEB2} = 40.74"	36.49"	419.5			0.0967	UPPER WEB $2 \times E_{ps2U}$ = 61.597
		180.0				LOWER WEB $2 \times E_{ps2L}$ = 26.344
δ_{WEB3} = 39.31"	62.46"	419.5				UPPER WEB $2 \times E_{ps3U}$ = 61.597
		180.0	"	"	"	LOWER WEB $2 \times E_{ps3L}$ = 26.344
						ΣE_{ps} = 233.779

CASE 4 - RIGHT ANGLE COLLISION - STRUCK BY 15° RAKED BOW

PLASTIC ENERGY DUE TO DECK DEFORMATION (E_d)

DEFORMATION AT LONG'L. NO.1 = 19497", $\varepsilon = 0.07902$

DEFORMATION AT DECK = $19497 + 39 \times \tan 15° = 20542" = 17.12'$

NO. OF DECK LONG'LS DAMAGED = $\frac{20542}{36} = 5.71$

$$E_{dx} = T \cdot e_t = A_s \times \frac{\sigma_y + \sigma_u}{2} \times L_d \times \varepsilon$$

$$E_{d_1} = 93.00 \times 50 \times 1008 \times .07902 \times \left(\frac{14\,12'}{17\,12'}\right)^2 = 251,949 \text{ IN-KIPS}$$

$$E_{d_2} = 68.25 \times 50 \times 1.008 \times .07902 \times \left(\frac{11\,12'}{17\,12'}\right)^2 = 14,676 \text{ IN-KIPS}$$

$$E_{d_3} = 68.25 \times 50 \times 1.008 \times .07902 \times \left(\frac{9\,12'}{17\,12'}\right)^2 = 61,147 \text{ IN-KIPS}$$

$$E_{d_4} = 68.25 \times 50 \times 1.008 \times .07902 \times \left(\frac{5\,12'}{17\,12'}\right)^2 = 24,311 \text{ IN-KIPS}$$

$$E_{d_5} = 68.25 \times 50 \times 1.008 \times .07902 \times \left(\frac{2\,12'}{17\,12'}\right)^2 = 4,168 \text{ IN-KIPS}$$

$$\Sigma E_{dx} = 456,251 \text{ IN-KIPS}$$

DECK MEMBRANE TENSION ENERGY

$$E_d = \Sigma E_{dx} \left(1 + \frac{.07044}{.07902} \frac{L_s}{L_d}\right)$$

$$= 456.251 \times 1.27 = 514,195 \text{ IN-KIPS}$$

3.5 CASE 5 - OBLIQUE COLLISION - STRUCK BY VERTICAL BOW

SUMMARY OF PLASTIC ENERGY ABSORBED BEFORE SHELL PLATE RUPTURE — STRUCK MIDSPAN BETWEEN WEB FRAMES & BULKHEADS BY VERTICAL BOW AT AN OBLIQUE ANGLE OF 70°, 7 WEB FRAME SPACES BETWEEN BULKHEADS

		ENERGY (IN-KIPS)
E_{bc} = PLASTIC BENDING ENERGY IN LONG'L. STIFFENED SIDE	=	8,642
E_{mt} = MEMBRANE TENSION PLASTIC ENERGY IN LONG'L STIFFENED SIDE	=	3,448,217
E_{ps} = SHEARING PLASTIC ENERGY IN WEB FRAMES	=	65,860
E_d = DECK MEMBRANE TENSION PLASTIC ENERGY	=	174,748
TOTAL ENERGY ABSORBED	=	3,697,467 (IN-KIPS)

SHELL - SINGLE

SIDE SHELL PLATE = 1¾ MS
DECK PLATE = 1⅜ MS.

CASE 5 - OBLIQUE COLLISION - STRUCK BY VERTICAL BOW

CONFIGURATION OF THE STRIKING & THE STRUCK SHIP

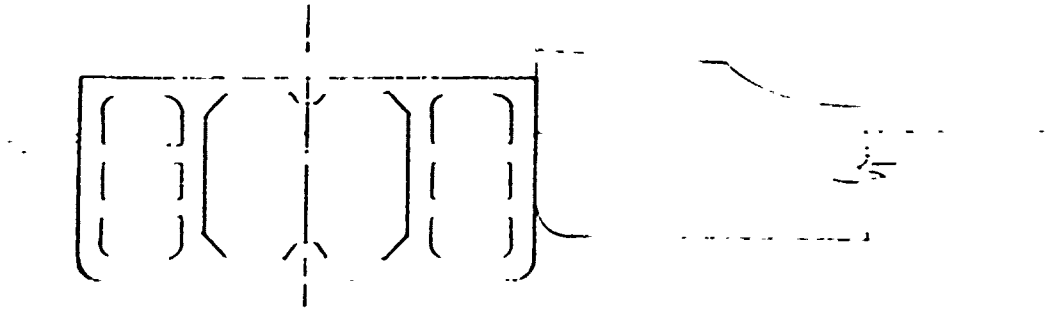

	STRUCK SHIP	STRIKING SHIP
TYPE	TANKER	TANKER
DWT	120,000 TONS	15,000 TONS
L	900.0 FT	500 FT
B	147.5 FT	68 FT
D	63.5 FT	39 FT
d	48.5 FT	30 FT

NOTE:

1. STRUCK SHIP'S WEB SPACING (L_S) EQUALS 12 FEET; SINGLE SHELL 1 3/4" M S
2. STRIKING SHIP HAS VERTICAL BOW
3. THE TANKER IS STRUCK MIDSPAN BETWEEN WEB FRAMES & BULKHEADS AT RIGHT ANGLE, DISTANCE BETWEEN ADJACENT BULKHEADS IS 7 WEB FRAME SPACES.
4. DECK PLATE = 1 3/8 M.S

CASE 5 - OBLIQUE COLLISION - STRUCK BY VERTICAL BOW

SCANTLINGS IN WAY OF WEB FRAME

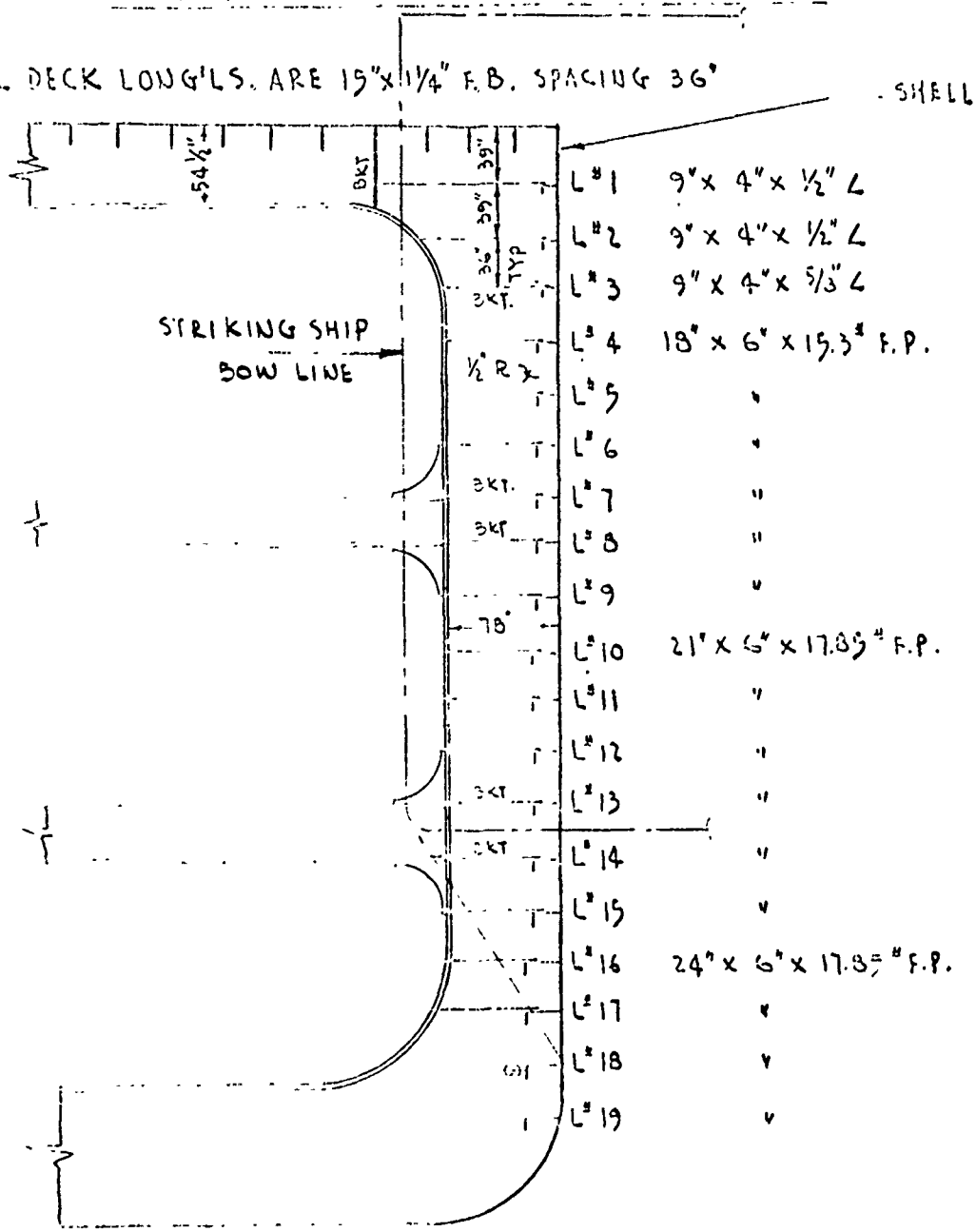

SIDE LONGITUDINAL SPACING = 36"
EXCEPT AS NOTED.

CASE 5 - OBLIQUE COLLISION - STRUCK BY VERTICAL BOW

SHELL LONGITUDINAL NO.	1	2	3	4	5	6	7	8	9	10	11	12	13	14	15	16	17	REMARK
BASIC DIMENSIONS	9"x4"x½" ∠	9"x4"x½" ∠	9"x4"x⅝" ∠	18"x6"x ½" F.P.	18"x6"x ½" F.P.	18"x6"x ½" F.P.	18"x6"x ½" F.P.	18"x6"x ½" F.P.	18"x6"x ½" F.P.	21"x6"x ½" F.P.	21"x6"x ½" F.P.	21"x6"x ½" F.P.	21"x6"x ½" F.P.	21"x6"x ½" F.P.	21"x6"x ½" F.P.	24"x6"x ½" F.P.	24"x6"x ½" F.P.	
A_s = SECTIONAL AREA OF LONG'L WITH PORTION OF SHELL PLT (IN²)	08.63	69.25	70.82	71.86	—	—	—	—	—	74.62	—	—	—	—	—	75.95	75.95	
I = MOMENT OF INERTIA OF LONG'L WITH PORTION OF SHELL PLT (IN⁴)	330.31	311.65	381.40	1,458.00	—	—	—	—	—	2,511.00	—	—	—	—	—	3,149.00	3,149.00	
b = BREADTH OF FLANGE (IN) = 2 × FLANGE OF F.P. OR ANGLE	8	8	8	12	12	12	12	12	12	12	12	12	12	12	12	12	12	
t_f = THICKNESS OF FLANGE (IN)	0.500	0.500	0.625	0.375	0.375	0.375	0.375	0.375	0.375	0.438	0.438	0.438	0.438	0.438	0.438	0.438	0.438	
b/t_f = BREADTH - THICKNESS RATIO	16.0	16.0	12.8	32.0	32.0	32.0	32.0	32.0	32.0	27.4	27.4	27.4	27.4	27.4	27.4	27.4	27.4	
d = DEPTH OF WEB OF LONGITUDINAL (IN)	9	9	9	18	18	18	18	18	18	21	21	21	21	21	21	24	24	
b/d = BREADTH - DEPTH RATIO	0.89	0.89	0.89	0.67	0.67	0.67	0.67	0.67	0.67	0.57	0.57	0.57	0.57	0.57	0.57	0.50	0.50	

CASE 5 - OBLIQUE COLLISION - STRUCK BY VERTICAL BOW

SHELL LONGITUDINAL NO.	1	2	3	4	5	6	7	8	9	10	11	12	13	14	15	16	17	REMARK
L_y = YIELD LENGTH FIG 2-3	12.0'	12.0'	12.0'	18.9'	18.9'	18.9'	18.9'	18.9'	18.9'	19.6'	19.6'	19.6'	19.6'	19.6'	19.6'	20.5'	20.5'	
L'	72.0"	—															—	
$\frac{2L_y}{L'}$	0.33	0.33	0.33	0.53	—				→	0.54	—				→	0.57	0.57	
$\frac{2L_y}{2L_y+L'}$	0.25	0.25	0.25	0.34	—				→	0.35	—				→	0.36	0.36	
CONSTANT A $\left(\frac{2L_y}{2L_y+L'}\right)\left(\frac{32.2\,\xi}{0.9\,D\sqrt{\sigma_y}}\right) \le \left(1-\frac{\sigma_y}{\sigma_u}\right)$	0.28	0.28	0.34	0.19	—				→	0.23	—				→	0.24	0.24	
CONSTANT B $\left(\frac{2L_y}{L'}\right)\left(\frac{51.2\,\xi}{0.9\,D\sqrt{\sigma_y}}\right) \le \left(\frac{\sigma_u}{\sigma_y}-1\right)$	0.36	0.36	0.45	0.29	—				→	0.35	—				→	0.37	0.37	
ROTATION CAPACITY CONST. $K = A(11.6+16.1B)$	4.87	4.87	6.41	3.09	—				→	3.96	—				→	4.21	4.21	
PLASTIC CURVATURE M_p/EI	312.0 $\times 10^{-6}$	256.0 $\times 10^{-6}$	245.5 $\times 10^{-6}$	109.0 $\times 10^{-6}$	—				→	94.9 $\times 10^{-6}$	—				→	85 $\times 10^{-6}$	85 $\times 10^{-6}$	THESE ARE CALCULATED VALUES, FIG. 2-6 MAY BE USED
PLASTIC ANGLE CHANGE CAP $\theta_p = K\left(\frac{M_p}{EI}\right)\left(\frac{L'}{2}\right)$	0.0547	0.0445	0.0507	0.0121	—			—	→	0.0135	—				→	0.0129	0.0129	
BENDING DEFLECTION CAP $\delta_{bc} = \theta_p \cdot L'$	3.94	3.20	4.08	0.87	—				→	0.97	—				→	0.93	0.93	
PLASTIC BENDING MOMENT M_p (IN-KIPS)	2,989	2,388	2,779	4,708	—				→	6,676	—				→	7,162	7,162	E = 29,000 KSI
PLASTIC BENDING ENERGY $E_{bc} = 5.72\, M_p \theta_p$	935	608	901	326	—				→	516	—				→	575	575	ΣE_{bc} = 8,642 IN-K CORRECTED $E_{bc} = \frac{2}{3}\frac{\delta_{bc}}{\delta_m}E_{bc}$ IF $\delta_{bc} > \delta_m$
LATERAL FORCE, (KIPS) (BENDING ONLY) $P_{bc} = E_{bc}/\delta_{bc}$	237	190	221	375	—				→	531	—				→	616	616	
FORCE OUTBOARD AT ENDS OF L_t (KIPS) $(P_{bc} + M_p/L_t)$	139	112	130	188	—				→	312	—				→	474	474	

CASE 5 · OBLIQUE COLLISION · STRUCK BY VERTICAL BOW

SHELL LONGITUDINAL NO.	1	2	3	4	5	6	7	8	9	10	11	12	13	14	15	16	17	REMARK
ε_r (WITHIN L_E)	0.10																	
MEMBRANE TENSION DEFL $\delta_{EC} = \frac{L_E^2}{2}(\varepsilon_r + \varepsilon_c) + \delta_{DC}$	23.11	22.99	23.15	22.78						22.79								
AVERAGE MEMBRANE TENSION FORCE AFT OF THE STRIKE $T_a = A_s\left(\frac{\sigma_y + \sigma_u}{2}\right)$	5457	3,466	3,545	3,597						3,735						3,798	3,798	
AVERAGE MEMBRANE TENSION FORCE FORWARD OF THE STRIKE T_b (ASSUME $T_b = T_{b_1}$)	2,719	1,733	1,773	1,799						1,868						1,899	1,899	
δ_m (DEFORMATIONS TO MATCH STRIKING BOW CONFIGURATION ARE LIMITED TO δ_{DC})	22.78													18.22	13.67	9.11	4.56	
NET LATERAL FORCE ON WEB FRAMES AFT OF THE STRIKE $\frac{2 P_m T_a}{L_E^2}$	1,720	1,096	1,122	1,138						1,182				945	709	480	240	
NET LATERAL FORCE ON WEB FRAMES FORWARD OF THE STRIKE $\frac{2 P_m T_b}{L_E^2}$	860	548	561	569						591				473	345	240	120	
$P_{WS} = \frac{2 \delta_m T_b}{L_E R_{mb}} = \frac{2 P_m T_a}{L_E R_{ma}}$	326	208	213	216						224				179	134	91	45	$R_{mb} = 5.277$ $R_{ma} = 2.659$ SEE SHEET NO. 5-72
CALCULATED NO OF WEB FRAME SPACES DAMAGED AFT OF THE STRIKE $\frac{2 \delta_m T_b}{L_E R_{mb}} - \frac{1}{2}$	5.5	5.5	5.5	5.5	5.5	5.5	5.5	5.5	5.5	5.5	5.5	5.5	5.5	5.5	5.5	5.5	5.5	ROUNDED OFF TO NEXT HIGHER HITBOOK +0.5
CALCULATED NO OF WEB FRAME SPACES DAMAGED FORWARD OF THE STRIKE $\frac{2 T_b \delta_m}{L_E R_{mb}} - \frac{1}{2}$	2.5	2.5	2.5	2.5	2.5	2.5	2.5	2.5	2.5	2.5	2.5	2.5	2.5	2.5	2.5	2.5	2.5	↓
ACTUAL NO OF WEB FRAME SPACES DAMAGED AFT OF THE STRIKE	3.5	3.5	3.5	3.5	3.5	3.5	3.5	3.5	3.5	3.5	3.5	3.5	3.5	3.5	3.5	3.5	3.5	
ACTUAL NO OF WEB FRAME SPACES DAMAGED FORWARD OF THE STRIKE	2.5	2.5	2.5	2.5	2.5	2.5	2.5	2.5	2.5	2.5	2.5	2.5	2.5	2.5	2.5	2.5	2.5	
$\delta_{1b} = \frac{P_{WS} \cdot L_E}{2 \cdot T_b}$	4.33													3.45	2.59	1.73	0.86	
$\delta_{1a} = \frac{P_{WS} \cdot L_E}{2 \cdot T_a}$	8.66													6.90	5.18	3.46	1.72	

CASE 5 - OBLIQUE COLLISION - STRUCK BY VERTICAL BOW

SHELL LONGITUDINAL NO.	1	2	3	4	5	6	7	8	9	10	11	12	13	14	15	16	17	REMARK
FINAL δ (DEFORMATION AT LONG'L NO. 1 SEE SHT NO 3-105, FOLLOWS BOW CONTOUR TO LONG'L NO. 13)	130.39													104.31	78.23	52.16	26.09	MAX BEND ANGLE = 10°-16' SEE SHT NO. 3-105
$\varepsilon_b = \frac{\delta^2 - 9433\, b_{ib}^2}{2.92 \cdot L_f \cdot L_{db}}$	0.07342													0.04819	0.02716	0.01207	0.00302	
$e_{tb} = L_{db} \cdot \varepsilon_b$	3.801													24.34	13.69	6.08	1.52	L_{db}=95=L_f=504"
$T_b e_{tb}\left(1 + \frac{0.01898\, t_s}{0.08505\, L_{db}}\right)$	261.425	166,694	170,453	172,993	172,993	172,993	172,993	172,993	172,993	179,589	179,589	179,589	179,589	115,001	64,682	29,211	7,305	Σ 2,970,805
THICKNESS OF WEB STIFF t_w	0.500	0.500	0.425	0.575						0.438								d = DEPTH OF WEB
(1) = $\frac{\sigma_y d}{R}$	63			126						147						168	168	RADIUS OF BEND AT NEUTRAL AXIS = R = 5 & σ_y = 35
(2) = d = t_w	45	45	3.6	60						9.2						10.5	10.5	
(3) = $\frac{\sigma_y \cdot R}{E \cdot d}$	0.0006			0.0003						0.0003						0.0003	0.0003	E = 29,000 KSI
(4) = (1 - (3))'	0.999			0.999														
(5) = $\frac{d - 0.5 t_f}{d}$	0.972	0.972	0.966	0.990						0.990						0.991	0.991	
(6) = $t_f(b - t_w)$	b=4 1.75	1.75	2.11	b=6 2.11						2.44						2.44	2.44	b = WIDTH OF FLANGE OF STIFF.
F_a = (1)[(1)(4)+(2)(3)·(5)]	390	390	481	1,119						1,306						2,168	2,168	
$F_z = \delta / \tan\theta$	18,508	18,508	22,827	33,105	33,105	33,105	33,105	33,105	33,105	80,963	80,963	80,963	80,963	64,769	48,575	41,158	20,587	ASSUME θ = 70° TAN θ = 2.7475 Σ = 877,614
$E_{mt} = T_b e_{tb}\left(1 + \frac{0.01898 t_s}{0.08505 L_{db}}\right) + \frac{F_a b}{\tan\theta}$	279,933	185,162	193,280	226,098	226,098	226,098	226,098	226,098	226,098	260,992	260,992	260,992	260,992	179,770	113,297	70,369	27,890	Σ E_{mt} = 3,448,217 IN-KIPS

CASE 5 - OBLIQUE COLLISION - STRUCK BY VERTICAL BOW

ANALYSIS OF WEB FRAMES

(LATERAL LOADS AFT OF THE STRIKE)

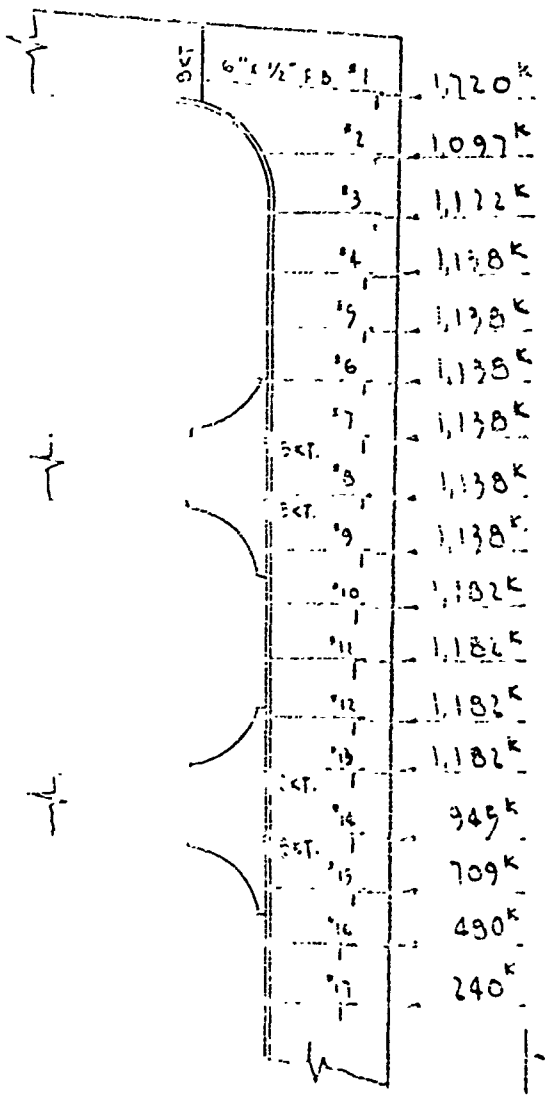

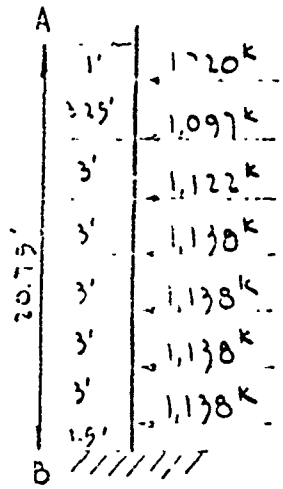

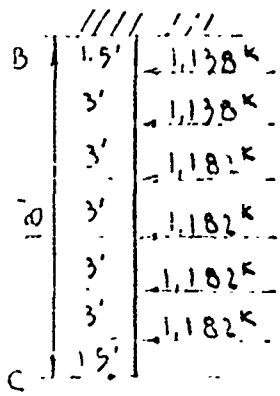

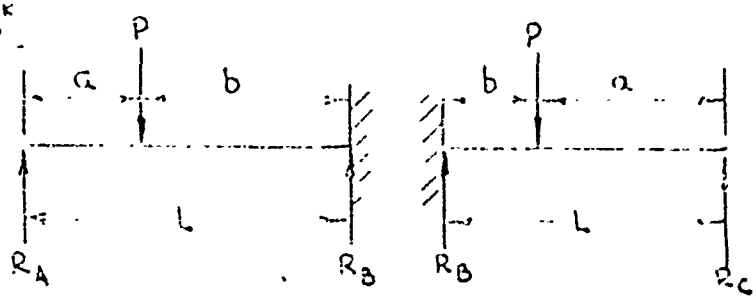

$$R_A = \frac{Pb^2}{2L^3}(a+2L), \qquad R_C = \frac{Pb^2}{2L^3}(a+2L)$$

$$R_B = \frac{Pa}{2L^3}(3L^2 - a^2)$$

CASE 5 - OBLIQUE COLLISION - STRUCK BY VERTICAL BOW

ANALYSIS OF WEB FRAMES
DETERMINATION OF R_A, R_B & R_C

LONG'LS	L	P/2	a	b	2L+a	L^3	$3L^2-a^2$	R_A	R_B	R_C
A	—	—	—	—	—	—	—	—	—	—
1	20.75	860.0	1.00	19.75	42.50	8,934.16	1,291	1,596	124	
2		548.5	4.25	16.50	45.75		1,274	765	333	
3		561.0	7.25	13.50	48.75		1,239	558	564	
4		569.0	10.25	10.50	51.75		1,187	363	775	
5		569.0	13.25	7.50	54.75		1,116	196	942	
6		569.0	16.25	4.50	57.75		1,028	74	1,064	
7		569.0	19.25	1.50	60.75		921	9	1,129	
B		—	—	—	—				4,930	—
8	18.00	569.0	16.50	1.50	52.50	5,832.00	700		1,127	12
9		569.0	13.50	4.50	49.50		790		1,041	98
10		591.0	10.50	7.50	46.50		862		917	265
11		591.0	7.50	10.50	43.50		916		696	486
12		591.0	4.50	13.50	40.50		952		434	748
13		591.0	1.50	16.50	37.50		970		147	1,035
C		—	—	—	—				4,363	
TOTAL								3,561	9,293	2,644

CASE 5 - OBLIQUE COLLISION - STRUCK BY VERTICAL BOW

SHEAR & BENDING MOMENT FOR THE UPPER PART OF THE WEB FRAME

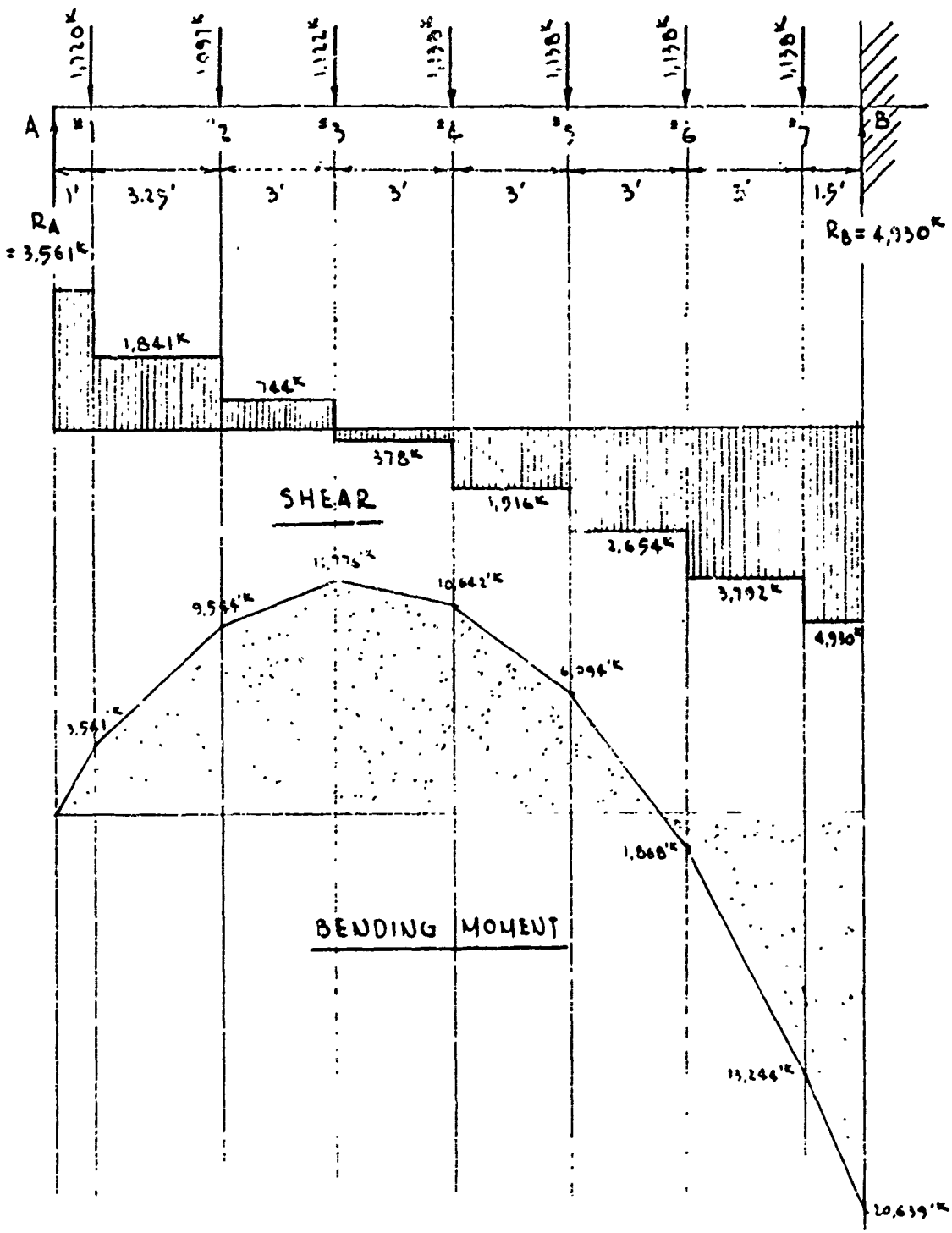

CASE 5 - OBLIQUE COLLISION - STRUCK BY VERTICAL BOW

SHEAR & BENDING MOMENT FOR THE LOWER PART OF THE WEB FRAME

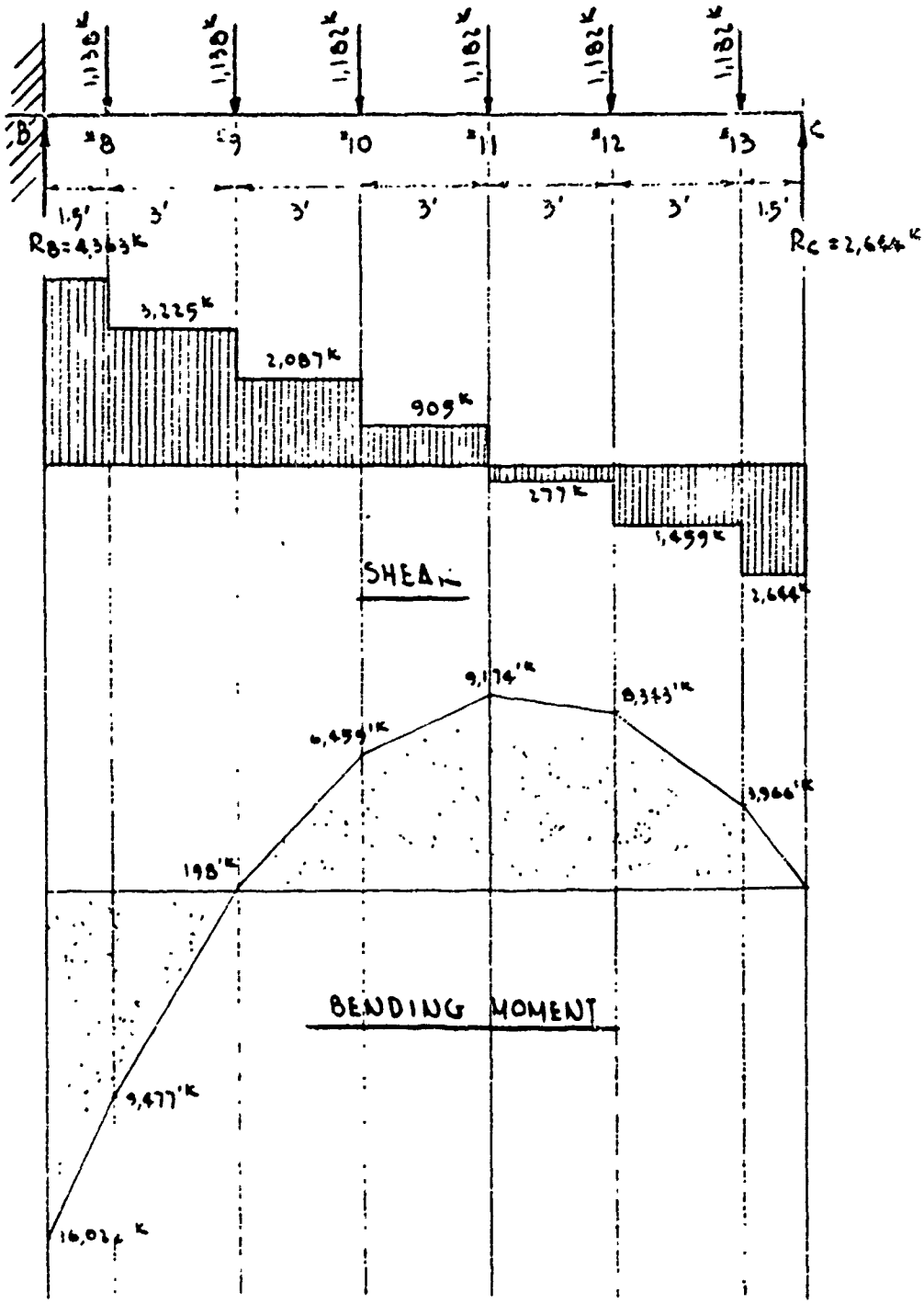

CASE 5 - OBLIQUE COLLISION - STRUCK BY VERTICAL BOW

SUMMARY OF "R"

LATERAL LOADS / STRENGTH OF WEB FRAME

LOCATION \ TYPE OF LOAD	R BENDING	R SHEAR	R CRUSHING	R COMPR.
A	—	—	—	—
1	—	—	3.554	—
2	1 345	2 336	2 266	—
3	1.660	0 944	—	—
4	1.500	1 923	2 351	—
5	0.859	3 368	2 351	—
6	0 263	4 812	2 351	—
7	—	—	—	—
8		—		5 277
8		—		—
9	0 028	4 092	2 351	—
10	0 910	2 648	2 442	—
11	1 293	1 149	2 442	—
12	1 176	1 851	2 442	—
13	0 559	—	2 442	—
C	—	—	—	1 501

MAX R = R_{mb} = 5 277; FOR $T_a = T_b/2$ R_{ma} = 5 277/2 = 2 639

FOR SUMMARY OF WEB FRAME STRENGTH SEE SHEET NO 3-93

CASE 5 - OBLIQUE COLLISION - STRUCK BY VERTICAL BOW

SHEARING PLASTIC ENERGY (E_{ps})

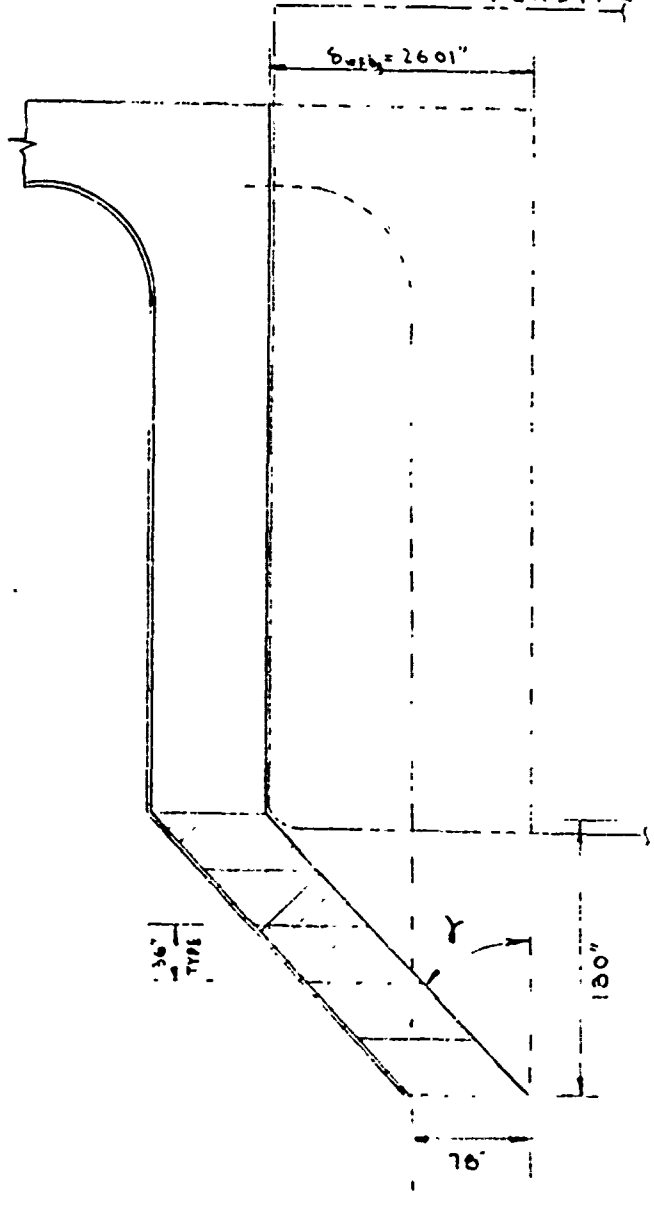

$\gamma = \tan^{-1} \frac{26.01"}{180"} = 0.1443$

$\gamma = 8.222° = 0.1435$ RADIAN

$\gamma_{m_1} = 0.0947$ RADIAN

$\gamma > \gamma_m$

WEB PANEL:

$a = 36"$

$d = 78"$

$t = 0.5"$

$d/a = 2.17$

$d/t = 156$

FROM FIG 2-6, $\bar{\tau}_{cr} = 27.0$, $\bar{\tau}_y = 20.2$

SINCE $\bar{\tau}_{cr} > \bar{\tau}_y$

$$E_{ps} = (a,d,t)\left(\gamma - \frac{\bar{\tau}_y}{11,150}\right)(\bar{\tau}_y) \times 5$$

$$= 180" \times 78" \times 0.5" \left(0.0947 - \frac{20.2}{11,150}\right) 20.2 \times 5$$

$= 65\,360$ IN-KIPS

* $\delta_{web_3} = \frac{\delta - 4\delta_{web}}{2.9} = \frac{150.39 - 4 \times 8.66}{2.9} = 38.30"$

$\delta_{web_3} = 26.01"$ WHICH IS THE LEAST DEFORMATION

CASE 5 - OBLIQUE COLLISION - STRUCK BY VERTICAL BOW

PLASTIC ENERGY DUE TO DECK DEFORMATION (Ed)

DEFORMATION AT LONG'L. NO.1 = 130.39, $\varepsilon = 0.08503$
= 10.87'

NO. OF DECK LONG'LS DAMAGED = $\frac{130.39}{36} = 3.62$

$Ed_x = T \cdot e_t = A_s \times \frac{\sigma_y + \sigma_u}{2} \times L_{dD} \times \varepsilon$

$Ed_1 = 93.00 \times 50 \times 504 \times 0.08503 \times \left(\frac{10.87'}{10.87'}\right)^2 = 104,459$ IN-KIPS

$Ed_2 = 68.25 \times 50 \times 504 \times 0.08503 \times \left(\frac{4.87'}{10.87'}\right)^2 = 29,354$ IN-KIPS

$Ed_3 = 68.25 \times 50 \times 504 \times 0.08503 \times \left(\frac{1.87'}{10.87'}\right)^2 = 4,328$ IN-KIPS

$\Sigma Ed_x = 138,141$ IN-KIPS

DECK MEMBRANE TENSION ENERGY

$$Ed = \Sigma Ed_x \left(1 + \frac{0.07898 \cdot L_s}{0.08503 \cdot L_{dD}}\right)$$

$= 138,141 \times 1.265 = 174,748$ IN-KIPS

3.6 CASE 6 - RIGHT ANGLE COLLISION - STRUCK BY VERTICAL BOW

SUMMARY OF PLASTIC ENERGY ABSORBED BEFORE SHELL PLATE RUPTURE — STRUCK MIDSPAN BETWEEN WEB FRAMES & BULKHEADS BY VERTICAL BOW, 7 WEB FRAMES SPACES BETWEEN BULKHEADS.

		ENERGY (IN-KIPS)
E_{bc} = PLASTIC BENDING ENERGY IN LONG'L. STIFFENED SIDE	=	6,517 6,260
E_{mt} = MEMBRANE TENSION PLASTIC ENERGY IN LONG'L. STIFFENED SIDE	=	5,744,419
E_{ps} = SHEARING PLASTIC ENERGY IN WEB FRAMES	=	65,860
E_d = DECK MEMBRANE TENSION PLASTIC ENERGY	=	542,997
OUTER SHELL DUCTILE TEARING ENERGY AS PENTRATION EXTENDED FROM 204.31 TO 282.31"	=	7,848
DECK DUCTILE TEARING ENERGY	=	4,658
TOTAL ENERGY ABSORBED	=	6,380,363 IN-KIPS

SHELL - DOUBLE
SIDE SHELL PLATE = 1" M S (OUTER)
SIDE SHELL PLATE = 3/4" M S (INNER)
DECK PLATE = 1 1/8" M S

CASE 6 - RIGHT ANGLE COLLISION - STRUCK BY VERTICAL BOW

CONFIGURATION OF THE STRIKING & THE STRUCK SHIP

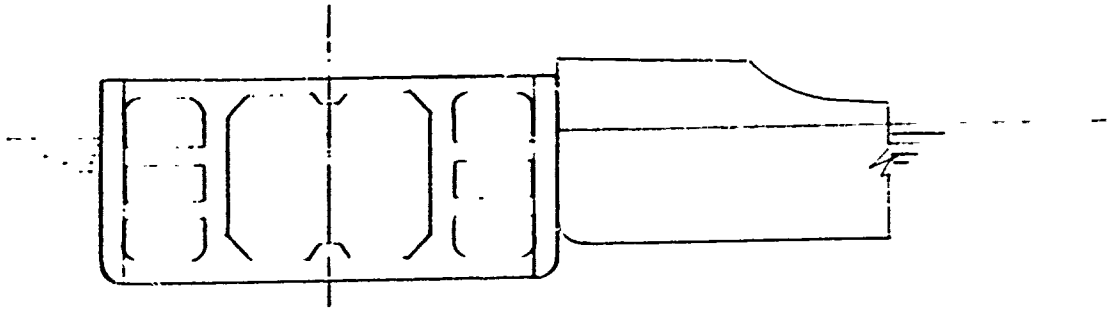

	STRUCK SHIP	STRIKING SHIP
TYPE	TANKER	TANKER
DWT	120,000 TONS	15,000 TONS
L	900.0 FT	500 FT
B	147.5 FT	68 FT
D	63.5 FT	39 FT
d	48.5 FT	30 FT

NOTE:

1. STRUCK SHIP'S WEB SPACING (L_S) EQUALS 12 FEET; DOUBLE SHELL - OUTER SHELL 1" M S, INNER SHELL ¾" M S, THEY ARE 7B APART
2. STRIKING SHIP HAS VERTICAL BOW
3. THE TANKER IS STRUCK MIDSPAN BETWEEN WEB FRAMES & BULKHEADS AT RIGHT ANGLE, DISTANCE BETWEEN ADJACENT BULKHEADS IS 7 WEB FRAME SPACES.
4. DECK PLATE = 1⅜" M S

CASE 6 - RIGHT ANGLE COLLISION - STRUCK BY VERTICAL BOW

SCANTLINGS IN WAY OF WEB FRAME

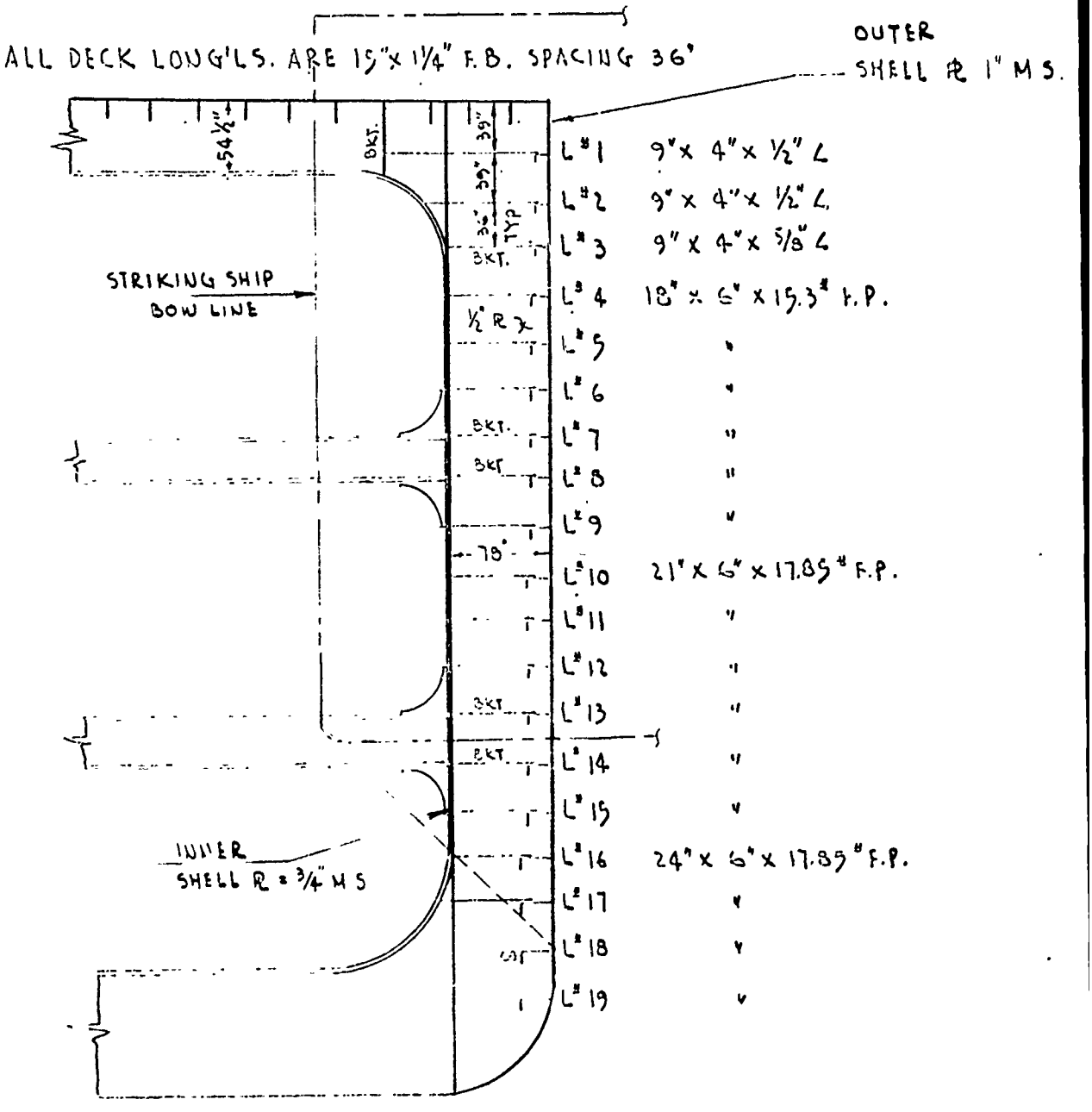

SIDE LONGITUDINAL SPACING = 36"
EXCEPT AS NOTED.

CASE 6 - RIGHT ANGLE COLLISION - STRUCK BY VERTICAL BOW

OUTER SHELL

SHELL LONGITUDINAL NO.	1	2	3	4	5	6	7	8	9	10	11	12	13	14	15	16	17	REMARK
BASIC DIMENSIONS	9"x6"x½" ∠	9"x6"x½" ∠	9"x6"x⅜" ∠	18"x6"x 19.5°F.P.	18"x6"x 19.5°F.P.	18"x6"x 19.5°F.P.	18"x6"x 19.5°F.P.	18"x6"x 19.5°F.P.	18"x6"x 19.5°F.P.	21"x6"x 17.85°F.P.	21"x6"x 17.85°F.P.	21"x6"x 17.85°F.P.	21"x6"x 17.85°F.P.	21"x6"x 17.85°F.P.	21"x6"x 17.85°F.P.	24"x6"x 17.85°F.P.	24"x6"x 17.85°F.P.	
A_{SG} = SECTIONAL AREA OF LOUGL WITH PORTION OF SHELL PLT (IN^2)	6.45	4.38	4.37	4.69	———	———	———	———	———	41.6	———	———	———	———	———	49.0	49.0	
I = MOMENT OF INERTIA OF LOUGL WITH PORTION OF SHELL PLT (IN^4)	2.74	2.61	3.07	1,263	———	———	———	———	———	2,060	———	———	———	———	———	2,836	2,836	
b = BREADTH OF FLANGE (IN) = 2 x FLANGE OF F.P. OR ANGLE	8	8	8	12	12	12	12	12	12	12	12	12	12	12	12	12	12	
t_f = THICKNESS OF FLANGE (IN)	0.900	0.500	0.425	0.375	0.375	0.375	0.375	0.375	0.375	0.438	0.438	0.438	0.438	0.438	0.438	0.438	0.438	
b/t_f = BREADTH - THICKNESS RATIO	16.0	16.0	12.8	32.0	32.0	32.0	32.0	32.0	32.0	27.4	27.4	27.4	27.4	27.4	27.4	27.4	27.4	
d = DEPTH OF WEB OF LOUGITUDINAL (IN)	9	9	9	18	18	18	18	18	18	21	21	21	21	21	21	24	24	
b/d = BREADTH - DEPTH RATIO	0.89	0.89	0.89	0.67	0.67	0.67	0.67	0.67	0.67	0.57	0.57	0.57	0.57	0.57	0.57	0.50	0.50	

CASE 6 - RIGHT ANGLE COLLISION - STRUCK BY VERTICAL BOW

OUTER SHELL

SHELL LONGITUDINAL NO.	1	2	3	4	5	6	7	8	9	10	11	12	13	14	15	16	17	REMARK
L_y = YIELD LENGTH FIG 2-3	12.0"	12.0"	12.0"	18.9"	18.9"	18.9"	18.9"	18.9"	18.9"	19.6"	19.6"	19.6"	19.6"	19.6"	19.6"	20.5"	20.5"	
L'	72.0"	—																
$\frac{2L_y}{L'}$	0.33	0.33	0.33	0.53	—				→	0.54	—				→	0.57	0.57	
$\frac{2L_y}{2L_y+L'}$	0.25	0.25	0.25	0.34	—				→	0.35	—				→	0.36	0.36	
CONSTANT A $\left(\frac{2L_y}{2L_y+L'}\right)\left(\frac{32.2\,\xi}{0.5D\sqrt{\sigma_y}}\right)\leq\left(1-\frac{\sigma_y}{\sigma_u}\right)$	0.28	0.28	0.34	0.19	—				→	0.23	—				→	0.24	0.24	
CONSTANT B $\left(\frac{2L_y}{L'}\right)\left(\frac{32.2\,\xi}{0.5D\sqrt{\sigma_y}}\right)\leq\left(\frac{\sigma_u}{\sigma_y}-1\right)$	0.36	0.36	0.45	0.29	—				→	0.35	—				→	0.37	0.37	
ROTATION CAPACITY CONST $K = A(11.6+16.1B)$	4.87	4.87	6.41	3.09	—				→	3.96	—				→	4.21	4.21	
PLASTIC CURVATURE M_p/EI	221 $\times 10^{-6}$	221 $\times 10^{-6}$	220 $\times 10^{-6}$	106 $\times 10^{-6}$	—				→	94 $\times 10^{-6}$	—				→	89 $\times 10^{-6}$	89 $\times 10^{-6}$	THESE ARE CALCULATED VALUES, FIG. 2-4 MAY BE USED
PLASTIC ANGLE CHANGE CAP $\theta_p = \epsilon\left(\frac{M_p}{EI}\right)\left(\frac{L'}{2}\right)$	0.0387	0.0387	0.0508	0.0118	—				→	0.0134	—				→	0.0129	0.0129	
BENDING DEFLECTION CAP $\delta_{BC} = \theta_p \cdot L'$	2.79	2.79	3.66	0.85	—				→	0.96	—				→	0.93	0.93	
PLASTIC BENDING MOMENT M_p (IN-KIPS)	1,756	1,675	1,959	3,892	—				→	5,616	—				→	6,991	6,991	E = 29,000 KSI
PLASTIC BENDING ENERGY $E_{BC} = 5.72\,M_p\theta_p$	388	370	569	263	—				→	430	—				→	516	516	$\Sigma E_{BC} = 6,517$ IN-K CORRECTED $E_{BC} = \frac{\Sigma}{\delta_{BC}} E_{BC}$ IF $\delta_{BC} > b$
LATERAL FORCE, (KIPS) (BENDING ONLY) $P_B = E_{BC}/\delta_{BC}$	139.1	132.6	155.5	309.4	—				→	447.9	—				→	554.8	554.8	
FORCE ON WEB AT ENDS OF L_p (KIPS) $\left(\frac{P_B}{2} + \frac{M_p}{L_p}\right)$	81.7	77.9	91.4	181.7	—				→	263.0	—				→	325.9	325.9	

CASE 6 - RIGHT ANGLE COLLISION - STRUCK BY VERTICAL BOW

OUTER SHELL

SHELL LONGITUDINAL NO.	1	2	3	4	5	6	7	8	9	10	11	12	13	14	15	16	17	REMARK
ε_r (WITHIN LE)	010	—	—	—	—	—	—	—	—	—	—	—	—	—	—	—	—	
MEMBRANE TENSION DEFL $\delta_{ec} = \frac{1}{2}(\varepsilon_r + \varepsilon_c) + \delta_{mc}^2$	3237	3237	3246	3226	—	—	—	—	—	—	—	—	—	—	—	3226	3226	
AVERAGE MEMBRANE TENSION FORCE $T = A_{sb}\sigma_y\left(\frac{\sigma_y + \sigma_u}{2\sigma_y}\right)$	3,229	2,167	2,187	2,247	—	—	—	—	—	2,382	—	—	—	—	—	2,496	2,496	
δ_m (DEFORMATIONS TO MATCH STRIKING BOW CONFIGURATION ARE LIMITED TO δ_m)	3226	—	—	—	—	—	—	—	—	—	—	—	—	29.81	19.38	12.96	6.49	
NET LATERAL FORCE ON LONG'L DUE TO MEMBRANE TENSION ONLY $P_{em} = 4T\,\delta_m/L_E$	2,892	1,942	1,960	2,015	—	—	—	—	—	2,134	—	—	—	1,704	1,283	880	440	

NOTE INITIAL WEB FRAME ANALYSIS (SHT NO 3-11) LOADED BY LATERAL FORCE DUE TO OUTER SHELL MEMBRANE TENSION ON THIS SHEET INDICATES THAT THE WEB FRAMES WILL YIELD UNDER COMPRESSION AT STRUT "B". AS RESULT OF SUCH OCCURENCE EACH SHELL IS ANALYZED SEPARATELY WITH BOTH IN UNISON.

CASE 6 - RIGHT ANGLE COLLISION - STRUCK BY VERTICAL BOW

INNER SHELL

SHELL LONGITUDINAL NO.	1	2	3	4	5	6	7	8	9	10	11	12	13	14	15	16	17	REMARK
BASIC DIMENSIONS	9"x6"x½" ∠	9"x6"x½" ∠	9"x6"x⅜" ∠	18"x6"x 19.5°FP	18"x6"x 19.5°FP	18"x6"x 19.5°FP	18"x6"x 19.5°FP	18"x6"x 19.5°FP	18"x6"x 19.5°FP	21"x6"x 17.05°FP	21"x6"x 17.05°FP	21"x6"x 17.05°FP	21"x6"x 17.05°FP	21"x6"x 17.05°FP	21"x6"x 17.05°FP	24"x6"x 17.05°FP	24"x6"x 17.05°FP	
A_{si} = SECTIONAL AREA OF LONG'L WITH PORTION OF SHELL PLT (IN²)	5.01	3.44	3.47	39.9	———	———	———	———	———	38.6	———	———	———	———	———	40.0	40.0	
I = MOMENT OF INERTIA OF LONG'L WITH PORTION OF SHELL PLT. (IN⁴)	2.66	2.63	2.63	1.185			———	———	———	1,920	———	———	———	———	———	2,640	2,640	
b = BREADTH OF FLANGE (IN) = 2 × FLANGE OF I.P OR ANGLE	8	8	8	12	12	12	12	12	12	12	12	12	12	12	12	12	12	
t_f = THICKNESS OF FLANGE (IN)	0.500	0.500	0.625	0.375	0.375	0.375	0.375	0.375	0.375	0.438	0.438	0.438	0.438	0.438	0.438	0.438	0.438	
b/t_f = BREADTH - THICKNESS RATIO	16.0	16.0	12.8	32.0	32.0	32.0	32.0	32.0	32.0	27.4	27.4	27.4	27.4	27.4	27.4	27.4	27.4	
d = DEPTH OF WEB OF LONGITUDINAL (IN)	9	9	9	18	18	18	18	18	18	21	21	21	21	21	21	24	24	
b/d = BREADTH - DEPTH RATIO	0.89	0.89	0.89	0.67	0.67	0.67	0.67	0.67	0.67	0.57	0.57	0.57	0.57	0.57	0.57	0.50	0.50	

CASE 6 - RIGHT ANGLE COLLISION - STRUCK BY VERTICAL BOW

INNER SHELL

SHELL LONGITUDINAL NO.	1	2	3	4	5	6	7	8	9	10	11	12	13	14	15	16	17	REMARK
L_y = YIELD LENGTH FIG 1-3	11.0'	12.0'	12.0'	18.9'	18.9'	18.9'	18.9'	18.9'	18.9'	19.6'	19.6'	19.6'	19.6'	19.6'	19.6'	20.5'	20.5'	
L'	72.0'																	
$\frac{2L_y}{L'}$	0.33	0.33	0.33	0.53						0.54						0.57	0.57	
$\frac{2L_y}{2L_y+L'}$	0.23	0.25	0.25	0.34						0.35						0.36	0.36	
CONSTANT A $\left(\frac{2L_y}{2L_y+L'}\right)\left(\frac{52.2}{0.9D\sqrt{\sigma_y}}\right)=\left(1-\frac{\sigma_y}{\sigma_u}\right)$	0.28	0.28	0.34	0.19						0.23						0.24	0.24	
CONSTANT B $\left(\frac{2L_y}{L'}\right)\left(\frac{52.2}{0.9D\sqrt{\sigma_y}}\right)=\left(\frac{\sigma_u}{\sigma_y}-1\right)$	0.36	0.36	0.45	0.29						0.35						0.37	0.37	
ROTATION CAPACITY CONST. $K=A(11.6+16.8B)$	4.87	4.87	6.41	3.09						3.96						4.21	4.21	
PLASTIC CURVATURE M_p/EI	213.10 $\times 10^{-6}$	221.10 $\times 10^{-6}$	220.20 $\times 10^{-6}$	106.27 $\times 10^{-6}$						94.38 $\times 10^{-6}$						92.98 $\times 10^{-6}$	92.98 $\times 10^{-6}$	THESE ARE CALCULATED VALUES, FIG. 2-6 MAY BE USED
PLASTIC ANGLE CHANGE CAP $\theta_p=K\left(\frac{M_p}{EI}\right)\left(\frac{L'}{2}\right)$	0.0.72	0.0387	0.0508	0.0118						0.0134						0.0141	0.0141	
BENDING DEFLECTION CAP $\delta_{BC}=\theta_p \cdot L'$	2.69	2.79	3.66	0.85						0.96						1.01	1.01	
PLASTIC BENDING MOMENT M_p (IN-KIPS)	1,644	1,550	1,807	3,657						5,255						7,119	7,119	E = 29,000 KSI
PLASTIC BENDING ENERGY $E_{BC}=5.72\,M_p\theta_p$	352	349	529	246						403						574	574	$2E_{BC}$ = 6,264 IN-K CORRECTED $E_{BC}=\frac{b}{\delta_{BC}}E_{BC}$ IF $\delta_{BC}>b$
LATERAL FORCE, (KIPS) (BENDING ONLY) $P_{BC}=E_{BC}/\delta_{BC}$	131	124	145	289	...					420						568	568	
FORCE ON WEB AT ENDS OF L_f (KIPS) $(P_{BC}/2+M_p/L_f)$	76	73	84	170						246						333	336	

CASE 6 - RIGHT ANGLE COLLISION - STRUCK BY VERTICAL BOW

OUTER SHELL & INNER SHELL DEFORMING IN UNISON

SHELL LONGITUDINAL NO.	1	2	3	4	5	6	7	8	9	10	11	12	13	14	15	16	17	REMARK
ε_r (WITHIN L_E)	010																010	
MEMBRANE TENSION DEFL. $\delta_{tc} = \frac{1}{2}(\varepsilon_r + \varepsilon_t) + \delta_{bc}^2$	3249	3241	3251	3226													3226	
AVERAGE MEMBRANE TENSION FORCE $T = (A_{s1} + A_{s2})\sigma_y\left(\frac{\sigma_y + \sigma_u}{2\sigma_u}\right)$	3730	3,910	3,920	4040						4,510						4,450	4,450	
δ_m (DEFORMATIONS TO MATCH STRIKING BOW CONFIGURATION ARE LIMITED TO δ_{bc})	3226													25.81	19.36	12.90	6.45	
NET LATERAL FORCE ON LONGL DUE TO MEMBRANE TENSION ONLY $P_{em} = 4T\,\delta_m/L_E$	3,135	3,504	3,512	3,620						3,860				3,090	2,318	1,595	797	
$P_{wf} = P_{em}/2 \div R_m$	305	208	208	215						229				183	137	95	47	$R_m = 8451$ SEE SHEET NO. 3-08
NO OF WEB FRAME SPACES DAMAGED $n = \left[\frac{-0.5 P_{em}}{P_{wf}}\right] \geq 1$	17	17	17	17	17	17	17	17	17	17	17	17	17	17	17	17	17	ROUNDED OFF TO NEXT HIGHER ODD INTEGER
ACTUAL n WEB FRAME SPACES DAMAGED $L_d = n L_s$	1008	---																
$\delta_1 = \frac{P_{wf} L_E}{2T}$	383	---												3.06	2.30	1.63	0.77	
FINAL δ (DEFORMATION AT LONG'L #1 SEE SHT NO 3-15 FOLLOWS CONTOUR #2 LONG'L NO 3-15)	20431													163.45	122.59	81.72	40.86	MAX. BEND. ANGLE = 18°-54' SEE SHT NO 3-15B
$\varepsilon = \frac{\delta^2 + 92.5^2}{35 L_E - a}$	003367													0.05355	0.03012	0.01362	0.00339	
$e_t = L_d \cdot \varepsilon$	9434	---												53.98	30.36	13.53	3.38	
$E_{mT} = T e_t\left(1 + \frac{0.07661 L_E}{0.08367 - a}\right)$	544,574	372,969	373,923	385,370	385,370	385,370	385,370	385,370	385,370	411,125	411,125	411,125	411,125	265,131	147,993	68,096	17,011	$\Sigma E_{mt} = 5,746,449$ LBS.

3-83

CASE 6 · RIGHT ANGLE COLLISION - STRUCK BY VERTICAL BOW

OUTER SHELL & INNER SHELL DEFORMING IN UNISON

ANALYSIS OF WEB FRAME

(LATERAL LOAD ½ Pcm)

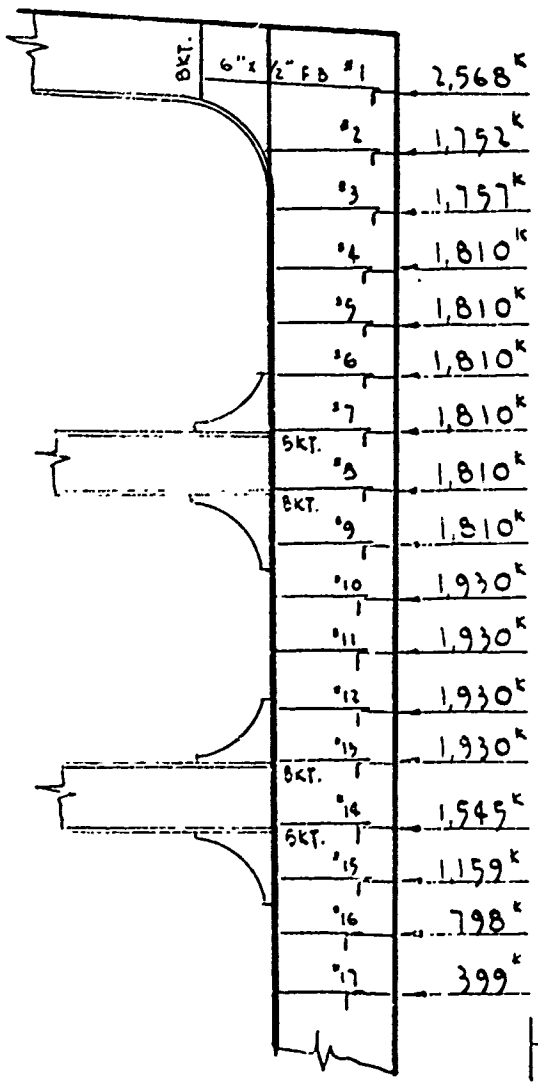

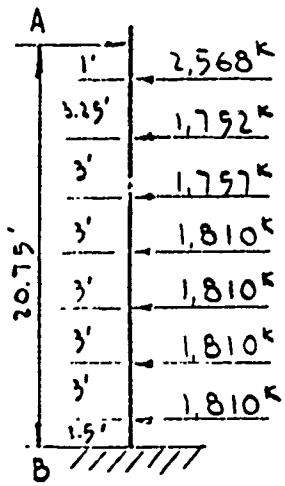

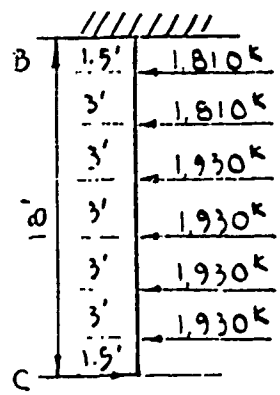

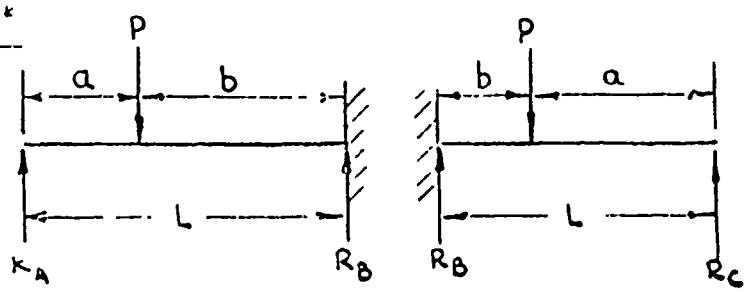

$$R_A = \frac{Pb^2}{2L^3}(a+2L), \qquad R_C = \frac{Pb^2}{2L^3}(a+2L)$$

$$R_B = \frac{Pa}{2L^3}(3L^2 - a^2)$$

CASE 6 - RIGHT ANGLE COLLISION - STRUCK BY VERTICAL BOW

ANALYSIS OF WEB FRAMES
DETERMINATION OF R_A, R_B & R_C

LONG'LS	L	P/2	a	b	2L+a	L^3	$3L^2-a^2$	R_A	R_B	R_C
A	—	—	—	—	—	—	—	—	—	—
1	20.75	1,284	1.00	19.75	42.50	3,934.16	1,291	2,383	185	
2		876	4.25	16.50	45.75		1,274	1,221	531	
3		879	7.25	13.50	48.75		1,239	874	884	
4		905	10.25	10.50	51.75		1,187	578	1,232	
5		905	13.25	7.50	54.75		1,116	312	1,498	
6		905	16.25	4.50	57.75		1,028	118	1,692	
7		905	19.25	1.50	60.75		921	14	1,796	
B		—	—	—	—				7.818	—
8	18.00	905	16.50	1.50	52.50	5,832.00	700		1,792	18
9		905	13.50	4.50	49.50		790		1,654	156
10		965	10.50	7.50	46.50		862		1,497	433
11		965	7.50	10.50	43.50		916		1,136	794
12		965	4.50	13.50	40.50		952		709	1,221
13		965	1.50	16.50	37.50		970		241	1,689
C		—	—	—	—				7.029	
TOTAL								5.500	14.847	4311

CASE 6 - RIGHT ANGLE COLLISION - STRUCK BY VERTICAL BOW

SHEAR & BENDING MOMENT FOR THE UPPER PART OF THE WEB FRAME

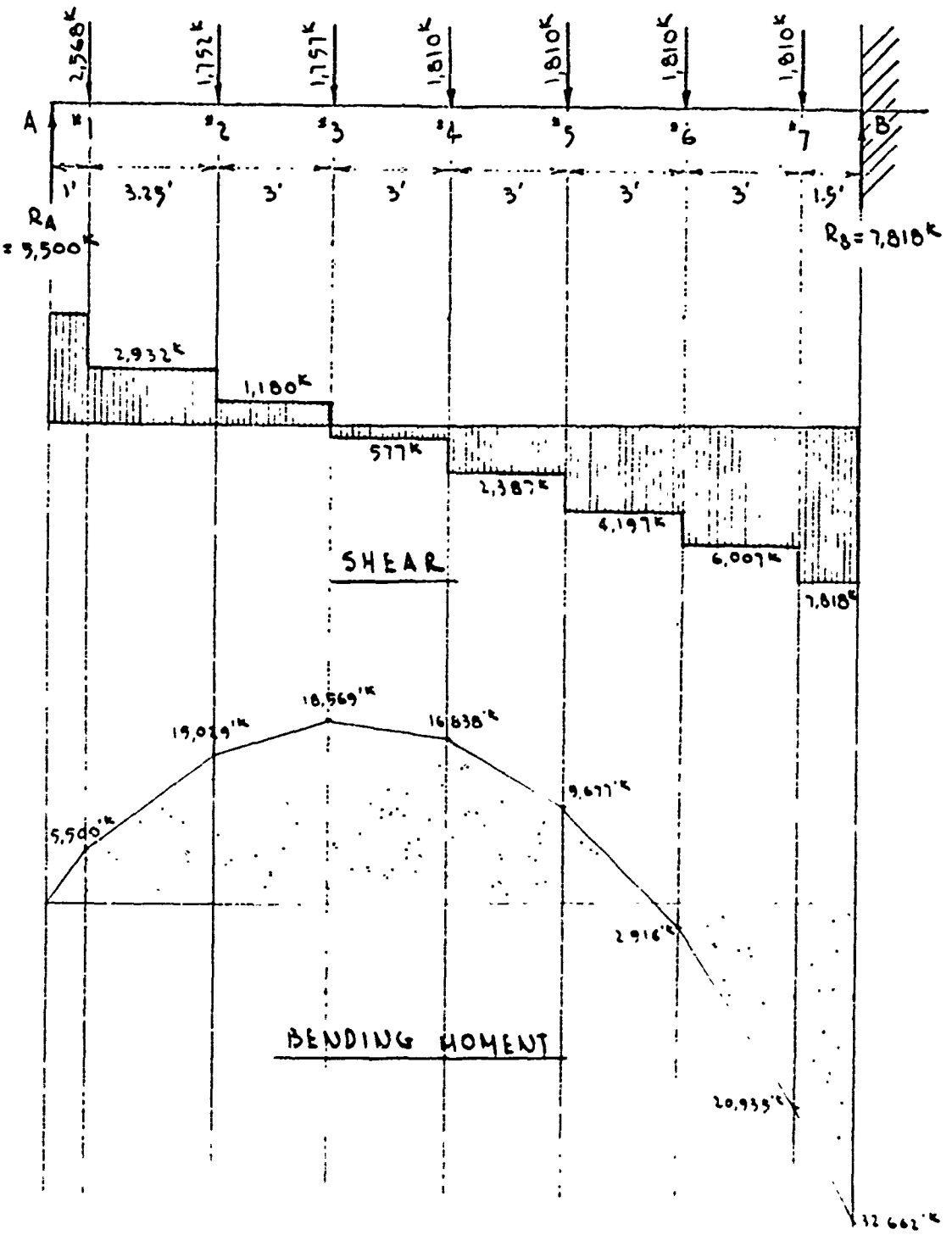

CASE 6 - RIGHT ANGLE COLLISION - STRUCK BY VERTICAL BOW

SHEAR & BENDING MOMENT FOR THE LOWER PART OF THE WEB FRAME

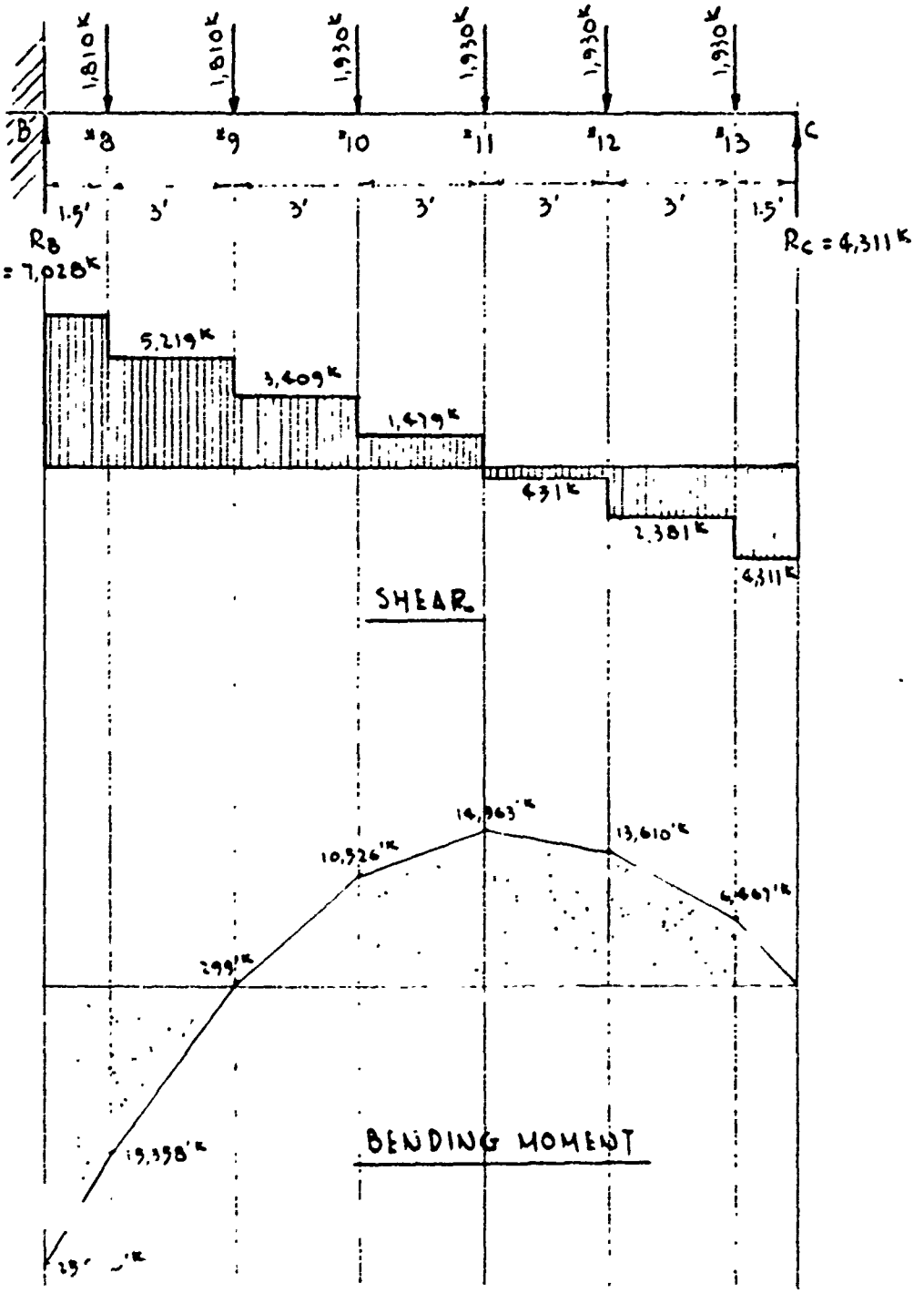

CASE 6 - RIGHT ANGLE COLLISION - STRUCK BY VERTICAL BOW

SUMMARY OF "R"

(LATERAL LOADS/STRENGTH OF WEB FRAME)

LOCATION \ TYPE OF LOAD	R BENDING	R SHEAR	R CRUSHING	R COMPR.
A	—	—	—	—
1	—	—	3.305	—
2	1.570	3.721	3.623	—
3	1.940	1.497	3630	—
4	1.760	3029	3739	—
5	1.012	5.326	3739	—
6	0305	7623	3739	—
7	—	—	—	—
8	—	—	—	3431
8		—	—	—
9	0.031	6623	3739	—
10	1100	4326	3987	—
11	1564	1877	3987	—
12	1.423	3021	3987	—
13		—		
C		—	—	2449

MAX R = 8431

FOR SUMMARY OF WEB FRAME STRENGTH SEE SHT NO 3-94

CASE 6 - RIGHT ANGLE COLLISION - STRUCK BY VERTICAL BOW

SHEARING PLASTIC ENERGY (E_{ps})

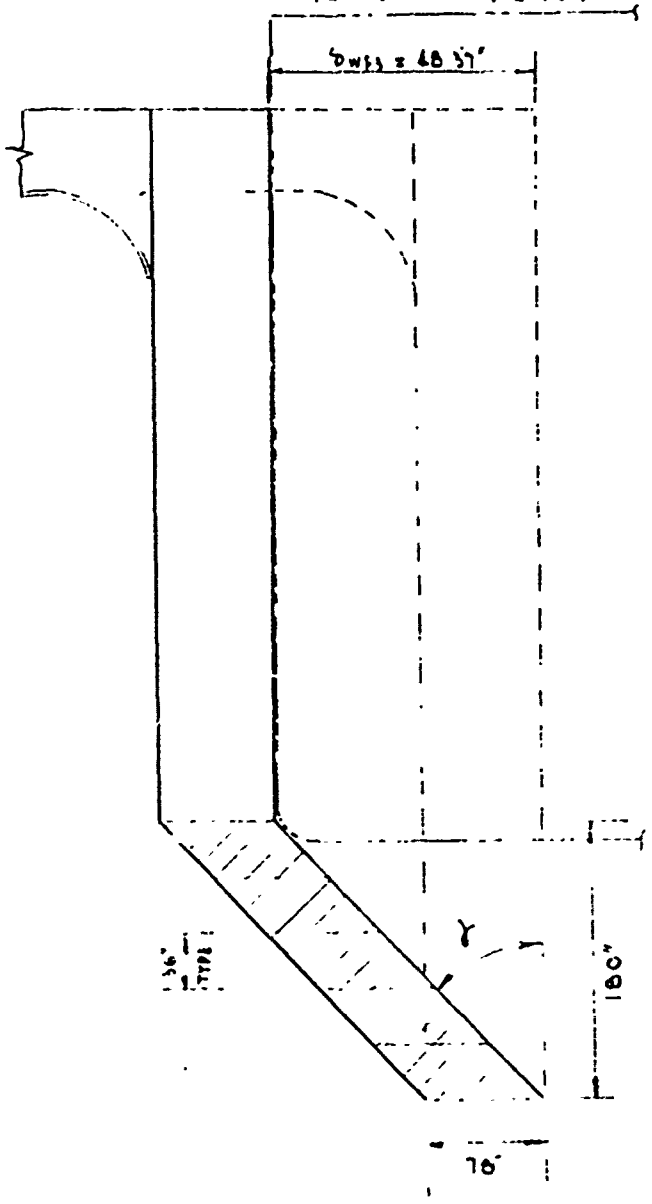

$$\gamma = \tan^{-1} = \frac{48.37"}{180"} = 0.2687$$

$$\gamma = 15.041° = 0.2625 \text{ RADIAN}$$

$$\gamma_m = 0.0947 \text{ RADIAN}$$

$$\gamma > \gamma_m$$

WEB PANEL :

$a = 36"$

$d = 78"$

$t = 0.5"$

$d/a = 2.17$

$d/t = 156$

FROM FIG. 2-6, $\tau_{cr} = 27.0$, $\tau_y = 20.2$

SINCE $\tau_{cr} > \tau_y$

$$E_{ps} = (a_1 d t)\left(\gamma - \frac{\tau_y}{11{,}150}\right)(\tau_y) \times 6$$

$$= 180" \times 78" \times 0.5" \left(0.0947 - \frac{20.2}{11{,}150}\right) 20.2 \times 6$$

$$= 65{,}860 \text{ IN-KIPS}$$

CASE 6 - RIGHT ANGLE COLLISION - STRUCK BY VERTICAL BOW

PLASTIC ENERGY DUE TO DECK DEFORMATION (E_d)

DEFORMATION AT LONG'L. NO. 1 = 20.31', $\varepsilon = 0.08367$.
= 17.03'

NO OF DECK LONG'LS DAMAGED = $\frac{20.31}{3.6} = 5.68$

$$E_{dx} = T\,\epsilon_t = A_s \times \frac{\sigma_y + \sigma_u}{2} \times L_d \times \varepsilon$$

$E_{d_1} = 93.00 \times 50 \times 1.008 \times 0.08367 \times \left(\frac{14.03'}{17.03'}\right)^2 = 266,176$ IN-KIPS

$E_{d_2} = 68.25 \times 50 \times 1.008 \times 0.08367 \times \left(\frac{11.03'}{17.03'}\right)^2 = 120,733$ IN-KIPS

$E_{d_3} = 68.25 \times 50 \times 1.008 \times 0.08367 \times \left(\frac{8.03'}{17.03'}\right)^2 = 63,989$ IN-KIPS

$E_{d_4} = 68.25 \times 50 \times 1.008 \times 0.08367 \times \left(\frac{5.03'}{17.03'}\right)^2 = 25,108$ IN-KIPS

$E_{d_5} = 68.25 \times 50 \times 1.008 \times 0.08367 \times \left(\frac{2.03'}{17.03'}\right)^2 = 4,089$ IN-KIPS

$$\Sigma E_{dx} = 480,095 \text{ IN-KIPS}$$

DECK MEMBRANE TENSION ENERGY

$$E_d = \Sigma E_{dx} \left(1 + \frac{.07661 \times L_s}{.08367 \times L_d}\right)$$

$= 480,095 \times 1.131 = 542,997$ IN-KIPS

CASE 6 - RIGHT ANGLE COLLISION - STRUCK BY VERTICAL BOW

OUTER SHELL DUCTILE TEARING ENERGY

= VERTICAL SIDE SHELL LENGTH x SIDE SHELL THICKNESS x 12 K/IN
TO LONG'L NO 19

= 654" x 1" x 12 K/IN = 7,848 IN-KIPS

DECK DUCTILE TEARING ENERGY

= (δ - 78") x DECK THICKNESS x 12 K/IN

= (204.31" + 78") x 1.375 x 12 K/IN = 4,698 IN-KIPS

(δ = 204.31" FROM SHT 3-104)

3.7 MISCELLANEOUS CALCULATIONS

WEB FRAME STRENGTH FOR CASES 1 & 2

SUMMARY OF WEB FRAME STRENGTH

LOCATION \ STRENGTH	BENDING IN-KIPS	SHEAR KIPS	CRUSHING KIPS	COMPR. KIPS
A	—	—	—	—
1	—	—	484	—
2	78,439	788	484	—
3	↓	↓	—	—
4	↓	↓	484	—
5	↓	↓	484	—
6	↓	↓	484	—
7	—	—	—	—
8	—	—	—	1,761
9	78,439	788	484	—
10	↓	↓	484	—
11	↓	↓	484	—
12	↓	↓	484	—
13	—	—	—	—
C	—	—	—	1,761

WEB FRAME STRENGTH FOR CASES 3, 4 & 5

SUMMARY OF WEB FRAME STRENGTH

STRENGTH / LOCATION	BENDING IN-KIPS	SHEAR KIPS	CRUSHING KIPS	COMPR. KIPS
A	—	—	—	—
1	—	—	484	—
2	85,142	788	484	—
3	↓	↓	—	—
4	↓	↓	484	—
5	↓	↓	↓	—
6	↓	↓	↓	—
7	—	—	—	—
8	—	—	—	1,761
8	—	—	—	—
9	85,142	788	484	—
10	↓	↓	↓	—
11	↓	↓	↓	—
12	↓	↓	↓	—
13	—	—	—	—
C	—	—	—	1,761

WEB FRAME STRENGTH FOR CASE 6

SUMMARY OF WEB FRAME STRENGTH

STRENGTH / LOCATION	BENDING IN-KIPS	SHEAR KIPS	CRUSHING KIPS	COMPR. KIPS
A	—	—	—	—
1	—	—	484	—
2	114,778	788	484	—
3			—	—
4			484	—
5				—
6				—
7	—	—	—	—
8	—	—	—	1,761
8	—	—	—	—
9	114,778	788	484	—
10				—
11				—
12				—
13	—	—	—	—
C	—	—	—	1,761

WEB FRAME STRENGTH FOR CASES 1 & 2

STRENGTH FOR BENDING AT LONG'LS. 2, 3, 4, 5, 6, 9, 10, 11, & 12

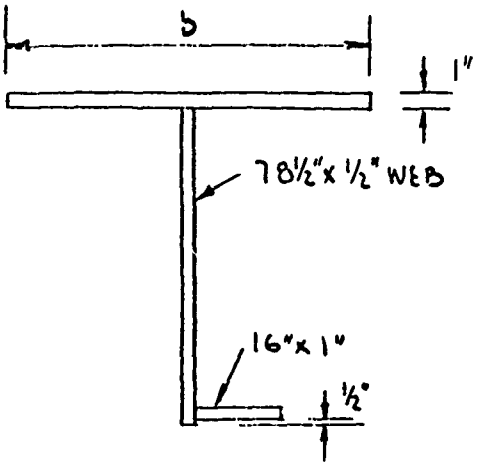

$a = 144"$, $t = 1"$

$a/t = 144$

FROM FIG 2-5, $b/t = 50.5$

$b = 50.5 \times 1" = 50.5"$

$i_o = 1/12 \times 0.5 \times 78.5^3 = 20,156\ IN^4$

	A - IN^2	d - IN	Ad - IN^3	Ad^2 - IN^4	i_o - IN^4
SHELL R	50 50	0.50	25.3	13	—
WEB	39.25	40 25	1,579.8	63,587	20,156
FLG.	16 00	78.50	1,2960	98,596	—
	10576	27.05	2,861 1	162,196	20,156

$20,156$

$182,352$

$- Ad^2 = 105.76 \times 27.05^2 = -77,385$

$I = 104,967\ IN^4$

$\frac{I}{C} = \frac{104,967}{52\frac{1}{2}} = 2001\ IN^3$

$M_{PWF} = 2,001 \times 35 \times 112 = \underline{78,639\ IN\text{-}KIPS}$

WEB FRAME STRENGTH FOR CASES 3, 4 & 5

STRENGTH FOR BENDING AT LONG'LS. 2, 3, 4, 5, 6, 9, 10, 11 & 12

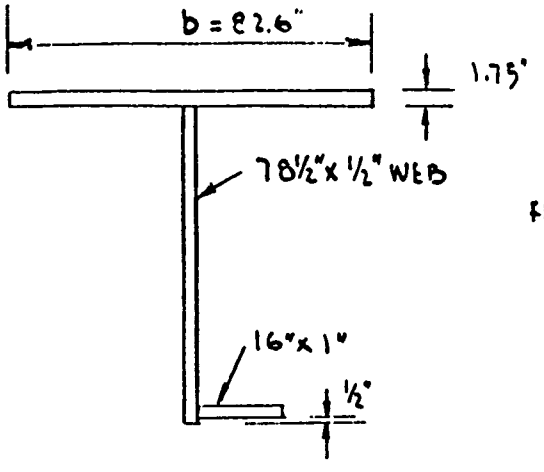

$a = 144"$, $t = 1.75"$

$a/t = 144/1.75 = 82.3$

FROM FIG. 2-5, $b/t = 47.2$

$b = 47.2 \times 1.75 = 82.6"$

SHELL R $i_o = \frac{1}{12} \times 82.6 \times 1.75^3 = 37$ IN⁴

WEB $i_o = \frac{1}{12} \times .5 \times 78.5^3 = 20,156$ IN⁴

	A - IN²	d - IN	Ad - IN³	Ad² - IN⁴	i_o - IN⁴
SHELL R	144.55	0.88	127.2	112	37
WEB	39.25	41.00	1,609.3	65,979	20,156
FLG.	16.00	79.25	1,268.0	100,489	—
	199.80	15.03	3,004.5	166,580	20,193

20,193

186,773

$-Ad^2 = 199.80 \times 15.03^2 = -\ 65,134$

$i = 141,639$

$\frac{I}{C} = \frac{141,689}{80.25 - 15.03} = \frac{141,689}{65.22} = 2,172$ IN³

$M_{PWF} = 2,172 \times 35 \times 112 = \underline{85,142 \text{ IN-KIPS}}$

WEB FRAME STRENGTH FOR CASES 6

STRENGTH FOR BENDING AT LONG'LS. 2, 3, 4, 5, 6, 9, 10, 11 & 12

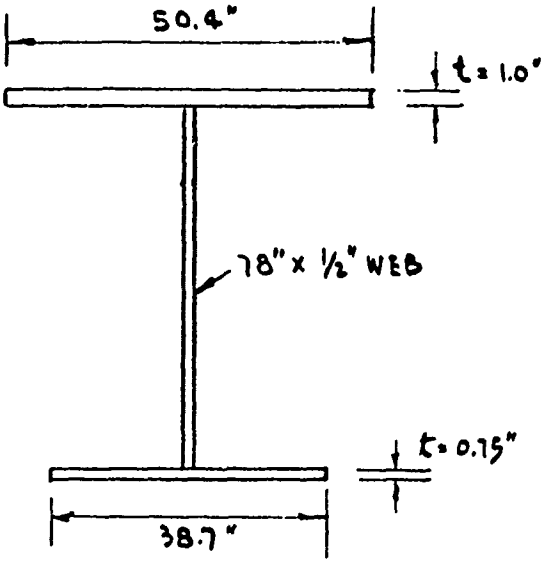

$a = 144"$, $a/t = 144$

FROM FIG. 2-5 $b/t = 50.4$

$b = 50.4"$

$a = 144"$, $a/t = \frac{144}{0.75} = 192$

FROM FIG. 2-5, $b/t = 51.6$

$b = 0.75 \times 51.6 = 38.7"$

$i_o = 1/12 \times 0.5 \times 78^3 = 19,773 \text{ IN}^3$

	A - IN²	d - IN	Ad - IN³	Ad² - IN⁴	i_o - IN⁴
OUTER SHELL	50.40	0.50	25.2	12.6	—
WEB	39.00	40.00	1,560.0	62,400.0	19,773
INNER SHELL	29.03	79.38	2,304.4	182,923.0	—
	118.43	32.84	3,889.6	245,336	19,773

19,773

265,109

- 127,746

$I = 137,363$

$C = 79.75 - 32.84 = 46.91$

$\frac{I}{C} = \frac{137,363}{46.91} = 2,928 \text{ IN}^3$

$M_{pwf} = 2,928 \times 35 \times 1.12 = \underline{114,778 \text{ IN·KIP}}$

WEB FRAME STRENGTH FOR CASES 1 THROUGH 6

STRENGTH FOR SHEAR AT LONG'LS. 2, 3, 4, 5, 6, 9, 10, 11 & 12

$d = 78"$, $a = 36"$, $t = 1/2"$

$\frac{d}{a} = \frac{78}{36} = 2.16$, $\frac{d}{t} = \frac{78}{0.5} = 156$

FROM FIG. 2-6, $\tau_{cr} = 27.0$ KSI

$\tau_y = 20.2$ KSI

SINCE $\tau_{cr} > \tau_y$

$V_p = \tau_y \cdot d \cdot t$

$= 20.2\ (78)(1/2) = 788$ KIPS

WEB FRAME STRENGTH FOR CASES 1 THROUGH 6.

STRENGTH FOR COMPRESSION AT STRUTS B & C

STRUTS.— 35 7/8" x 16½" x 230 # I

$r_m = 3.59$

$A_c = 67.73\ IN^2$

$L_c = 27.50\ FT = 330"$

$L_c/r_m = 330/3.59 = 91.9$

FROM FIG. 2-8. $P_m/A_c = 26.0\ KSI$

$P_m = 26.0 \times 67.73 = \underline{1,761\ KIPS}$

WEB FRAME STRENGTH FOR CASES 1 THROUGH 6

STRENGTH FOR CRUSHING AT LONG'LS. 1, 2, 4, 5, 6, 9, 10, 11, & 12

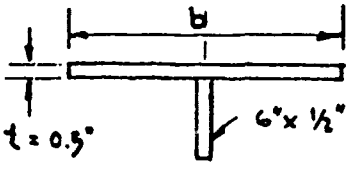

$a/t = \frac{39}{0.5} = 78$

FROM FIG. 5, $b/t = 47$

$b = 47 \times 0.5 = 23.5"$

$A_c = 14.75\ IN^2$, $r_m = 1.53"$

$L_c = 69"$, $L_c/r_m = 45.1$

FROM FIG. 2-8, $P_m/A_c = 32.8\ KSI$

$P_m = 32.8 \times 14.75 = \underline{484\ KIPS}$.

DETERMINATION OF δ, ε_r AND BEND ANGLE

FOR CASE 2 - $L_t = L_s = 144"$ & $L_d = 5 \times L_s = 720"$

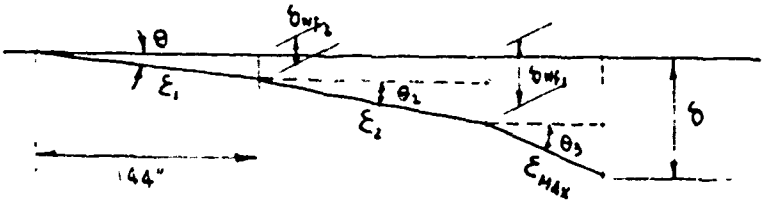

THE FOLLOWING EQUATIONS WERE USED

$$\delta = \sqrt{2.5\, L_t L_d (\varepsilon + \varepsilon_c)} - 14\delta_1^2$$

$$\delta_{WF_2} = \frac{\delta - 4\delta_1}{2.5}$$

$$\delta_{WF_1} = 2\delta_{WF_2} + 2\delta_1$$

$$\text{TAN}\theta_1 = \frac{\delta_{WF_2}}{L_s}$$

$$\text{TAN}\theta_2 = \frac{\delta_{WF_1} - \delta_{WF_2}}{L_s}$$

$$\text{TAN}\theta_3 = \frac{2(\delta - \delta_{WF_1})}{L_s}$$

$$\varepsilon_2 = \varepsilon_{MAX}\left[1 - \left(1 - \frac{\cos\theta_3}{\cos\theta_1}\right)^{1/2}\right]$$

$$\varepsilon_1 = \varepsilon_{MAX}\left[1 - \left(1 - \frac{\cos\theta_3}{\cos\theta_1}\right)^{1/2}\right]$$

$$\varepsilon_{AVERAGE} = \left[\varepsilon_{MAX} + 2\varepsilon_2 + 2\varepsilon_1\right] \div 5$$

DETERMINATION OF δ, ε_f AND BEND ANGLE

FOR CASES 1, 3, 4 & 6 — $L_t = L_s = 144"$ & $L_d = 7 \times L_s = 1,008"$

FOR CASE 5 — $L_t = L_s = 144"$ & $L_d = 3.5 \times L_s = 504"$

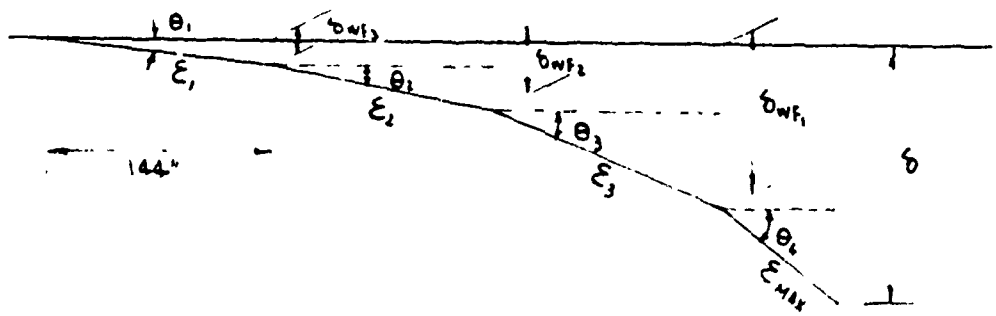

THE FOLLOWING EQUATIONS WERE USED

FOR CASES 1,3,4,&6 $\delta = \sqrt{3.50 L_t L_d (\varepsilon + \varepsilon_c) - 5200 \theta_1^2}$

FOR CASE 5 $\delta = \sqrt{2.92 L_t L_d (\varepsilon + \varepsilon_c) - 54.33 \theta_1^2}$

$$\delta_{WF_3} = \frac{\delta - 9\theta_1}{3.5}$$

$$\delta_{WF_2} = 2\delta_{WF_3} + 2\theta_1$$

$$\delta_{WF_1} = 3\delta_{WF_3} + 6\theta_1$$

$$\text{TAN}\theta_1 = \frac{\delta_{WF_3}}{L_s}$$

$$\text{TAN}\theta_2 = \frac{\delta_{WF_2} - \delta_{WF_3}}{L_s}$$

$$\text{TAN}\theta_3 = \frac{\delta_{WF_1} - \delta_{WF_2}}{L_s}$$

$$\text{TAN}\theta_4 = \frac{2(\delta - \delta_{WF_1})}{L_s}$$

$$\varepsilon_3 = \varepsilon_{MAX}\left[1 - \left(1 - \frac{\cos\theta_4}{\cos\theta_3}\right)^{1/2}\right]$$

$$\varepsilon_2 = \varepsilon_{MAX}\left[1 - \left(1 - \frac{\cos\theta_4}{\cos\theta_2}\right)^{1/2}\right]$$

$$\varepsilon_1 = \varepsilon_{MAX}\left[1 - \left(1 - \frac{\cos\theta_4}{\cos\theta_1}\right)^{1/2}\right]$$

$$\varepsilon_{AVERAGE} = \left[\varepsilon_{MAX} + 2\varepsilon_3 + 2\varepsilon_2 + 2\varepsilon_1\right] \div 7$$

INITIAL DETERMINATION

ASSUME $\varepsilon_c = 0$ & $\varepsilon_y = 0.10$

	CASE 1	CASE 2	CASE 3	CASE 4	CASE 5	CASE 6
δ_1	6.91	10.77	4.33	6.40	4.33	3.83
δ	219.82	155.87	223.27	220.62	142.03	223.70
δ_{WF3}	45.04	——	52.68	46.58	29.45	54.07
δ_{WF2}	103.90	45.12	114.00	105.96	67.56	115.80
δ_{WF1}	176.58	111.78	183.97	178.14	114.33	185.19
TAN θ_1	0.3128	0.3133	0.3658	0.3235	0.2045	0.3155
TAN θ_2	0.4088	0.4629	0.4258	0.4124	0.2647	0.4287
TAN θ_3	0.4839	0.6124	0.4859	0.5013	0.3248	0.4819
TAN θ_4	0.6006	——	0.5458	0.5900	0.3847	0.5349
θ_1	17°~22'	17°~24'	20°~5'	17°~56'	11°~33'	20°~35'
θ_2	22°~14'	24°~50'	23°~4'	22°~25'	14°~49'	23°~12'
θ_3	25°~49'	31°~29'	25°~55'	26°~37'	18°~0'	25°~44'
θ_4	30°~59'	——	28°~38'	30°~32'	21°~3'	28°~8'
ε_3	0.07818	——	0.08487	0.08087	0.08633	0.08547
ε_2	0.07282	0.07544	0.07921	0.07385	0.08140	0.07988
ε_1	0.06811	0.06738	0.07525	0.06921	0.07823	0.07592
ε AVERAGE	0.07689	0.07713	0.08214	0.07827	0.08456	0.08322

2ND. DETERMINATION BASED ON ε OBTAINED FROM PREVIOUS SHEET

	CASE 1	CASE 2	CASE 3	CASE 4	CASE 5	CASE 6
δ_1	6.91	10.77	4.33	6.40	4.33	3.83
δ	191.26	135.53	201.89	193.99	130.01	203.75
δ_{WF3}	36.88	—	46.57	38.97	26.01	48.37
δ_{WF2}	87.58	36.98	101.79	90.74	60.68	104.40
δ_{WF1}	152.10	95.50	165.64	155.31	104.01	168.09
TAN θ_1	0.2561	0.2568	0.3234	0.2706	0.1806	0.3359
TAN θ_2	0.3521	0.4064	0.3834	0.3595	0.2408	0.3891
TAN θ_3	0.4481	0.5560	0.4434	0.4484	0.3010	0.4423
TAN θ_4	0.5439	—	0.5035	0.5372	0.3611	0.4953
θ_1	14°~22'	14°~24'	17°~55'	15°~9'	10°~14'	18°~34'
θ_2	19°~24'	22°~7'	21°~0'	19°~46'	13°~32'	21°~16'
θ_3	24°~8'	29°~4'	23°~55'	24°~9'	16°~45'	23°~52'
θ_4	28°~32'	—	26°~44'	28°~15'	19°~51'	26°~21'
MAX. SEND ANGLE	14°~22'	14°~24'	17°~55'	15°~9'	10°~14'	18°~34'
ε_3	0.08066	—	0.08487	0.08140	0.08666	0.08582
ε_2	0.07381	0.07621	0.07921	0.07472	0.08197	0.08040
ε_1	0.06949	0.06875	0.07525	0.07044	0.07898	0.07661
ε AVERAGE	0.07465	0.07198	0.08266	0.07552	0.08503	0.08367

FINAL DETERMINATION OF δ BASE ON ε_r OBTAINED FROM ABOVE

	CASE 1	CASE 2	CASE 3	CASE 4	CASE 5	CASE 6
δ	193.08	136.34	202.52	194.97	130.39	204.31

* SEE PAGE 3-105 FOR FURTHER DISCUSSION

DEFLECTIONS AND STRAINS

The geometry and strains given on page 3-104 must be viewed in light of the assumptions of the procedure.

Using Case 1 as an example, if the strains within the damaged web frame spaces are computed, based on the calculated deflections and intact web frame spacing, the following results:

e_{max} = elongation in half of struck web frame space

$$= \frac{(\delta - \delta_{wf_1})^2}{L_s} = \frac{(193.08 - 152.10)^2}{144} = 11.66$$

$$\varepsilon_{max} = \frac{11.66}{72} = 0.162$$

$$\varepsilon_3 = \frac{(\delta_{wf_1} - \delta_{wf_2})^2}{2L_s} = \frac{(152.10 - 87.58)^2}{2 \times 144} = 14.45$$

$$\varepsilon_3 = \frac{14.45}{144} = .1004$$

and similarly, $\varepsilon_2 = .062$ and $\varepsilon_1 = .033$, so that in comparison,

Case 1	From Page 3-104	Calculated Above
ε_{max}	.100	.162
ε_3	.08066	.1004
ε_2	.07381	.062
ε_1	.06949	.033

The method used to calculate the strains above is not consistent with the procedure assumptions, however, and it is for this reason that "apparent strains" greater than the maximum allowable of .10 occur.

The assumptions of the procedure include fore and aft movement of the web frames once they distort. Therefore the original intact web frame spacing cannot be used to correctly calculate strains. Precisely, the web frames of Case 1 move the distances shown below in the fore and aft direction; and the resultant actual strains are those given on page 3-104.

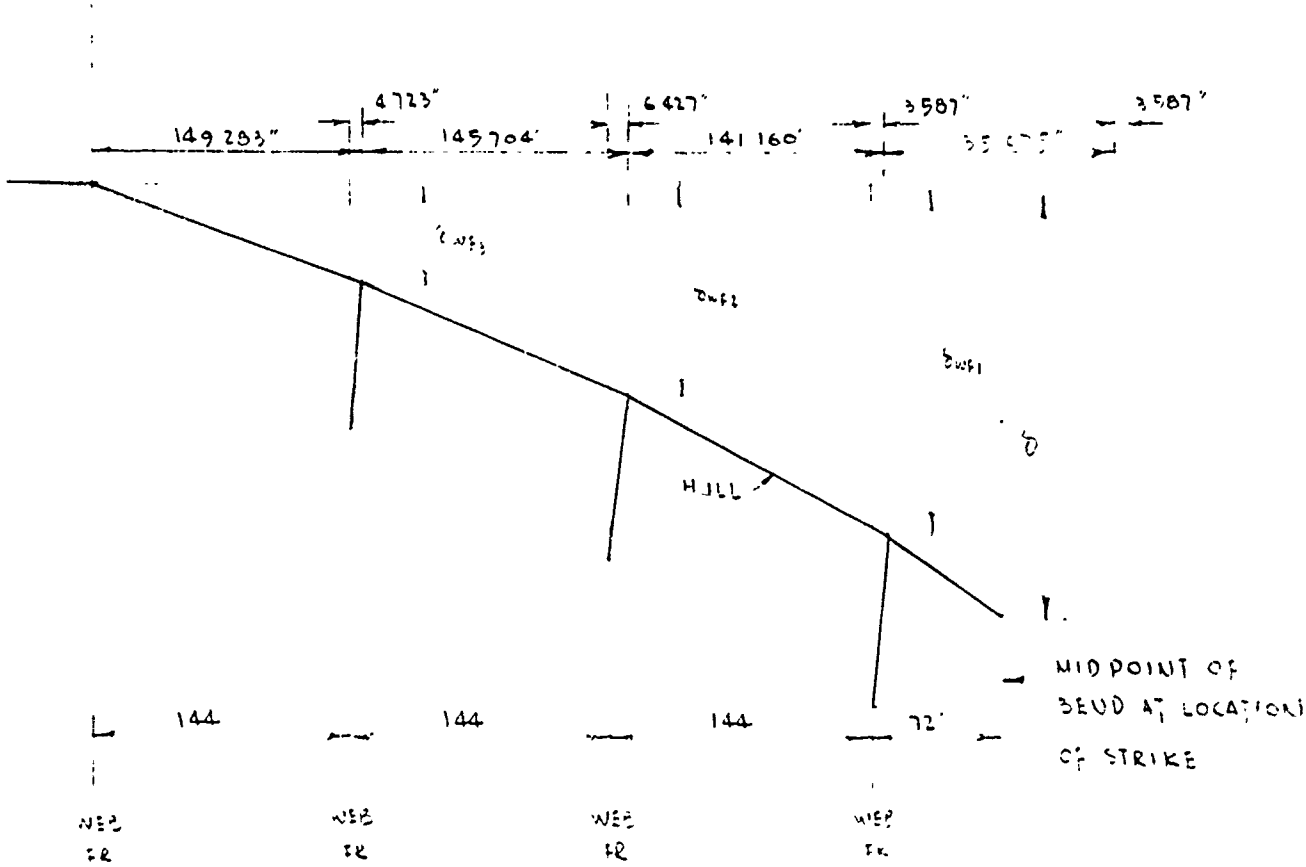

ACTUAL DISTANCE BETWEEN WEB FRAMES AFTER DAMAGED

It is of interest to note that the actual values of ε_1 and ε_2 are larger than the apparent as a result of increased stretching in these web frame spaces while for the web frame spaces closer to the strike the actual is less than the apparent.

PART III

TANKER STRUCTURAL ANALYSIS
COLLISION INSPECTION REPORTS

Preceding page blank

TABLE OF CONTENTS

		Page
1.	INTRODUCTION	1-1
2.	OBSERVATIONS	2-1
3.	CONCLUSIONS	3-1
4.	REFERENCES	4-1

APPENDIX A - COLLISION INSPECTION REPORTS

A-1	COLLISION INSPECTION REPORT FOR CASE 1 - Longitudinally Stiffened Single-Hull Barge	A-1
A-2	COLLISION INSPECTION REPORT FOR CASE 2 - Double-Hull Barge	A-15
A-3	COLLISION INSPECTION REPORT FOR CASE 3 - Transversely Framed Cargo Ships	A-44
A-4	COLLISION INSPECTION REPORT FOR CASE 4 - Longitudinally Stiffened Single-Hull Barge	A-74
A-5	COLLISION INSPECTION REPORT FOR CASE 5 - Longitudinally Framed Double-Hull Barge	A-91
A-6	COLLISION INSPECTION REPORT FOR CASE 6 - Transversely Framed Containership and Longitudinally Framed Tanker	A-109

Preceding page blank

1. INTRODUCTION

During the course of the project on the Evaluation of Tanker Structure in Collision (1,2)* investigations of actual collisions were performed in order to determine the validity of many assumptions which were made.

The objectives of the inspections were to obtain first-hand knowledge of the collision condition, the structural failure mechanisms, and extent of damage. The knowledge gained from the actual collisions was to be incorporated in the plastic energy evaluation procedure as judged desirable.

Although only six cases of collision damage were available for inspection, the information gained was considerable. None of the cases involved an ocean tanker with minor or moderate damage, and none included damage of horizontally stiffened web frames, which were of particular interest for the formulation of the analysis procedure. The six collision cases that were inspected are as follows:

1. Collision of a longitudinally stiffened single-hull barge with concrete dolphin adjacent to railroad bridge pier in the Mississippi River at Burlington, Iowa. Inspected on October 30, 1971, in Hartford, Illinois.

2. Collision of a longitudinally framed double-hull barge for compressed chlorine gas with piers on a dam on the Ohio River. Inspected on May 17, 1972, in Louisville, Kentucky.

3. Collision between two transversely framed cargo ships, the Aegean Sea and the C.E. Dant. The ships were inspected September 8, 1972, in Victoria, British Columbia, and Seattle, Washington, respectively.

*Numbers in brackets designate references in the Reference Section.

Preceding page blank

4. Collision between a tugboat and a longitudinally framed sulphuric acid barge. Inspected October 24, 1972, in Edgemore, Delaware.

5. Collision of a longitudinally framed double-hull chemical barge with a bridge pier inspected May 30, 1973, in Port Allen, Louisiana.

6. Collision between a longitudinally framed tanker, the Esso Brussels, and a transversely framed containership, the C.V. Sea Witch. The ships were inspected June 28, 1973, in Hoboken, New Jersey, and New York, New York, respectively.

2. OBSERVATIONS

2.1 Overall Extent of Damage

The longitudinal extent of damage appeared to be somewhat limited in two collisions (Nos. 4 and 6), but to be of the general magnitude expected of longitudinally framed ships in three other collisions (Nos. 1,2,and 5), although theoretical calculations were not made for direct comparison. Collision No. 3 was between two transversely framed ships; the apparent "brittleness" of that particular collision in comparison with Collision Nos. 1, 2, and 5 suggests that the damaged length and the extent of incursion before hull rupture will tend to be greater for a longitudinally framed ship than for a comparable transversely framed ship. The limited extent of the damage to the longitudinally-stiffened shell and outboard structure of the struck ship (tanker) in collision No. 6 may possibly be explained by the fact that it was an oblique collision, and the portion of the hull behind the strike, where plastic membrane tension strains may be expected to occur in oblique collisions, was rigidly supported during the initial stages of the collision by a transverse bulkhead. The longitudinal bulkhead was also ruptured and seemed to have developed membrane tension prior to rupture.

"Hard points," such as the transverse bulkheads and/or strong web frames that define the ends of the overall length of damage have a significant effect on limiting the plastic deformation of a struck ship. In most collisions, there appears to be more of a tendency for ruptures to occur at hard points before occurring at the imprint of the striking bow.

Considerably more plastic distortion is exhibited in a stiffened hull that is struck about midway between transverse bulkheads than one that is struck near to a transverse bulkhead.

The deck and the ship bottom seem to act as "hard lines" in resisting side incursions, and ruptures generally occur in the hull at the deck and bilge elevations. This suggests that the strength of the deck and the ship bottom in resisting side incursions may have a very significant effect on collision phenomena.

2.2 Longitudinally Stiffened Hull Plates

At the location of greatest incursion by the striking ship, the hull longitudinal stiffeners of the struck ship tend to trip and in many cases, there are ruptures of the welds connecting the stiffeners to the hull plate. As a result, the bending strains in the stiffeners are not as great as they would be if the stiffeners remained in their normal geometric position. Consequently, large incursions are resisted primarily by membrane tension in the side plate and longitudinal stiffeners and not by bending.

2.3 Deck or Bilge Areas

When the striking bow does not directly bear against a deck or the bilge area of the struck ship, the deck or bilge area is likely to survive (without extensive damage) a significant incursion of the hull. If the deck or bilge area is struck directly or if the struck hull is extensively damaged, the deck or bilge area will tend to fail by first forming a series of longitudinal folds (each typically only one or two feet deep) and eventually forming transverse ruptures across the folds.

Such transverse ruptures indicate that ultimately the primary strains in a distorted deck or bilge area are longitudinal membrane tension strains.

2.4 Transverse Structure

The transverse structure of a longitudinally framed tanker generally consists of transverse bulkheads and intermediate transverse web frames. Generally, the transverse bulkheads do not suffer any significant damage unless the striking ship has actually "plowed" through them. Conversely, the transverse web systems are generally quite vulnerable to collisions. Web trusses as opposed to web plates buckle under relatively minor side distortions, without much overall straining. Web trusses between the outer and inner plating of double-skin ships appear to be particularly ineffective in causing the two platings to distort in unison (or parallel) during a collision; web plates appear to be more effective for causing the two hulls to distort in unison.

In single-skin tank barges vertical web plates without attached horizontal stiffeners tend to fail in a crushing mode by developing vertical folds. In larger single-skin ships vertical web frames with attached horizontal stiffeners offer significant in-plane resistance to inward movement of the hull and eventually will fail by rupturing and/or overall twisting rather than by crushing.

2.5 Oblique Collisions

In oblique collisions the struck hull back of the strike (shell area transversed by the striking bow) tends to be in nearly a

single flat plane. This indicates that the collision angle (the acute angle between the centerlines of the colliding ships) tends to remain practically constant during a collision. Whereas the hull in back of the strike generally appears to be stretched fairly straight in membrane tension, the hull ahead of the location of greatest incursion tends to develop vertical folds. This indicates that in an oblique collision it is most reasonable to assume plastic longitudinal strains in the hull in back of but not ahead of the location of maximum incursion.

2.6 Striking Bows

The striking bows generally are relatively undistorted except where they encounter stiff horizontal resistance at a deck or bilge area of the struck ship. At such elevations, the horizontal structure of the struck ship tends to "knife through" the striking bow.

3. CONCLUSIONS

Analyses of the results of the six ships' collision inspection cases have brought forth the following generalized conclusions:

(1) The bow of the striking ship distorts significantly only if it encounters relatively stiff horizontal resistance at a deck or bilge.

(2) The longitudinal extent of damage is the same for the deck, shell plate, and all damaged longitudinals.

(3) The energy absorption capacity of a longitudinally framed ship is generally greater than that of a comparable transversely framed ship.

(4) The longitudinal extent of damage is likely to be restricted between the transverse bulkheads and/or strong web frames.

(5) The deck and bilge area are "hard points" in resisting side incursion unless the striking bow directly bears against them.

(6) The relative location of strike to the transverse bulkhead has a significant effect on energy absorption.

(7) For a longitudinally stiffened hull, the collision energy is primarily absorbed by membrane tension in the side shell plate and longitudinal stiffeners.

(8) For a double-skin struck ship, web plates are more effective than web trusses for causing the two skins to distort in unison.

(9) In an oblique collision, the angle of collision remains constant throughout the collision.

(10) For oblique collisions, plastic membrane-tension strains occur in the portion of hull behind the strike.

(11) The damaged deck forms a series of small-pitch accordion folds extending in the longitudinal direction.

4. REFERENCES

1) U.S. Department of Transportation - U.S.C.G., "Tanker Structural Analysis for Minor Collisions," prepared by M. Rosenblatt & Son, Inc. and U.S. Steel Corp., MR&S Report No. 2087-18, December, 1975.

2) U.S. Department of Transportation - U.S.C.G., "Tanker Structural Analysis Procedure Primer," prepared by M. Rosenblatt & Son, Inc. and U.S. Steel Corp., MR&S Report No. 2087-19, December, 1975.

Preceding page blank

APPENDIX A

COLLISION INSPECTION REPORTS

Preceding page blank

A-1. COLLISION INSPECTION REPORT FOR CASE 1

Longitudinally Stiffened Single Hull Barge

by J. F. McDermott, USS Engineers and Consultants

Barge: BGE-102, with longitudinally stiffened single-hull plate.

Owners: Marine Transportation Co., St. Louis, Missouri.

Barge Built: Approximately 2-1/2 years previously at Nashville Bridge Shipyard, Nashville, Tennessee.

Towing Vessel: M/V (Motor Vessel) Marine.

Damaged by: Collision with concrete dolphin adjacent to railroad bridge pier in the Mississippi River at Burlington, Iowa.

Visited Damaged Barge at: National Marine Service Repair Plant, Hartford, Illinois, October 30, 1971. Attended by R. W. Haskew, Yard Supt.

Local Coast Guard Office: Marine Inspection Office
Second Coast Guard District
Suite 1118
210 N. 12th Street
St. Louis, Missouri 63101
Represented by
CWO-3 George M. Miley, Jr.
Duty Officer.

External Damage: Approximately 25- by 8-foot area (plate 1/2 inch thick) with approximately 1-foot indention and an 18-inch horizontal rupture within a 16- by 4-foot elliptical area, in the transition portion at the No. 1 starboard cargo compartment.

Preceding page blank

Internal Damage: Extensive twisting of longitudinal stiffeners within three web-frame spaces, but only one longitudinal stiffener ruptured; some rupture of intermittent fillet welds connecting longitudinal stiffeners to hull plate. Four web frames dished in (maximum out-of-plane deflection approximately 1 inch, 4-1/2 inches, 4-1/2 inches, and 3 inches, respectively). However, inboard flanges of web frames were not significantly distorted (3/4-inch maximum out-of-line deflection).

Tentative General Observations:

(1) The maximum permanent set in the hull plate was only of the order of 1 to 5 percent strain, which cannot explain the 18-inch rupture.

(2) The longitudinally stiffened hull plate loaded in bending until the stiffener flanges buckled, then loaded in membrane tension to result in the final distortion, as generally predicted by the analysis developed by M. Rosenblatt & Son—USS Engineers and Consultants.

(3) The web frames folded and crushed, but did not exhibit any in-plane shearing, perhaps because the stiffener-to-web frame fillet-weld connections were along the stiffener flanges rather than along the stiffener webs.

Note: The following twelve sheets are photographs of the damaged barge.

General view of transverse frame, showing
vertical, transition, and horizontal members.
Note the predominance of rolling and dishing types of failures.

252 (373)

Column failures of transverse diagonal struts
and end crippling of transverse horizontal strut.

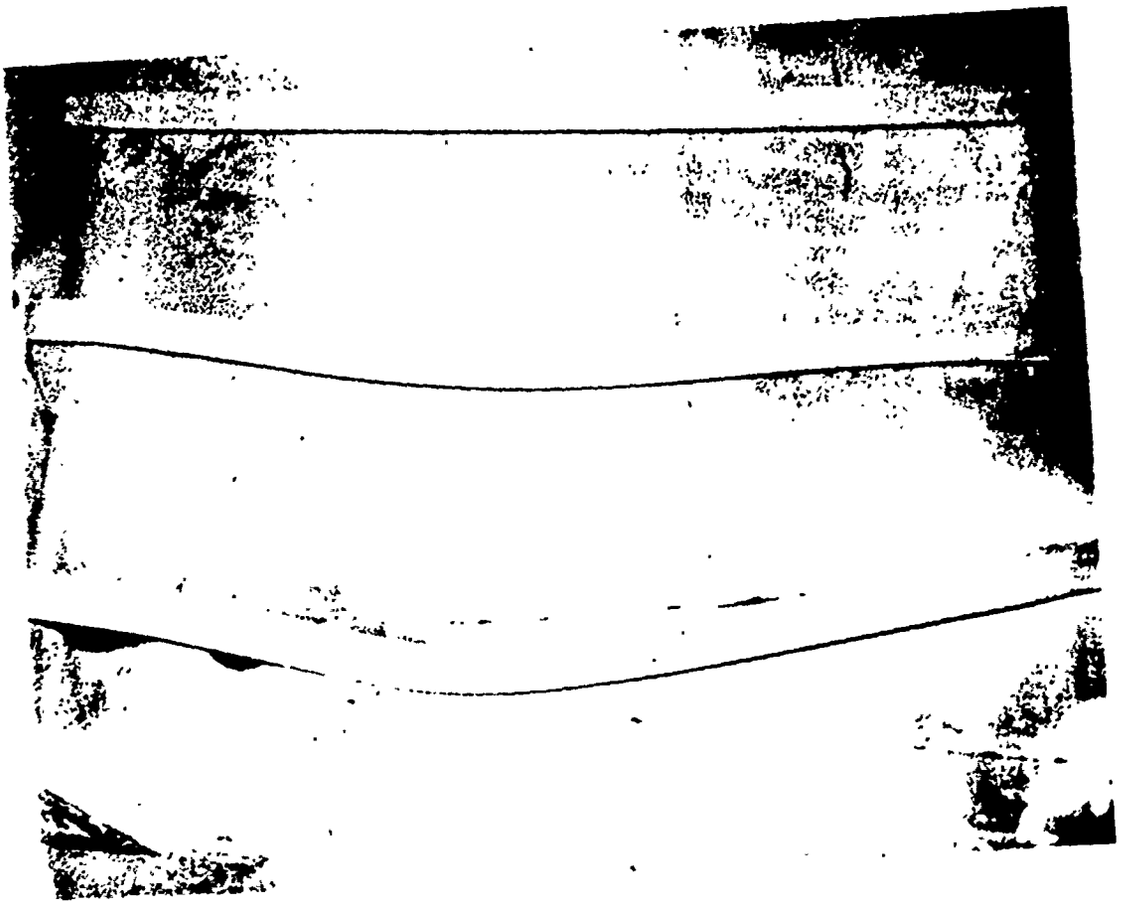

Typical rolling buckle of longitudinal stiffeners.

Transition transverse frame member torn at connection with vertical member and bent like a buckled column.

L5L (316)

Transition transverse frame member torn at connection with horizontal member and bent like a buckled column.

Vertical transverse frame member folded in, but with no appreciable in-plane shearing or bending. Note that the longitudinal stiffeners are only connected to the vertical member by fillet welds on the outstanding legs of the longitudinal stiffeners. Note one longitudinal stiffener rupture, lower right.

Typical dishing of vertical transverse frame member. The rupture of one longitudinal stiffener is evidenced by the kink in the foreground.

Rupture of one longitudinal stiffener. The connection welds are intact forward but ripped aft, and the longitudinal stiffener is severely rolled.

252 (380)

Horizontal side plate tear about 18 inches long. The intermittent welds of the adjacent longitudinal stiffener are ripped, and the longitudinal stiffener is severely rolled. The vertical transverse frame member is folded and dished out of plane, but with no appreciable in-plane shearing or bending. There is slight crippling at the end of the diagonal strut.

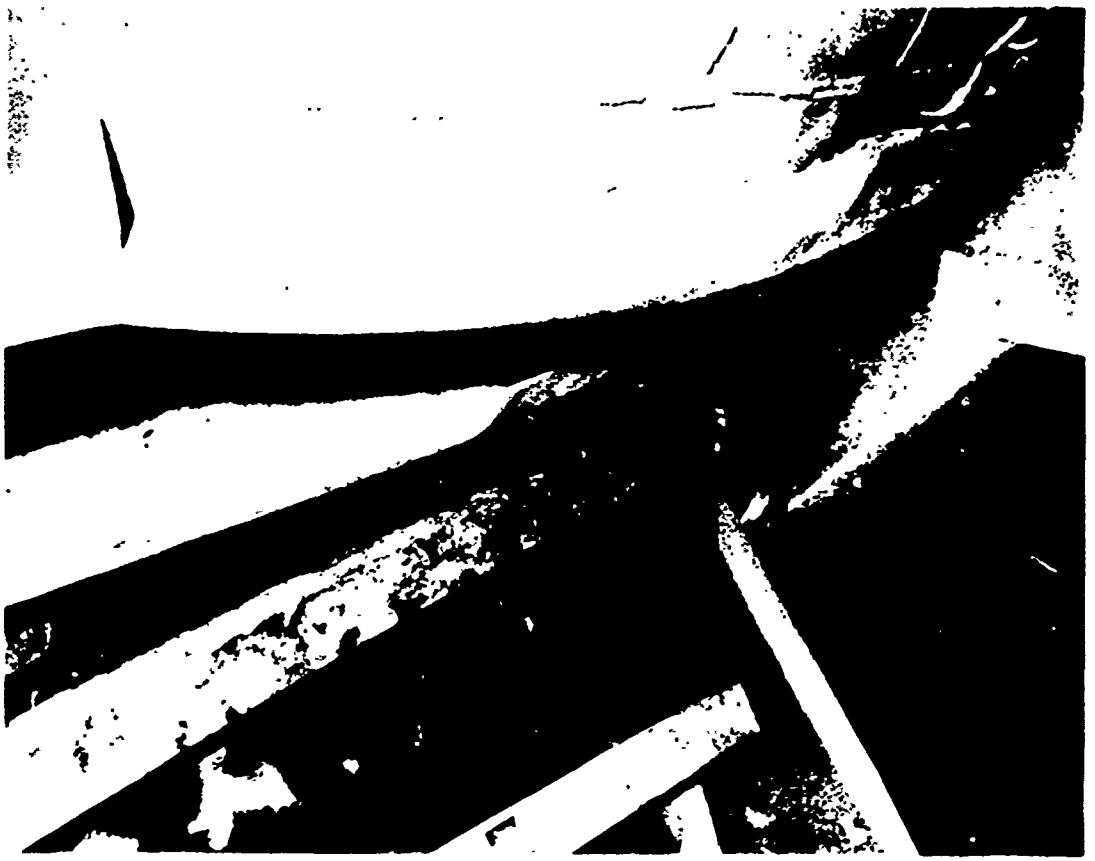

Portion of longitudinal stiffener with connection welds ripped, between rupture of stiffener and tear of side plate.

Horizontal tear in side plate near severe folding of vertical transverse frame member.

Severe dishing of vertical transverse frame member, but with no apparent in-plane shearing or bending. Note rip of fillet welds connecting longitudinal stiffener to side plate. The longitudinal stiffener is severely rolled and twisted, but is not ruptured.

A-2. COLLISION INSPECTION REPORT FOR CASE 2

Double-Hull Barge

by J. F. McDermott, USS Engineers and Consultants

Barge: Double-Hull (Originally 175 ft. x 26 ft. x 11 ft. Single-Hull) Barge for Transporting Compressed Chlorine Gas (Original Design 1957, Revised Design 1967).

Owner: U. S. Army Corps of Engineers

Damaged by: Collision with piers on dam in the Ohio River, Louisville, Kentucky.

Visited Damaged Barge at: Jeffboat Inc.
Jeffersonville, Indiana
May 17, 1972.

Participants of Detailed Inspection and Field Measurements:

E. L. Jones, Lt. Cmdr., U. S. Coast Guard

W. P. Chaing, M. Rosenblatt & Son

J. F. McDermott, USS Engineers and Consultants

Field Data

Figures 1 to 17, inclusive, are photographs taken May 17, 1972, of the starboard-side, midship damaged portion of the chlorine barge. This portion engaged a 5-foot-radius vertical end of a concrete pier during the time it was caught in the dam spillway. Figure 18 gives offset measurements made at the time of the photographs to document the lateral distortions in this damaged portion.

As illustrated in Figures 1 through 18, some pertinent observations are as follows:

(1) The major portion of the damaged area extended between two consecutive wing-tank bulkheads, spaced 30 feet apart; one wing-tank bulkhead was in line with the main transverse bulkhead amidships and the other was in line with a web frame backing up the inner null.

(2) The outer hull plate was ruptured at the center of the damaged area, (Figures 1, 2, 3, 4, and 6), but not at the ends of the damaged area (Figures 1, 2, and 3) except (Figure 7) near the upper portion of the distorted (Figure 8) midship wing-tank bulkhead. The inner hull plate apparently was not ruptured except for cracks near the deck.

(3) Within the central portion of the damaged area, the outer hull was formed to a cylindrical depression (Figures 3, 4 and 6), apparently conforming to the curvature of the dam pier.

(4) At various stations, the deck plate ruptured along lines at right angles to the ship side and then buckled into folds. (Figures 3, 4, and 5). In the central portion of the damaged area, the average fold height (of five 180-degree folds) was about one foot.

(5) In the central portion of the damaged area, the bilge plate ruptured transversely and formed one fold (Figure 6), projecting downward about one foot below the bottom of the barge.

(6) In the central portion of the damaged area, the longitudinal stiffeners of the outer hull were tripped, with the outer edges of the outstanding legs bearing against the inboard face of the outer hull plate (Figure 6). However, the stiffeners were not ruptured at the locations where the outer hull plate was ruptured.

(7) Instead of ruptures occurring in the stiffeners at the maximum incursion, as predicted by plastic analysis theory, premature failures occurred in the end connections to the stiffeners for both the outer (Figure 10) and inner (Figure 17) hull plates. Also, failures occurred in the butt-welded joints of the inner-hull longitudinal stiffeners close to the wing bulkhead (Figure 16).

(8) Many gusset plates were grossly distorted (Figures 12 and 16), resulting in prying actions at the connections, which would tend to reduce the strengths of the connections.

(9) The two wing frames within the area of major damage (Figures 9 and 10) were crumpled beyond any configuration capable of resisting any significant forces.

(10) Folding action dominated the distortion behavior of the midship wing-tank bulkhead (Figure 8), the main midship bulkhead (Figure 11), and the intermediate web frame which backed up the inner hull in the damaged area (Figures 13 and 14).

(11) The tendency of the web frames to fold rather than be rigid allowed the web frames in the damaged area to fold around the chlorine tank (Figures 13 and 14), even lifting the tank off its saddle (Figure 15) without puncturing or significantly distorting the tank. This suggests that the horizontal crushing (column action) force (computed to be 0.56 kip per inch of web frame) offered by one intermediate 5/16-inch-thick web plate on the inner hull did not exceed the force that would be required to produce inelastic deformation in the chlorine tank thus loaded.

(12) At the station of greatest incursion, the inner-hull longitudinal stiffeners were severely bent but not tripped (Figure 17).

(13) As tabulated in Figure 18, the inward distortions of the hull plates were as follows, indicating a very tight fit of the outer hull against the inner hull over most of the depth of the barge:

Location	Maximum Offset, inches	
	Outer Hull Plate	Inner Hull Plate
Just below deck	70.5	81.5
Top lap joint	71	73.2
Midway between lap joints	62	64.5
Bottom lap joint	62	64.7
Bilge	52	—

Analysis Assumptions Based on Field Data

From these observations, the following empirical assumptions are derived which are pertinent for approximate theoretical analyses of the collision:

(1) The radius of bend induced by the long-term contact with the dam pier should be considered in the distortion geometry.

(2) The structural contribution of the crumpled wing frames and of the outer-hull longitudinal stiffeners, which separated from their end connections, can be neglected. (In fact, if the longitudinal stiffeners had continued to act monolithically with the outer hull plate, they theoretically would have ruptured in the bent portion.)

(3) An approximate evaluation of the resistance of the intermediate web plates to inward movement of the inner hull is obtained by considering the web plates to be stiffened (at the deck and bottom) plates in axial compression, with the axial direction horizontal. For a yield stress of 35 ksi, the "effective width" of a 132-inch by 5/16-inch web plate

is 18 inches, half of which is considered concentrated near the deck and half near the bottom. Multiplying this effective width times the theoretical horizontal crushing force of 0.56 kip per inch gives a total horizontal resisting force equal to 10 kips per intermediate web plate. Because this resisting force is relatively small and is concentrated at the extremities of the web plate, it may be neglected in calculations of membrane tension equilibrium of the hull plate.

(4) Because the major portion of the damage is confined between two consecutive wing-tank bulkheads, it may be assumed that these wing-tank bulkheads, which are backed up by either the midship bulkhead or a web frame, can resist the loads from the hulls.

(5) Because of the transverse cracks and subsequent folding of the deck and bilge plates, the transverse bending and/or membrane-tension resistance of those plates very likely was terminated before rupture of the outer hull. Since the resistance of these plates to shearing and folding was relatively small, the resistance of the deck and bilge plates to incursion may be neglected.

Approximate Theoretical Analyses

With these empirically derived assumptions—plus the simplifying assumption that the wing tank bulkheads, spaced at 30 feet, do not distort or move together by any amount—approximate theoretical analyses are given in Figures 19, 20, and 21. The

analyses are concerned with forces and distortions, rather than energy, since the accident was a long-term steady-state phenomenon.

Figures 19 and 20 give the theoretical membrane tension capacities of the outer and inner hull acting separately. Based on a normal encounter with the dam pier, Figure 21 gives the theoretical horizontal geometry and forces in the barge at the instant of rupture of the outer hull plate. The incursion at rupture theoretically was 52.5 inches. The 62-inch offset measured at the lower plate lap, Figure 18, corresponds to an additional incursion after rupture of 9.5 inches, which would cause about a 6-inch separation of the ruptured edges. Adding a 4-inch spring back (after relief of membrane tension) gives a predicted opening of 10 inches, compared to a measured opening of 13 inches at this location, Figure 18.

The total of the resisting forces offered by the stiffened hulls (neglecting the resistances of intermediate web plates) at the instant of outer hull rupture was calculated to be 1970 kips, Figure 21. To this may be added 10 kips resistance from each of the two intermediate web frames to give a total resisting force of 1990 kips. However, the maximum resisting force probably was considerably less because of (1) the distortions of the supporting midship bulkheads (Figure 8 and 11), (2) the tendency for the membrane tension in the hull plates to be reduced because of lateral bending of the entire ship cross section, and (3) the reported list (about 6 degrees) of the barge against the dam pier, which would tend to initiate earlier rupture near the deck of the barge.

Comparison of Double-Hull and Single-Hull Capacities

In spite of the probability that the forces are thus overestimated, the analyses in Figures 19, 20, and 21 afford a comparison of the resistances of double-hull and single-hull construction to such an accident. Compared to the resisting force immediately before the rupture of the outer hull plate (1990 kips), the maximum resisting force afterwards was theoretically only capable of being roughly eight-tenths as great (1588 + 20 = 1608 kips), i.e., equal to the capacity of the barge as originally constructed with only a single hull. However, the barge apparently was subjected to a steady-state loading, without significantly increasing distortions, for a considerable time after the rupture of the outer hull plate. This could possibly be explained by a transfer of forces between the inner and outer hulls by friction, due to the very tight fit between the hulls at the center of the damaged area.

The forces calculated in the analyses afford an indication of how the efficiency of a double hull in resisting a normal collision can be increased by constructing the inner hull nearer to the outer hull. Based on the assumptions listed above, the horizontal resistance up to rupture of the outer hull generally could be expected to vary from roughly 1990 kips for the barge investigated to roughly 1-3/4 times as great (1884 + 1608 = 3492 kips) if the flanges of the outer-hull stiffeners touched the inner hull along the full length of the barge so that both hulls would be forced to deflect simultaneously under an incursion.

General view, looking forward.

Figure 1.

252 393

General view, looking aft.

Figure 2.

View from upper deck of dry dock,
looking forward.

Figure 3.

252 (395)

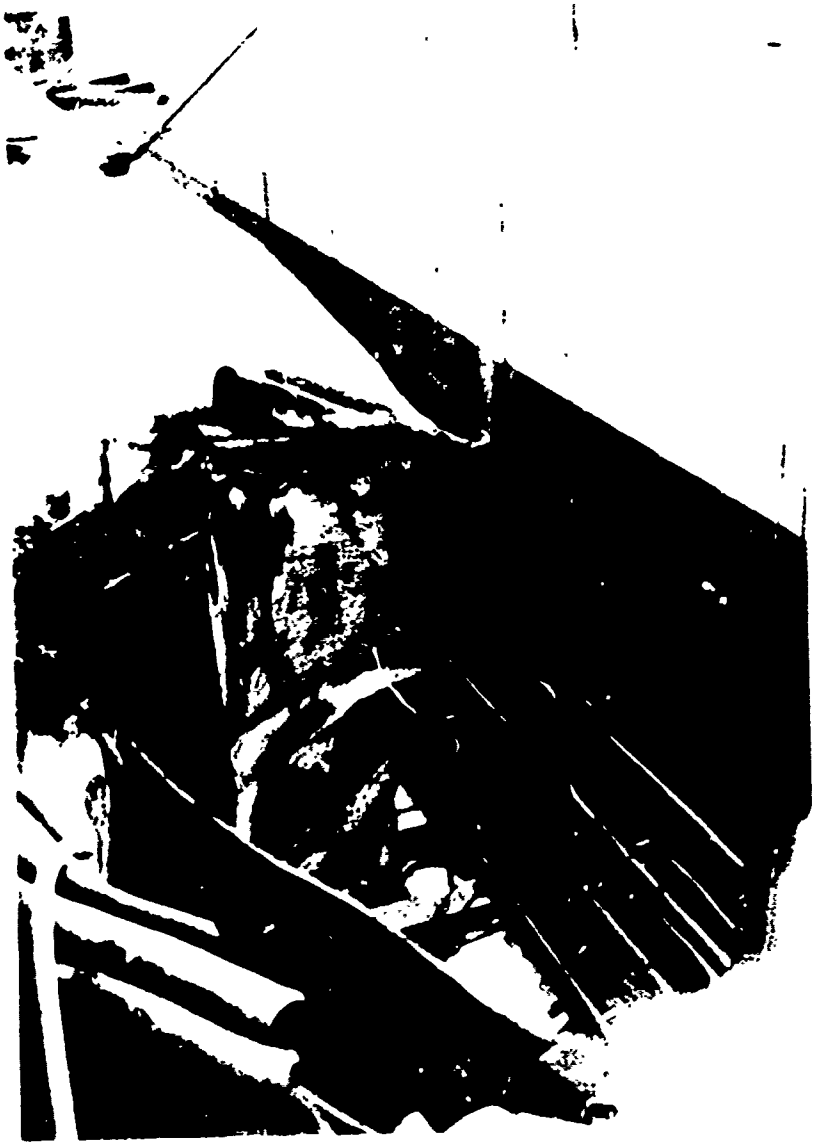

Top view of ruptures and folds.

Figure 4.

Rupturing and folding of deck plate,
looking forward.
(Note hole burned in deck plate,
foreground, to arrest spread of rupture.)

Figure 5.

252 (397)

Bottom portion of ruptured outer hull.
(Note that the longitudinal stiffeners are tripped,
with the outer edges of the outstanding legs
bearing against the inboard face of the outer hull plate;
the bilge plate is folded, projecting about one
foot below the bottom of the barge.)

Figure 6.

Bend line and plate ruptures of outer hull just forward of midship wing-tank bulkhead.

Figure 7.

252 (399)

Midship wing-tank bulkhead,
looking forward.

Figure 8.

Crumpled wing frame 10 feet forward of midships, looking aft. (Note 90-degree trip in vertical channel and 90-degree horizontal bend in horizontal channel.)

Figure 9.

Crumpled wing frame 20 feet forward of midships, looking forward. (Note vertical channel tripped 90 degrees, no trace of horizontal gusset plate connecting square ends of longitudinal stiffener angles.)

Figure 10.

Vertical fold in midship bulkhead,
looking aft.
(Note cracks at top of fold.)

Figure 11.

Bent gusset plates connecting longitudinal stiffeners to midship bulkhead, looking aft.

Figure 12.

Web plate 10 feet forward of midships dished 11 inches (in 22 inches), with inboard edge folded to contour of chlori e tank (about two inches cle rance to tank.)

Figure 13.

Web plate 10 feet forward of midships
ıished and folded, looking forward.

Figure 14.

252 (406)

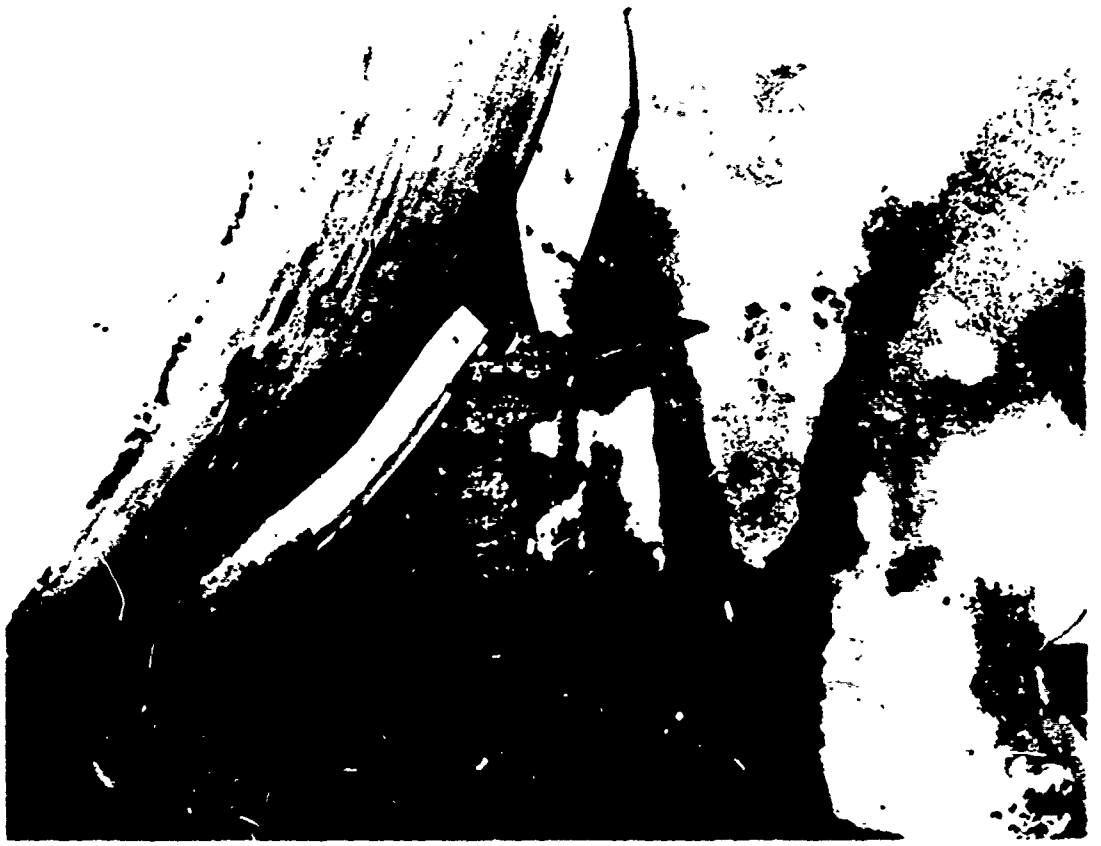

Forward starboard chlorine tank with two-inch clearance to starboard edge of aft saddle plate. (Note vertical bend in saddle.)

Figure 15.

252 (407)

Inner hull longitudinal stiffener angles ruptured at welded joint near web plate 10 feet forward of midships, looking aft.

Figure 16.

Bowed inner hull plate and stiffener angles in space just forward of the web plate 10 feet forward of midships, looking aft.

Figure 17.

252 (404)

INSPECTION OF DAMAGED CHLORINE BARGE AT JEFFBOAT, JEFFERSONVILLE, IND., 5-17-72

OFFSET MEASUREMENTS OF MIDSHIP DISTORTIONS

FIGURE 18

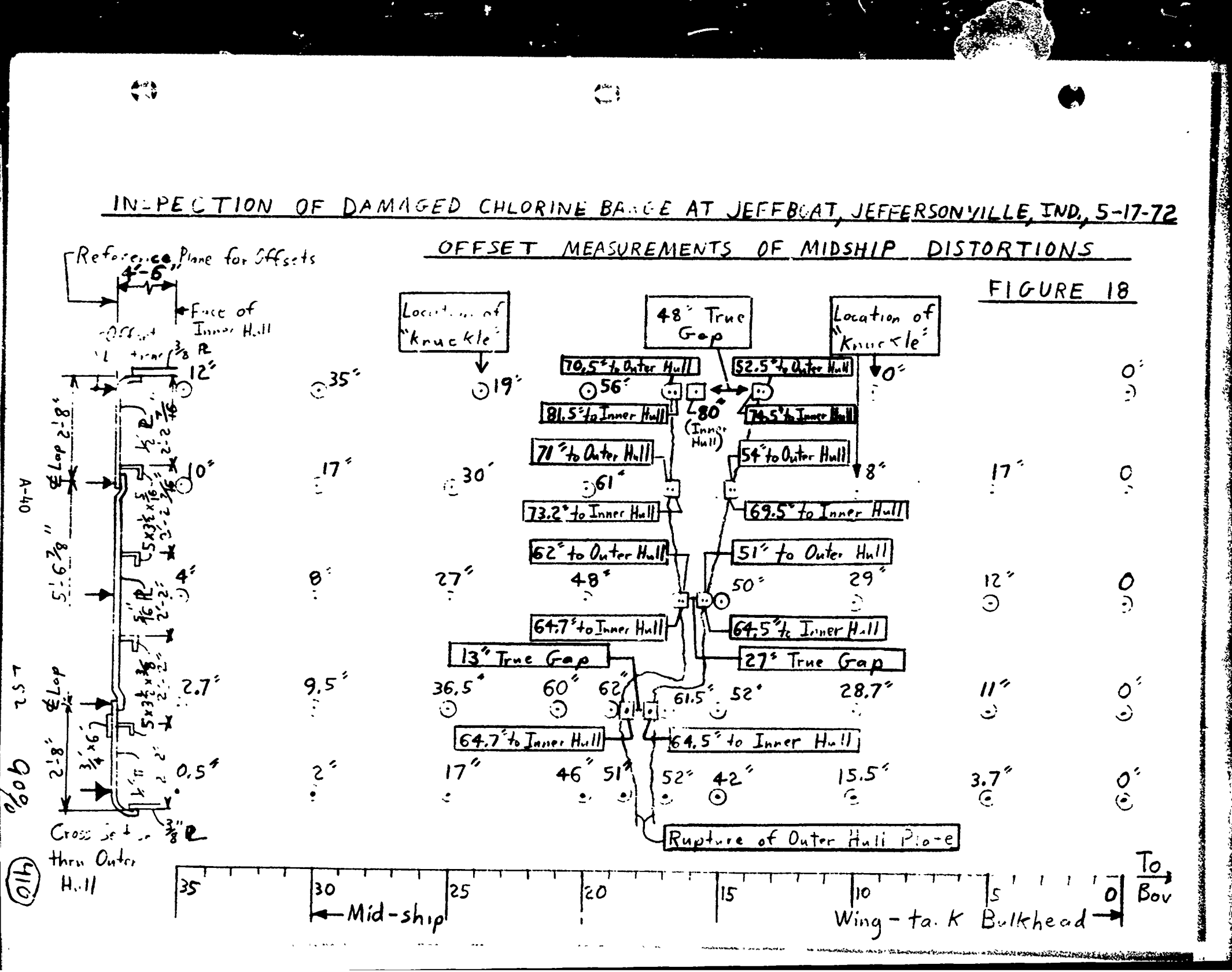

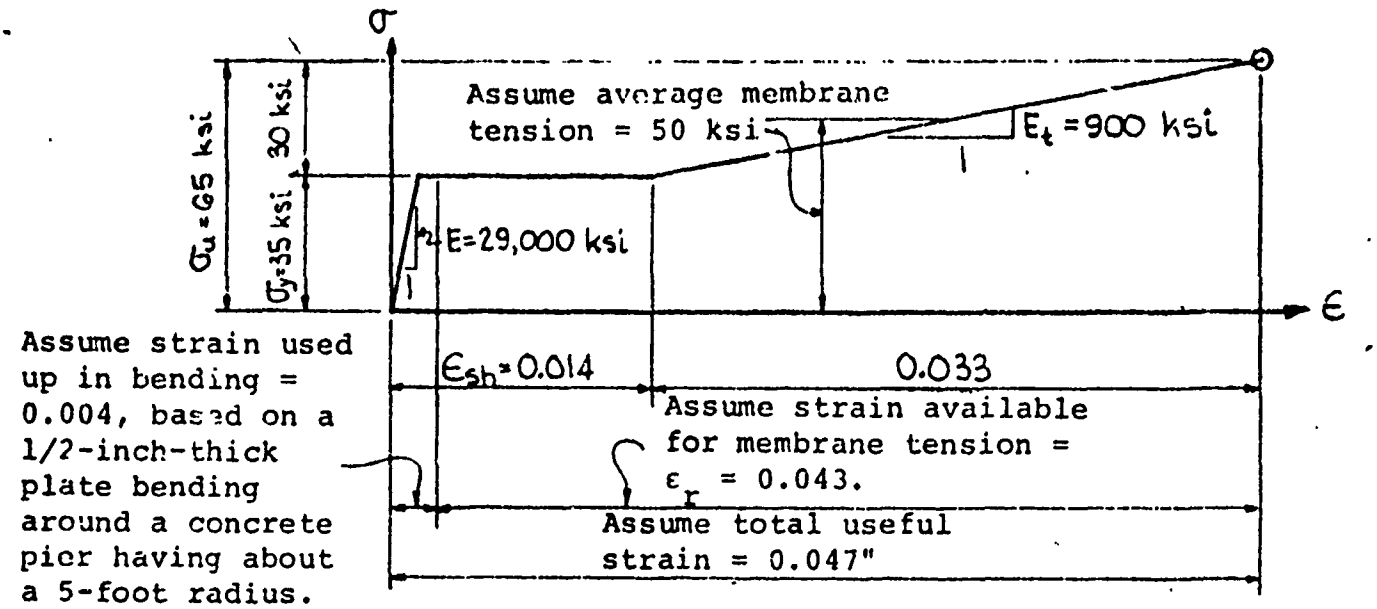

IDEALIZED STRESS-STRAIN CURVE

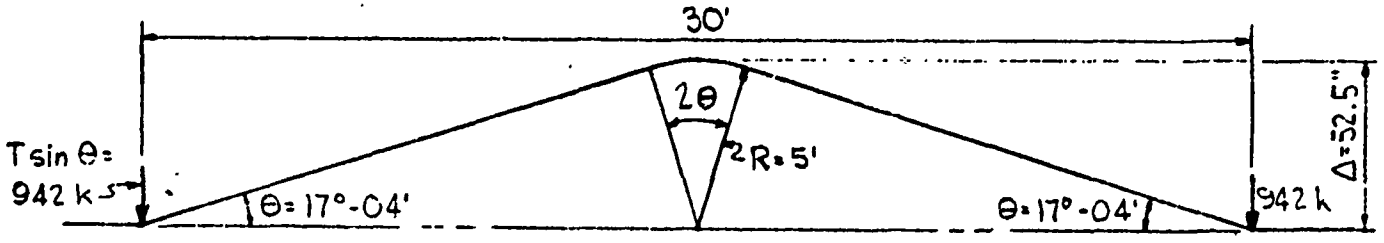

Notes:

(1) The calculations neglect the longitudinal stiffeners, which did not rupture where the hull plate ruptured, Figure 6, and which separated from their end connections, Figure 10. The calculations are based on the idealized stress-strain curve.

(2) Bending strains at the bend lines at the ends of the damaged area are neglected since major ruptures did not occur at the ends of the damaged area, Figure 1.

(3) Average membrane tension strain = $\epsilon_r = \dfrac{\frac{15}{\cos\theta - 5\tan\theta + 5\theta - 15}}{15} = 0.043$

(4) Maximum incursion = $\Delta = 5 + 15\tan\theta - \dfrac{5}{\cos\theta}$

(5) Total membrane tension thrust = T = 3209K (assuming longitudinal stiffeners have tripped and slipped and deck and bottom plating have ruptured, leaving only 37" x 1/2", 68-7/8" x 5/16", and 39-5/16" x 1/2" plates and a 6" x 3/4" rub bar all under an average tension of 50 ksi).

THEORETICAL MEMBRANE TENSION CAPACITY OF OUTER HULL ASSUMING WING-TANK BULKHEADS DO NOT DISTORT

Figure 19

411

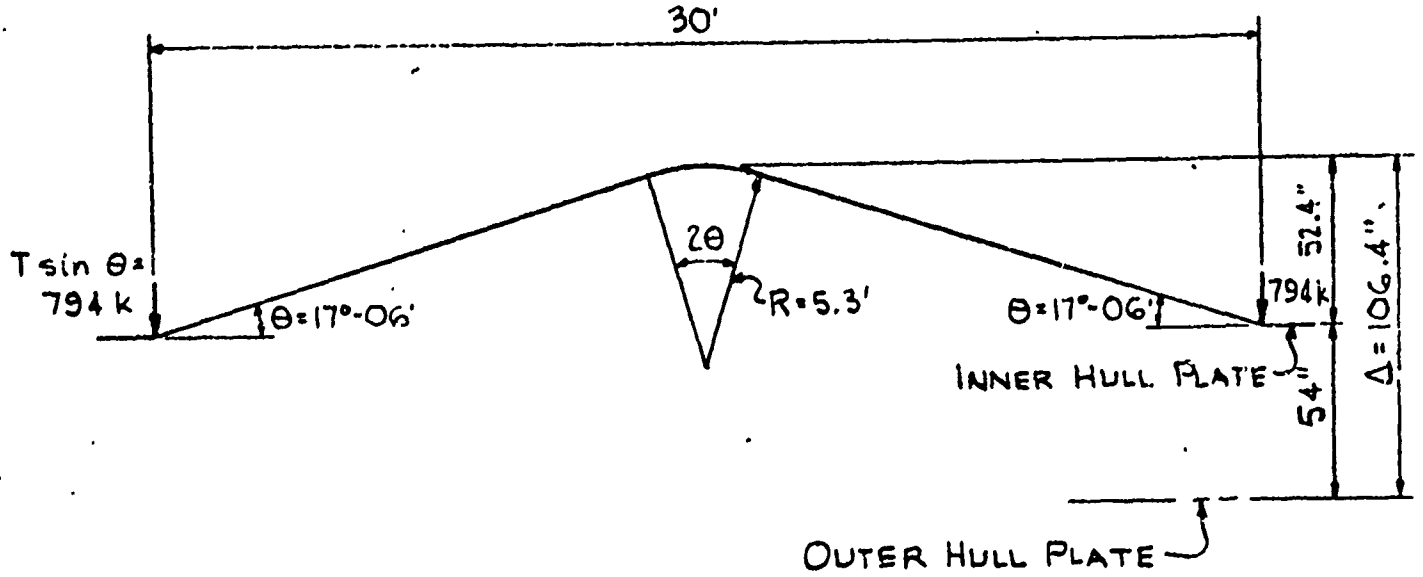

Notes:

(1) The calculations neglect (a) the longitudinal stiffeners, which tend to separate from their end connections, Figure 17, and (b) the intermediate web plates near the central portion of the damaged area, which tend to fail by folding (Figures 13 and 14). The calculations are based on the idealized stress-strain curve, Figure 19.

(2) Bending strains at the bend lines at the ends of the damaged area are neglected as for the outer hull, Figure 19.

(3) Average membrane tension strain = $\varepsilon_r = \frac{\frac{15}{\cos\theta - 5.3\tan\theta + 5.3\theta - 15}}{15} = 0.043$

(4) Portion of incursion extending into inner hull = $(\Delta - 54) = 5.3 + 15\tan\theta - \frac{5.3}{\cos\theta}$

(5) Total membrane tension thrust = T = 2700K (assuming longitudinal stiffeners have tripped and slipped and deck and bottom plating have ruptured, leaving only a 132" x 3/8" plate and a 6" x 3/4" rub bar under an average tension of 50 ksi).

THEORETICAL MEMBRANE TENSION CAPACITY OF INNER HULL ASSUMING WING-TANK BULKHEADS DO NOT DISTORT

Figure 20

42

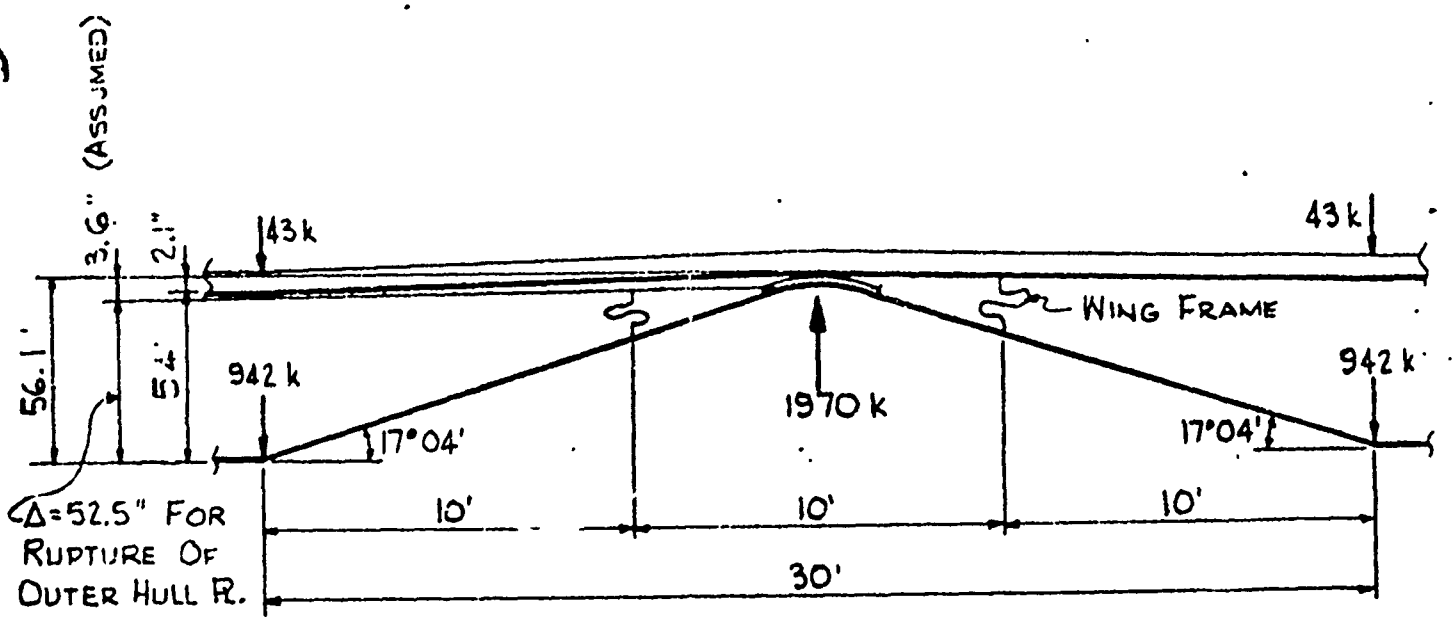

Notes:

(1) It is assumed that the wing frames are completely crumpled, offering no significant resistance.

(2) It is assumed that the longitudinal stiffeners attached to the outer hull plate have tripped and slipped, thereby offering no membrane tension resistance.

(3) The 942K bulkhead reaction on the outer hull is as computed in Figure 19.

(4) The 43K bulkhead reaction on the inner hull corresponds to the plastic bending phase (extending up to 6.4 inches central deflection) of the stiffened inner hull plate (based on a cross section including only 5 angles 6" x 3-1/2" x 3/8", one 132" x 3/8" plate, and a 6" x 3/4" bar, all stressed at 50 ksi in monolithic plastic bending.

THEORETICAL HORIZONTAL GEOMETRY AND FORCES AT RUPTURE OF OUTER HULL PLATE STRUCK NORMALLY AGAINST A 5-FOOT-RADIUS PIER ASSUMING WING-TANK BULKHEADS DO NOT DISTORT

Figure 21

A-3. COLLISION INSPECTION REPORT FOR CASE 3

Transversely Framed Cargo Ships

(Note: The inspection described below was conducted by permission of the ships' owners under the condition that the information obtained be kept for use solely by the United States Coast Guard)

Date of Collision: 9/5/72

Date of Inspection: 9/8/72

Inspection by: John C. Daidola, M. Rosenblatt & Son, Inc.
John F. McDermott, U. S. Steel Corp.

Ships Involved:

C. E. Dant - Transversely framed cargo ship (striking vessel)

Agean Sea - Transversely framed cargo ship (struck vessel)

C. E. Dant	Agean Sea
Type: C4 with bulbous bow	
Built: San Diego, Calif.	Built: France
Owner: States Steamship Co.	Owner: Yick Fung Shipping & Enterprises LTD, Hong Kong
Length: 565' - LOA, 528' - LBP	Length: 525'-7" - LOA, 492'-3" - LBP
Beam: 76'	Beam: 65'-9"
Draft: 31'-7-1/8"	Draft: 26'-7" (max. 32'-6-1/2")
Displ.: About 22,000 tons (loaded)	Displ.: About 16,000 tons
Light Ship: 7680 tons	Light Ship: About 6800 tons
No. of Screws/Power: 1/17,500 SHP	No. of Screws/Power: 1/7500 SHP
Cargo: Dry Cargo	Cargo: Dry Cargo (deep tanks also)
Classification: A.B.S.	Classification: Lloyds

11/4

Location of Ships:

C. E. Dant - Todd Shipyards
Harbor Island
Seattle, Washington
U. S. A.
(ship afloat)

Agean Sea - Yarrous Shipyard
Victoria, British Columbia
Canada
(ship dry docked)

Local Coast Guard Office:

Office of Marine Inspection
618 Second Avenue
Seattle, Washington

Inspection:

Summary

The subject collision represents an example of two transversely framed ships striking at an oblique angle. Because of the current structural configuration of tankers, the Tanker Collision Study has been limited to longitudinally framed ships. The reason for inspecting a collision involving transversely framed ships is that it was anticipated that fundamental information on various modes of failure could be learned from such a study.

Because of restriction of information pending a forthcoming inquiry, it was not possible at the time of inspection to know the actual courses, speeds, and motions of the ships during the collision. From the inspection and newspaper photographs of the ships, it appears that the collision angle was 50° - 55° from the perpendicular

to the ship center line; the relative speed of the ships to each other must have been significant; and the angle of collision did not change significantly during the collision.

Some aspects of the subject collision are pertinent to evaluations of the analysis procedure developed for longitudinally framed ships under the subject contract. The deck did not lift from the transverse frames but instead ripped and compressed. The striking ship in effect had a rigid bow, except where it was sliced by the main and second decks. The double bottom was extensively damaged, thus indicating that the assumption of a non-yielding bilge may not be accurate, but the major portion of the bottom damage apparently occurred after the hull ruptured.

Beside the items discussed above, several other observations were of particular interest. The salient characteristic of the struck ship was the localized extent of damage with consequent small energy absorption before side-plate rupture. The outline of the penetration was the same as that of the striking ship bow, and the damage extended only a few inches from the outline. The shear line along the decks of the struck ship, made by the striking ship cutting them, was straight, which indicates the direction of the ships relative to each other didn't change significantly during the collision.

Details of Damage

Agean Sea (Struck Ship)

The center of the damage was located approximately 80 feet from the bow, at the foward shoulder of the parallel middle body.

Damage sustained by the struck ship is illustrated in Figures 1 through 18. Overall views appear in Figures 1 through 4; typical transverse framing (undamaged) is shown in Figures 5 and 6; the relation of the damage to the transverse framing is illustrated in Figures 7, 8, and 9; damage imparted by the starboard side of the striking ship is shown in Figures 10, 11, and 12; typical deck plate failures are illustrated in Figures 13 and 14; and views defining the incursion appear in Figures 15 through 18.

Extent of Hull Damage. The most significant difference between the hull damage sustained by the transversely stiffened struck ship of the present collision and the longitudinally stiffened struck ships of the two previously reported collisions* is the extent of damage beyond the hull plate rupture. Figures 1 through 4, 7, and 8 indicate that the hull plates were not noticeably deformed either forward of the forward rupture line or aft of the plate folds at the aft rupture line. This demonstrates the

---

*"Collision Inspection Report, Barge: BGE-102, with Longitudinally Stiffened Single-Hull Plate," October 30, 1971: "Collision Inspection Report, Double-Hull Barge for Transporting Compressed Chlorine Gas," May 17, 1972.

stiffness of transversely framed hulls in bending of the stiffened side, Figure 7, and in arch action, Figure 8, resulting in relatively little energy being consumed in deforming the hull plates beyond the areas of gross damage. In contrast, the plastic distortions of longitudinally stiffened hulls beyond the rupture locations are generally extensive, resulting in plastic membrane-tension straining in large portions of the stiffened hull plate. Thus, the present collision demonstrated that transversely stiffened hulls are not capable of absorbing, before rupture, the energy that can be absorbed by longitudinally stiffened hulls of the same general size.

Figures 9 and 11 indicate a tendency for the transverse stiffenars to be easily ripped away from the hull plate during the flexing of the plate-stiffener joint that occurs during a collision. This suggests that welded connections in ships should, in addition to usual design requirements, be evaluated for such flexing action.

Deck Crushing. As viewed in Figures 1 and 2, no general lifting of the decks was exhibited. Instead, the deck plates were crumpled into small-pitch folds, Figures 13 and 14. Figure 19 suggests that the bow of the striking ship extended above the decks of the struck ship, and that the decks of the struck ship knifed into the striking ship. Subsequently, the vertical wedging action offered by the structure of the striking ship apparently precluded general lifting of the decks of the struck ship.

Geometry of Incursion. Figures 15 through 18 indicate that the angle between the colliding ships did not vary significantly during the incursion. Figures 15 and 16 suggest that this was due to the striking ship being firmly wedged into the struck ship after the hull of the struck ship was penetrated. Because of the wedging action, the striking ship could not, on its own power, withdraw from the struck ship. On the acute-angle side of the incursion, tensile and shearing failures were generally exhibited, Figures 1, 3, 7, 8, 9, and 17. On the obtuse-angle side of the incursion, compression buckling and folding failures were generally exhibited, Figures 2, 4, 10, 11, 12, and 18. Thus, relative to the progression of the strike along the side of the struck ship, the material of the struck ship was compressed ahead of the strike and tensioned behind the strike.

Bottom Damage. As shown in Figures 4 and 12, the double bottom of the struck ship was crushed inward during the incursion, presumably because the forefoot of the striking bow extended below the bottom of the struck ship. Mostly plate folding and buckling was exhibited in the damaged double bottom structure.

C. E. Dant (Striking Ship)

Damage sustained by the striking ship is illustrated in Figures 19 through 23. Overall views appear in Figures 19 and 20, and failure details appear in Figures 21, 22, and 23.

414

Rigid Bow Assumption. Figures 19 and 20 indicate that the assumption of a rigid striking bow is realistic in the analysis of the struck hull but not in the analysis of the struck decks. Apparently, the first and second decks of the struck ship knifed into the bow of the striking ship, but elsewhere the striking bow was hardly dented. Furthermore, the bottom portion of the striking bow crushed the double bottom of the struck ship without sustaining major damage. At the time of the inspection, this ship was still afloat. However, after dry docking, some dishing on the port side of the bulbous bow was noticed.

Failures Within Striking Bow. Most of the failures within the striking bow involved folding and subsequent compression of the hull plates, Figure 21. No significant deformation of the framing members in the striking bow was observed, although localized tripping and buckling failures were observed, Figures 22 and 23.

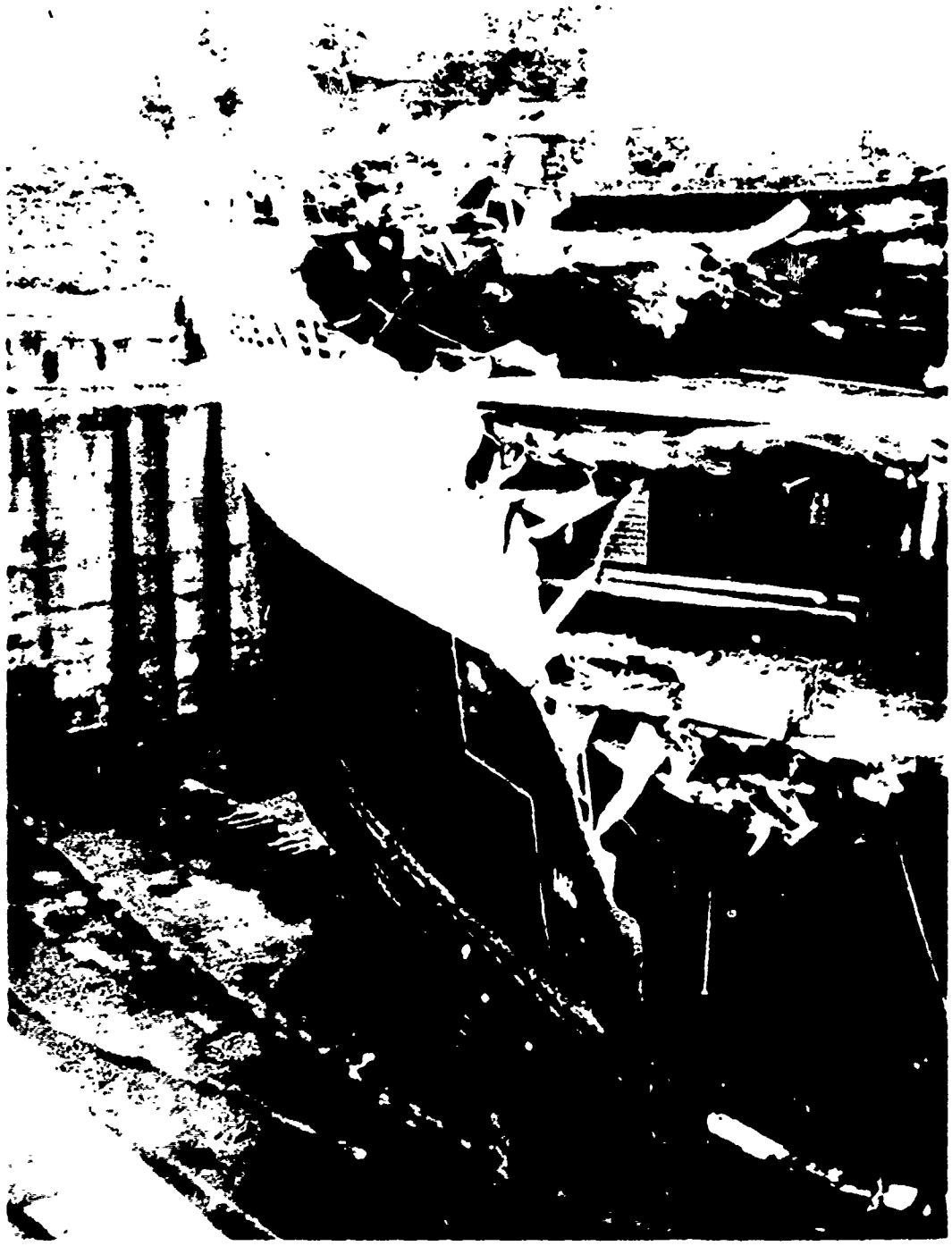

Fig. 1 Struck ship, looking forward. Note that the hull plates are not noticeably deformed forward of the rupture.

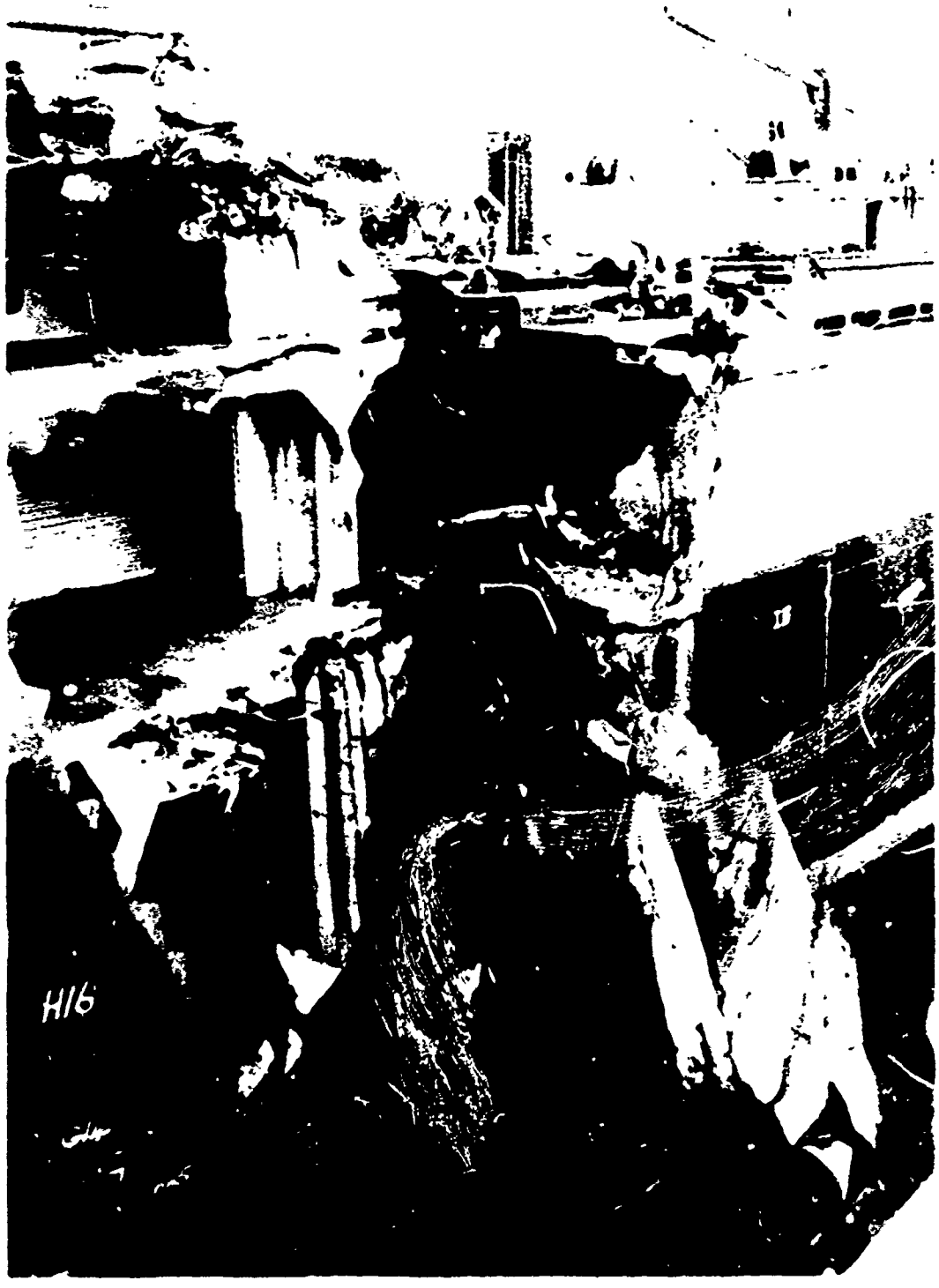

Fig. 2 Struck ship, looking aft. Note that the hull plates are not noticeably deformed aft of the rupture.

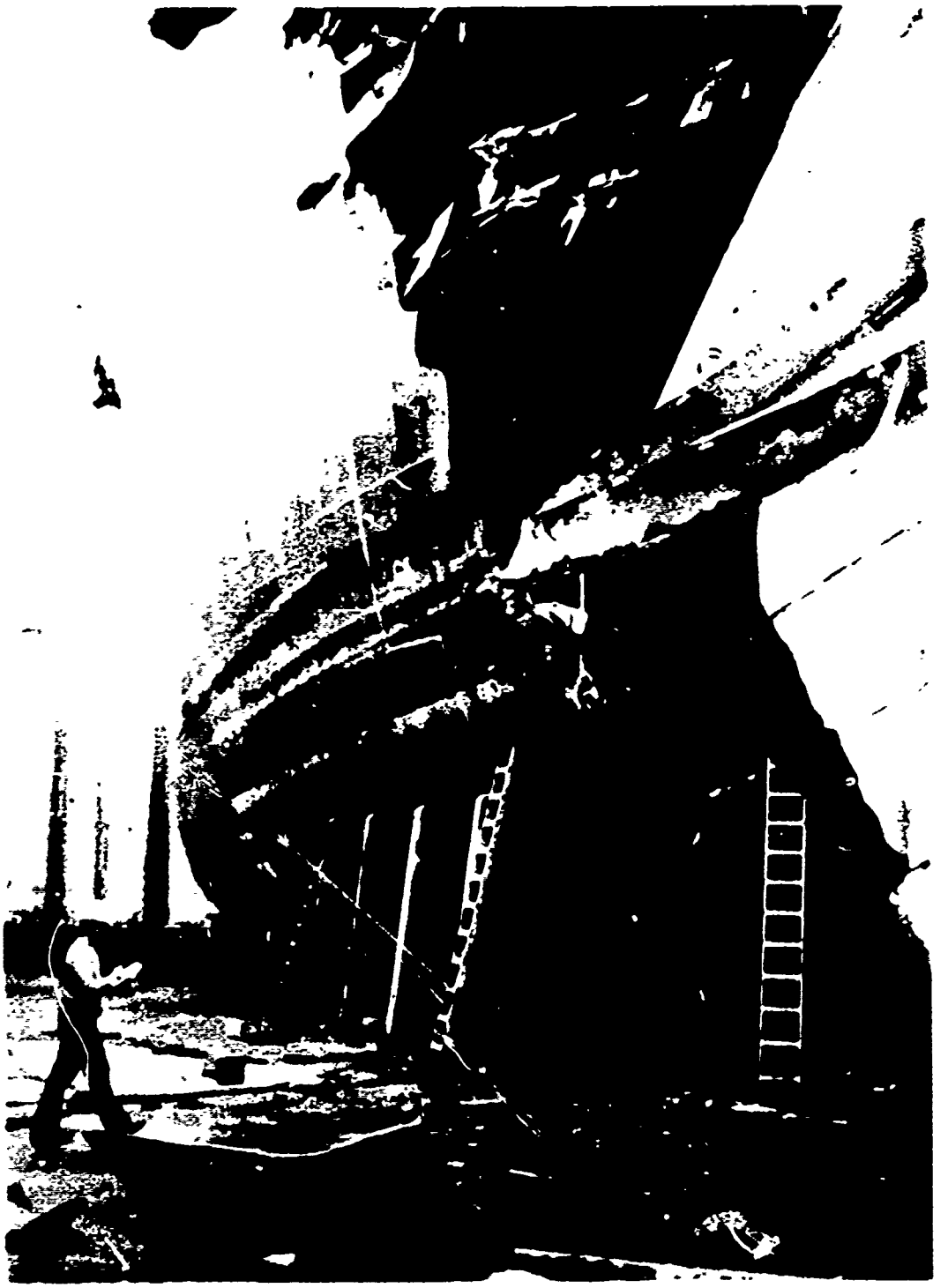

Fig. 3 View from dry dock, looking forward.

(423)

Fig. 4 Hull failure sharply limited on starboard side of strike. Bottom damage shown on port side of strike.

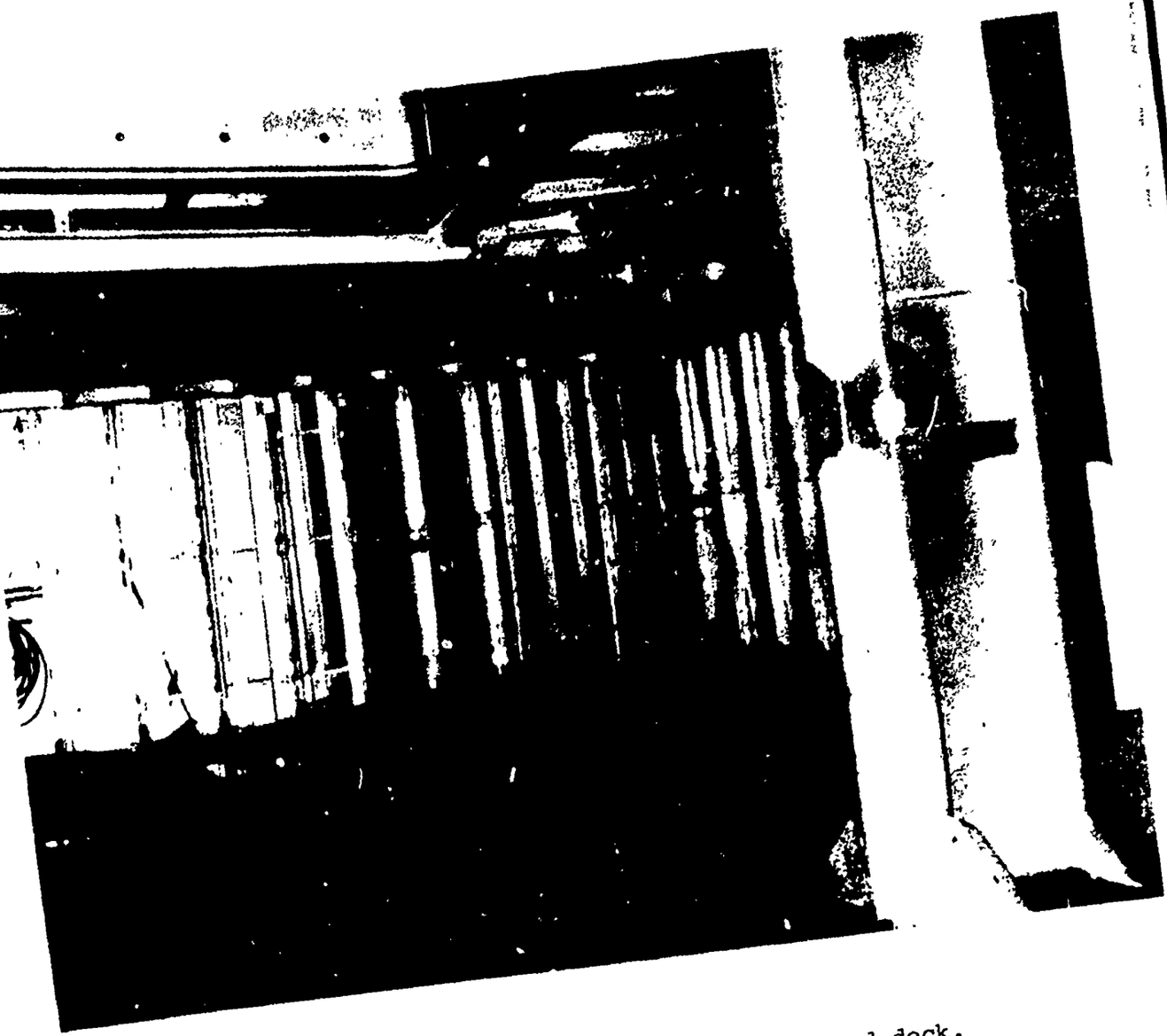

Fig. 5 Typical side structure at second deck.

(425)

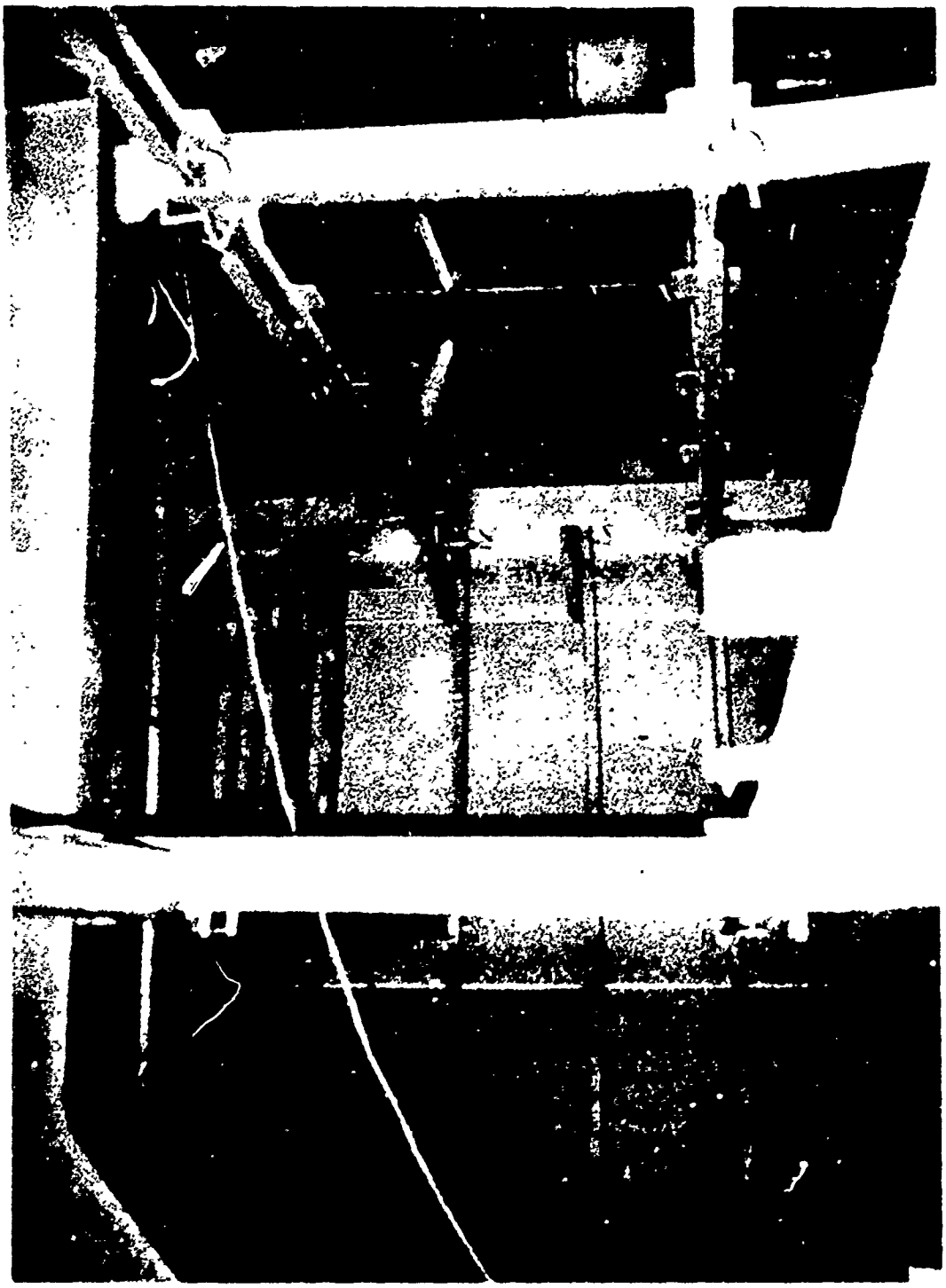

Fig. 6 Typical framing in hold (deep tank) of struck ship.

Fig. 7 Transverse framing, which prevented extension of damage along hull beyond shearing failure, at second deck.

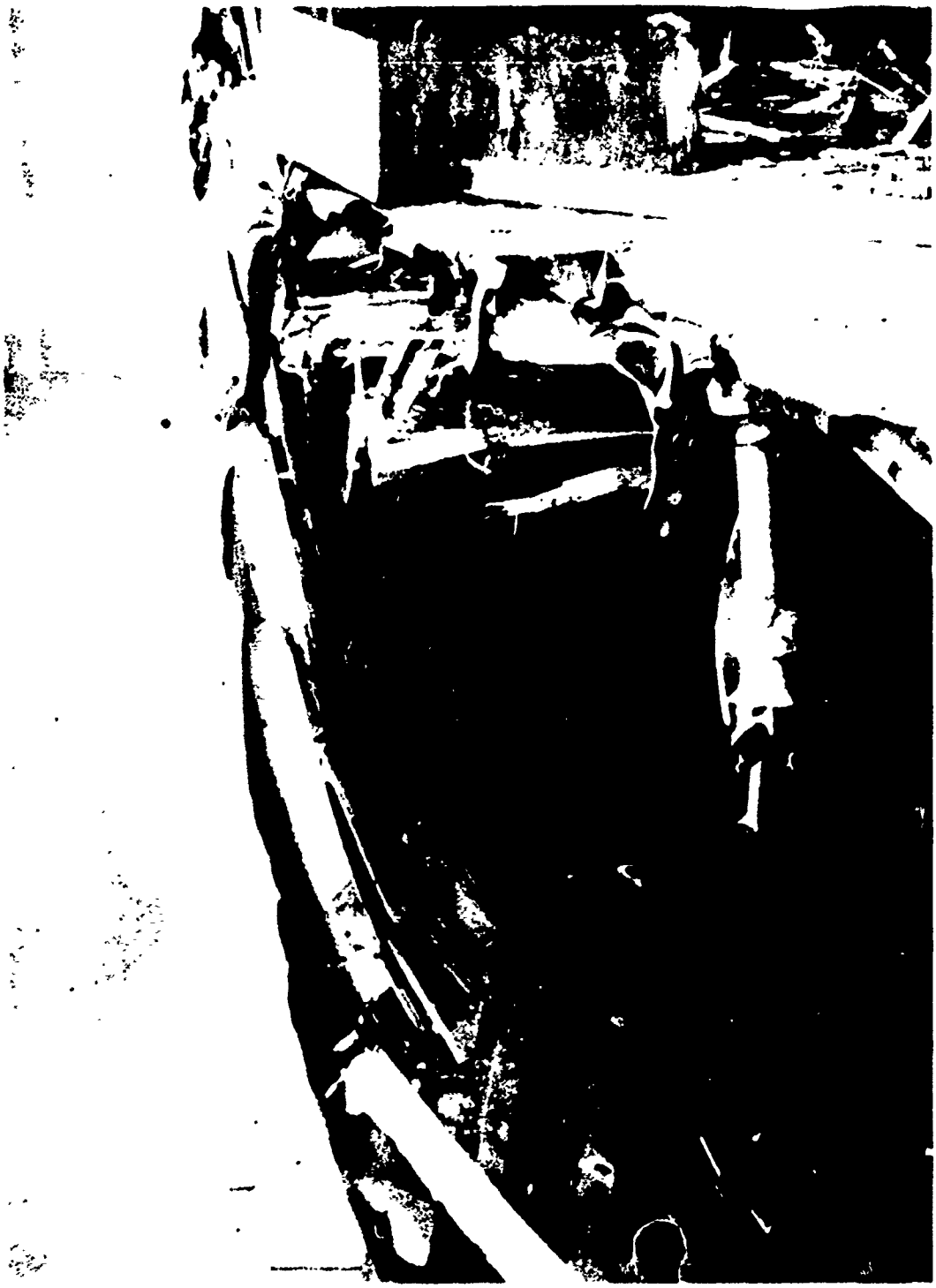

Fig. 8 Transverse framing, which prevented extension of damage along hull beyond shearing failure, at bottom of hull.

Fig. 9 Buckling of transverse framing
near edge of damaged area.

Fig. 10 Folded hull plates in advance of strike, looking aft.

Fig. 11 Damage in direction of strike. Note framing members torn loose from hull plate at the bottom.

Fig. 12 Bottom failure on starboard side of strike.

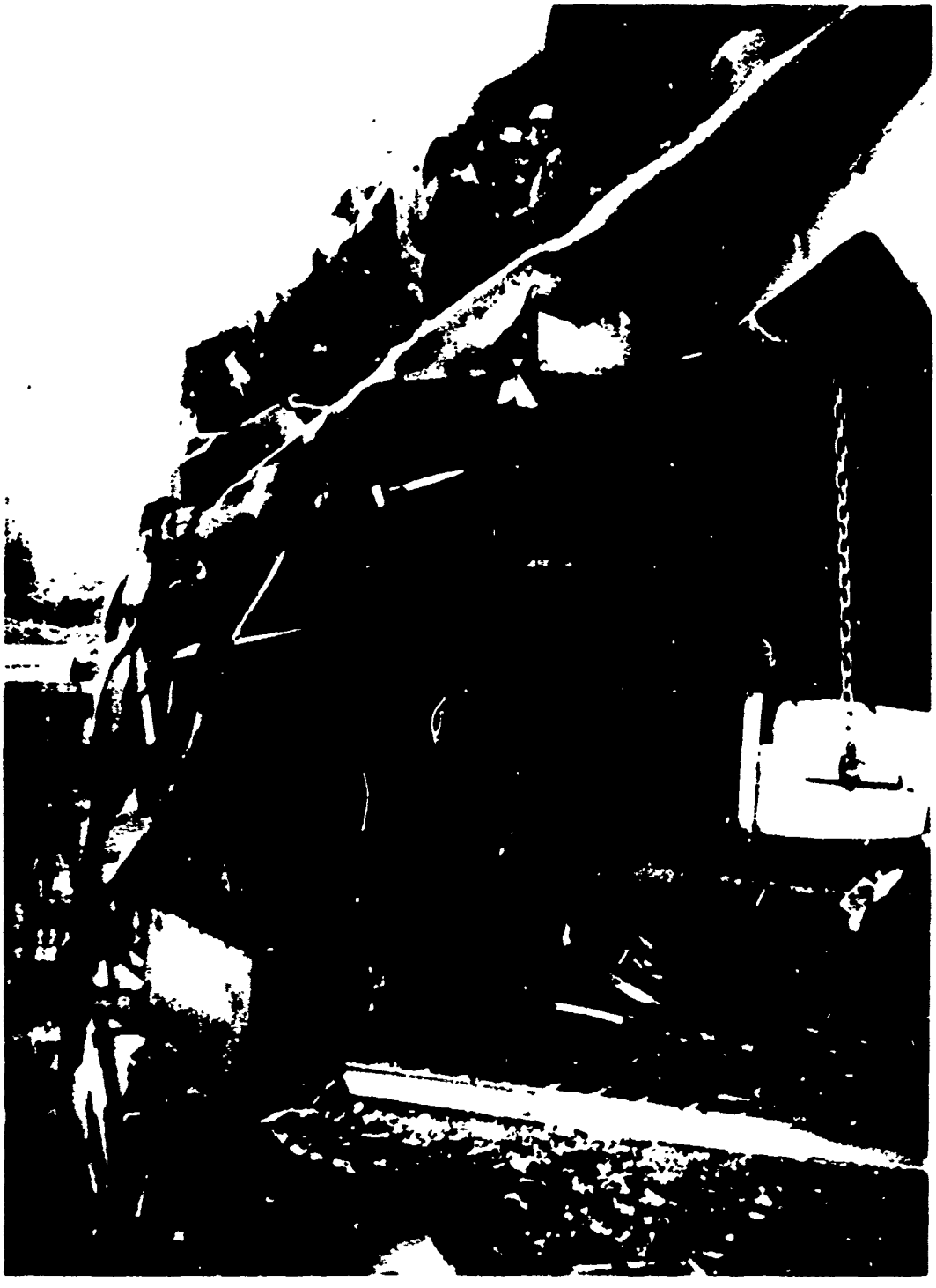

Fig. 13 Typical folding of deck plates.

14 Typical folding and crushing.

Fig. 15 Incursion viewed from edge of dry dock.

Fig. 16 View on second deck, looking outward from point of maximum incursion.

Fig. 17 Second deck sheared along a nearly straight line on the port side of the incursion.

Fig. 18 Material pushed back to a nearly straight plane at the starboard side of the incursion.

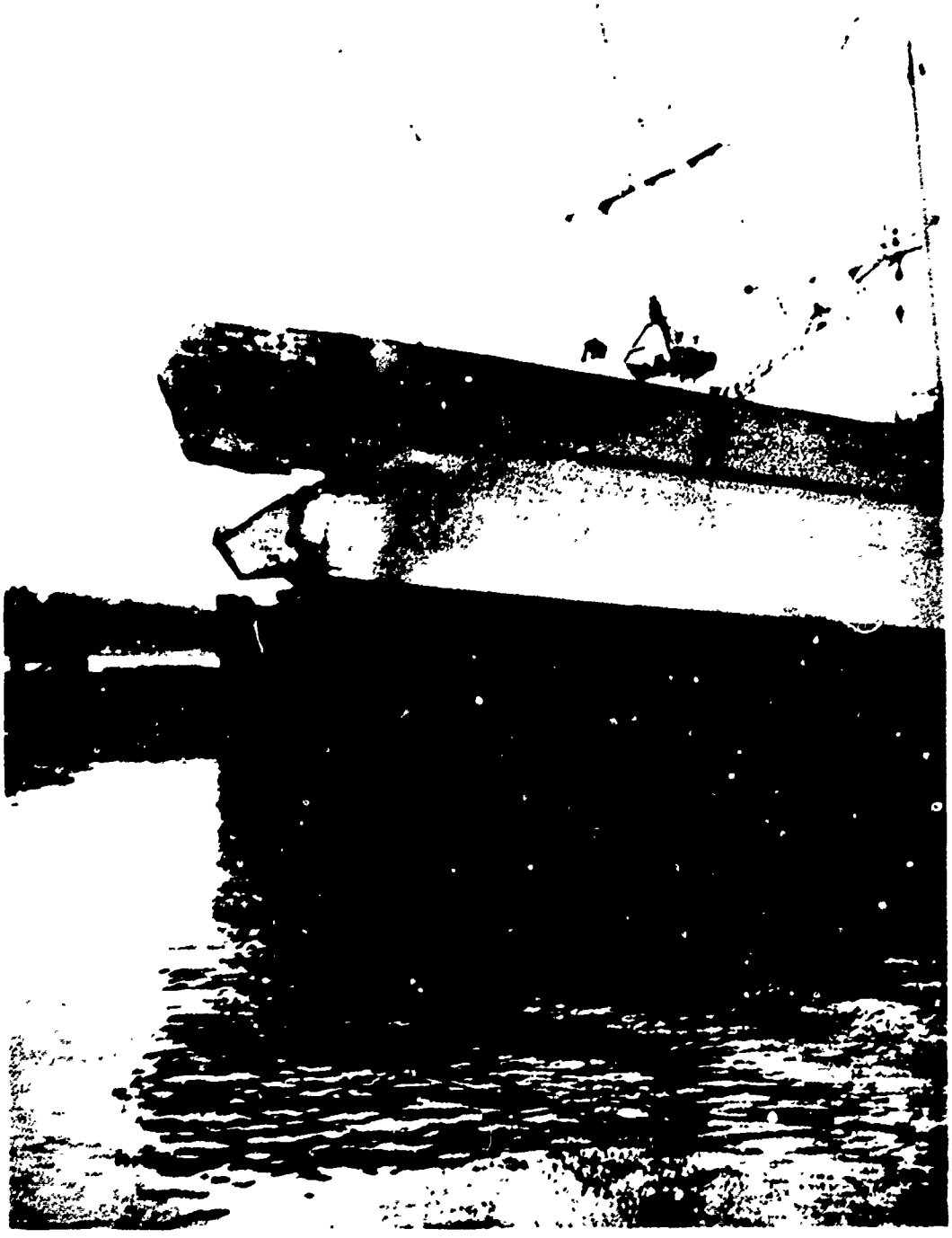

Fig. 19 Striking ship. Incursions into striking ship appear to match deck levels of struck ship.

Fig. 20 Bow of striking ship.

440

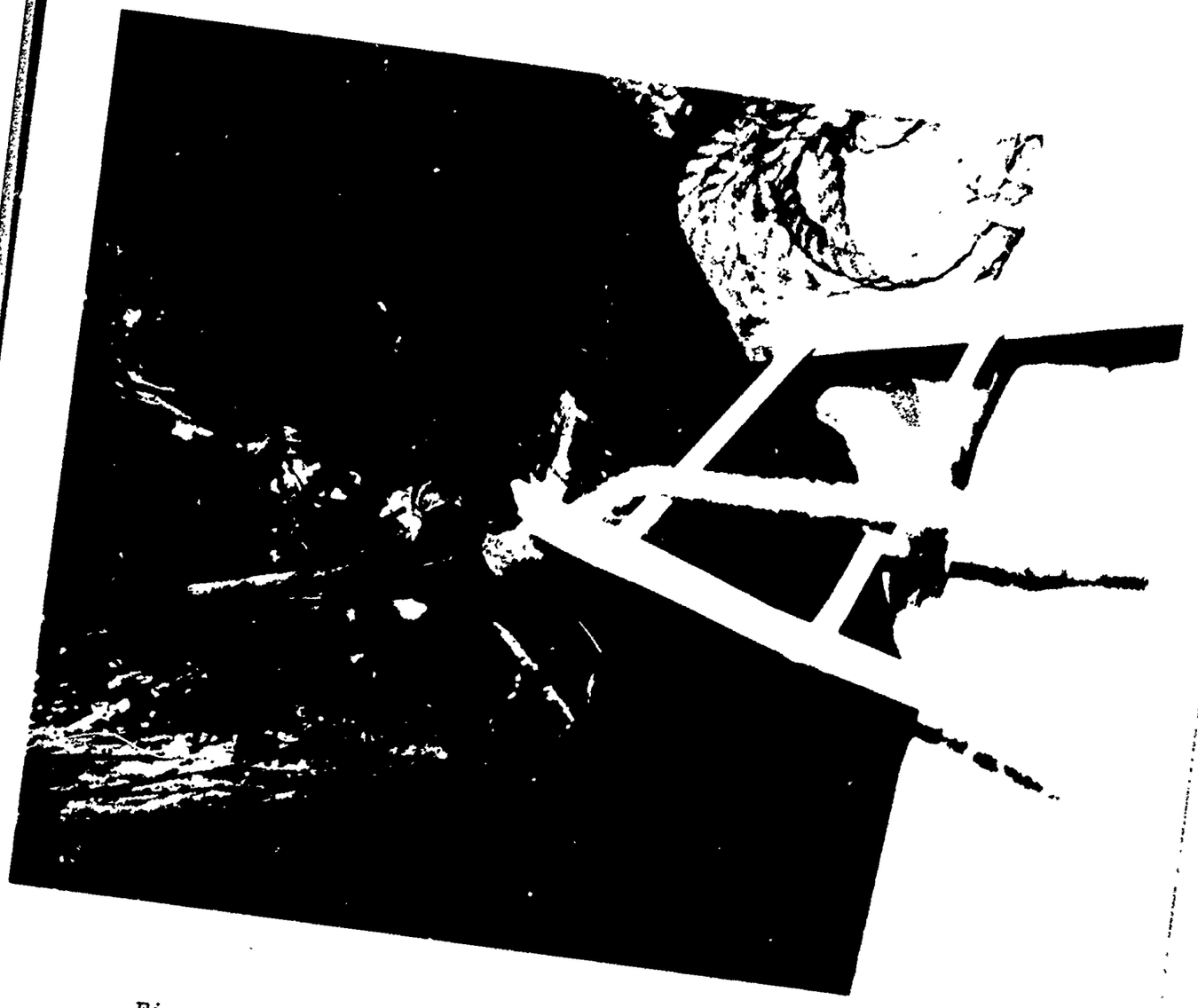

Fig. 21 Looking down on portion of bow of striking ship that was damaged by main deck of struck ship. Note plates are folded over.

Fig. 22 Hull plate tearing and stiffener tripping and buckling in bow of striking ship.

Fig. 23 Stiffener distortions aft of damaged bow in striking ship. At top, transverse frame is folded near its connection with the hull plate. In the lower half, the vertical leg of the longitudinal stiffener is buckled.

A-4. COLLISION INSPECTION REPORT FOR CASE 4

Longitudinally Stiffened Single-Hull Barge

Date of Collision: (Not known)

Date of Inspection: 10-24-72

Location of Inspection: du Pont Plant Terminal, Edgemore, Delaware

Inspection by: N. M. Maniar, M. Rosenblatt & Son, Inc.
R. G. Kline, U. S. Steel Corp.
J. F. McDermott, U. S. Steel Corp.

Ships Involved:

Striking ship - Tug boat (not identified)

Struck ship - Edge Moor 1, du Pont Corp. barge for transporting sulphuric acid out to sea for dumping; barge approximately 250 feet long by 20 feet deep.

Side construction of struck ship
- Longitudinally stiffened single hull.
- Unstiffened web frames at 7'-4" spacing.
- Longitudinal angle stiffeners 6" x 3-1/2" x 1/4" or 5/16", spaced at 24".
- Shear strake 5/8" thick (measured).
- Hull plate 1/2" thick (estimated).

Damage to struck ship
- 2-1/8" permanent-set circular-arc inward bowing of hull between a transverse bulkhead and an adjacent web frame; no apparent damage fore or aft of this area, Figures 1, 2, 3, and 4.
- No rupture of material, Figures 1 and 2.
- Slight permanent-set in-plane bending of a web frame, Figures 5, 6, 7, and 8.
- Local buckle in a diagonal transverse bracing strut, Figures 5 and 7.
- Local buckles in horizontal gusset plates connecting longitudinal stiffeners to transverse bulkhead, Figures 2 and 9.
- Vertical legs of longitudinal stiffeners depressed at gusset plates but slightly elevated near to the web frame, Figures 2, 3, and 9.

Discussion

Because the damage was slight, Figures 1 and 2, the collision was possibly a "glancing blow." However, the initial angle of collision is not known. Thus, the collision could have been a slow-moving oblique collision.

Although the theoretical plastic analyses for both right-angle and oblique collisions have, to date, assumed that the stiffened hull plate plastically distorts to a vee-shaped horizontal profile, the actual horizontal profiles of the distorted longitudinal stiffeners of the present barge were more nearly approximated by circular or parabolic curves, Figures 3 and 4. This was also observed in the damage resulting from another oblique (or glancing blow) collision.* This means that as the striking bow moves along the struck ship, it does not completely "straighten out" the distorted hull after it moves to another station. Instead, there is a superposition of the plastic bending that results from incursion of the striking bow at different stations along the struck hull, as shown in Figure 10.

As shown in Figure 4, the white paint flaked off the flanges (vertical legs) of the horizontal angle stiffeners mostly at the web frame and the middle portion of the span between web frames. This indicated that the flange yielded in compression at the web frame and in tension at midspan, as would be predicted for the bending phase (as opposed to the membrane-tension phase) of the structural deformation. Overall membrane-tension yielding of the stiffener flanges was not apparent, Figure 2. As shown in Attachment I, the plastic analysis—considering only a strike at midspan—predicts that flange buckling will occur at the web frame when the midspan lateral deflection is about 0.94 inch (for either a normal or oblique collision). A lateral deflection without flange buckling equal to 1.1 inches is computed by the moving-load bending analysis given in Figures 10 and 11 and Attachment II, in which it is assumed that the striking bow scrapes over three-fourths of the distance between the web frame and the transverse bulkhead. According to Attachment I, midspan rupture at the end of the membrane-tension phase can be expected when the deflection is about 8.2 inches for a normal collision or 5.8 inches for an oblique collision.

Because the collision history is not known, the realism of assuming a strike only at midspan cannot be evaluated. The calculations of Attachment I considering only a strike at midspan and the

---

* "Collision Inspection Report, Barge: BGE-102, With Longitudinally Stiffened Single Hull Plate," October 30, 1971.

745

calculations of Figures 10 and 11 and Attachment II considering a moving load both predict bending distortions less than occurred (i.e., roughly 1 inch compared with a measured permanent-set lateral deflection of 2-1/8 inches that occurred without flange buckling).

Although the side longitudinal stiffeners were continuous at the web frame, they terminated at the transverse bulkhead. Furthermore, the end connections of the stiffeners at the transverse bulkhead did not provide the idealized fixed-end-condition generally assumed in the plastic analysis. The horizontal gusset plates within the damaged area were all buckled downward allowing some end rotation in the horizontal plane, Figures 2 and 9. Therefore, the calculations in Attachment I do not consider that plastic bending will occur near the transverse bulkhead. Since the gusset plates allowed the ends of the angle stiffeners to rotate, angle-stiffener webs possibly acted as the spring systems of elastic foundations supporting the stiffener flanges, causing the flanges to assume an undulating elevation, Figure 2. However, in spite of this disturbance, there was no strong tendency for the angle stiffeners to trip when subjected to the distortions experienced during the collision.

Figure 1. Exterior view of damaged area.

Figure 2. Interior view of damaged area.

Figure 3. Inward bowing of longitudinal angle stiffener, 2-1/8 inches.

Figure 4. View of longitudinal stiffeners from below.

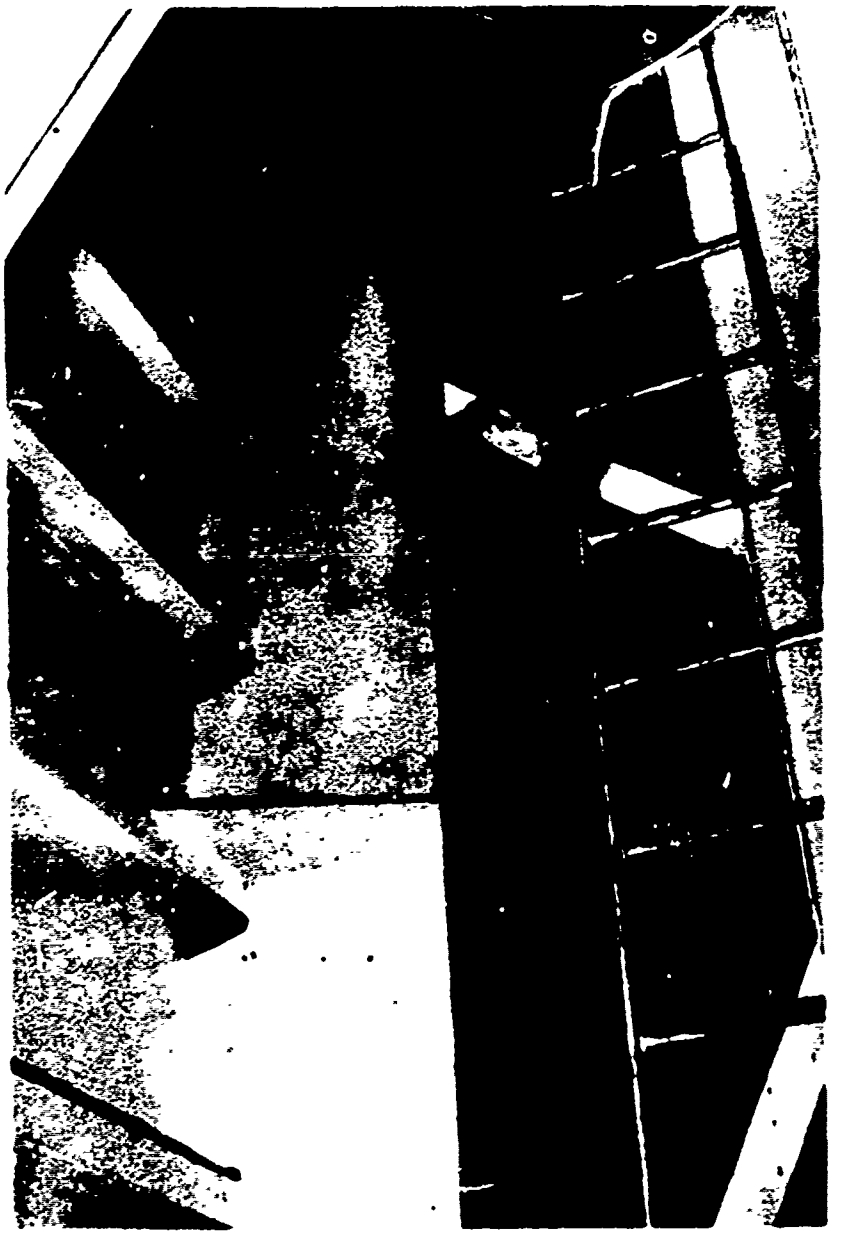

Figure 5. Upper portion of transverse web frame.

Figure 6. Lower portion of transverse web frame.

452

Figure 7. View looking up, showing permanent-set transverse deflection of flange of web frame.

Figure 8. Lateral deflection of flange of web frame.

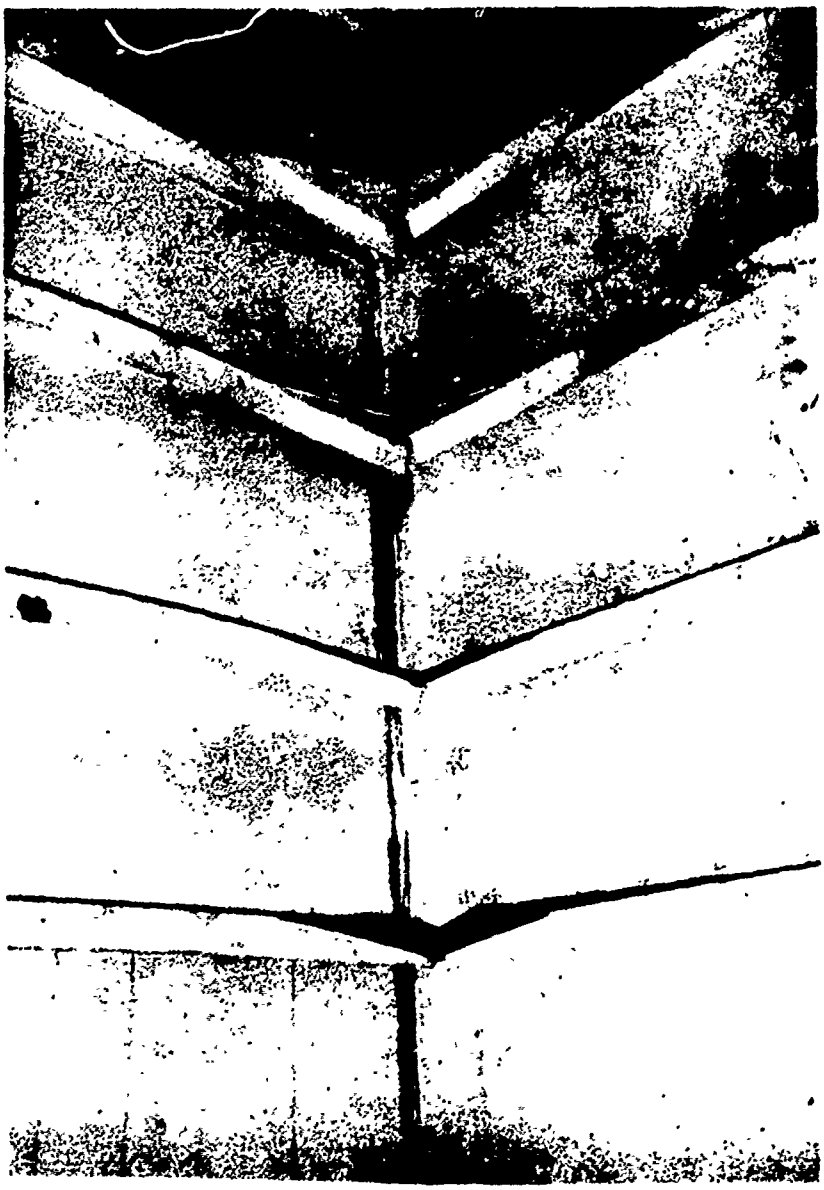

Figure 9. Buckling of gusset plates connecting longitudinal stiffeners to transverse bulkhead.

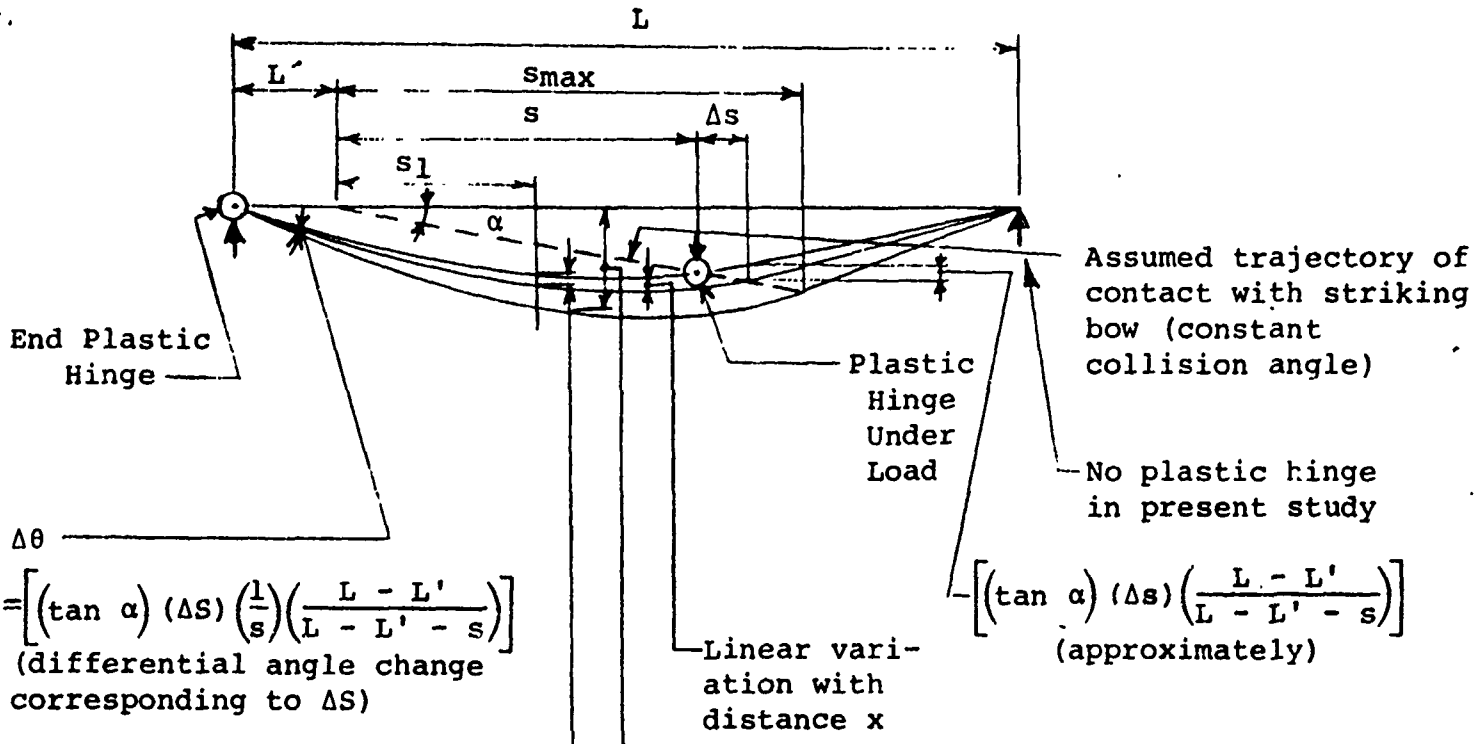

s_1	Value of Load P When It Is s_1 From End	Deflection at Position s_1 From End When L' = 0 and Load Is at Position s_{max} = 0.75L From End*
0.125L	17.14 M_p/L	0.506 L tan α
0.250L	9.33 M_p/L	0.799 L tan α
0.375L	6.93 M_p/L	0.979 L tan α
0.500L	6.00 M_p/L	1.049 L tan α
0.625L	5.87 M_p/L	0.992 L tan α
0.750L	6.67 M_p/L	0.750 L tan α

* The solution is not defined for $s_1 = 0$. Also, the structure is not bending plastically when s_1 is near zero.

FIGURE 10 - CURVED DEFLECTION PRODUCED IN STRUCK HULL BEHIND A STRIKING LOAD MOVING LONGITUDINALLY

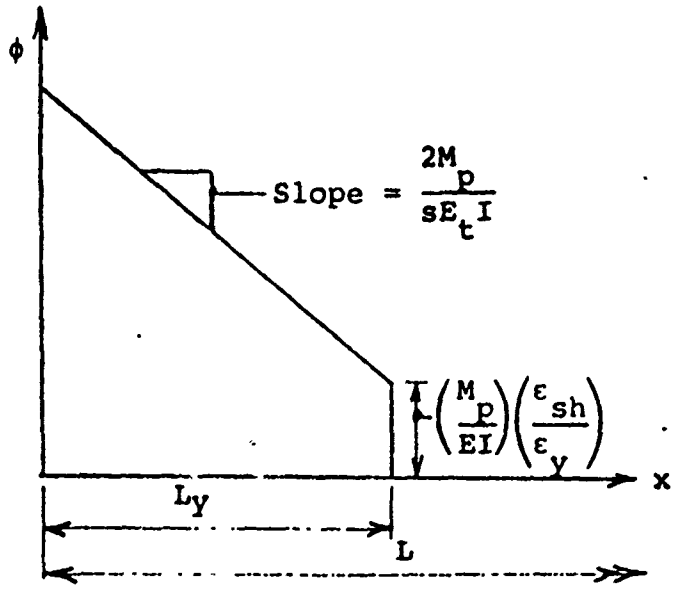

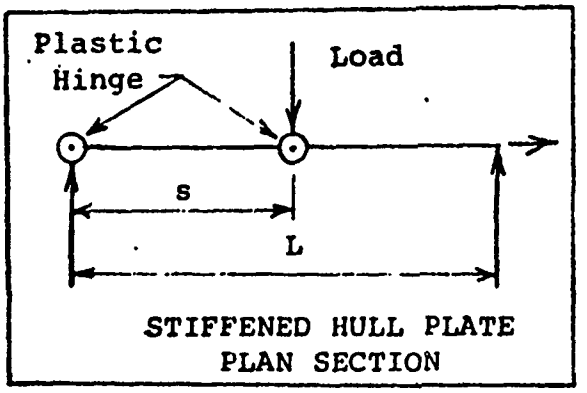

CURVATURE WITHIN END PLASTIC HINGE FOR LOAD AT ONLY ONE STATION

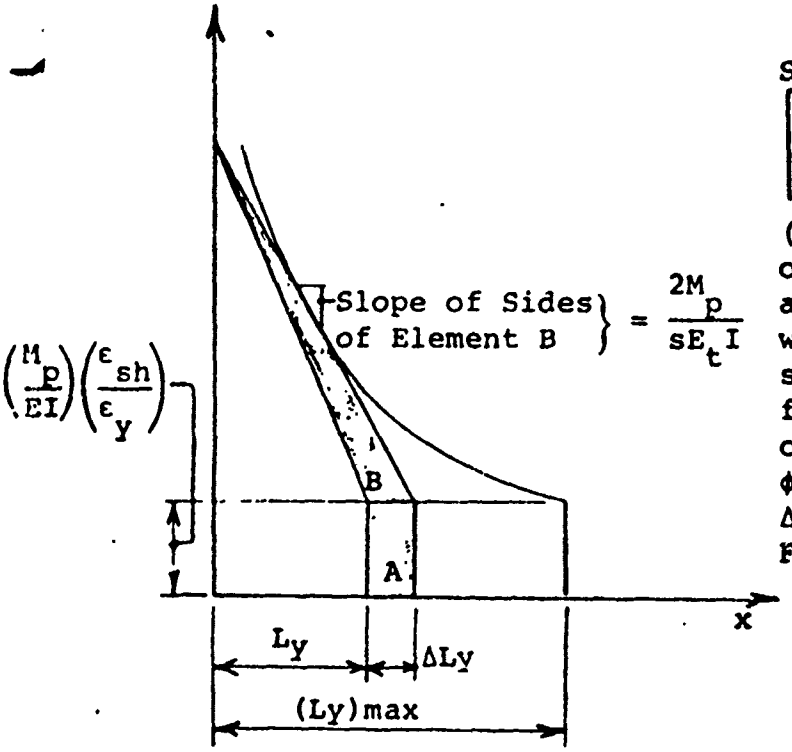

Shaded Area (A + B) = $\Delta\theta$ =

$$\left[\left(\frac{M_p}{E_tI}\right)\left(\frac{L_y}{s}\right) + \left(\frac{M_p}{EI}\right)\left(\frac{\epsilon_{sh}}{\epsilon_y}\right)\right]\Delta L_y$$

(The slope of the ϕ - x curve depends on the rate of change of L_y with s and would be a straight line if L_y were directly proportional to s. The shaded-area elements overestimate $\Delta\theta$ for a concave ϕ - x curve, as shown, or underestimate $\Delta\theta$ for a convex ϕ - x curve.) Setting this value of $\Delta\theta$ equal to the expression for $\Delta\theta$ in Figure 10 gives

$$\frac{\Delta L_y}{\Delta s} = \frac{\left(\tan\alpha\right)\left(\frac{1}{s}\right)\left(\frac{I - L'}{L - L' - s}\right)}{\left(\frac{M_p}{E_tI}\right)\left(\frac{L_y}{s}\right) + \left(\frac{M_p}{EI}\right)\left(\frac{\epsilon_{sh}}{\epsilon_y}\right)}$$

CURVATURE WITHIN END PLASTIC HINGE RESULTING FROM LOAD MOVING ACROSS SPAN

FIGURE 11 - ANGLE CHANGE WITHIN END PLASTIC HINGE RELATED TO STRUCTURAL PROPERTIES

ATTACHMENT I

BENDING ANALYSIS FOR STRIKE ONLY AT MIDSPAN

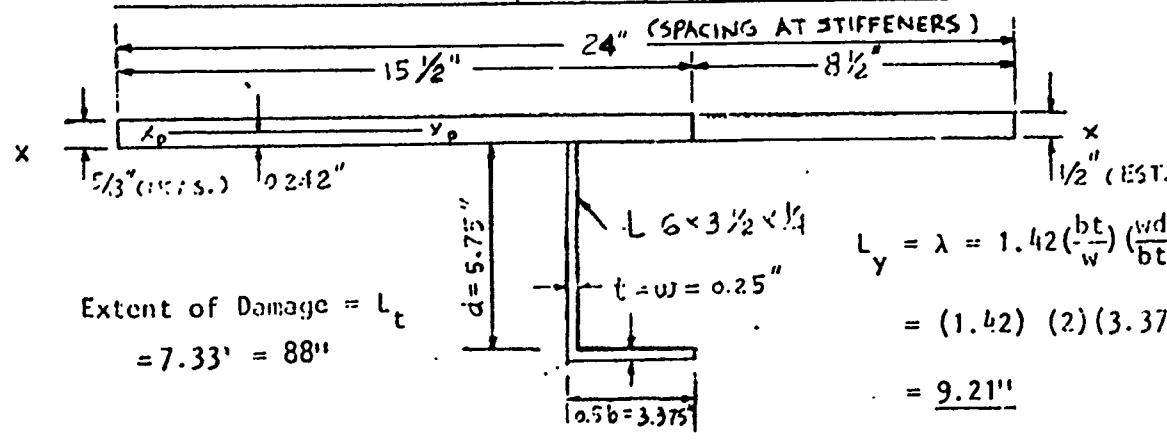

Extent of Damage = L_t

$= 7.33' = 88"$

$$L_y = \lambda = 1.42\left(\frac{bt}{w}\right)\left(\frac{wd}{bt}\right)^{\frac{1}{2}}$$

$$= (1.42)\ (2)(3.375)\left[\frac{5.75}{(2)(3.375)}\right]^{\frac{1}{2}}$$

$$= \underline{9.21"}$$

Properties about X-X Axis

Part	A	d	Ad	I
5/8" ℄	9.69	+0.312	+3.02	1.26
1/2" ℄	4.25	+0.250	+1.06	0.35
Angle	2.31	-4.01	-9.26	37.15
				8.86
Total	16.25	-0.319	-5.18	47.62

$(-0.319) \times (5.18) = -1.65$

$$I_{x_g - x_g} = \underline{45.97\ in^4}$$

Properties about X_p Axis

Part	A	d	Ad
Outer Part of 5/8" ℄	5.94	+0.191	1.135
Outer Part of 1/2" ℄	2.19	+0.129	0.282
Inner Part of ℄ s	5.81	-0.121	0.703
Angle	2.31	-4.252	9.822
Total	16.25		11.942

$$M_p = |Ad|\sigma_y = (11.942)(35) = \underline{418\ K\text{-}in}$$

$$\frac{VL_y}{M_p} = \frac{VL_y}{VL_t/4} = \frac{9.21}{22} = \underline{0.419}, \quad \frac{VL_y}{VL_y + M_p} = \frac{9.21}{31.21} = \underline{0.295}, \quad \frac{52.2t}{0.5b\sqrt{\sigma_y}} = \frac{(52.2)(0.25)}{3.375\sqrt{35}} = \underline{0.654}$$

$$A = \left(\frac{VL_y}{VL_y + M_p}\right)\left(\frac{52.2t}{0.5b\sqrt{\sigma_y}}\right) = (0.295)(0.654) = \underline{0.1929}$$

$$B = \left(\frac{VL_y}{M_p}\right)\left(\frac{52.2t}{0.5b\sqrt{\sigma_y}}\right) = (0.419)(0.654) = \underline{0.274}$$

$$k = A\left\{\left(\frac{\varepsilon_{sh}}{\sigma_y/E}\right) + B\left(\frac{E}{2E_t}\right)\right\} = 0.1919\left[11.6 + (0.274)(16.1)\right] = \underline{3.09}$$

$$\theta_p = k\left(\frac{M_p}{EI}\right)\left(\frac{L_t}{4}\right) = 3.09\left[\frac{418}{(29{,}000)(45.97)}\right](22) = \underline{0.0213\ \text{radians}}$$

Midspan deflection at occurrence of flange buckling at web frame =

$$\delta_{bc} = \frac{\theta_p L_t}{2} = (0.0213)(44) = \underline{0.937\ \text{inch}}$$

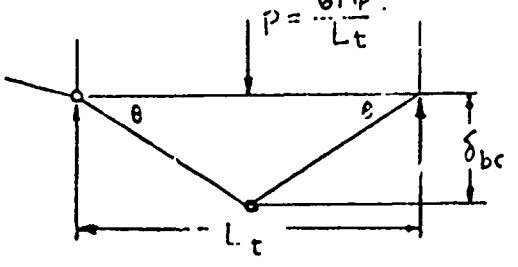

Shear in stiffener near web frame =

$$V = \frac{6M_p}{L_t} - \frac{M_p}{0.5L_t} = \frac{4M_p}{L_t},$$

$$\text{or } M_p = VL_t/4$$

Membrane Tension Analysis for Strike only at Midspan

$$\epsilon_r = \frac{\delta_y}{E_t}\left[\left(\frac{\sigma_u}{\sigma_y} - 1\right) - \left(\frac{VL_y}{M_p}\right)\right] = (0.0389)\left[0.857 - 0.419\right] = \underline{0.0170 \text{ in/in}}$$

On the basis of a right-angle collision (membrane tension yielding on both sides of the strike), midspan deflection at occurrence of flange rupture =

$$\delta_{tc} = \sqrt{\frac{L_t^2}{2}(\epsilon_r) + \delta_{bc}^2} = \sqrt{\frac{(88)^2}{2}(0.0170) + (0.937)^2} = \underline{8.17 \text{ inches}}$$

On the basis of an oblique collision (membrane tension yielding on only one side of the strike), midspan deflection at occurrence of flange rupture =

$$\delta_{tc} = \sqrt{\frac{L_t^2}{4}(\epsilon_r) + \delta_{bc}^2} = \sqrt{\frac{(88)^2}{4}(0.0170) + (0.937)^2} = \underline{5.81 \text{ inches}}$$

Attachment II

MOVING LOAD BENDING ANALYSIS BASED ON PLASTIC ACTION OCCURRING ONLY WHEN THE STRIKING BOW IS CONTACTING THREE-FOURTHS OF THE SPAN STARTING NEAR THE WEB FRAME

On basis of midspan lateral deflection = 1.1 inch, the expression in Figure 10 gives

$$\tan \alpha = \frac{1.1}{1.049L} = \frac{1.1}{(1.049)(88)} = \underline{0.0119}$$

$$\alpha = \underline{0° - 41'}$$

$$(\tan \alpha)\left(\frac{1}{s}\right)\left(\frac{L - L'}{L - L' - s}\right) = (0.0130)\left(\frac{1}{s}\right)\left(\frac{L}{L - s}\right)$$

$$\left(\frac{M_p}{E_t I}\right)\left(\frac{L_y}{s}\right) + \left(\frac{M_p}{EI}\right)\left(\frac{\varepsilon_{sh}}{\varepsilon_y}\right) = \left[\frac{418}{(900)(45.97)}\right]\left(\frac{L_y}{s}\right) + \left[\frac{418}{(29,000)(45.97)}\right] \quad (11.6)$$

$$= 0.0101\left(\frac{L_y}{s}\right) + 0.00364$$

Assume L_y is the critical value, 9.21 inches (see Attachment I), when $s = s_{max} = 0.75L = 66$ inches.

Then, changes in L_y, proceeding backward from s = 0.75L to s = 0.125L, are computed using (see Figure 11)

$$\Delta L_y = \frac{(\tan \alpha)\left(\frac{1}{s}\right)\left(\frac{L}{L - s}\right)\Delta s}{\left(\frac{M_p}{E_t I}\right)\left(\frac{L_y}{s}\right) + \left(\frac{M_p}{EI}\right)\left(\frac{\varepsilon_{sh}}{\varepsilon_y}\right)} = \left[\frac{0.0119\left(\frac{1}{s}\right)\left(\frac{L}{L - s}\right)}{0.0101\left(\frac{L_y}{s}\right) + 0.00364}\right]\Delta s$$

s, inches	L_y, inches	Δs, inches	ΔL_y, inches, Based on Greater Values of s and L_y
66.0	9.21	11.0	1.57
55.0	7.64	11.0	1.26
44.0	6.38	11.0	1.17
33.0	5.21	11.0	1.21
22.0	4.00	11.0	1.45
11.0	2.55	11.0	2.27

Reasonable Check

.us, the critical value L_y = 9.21 inches would be expected to be attained, with subsequent flange buckling, with a midspan deflection = 1.1 inches. Because the variation of L_y with s is not greatly different from linear, the overestimation of elements $\Delta\theta$, Figure 11, is not significant.

A-5. COLLISION INSPECTION REPORT FOR CASE 5

Longitudinally Framed Double-Hull Barge

(Note: the inspection described below was conducted by permission of the ship's owners under the condition that the information obtained be kept for use solely by the United States Coast Guard.)

Date of Collision:	5-25-73
Date of Inspection:	5-30-73
Inspected by:	James Dwyer, U. S. Coast Guard John C. Daidola, M. Rosenblatt & Son, Inc. John F. McDermott, U. S. Steel Corp.
Ship Involved:	FT-4 - Longitudinally framed double-hull barge
Type:	Chemical Cargo Barge
Built:	Dravo Corp. (Neville Island, Pennsylvania, 1968)
Owner:	Frank Thomas
Leased to:	Dow Chemical Corp.
Length:	195 feet LOA
Beam:	35 feet
Depth:	12.5 feet
Displacement:	800 tons
Cargo:	3 Cargo Holds for Chemicals
Striking Object:	Pier of Bridge over Mississippi River at Vicksburg, Mississippi
Location of Ship:	Port Allen Marine Service Port Allen, Louisiana
Local Coast Guard Office:	Marine Inspection Office Baton Rouge, Louisiana

Summary:

The subject collision consisted of a barge hitting and scraping along a bridge pier. At the time of the collision, the barge was part of a larger tow, and it appears that the tow had lateral as well as forward motion relative to the bridge pier. From the damage, it appears that the collision angle, measured between the trajectory of the incursion and the original position of the side of the barge, was between 10 and 20 degrees, Figure 1. Aft of the location of maximum incursion, the angle between the damaged side and the original position of the side of the barge was between 30 and 45 degrees. (The captain of the tow boat involved in the accident was not available for comment.)

Thus, the collision was representative of a rather "flat" oblique collision in which a very stiff bow (the pier) "struck" a longitudinally framed double-hull tank ship (the barge). The oblique incursion progressed in practically a straight path, Figure 1. (This is assumed in the theoretical plastic analysis.) Near the beginning of the incursion, the inner hull distorted parallel to the outer hull, indicating that for moderate distortions the truss web frames, Figure 2, satisfactorily caused the inner and outer hulls to act in unison. However, after roughly the mid-distance of the incursion, the web frames collapsed and the outer hull approached very close to the inner hull, Figures 3, 4, 5, and 6. This indicated that for the larger hull distortions the

web frames were not strong enough to cause the inner and outer hulls to act in unison. (Energy absorption will generally be maximized when both hulls distort in unison.) The vertically corrugated transverse bulkhead just aft of the location of maximum incursion, Figure 3, exhibited no significant distortion.

As seen in Figure 7, there were no gross ruptures of the outer hull, except for longitudinal ruptures along the bilge; some short ruptures occurred in the outer hull at the locations of welded connections to web frames, and some ruptures occurred at the junction with the deck, Figure 1. The short ruptures in the weld zones may have indicated that the ductility of the outer hull was almost exhausted at the location of maximum incursion.

There were short ruptures of the inner hull at the location of maximum incursion at the bottom and top of the tank. As a result, the tanks on either side of the transverse bulkhead near there were flooded shortly after the accident. It is probable that these ruptures would not have occurred for a lesser incursion.

There was a very pronounced overall horizontal bending of the barge that was much greater than just an elastic overall bending. (Only elastic bending is assumed in the theoretical plastic analysis.) This was obvious from the top views of the barge, Figures 8 and 9. Furthermore, deep transverse buckles were exhibited in both the deck, Figures 10 and 11, and the bottom, Figure 12. Since the bottom transverse buckles tapered out only

4/6

at the leeward inner hull (opposite to the struck side), it appeared that the neutral vertical plane for the horizontal bending was very close to the leeward inner hull.

On the struck side the bilge, the bottom in the vicinity of the bilge, and the deck developed extensive folding with longitudinal fold lines, Figures 1, 13, and 14. Transverse ruptures, apparently from membrane tension, were exhibited in a few locations in the bilge and the bottom in the vicinity of the bilge, Figures 13 and 14. Because of the ruptures, it appears that most of the energy absorbed in such distortions of the deck or bottom may be from membrane-tension straining, which can be evaluated by considering the stretching of longitudinal elements of the ship structure extending from the location of maximum incursion to the limits of gross distortions in the deck or bottom.

Struck side looking forward, showing a practically straight-line incursion trajectory along the outer hull. The principal damage extended from a location about 20 feet from the bow to a location about 70 feet from the bow.

Figure 1

Typical truss web frame, located two web frame spaces aft of the location of maximum incursion.

Figure 2

(46)

Inside hull plate in damaged area. The crease showing in the right foreground apparently occurred at a web bulkhead, and divided the two areas of damage exhibited in the inner hull plate. Forward (to the right) of the crease the deflected inner hull was roughly parallel to the outer hull, with web frames slightly distorted. Aft (to the left) of the crease the web frames were collapsed and the inner hull was close to the outer hull. Note that no rupture of the inner hull appears in the photograph, even at the location of maximum incursion, and the vertically corrugated transverse bulkhead, in the background, was not significantly distorted.

Figure 3

(467)

Collapsed truss web frame, within area where the inner hull was close to the outer hull.

Figure 4

4(5

View through top portion of truss web frame looking forward between outer hull (on left) and inner hull (on right) to the location of maximum incursion near the collapsed web frame.

Figure 5

View through bottom portion of truss web frame looking forward between outer hull (on left) and inner hull (on right) to the location of maximum incursion near the collapsed web frame.

Figure 6

Struck side at the location of maximum incursion, showing outer hull rupturing to be limited to longitudinal tearing along the bilge, tearing at the deck, and short ruptures at the locations of welded connections to web frames.

Figure 7

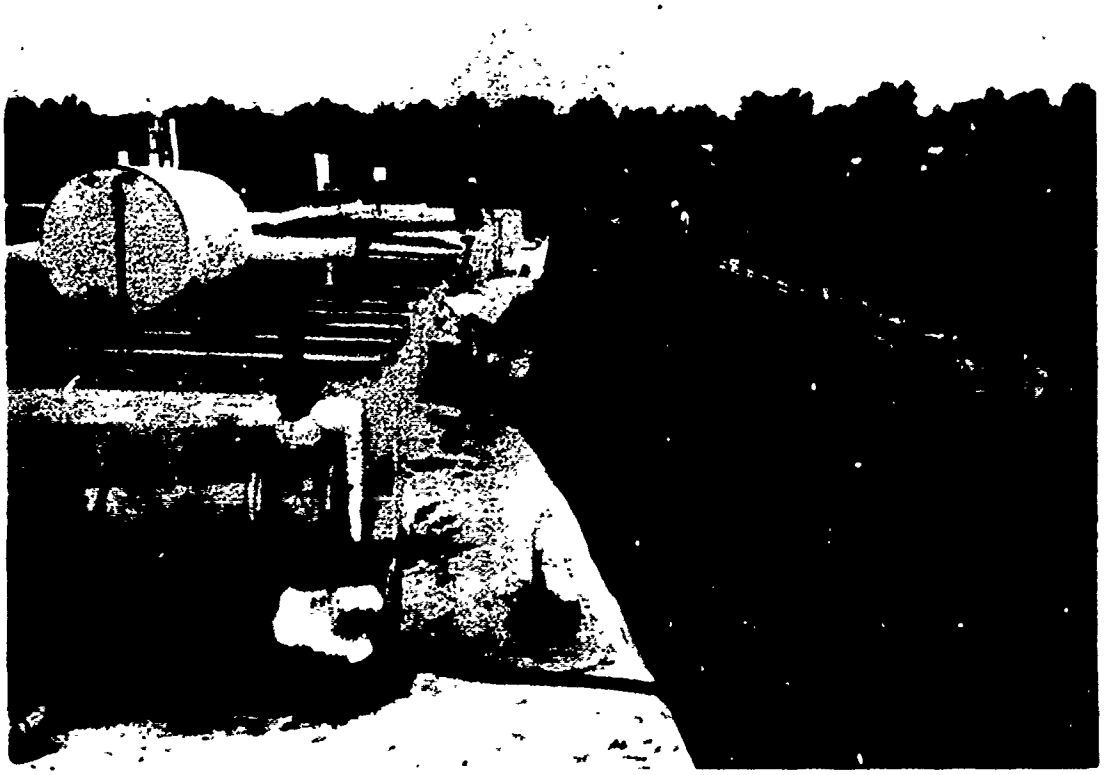

Fdge of deck on struck side, looking aft and showing buckling and other "compression" effects of horizontal bowing of the barge.

Figure 8

Edge of deck on leeward side, looking aft and showing permanent-set "tension" effects of horizontal bowing of the barge.

Figure 9

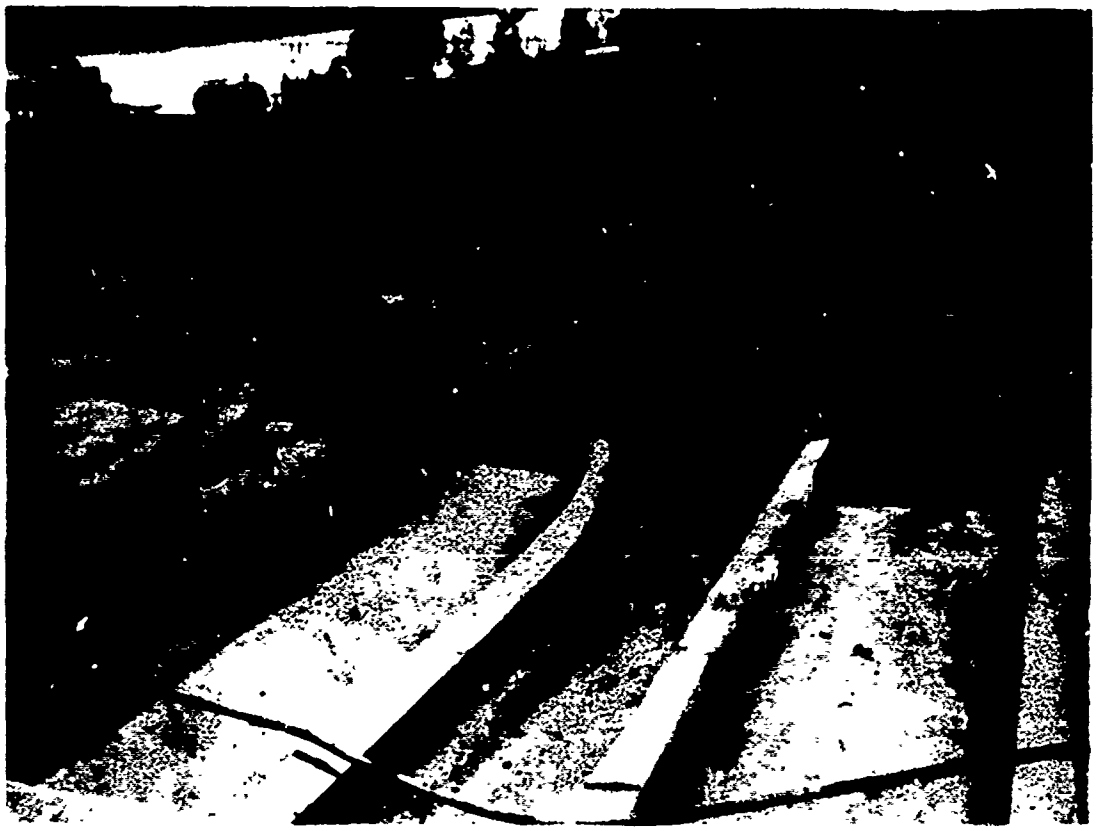

Buckled deck, looking toward struck side.

Figure 10

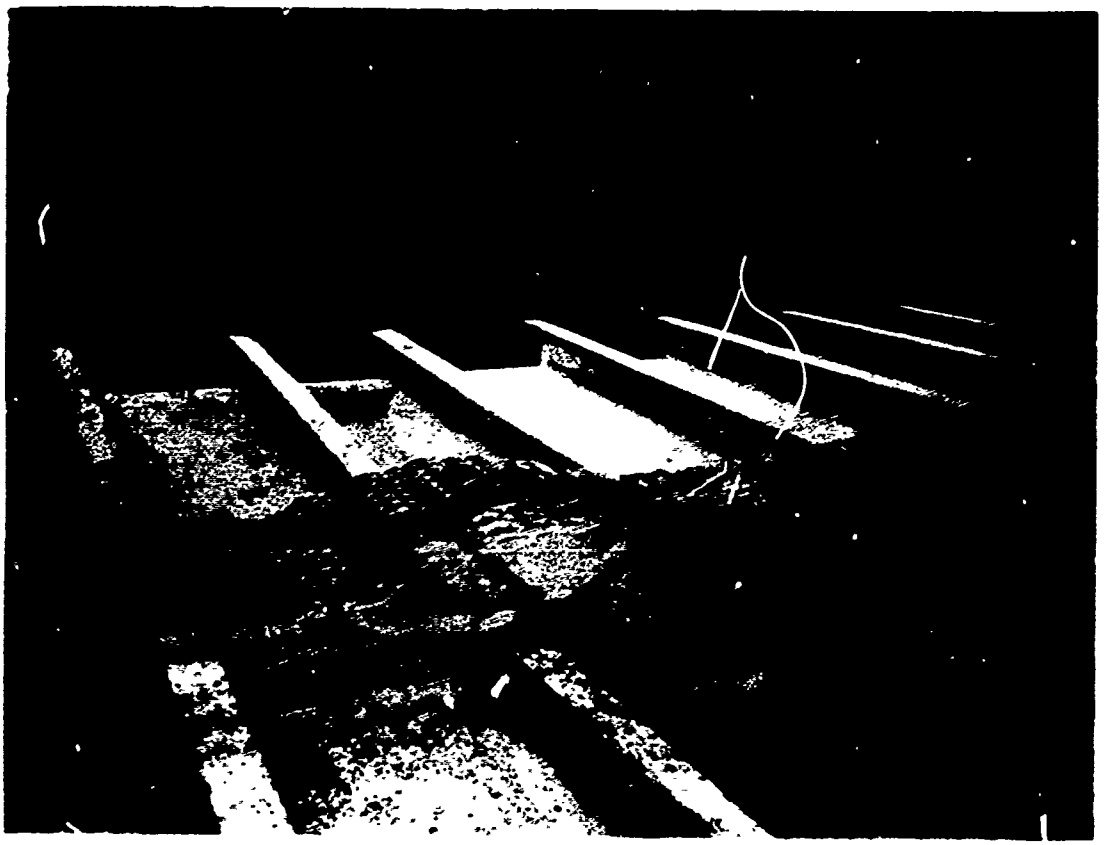

Buckled deck, looking toward leeward side. Buckles extend all the way to the leeward edge shown in the photograph.

Figure 11

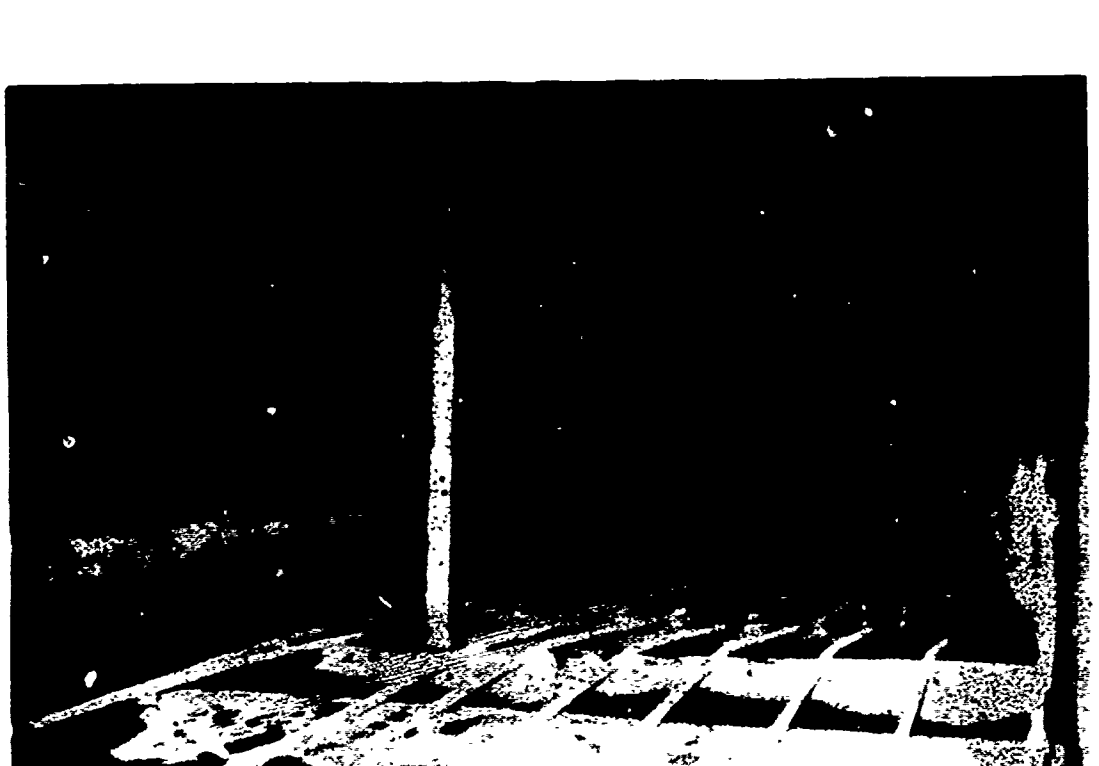

Transverse bottom buckles extend over to the leeward inner hull, tapering out at that location. The inward distortion of the inner hull appears at the right.

Figure 12

Bottom and bilge damage, including extensive folding with longitudinal fold lines, a transverse tear, and a 1-1/2-foot-deep downward transverse buckle (shown in the upper right).

Figure 13

Bottom and bilge damage, including extensive folding with longitudinal fold lines, transverse tears, and a 1-1/2-foot-deep downward transverse buckle (shown in the left).

Figure 14

475

A-6. COLLISION INSPECTION REPORT FOR CASE 6

Transversely Framed Containership and Longitudinally Framed Tanker

(Note: The inspection described below was conducted by permission of the ship's owners under the condition that the information obtained be kept for use solely by the United States Coast Guard.)

Date of Collision: 6/2/73

Date of Inspection: 6/28/73

Inspection by: John C. Daidola, M. Rosenblatt & Son, Inc.
James Dwyer, U. S. Coast Guard
John F. McDermott, U. S. Steel Corporation

Ships Involved:

C. V. Sea Witch - Containership with transversely framed bow (striking vessel)

Esso Brussels - Longitudinally framed oil tanker (struck vessel)

	C. V. Sea Witch	Esso Brussels
Type:	Containership (with bulb—4-1/2 ft. protrusion forward of FP)	Tanker
Built:	Bath Iron Works, Maine (1968)	Kockuns Mekaniska Verkstad A-B, Sweden (1960)
Owner:	American Export Lines	Esso Maine (Belgium) S. A.
Length:	594.2 ft. LBP	677.4 ft. LBP
Beam:	78.2 ft.	97.3 ft.
Depth:	49. 5 ft.	49.2 ft.
Draft:	31.6 ft. (full load)	38.0 ft. (full load)
Displacement:	26,670 long tons	
Deadweight:		47,220 long tons
No. of Screws/Power:	1/17,500 SHP	1/16,500 SHP
Cargo:	Containers	Petroleum, crude
Classification:	A.B.S.	A.B.S.

Location of Ships:

C. V. Sea Witch - Anchored south of Verrazano Narrows Bridge
New York, New York

Esso Brussels - Bethlehem Steel Shipyard
Hoboken, New Jersey
(ship dry docked)

Local Coast Guard Office:

Marine Inspection Office
New York, New York

Summary

The subject collision consisted of a containership with a transversely framed bow striking a longitudinally framed oil tanker. The containership was traveling at a significant speed and struck the side of the tanker near midships, while the tanker lay at anchor. The collision angle, measured between the longitudinal centerlines of the ships, is estimated to have been about 60 degrees.

Esso Brussels (Struck Ship)

The collision was considered "severe" since both the outer hull, Figure 1, and the longitudinal bulkhead, Figure 2, of the struck ship ruptured and distorted excessively. The strike occurred in the vicinity of a transverse bulkhead, Figure 3. As a result, the failure of the outer hull exhibited less membrane stretching than it probably would have had the strike occurred further from the transverse bulkhead. The stiffened hull plate ahead of the strike was crumpled into a folded configuration, Figure 4, but the hull plate

and longitudinal stiffeners behind the strike (and near the transverse bulkhead) ruptured without much apparent distortion, Figure 3.

The transverse "oiltight" bulkhead near the strike was ruptured and considerably distorted, Figure 5, probably because the striking ship proceeded through the bulkhead during the oblique collision. The web frame just behind the strike was relatively undamaged, Figure 6. However, web frames ahead of the strike buckled and ripped away from the outer hull and, to some extent, the longitudinal bulkhead, particularly the web frames flanking the longitudinal-bulkhead rupture, Figure 7.

The failure of the longitudinal bulkhead exhibited more bending and stretching than the failure of the outer hull, Figures 2, 7, and 8. This behavior of the longitudinal bulkhead could possibly be explained by the fact that the outer hull ruptured early (due to the proximity of the transverse bulkhead) while the longitudinal bulkhead (because of the strike location) was able to stretch considerably before rupturing.

The damage extended vertically from about the 10-foot draft mark, Figure 9, to the deck, Figure 10, but the deck exhibited only a folding type of failure and not a lifted configuration, Figure 11.

C. V. Sea Witch (Striking Ship)

The horizontally extending slit in the bow of the striking ship, Figures 12, 13, and 14, apparently was at the elevation of the

deck of the struck ship during the collision. Consequently, the top portion of the bow of the striking ship was damaged relatively little. F tween the horizontal slit and the water line, the striking bow was extensively crushed. However, considering the damage to the struck ship, it is doubtful that the crushing extended much further down. The damage of the striking ship below the water lines was inaccessible for inspection.

Figure 1. Overall view of struck ship, looking aft.

Figure 2. Ruptured longitudinal bulkhead of struck ship.

Figure 3. Brittle failure of outer hull at transverse bulkhead.

Figure 4. Outer hull folded ahead of the strike.

Figure 5. Failed transverse bulkhead.

Figure 6. Web frame only slightly damaged near failed transverse bulkhead.

4188

Figure 7. Details of failures of longitudinal bulkhead and web frames.

459

Figure 8. Details of failures of longitudinal bulkhead and web frames.

Figure 9. View showing vertical extent of damage to struck ship.

Figure 10. View of deck damage above side penetration.

Figure 11. Top view of deck above side penetration.

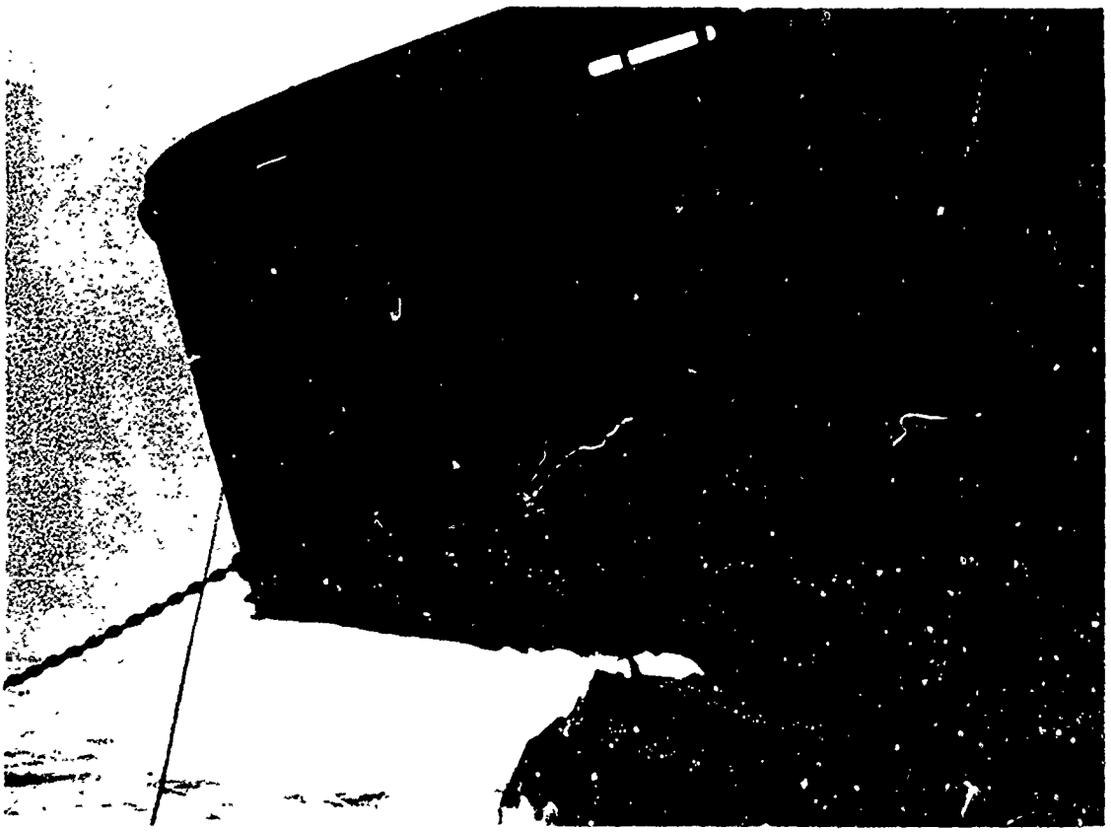

Figure 12. Overall view of bow of striking ship.

Figure 13. View of damage to bow of striking ship, looking forward.

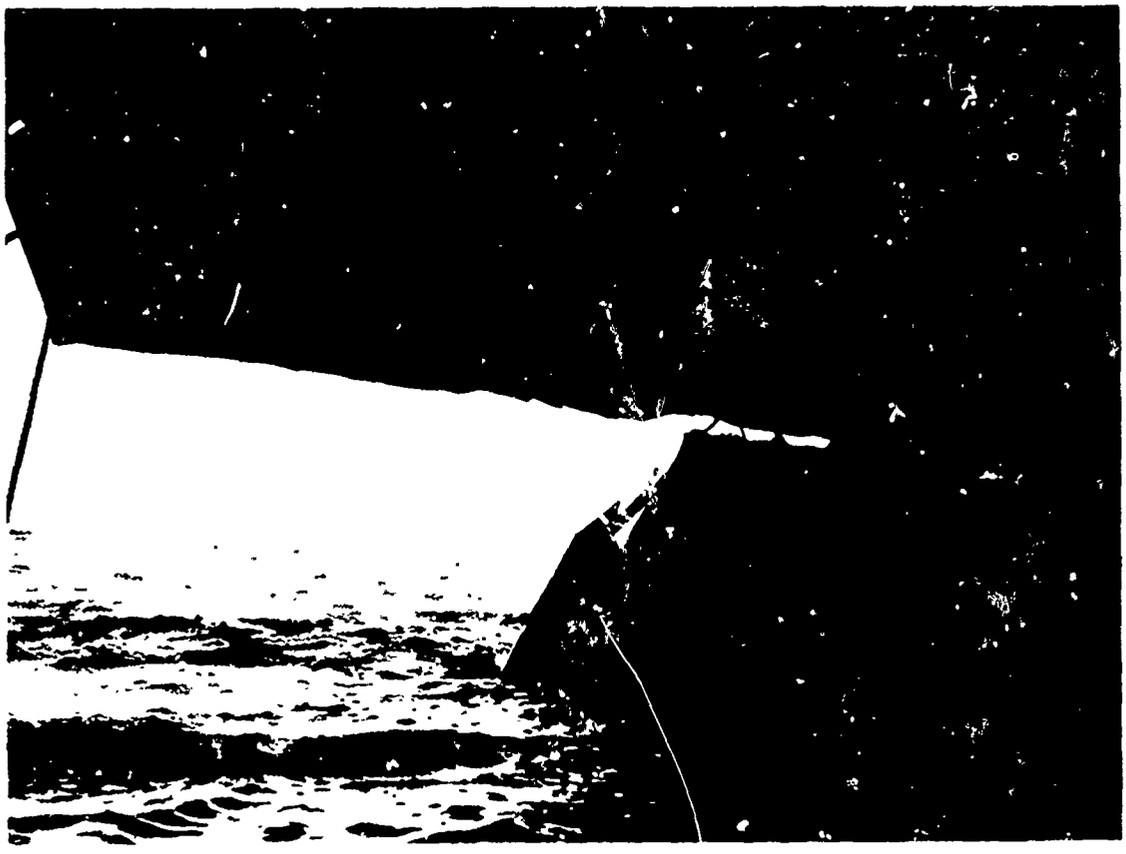

Figure 14. View of damage to bow of striking ship, looking normal to the ship side.

PART IV

EVALUATION OF AN LNG SHIP STRUCTURE IN COLLISION

NOTICE

The work reported on herein was performed as part of a research project done by M. Rosenblatt & Son for the U. S. Coast Guard Office of Research and Development. It is extremely preliminary and theoretical in nature and therefore must be considered as such. The U. S. Coast Guard does not endorse or approve of the methods utilized in this report.

TABLE OF CONTENTS

		Page
1.	INTRODUCTION	1-1
2.	COLLISION ANALYSIS PROCEDURE	2-1
	2.1 The LNG Ship	2-1
	2.2 Fundamental Differences Between the Side Structures of the LNG Ship and Typical Tankers	2-1
	2.3 Changes in Plastic Analysis for a Right-Angle Strike at The Centerline of Tank	2-5
	2.4 References	2-14
3.	ANALYSIS PROCEDURE APPLICATION	3-1
	3.1 General	3-1
	3.2 Membrane Tension Energy for Arbitrary Strike Location	3-3
	3.3 Results	3-7
4.	CONCLUSIONS	4-1
5.	RECOMMENDATIONS	5-1
6.	ACKNOWLEDGEMENTS	6-1
	GLOSSARY OF SYMBOLS	7-1
	APPENDIX - CALCULATIONS	

1. INTRODUCTION

This report is on a separate task accomplished within the research and development project related to the evaluation of the structure of tankers in collision from the viewpoint of the protection afforded to the cargo. The tanker project has developed to date an analytical procedure for estimating the plastic energy absorbed prior to side shell rupture by a longitudinally framed tanker when involved in collision, both right angle and oblique, with ships with rigid bows. The procedure appears in the following reports:

1. Tanker Structural Evaluation, Prepared for Department of Transportation, U.S. Coast Guard, by M. Rosenblatt & Son, Inc., New York and USS Engineers & Consultants, Pittsburgh, Pa., MR&S Report No. 2087, April 1972, (USCG Project 72-33-2I).

2. Evaluation of Tanker Structure in Collision Prepared for Department of Transportation, U.S. Coast Guard, by M. Rosenblatt & Son, Inc. New York and U.S. Steel Corporation, Monroeville, Pa. MR&S Report No. 2087-15, November 1973

It appeared that the tanker procedure was sufficiently general that with judicious modification it could be employed to evaluate the structure of other ships such as LNG vessels and nuclear powered ships. In order to test such an adaptability of the procedure it was decided to attempt its application to a 125,000 M^3 LNG Ship designed with spherical aluminum cargo tanks.

This report describes the modifications made to the tanker procedure to suit the LNG ship and presents the numerical calculations made for the energy absorbed when the ship is struck at right angles by the 20,000 ton displacement vessel with a plumb (vertical) bow.

2.COLLISION ANALYSIS PROCEDURE

2.1 The LNG Ship

The ship analyzed is a 125,000 cubic meter LNG carrier employing independent spherical cargo tanks (Fig.2-1). Ship data were provided by the Quincy shipbuilding Division of General Dynamics. Although this ship is longitudinally framed, the geometry of the side structure is fundamentally different from that of the oil tankers previously studied. For example, the deck width varies from a narrow strip in way of the spherical tanks to the full width of the ship at the transverse bulkhead, and a tank-top provides support to the web frames at an elevation of 25 feet above the keel. Such differences necessitate changes in the plastic analysis.

2.2 Fundamental differences between the Side Structures of the LNG Ship and Typical Tankers

2.2.1 Web Frame Construction

A schematic cut-away view of the midship portion of the LNG ship is given in Figure 2-2. One principal difference between the structure of the LNG ship and that of a typical longitudinally framed tanker is that a tank top at Elevation 25'-5", which is integral with parts of thebottom web frames (spaced at 7'-2"), will provide effective horizontal reactions against the vertical webs (spaced at 14'-4") that connect the outer hull and the longitudinal bulkhead.

Consequently, each full-height vertical web, consisting of a vertical plate above the upper level of the tank top and the vertical portion of the bottom web frame, has three horizontal supports: (1) at the top "box girder" comprised of the main deck, the deck below the main deck, the sheer strake, and the upper portion of the longitudinal bulkhead, (2) at the upper level of the tank top, and (3) at the upper turn of the bilge. Failure of a full-height vertical web, concomitant with lateral loading P_{wf}, may result from either a failure of the material in the full-height vertical web or a failure of one of the three horizontal supports. As defined in the November 1973 tanker report and as used herein, P_{wf} is the value, during the crippling of a web frame, of the transverse resistance(s) exerted by the web frame against the most highly strained tee-beam unit(s) of the stiffened hull and/or longitudinal bulkhead.

For the LNG ship struck by a typical tanker, failure of the top box-girder support and the middle support—provided by the tank top and integral bottom web frame—are both important considerations, in addition to possible failure of the vertical web. It is assumed that the bilge does not fail. The failure of the middle support would result from a failure of the bottom web frame.

Consider the set of constants R_m. For any given failure mode, R_m is the ratic of (1) the loading first assumed in analyzing that and all other failure modes to (2) the loading causing the given failure mode. For the LNG ship, R_m should be calculated for every possible failure mode of

the top box girder and both the full-height vertical web and the bottom web frame. Then, at the location of the most highly strained tee-beam unit of the stiffened hull, P_{wf} is the lateral loading first assumed in analyzing all failure modes divided by the greatest value of R_m.

2.2.2 Effective Cross Sections of Web Frames for Calculations

In the calculations of R_m, it is necessary to consider what effective widths of hull plate and longitudinal bulkhead plate act integrally with each full-height vertical web. If the mode of web failure is not bending, it is conservative and satisfactory to neglect the longitudinal stiffeners in effective-width calculations. References 1 and 2 may be utilized for such calculations.

To determine the effective width more accurately, as would be desirable if web bending failure should govern, the second step is to compute the critical buckling stress for in-plane plate thrust. For calculations of in-plane bending and shearing of the web frames, the thrusts in these plates are perpendicular to the longitudinal stiffeners attached to the plates. Hence, although the longitudinal stiffeners do not contribute to the effective cross sectional area, they do help to stiffen the plate relative to tendencies for buckling. Consequently, the critical buckling stress in each plate may be approximated by the following equation:[3]*

*See References

$$\sigma_{cr} = \frac{\pi^2 D}{b^2 t}\left[\frac{(m^2 + \beta^2)}{\beta^2 m^2} + \frac{r\beta EI}{m^2 bD}\right]$$

where b is the spacing of the webs (7'-2" or 14'-4"), β = b/a where a is the unsupported width of the stiffened plate in the direction perpendicular to the longitudinal direction, t is the plate thickness, r is the number of spaces between stiffeners within distance a, E is the modulus of elasticity, I is the moment of inertia of a longitudinal stiffener about its interface with the plate, $D = Et^3/10.92$, and m is an integer that may vary from 1 to r. The value of m should be chosen to minimize the calculated value of σ_{cr}. For relatively large values of EI/bd, as are typical of the stiffened plates of the ship, σ_{cr} would be expected to be minimized by assuming m = r. However, it is necessary to test this assumption by evaluating the expression for σ_{cr} assuming m = r - 1, etc.

After σ_{cr} is computed, it is compared to the yield strength, σ_y, of the plate. If $\sigma_{cr} = \sigma_y$, the effective width of the plate is b. If $\sigma_{cr} < \sigma_y$, the effective width is $\frac{b\sigma_{cr}}{\sigma_y}$. Finally, the effective width is the lesser of $\frac{b\sigma_{cr}}{\sigma_y}$ and result obtained from calculations based on references 1 and 2.

In the calculations of R_m for the bottom web frame, the neutral axis of frame bending may be conveniently assumed to be at the interface of the web plate with the tank-top or shell plate, and the moment of inertia of the tank-top or shell plate may be neglected.

2.2.3 Alternate Available Modes of Support at Elevation 25'-5"

Relative to failure of the middle support of each full-height vertical web, there will be two critical values of R_m. One, $(R_m)_1$ relates to failure of the upper level of the tank top in an in-plane shearing mode or a crushing mode. A crushing mode would consist of folding of the tank-top horizontal plate and "gathering" of the attached longitudinal stiffeners, with longitudinal membrane tension subsequently predominating in the plate and stiffeners. The other, $(R_m)_2$, relates to failure of the bottom web frame itself, in a shearing, bending, or crushing mode, whichever would occur at the lowest loading; $(R_m)_2$ is the largest value of R_m for the bottom web frame. However, only the least of the two values $(R_m)_1$ and $(R_m)_2$ should be included in the set of values of R_m of which the greatest determines p_{wf} because, if there is a tendency for either horizontal support system (the stiffened tank-top plate or the bottom web frame) to fail, the other system will provide the necessary horizontal support. In either case, membrane tension resistance of the longitudinally stiffened plates should preclude any gross movement of the upper inside corner of the bottom web frame toward the LNG tank.

2.2.4 Horizontal Flare of Main Deck

Over a length of three web-frame spaces at the widest portion of each LNG tank, Figure 2-2, the main deck on each side of the ship is only as wide as the distance between the outer hull and the longitudinal bulkhead. It would be expected that the LNG ship would

be most vulnerable to a strike within this 43-foot length. Beyond this length, the main deck and the deck immediately below the main deck (which extends over the same area as the main deck) flares horizontally such that the net width of deck is considerably increased. These horizontally flared portions of the main deck and the deck below therefore act as "abutments" providing resistance to (1) transverse and longitudinal forces exerted by the 43-foot-long portion of top "box girder" extending between the "abutments," and (2) transverse forces exerted by the top of the full-height vertical web positioned at the beginning of the deck flare. During the early stages of a collision, the "abutments" may be capable of resisting forces without being overstressed. However, this should be verified at various stages of the analysis, utilizing a digital computer program as suggested in Figure 2-3.

2.3 Changes in Plastic Analysis for a Right-Angle Strike at the Centerline of Tank

Consider a right-angle strike in a plane through the centerline of a spherical tank. The steps involved in modifying the plastic analysis of the November 1973 tanker report to apply to such a collision are as follows.

2.3.1 Only Three Web Frame Spaces Damaged

To start, consider that the outer hull and possibly the longitudinal bulkhead within only the three web-frame spaces at the narrow portion of the deck deflect laterally, Figure 2-2, that is,

that the damaged length does not exceed three web frame spaces. This presumes that the full-height vertical webs at the beginning of the horizontal flare of the top deck resist the lateral forces from the hull and longitudinal bulkhead without yielding or buckling of the vertical webs or bottom web frame. The flow diagram in Figure 2-4 for a strike midway between two web frames indicates the analyses that should be made initially. Figures 2-5 and 2-6 of the present report and Figures 4-2, 4-3, and 4-6 of the November 1973 tanker report define procedures of various analysis steps in Figure 2-4. The symbols appearing in Figures 2-5 and 2-6 correspond to the symbols used in the November 1973 tanker report.

First, using the analysis figures previously developed for the plastic analysis and appearing in the April 1972 and November 1973 reports, complete an analysis assuming only one web-frame space is damaged.

The stiffened grid analysis, which follows, is merely a bending analysis that considers the full-height vertical webs flanking the strike (with effective widths of outer hull and longitudinal bulkhead acting as integral flange plates) behaving as vertically extending beams that are supported transversely by the top box girder, the upper level of the tank top, and the upper turn of the bilge, as discussed previously. The aim of the stiffened grid analysis is to determine the load P_{wf} and the other concomitant lateral loads over the vertical extent of the ship side that would cause

failure of either the full-height vertical webs flanking the strike or the horizontal supports of these webs. The forces applied to the grid are proportional to the forces P_{tc} that would result in hull rupture if only one web frame space were damaged. The top box girder, which includes all elements above Elevation 71'-5-1/4" that appear in a transverse cross section, is analyzed as a fixed-end beam subjected to lateral loads applied from the vertical webs. The resistances of the tank top and/or bottom web frame are determined as discussed previously.

Where the bow of the striking ship is below the top box girder of the LNG ship, it could be assumed that above the strike the hull will assume a triangularly shaped distortion profile. With such an assumption, hypothetical lateral forces would vary linearly from a maximum value at the top of the striking bow to zero at Elevation 71'-5-1/4". In the present analysis, however, no such hypothetical lateral forces were considered.

In the flow diagram in Figure 2-4, it is presumed that once the full-height vertical webs flanking the strike begin to fail—whether it be by failure of the vertical webs or failure of the systems supporting the webs, the full-height vertical webs will continue to fail at a constant resistance. This implies that the tank top is "knifing" through the striking bow if the tank top does not fail. The longitudinal bulkhead will participate by distorting transversely in a longitudinal-membrane-tension modeonly if the full-height vertical webs do not fail by crushing.

If a failure of the full-height vertical webs flanking the strike is indicated in the analysis for a strike midway between two web frames, it may be desirable to make an analysis as indicated in the steps in Figure 2-4 for a strike at a web frame.

2.3.2 Five Web Frame Spaces Damaged

In the above calculations for only three web frame spaces damaged, Figure 2-5, the full-height vertical webs at the beginning of the horizontal flare of the top deck receive lateral loads, $(T_1 + T_2)$ times (δ_{wf}/L_s), from the outer hull and the longitudinal bulkhead. These "end" webs (designated by the subscript "wfe" rather than "wf") must be analyzed to determine whether they can withstand the imposed lateral loads. Generally, there is a lateral load exerted on the full-height vertical web by each longitudinal T-beam unit (longitudinal element of the outer hull and longitudinal bulkhead) that is plastically distorted. In the analyses of these particular webs, it may be desirable to perform a strength analysis, such as is suggested in Figure 2-3, to determine the capacity of the horizontally flared portion of the main deck and the deck below to resist the top "end reaction" of the full-height vertical web.

If none of these calculations indicate failures, the damage should extend over only three web frame spaces. Otherwise, the damage should be assumed to extend over five web frame spaces, and the analysis given in Figure 2-6 should be performed, utilizing the values of P_{wf} for the web flanking the strike and P_{wfe} for the webs at the beginning of the horizontal flare of the top deck.

2.3.3 More Than Five Web Frame Spaces Damaged

The damaged length will extend beyond five web frame spaces if $(T_1 + T_2)(\delta_{wfe}/L_s)$, Figure 2-6, exceeds the lateral force that is concomitant with failure of the web frames at the end of the damaged length. As an approximation, lateral deflections of the outer hull with a damaged length exceeding five web frames spaces are determined by the following steps:

1. Compute the lateral offsets in the web frame spaces that are outside of the central five web frame spaces by assuming that the offsets decrease progressively (proceeding away from the strike) by a constant value. This value is equal to the difference, $\delta_{wf} - \delta_{wfe}$, using the values of δ_{wf} and δ_{wfe} computed by the analysis of Figure 2-6. Then, the angle change in the damaged hull is approximately the same at every web frame within the damaged length but excluding the web frames flanking the strike and at the end of the damaged length. As discussed on pages D-3 and D-4 of the April 1972 report, this corresponds to the assumption, for struck single-hull ships, that the angle change in the hull at a crippled web frame is a constant value depending only on the ratio of the hull membrane tension to the resisting force offered by the web frame.
2. Combine these calculations with the results of Figure 2-6 to give a lateral deflection profile. For nine web frame spaces damaged, summing the offsets would result in a

maximum lateral deflection of the outer hull

$$\delta = \delta' + \delta_{wf} + \delta_{wfe} + (2\delta_{wfe} - \delta_{wf}) + (3\delta_{wfe} - 2\delta_{wf})$$

$$= \delta' + 6\delta_{wfe} - 2\delta_{wf}$$

where δ' is the offset within the struck web frame space. Corresponding to that lateral deflection profile, the membrane tension elongation in the outer hull would be $e_{to} =$

$$2\left[\frac{(\delta')^2}{L_s} + \frac{\delta_{wf}^2 + \delta_{wfe}^2 + (2\delta_{wfe}-\delta_{wf})^2 + (3\delta_{wfe}-2\delta_{wf})^2}{2L_s}\right] - 9L_s\varepsilon_c \leq 9L_s\varepsilon_r$$

and the membrane tension elongation in the inner hull (longitudinal bulkhead) would be $e_{ti} =$

$$\frac{1}{L_s}\left[\delta_{wf}^2 + \delta_{wfe}^2 + (2\delta_{wfe} - \delta_{wf})^2 + (3\delta_{wfe} - 2\delta_{wf})^2\right] - 9L_s\varepsilon_c \leq 9L_s\varepsilon_r$$

3. If the incursion δ thus computed results in a strain greater than ε_r or a rupture of the LNG tank (see below), reduce all of the offset terms by the same percentage and recompute e_{to} and e_{ti}.

2.3.4 Modifications for Limitations Imposed by Proximity of LNG Sphere

The analyses should be modified, as necessary, to reflect the limitations imposed by the proximity of the LNG sphere. The sphere can distort inward to some limited extent during a collision, but the incursion of the striking ship and distortion of the structure

of the struck ship should be limited to what would cause the sphere to rupture. The support system for the LNG tank may allow it to move away from the incursion some distance without being significantly stressed. If such a critical distance can be established, the incursion that initially causes an external force on the sphere can be determined. Then, the theory for shallow spherical shells can be applied to relating sphere stresses and yielding to deflections of the sphere resulting from a greater incursion. The limited information applicable to this problem has been developed for radial deflections of spheres, as given in References 4, 5, 6, and 7.

References 4 and 5, which consider a radial axial load applied through a solid cylinder welded to the sphere, are easiest to apply, although such a circular contact area simulates only very approximately the contact that would be exerted during an LNG ship collision. For different magnitudes assumed for the radius of the contact area, Figure A-7 compares the radial deflection (at the edge of the circular contact area) under given radial loads with the bending moments, membrane forces, and yield criteria at that critical location.[4,5] As a result, it is observed (see the right-hand column in Figure A-7) that the deflection corresponding to the yield criterion is not very sensitive to the radius of the contact area, and may be approximated as

$$\delta_s = \frac{0.2R\sigma_y}{E}$$

where, for the sphere, R is the midplane radius, σ_y is the yield strength, and E is the modulus of elasticity. Similarly, the radial load causing the sphere to yield (see the second-from-the-left column in Figure 2-7) may be approximated as

$$P_s = 3 \frac{ET^2}{R} \delta_s$$

where t is the thickness of the sphere wall. With bending stresses predominating, it is conservative yet realistic to assume that the "permissible" radial deflection of the sphere in Figure 2-8, defined as the deflection at rupture, is the deflection at onset of yielding times $\varepsilon_{ts}/\varepsilon_y$, where ε_{ts} is the strain at the tensile strength and ε_y is the strain at onset of yielding. The sketches in Figure 2-8 relate the incursion to the inward deflection of the sphere.

If a more realistic evaluation of radial distortions, corresponding to a "line loading" rather than a loading assumed over a circular contact area, is desired, the "influence surface" charts of Reference 6 can be utilized. These nondimensional charts, which are dimensionalized by the use of a scale factor, $\ell = \sqrt{Rt}/\sqrt[4]{12\ (1 - \mu^2)}$, readily give radial-deflection, bending-moment, and membrane-force coefficients at locations away from load points, and suitable integrations could compare deflections and stresses for line loadings. However, the charts do not afford a direct solution for calculating line loads corresponding to a given "line" deflection, and the bending stresses are very sensitive to the "width" of the line loading, theoretically being infinite directly under a "knife-edge" loading.

2.4 References

1. Shade, H. A., "The Effective Breadth Concept in Ship-Structure Design," Transactions of the Soc. of Naval Architects and Marine Engineers, Vol. 61, 1953, p. 410-430.
2. Shade, H. A., "The Effective Breadth of Stiffened Plating Under Bending Loads," Transactions of the Soc. of Naval Architects and Marine Engineers, Vol. 59, 1951, p. 403-420, 429, and 430.
3. Timoshenko, S. P. and Gere, J. M., Theory of Elastic Stability, McGraw-Hill Book Co., New York, 1961, Equation 9-22, pg. 402.
4. Bijlaard, P. P., "Computation of the Stresses From Local Loads in SphericalPressure Vessels or Pressure Vessel Heads," Welding Research Council Bulletin, No. 34, March 1957.
5. Bijlaard, P. P., "Local Stresses in Spherical Shells from Radial or Moment Loadings," The Welding Journal, 36(5), Research Suppl., 240-s to 243-s (1957).
6. Chinn, J., "Influence Charts for Deflections and Stresses in Shallow Spherical Shells," Paper Presented at the International Symposium on Shell Structures in Engineering Practice, Budapest, Hungary, August 31 to Sept. 3, 1965. (Limited number of copies available from University of Colorado, Boulder, Colorado)
7. Tooth, A. S., Kenedi, R. M., and Hossack, J. D. W., "The Use of Semi-Graphical Methods in the Stress and Deformation Analysis of Shell Forms," The Structural Engineer, April 1960, pg. 129-137.

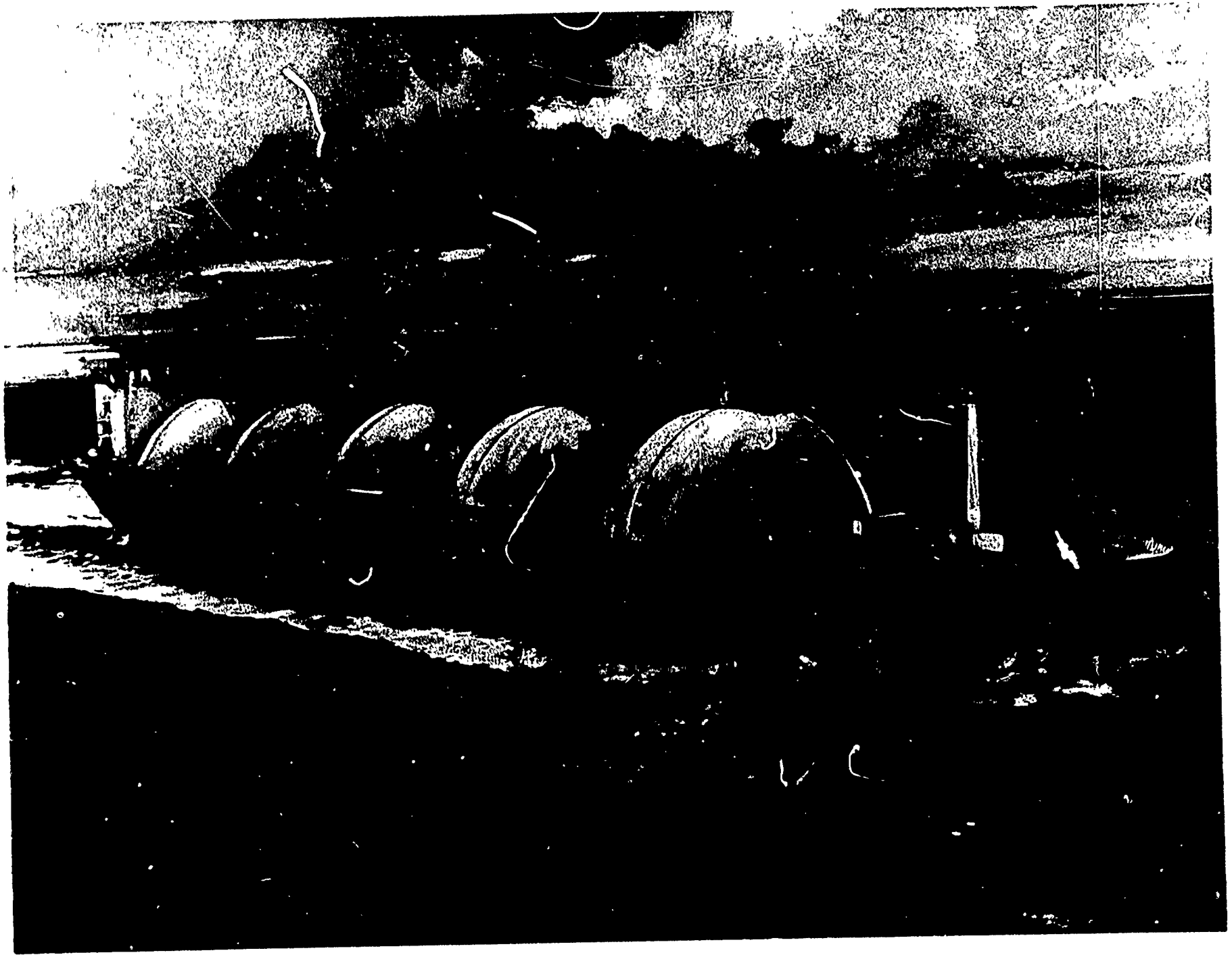

Fig. 2-1

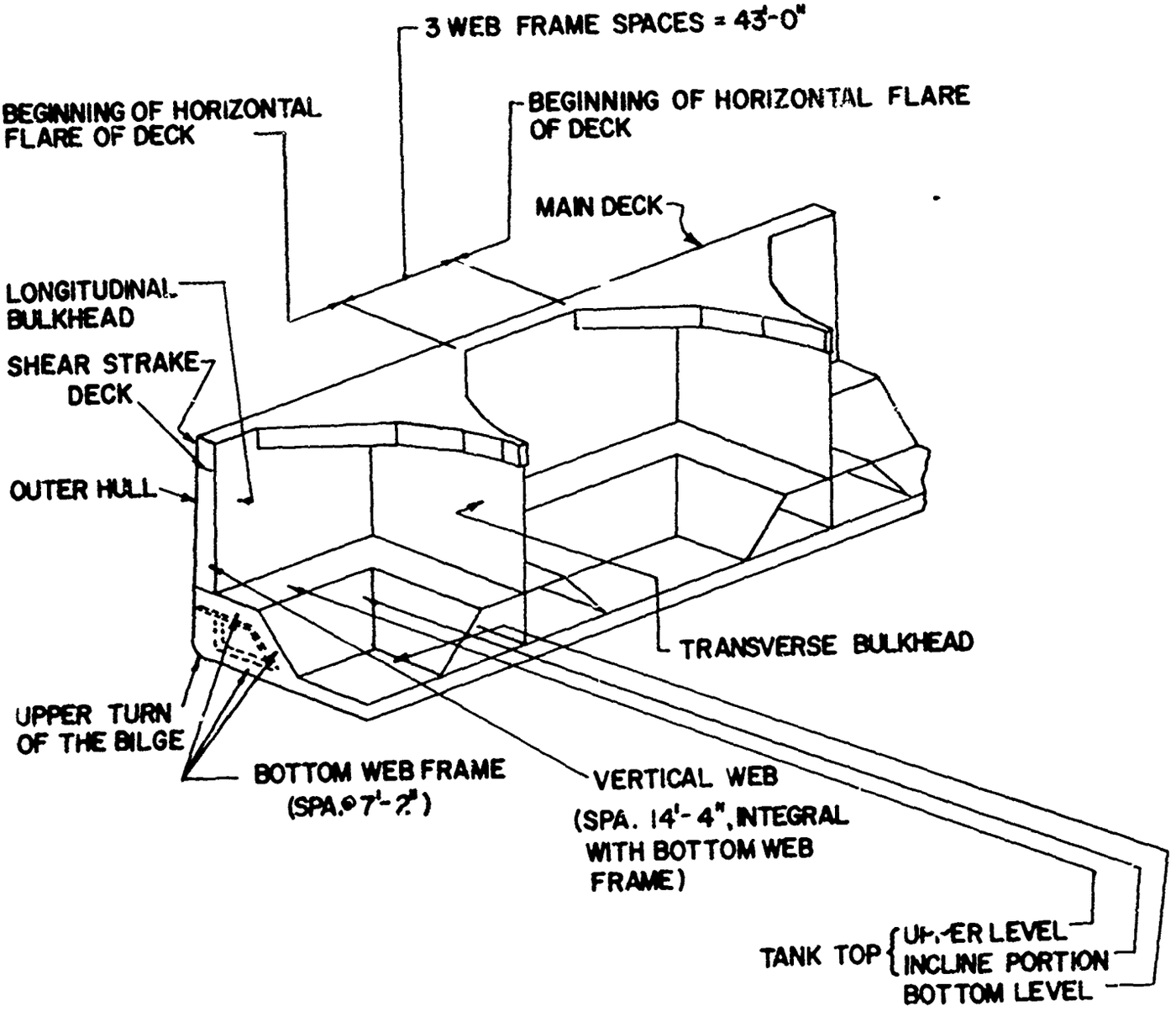

SCHEMATIC CUT-AWAY VIEW OF MIDSHIP PORTION OF GENERAL DYNAMICS 125,000 M^3 LNG SHIP

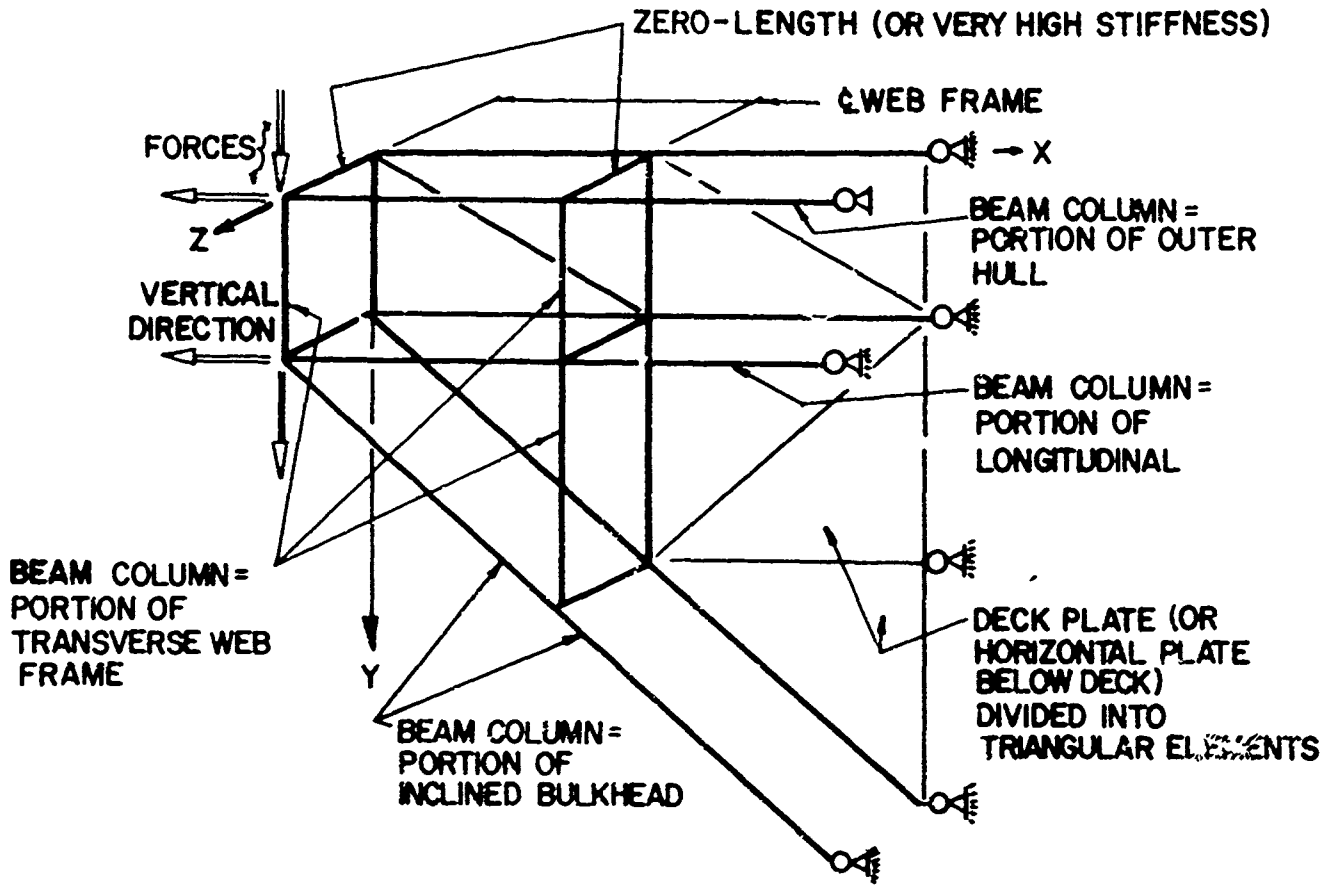

TYPICAL STRUCTURAL MODEL FOR BEAM-COLUMN AND PLATE ELEMENTS COMBINED IN A SINGLE PLANE

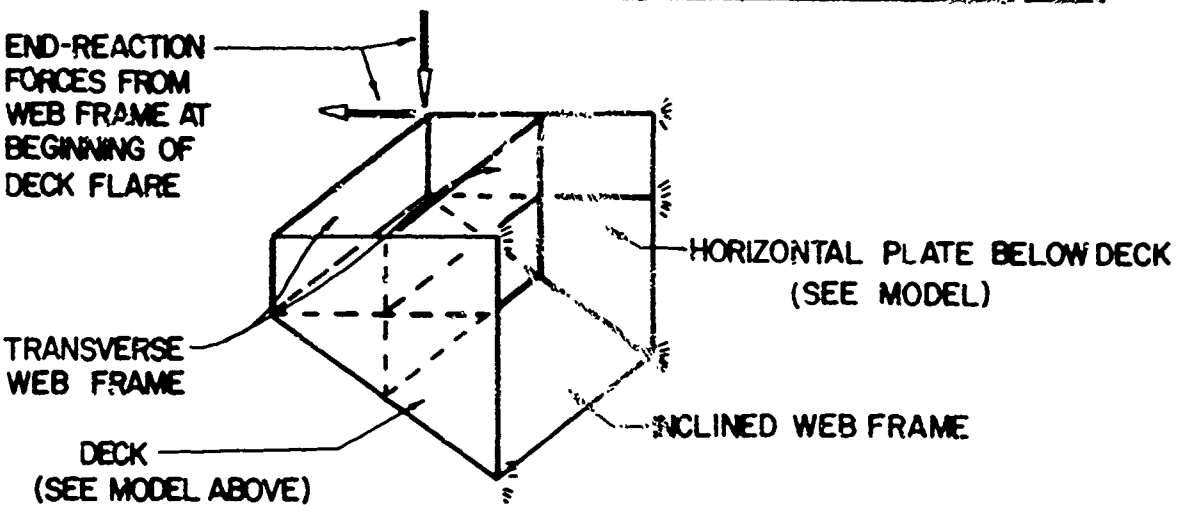

STRUCTURE TO BE ANALYZED BY A STIFFNESS-MATRIX ENGINEERING ANALYSIS COMPUTER PROGRAM, SUCH AS ANSYS

SUGGESTED ANALYSIS FOR DETERMINING STRESSES IN DECK FROM

END-REACTION FORCES FROM WEB FRAME AT BEGINNING OF DECK FLARE

Fig. 2-3

MACRO FLOW DIAGRAM FOR SIDE COLLISION
PLASTIC ENERGY ANALYSIS OF LNG SHIP
ASSUMING DAMAGED AREA EXTENDING ONLY
OVER THREE WEB FRAME SPACES AT
THE NARROW PORTION OF THE DECK

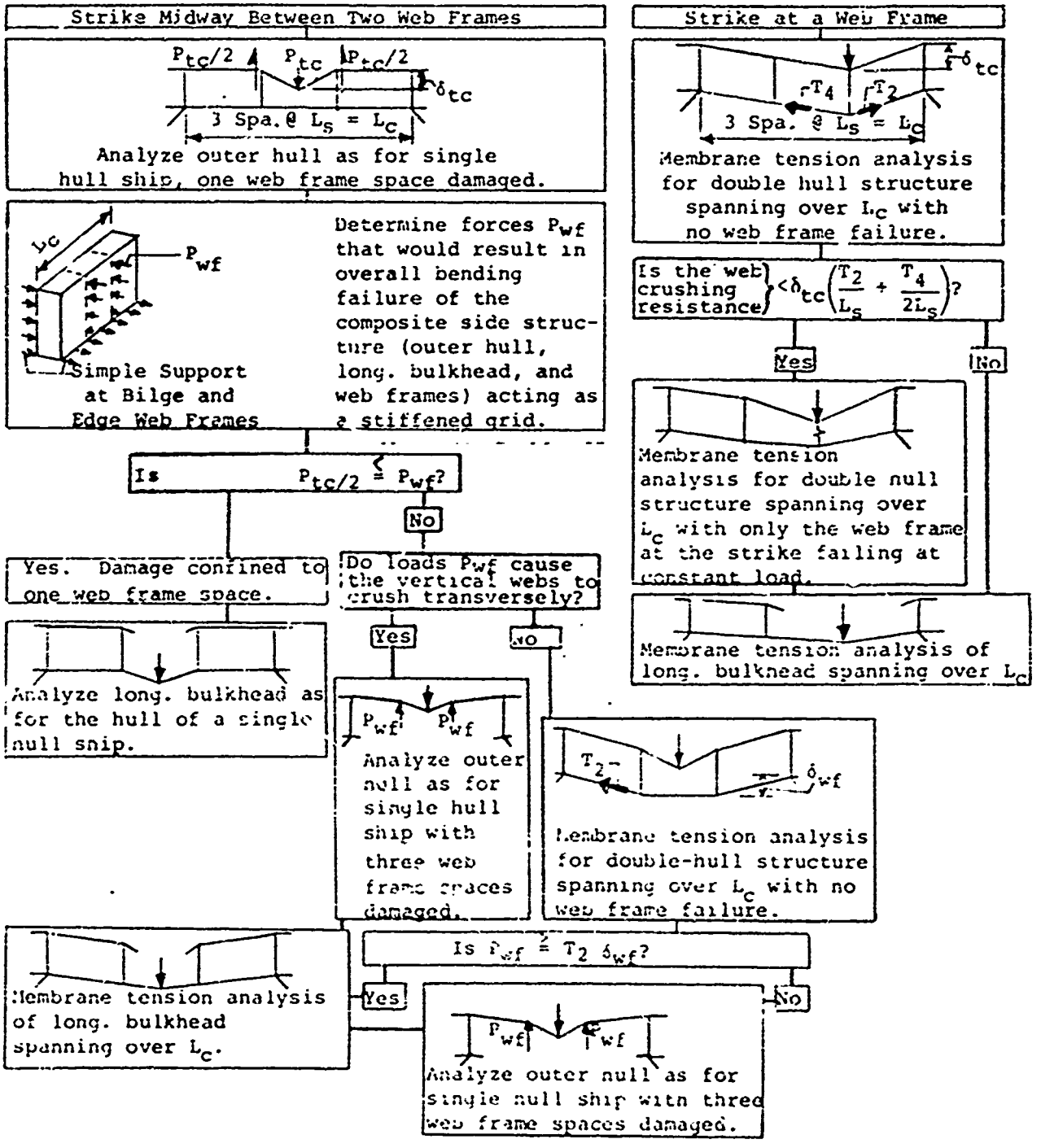

FIGURE 2-4

RIGHT-ANGLE COLLISION

MEMBRANE TENSION ANALYSIS OF DOUBLE-HULL STRUCTURE SPANNING LONGITUDINALLY OVER THREE WEB FRAME SPACES — STRIKE MIDWAY BETWEEN WEB FRAMES — NO WEB FRAME FAILURES

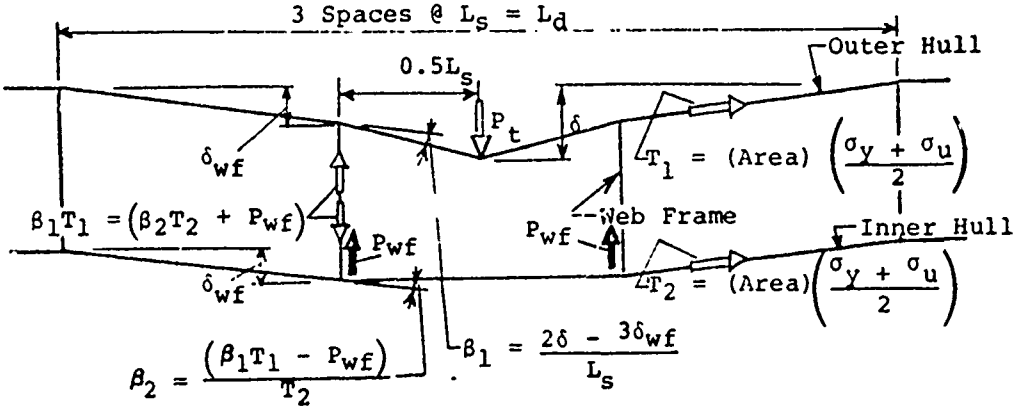

Geometry Assuming Small-Angle Theory (Angle = Sine = Tangent)

$$\text{From } \beta_2 = \frac{\delta_{wf}}{L_s},\ \delta_{wf} = \frac{2\delta - P_{wf}\, L_s/T_1}{3 + T_2/T_1}$$

This expression is substituted for δ_{wf} in the following inequality.

Membrane Tension Elongation in Outer Hull

$$e_{to} = 2\left[\frac{\delta_{wf}^2}{2L_s} + \frac{(\delta - \delta_{wf})^2}{L_s}\right] - 3L_s\varepsilon_c \leq 3L_s\varepsilon_r$$

This used as an equation gives $\delta = \delta_c$ = deflection at rupture.

Membrane Tension Elongation in Inner Hull

$$e_{ti} = \frac{\delta_{wf}^2}{L_s} - 3L_s\varepsilon_c \leq 3L_s\varepsilon_r$$

Membrane Tension Plastic Energy (including energy in flanking spans)

$$E_{mt} = 1.33(T_1 e_{to} + T_2 e_{ti})$$

Normal Forces

$$P_t = \frac{4T_1}{L_s}(\delta - \delta_{wf})$$

$$\text{End Reaction} = (T_1 + T_2)(\delta_{wf}/L_s)$$

FIGURE 2-5

RIGHT-ANGLE COLLISION

MEMBRANE TENSION ANALYSIS OF DOUBLE-HULL STRUCTURE WITH DAMAGE EXTENDING OVER FIVE WEB FRAME SPACES—STRIKE MIDWAY BETWEEN CENTRAL WEB FRAMES—WEB FRAMES AT BEGINNING OF DECK FLARE FAILING WITHOUT CRUSHING

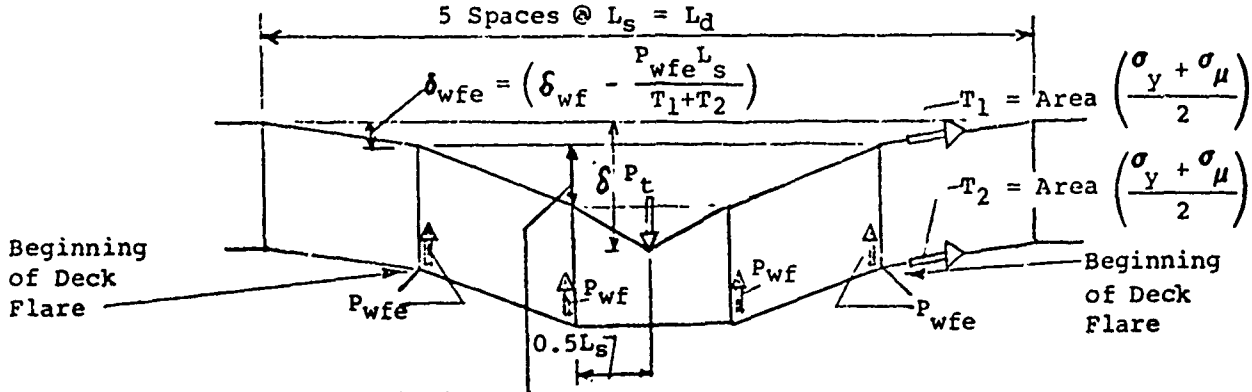

From the analysis for only three web frame spaces damaged, Figure 4,

$$\delta_{wf} = \left[\frac{2(\delta - \delta_{wfe}) - \frac{P_{wf} L_s}{T_1}}{3 + \frac{T_2}{T_1}}\right]$$

This expression is substituted for δ_{wf} in the above expression for δ_{wfe}, and both expressions are substituted in the inequality below so that the only unknown value is for δ_{wfe}.

Membrane Tension Elongation in Outer Hull

$$e_{to} = 2\left[\frac{\delta_{wfe}^2}{2L_s} + \frac{\delta_{wf}^2}{2L_s} + \frac{(\delta - \delta_{wfe} - \delta_{wf})^2}{L_s}\right] - 5L_s\epsilon_c \leq 5L_s\epsilon_r$$

This used as an equation gives $\delta = \delta_c$ = deflection at rupture.

Membrane Tension Elongation in Inner Hull

$$e_{ti} = \frac{\delta_{wfe}^2}{L_s} + \frac{\delta_{wf}^2}{L_s} - 5L_s\epsilon_c \leq 5L_s\epsilon_r$$

Membrane Tension Plastic Energy (including energy in flanking spans)

$$E_{mt} = 1.17(T_1 e_{to} + T_2 e_{ti})$$

Normal Forces

$$P_t = \frac{4T_1}{L_s}(0.5\delta_{wfe} + \delta_1 - \delta_{wf})$$

$$\text{End Reaction} = (T_1 + T_2)(\delta_{wfe}/L_s)$$

FIGURE 2-6

Radial Deflection at Onset of Yielding of LNG Sphere Under a Concentrated Radial Load

References: Bijlaard, P. P., "Computation of the Stresses from Local Loads in Spherical Pressure Vessels or Pressure Vessel Heads," Welding Research Council Bulletin, No. 34, March 1957.

Bijlaard, P. P., "Local Stresses in Spherical Shells from Radial or Moment Loadings," The Welding Journal, 36(5), Research Suppl., 240-s to 243-s (1957).

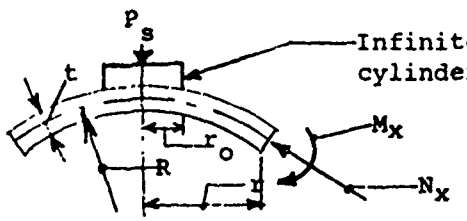

Section Through Centerline

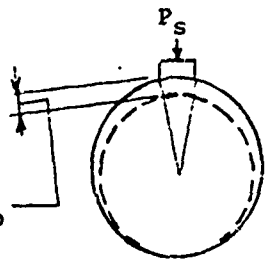

	Conditions at $r = r_o$						
$1.82\frac{r_o}{R}\sqrt{\frac{R}{t}}$	Radial Deflection $\frac{\delta_s}{\frac{R}{Et^2}P_s}$	Radial Bending Moment per Unit Width $\frac{M_x}{P_s}$	Radial Membrane Force per Unit Width $\frac{N_x}{P_s/t}$	Tangential Bending Moment* per Unit Width $\frac{M_y}{P_s}$	Tangential Membrane Force* per Unit Width $\frac{N_y}{P_s/t}$	Von Mises-Huber Yield Criterion** $\frac{P_s}{t^2\sigma_y}$	$\frac{\delta_s}{R\sigma_y/E}$
0.1	0.388	0.383	0.298	0.120	0.090	0.435	0.169
0.2	0.346	0.287	0.273	0.082	0.082	0.562	0.194
0.4	0.288	0.180	0.224	0.052	0.067	0.861	0.248
0.6	0.233	0.128	0.181	0.038	0.054	1.185	0.276
0.8	0.191	0.095	0.149	0.029	0.044	1.566	0.299
1.0	0.158	0.075	0.124	0.022	0.037	1.957	0.309
1.5	0.102	0.043	0.081	0.013	0.025	3.322	0.339
2.0	0.073	0.029	0.056	0.009	0.017	4.904	0.358

Conclusion from Calculated Data

At onset of yielding, δ_s will be a value approximately in the range $\frac{0.2R\sigma_y}{E}$ to $\frac{0.3R\sigma_y}{E}$

* Acting in the circumferential direction.

** Based on the octrahedral shearing stress =

$$\frac{\sqrt{2}}{3}\sigma_y = \frac{1}{3}\sqrt{\left(\frac{6M_x}{t^2} + \frac{N_x}{t} - \frac{6M_y}{t^2} - \frac{N_y}{t}\right)^2 + \left(\frac{6M_x}{t^2} + \frac{N_x}{t}\right)^2 + \left(\frac{6M_y}{t^2} + \frac{M_y}{t}\right)^2}$$

FIGURE 2-7

Adaptation of Plastic Analysis Procedure
for LNG Ship Considering Incursion
of the Sphere Containing the LNG

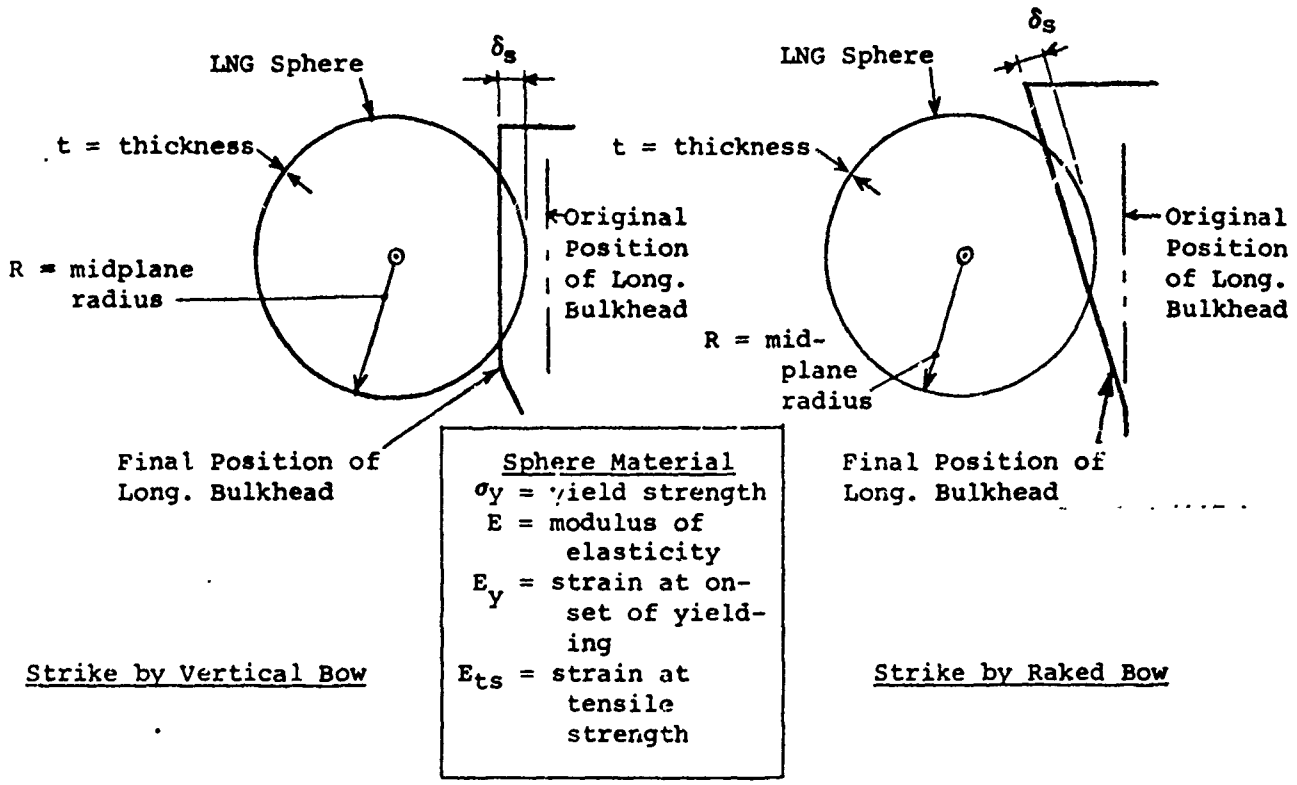

1. For maximum incursion not considering the LNG sphere, determine δ_s from the geometry of the ship structure.

2. Compare this to a "permissible" value

$$\delta_s = 0.2 \frac{R\sigma_y}{E} \frac{\epsilon_{ts}}{\epsilon_y}$$

which results from the calculated data in Table III. This is based on the assumption that, under the line loading exerted by a striking bow, the maximum deflection should not be greater than the radial deflection concomitant with rupture of the sphere under a concentrated radial load transmitted through a solid cylinder end-welded to the sphere; the radius of the cylinder $\geq 0.11\sqrt{Rt}$. Also, with bending stresses predominating, it is conservative yet realistic to assume that the deflection at rupture is the deflection at onset of yielding times ϵ_{ts}/ϵ_y.

3. If the permissible value is exceeded, recalculate the incursion geometry so that δ_s is equal to the permissible value.

FIGURE 2-8

3. ANALYSIS PROCEDURE APPLICATION

3.1 General

Based on the procedure presented in Chapter 2, a set of calculations were performed to obtain the plastic energy absorbed prior to cargo tank rupture when the LNG ship in the fully loaded condition is struck beam on (90 degrees) between web frames coincident with midpoint between two adjacent bulkheads by a 20,000 ton displacement ship with a plumb bow. Using the value of the energy absorbed in the midpoint strike as reference, very approximate estimates were made for the energy absorbed in strikes at other points along the length between bulkheads. The approximation method is described in section 3.2. Elevation sketch of the collision, Figure 3-1, shows the vertical extent of the LNG ship intercepted by the striking bow. It is important to note that the main deck is not intercepted.

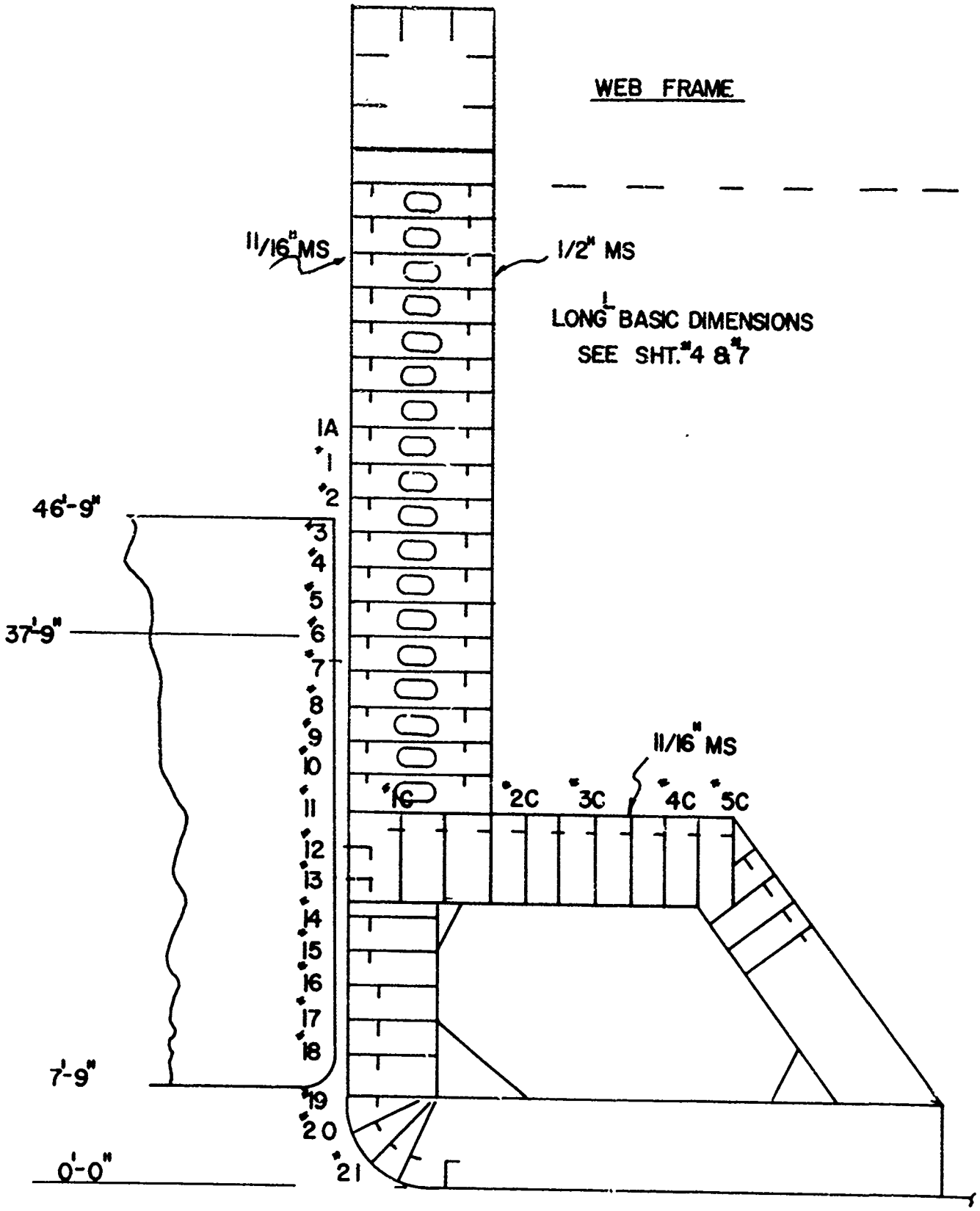

ELEVATION SKETCH OF COLLISION

Fig. 3-1

3.2 Membrane Tension Energy for Arbitrary Strike Location

An examination of the results of the energies in the component structures tests, (see MR&S report 2087-15, Evaluation of Tanker Structure in Collision, November 1973.) Figure 3-21, and of a hypothetical case of a damaged length extending over seven web frame spaces, Figures 3-3 and 3-4, suggests that the following could possibly be reasonable for a rough approximation of the membrane tension energy with the distance from a transverse bulkhead.

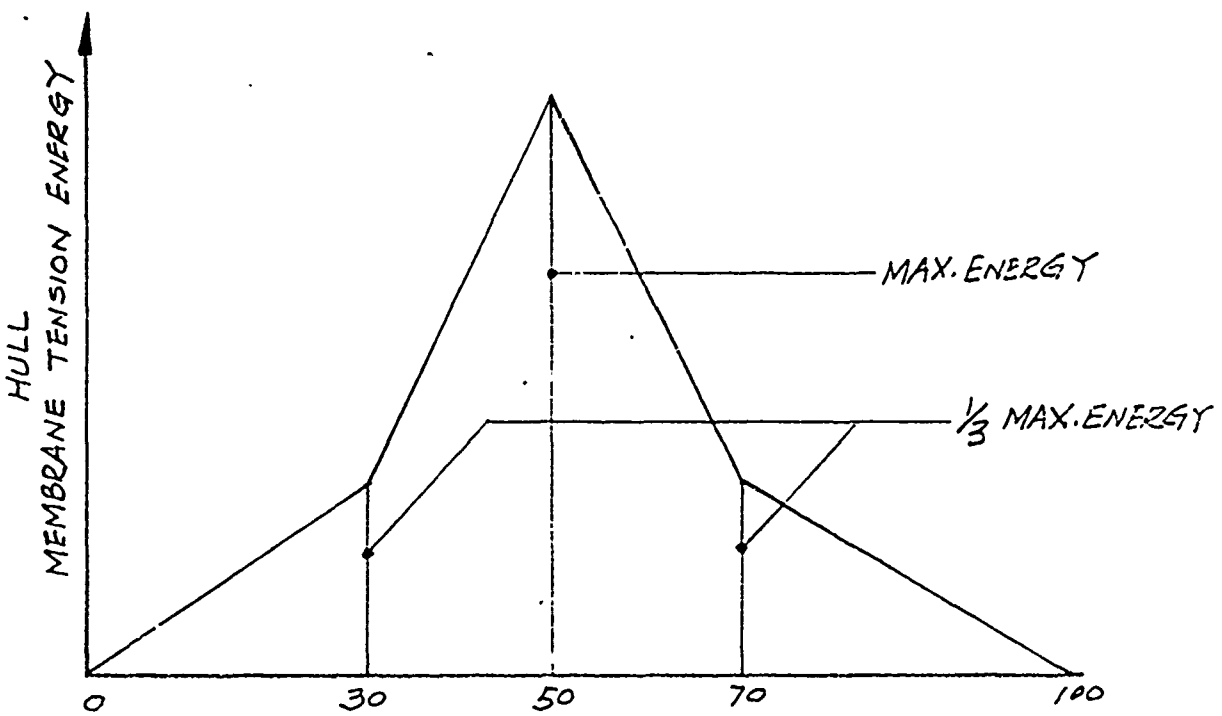

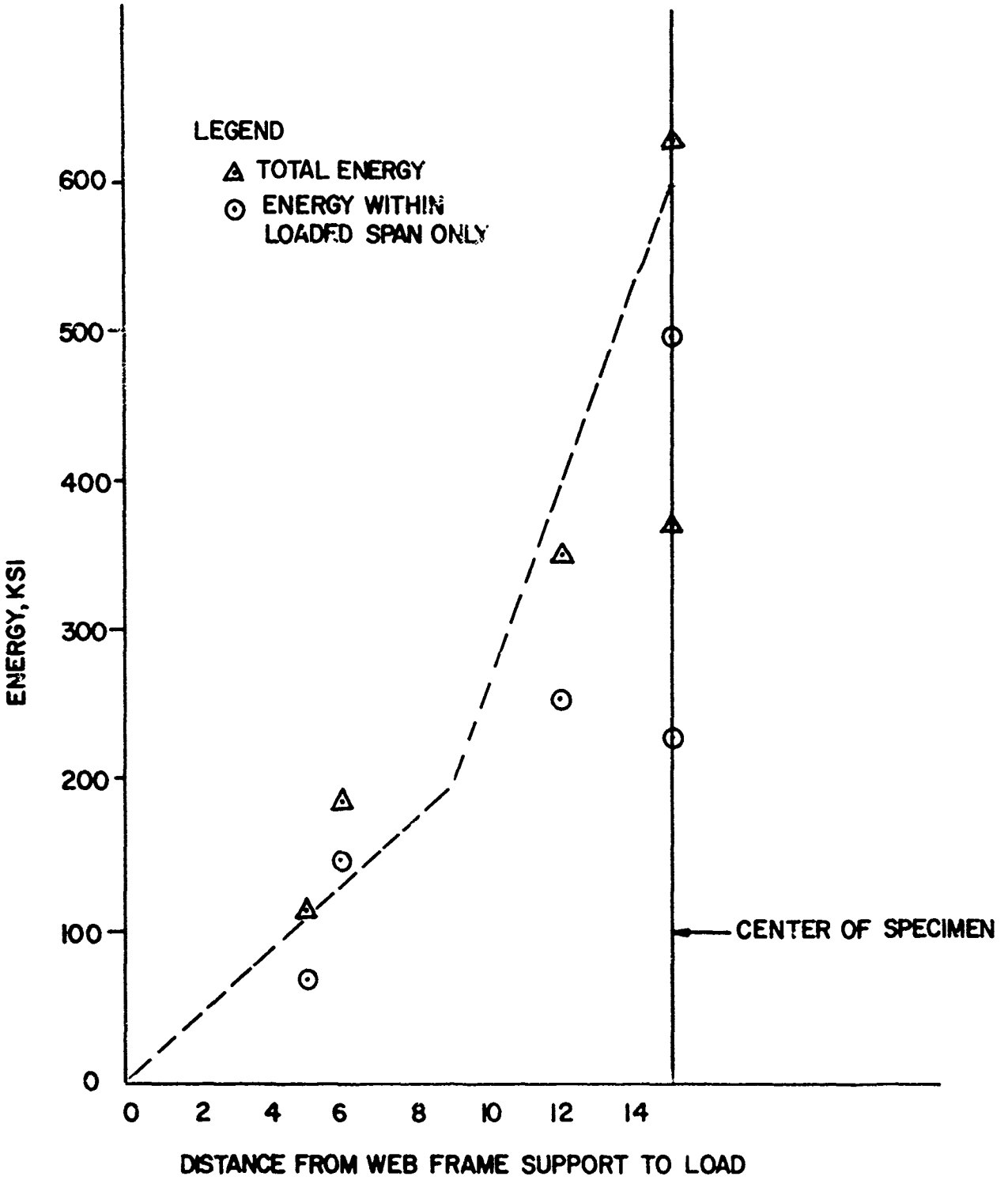

PLASTIC ENERGIES EXHIBITED AT RUPTURE IN COMPONENT STRUCTURE TESTS

Fig. 3-2

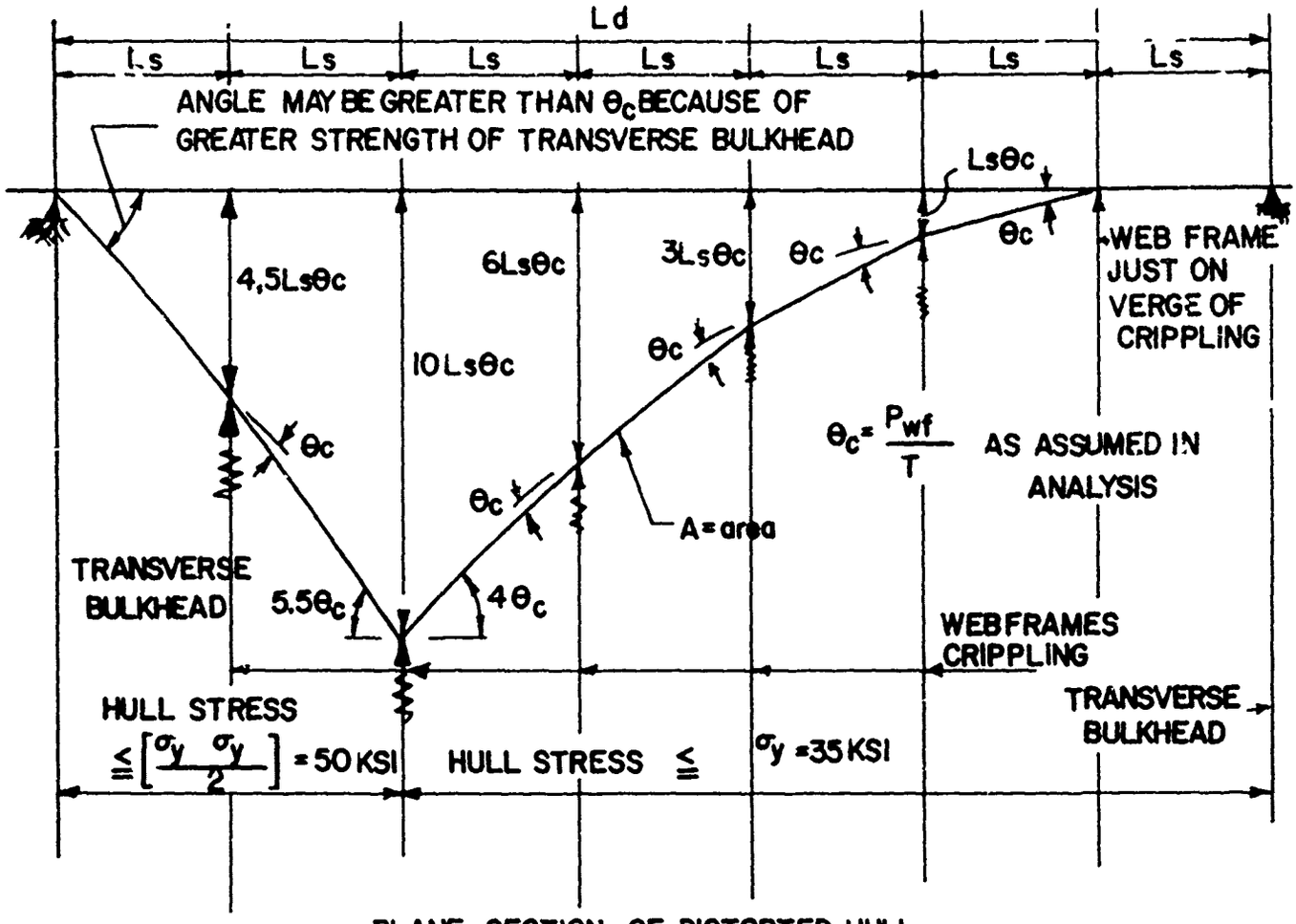

PLANE SECTION OF DISTORTED HULL

ASSUME $4\theta c = 36.5^\circ$ THEN $5.5\theta c = 50^\circ$

THEN, LONGITUDINAL COMPONENT OF MEMBRANE TENSION LEFT OF THE LOAD $= 50A\cos 50^\circ = 32A$

CLOSE ENOUGH CHECK

LONGITUDINAL COMPONENT OF MEMBRANE TENSION RIGHT OF THE LOAD $= 35A\cos 36.5^\circ = 28A$

ANGLE AT TRANSVERSE BULKHEAD $= 4.5\theta = 41^\circ$ (THIS IS THE MAXIMUM BEND ANGLE PERMITTED AWAY FROM STRIKE FOR ABS STEEL.)

JUST BARELY YIELDING IN HULL ON ONE SIDE OF STRIKE FOR A HYPOTHETICAL CASE WITH SEVEN WEB FRAME SPACES DAMAGED UNDER A LOAD 0.29LD FROM A TRANSVERSE BULKHEAD

FIGURE 3-3

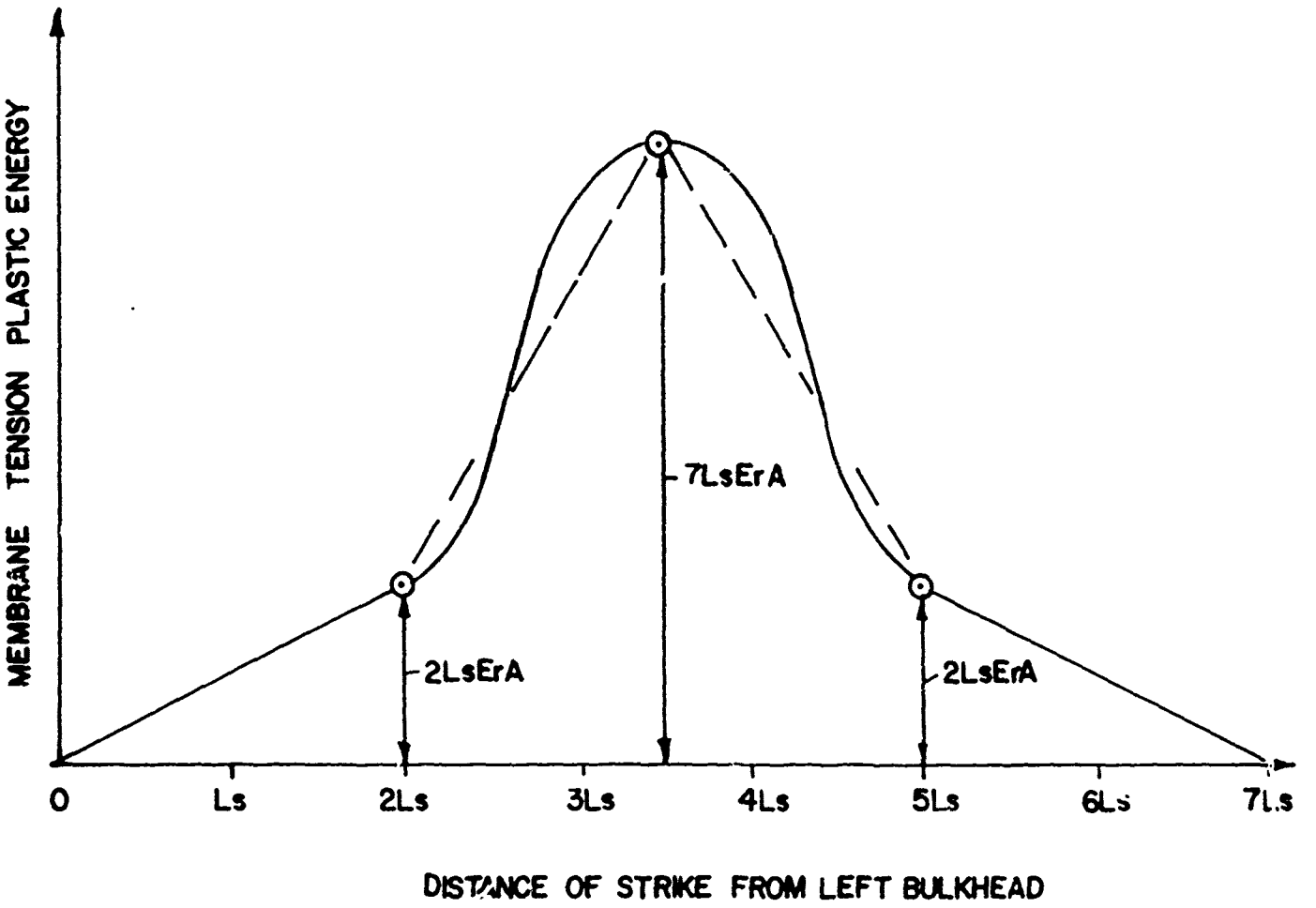

VARIATION OF MEMBRANE TENSION PLASTIC ENERGY WITH LOCATION OF STRIKE (CORRESPONDING TO ASSUMPTIONS OF FIGURE 3-3)

FIGURE 3-4

3.3 Results

The results of the calculations are summarized in table 3-I and Figures 3-5 and 3-6. Table 3-I gives the average of the plastic energy developed prior to shell plate rupture for strike location anywhere between adjacent bulkheads. The average value is equivalent to collision energy imparted by the striking ship travelling at approximately 7.4 knots.

The variation of the energy with strike location and the energy for strike midway between bulkheads are shown in Figure 3-5. The extreme variation of energy is apparent.

The significant boundary condition imposed on the calculation was that the total incursion of the striking vessel would be limited to the distance between the shell and the cargo tank plus 16 inches. The 16 inches is due to the allowable deflection of the tank and it is based on rough calculation only since the investigation of the cargo tank structure was outside the scope of work. Of course, this total allowable incursion limitation becomes trivial when the shell and or the inner skin fail before the total incursion is reached.

The variation in the energy absorbed along the length is due to the number of webs involved in the damage and consequently the resulting damage length over which the plastic membrane tension can be developed, as well as the permissable incursion or strain before the LNG containment tank is ruptured. Close to a bulkhead

due to location and spherical shape of the cargo tank the allowable incursion is high but the available damage length is low, whereas, the conditions are reversed toward the center of cargo space (see Figure 3-6.

The foregoing discussion brings out the point that except for strikes within two web spaces of the bulkheads the LNG cargo tank will rupture (assuming the estimate of 16 inch tank deflection prior to rupture is reasonable) before the maximum strains in the outer and inner skin are developed. This implies that the closeness of the tank to the shell and allowable strain in the tank limits the energy developed in a collision.

Striking Ship Bow	Vertical
Hit Angle	90°
Case No.	12a
Shell Plate Thickness	Inner shell 1/2" M.S. Outer shell 11/16 M.S.
Energy Absorbed (Average) in - Kips	1,309,700
Energy Absorbed (Average) Ft - Tons	48,730
Equivalent Striking Speed of A 20,000 T Ship (knots)	7.4

Table - I

SUMMARY OF AVERAGE PLASTIC ENERGY ABSORBED BEFORE SHELL PLATE RUPTURE

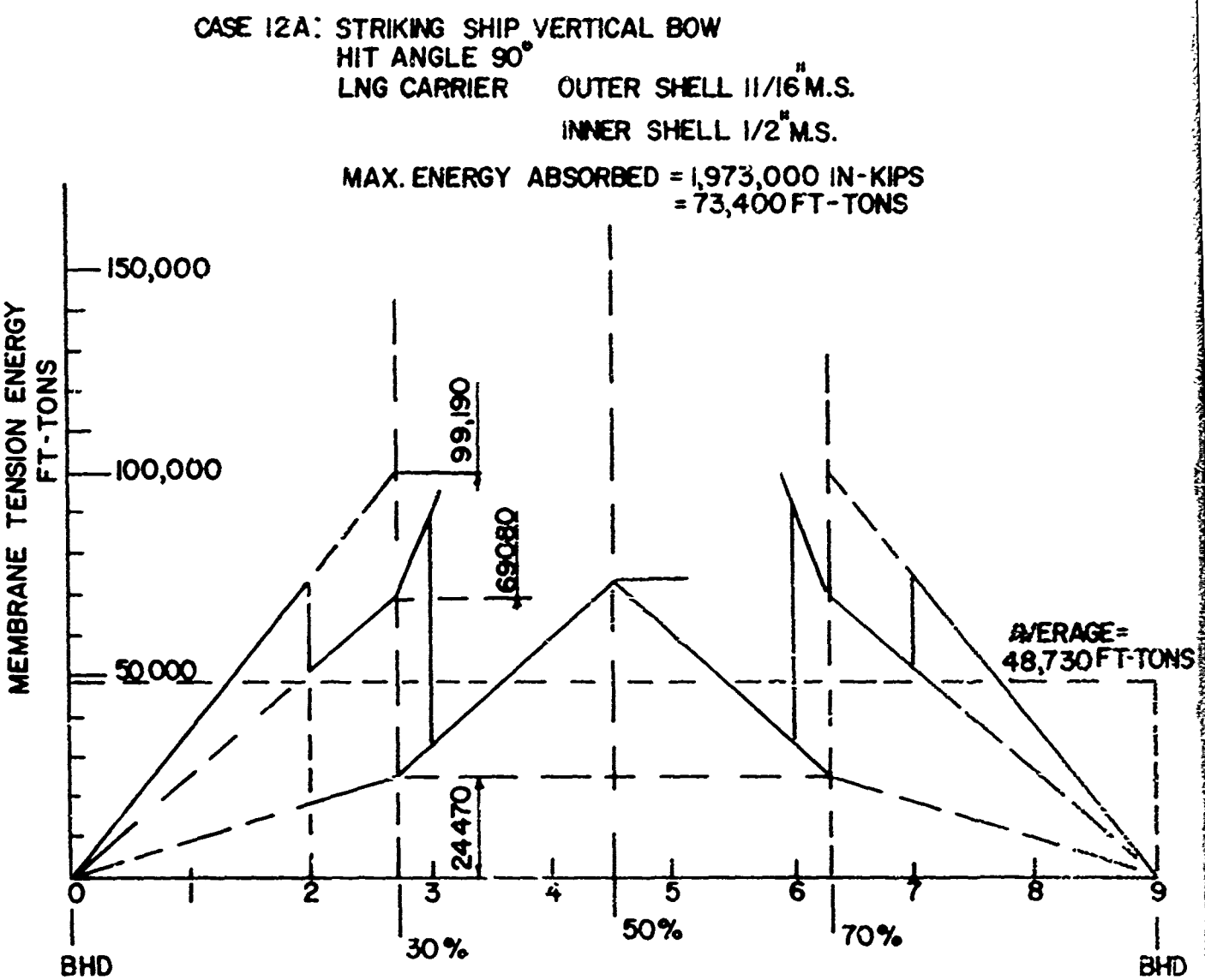

VARIATION OF ENERGY WITH LOCATION OF STRIKE

Fig. 3-5

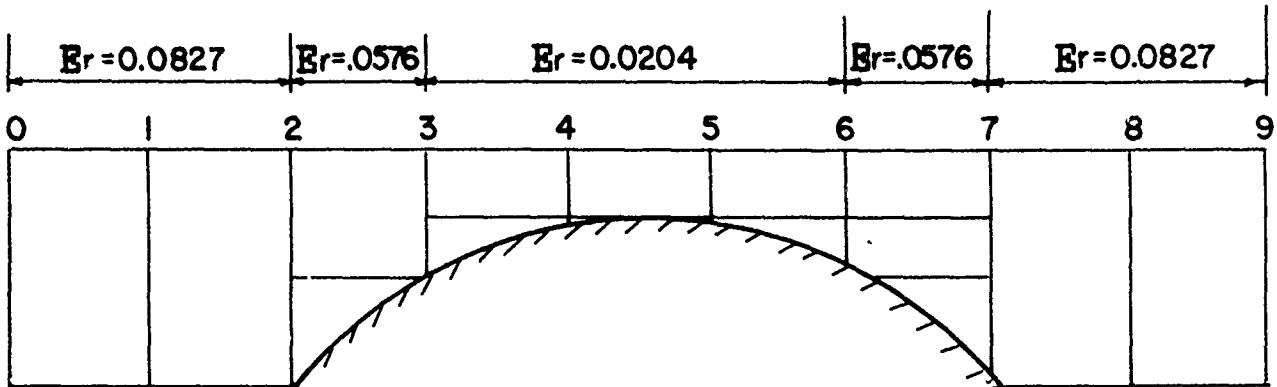

MAX. ENERGY ABSORBED
=1,973,000 IN-KIPS
=73,400 FT-TONS

Er	MAX. ENERGY FT - TONS	1/2 MAX. ENERGY FT-TONS
0.0204	73,400	24,470
0.0576	207,247	69,080
0.0827	297,558	99,190

VARIATION OF AVERAGE PLASTIC STRAIN (Er) WITH LOCATION OF STRIKE

Fig. 3-6

4. CONCLUSIONS

1. The attempt to modify the procedure for the evaluation of tanker structure in collision to suit the LNG ship was successful.

2. The following limitations of the procedure developed for the LNG ship should be recognized.

- The procedure is based on a static analysis.
- The procedure assumes that the striking bows are infinitely rigid.
- The damage to the struck ship does not extend into the bilge area.
- The procedure employs a very approximate method for estimating allowable deflection in the cargo tank before rupture.

5. RECOMMENDATIONS

1. Perform numerical calculations for raked striking bow and oblique collision.

2. Perform calculation for strike anywhere between adjacent bulkheads by applying the detail procedure.

3. Update procedure to reflect non-rigid striking bows and dynamic analysis and extend procedure to include damage to bilge area.

Preceding page blank

6. ACKNOWLEDGEMENTS

The LNG structure evaluation task was sponsored by the United States Coast Guard under Contract DOT-10,605A. The technical representatives of the U.S. Coast Guard were Commander Emlyn Jones, USCG, Commander Charles Loosmore, USCG and Mr. James Dwyer. The prime contractor was M. Rosenblatt & Son, Inc. and the subcontractor was United States Steel Corporation, Research Laboratory in Monroeville, Pa. Contributors to the MR&S effort were Messrs. Wei P. Chiang, John Daidola, George Chi and Naresh M. Maniar. Contributors to the U.S. Steel Corporation effort were Messrs. Roger Kline and John F. McDermott.

Preceding page blank

7. GLOSSARY OF SYMBOLS

b = effective design width of a plate, except for the flange of a stiffener, for which 0.5b is the width of the outstanding leg, measured from the center of the web

d = depth of the web of a stiffener or clear depth of web plate

e_t = total membrane-tension elongation of a stiffened-plate T-beam unit

t_F or t = thickness of a stiffener flange

t_W or w = thickness of the web of a stiffener

A, B, and k = material property constants relating to when buckling rupture will occur during plastic bending

A_f = area of stiffener flange

A_w = area of stiffener web

D = tensile test ductility

E = modulus of elasticity

E_{bc} = maximum value of bending plastic energy in stiffened-plate T-beam unit, occurring when a longitudinal stiffener flange buckles or ruptures

E_d = membrane tension plastic energy in deck

E_{mt} = membrane tension plastic energy in ship side

E_t = tangent modulus

F = force required to propagate longitudinally the yield line at the strike

I = moment of inertia about the axis of bending

K = $\varepsilon/\varepsilon_r$

L' = distance from the load to the nearest support for a right angle collision, or distance from the load to the support behind the load (in the direction opposite to the longitudinal direction of the strike) for an oblique collision

L'' = $L_t - L'$

L_d = length of damage, measured in the longitudinal direction

L_s = space between two consecutive web frames or swash bulkheads

Preceding page blank

L_t = value of L_a when the length of damage is only one or two spaces between web frames or swash bulkheads

L_y = yielded length of flange at beginning of local buckling of a stiffener flange

M_p = plastic bending moment in a stiffened-plate T-beam unit

P_b = load on a stiffened-plate T-beam unit that will occur during plastic bending

P_{tm} = a maximum value of the load on a stiffened-plate T-beam unit that will occur during membrane tension

P_{wf} = load exerted by the most highly strained stiffened-plate T-beam unit on a web frame at the instant that the web frame yields or buckles

R (with number subscript) = ratio of force (shear, moment, or thrust) within a web frame, subjected to a given lateral load, to the ultimate force

R_m = maximum value of R (with number subscript)

T = total membrane-tension thrust in a stiffened-plate T-beam unit after yielding

δ = a specified lateral deflection; also, the deflection of the centroid of a stiffened-plate T-beam unit

δ_{bc} = maximum value of δ during the bending phase

δ_m = maximum value of δ during the membrane-tension phase

δ_{tc} = value of δ at the instant of rupture, during the membrane-tension phase, when only one or two web-frame spaces are damaged

ε = longitudinal strain in hull

ε_c = longitudinal compression strain that results from elastic bending of the entire ship cross section

ε_ℓ = average strain over L"

ε_m = maximum bending-plus-membrane-tension strain at hull rupture

ε_r = $0.10 \left(\frac{D}{328} \right)$

L_t = value of L_a when the length of damage is only one or two spaces between web frames or swash bulkheads

L_y = yielded length of flange at beginning of local buckling of a stiffener flange

M_p = plastic bending moment in a stiffened-plate-T-beam unit

P_b = load on a stiffened-plate T-beam unit that will occur during plastic bending

P_{tm} = a maximum value of the load on a stiffened-plate T-beam unit that will occur during membrane tension

P_{wf} = load exerted by the most highly strained stiffened-plate T-beam unit on a web frame at the instant that the web frame yields or buckles

R (with number subscript) = ratio of force (shear, moment, or thrust) within a web frame, subjected to a given lateral load, to the ultimate force

R_m = maximum value of R (with number subscript)

T = total membrane-tension thrust in a stiffened-plate T-beam unit after yielding

δ = a specified lateral deflection; also, the deflection of the centroid of a stiffened-plate T-beam unit

δ_{bc} = maximum value of δ during the bending phase

δ_m = maximum value of δ during the membrane-tension phase

δ_{tc} = value of δ at the instant of rupture, during the membrane-tension phase, when only one or two web-frame spaces are damaged

ε = longitudinal strain in hull

ε_c = longitudinal compression strain that results from elastic bending of the entire ship cross section

ε_ℓ = average strain over L"

ε_m = maximum bending-plus-membrane-tension strain at hull rupture

ε_r = $0.10 \left(\frac{D}{328} \right)$

APPENDIX

CALCULATIONS

Preceding page blank

LNG CARRIER DAMAGE ANALYSIS

(PLASTIC ENERGY ANALYSIS)

Preceding page blank

Subject LNG CARRIER DAMAGE ANALYSIS

Ship or Project RIGHT ANGLE COLLISION - STRUCK BY VERTICAL BOW

Section B5DD Prepared by MC Date 10-1-73 Checked Reviewed

CONTENTS

1. CASE NO. 12a — RIGHT ANGLE COLLISION, $\frac{11}{16}$" OUTER SHELL, $\frac{1}{2}$" INNER SHELL PLATE, STRUCK BY VERTICAL BOW

1-1 → 1-42

2. AVERAGE ENERGY ABSORPTIONS OF CASE 12a

2-1 → 2-3

Preceding page blank

Subject LNG DAMAGE ANALYSIS

Ship or Project RIGHT ANGLE COLLISION - STRUCK BY VERTICAL BOW

Section BSDD Prepared by M.C Date 10-1-73 Checked Reviewed

CASE 12a

A. SUMMARY OF PLASTIC ENERGY ABSORBED BEFORE SPHERICAL LNG CONTAINMENT RUPTURE, STRUCK BY VERTICAL BOW.

ENERGY (IN-KIPS)

E_{bc} = PLASTIC BENDING ENERGY IN LONGL STIFFENED SIDE = 56718

E_{INT} = MEMBRANE TENSION PLASTIC ENERGY IN LONGL STIFFENED SIDE = 1,757,500

E_{PS} = SHEARING PLASTIC ENERGY IN NEB FRAMES = 84,576

E_d = DECK MEMBRANE TENSION PLASTIC ENERGY = 74,495

TOTAL ENERGY ABSORBED = 1,973,289 IN-KIPS

SHELL - DOUBLE

OUTER SHELL PLATE = $\frac{11}{16}$" MS

INNER SHELL PLATE = $\frac{1}{2}$" MS

DECK PLATE AT 25'-0" LEVEL = $\frac{11}{16}$" MS

M. Rosenblatt & Son, Inc.
DESIGN CALCULATION SHEET

No. 2087-12
Sheet 1 of 4-?

Subject LNG DAMAGE ANALYSIS

Ship or Project RIGHT ANGLE COLLISION - STRUCK BY VERTICAL BOW

Section BSDD Prepared by M.C Date 10-1-73 Checked Reviewed

CASE 12a

SUMMARY OF PLASTIC ENERGY ABSORBED BEFORE SPHERICAL LNG CONTAINMENT RUPTURE, STRUCK BY VERTICAL BOW.

ENERGY IN - KIPS

E_{bc} = PLASTIC BENDING ENERGY IN LONGL STIFFENED SIDE = 56718

E_{MT} = MEMBRANE TENSION PLASTIC ENERGY IN LONGL STIFFENED SIDE = 1.757,500

E_{PS} = SHEARING PLASTIC ENERGY IN WEB FRAMES = 84,576

E_d = DECK MEMBRANE TENSION PLASTIC ENERGY = 74,495

TOTAL ENERGY ABSORBED = 1,973,289 IN-KIPS

SHELL - DOUBLE

OUTER SHELL PLATE = $\frac{11}{16}$" MS

INNER SHELL PLATE = $\frac{1}{2}$" MS

DECK PLATE AT 25'-0" LEVEL = $\frac{11}{16}$" MS

M. Rosenblatt & Son, Inc.
DESIGN CALCULATION SHEET

No. 2087-12
Sheet 3 of 42

Subject LNG DAMAGE ANALYSIS
Ship or Project RIGHT ANGLE COLLISION - STRUCK BY VERTICAL BOW
Section BSOD Prepared by MC Date 8/28/79 Checked Reviewed TMS

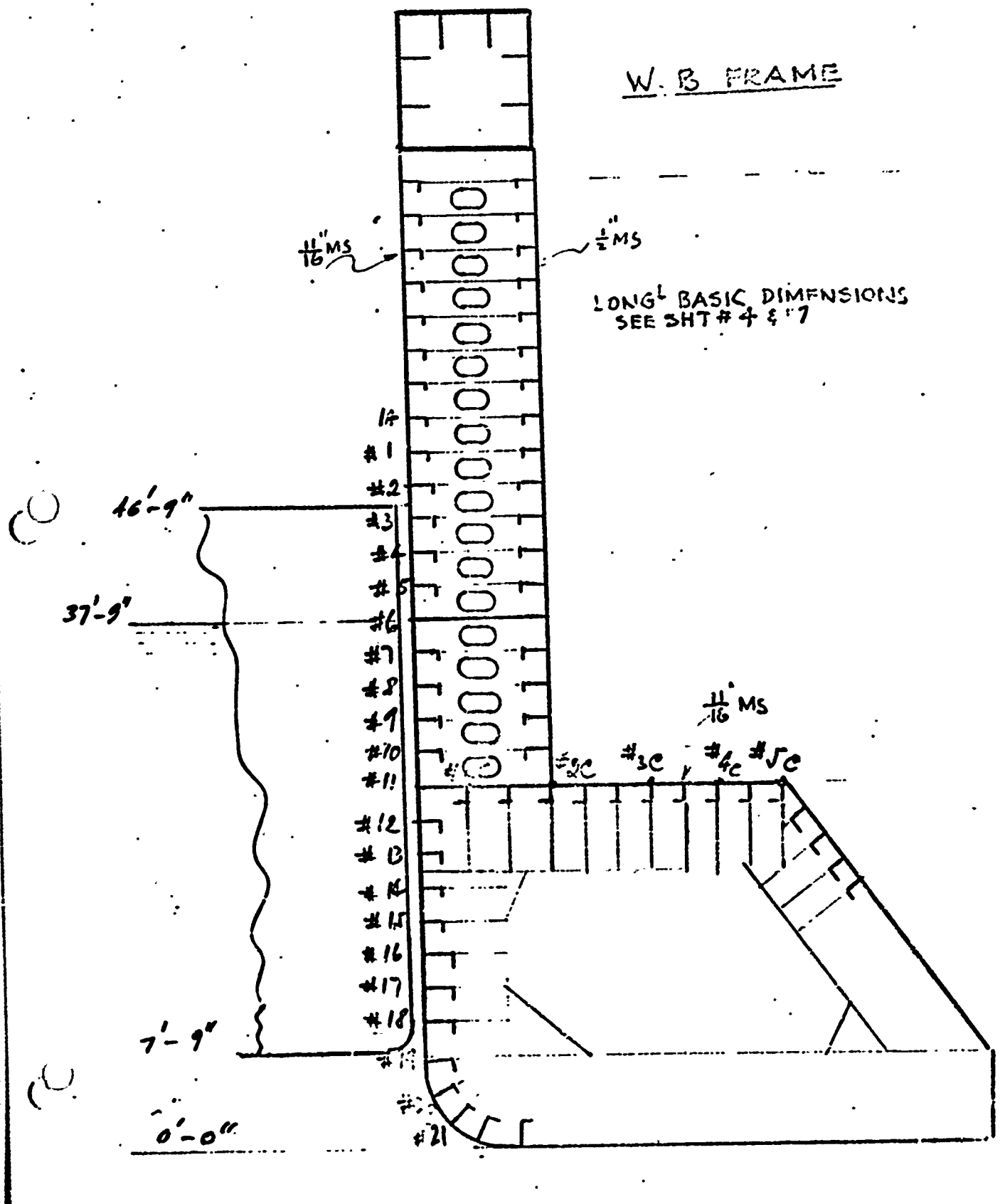

Inc.

T

No. 2087-12a

Sheet 4 of 42

AMAGE ANALYSIS

E COLLISION - STRUCK BY VERTICAL BOW

ed by MC Date 9/6/73 Checked Reviewed JLK

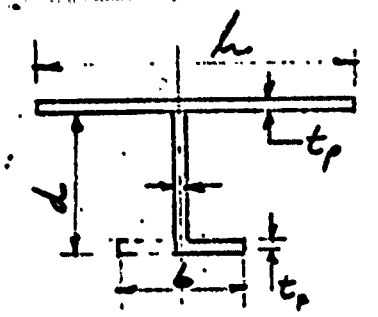

OUTER SHELL

*) ASSUMPTION

DOUBLE HULL

	1	2	3	4	5	6 *)	7	8	9	10	11 *)	12	13	14	15	16	17	18	19	20	21
S (IN)	11/16 t	13/16 - 1/2 t 6 3/16 - 5/8 t	—	—	—	11/16 t	19/16 - 1/2 t 6 3/16 - 5/8 t	—	—	—	11/16 t	10 - 1/2 t 6 3/16 - 1/2 t	—	—	→	14 5/16 - 1/2 t 6 3/16 - 1/2 t	—	—	—		→
THE T TO (IN)	11/16	—	—	—	—	—	—	—	—	—	—	—	—	—	—	—	—	—	→	1"	1"
STEEL TO (IN)	27.5	—	—					—	—	—			—	—	—		—	—	—	50.	50.
(IN²)	71.5	33.8	—	—	→	55.	33.8			→	55.	29.3	—	—	→	30.7	—	—	→	60.	60.
ERIA	950	1,900	—	—	→	58,500	1,900	—	—	→	58,500	381.	—	—	→	858.	—	—	→	980.	980.
KE	12	—	—	—	→	1.3	12.	—	—	→	1.3	12.	—	—	—	—	—	—	—	—	→
NESS	1/2	—	—	—	—	→	.625	—	—	→	1/2	—	—	—	—	—	—	—	—	—	→
E	24.	—	—	—	→	2.6	24.	—	—	→	2.6	24.	—	—	—	—	—	—	—	—	→
OF	14.6	19.25	—	—	→	94.	19.25	—	—	→	94.	10.	—	—	→	14.6	—	—	—	—	→
TH	.82	.62	—	—	→	.12	.62	—	—	→	.12	1.2	—	—	→	.82	—	—	—	—	→

M. Rosenblatt & Son, Inc.

No. 2087-129

DESIGN CALCULATION SHEET

Sheet 4 of 42

Subject LNG DAMAGE ANALYSIS

Ship or Project RIGHT ANGLE COLLISION - STRUCK BY VERTICAL BOW

Section B500 Prepared by MC Date 9/6/73 Checked Reviewed JHS

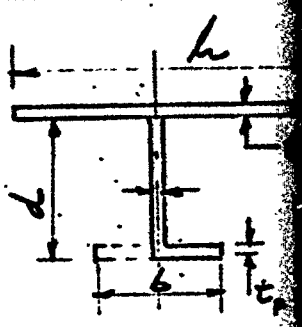

OUTER SHELL

*) ASSUMPTION

DOUBLE HULL

LONG'L NO.	1	2	3	4	5	6 *)	7	8	9	10	11 *)	12	13	14	15	16
LONGITUDINAL BASIC DIMENSIONS (IN)	17 1/2 x 1/2 6 3/16 x 5/8	19 1/4 x 1/2 6 3/16 x 5/8	—	—	—	11/16 PL	19 1/4 x 1/2 6 3/16 x 5/8	—	—	—	11/16 PL	10 x 1/2 6 3/16 x 1/2	—	—	→	17 1/2 x 1/2 6 3/16 x 5/8
t_p - THICKNESS OF THE SHELL PLATE ADJACENT TO LONGITUDINAL (IN)	11/16	—	—	—	—	—	—	—	—	—	—	—	—	—	—	—
h - WIDTH OF THE SHELL PLATE ADJACENT TO LONGITUDINAL (IN)	29.5	—	—	—	—	—	—	—	—	—	—	—	—	—	—	—
A_s - SECT. AREA OF LONGITUD. WITH SHELL PLATE (IN^2)	21.5	33.8	—	—	→	55.	33.8	—	—	→	55.	29.3	—	—	→	30.7
I - MOMENT OF INERTIA OF LONG'L WITH SHELL PLATE (IN^4)	950	1,900	—	—	→	58,500	1,900	—	—	→	58,500	381.	—	—	→	858.
b - BREADTH OF FLANGE = 2 x FLANGE OF F.B OR SINGLE (IN)	12	—	—	—	→	1.3	12.	—	—	→	1.3	12.	—	—	—	—
t_f - FLANGE THICKNESS (IN)	1/2	—	—	—	→	.625	—	—	—	→	1/2	—	—	—	—	—
b/t_f - BREADTH - TO RATIO.	24.	—	—	—	→	2.6	24.	—	—	→	2.6	24.	—	—	—	—
d - DEPTH OF WEB OF LONGITUD (IN)	14.6	19.25	—	—	→	94.	19.25	—	—	→	94.	10.	—	—	→	14.6
b/d - BREADTH - DEPTH RATIO	.82	.62	—	—	→	.138	.62	—	—	→	.138	(1).2	—	—	→	.82

No. 2087-12a

Sheet 5 of 42

CE ANALYSIS

LLISION - STRUCK BY VERTICAL SAW

MC Date 9/10/73 Checked Reviewed JAB

UTER SHELL.

Final

1	2	3	4	5	6	7	8	9	10	11	12	13	14	15	16	17	18	19	20	21
17.	19.	----	———	→	28.4	19.	———	———	→	28.4	16.	———	———	→	18.	———	———	———	———	→
172.	———	———	———	———	———	———	———	———	———	———	———	———	———	———	———	———	———	———	———	→
.41	.42	———	———	→	.67	.42	———	———	→	.67	.38	———	———	→	.41	———	———	———	———	→
.30	.32	———	———	→	.40	.32	———	———	→	.40	.27	———	———	→	.30	———	———	———	———	→
.23	.25	———	———	→	.462	.25	———	———	→	.462	.21	———	———	→	.25	———	———	———	———	→
.71	.32	———	———	→	.857	.32	———	———	→	.857	.28	———	———	→	.31	———	———	———	———	→
3.8	4.2	———	———	→	11.7	4.2	———	———	→	11.7	3.4	———	———	→	3.8	———	———	———	———	→
120.	100.	———	———	→	70.	100.	———	———	→	70.	180.	———	———	→	120.	———	———	———	———	→
0.0212	.0181	———	———	→	0.0352	.0181	———	———	→	.0352	.0263	———	———	→	.0212	———	———	———	———	→
1.82	1.56	———	———	→	3.0	1.56	———	———	→	3.0	2.26	———	———	→	1.82	———	———	———	———	→
[illegible]	[illegible]	———	———	→	[illegible]	[illegible]	———	———	→	[illegible]	[illegible]	———	———	→	[illegible]	———	———	———	———	→
[illegible]	570.	———	———	→	[illegible]	570.	———	———	→	[illegible]	300.	———	———	→	439.	———	———	———	———	→
8	365	———	———	→	8,000	365.	———	———	→	8000	132.	———	———	→	238	———	———	———	———	→
140.	214.	———	———	→	4,692	214.	———	———	→	4,692	77.6	———	———	→	140.	———	———	———	———	→
[illegible]	———	———	———	———	———	———	———	———	———	———	———	———	———	———	———	———	———	———	———	→

M. Rosenblatt & Son, Inc.

No. 2087-12a

DESIGN CALCULATION SHEET

Sheet 5 of 42

Subject MID DAMAGE ANALYSIS

Ship or Project 90° ANGLE COLLISION - STRUCK BY VERTICAL BOW

Section BSDD Prepared by MC Date 9/10/73 Checked Reviewed

OUTER SHELL

LONG'L NO.	1	2	3	4	5	6	7	8	9	10	11	12	13	14	15	16
L_y - FIELD LENGTH FIG. D-2 FOR U_y=35	12.	19.	—	—	→	28.4	19.	—	—	→	28.4	16.	—	—	→	18.
$L_t = L_J = L_s$	172.	—	—	—	—	—	—	—	—	—	—	—	—	—	—	—
VL_y/M_p FIG. D-3	.41	.49	—	—	→	.67	.42	—	—	→	.67	.38	—	—	→	.41
$VL_y/(VL_y+M_p)$	.30	.32	—	—	→	.40	.32	—	—	→	.40	.27	—	—	→	.30
CONST. A FOR U_y=35 FIG. D-4	.23	.25	—	—	→	.462	.25	—	—	→	.462	.21	—	—	→	.25
CONST. C FOR U_y=35	.11	.32	—	—	→	.857	.32	—	—	→	.857	.28	—	—	→	.31
[illegible]	3.8	4.2	—	—	→	11.7	4.2	—	—	→	11.7	3.4	—	—	→	3.8
PLASTIC [illegible]	130.	100.	—	—	→	70.	100.	—	—	→	70.	180.	—	—	→	12
PLASTIC MOMENT	0.0212	.0181	—	—	→	0.0352	.0121	—	—	→	.0352	.0263	—	—	→	.021
$L_{ft} = (L_y + L_t)/2$	1.82	1.56	—	—	→	3.0	1.56	—	—	→	3.0	2.26	—	—	→	1.8
MOMENT OF INERTIA	2.2×10^3	5.51×10^3	—	—	→	11.9×10^3	5.51×10^3	—	—	→	11.9×10^3	$2.\times10^3$	—	—	→	3.58×10^3
PLASTIC [illegible]	404.	570.	—	—	→	23,960.	570.	—	—	→	23,960.	300.	—	—	→	439.
[illegible]	8	365	—	—	→	8,000	365.	—	—	→	8000	132.	—	—	→	238
[illegible]	140.	214.	—	—	→	4,692	214.	—	—	→	4,692	77.6	—	—	→	14
E [illegible]	29×10^6	—	—	—	—	—	—	—	—	—	—	—	—	—	—	—

Inc.

No. 2087-12a

T 1 Sheet 6 of 42

RAMP ANALYSIS

ON - STRUCK BY VERTICAL SOW

ed by M. C. Date 9/6/73 Checked Reviewed JVB

Final

OUTER SHELL

	1	2	3	4	5	6	7	8	9	10	11	12	13	14	15	16	17	18	19	20	21
	0.1	—	—	—	—	—	—	—	—	—	—	—	—	—	—	—	—	—	—	—	→
DEFL. = 3.2 IN.	38.5																				→
	1,575	1,690	—	—	→	2,750	1,690	—	—	—	2,717	1,465	—	—	→	1,535			→	3,000	3,000
SC.	3.64	31.6	38.5	—	—	—	—	—	—	—	—	—	—	—	—	—	—	—	→	29.5	5.27
ON FACE IN.	133.	1,240	1,520	—	→	2,470	1,520	—	—	—	2,470	1,310	—	—	→	1,372		—	→	2,060	367.
HULL ND)	67.	620.	760.		—	1,235	760			—	=										
HULL TION)	"											327.	—	—	→	343.		—	→	515	92.
= 5.0	13.4	124.	152.	—	→	249.	152.	—	—	→	249.	65.4	—	—	→	68.6	—	—	→	103.	18.4
(IN)	0.73	6.3	7.7	—	→	7.8	7.7	—	—	→	7.8	3.9	—	—	→	3.9	-	—	—	4.0	.53

M. Rosenblatt & Son, Inc.

No. 2087-12a

DESIGN CALCULATION SHEET

Sheet 6 of 42

Subject LNG DAMAGE ANALYSIS

Ship or Project EIGHT ASSET CARRIER - STRUCK BY VERTICAL BOW

Section B500 Prepared by M.C. Date 9/6/73 Checked Reviewed MG

OUTER SHELL

LONG'L NO.	1	2	3	4	5	6	7	8	9	10	11	12	13	14	15	16
ε_R	0.1	—	—	—	—	—	—	—	—	—	—	—	—	—	—	—
MEMBRANE TENSION DEF. CAPACITY $\delta_{TC} = \sqrt{\frac{L^2}{C}(\varepsilon_u - \varepsilon_0) + \delta_{BC}^2}$	38.5															
AVERAGE MEMBRANE TENSION FORCE $T = A_S \sigma_y$ Equation	1,575	1690	—	—	→	2,750	1,690	—	—	—	2,710	1,465	—	—	→	1,5
δ_m = LESSER δ OR δ_{TC}	3.64	31.6	38.5	—	—	—	—	—	—	—	—	—	—	—	—	
NET LATERAL FORCE ON LONG'L DUE TO MEMBRANE TENSION ONLY $P_{tm} = 4T_0 \sin \frac{\theta}{2}$	133.	1,240	1,520	—	→	2,470	1,520	—	—	—	2,410	1,310	—	—	→	1,3
$P_L / 2$ (DOUBLE HULL SECTION)	67.	620.	760.		—	1,235	760			—	=					
P_{Lm} / ψ (SINGLE HULL SECTION)												327.	—	—	→	34
$P_{Lt} = \frac{P_{tm}}{2k_m}$ or $\frac{P_{Lm}}{+k_m}$ where $k_m = 5.0$	13.4	124.	152.	—	→	249.	152.	—	—	→	249.	65.4	—	—	→	68
$\delta_1 = \frac{P_{Lt} L_t}{2T}$ (IN)	0.73	6.3	7.7	—	→	7.8	7.7	—	—	→	7.8	3.9	—	—	→	3.

No. 2087-12a
Sheet 7 of 42

...F ANALYSIS
COLLISION - STRUCK BY VERTICAL BOW
...C Date 9/6/73 Checked Reviewed

...ER SHELL

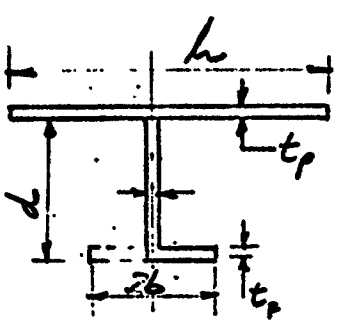

1	2	3	4	5	6 *)	7	8	9	10	11	12	13	14	15	16	17	18	19	
14 5/8 x 1/2 6 3/16 x 5/8	19 1/4 x 1/2 6 3/16 x 5/8	—	—	—	11/16 FL	19 1/8 x 1/2 6 3/16 x 1/2	—	—	→										
1/2	7/16	—	—	—	—	→	5/8	—	→										
20.		—	—	—	—	—	—	—	→										
26.0	29.2	—	—	→	55.	29.2	—	—	→										
1+0.	1900	—	—	→	51,500	1900	—	—	→										
12	—	—	—	→	1.3	12.	—	—	→										
1/2	—	—	—				—	—	→										
24	—	—	—	→	2.6	24	—	—	→										
14.6	19.25	—	—	→	94.	19.25	—	—	→										
.82	.62	—	—	→	.138	.62	—	—	→										

Gibbs & Cox, Inc.

DESIGN CALCULATION SHEET

No. 2087-12a

Sheet 7 of 42

Subject LIFE DAMAGE ANALYSIS

Ship or Project RIGHT ANGLE COLLISION - STRUCK BY VERTICAL BOW

Section ESDD Prepared by RLC Date 9/6/72 Checked Reviewed ZJG

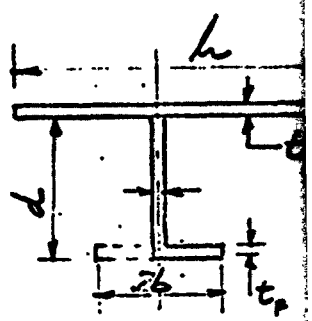

INNER SHELL

LONG'L NO.	1	2	3	4	5	6 *)	7	8	9	10	11	12	13	14	15	16
LONGITUDINAL BASIC DIMENSIONS (IN)	14 5/8 x 1/2 / 6 1/2 x 5/8	19 1/4 x 1/2 / 6 3/16 x 5/8	—	—	—	11/16 FB	19 1/4 x 1/2 / 6 1/16 x 1/2	—	—	→						
t_p - THICKNESS OF THE SHELL PLATE ADJACENT TO LONGITUDINAL (IN)	1/2	9/16	—	—	—	—	→	5/8	—	→						
h - WIDTH OF THE SHELL PLATE ADJACENT TO LONGITUDINAL (IN)	20.		—	—	—	—	—	—	—	→						
A_s - SECT. AREA OF LONGITUD. WITH SHELL PLATE (IN^2)	26.0	29.2	—	—	→	55.	29.2	—	—	→						
I - MOMENT OF INERTIA OF LONG'L WITH SHELL PLATE (IN^4)	1:0.	1900	—	—	→	58,550	1900	—	—	→						
b - BREADTH OF FLANGE = 2 xFLANGE OF F.B OR ANGLE (IN)	12	—	—	—	→	1.3	12.	—	—	→						
t_F - FLANGE THICKNESS (IN)	1/2	—	—	—	—	—	—	—	—	→						
b/t_f - BREADTH - TK RATIO.	24	—	—	—	→	2.6	24	—	—	→						
d - DEPTH OF WEB OF LONGITUD (IN)	14.6	19.25	—	—	→	99.	19.25	—	—	→						
b/d - BREADTH - DEPTH RATIO	.82	.62	—	—	→	.128	.62	—	—	→						

Inc.

No. 2087-12a
Sheet 13 of 4-2

CE ANALYSIS

GLE COLLISION - STRUCK BY VERTICAL BOW

ed by MC Date 9/6/73 Checked Reviewed

INNER SHELL

	1	2	3	4	5	6	7	8	9	10	11	12	13	14	15	16	17	18		
	0.1	—	—	—	—	—	—	—	—	→										
EFL.	38.5	—	—			—	—	—	—	→										
s x St.	1,800	1,415	—	—	—	→	2,250	1,415	—	—	→									
	3.6	31.6	38.5						—	→										
ow E/L.	110.	1,060	1,265	—		→	2,470	1,265	—	—	→									
	55.	520.	633	—	—	→	1,235	633.		—	→									

M. Rosenblatt & Son, Inc.

No. 2087-12a

DESIGN CALCULATION SHEET

Sheet 13 of 4-2

Subject LONG'L DAMAGE ANALYSIS

Ship or Project RIGHT ANGLE COLLISION - STRUCK BY VERTICAL BOW

Section BSVD Prepared by MC Date 9/6/73 Checked Reviewed WHG

INNER SHELL

LONG'L NO.	1	2	3	4	5	6	7	8	9	10	11	12	13	14
ε_2	0.1	—	—	—	—	—	—	—	—	→				
MEMBRANE TENSION DEFL. CAPACITY $c_{TC} = \sqrt{\frac{L^2}{\pi^2}(\varepsilon_y + \varepsilon_c)} + \delta_{LE}$	38.5	—	—	—	—	—	—	—	—	→				
INFLUENCE MEMBRANE TENSION FORCE $T_2 = H_2 C_{TC} \frac{\varepsilon - \varepsilon_{TC}}{\varepsilon_y - \varepsilon_{TC}} = H_2 \times 51.$	1,200	1,415	—	—	→	2,250	1,415	—	—	→				
c_{TC} - MIN c_{TC}	3.6	31.6	38.5						-	→				
NET LATERAL FORCE ON LONG'L DUE TO MEMBR TENSION ONLY $P_{LM} = 4T_2\delta_m/L$	110.	1,040	1,265	—	→	2,470	1,265	—	—	→				
$P_L/2$	55.	520.	633	—	→	1,235	633.		—	→				

No. 2097-12

Sheet 9 of 42

ANALYSIS

COLLISION - STRUCTURAL BOW

Date 1/24/72 Checked Reviewed

SPACE CONFIGURATION

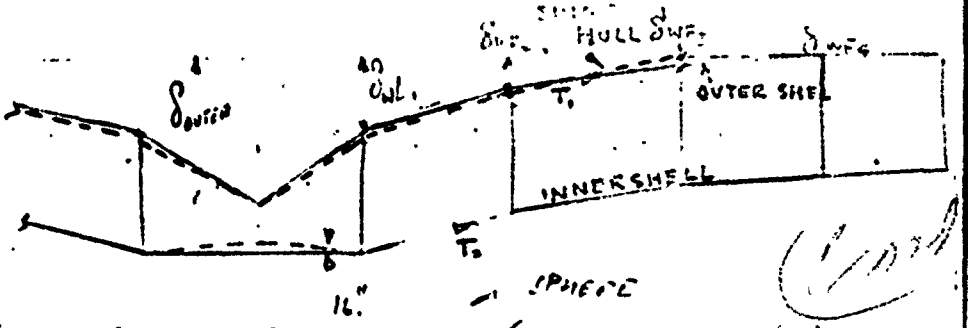

DOUBLE HULL SECTION + SINGLE HULL SECTION

1	2	3	4	5	6	7	8	9	10	11	12	13	14	15	16	17	18	19	20	21	REFERENCE
		100.	—	—	—	—	—	—	—	→											SHEET 1-33
3.4	116.7	142.3	—	—	—	—	—	—	—	—	—	—	—	—	—			→	109.0	19.4	SHEETS 1-6 & 1-34
023	.0198	.0242	—	—	—	—	—	—	—	→	/										SHEETS 1-6 & 1-35
010	.0088	.0107	—	—	—	—	—	—	—	→	/										SHEETS 1-6 & 1-36
											.0263	—	—	—	—	—	—	→	.0201	.0036	SHEETS 1-6 & 1-35
.52	30.72	37.44	—	—	—	—	—	—	—	→	//										
56	13.58	16.56	—	—	—	—	—	—	—	→											
											40.72	—	—	—	—	—	—	→	31.19	5.54	
400	79000	96,100	—	→	165,000	96,400	—	—	→	165,000											
											66300	—	—	→	69,400	—	—	→	104,000	18,500	

M. [illegible] & Son, Inc.

No. 2087-12 Q

DESIGN CALCULATION SHEET

1 Sheet 9 of 42

Subject [illegible] ANALYSIS

Ship or Project [illegible] COLLISION - STATIONAL SUM

Section [illegible] Prepared by [illegible] Date 1/24/73 Checked Reviewed [illegible]

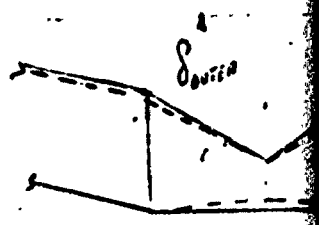

T- FRAME SPACE CONFIGURATION

DOUBLE HULL SECTION | SINGLE

LONG'L NO.	1	2	3	4	5	6	7	8	9	10	11	12	13	14	15
[illegible] = [illegible]			100.	---	---	---	---	---	---	---	→				
[illegible] = 142.3 [illegible]	13.4	116.7	142.3	—	—	---	--	---	—	—	—	---	---	---	---
[illegible] .0212 [illegible]	.0023	.0198	.0212	---	--	---	---	---	—	—	→				
[illegible] .0107 [illegible]	.0010	.0097	.0107	—	—	—	—	—	—	—	→				
[illegible] .0263 [illegible]												.0263	—	—	—
[illegible] - 9 [illegible]	3.52	30.72	37.46	---	---	—	—	—	—	—	→				
[illegible] 9 [illegible]	1.56	13.58	16.36	—	—	---			—	—	→				
[illegible]												40.72	—	---	---
[illegible]	3400	79000	96,100	—	→	165,000	96,400	—	—	→	165,000				
[illegible] 1.111 [illegible]												66300	.	---	→
ΣF = 1757.500															

M. Rosenblatt & Son, Inc.
DESIGN CALCULATION SHEET

No. 2037-12.4
Sheet 10 of 47

Subject LNG DAMAGE ANALYSIS

Ship or Project RIGHT ANGLE COLLISION - STRUCK BY VERTICAL BOW

Section BSDD Prepared by M. C Date 9/24/73 Checked Reviewed JHH

SUMMARY OF FORCES & R's

Logic No.	CAPACITY OF STRUCT. TO ABSORB FOLLOWING FORCES BEFORE FAILING			STRUCTURAL FORCES DUE TO $P_{tm}/2$ LOADS			CORRESPONDING R's				P_{tm} LOAD
	BENDING MOMENT (FT-K)	SHEAR (K)	CRUSHING (K)	= $P_{tm}/2$ or $P_{tm}/4$	BEND M. (K-FT)	SHEAR (K)	R_{SH}	R_{BEND}	R_{CRUSH}		$P_{tm}/2$ or $P_{tm}/4$
1	13,280	717	352		17,500	1560	2.18	.22			
2					20,200	1,760	2.18	1.57			
3				760.	22,200	1,300	1.82	1.67	2.16		760
4					22,500	650	.91	1.72	2.16		
5			↓	↓	21,400	350	.49	1.76	2.16		↓
6			1,048	2,470	23,200	800	1.11	1.79	2.36		2,470
7			352.	760	15,200	1,500	2.09	1.15	2.16		760
8					7,000	2,200	3.07	.53			
9					6000	2,900	4.05	—			
10		↓	↓		8700.	3,600	5.02	.66	↓		↓
11		950.	1350	2,470	17,100	4,300	4.53	1.29	1.83		2,470
12	↓		↓	327	12,000	1,700	1,79	.98	.24		327
13	2,230	↓	453		10,500	1,500	1.58	4.7	.72		
14		794.			8,000	1,250	1.57	3.59			
15				↓	5,500	950.	1.2	2.47	0		0
16				343	3,000	700	.88	1.35	.76		343
17					1,200			.54	↓		
18					1,520			.61			
19				↓	1,700			.76	↓		↓
20				515.	1,500			.81	.35		515
21		↓	↓	92.	1,900			.55	.2		92
1C			1,256	4,660	5,800	260					
2C				2,840	4,000	150					
3C	↓		↓	1,575	1,428	90					

M. Rosenblatt & Son, Inc.

DESIGN CALCULATION SHEET

No. 2047-12a

Sheet 11 of 42

Subject LNG SITING ANALYSIS

Ship or Project 2 GIT ANGLE COLLISION

Section BSDD Prepared by [illegible] Date [illegible] Checked Reviewed [illegible]

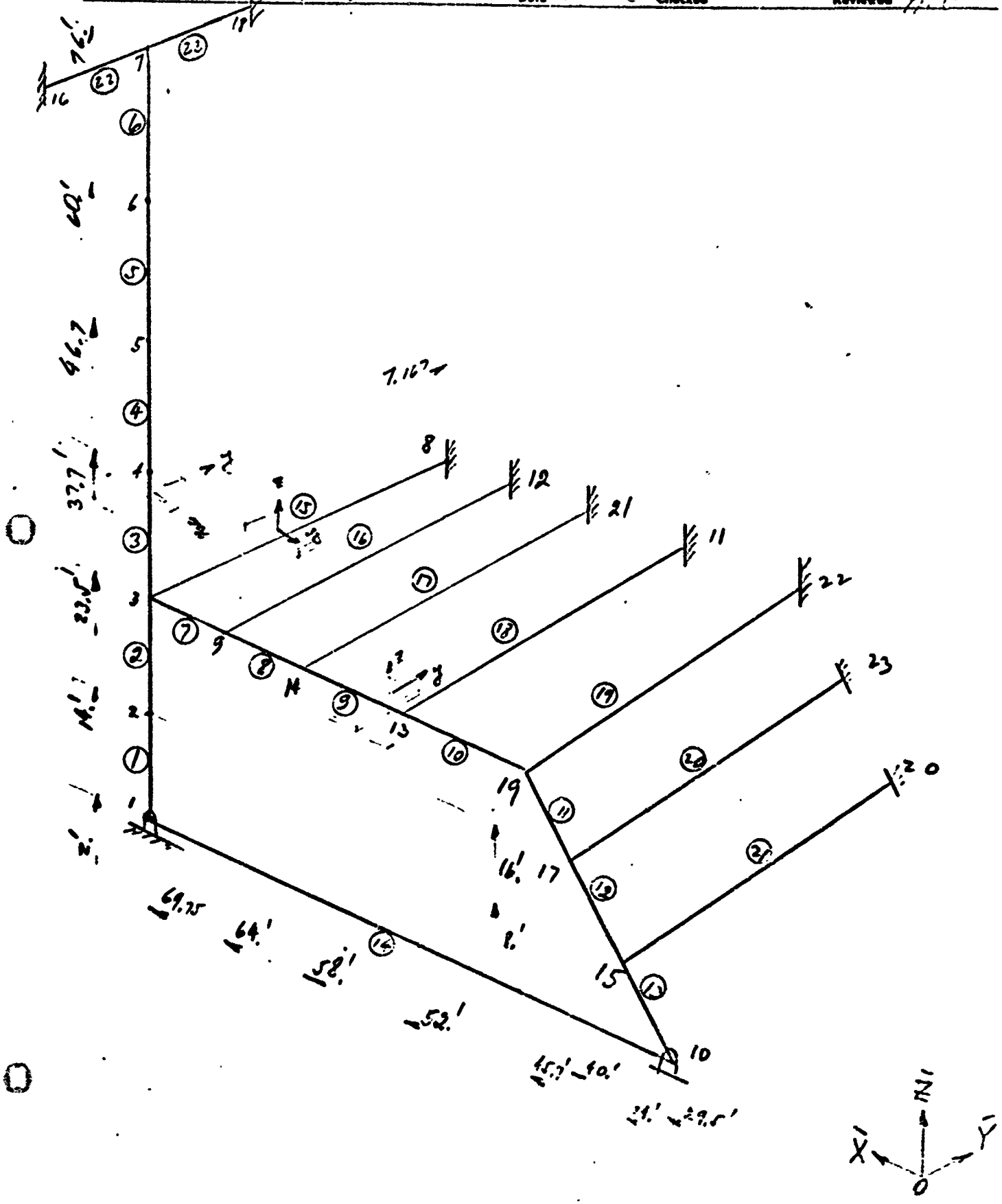

2087-12a

M. Rosenblatt & Son, Inc.
DESIGN CALCULATION SHEET

SHT 12 OF 42

Subject LNG DAMAGE ANALYSIS

Ship or Project RIGHT ANGLE COLLISION - STRUCK BY [illegible]

Section B5DD Prepared by M.C. Date 9/24/92 Checke

LOAD DIAGRAM

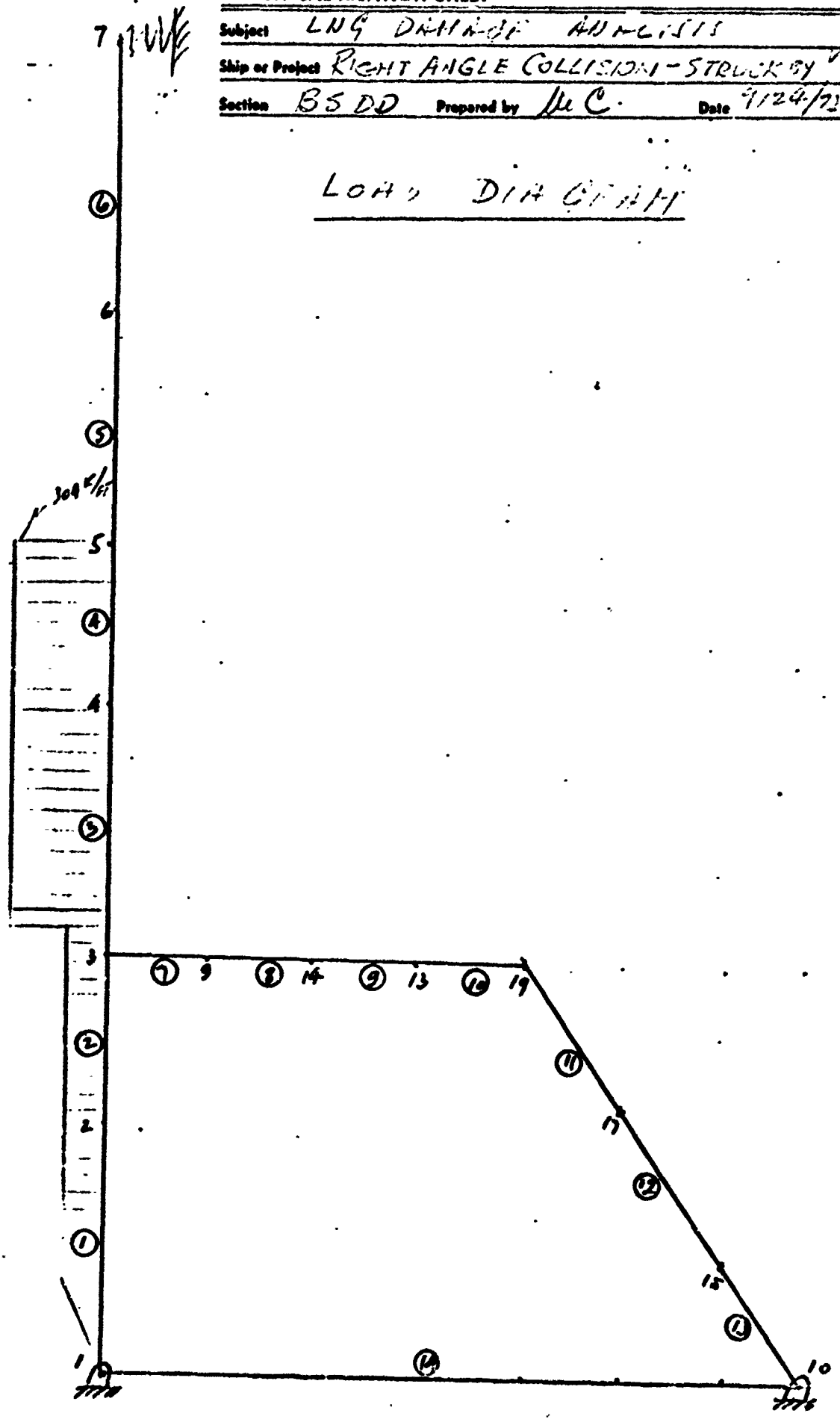

M. Rosenblatt & Son, Inc.
DESIGN CALCULATION SHEET

Subject LNG DAMAGE ANALYSIS

Ship or Project RIGHT ANGLE COLLISION - STRUCK BY VERT BOW

Section BSDD Prepared by M.C. Date 9/24/73 Checked JHS

LOADING DIAGRAM OF WEB FRAMES

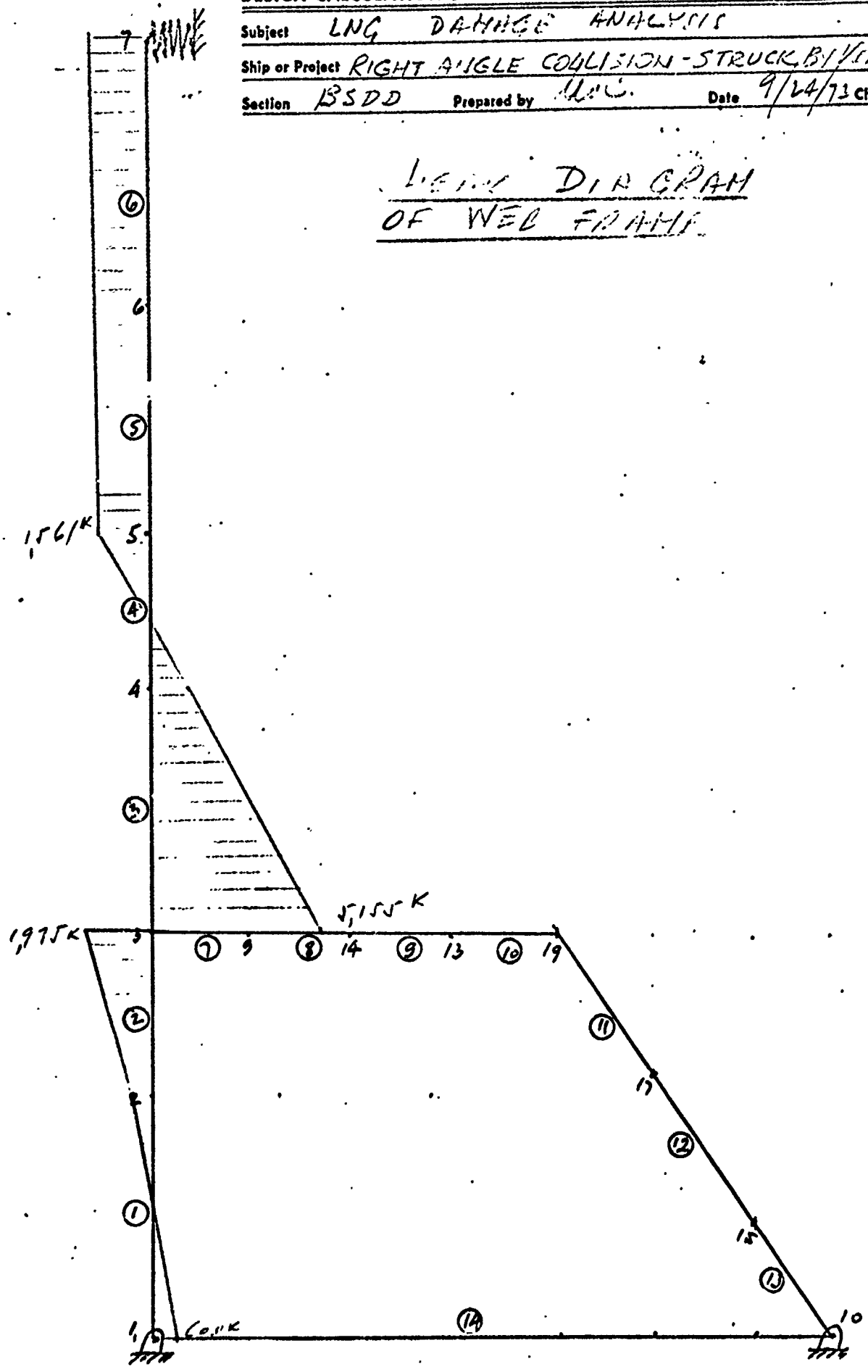

M. Rosenblatt & Son, Inc.

DESIGN CALCULATION SHEET

2021-120

SHT 14 OF 42

Subject 23,270 LNG DAMAGE ANALYSIS

Ship or Project 90° RIGHT ANGLE COLLISION-STATIONARY

Section 3500 Prepared by MC Date 9/24/72 Chec

MOMENT DIAGRAM OF THE WEB FRAME

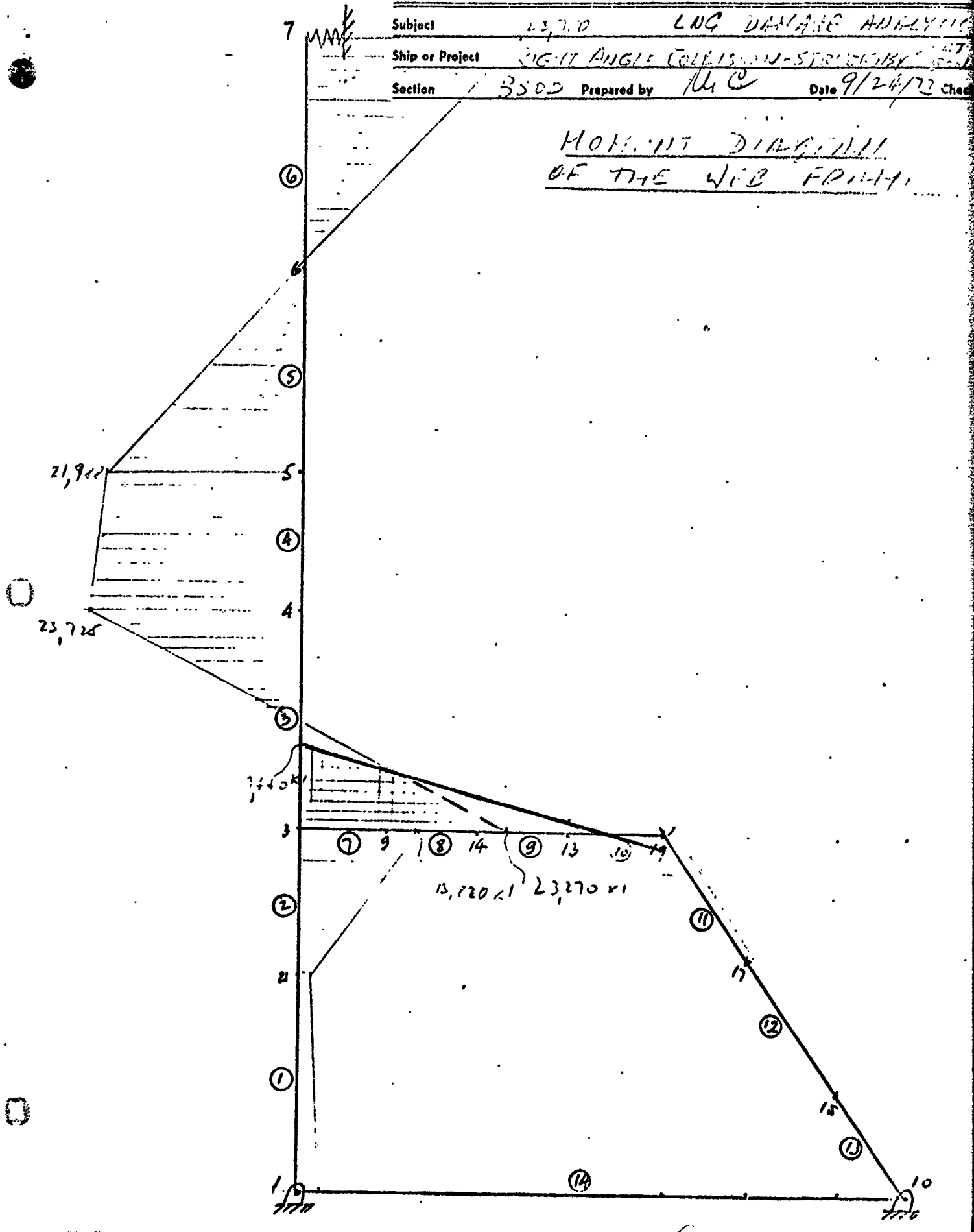

Subject LNG DAMAGE ANALYSIS

Ship or Project RIGHT ANGLE COLLISION

Section B500 Prepared by MC Date 9/6/73 Checked Reviewed JHB

(A) BENDING AT #1 — #12 (BASED ON D-15 CRITERIA)

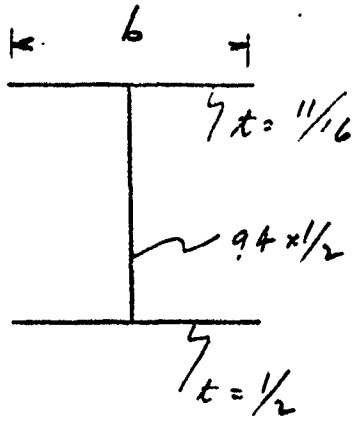

$a = 172$ IN
$t = 11/16$ IN

$\frac{a}{t} = \frac{172}{11/16} = 250$

FROM FIG D-15

$\frac{b}{t} = 52$

$b = \frac{11}{16} 52 = 35.7$ IN

	A	y	A_y	A_y^2	i_o
35.7 x 11/16	24.6	94.	2,310	217,000	-
94. x 1/2	47.	47.	2,210	103,800	34,610
35.7 x 1/2	17.90	-	-	-	
	88.5	51.2	4,520	320,800	
				+ 34610	
				355,410	
				231,900	

$I_{xx} = 123,310$ IN^4

$SM_1 = \frac{123,310}{51.2} = 2,410$ IN^3

$M_{PNF} = \frac{35.0 \times 2,410 \times 1.12}{12} = 7,860$ ft-K

M. Rosenblatt & Son, Inc. No. 2287-12A
DESIGN CALCULATION SHEET Sheet 1 of 42

Subject LNG DAMAGE ANALYSIS

Ship or Project RIGHT ANGLE COLLISION - STRUCK BY VERTICAL BOW

Section BSDD Prepared by M C Date 9/6/73 Checked Reviewed JJH

BENDING AT #13 - #19 (BASED ON D-√ CRITERIA)

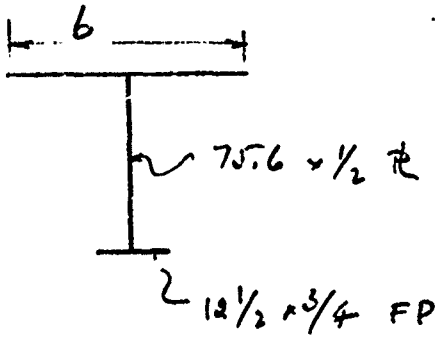

$$\frac{a}{t} = \frac{86}{11/16} = 125$$

$$\frac{b}{t} = 50$$

$$b = 50 \times 11/16 = 34.4 \text{ IN}$$

	A	y	Ay	Ay²	i_o
34.4 × 11/16	23.65	76.	1,800	136,600	—
75.6 × 1/2	37.80	38.5	1,455	56,000	18,000
12.5 × .75	9.38	—	—	—	—
	60.83	53.5	3,255	192,600	18,000

$$\frac{18,000}{210,600}$$

$$- \frac{174,000}{36,600 \text{ IN}^4}$$

$$I = 36,600 \text{ IN}^4$$

$$SM_{bott.} = \frac{36,600}{53.5} = 685. \text{ IN}^3$$

$$M'_{PNF} = \frac{35. \times 685 \times 1.12}{12} = \underline{2230} \text{ ft-K}$$

$$SM_{TOP} = \frac{36,600}{22.1} = 1,660 \text{ IN}^3$$

$$M''_{PNF} = \frac{35. \times 1660 \times 1.12}{12} = 5,420$$

M. Rosenblatt & Son, Inc.
DESIGN CALCULATION SHEET

No. 2027-1
Sheet 17 of 42

Subject LNG DAMAGE ANALYSIS

Ship or Project RIGHT ANGLE COLLISION - STRUCK BY VERTICAL BOW

Section B-500 Prepared by Date Checked Reviewed

(B) BENDING AT #1 - #2 (BASED ON 40% OF 14'-4" SPACING)

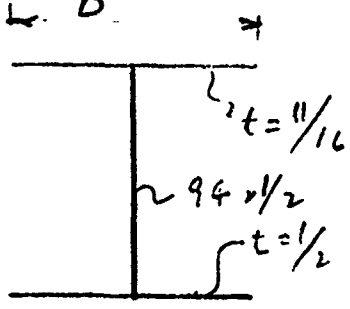

$b = 0.40 \times 172$
$= 68.8$ IN

	A	y	Ay	Ay^2	i_o
68.8 x 11/16	47.3	94.	4450	418,000	—
94 x 1/2	47.0	47.	2210	103,800	34,600
68.8 x 1/2	34.4	—			
	128.7	$\sqrt{1.8}$	6,660	$\sqrt{521,800}$	
				34,600	
				$\sqrt{556,400}$	
				346,000	
				$I_{xx} = 210,400$ IN^4	

$SM_{top} = \frac{210,400}{42.2} = 4,990$ IN^3; $SM_{bot} = \frac{210,400}{\sqrt{1.8}} = 4,060$ IN^3

$M'_{PW} = \frac{3\sqrt{\ } \times 4,060 \times 1.12}{12} = \frac{13280}{}$ K-ft

$M_{PW} = \frac{3\sqrt{\ } \times 4,990 \times 1.12}{12} = 16,300$ K-ft.

Subject LUG DAMAGE ANALYSIS

Ship or Project RIGHT ANGLE COLLISION, STRUCK BY VERTICAL BOW

Section B500 Prepared by [illegible] Date [illegible] Checked Reviewed J.H.G.

SHEAR LOADS @ #1 – #10

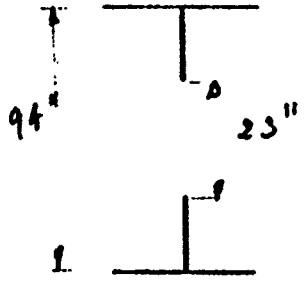

SHEAR AREA:

$A_s = (94 - 23) \times 1/2 = 35.5\ in^2$

$\tau_a = 20.2\ KSI$

$V_{SHEAR} = 35.5 \times 20.2 = \underline{717}\ K$

SHEAR LOADS @ #11 – #13

$A_{sh} = 94 \times 1/2 = 47.\ in^2$

$V_{shear} = 47. \times 20.2 = 950.\ KIPS$

SHEAR LOADS @ #14 – #21

$d = 75.6"$

$a = 29.5"$; $\frac{d}{a} = \frac{75.6}{29.5} = 2.56$; $\frac{d}{t} = 151$

from Fig D-8

$\tau_a = 20.2$; $\sigma_{ta} = 0$

$V_p = 20.2 \times dt = 20.2 \times 78.6 \times 1/2 = \underline{794}\ K.$

Subject L.N.G. DAMAGE ANALYSIS

Ship or Project RECTANGULAR COLLISION ATTACK BY VERTICAL BOW

Section 3000 Prepared by MC Date 9/10/73 Checked Reviewed TWK

COMPRESSION AT # 1C

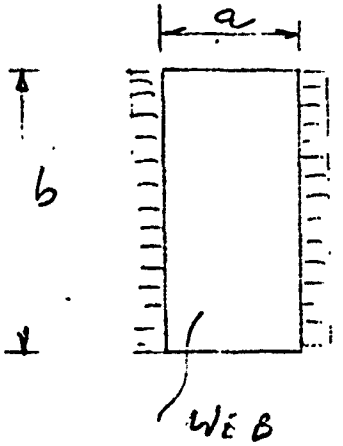

(Ref.: "A Design Manual on the Buckling Strength of Metal Structures" by Bleich; SNAME Bull. #22, Page 8)

$t = 1/2"$; $b = 29.5"$; $a = 29.5"$

ASSUMPTION
ONE UNLOADED EDGE SIMPLY SUPPORTED THE OTHER FIXED

$$\frac{\sigma_c}{\eta} = 26,750,000 \left(\frac{0.5}{29.5}\right)^2 \left(\left(\frac{29.5}{29.5}\right)^2 + 2.28 + 2.46\left(\frac{29.5}{29.5}\right)^2\right)$$

$$= 10,800 \text{ psi}$$

$$F'_{PNF} = 10.8 \times 29.5 \times 0.5 = 408 \text{ KIPS}$$

(CAPACITY of WEB)

LOWER DECK PANELS

$b = 172$; $a = 29.5"$; $t = 11/16"$

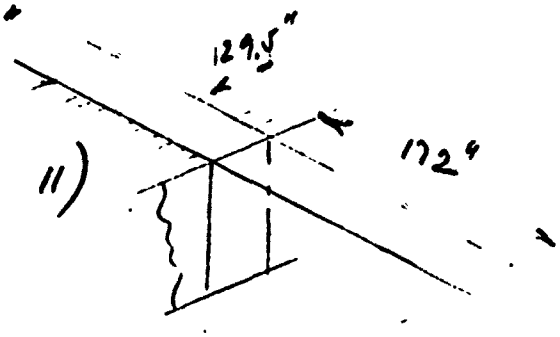

ALL EDGES FIXED
(see ABOVE REFERENCE Page 11)

$$\frac{a}{b} = \frac{29.5}{172} = 0.172$$

Let $k = 1.3$

$$\frac{\sigma}{\eta} = 26,750,000 \left(\frac{0.5}{29.5}\right)^2 1.3 = 10,400 \text{ psi}$$

$$F''_{PNF} = 10.0 \times 172 \times 0.8 \times 11/16 = 948 \text{ KIPS}$$

TOTAL $F_{PNF} = F'_{PNF} + F''_{PNF} = 408 + 948 = \underline{1356 \text{ KIPS}}$

Subject LNG DAMAGE ANALYSIS

Ship or Project SUBTANGLE COLLISION, STRUCK BY VERTICAL BOW

Section B3DD Prepared by [illegible] Date [illegible] Checked Reviewed [illegible]

CRUSHING LOAD @ #11

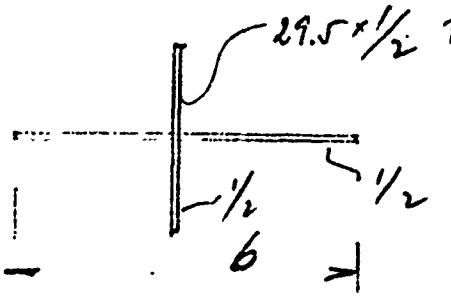

$a = 172$

$t = 11/16$

$$\frac{a}{t} = \frac{172}{11/16} = 250$$

$$\frac{b}{t} = \sqrt{3}$$

$$b = \sqrt{3} \cdot 11/16 = 36.4''$$

$$A_c = 29.5 \times 1/2 + 36.4 \times 11/16 = 39.75 \text{ in}^2$$

$$I = \frac{0.5 \times 29.5^3}{12} = 1,070 \text{ in}^4$$

$$r = \sqrt{\frac{1,070}{39.75}} = 5.19$$

$$\frac{l}{r} = \frac{94}{5.7} = 18.1$$

From fig D-14

$\sigma_a = 34.$ KSI

$P_{crushing} = 34.0 \times 39.75 = 1350$ KIPS

Subject LNG DAMAGE ANALYSIS

Ship or Project RIGHT ANGLE COLLISION, STOCK BY VERTICAL BOW

Section BSDD Prepared by M.C Date 9/6/73 Checked Reviewed JHB

CRUSHING AT 13 - 20

$$\frac{a}{t} = \frac{29.5}{0.5} = 59$$

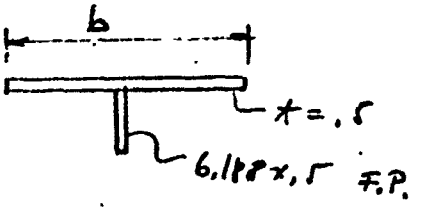

FROM FIG D-15

$$\frac{b}{t} = 42.5$$

$$b = 42.5 \times 0.5 = 21.25 \text{ IN}$$

$$A_c = 21.25 \times 0.5 + 6.188 \times 0.5 =$$

$$= 13.72 \text{ IN}^2$$

$$F_{cr} = 13.72 \times 33 = \underline{453 \text{ KIPS}}$$

M. Rosenblatt & Son, Inc.

No. 2037-12R

DESIGN CALCULATION SHEET

Sheet 27 of 42

Subject LNG DAMAGE ANALYSIS

Ship or Project RIGHT ANGLE COLLISION - TRUCK HIT VERTICAL BOW

Section ESDD Prepared by MC Date 9/12/77 Checked Reviewed

CRUSHING FORCE @ #6

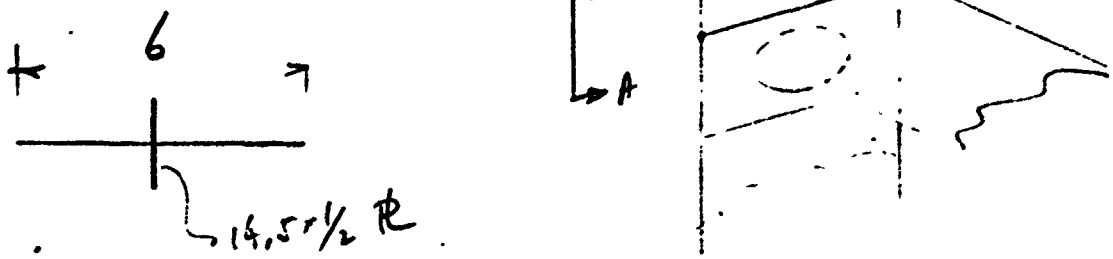

$a = 172$; $t = 11/16$

$\frac{a}{t} = \frac{172}{11/16} = 250$

$\frac{b}{t} = \sqrt{3}$; $b = \sqrt{3} \times \frac{11}{16} = 36.4$

$A_c = 14.5 \times 1/2 + 36.4 \times 11/16 = 32.25\ in^2$

$I = \frac{0.5 \times 14.5^3}{12} = 127\ in^4$

$r = \sqrt{\frac{127}{32.25}} = 1.985\ in$

$L_c = 94$

$\frac{L_c}{r} = \frac{94}{1.985} = 47.3$

$\sigma_{cr} = 32.5$ (FIG D-14)

$P_{crush} = 32.5 \times 32.25 = 1047\ kips$

M. Rosenblatt & Son, Inc. No. 2067-12

DESIGN CALCULATION SHEET Sheet 23 of 47

Subject LNG DAMAGE ANALYSIS

Ship or Project RIGHT ANGLE COLLISION, STRUCK BY VERTICAL BOW

Section BSDD Prepared by JMC Date 4/3/73 Checked Reviewed

CRUSHING LOAD @ #1-#5 & #7-#10

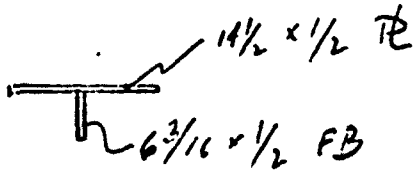

	A	y	Ay	Ay²	i
14.5 x .5	7.25	0.25	1.8	—	
6.188 x .5	3.09	3.59	11.1	39.8	9.9
	10.34	1.25	12.9	39.8	
				+ 9.9	
				49.7	
				− 16.2	
				I = 33.5 in⁴	

$$h = \sqrt{\frac{33.5}{10.34}} = 1.8$$

$$\frac{kl}{h} = \frac{1 \times 64}{1.8} = 35.5$$

FIG D-14

$\sigma_c = 34.$ KSI

$P_{cc} = 34.0 \times 10.34 = 352.$ KIPS

Subject LNG DOCKING ANALYSIS

Ship or Project RIGHT ANGLE COLLISION, STRUCK BY VERTICAL BOW

Section BSDD Prepared by MLC Date 7/83 Checked Reviewed BJL

STRESS IN THE BOX GIRDER DUE TO HIS FRAME LOADINGS

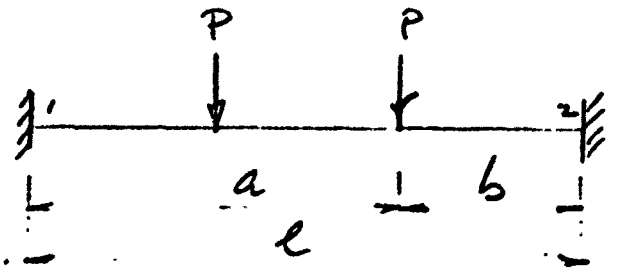

$a = \frac{2}{3}\ell$; $b = \frac{\ell}{3}$; $\ell = 3 \times 172 = 516$ IN

@ support 1"

$$M_1 = M_1' + M_1'' = \frac{Pab^2}{\ell^2} + \frac{Pb^2a}{\ell^2}$$

$$= \frac{Pab}{\ell^2}(a+b) = \frac{P\frac{2\ell}{3}\cdot\frac{\ell}{3}\cdot\ell}{\ell^2} = \frac{2}{9}P\ell$$

Since $SM = 36{,}200\ IN^3$

$$\sigma = \frac{\frac{2}{9}P\ell}{36{,}200} = 0.0031P$$

Subject LIVE LOADING ANALYSIS

Ship or Project EIGHT MILE CREEK BRIDGE / STRUCK BY NATIONAL GUARD

Section BSOD Prepared by [illegible] Date [illegible] Checked [illegible] Reviewed [illegible]

BOX GIRDER

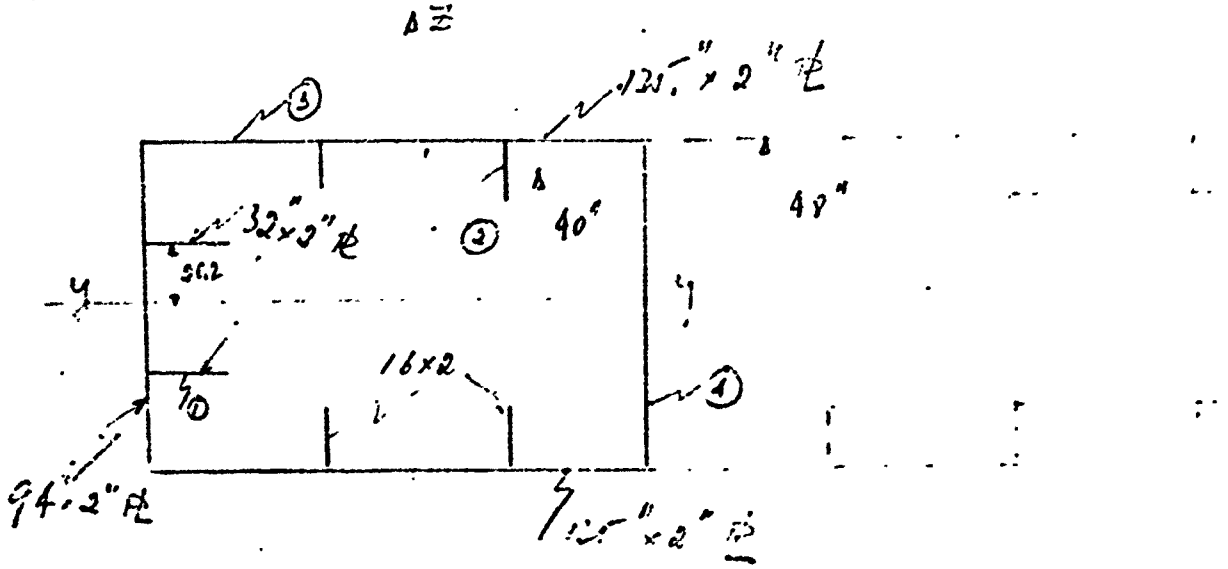

$$A = 2\times(135. + 32. + 32. + 2\times16)\times2$$
$$= 1{,}16+\ IN^2$$

$$I_{xx} = 2\left[32\times2\times\overline{20.2}^2 + 2(16\times2)\times\overline{40}^2 + \frac{2\times\overline{94}^3}{12} + 135.\times2\times\overline{48}^2\right]$$
$$= 2\left[26{,}100 + 102{,}400 + 138{,}600 + 620{,}\text{---}\right]$$
$$\approx 1{,}77\text{-}{,}\text{---} \ IN^4 \approx 12{,}3\text{--} \ IN^2 FT^2$$

$$I_x = \frac{2t^2(12.-2)^2 3+^2}{132\times2 + 94\times2 - 2\times2^2} = 2{,}10\text{-}{,}\text{---} \ IN^4 \approx \underline{1\text{-},\text{---} \ IN^4}$$

$$SM_{xx} = -\frac{177{,}\text{---}}{49.} = 36{,}200 \ IN^3$$

M. Rosenblatt & Son, Inc. No. 7047-126

DESIGN CALCULATION SHEET Sheet 7 of 47

Subject LIP DAMAGE ANALYSIS

Ship or Project EIGHT KNOT COLLISION, STRUCK BY VERTICAL BOW

Section BSDD Prepared by [illegible] Date 5/3/73 Checked Reviewed JHK

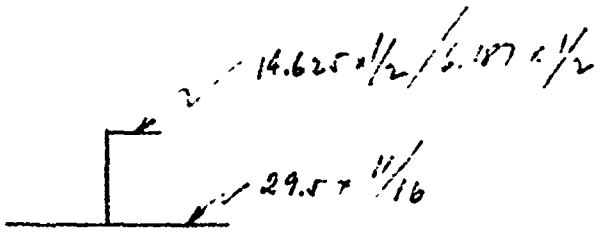

	A	y	Ay	Ay²	i₀
29.5 x 0.688	20.3	0.344	7.0	2.4	
14.625 x 1/2	7.31	8.00	58.5	467.8	44.
6.187 x 1/2	3.096	16.5	51.	743.8	
	30.71	3.7	113.5	1,217	
				44	
				1,258	
				− 420	

I = 838. in⁴

A = 30.71

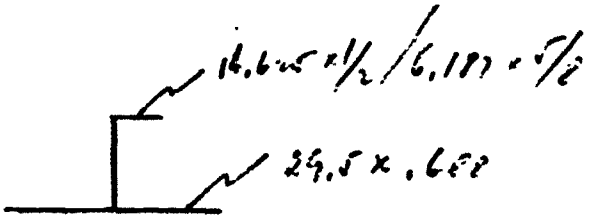

	A	y	Ay	Ay²	i₀
29.5 x 0.688	20.3	0.344	7.0	2.4	—
14.625 x 1/2	7.31	8.0	58.5	467.8	44.
6.187 x .625	3.86	16.6	60.3	940.	—
	31.47	4.0	126.8	1,410	
				44	
				1454	
				504	

I = 950. in⁴

A = 31.47 in²

Subject LUG DAMAGE ANALYSIS

Ship or Project RIGHT ANGLE COLLISION, STRUCK BY VERTICAL BOW

Section RSDD Prepared by W.S. Date 2/6/73 Checked Reviewed JWK

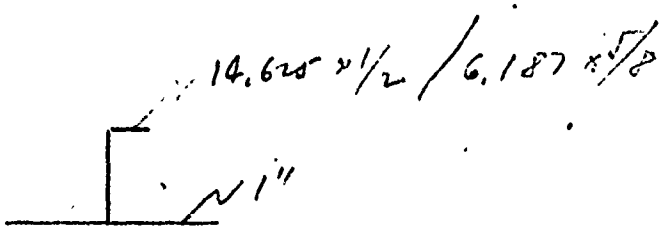

	A	y	Ay	Ay²	i_o
50 x 1"	50.	.5	25.	12.5	—
14.625 x 1/2	7.31	8.0	58.5	467.9	44
6.187 x 1/2	3.096	15.5	48.	743.8	—
	60.406	2.18	131.5	1,224	44.
				44	
				1,268	
				287	

$I = 981.1 in^4$

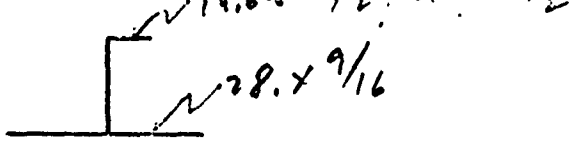

	A	y	Ay	Ay²	i_o
28 x 9/16	15.7	.28	4.4	1.	—
14.625 x 1/2	7.3	8.	58.5	467.1	44
6.187 x 1/2	3.1	15.5	48	743.8	
	26.1	4.25	110.9	1212.6	
				44.	
				1256.6	
				470.	

$I = 786.6 in^4$

Subject LNG DAMAGE ANALYSIS

Ship or Project RIGHT ANGLE COLLISION, STRUCK BY VERTICAL BOW

Section B.S.D.D. Prepared by M.C. Date 9/6/73 Checked Reviewed

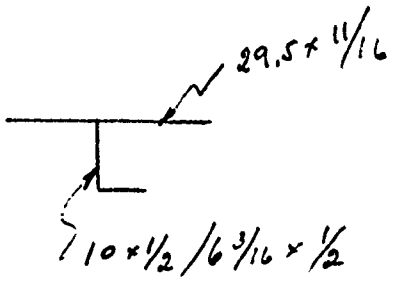

	A	y	I_y	I_y'	i_o
29.5 x 0.688	20.3	10.35	210.1	2.75	—
10 x 1/2	5.0	5.	25.	125	41.
6.187 · 0.5	3.09	.25	.8		—
	28.4	8.31	235.9	2,300	
				41	
				2,341	
				− 1,960	
				I = 381 IN^4	

#6 & #11

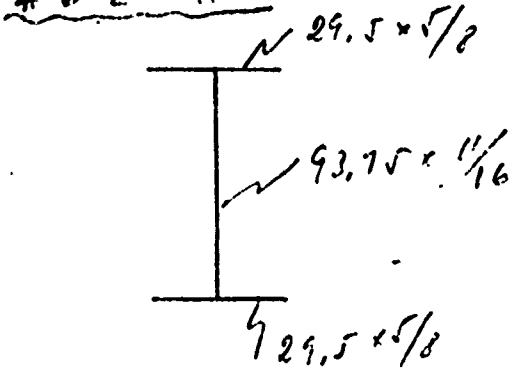

$A = 2(29.5 \times 5/8) + 93.75 \times 11/16$

$= 37. + 64 = 111.$ IN^2

$A' = 55.5$

$I = 2\left(29.5 \times \frac{5}{8}\right) \cdot 47.18^2 + \frac{11}{16}\frac{93.75^3}{12}$

$= 117,$ IN^4

$I' = \frac{I}{2} =$ 58,500 IN^4

M. Rosenblatt & Son, Inc. No. 2027-12

DESIGN CALCULATION SHEET Sheet 29 of 42

Subject LNG DRIVER ANALYSIS

Ship or Project RIGHT ANGLE COLLISION - STRUCK BY VERTICAL RAM

Section BSDD Prepared by M.C Date 9/5/73 Checked Reviewed TH-6

(13) - (16) & (18) - (21)

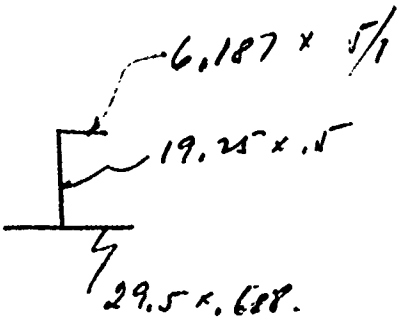

	A	y	Ay	Ay^2	i_o
29.5 x .688	20.3	.344	7.0	2.4	
19.25 x .5	9.625	10.31	99.2	1,022.8	297.
6.187 x .625	3.866	20.25	78.3	1,585.2	
	33.7	.546	184.5	2,610	
				+ 297	
				2,907	
				- 1,008	

$A' = 33.8\ in^2$

$I' = 1,819\ in^4 \approx 1,800\ in^4$

M. Rosenblatt & Son, Inc.
DESIGN CALCULATION SHEET

No. 2057-12a
Sheet 30 of 42

Subject LNG DAMAGE ANALYSIS
Ship or Project RIGHT ANGLE COLLISION STRUCK BY VERTICAL BOW
Section B.S.D.D. Prepared by M.C. Date 9/10/73 Checked Reviewed

TAPER OF DEFORMATION ABOVE STRICKING SHIP TOP

(Ref.: PAGE D-27)

$$H_1 = \frac{t\Delta_1\sigma_y}{h_1} = \frac{t\Delta_1^3 E}{2h_1^3}$$

$$\Delta_1 = 1.42''$$

1 - 1
2 - 2
3 - 3

$$H_2 - H_1 = \left(\frac{\Delta_2}{h_2} - \frac{\Delta_1}{h_1}\right) t\sigma_y = \frac{2\pi^2 E A_2 (\Delta_1)^3}{L_d^4}$$

$$A_2 = A_3 = 33.8\ in^2$$

$$L_d = 172''$$

$$H_2 - H_1 = \frac{3 \times \pi^2 \times 30{,}000 \times 33.8 \times 1.42^3}{(172)^4} = .0981$$

$$\Delta_2 = 29.5\left(\frac{.0981}{0.688 \times 35} + \frac{1.42}{29.5}\right) = 1.53''$$

$$H_3 - H_2 = \frac{2\pi^2 E A_1 (\Delta_1 + \Delta_2)^3}{L_d^4} = \frac{2\pi^2 \times 30{,}000 \times 31.5\ (1.42 + 1.53)^3}{172^4}$$

$$= 0.82$$

$$H_3 - H_2 = \left(\frac{\Delta_3}{h_3} - \frac{\Delta_2}{h_2}\right) t\sigma_y =$$

$$\Delta_3 = \left(\frac{0.82}{0.688 \times 35} + \frac{1.53}{29.5}\right) 29.5 = 2.53''$$

Subject LNG DAMAGE ANALYSIS

Ship or Project RIGHT ANGLE COLLISION. STRUCK BY VERTICAL BOW

Section BSDD Prepared by MC Date 9/10/73 Checked Reviewed

$$H_4 - H_3 = \frac{2\bar{u}^2 E A_3 (\Delta_1 + \Delta_2 + \Delta_3)^3}{L_{a1}^4} = 5.64$$

$$\Delta_4 = \left(\frac{5.64}{0.188 \times 35} + \frac{2.53}{29.5} \right) 29.5 = 10.73 \text{ IN}^3$$

$$\Delta_1 + \Delta_2 + \Delta_3 + \Delta_4 = 16.21 \text{ IN}$$

$$\Delta_1' = 38.46 \left(\frac{1.42^{1.5}}{1.42^{1.5} + 1.53^{1.5} + 2.53^{1.5} + 10.73^{1.5}} \right) = 1.5''$$

$$\Delta_2' = 38.46 \times \frac{1.53^{1.5}}{\sum_1^4 \Delta_i'} = 1.68''$$

$$\Delta_3' = 38.46 \cdot \frac{2.53^{1.5}}{\sum_{i=1}^4 \Delta_i'} = 3.64''$$

$$\Delta_4' = 38.46 \frac{10.73^{1.5}}{\sum_1^4 \Delta_i'} = 31.6''$$

Subject LNG DAMAGE ANALYSIS

Ship or Project RIGHT ANGLE COLLISION - STRUCK BY VERTICAL BOW

Section BSDD Prepared by MC Date 9/10/73 Checked Reviewed JHL

TAPER OF DEFORMATION BELOW TOP OF FOREFOOT OF STRIKING SHIP

$$H_1 = \frac{t\,\Delta_1 \sigma_y}{L_1} = \frac{t\,\Delta_1^3 E}{2L_1^3}$$

$$\Delta_1 = 1.42''$$

$$H_2 - H_1 = \left(\frac{\Delta_2}{L_2} - \frac{\Delta_1}{L_1}\right) t\,\sigma_y =$$

$$= \frac{3\bar{u}^2\, 30{,}000 \times 40.0 \times \overline{1.42}^3}{(86.)^4} = 1.42$$

Since $L_1 = 86$

$A_1 = 20.7$

$$\Delta_2 = 29.5 \times \left(\frac{1.42}{0.688 \times 35.} + \frac{1.42}{29.5}\right) = 3.16$$

$$H_3 - H_2 = \frac{3\bar{u}^2 E A (\Delta_1 + \Delta_2)^3}{L_1^4} = \frac{2\bar{u}^2 30{,}000 \times 40.0\,(4.58)^3}{86^4}$$

$$= 61.3 \text{ TO HIGH}$$

USE ONLY $\Delta_1 = 1.42''$; $3.16''$

$$\Delta_1' = 38.46 \frac{\Delta_1^{1.5}}{\Delta_1^{1.5} + \Delta_2^{1.5}} = 38.46 \times \frac{1.42^{1.5}}{1.42^{1.5} + 3.16^{1.5}}$$

$$= 5.27''$$

$$\Delta_2' = 38.46 \frac{3.16^{1.5}}{9.25} = 29.5''$$

FLOW CHART OF THE CALCULATION PROCEDURE OF THE DOUBLE HULL PLASTIC DEFORMATION

MAX. DEFLECTION OF THE INNER HULL

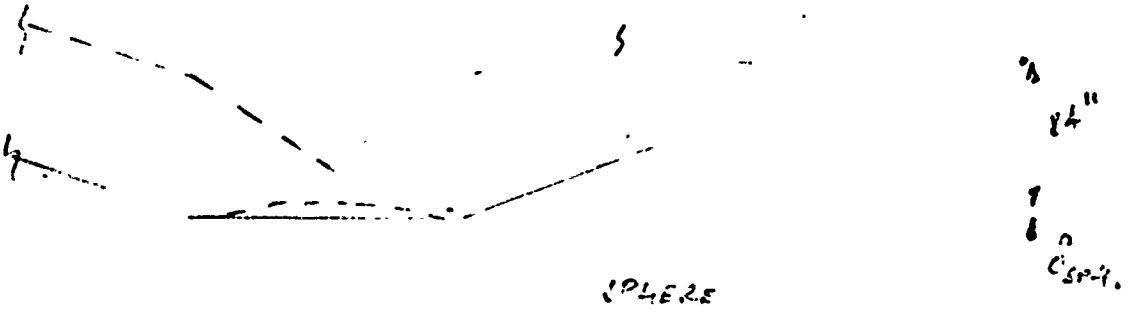

INNER SHELL INCURSION INTO SPHER

$$\delta_{SPH} = 0.2 \frac{R}{E} \sigma_y \frac{\varepsilon_{ts}}{\varepsilon_y}$$

where $R = 729.5"$

$E = 11.2 \times 10^3$ KSI

$\sigma_y = 20.$ KSI

$\varepsilon_y = \frac{20.}{11.2 \times 10^3} + 0.002 = 0.00378$

$\varepsilon_{ST} = 0.23$

$$\delta_{SPH} = 0.2 \times \frac{729.5" \times 20.}{11.2 \times 10^3} \times \frac{0.23}{0.00378} = 15.85 \text{ IN} \cong \underline{16.}"$$

MAX. DEFLECTION OF INNER SHELL:

$\delta_{INNER} = 24 + 16. = \underline{100.}$ IN

M. Rosenblatt & Son, Inc.
DESIGN CALCULATION SHEET

No. 20-[illegible]
Sheet 24 of [illegible]

Subject LNG DAMAGE ANALYSIS

Ship or Project [illegible] COLLISION - [illegible] BY VERTICAL [illegible]

Section BSDD Prepared by [illegible] Date 10-1-73 Checked [illegible] Reviewed [illegible]

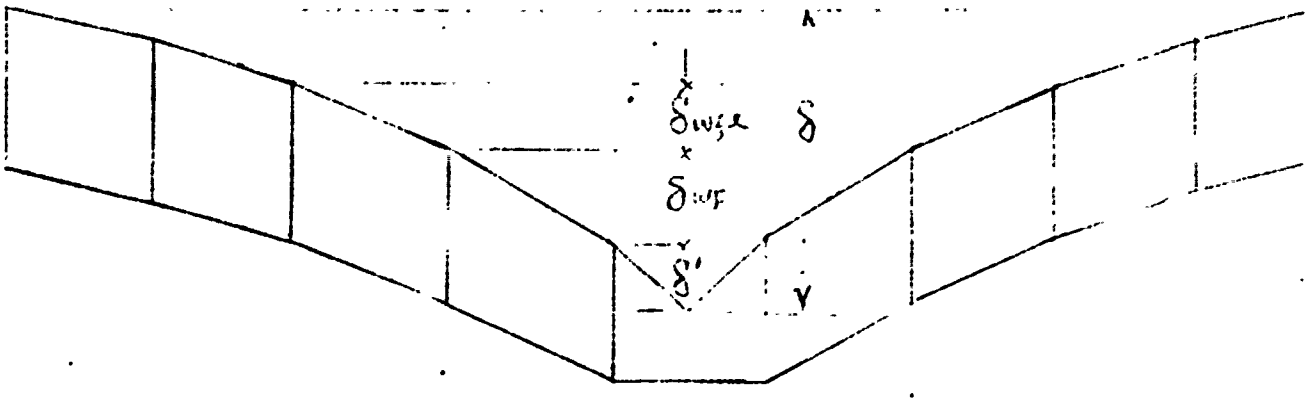

$\delta = \delta' + 6\delta_{WFe} - 2\delta_{WF}$, REF SECT 2·3·3)

$\delta - \delta' = 6\delta_{WFe} - 2\delta_{WF} = 100''$

$\delta_{WF} = \delta_{WFe} + \frac{P_{WF} L_S}{T_1 + T_2} = \delta_{WFe} + \frac{15.2 \times 172}{1690 + 1415}$

$\delta_{WF} = \delta_{WFe} + 8.4$

$4\delta_{WFe} - 16.8 = 100''$

$\delta_{WFe} = \frac{116.8}{4} = 29.2''$

$\delta_{WF} = 29.2 + 8.4 = 37.6''$

$\delta_{WF} = \frac{2(\delta + 3\delta_{WF} - 6\delta_{WFe}) - P_{WF} L_S / T_1}{3 + T_2/T_1}$

$= \frac{2(\delta + 112.8 - 175.2) - 15.4}{3.84} = 37.6''$

$\delta = \frac{37.6 \times 3.84 + 15.4}{2} + 62.4 = 142.3''$

$\frac{4 \times 1690 \times 142.3}{172 \times 152} - 1 = 1.29 \text{ OK}$

FOR OUTER SHELL (DOUBLE SHELL)

(REF SECT 2.3.3) $\epsilon_r = \frac{1}{9L_s^2}\left[2(\delta')^2 + (\delta_{WF})^2 + (\delta_{WFe})^2 + (2\delta_{WFe} - \delta_{WF})^2 + (3\delta_{WFe} - 2\delta_{WF})^2\right]$

$$\epsilon_r = \frac{1}{9(172)^2}\left[2(42.3)^2 + (37.6)^2 + (29.2)^2 + (20.8)^2 + (12.4)^2\right]$$

$$= \frac{6431}{266,256} = 0.0242$$

FOR OUTER SHELL (SINGLE SHELL)

$$\delta = \delta' + 6\delta_{WFe} - 2\delta_{WF}$$

$$\delta_{WF} = \delta_{WFe} + \frac{P_{WF} L_s}{T_1} = \delta_{WFe} + \frac{152 \times 172}{1690} = \delta_{WFe} + 15.4$$

$$\delta_{WF} = \frac{2(\delta + 3\delta_{WF} - 6\delta_{WFe}) - P_{WF} L_s / T_1}{3}$$

$$1.5\,\delta_{WF} = \delta + 3\delta_{WF} - 6\delta_{WFe} - 15.4$$

$$\delta = 6\delta_{WFe} - 1.5\delta_{WF} + 15.4 = 4.5\delta_{WFe} - 7.7$$

$\delta = 142.3$ $\delta_{WFe} = 33.3$ $\delta_{WF} = 48.7$

$\delta' = 39.9$

$$\epsilon_r = \frac{1}{9L_s^2}\left[2(\delta')^2 + (\delta_{WF})^2 + (\delta_{WFe})^2 + (2\delta_{WFe} - \delta_{WF})^2 + (3\delta_{WFe} - 2\delta_{WF})^2\right]$$

$$= \frac{1}{9L_s^2}\left[2(39.9)^2 + 48.7)^2 + (33.3)^2 + (17.9)^2 + (2.5)^2\right)$$

$$= \frac{6991}{266.256} = 0.0263$$

INNER SHELL

$$\epsilon_1 = \frac{1}{9L_s^2}\left[(\delta_{WF})^2 + (\delta_{WFR})^2 + (2\delta_{WFR} - \delta_{WF})^2 + (3\delta_{WFR})^2\right]$$

$$= \frac{1}{9(172)^2}\left[(37.6)^2 + (29.2)^2 + (20.8)^2 + (12.4)^2\right]$$

$$= \frac{2853}{266256} = 0.0107$$

Subject LNG DAMAGE ANALYSIS

Ship or Project PIGHT ANGLE COLLISION, STRUCK BY [illegible]

Section B.B.D. Prepared by MC Date 10-1-78 Checked Reviewed JJK

PLASTIC ENERGY DUE TO DECK DEFORMATION (E_d)
(AT 25'-5" ABL)

$$\delta_1 = \frac{P_{WF_1} L_t}{2T_1} = \frac{152 \times 172}{2 \times 1690} = 7.7''$$

$$\delta_{WF_1} = 1.00''$$

$$\delta = 142.3'' \qquad \epsilon_y = .0242$$

$$E_{d_x} = T\epsilon_t = A_s \times \frac{\sigma_y + \sigma_u}{2} \times L_d \times \epsilon_y$$

IN-KIPS

$$E_{d_1} = 36.6 \times 50 \times 1548 \times .0242 \left(\frac{109.3}{142.3}\right)^2 = 40381$$

$$E_{d_2} = 24.2 \times 50 \times 1548 \times .0242 \left(\frac{79.3}{142.3}\right)^2 = 14044$$

$$E_{d_3} = 28.7 \times 50 \times 1548 \times .0242 \left(\frac{49.3}{142.3}\right)^2 = 6439$$

$$E_{d_4} = 21.9 \times 50 \times 1548 \times .0242 \left(\frac{19.3}{142.3}\right)^2 = 754$$

$$E_5 = 32.9 \times 50 \times 1548 \times .0107 \left(\frac{43}{175}\right)^2 = 5034$$

$$E_6 = 28.7 \times 50 \times 1548 \times .0107 \left(\frac{13}{130}\right)^2 = 400$$

$$\Sigma E_d = 67052$$

DECK MEMBRANE TENSION ENERGY

$$E_d = 1.111 \times 67052 = 74{,}495 \text{ IN-KIPS}$$

STRUCTURE •LNG COLLISION MODEL
TYPE SPACE FRAME
NUMBER OF JOINTS 23
NUMBER OF MEMBERS 23
NUMBER OF SUPPORTS 11
NUMBER OF LOADINGS 1
TABULATE ALL
JOINT COORDINATES
1 X 69.75 Y 0.0 Z 2.0 S
2 X 69.75 Y 0.0 Z 14.0
3 X 69.75 Y 0.0 Z 23.5
4 X 69.75 Y 0.0 Z 37.7
5 X 69.75 Y 0.0 Z 46.7
6 X 69.75 Y 0.0 Z 60.0
7 X 69.75 Y 0.0 Z 76.0
8 X 69.75 Y 7.167 Z 23.5 S
9 X 64.0 Y 0.00 Z 23.5
10 X 29.5 Y 0.00 Z 2.0 S
11 X 59.0 Y 7.167 Z 23.5 S
12 X 64.0 Y 7.167 Z 23.5 S
13 X 59.0 Y 0.0 Z 23.5
14 X 53.0 Y 0.0 Z 23.5
15 X 34.0 Y 0.0 Z 8.0
16 X 69.75 Y -21.5 Z 76. S
17 X 40.0 Y 0.0 Z 16.0
18 X 69.75 Y 21.5 Z 76. S
19 X 45.7 Y 0.000 Z 23.5
20 X 34.0 Y 7.167 Z 8.0 S
21 X 59.0 Y 7.167 Z 23.5 S
22 X 45.7 Y 7.167 Z 23.5 S
23 X 40.0 Y 7.167 Z 16.0 S
MEMBER INCIDENCES
1 1 2
2 2 3
3 3 4
4 4 5
5 5 6
6 6 7
7 0 3
8 14 9
9 13 14
10 19 13
11 17 19
12 15 17
13 10 15
14 10 1
15 3 8
16 8 12
17 14 21
18 13 11
19 19 22
20 17 23
21 15 20
22 7 13
23 16 7
JOINT RELEASES
1 MOMENT Y
13 MOMENT Y
VERTICAL PROPERTIES OF STIC
1 AREA 32.6 IY 37.5 IZ 35.7 IX 1.0 IY 37. IZ 5.

```
2  AX 82.6  AY 37.5  AZ 35.7  IX 10.  IY 477.  IZ 5000.
3  AX 112.  AY 65.   AZ 47.0  IX 20.  IY 1237. IZ 5000.
4  AX 112.  AY 65.   AZ 47.0  IX 20.  IY 1237. IZ 5000.
5  AX 112.  AY 65.   AZ 47.0  IX 20.  IY 1237. IZ 5000.
6  AX 112.  AY 65.   AZ 47.0  IX 20.  IY 1237. IZ 5000.
7  AX 82.6  AY 37.5  AZ 35.7  IX 10.  IY 477.  IZ 5000.
8  AX 82.6  AY 37.5  AZ 35.7  IX 10.  IY 477.  IZ 5000.
9  AX 82.6  AY 37.5  AZ 35.7  IX 10.  IY 477.  IZ 5000.
10 AX 82.6  AY 37.5  AZ 35.7  IX 10.  IY 477.  IZ 5000.
11 AX 82.6  AY 37.5  AZ 35.7  IX 10.  IY 477.  IZ 5000.
12 AX 82.6  AY 37.5  AZ 35.7  IX 10.  IY 477.  IZ 5000.
13 AX 82.6  AY 37.5  AZ 35.7  IX 10.  IY 477.  IZ 5000.
14 AX 82.6  AY 37.5  AZ 35.7  IX 10.  IY 477.  IZ 5000.
15 AX 73.5  AY 57.5  AZ 10.  IX 1.0   IY 1.0   IZ 5000.
16 AX 88.   AY 72.   AZ 20.  IX 1.0   IY 1.0   IZ 5000.
17 AX 104.  AY 89.   AZ 30.  IX 1.0   IY 1.0   IZ 5000.
18 AX 88.   AY 72.   AZ 20.  IX 1.0   IY 1.0   IZ 5000.
19 AX 147.  AY 94.   AZ 30.  IX 1.0   IY 1.0   IZ 5000.
20 AX 168.  AY 120.  AZ 30.  IX 1.0   IY 1.0   IZ 5000.
21 AX 156.  AY 108.  AZ 30.  IX 1.0   IY 1.0   IZ 5000.
22 AX 1164. AY 540.  AZ 376.  IX 19500. IY 90000. IZ 99999.
23 AX 1164. AY 540.  AZ 376.  IX 19500. IY 90000. IZ 99999.
CONSTANTS E 30000. ALL G 12000. ALL
LOADING 1
MEMBER LOADS
1 FORCE Z UNIFORM = 68. LA 0.0 LB 5.0
1 FORCE Z UNIFORM = 136. LA 5. LB 12.
2 FORCE Z UNIFORM = 136.
3 FORCE Z UNIFORM = 136. LA 0.0 LB 2.0
3 FORCE Z UNIFORM = 304. LA 7.0 LB 14.2
4 FORCE Z UNIFORM = 304.
SOLVE
PROBLEM CORRECTLY SPECIFIED. EXECUTION IS PROCEED.
```

STRUCTURE SLAG COLLISION MODEL

LOADING 1

MEMBER FORCES

MEMB	JOINT	AXIAL FORCE	SHEAR FORCE Y	SHEAR FORCE Z	TORSION MOMENT	MOMENT Y	MOMENT Z
1	1	-310.514	5.609	-608.466	1.85	1931.89	76.94
1	2	310.514	-5.609	608.534	-1.85	-1191.41	-9.63
2	2	-310.514	5.609	608.532	1.85	1191.41	9.63
2	3	310.514	-5.609	-1875.538	-1.85	-13821.98	43.65
3	3	148.347	-2.580	-5155.771	-1.51	23272.31	-75.12
3	4	-148.347	2.580	1174.372	1.51	23725.55	35.48
4	4	148.347	-2.580	-1174.944	-1.51	-23725.50	-35.48
4	5	-148.347	2.580	1561.016	1.51	21900.40	15.26
5	5	148.347	-2.580	1561.016	-1.51	-21990.39	-15.26
5	6	-148.347	2.580	-1561.016	1.51	-1225.88	-4.53
6	6	148.347	-2.580	1561.013	-1.51	-1226.56	19.05
6	7	-148.347	2.580	-1561.013	1.51	-23746.34	-60.33
7	8	4666.601	-108.056	461.358	40.42	6787.38	1263.19
7	3	-4666.601	108.058	-461.358	-40.42	-8438.40	-1288.82
8	14	2843.774	-101.562	451.716	13.99	4071.79	1503.23
8	9	-2843.776	101.562	-451.716	-13.99	-8762.69	-2118.75
8	13	1575.772	-74.147	440.414	-15.45	1425.13	1435.40
9	14	-1575.772	74.147	-440.414	15.45	-4.74	-788.39
10	19	953.613	-51.325	437.254	-36.38	-1294.31	562.89
10	13	-953.613	51.325	-432.258	36.38	-2462.31	-338.1
11	17	642.608	-5.581	-140.154	1.19	25.82	19.12
11	18	-642.608	5.581	140.154	-1.19	1283.51	-71.89
12	15	544.930	-1.316	-21.643	0.39	242.93	23.47
12	17	-544.930	1.316	21.643	-0.39	-25.23	-36.64
13	18	547.286	-1.421	-28.311	-0.04	455.43	28.17
13	15	-547.286	0.421	28.311	0.04	-243.39	-32.16
14	1	0.000	0.000	59.294	0.00	-455.43	0.00
14	1	0.000	0.000	-59.294	0.00	-1631.00	0.00
15	9	-99.868	2464.695	2.917	-1.44	-0.05	1.87
15	8	99.868	-2464.695	-2.917	1.44	-5.03	1537.00
16	9	4.455	1822.727	-3.641	-4.95	26.47	5.00
16	12	-6.455	-1822.712	3.641	4.95	42.65	-2213.00
17	14	27.455	176.01	-11.01	-1.17	49.45	176.01
17	21	-27.455	-176.01	11.013	1.17	51.55	176.00
18	13	21.75	0.154	-0.15	.75	1.00	-1.00
18	11	-21.75	-0.154	0.154	-.75	1.00	1.00
19	17	45.144	45.077	-0.01	0.	1.00	0.
19	22	-45.144	-45.077	0.01	-0.	1.00	0.
20	17	4.144	44.077	-0.01	0.	1.00	0.
20	23	-4.144	-44.077	0.01	-0.	1.00	0.

21	15	[illegible]	-6.771	-2.007	[illegible]	7.18	[illegible]
21	20	-0.896	6.771	2.007	-.26	7.20	-53.35
22	7	-1.290	780.493	73.742	11874.67	-817.20	8389.68
22	18	1.290	-780.493	-73.742	-11874.67	-816.27	8390.92
23	16	1.29	-780.52	-74.604	-11874.67	776.46	-8382.97
23	7	-1.290	780.520	74.604	11874.67	827.53	-8391.20

APPLIED JOINT LOADS, FREE JOINTS

JOINT	FORCE X	FORCE Y	FORCE Z	MOMENT X	MOMENT Y	MOMENT Z
2	0.000	0.000	-0.000	0.00	-0.00	0.00
3	0.007	0.000	0.000	-0.00	0.00	-0.00
4	0.012	0.000	0.000	0.00	0.00	0.00
5	-0.203	-0.000	0.000	-0.00	0.01	0.00
6	0.002	-0.000	0.000	0.00	0.01	0.00
7	-0.000	0.000	-0.000	-0.00	0.00	-0.00
9	0.001	0.000	0.000	-0.00	0.00	0.00
13	0.001	-0.000	0.001	-0.00	-0.00	-0.00
14	0.004	0.000	-0.000	-0.00	0.00	-0.01
15	0.000	-0.000	0.000	-0.01	0.00	0.00
17	0.000	-0.000	0.001	0.00	-0.00	-0.00
18	-0.011	0.000	-0.000	-0.00	-0.00	-0.00

REACTIONS, APPLIED LOADS SUPPORT JOINTS

JOINT	FORCE X	FORCE Y	FORCE Z	MOMENT X	MOMENT Y	MOMENT Z
1	609.466	5.609	-369.826	-76.94	0.00	1.85
8	2464.695	99.968	-2.467	8.93	10.44	15776.57
10	351.023	-0.420	486.132	-23.28	0.00	17.34
11	622.156	-22.782	8.158	-37.04	-0.75	5038.85
12	1322.722	-6.495	2.641	-42.66	4.98	12213.38
16	780.520	1.290	-74.604	-776.46	-11874.67	-8389.97
18	780.493	1.290	-73.742	818.27	-11874.67	8390.92
20	-6.770	-0.496	2.007	-7.20	-0.26	-53.35
21	1268.100	-27.455	11.303	-51.55	1.17	8721.41
22	453.277	-45.743	5.379	-18.98	-0.80	3766.93
23	156.266	-4.264	4.225	-14.36	-0.10	1108.35

FREE JOINT DISPLACEMENTS

JOINT	X DISPL	Y DISPL	Z DISPL	X-ROTAT	Y-ROTAT	Z-ROTAT
2	-0.246	[illegible]	[illegible]	[illegible]	[illegible]	[illegible]
3	-0.0272	[illegible]	[illegible]	[illegible]	[illegible]	[illegible]
4	-0.2165	[illegible]	[illegible]	[illegible]	[illegible]	[illegible]
5	-0.2142	[illegible]	[illegible]	[illegible]	[illegible]	[illegible]
6	-0.1177	[illegible]	[illegible]	[illegible]	[illegible]	[illegible]
7	[illegible]	[illegible]	[illegible]	[illegible]	[illegible]	[illegible]
9	[illegible]	[illegible]	[illegible]	[illegible]	[illegible]	[illegible]
13	[illegible]	[illegible]	[illegible]	[illegible]	[illegible]	[illegible]
14	[illegible]	[illegible]	[illegible]	[illegible]	[illegible]	[illegible]
15	[illegible]	[illegible]	[illegible]	[illegible]	[illegible]	[illegible]
17	[illegible]	[illegible]	[illegible]	[illegible]	[illegible]	[illegible]

10 -0.0053 [illegible]

SUPPORT JOINT DISPLACEMENTS

JOINT	X DISPL	Y DISPL	Z DISPL	X-ROTAT	Y-ROTAT	Z-ROTAT
1	0.0000	[illegible]	[illegible]	[illegible]	-0.0017	0.0000
8	0.0000	[illegible]	[illegible]	[illegible]	0.0000	0.0000
10	0.0000	[illegible]	[illegible]	[illegible]	0.0003	0.0000
11	0.0000	[illegible]	[illegible]	[illegible]	0.0000	0.0000
12	0.0000	[illegible]	[illegible]	[illegible]	0.0000	0.0000
16	0.0000	[illegible]	[illegible]	[illegible]	0.0000	0.0000
18	0.0000	[illegible]	[illegible]	[illegible]	0.0000	0.0000
20	0.0000	[illegible]	[illegible]	[illegible]	0.0000	0.0000
21	0.0000	[illegible]	[illegible]	[illegible]	0.0000	0.0000
22	0.0000	0.0000	0.0000	0.0000	0.0000	0.0000
23	0.0000	0.0000	0.0000	0.0000	0.0000	0.0000

2087-14A
COVER PAGE

AVERAGE ENERGY ABSORPTIONS OF CASE 12-A

M. Rosenblatt & Son, Inc.
DESIGN CALCULATION SHEET

No. 2097-12a
2 Sheet 1 of 3

Subject LNG DAMAGE ANALYSIS (DOUBLE HULL)
Ship or Project RIGHT ANGLE COLLISION - STRUCK BY VERTICAL BOW
Section BSDD Prepared by G. CHI Date 11-9-73 Checked Reviewed

TABLE - 1

SUMMARY OF AVERAGE PLASTIC ENERGY ABSORBED BEFORE SHELL PLATE RUPTURE =

STRIKING SHIP BOW	VERTICAL
HIT ANGLE	90°
CASE NO.	12a
SHELL PLATE THICKNESS	INNER SHELL ½" M.S. OUTER SHELL 11/16" M.S.
ENERGY ABSORBED (AVERAGE) IN - KIPS	1,309,700
ENERGY ABSORBED (AVERAGE) FT - TONS	48,730
EQUIVALENT STRIKING SPEED OF A 20,000 T SHIP (KNOTS)	7.4

Subject LNG DAMAGE ANALYSIS (DOUBLE HULL)
Ship or Project RIGHT ANGLE COLLISION - STRUCK BY VERTICAL BOW
Section BSDD Prepared by G. CHI Date 11-9-73 Checked Reviewed

CASE 12a : AVERAGE ε_r AT THE LOCATION OF STRUCK.

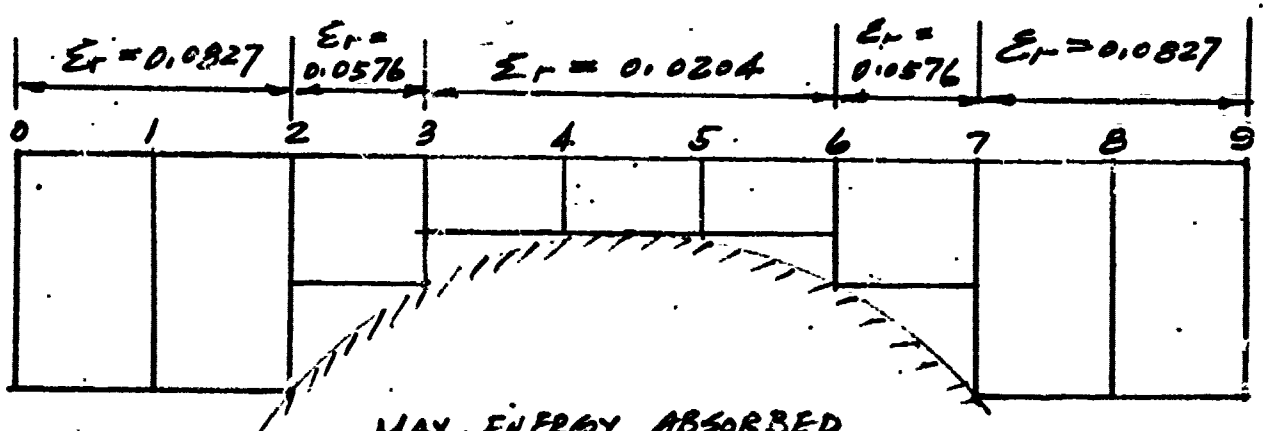

MAX. ENERGY ABSORBED
= 1,973,000 IN-KIPS
= 73,400 FT-TONS

ε_r	MAX. ENERGY FT-TONS	½ MAX. ENERGY FT-TONS
0.0204	73,400	24,470
0.0576	207,247	69,080
0.0827	297,558	99,190

Subject LNG DAMAGE ANALYSIS

Ship or Project RIGHT ANGLE COLLISION — STRUCK BY VERTICAL BOW

Section BS DD Prepared by G. CHI Date 11-9-73 Checked Reviewed

CASE 12a

STRIKING SHIP VERTICAL BOW
HIT ANGLE 90°
LNG CARRIER OUTER SHELL 11/16" M.S.
INNER SHELL ½" M.S.
MAX. ENERGY ABSORBED = 1,973,000 IN-KIPS
= 73,400 FT-TONS

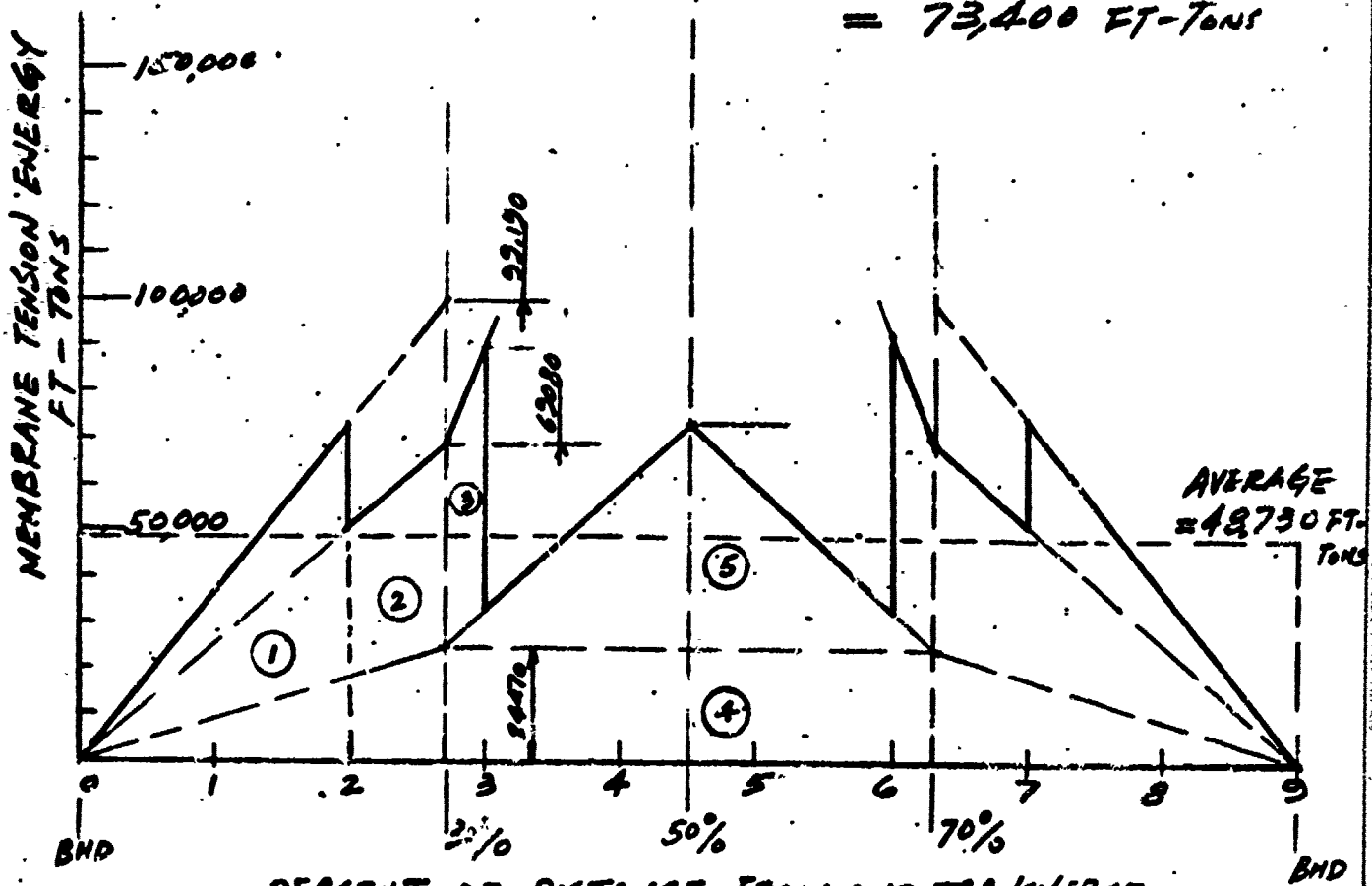

AREA ①	= ½ × 73474 × 6 × 2	=	440,844
" ②	= ½ (69020 + 51170) × 2.1 × 2	=	252,525
" ③	= ½ (44610 + 59483) × 0.9 × 2	=	93684
" ④	= 24470 × 10.8	=	264276
" ⑤	= ½ × 48930 × 10.8	=	264222
		27	1,315551

AVERAGE ENERGY = 48730 FT-TONS
= 1,309,700 IN-KIPS

PART V

NON-STANDARD STRUCTURAL SCHEMES FOR INCREASED COLLISION RESISTANCE OF TANKERS

NOTICE

The work reported on herein was performed as part of a research project done by M. Rosenblatt & Son for the U. S. Coast Guard Office of Research and Development. It is extremely preliminary and theoretical in nature and therefore must be considered as such. The U. S. Coast Guard does not endorse or approve of the methods utilized in this report.

TABLE OF CONTENTS

		Page
1.	BACKGROUND	1-1
2.	SCHEMES FOR ENERGY ABSORPTION	2-1
	2.1 Main Structure Energy Absorbers	2-1
	2.2 Dashpot Energy Absorbers	2-3
3.	APPENDIX - CALCULATIONS	

1. BACKGROUND

This report is on a separate task accomplished within the research and development project related to the evaluation of the structure of tankers in collision from the viewpoint of the protection afforded to the cargo. The tanker project has developed to date an analytical procedure for estimating the plastic energy developed by a longitudinally framed tanker when involved in collision, both right angle and oblique, with ships with rigid bows. The procedure is reported in the following reports:

Part I. Tanker Structural Evaluation, Prepared for Department of Transportation, U.S. Coast Guard, by M. Rosenblatt & Son, Inc., New York and USS Engineers & Consultants, Pittsburgh, Pa., MR&S Report No. 2087, April 1972, (USCG Project 72-33-21).

Part II. Evaluation of Tanker Structure in Collision Prepared for Department of Transportation, U.S. Coast Guard by M. Rosenblatt & Son, Inc. New York and U.S. Steel Corporation, Monroeville, Pa., MR&S Report No. 2087-15, November 1973.

The application of the conservative procedure of Part I showed that a typical oil tanker could only withstand side shell rupture and subsequent loss of cargo to the environment if the speed of the 20,000 ton displacement striking ship was limited. This indicated that some way of absorbing considerably more energy was needed for cargo protection. It was recognized that a limit existed as to the modifications that could be incorporated in standard ship design to improve cargo protection in the event

of collision. Hence it was felt essential that non-standard structural schemes be examined to enhance collision protection. These are not to be confused with non-structural schemes, collision avoidance equipment or operational practices.

Several non-standard structural schemes have been hypothesized. These may be considered "brain storms" since the level of effort was only to formulate a configuration and assume it would function as hypothesized without considering possible problem areas, no matter how obvious.

The various schemes fall into two categories depending on their main energy absorbing mechanism. The first group consists of designs wich absorb energy in the deformation of the main structural members while the second includes those which use some secondary mechanism like a dashpot, activated by the main structural system, to absorb the greater part of the energy. Economics have not been considered. A brief schematic sketch of each of the schemes is given in Figs. 1-3. Calculations for the various schemes can be found in the Appendix. The second category holds the most promise for large energy absorption.

Each of the schemes have been compared with theoretical collision calculations from Part I. Even though the theory of structural deformation as applied to standard structures has since been modified as described in Part II, the comparisons should remain valid since only the difference in energy absorption between standard and non-standard structures was considered. It should be noted that depending on the extent of damage that a particular standard structured ship can withstand, the additional protection of the non-standard structure will vary. Therefore in practice the advantage of non-standard structure should be evaluated independently for any particular ship.

Although considerable development is still required before any of the schemes can be considered, it has been indicated by the comparisons that the dashpot energy absorbers employing a multi-directional force dispersing medium as the energy absorber show encouraging characteristics.

2. ENERGY ABSORBING SCHEMES

2.1 Main Structure Energy Absorbers

2.1.1 Weakened Web Frames

The objective of this approach is to make the web frames less resistant to failure under the high collision loads (i.e., increase R_m, which for any given failure mode is the ratio of (1) the loading first assumed in analyzing that and all other failure modes to (2) the loading causing the failure mode) while maintaining their operational structural integrity. This will result in greater side shell deformation and therefore larger membrane energy absorption. As an example of how this can be done, consider the web frames of the CMX tanker used for the parametric study. By removing the flat bar stiffeners attached to the longitudinals and removing the web frame struts, while maintaining structural strength for operational loads, a wide unstiffened web will result. This web will be prone to local buckling behind the longitudinals when load is transmitted to it from them. The web frames can be designed to fail immediately after the maximum design load due to static and dynamic non-collision forces is surpassed. This will require rigorous calculations of hull strength. A.B.S. and other Classification Societies rules must also be met.

Calculations for a particular ship with weakened web frames showed that R_m increased by 120% and the energy absorption increased by 80% over the same ship with normal web frames.

2.1.2 Wire Ropes Inboard or Outboard of Side Shell

This scheme is intended to make use of higher strength steels (greater than 100 ksi yield) which are too non-ductile for side shell plating. By anchoring the high strength steel wire rope at the ends of the ship or other suitable point, and allowing it to pass and slide through web frames and bulkheads, (if inboard)

large deflections can be realized in the wire rope during a collision. Of great importance is the fact that although the deflection of the rope may be large, the strains will be small because of its long length. Of course this is necessary since the non-ductile rope can only withstand elastic deformation. The rope should be constructed so that stretching not due to straining of the steel is precluded.

The comparison of the energy absorption for a ship with and without wire ropes of high strength steel shows no advantage of the former over slightly increased plate thickness in the ship without wire ropes. This is attributable to the fact that the force in the rope must increase from zero to its maximum value at yield, while the force in the plating quickly reaches a value corresponding to yield and then remains fairly constant throughout the major part of the total plastic membrane deflection.

2.1.3 Double Hull Acting in Parallel

By constructing a stiff web between the parallel hulls so that during collision deformation the two hulls act together instead of in series, it was hoped greater forces on the inboard web frames would be produced and therefore an increase in the extent of damage and energy absorption could be realized.

Because the membrane stretching energy is proportional to the side shell thickness, the membrane energy absorbed by the double hull acting in parallel will be the same as that for a single hull of the same total side shell thickness. The additional energy of the double skin configuration will come from greater deck damage and destruction of the outer hull. These are small in relation to the membrane energy. However, there will be the added protection of an inside skin.

For the comparison a single hull ship was used as representative of the parallel acting double hull. The comparison between this and a series acting double hull of the same total shell thickness showed little difference in energy absorption between the two. Therefore no appreciable advantage is foreseen in considering a parallel acting double hull over a series acting double hull.

2.2 Dashpot Energy Absorbers

2.2.1 Dashpot Within the Main Hull

Constructing a controlled pressure fluid chamber integral with the side shell can result in large energy absorption due to expansion of the chamber fluid through orifices or valves during a collision. Relieving can be done into cargo tanks if the pressurized fluid is cargo oil, or outboard if the fluid is water.

The maximum allowable pressure within the chamber would depend on the strength of the side shell which forms one of the chamber walls. By estimating a collision time and maximum structural deformation, a flow rate can be calculated to preclude bursting of the chamber. Check valves or orifices may be used. However, only the valves will insure constant chamber fluid pressure, and therefore are preferred.

For a ship fitted with the dashpots 420% more energy was absorbed than with the same ship without the dashpots.

It should be noted that the chamber could be filled by cargo oil or sea water depending on the location of the orifices or valves. The former allows the tank space to be used for cargo carrying, while the latter affords greater safety during a collision if by chance the outer skin of the ship should fail.

2.2.2 Honeycombing Within the Main Hull

In this scheme the chamber fluid of 2.2.1 has been replaced with a metalic honeycomb.

Unless the load is evenly distributed over the honeycombing and parallel to its grain, the honeycombing will buckle instead of crush. The energy absorption in this mode of failure is much less than in compression. Because of the flexibility of the ship's side the collision load will be transferred to the honeycombing in such a fashion that it will cause buckling, so that high energy absorption will not be realized. Some experimental verification may be needed here.

2.2.3 External Honeycombing

By placing a specified thickness of honeycombing outside the main hull, and covering it with a thick plate capable of moving perpendicular to the side shell, and of such rigidity that it will transmit the line load of collision as a distributed load, large amounts of honeycombing can be crushed with significant energy absorption.

Calculations show that any reasonable plate thickness will not give the desired result.

2.2.4 Solid Absorber Inside Main Hull

If a solid energy absorber can be developed that will absorb equal amounts of energy regardless of the direction of load application (for instance a plastic foam or a metallic structure like honeycombing but with a granular rather than tubular structure), in theory, the results of 2.2.1 could be approached. The same amount of energy absorption probably could not be attained because of the rapid force transmitting capability of the fluid.

DOUBLE SKIN HULLS

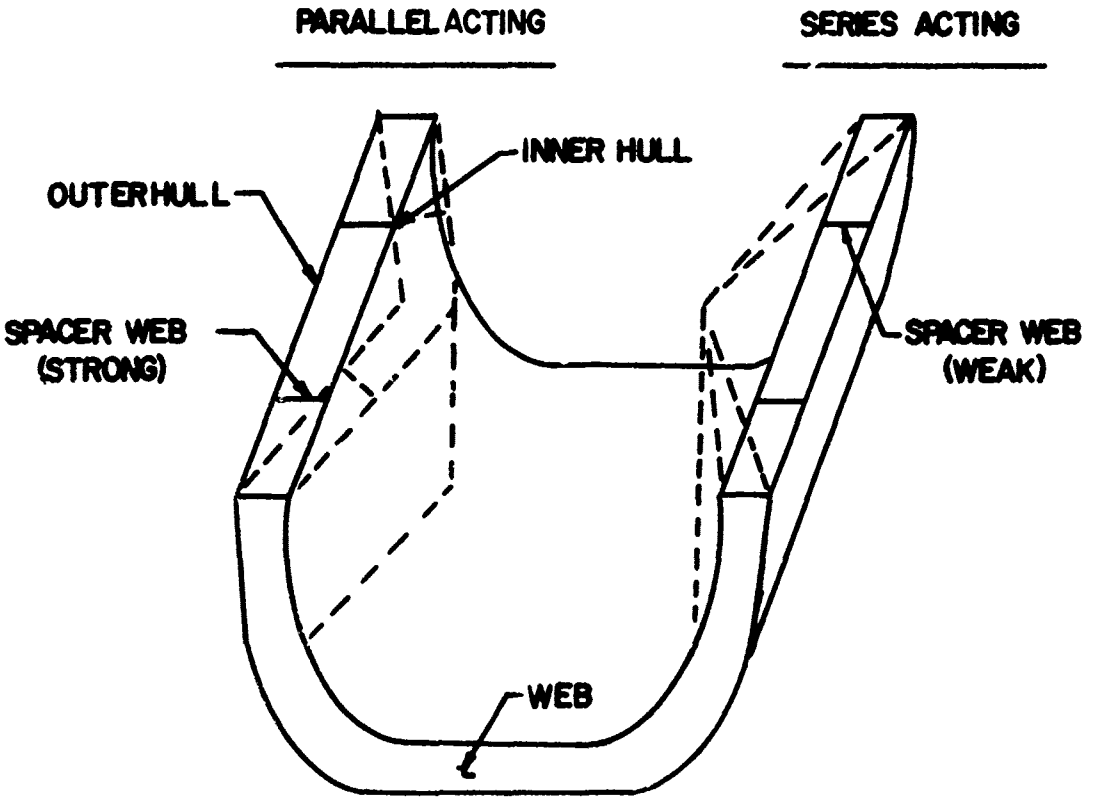

NOTE: DOTTED LINES INDICATE COLLISION INCURSION

Fig. 1

NON-STANDARD STRUCTURAL SCHEMES

WIRE ROPES INBOARD OF SIDE SHELL

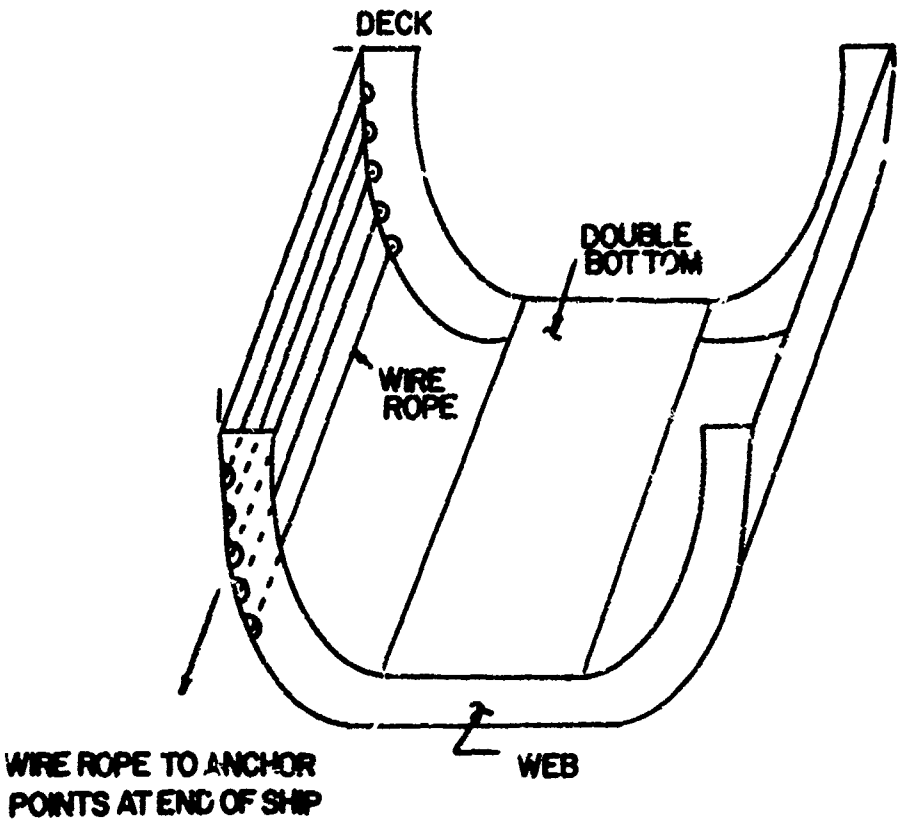

Fig. 2

NON-STANDARD STRUCTURAL SCHEMES

DASHPOT WITHIN THE MAIN HULL

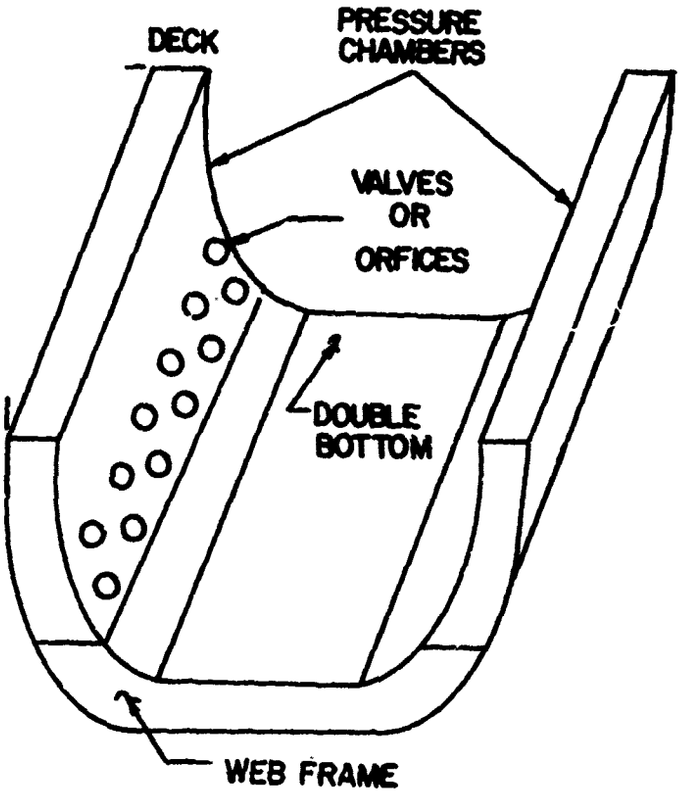

Fig. 3

NON-STANDARD STRUCTURAL SCHEMES

APPENDIX

M. Rosenblatt & Son, Inc. No. 2087

DESIGN CALCULATION SHEET Sheet 1 of

Subject WEAKENED WEB FRAMES

Ship or Project NON-STANDARD STRUCTURE

Section BSDD Prepared by JCD Date Checked Reviewed

THE 1972 A.B.S. RULES CONCERNING VESSELS INTENDED TO CARRY OIL IN BULK PUT NO RESTRICTION ON THE LENGTH OF TANKS OTHER THAN THEY BE ARRANGED TO AVOID EXCESSIVE DYNAMIC STRESSES IN THE HULL STRUCTURE.

MANY OF TODAY'S TANKERS ALREADY HAVE TANKS OF THE 100 FT. RANGE. THEREFORE WITHIN THIS DISTANCE ONLY DEEP WEB FRAMES AND WASH BULKHEADS ARE FOUND. BOTH HAVE SIMILAR STRUCTURE ABOVE THE BILGE AREA.

MAIN BULKHEADS HAVE LONGITUDINALS USUALLY RUNNING VERTICALLY ALONG THE BULKHEAD PLATE. THIS TYPE OF STRUCTURE IS DIFFERENT THAN THAT OF THE WEB FRAMES AND WASH BULKHEADS. HOWEVER, BEFORE THE FIRST STIFFENER IS MET, THE STRUCTURE ALONG THE SIDE PLATE IS THE SAME FOR BOTH.

THEREFORE IT IS PROPOSED TO DEVELOP A WEB FRAME-WASH BULKHEAD STRUCTURAL ARRANGEMENT, WITH ACCEPTABLE S.M. ACCORDING TO A.B.S., THAT WILL DEFLECT READILY UNDER COLLISION LOADS. ALTHOUGH BULKHEAD FAILURE HAS NOT BEEN ANALYZED HERE, IT IS ANTICIPATED SIMILAR RESULTS CAN BE ACHIEVED.

IT IS HOPED THAT WEB FRAMES AND ALL BULKHEADS WILL FAIL SUCH AS TO ALLOW A LARGE AMOUNT OF DEFLECTION AND MEMBRANE ACTION.

IT ALSO SHOULD BE NOTED THAT A DETAILED STRUCTURAL ANALYSIS OF SHIPS

Subject WEAKENED WEB FRAMES

Ship or Project NON-STANDARD STRUCTURE

Section BSDD Prepared by JJD Date Checked Reviewed

IS NOT THE SCOPE OF THIS PROJECT. IF IT IS FOUND THAT A SUITABLE WEB FRAME CAN BE DESIGNED, IT WILL HAVE TO BE UP TO INDIVIDUAL DESIGNERS TO CALCULATE AND HAVE APPROVED THEIR WEB FRAME SPACING AND BULKHEAD SPACING, (ALL SHOULD BE MAXIMIZED). AND SCANTLINGS.

Subject WEAKENED WEB FRAMES

Ship or Project NON STANDARD STRUCTURE

Section BSDD Prepared by JCD Date Checked Reviewed

FROM ABS: $SM = .0025\, ch\, s\, l_b^2\ in.^3$
(FOR WEB NEXT TO SIDE SHELL)

FOR CMX DESIGN:

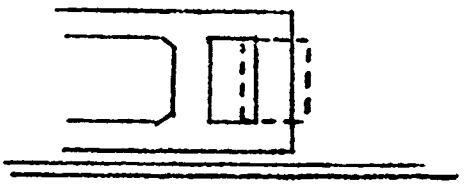

C = .65 (SIDE TRANSVERSE WITH TWO HORIZONTAL STRUTS)

h = THE VERTICAL DISTANCE IN FEET FROM THE CENTER OF THE AREA SUPPORTED TO 8 FT. ABOVE THE DECK AT SIDE AMIDSHIPS.
= 37.0

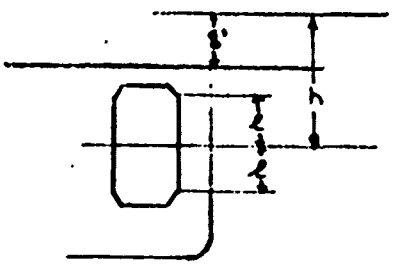

S = SPACING OF TRANSVERSES
= 144" = 12'

l_b = 540 in. = 45'

$$SM = .0025(.65)(37.0)(12')(45')^2$$

$$= 1457.\ in.^3$$

Subject WEAKENED WEB FRAMES

Ship or Project NON STANDARD STRUCTURE

Section BSDD Prepared by JCD Date Checked Reviewed

ACTUAL CALCULATION OF SECTION MODULUS ON CMX DESIGN:

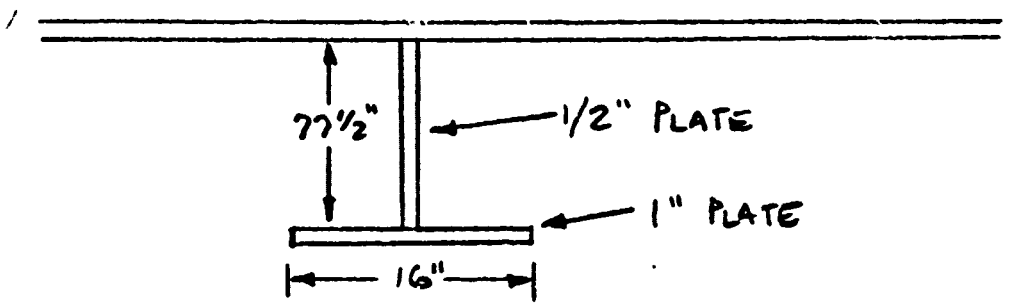

EFFECTIVE WIDTH OF STIFFENED PLATE IN AXIAL COMPRESSION (FOR SIDE SHELL).

$$\frac{b}{t} = \frac{326}{\sqrt{\sigma_y}}\left[1 - \frac{81.6}{(a/t)\sqrt{\sigma_y}}\right]$$

$$= \frac{326}{\sqrt{35}}\left[1 - \frac{81.6}{(144)\sqrt{35}}\right]$$

$$= 50.$$

$b = 50.$ (FOR $t = 1"$)

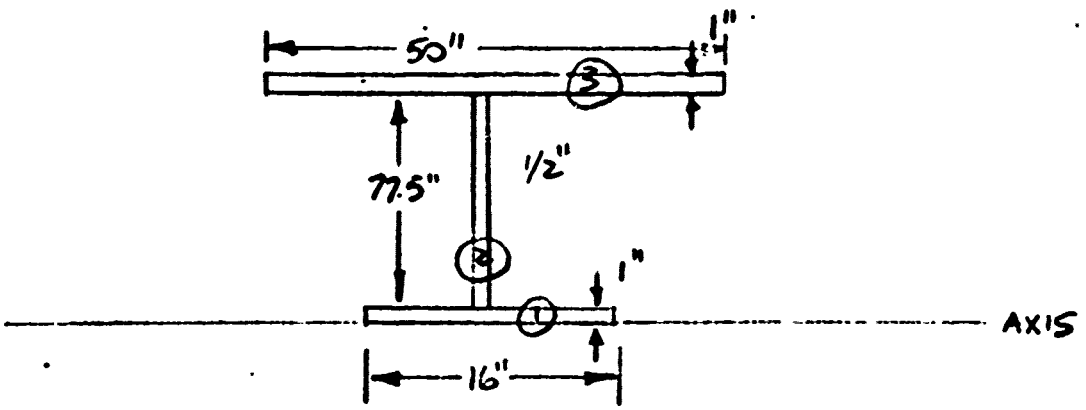

M. Rosenblatt & Son, Inc. No. 2087
DESIGN CALCULATION SHEET Sheet 5 of

Subject WEAKENED WEB FRAMES

Ship or Project NON STANDARD STRUCTURE

Section BSDD Prepared by JCD Date Checked Reviewed

MEMBER	A AREA	d ARM ABOUT AXIS	Ad	Ad^2
①	16.	.5	8.	4.
②	38.75	39.75	1502.	59687.
③	50.	79.	3950.	312050.
	104.75		5460.	371741.

$$C.G. = \frac{5460}{104.75} = 52. \qquad A\cdot(C.G.)^2 = 283244.$$

UPPER S.M. : $371741. - 283244. = I$

$= 88497$

$$\frac{I}{C} = \frac{8849?}{27.5} = 3218.\ in^3.$$

LOWER S.M. : $\frac{I}{C} = \frac{88497}{52.} = 1702.\ in^3$

$1702. > 1457$

M. Rosenblatt & Son, Inc. No. 2067

DESIGN CALCULATION SHEET Sheet of

Subject WEAKENED WEB FRAMES

Ship or Project NON-STANDARD STRUCTURE

Section BSDD Prepared by JCD Date Checked Reviewed

NET SECTIONAL AREA OF THE WEB PORTION (VIA A.B.S.)

q = ALLOWABLE AVERAGE SHEARING STRESS IN THE WEB

s = SPACING OF STIFFENERS OF DEPTH OF WEB PLATE, WHICHEVER IS LESS. = 36"

t = THICKNESS OF WEB PLATE = .5"

$s/t = 72.0 \quad \therefore \quad q \sim 5.5$ TONS/IN.^{2}

F= SHEARING FORCE

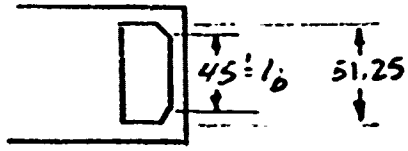

$$F_{\text{LOWER SIDE TRANSVERSE}} = .0285\,[12]\left[.43(51.25)(48.25) - 3.25\left(48.25 + \frac{51.25}{2} - \frac{3.25}{2}\right)\right]$$

$$= 283.35$$

$$F_{\text{UPPER SIDE TRANSVERSE}} = .0285\,[12]\left[.20(51.25)(33.75) - (3.25)\left(48.25 - \frac{51.25}{2} + \frac{3.25}{2}\right)\right]$$

$$= 91.36$$

$$\therefore A = \frac{F}{q} = \frac{283.35}{5.5} = 51.5 \text{ IN.}^2$$

$A = 38.75$ IN^2 ON AMX DESIGN [MUST HAVE SHOWN SHEAR TO BE LESS THAN ABS FORMULA]

M. Rosenblatt & Son, Inc. No. 2087
DESIGN CALCULATION SHEET Sheet 7 of

Subject WEAKENED WEB FRAMES

Ship or Project NON-STANDARD STRUCTURE

Section BSDD Prepared by JCD Date Checked Reviewed

CHANGES TO WEB FRAMES

IN EVENT OF COLLISION, IT IS DESIRED THAT WEB FRAMES YIELD AS SOON AS POSSIBLE. TO ACCOMPLISH THIS FOR MOST OF THE WEB FRAME, IT IS FELT THAT ALL STRUTS (SHOULD) BE REMOVED (EXCEPT FOR DECK AND BOTTOM OF COURSE), AND THAT ALL LONGITUDINAL FRAME STIFFENERS BE REMOVED (HORIZONTAL FLAT BARS).

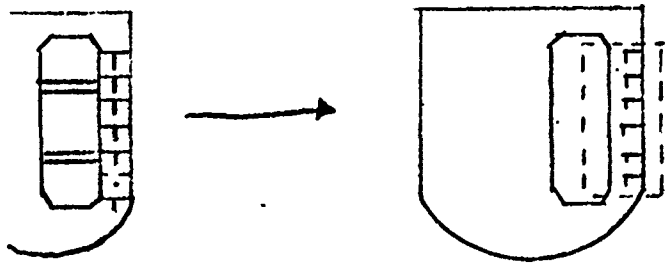

IN THIS CONFIGURATION, FOR ALL LONGITUDINALS AWAY FROM THE DECK AND BOTTOM STRUTS, THE MODE OF FAILURE WILL BE EITHER LOCAL CRUSHING (OR BUCKLING) DUE TO LOADS ON THE LONGITUDINALS OR GROSS BUCKLING OF THE SIDE TRANSVERSE. HOWEVER, CARE MUST BE TAKEN THAT THE ABOVE CONFIGURATION RESIST NORMAL OPERATING LOADS.

ALSO, PREVIOUS COLLISION CALCULATONS SHOW THAT SHEAR WAS AN IMPORTANT CONSIDERATION THEREFORE THIS MAY BE A MODE OF FAILURE AND MUST BE CONSIDERED.

Subject WEAKENED WEB FRAMES

Ship or Project NON-STANDARD STRUCTURE

Section BSDD Prepared by JCD Date Checked Reviewed

FIRST A NEW WEB FRAME WILL BE DEVELOPED AND THEN CHECKED FOR ALL THE ABOVE.

A) LOADING ON THE HULL GIRDER.

THERE ARE VARIOUS TYPES OF LOADING, WHICH WILL CONTRIBUTE TO STRESSES IN THE TRANSVERSE MEMBERS, IN ORDER TO APPROXIMATE HYDROSTATIC LOADING A HEAD DUE TO FULL LOAD DRAFT PLUS ONE HALF THE HEIGHT OF A 1.1 $\sqrt{L}$ WAVE WILL BE ASSUMED.

$$\text{HEAD} = \text{DRAFT} + 1/2\,(1.1\sqrt{L})$$
$$= 48.5 + .5\,(1.1)(\sqrt{700})$$
$$= 48.5 + 16.5 = 65' \quad (\text{DEPTH MLD} = 63.5)$$

MOMENTARY SLAMMING PRESSURES, RACKING, AND TORSION WILL NOT BE CONSIDERED HERE. (SINCE THE HEAD ALONE WILL NEVER REALLY BE REACHED, IT CAN BE ASSUMED TO COVER SOME OF THE EFFECTS OF THE ABOVE DISTORTION AND FORCES).

$$\text{WATER PRESSURE} = \frac{64\ \text{lbs}}{ft^3}\ ft = \frac{64\ \text{lbs}}{ft^3}/ft.$$

M. Rosenblatt & Son, Inc.

DESIGN CALCULATION SHEET

No. 7087

Sheet 9 of

Subject WEAKENED WEB FRAMES

Ship or Project NON-STANDARD STRUCTURE

Section BSDD Prepared by JCD Date Checked Reviewed

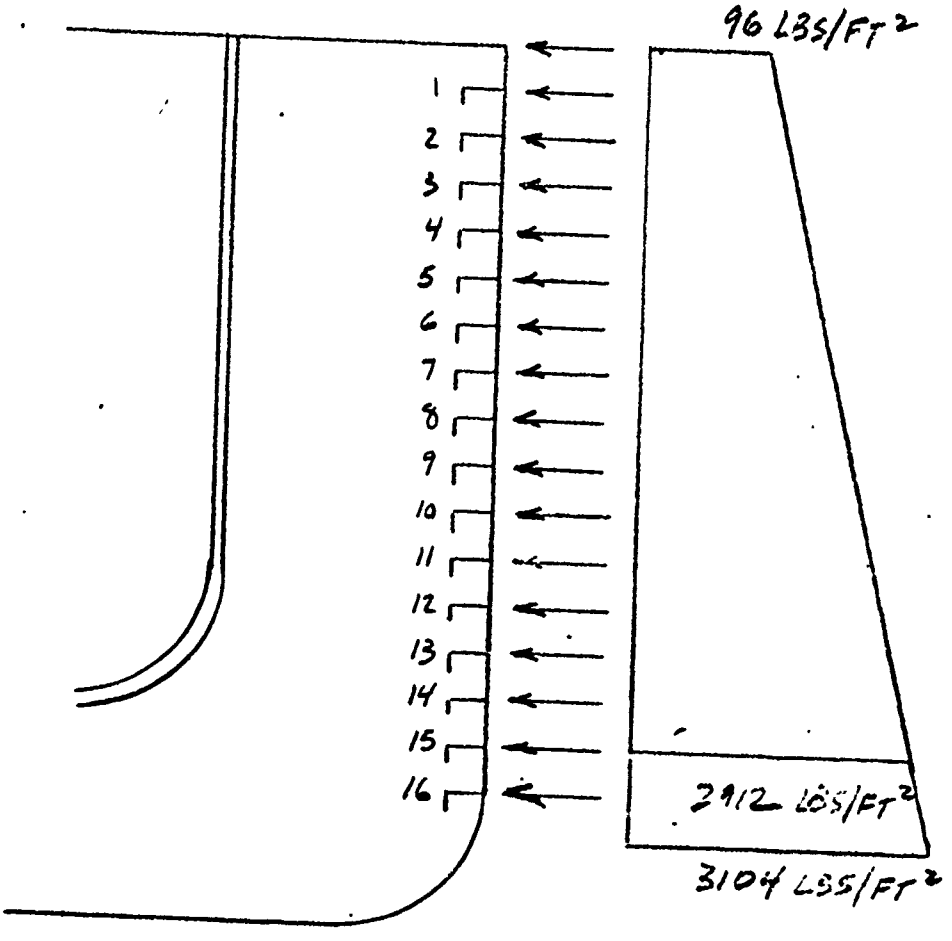

MAX FORCE OCCURS AT #15 [FOR OLD PARAMETRIC STUDY – SINCE #16 REMAINED UNDEFORMED]

FORCE = PRESSURE X LONG. STIFFENER SPACING X WEB FRAME SPACING

= 2912 LBS/FT² X 3.0 FT X 12.0 FT.

= 104,832. LBS. = 105 KIPS

∴ P_F = 105 KIPS

Subject WEAKENED WEB FRAMES

Ship or Project NON-STANDARD STRUCTURE

Section BSDD Prepared by JCD Date Checked Reviewed

B. WEB

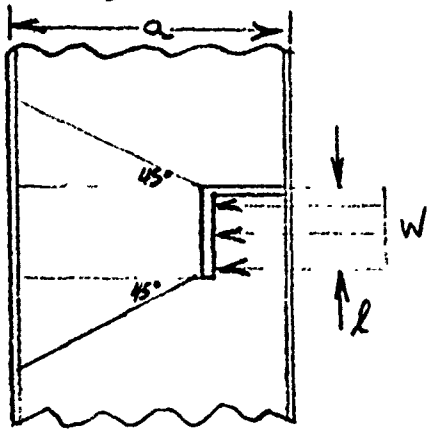

$W_\ell = P_F = 105$ KIPS

FIRST DIMENSION "a" AND THE THICKNESS OF THE WEB MUST BE DETERMINED.

THE THICKNESS OF THE WEB WILL BE DETERMINED BY THE LENGTH ℓ AND THE MAGNITUDE OF P_F AT FIRST CONSIDERATION. LATER BUCKLING OF THE WEB WILL BE HEAVILY DEPENDENT ON ITS THICKNESS.

THE SAME LONGITUDINALS WILL BE USED AS IN ANIX DESIGN, SINCE THEY WERE SATISFACTORY THERE.

ALLOWABLE COMPRESSIVE STRESS VIA ABS
ASSUMED = 20 $\frac{\text{KIPS}}{\text{IN.}^2}$

$$P = \ell + \sigma_{comp}$$

$$t = P/\ell\sigma_{comp} = \frac{105}{20.6} = .875 \text{ IN.}$$

$\therefore$ TRY A WEB 1.0 IN. THICK

Subject WEAKENED WEB FRAMES

Ship or Project NON-STANDARD STRUCTURE

Section BSOD Prepared by JCD Date Checked Reviewed

THE WIDTH "a" OF THE WEB WILL BE DETERMINED BY THE REQUIRED SECTION MODULUS.

FROM ABS RULES THE REQUIRED MODULUS IS 1457. IN^3 AND FROM AMX 1702.

FROM ABS:

C = 1.50 (SIDE TRANSVERSE WITHOUT STRUTS)
h = 37.0'
s = 144"
l_b = 45'

$$S.M. = .0025(1.5)(37.0)(12.0)(45.)^2$$

$$= 3372.$$

MEMBER	A AREA	d ARM ABOUT AXIS	Ad	Ad^2
①	16	.5	8	4.
②	1.0 x 130 130.	66.	8580.	566280.
③	50.	131.5	6575.	864613.
	196.		15163.	1,430,897

$$C.G. = \frac{15163.}{196.} = 77.$$

$$A(C.G.)^2 = 1,162,084. = 268813.$$

$$I = \text{LOWER S.M.} = \frac{268813}{77} = 3491.$$

Subject WEAKENED WEB FRAMES

Ship or Project NON-STANDARD STRUCTURE

Section BSDD Prepared by JCD Date Checked Reviewed

∴ WEB FRAME

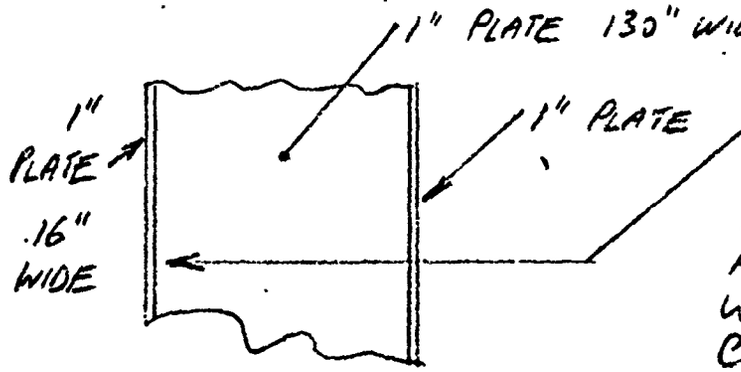

NOTE: THIS FLANGE OR SIDE COULD HAVE BEEN MADE LARGER TO GET S.M. BUT AT THIS STAGE ONLY WIDENING THE WEB WILL BE CONSIDERED.

NEXT, THE BUCKLING CAPABILITIES OF THE LOCAL WEB PLATE WILL BE ANALYZED.

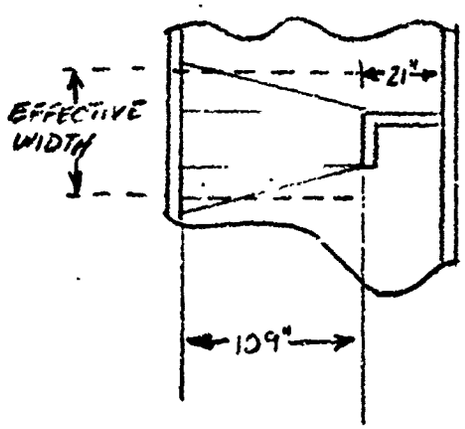

THIS WILL BE DONE BY FINDING AN EFFECTIVE WIDTH FOR THE BUCKLED PLATE AND ASSUMING THE EDGE CONSTRAINT (INBOARD & OUTBOARD) TO BE FIXED - FIXED (CONSERVATIVE ASSUMPTION)

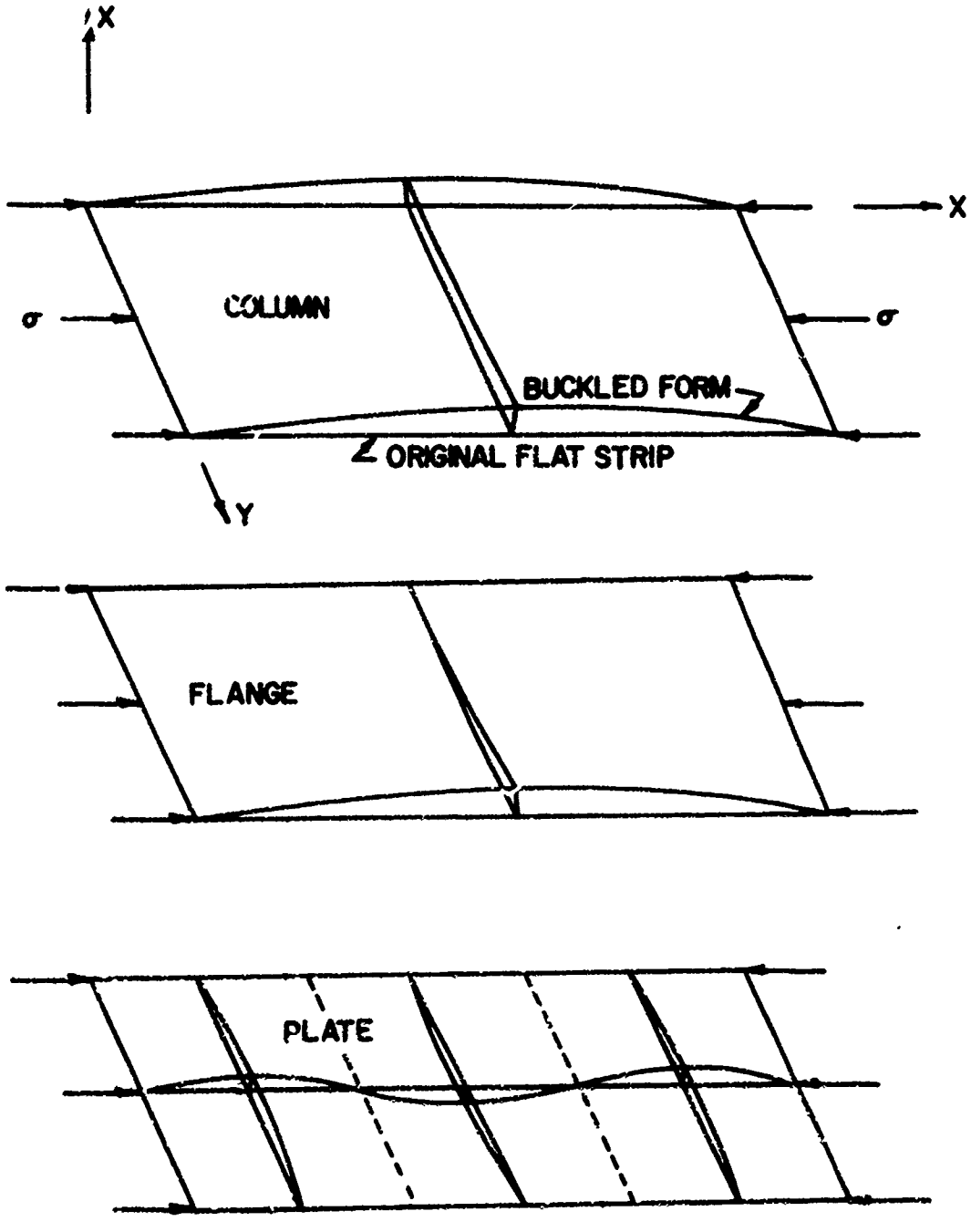

FIGURE 1. TRANSITION FROM COLUMN PLATE AS SUPPORTS ARE ADDED ALONG UNLOADED EDGES. NOTE CHANGES IN BUCKLE CONFIGURATIONS.

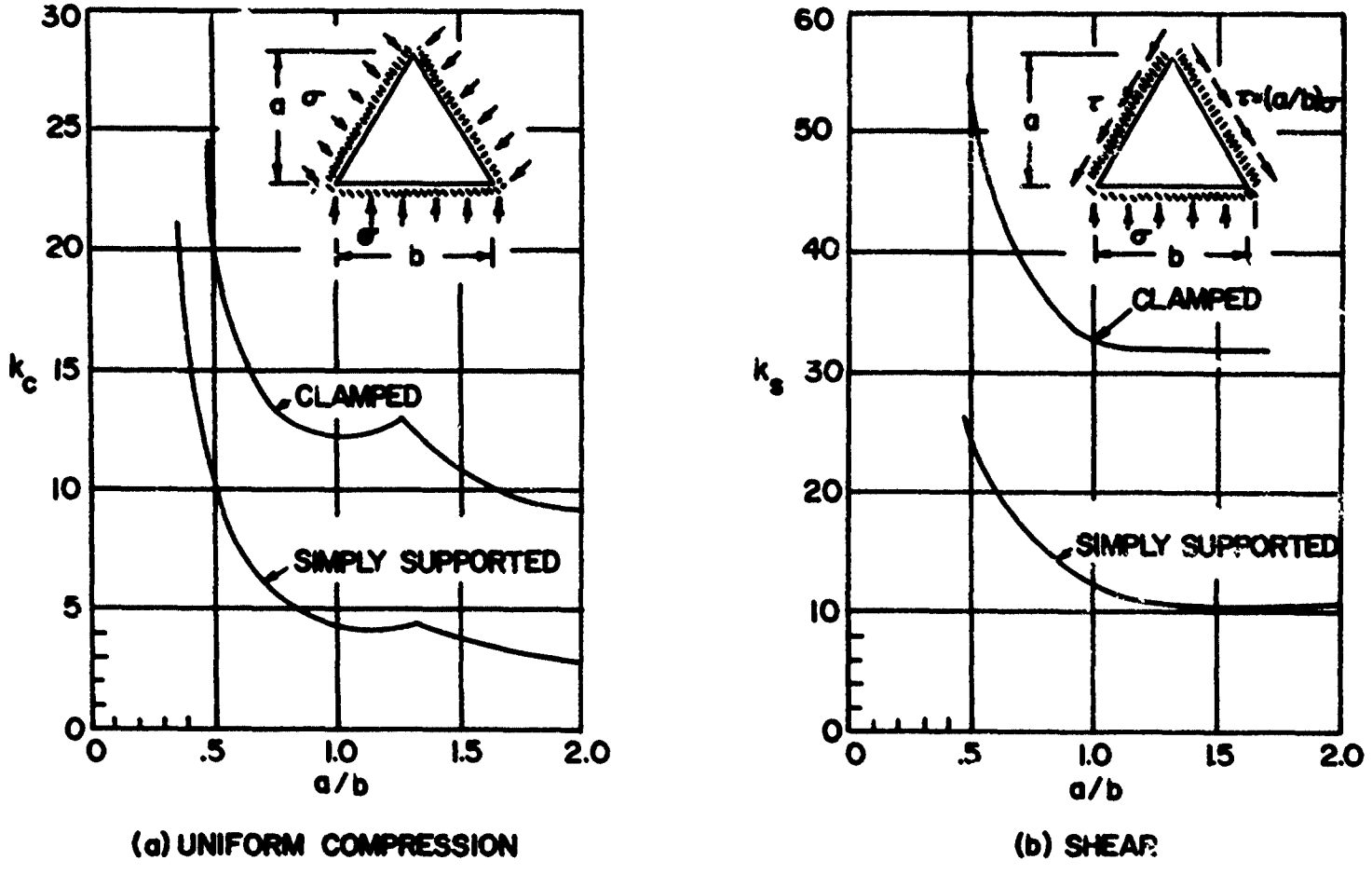

FIGURE 34. BUCKLING COEFFICIENT FOR ISOSCELES TRIANGULAR PLATES

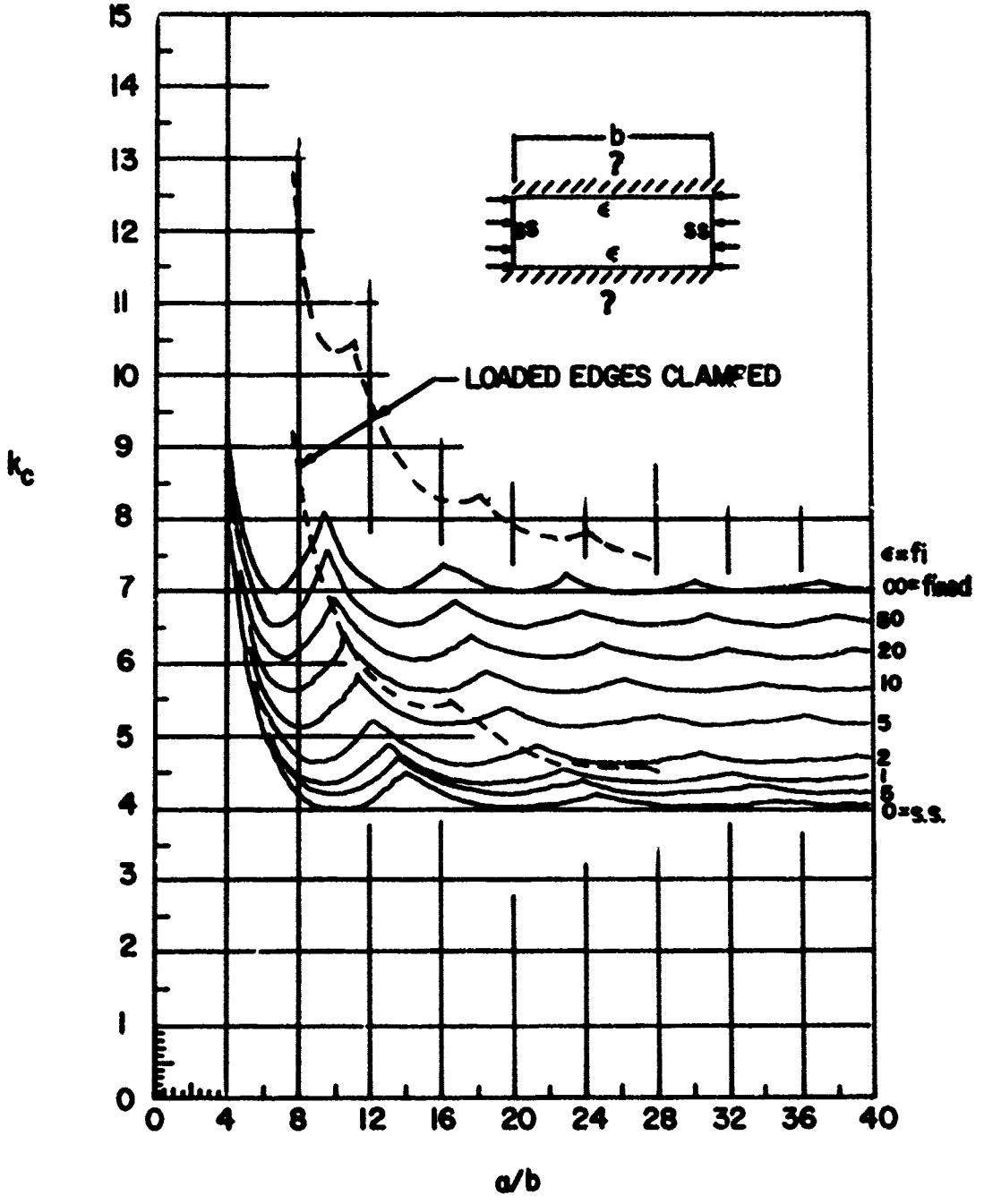

Figure 16. - Compressive-buckling-stress coefficient of plates as a function of a/b for various amounts of edge rotational restraint.

$$\epsilon = \frac{\text{rotational rigidity of sides}}{\text{rotational rigidity of plate}}$$

Subject WEAKENED WEB FRAMES

Ship or Project NON-STANDARD STRUCTURE

Section BSDD Prepared by JCD Date Checked Reviewed

PAGE 15 SHOWS K_c VALUES FOR VARIOUS EDGE ROTATIONAL RESTRAINTS. IN OUR CASE $\epsilon = 1$ SINCE PLATE IS THE ONLY EDGE. HOWEVER, SINCE FORE AND AFT DEFLECTION OF THE WEB IS POSSIBLE, THE ROTATIONAL CONSTRAINT IS MODIFIED. HOWEVER, IT IS FELT THAT THE FIG. ON PAGE 15 SHOWS THAT UNLESS EDGES ARE OF SIGNIFICANTLY GREATER RIGIDITY THAN THE PLATE ITSELF, K_c EQUAL TO THE VALUE FOR NO ROTATION (RIGIDITY) WILL BE CLOSE TO THE EXACT VALUE. EXTENDING TO THE PARTICULAR CASE AT HAND, SINCE DEFLECTION IN FORE AND AFT DIRECTION IS ALSO POSSIBLE, IT IS FELT THAT K_c FOR FREE-FREE (COLUMN) WILL NOT BE FAR FROM THE TRUE VALUE.

IT IS ENVISIONED THAT AS LOAD IS APPLIED BY THE LONGITUDINAL, INTERNAL STRESSES WILL BE BUILT UP IN THE WEB THAT RADIATE OUTWARDLY TOWARD THE INBOARD FLANGE.

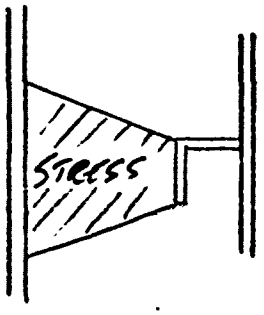

Subject WEAKENED WEB FRAMES

Ship or Project NON-STANDARD STRUCTURES

Section RSDD Prepared by JCD Date Checked Reviewed

IT IS ALSO EXPECTED, THAT THE PLATE IS OF SUCH SMALL RIGIDITY THAT NO LOCAL BUCKLING CAN TAKE PLACE UNTIL INTENSE STRESSES HAVE DEVELOPED TO THE INBOARD FLANGE. BECAUSE OF THE RIGIDITY OF THE INBOARD FLANGE, IT WILL GREATLY RESIST MOVEMENT, IMPOSE A LARGE REACTIVE AND OPPOSITE LOAD TO THAT OF THE LONG., AND CONDITION FOR BUCKLING WILL BE DEVELOPED. THE PLATE WIDTH FOR BUCKLING WILL BE ASSUMED TO BE THE "EFFECTIVE" WIDTH OF THE TRAPEZOIDAL AREA, WITH LOADED EDGES FIXED AND SIDE EDGES FREE.

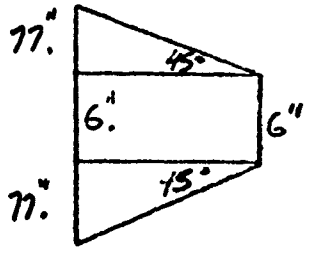

$$\text{EFFECTIVE WIDTH} = \frac{77.+77.+6.+6.}{2}$$

$$= 83.0"$$

$$9/6 = 109./83. = 1.31$$

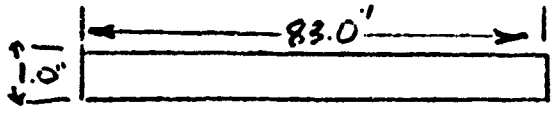

$$I = \frac{83.(1.)^3}{12.0} = 6.92$$

$$r = \sqrt{\frac{6.92}{83}} = .29$$

Subject WEAKENED WEB FRAMES

Ship or Project NON-STANDARD STRUCTURE

Section BSDD Prepared by JCD Date Checked Reviewed

L = COLUMN LENGTH. = 109.

K = EFFECTIVE LENGTH COEFFICIENT = .65
(ROTATION FIXED - APPROXIMATED IDEAL CONDITIONS)

$$\text{BUCKLING STRESS} = \frac{\pi^2 E}{(KL/r)^2} = \frac{\pi^2 \times 29 \times 10^6}{[.65(109.)/.29]^2}$$

$$= 4.79 \text{ KSI} \quad (\text{NOT DEPENDENT ON PLATE WIDTH})$$

NOTE THAT UP TO HERE THE ASSUMED WIDTH OF THE PLATE DOES NOT MAKE ANY DIFFERENCE EVEN THOUGH IT WAS USED IN THE CALCULATION.

∴ ASSUME A 30° OUTWARD RADIATION OF STRESSES IS MORE REPRESENTATIVE THAN A 45° RADIATION.

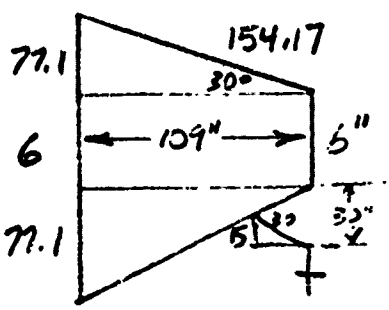

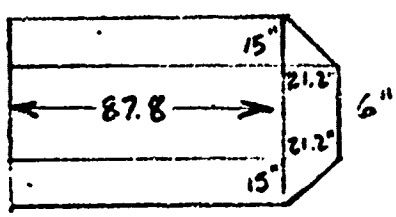

$$AREA = (87.8)(6.0) + (21.2)(6.0) + (20)(15.0)(87.8) + (5)(2.0)(21.2)(15.)$$

$$= 526.8 + 127.2 + 2634. + 318.$$
$$= 3606$$

$$EFFECTIVE\ WIDTH = \frac{3606.}{109.} = 33.1''$$

$$P_{CRIT} = 33.1'' \times 1'' \times 4.79\ KSi = \underline{158.5\ KIPS}$$

P_{CRIT} IS LARGER THAN THE DESIGN LOAD OF 105 KIPS, BUT IT WILL BE ASSUMED THAT THE INBOARD FLANGE WIDTH AND THICKNESS CAN BE INCREASED OR STRUTS PUT BACK IN IN ORDER TO GET THE P_{CRIT} TO JUST ABOVE 105 KIPS. NOTE THAT COLUMNS (STRUTS) WERE TAKEN OUT, BUT THAT DOES NOT SEEM TO BE TOO IMPORTANT, SINCE THE WEB FRAME CAN ARBITRARILY BE MADE WIDER.

Subject WEAKENED WEB FRAMES
Ship or Project VON - STANDARD STRUC. RE
Section BSDD Prepared by JCD Date Checked Reviewed

NOW ONE MUST NOTE THAT ALL PLATE ABOVE THE SECTION CONSIDERED WILL FAIL AT THE SAME TIME OR SOONER (EXCEPT FOR DECK AREA). FROM COLLISION CASE 5, TYPICAL FORCE VALUES FOR THE WEB FRAME REACTION WERE 380 KIPS

$$\therefore \quad \frac{380}{105} = 3.62 = R_m$$

AS COMPARED TO THE $1.67 = R_m$ FOR CASE 5. THIS REPRESENTS A SIGNIFICANT INCREASE IN WEB FRAME YIELDING.

SHEAR AT THE ENDS WILL NOT BE A PROBLEM SINCE THEY CAN BE STIFFENED AGAINST THIS WITHOUT HARMING BUCKLING CHARACTERISTICS.

Subject UNEARENED WEB FRAMES

Ship or Project NON-STANDARD STRUCTURE

Section BSDD Prepared by JCD Date Checked Reviewed

[NOTE THE SHEAR GAVE THE NEXT LARGEST RM IN CASE 5]

USING AN RM= 3.62 THE ENERGY OF CASE 5 WILL BE RECALCULATED.

BENDING ANALYSIS OF SIDE LONGITUDINALLY STIFFENED PLATE FOR ONLY ONE WEB FRAME SPACE DAMAGE IS THE SAME AS CASE 5.

FOR 5 WEB FRAME SPACES

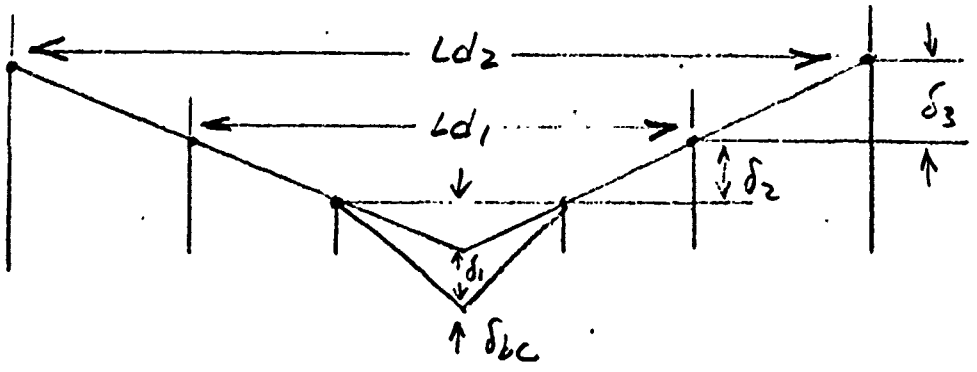

$$\delta_1 = \frac{P_{WF}}{P_b/2}\,\delta_{bc} = \frac{105}{264.2}(.96) = .38$$

$$\delta_2 = (\delta_{bc} - \delta_1)\left(\frac{3L_s}{L_x} - 1\right) = (.96 - .38)(2.) = 1.16$$

$$\delta_1' = \left(\frac{L_{d_1}}{2L_s}\right)\left[\frac{P_{WF}}{P_b/2 - P_{WF}}\right]\delta_2 = \left(\frac{3}{2}\right)\left[\frac{105}{264.2 - 105}\right]1.16 = 1.14$$

$$\delta_3 = \frac{L_{d_1}}{2L_s}\,\delta_2 + \delta_1'\left(\frac{L_{d_2}}{L_{d_1}} - 1\right)\Big] = \left(\frac{3}{2}\right)1.16 - 1.14\left(\frac{5}{3} - 1\right)$$

$$= .98$$

No.

Sheet 22 of

Date Checked Reviewed

OF SIDE LONGITUDINALLY STIFFENED

RAME SPACE DAMAGED

SAME AS COLLISION CASE 5

3	4	5	6	7	8	9	10	11	12	13	14	15	16	17	18		
							.0123										
							11.5										
							2,380										
							11.5										
693	717						760										
							380										

M. Rosenblatt & Son, Inc.

DESIGN CALCULATION SHEET

No.

Sheet 22 of

Subject TANKER DAMAGE ANALYSIS

Ship or Project 120,000 DWT TANKER

Section BSDD Prepared by Date Checked Reviewed

MEMBRANE TENSION ANALYSIS OF SIDE LONGITUDINALLY STIFFENED PLATES FOR ONLY ONE WEB FRAME SPACE DAMAGED

SAME AS COL

SHELL LONGITUDINAL NO.	1	2	3	4	5	6	7	8	9	10	11	12	13
$\varepsilon_r = \frac{\sigma_y}{E_t}\left[\left(\frac{\sigma_a}{\sigma_y}-1\right)-\left(\frac{VL_x}{M_p}\right)\right]$										.0123			
MEMBRANE TENSION DEFL. CAPACITY $\delta_{tc} = \sqrt{\frac{L_t^2}{2}(\varepsilon_r+\varepsilon_a)+\delta_{bc}^2}$										11.5			
AVERAGE MEMBRANE TENSION FORCE $T = A\sigma_y\left(\frac{\sigma_y+\sigma_a}{2\sigma_y}\right)$										2,380			
δ_m = LESSER OF δ OR δ_{tc}										11.5			
NET LATERAL FORCE ON LONG'L DUE TO MEMBRANE TENSION ONLY $P_{tm} = 4T\delta_m/L_t$	1034	700	698	717						760			
$P_{tm}/2$										380			

SHELL LONGITUDINAL NO.	1	2	3	4	5	6	7	8	9	10	11	12		
$\varepsilon_r = \frac{\sigma_y}{E_t L}\left[\left(\frac{\sigma_u}{\sigma_y}-1\right)-\left(\frac{VL_y}{M_p}\right)\right]$										.0123				
MEMBRANE TENSION DEFL. CAPACITY $\delta_{tc} = \sqrt{\frac{L_t^2}{4}(\varepsilon_r+\varepsilon_c)+\delta_{bc}^2}$										11.5				
AVERAGE MEMBRANE TENSION FORCE $T = A\sigma_y\left(\frac{\sigma_y+\sigma_u}{2\sigma_y}\right)$										2,380				
δ_m = LESSER OF δ OR δ_{tc}										11.5				
NET LATERAL FORCE ON LONG'L DUE TO MEMBRANE TENSION ONLY $P_{tm} = 4T\delta_m/L_t$	1034	700	698	717						760				
$P_{tm}/2$										380				

FIGURE E-4

4	5	6	7	8	9	10	11	12	13	14	15	16	17	18		
						.0123										
						11.5										
						2,380										
						11.5										
717						760										
						380										

No. 2087-
Sheet 23

Checked Reviewed

F SIDE LONGITUDINALLY
MORE WEB FRAME

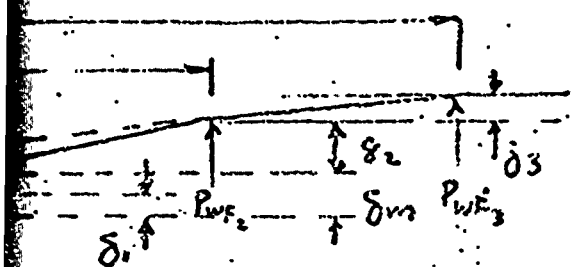

ASSUME FRAME #10 : TO BE AN AVERAGE FRAME
WITH $P_{tm} = 730$
$P_{tm}/2 = 365$.
T = 2,300 KIPS

3	4	5	6	7 8	9	10	11	12	13	14	15
						105					
						3.31					
						16.38					
						105					
						9.86					
						9.81					

M. Rosenblatt & Son, Inc.

No. 2087-

Sheet 23

DESIGN CALCULATION SHEET

Subject TANKER DAMAGE ANALYSIS

Ship or Project 120,000 DWT TANKER

Section E E D D Prepared by Date Checked Reviewed

MEMBRANE TENSION ANALYSIS OF SIDE LONGITUDINALLY STIFFENED PLATES FOR THREE OR MORE WEB FRAME SPACE DAMAGED

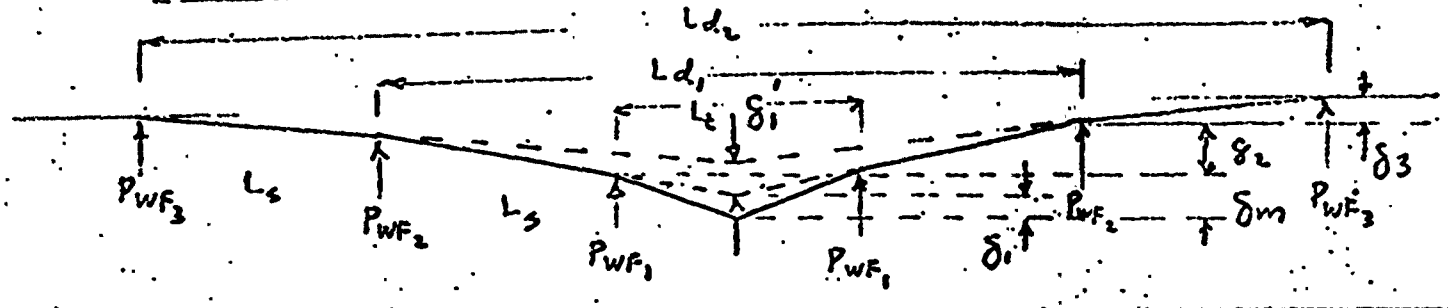

ASSUME FR

WITH $P_{tm} =$

$P_{tm}/2$

$T =$

SHELL LONG'L NUMBER	1	2	3	4	5	6	7	8	9	10	11
RESISTANCE OF FIVE 3 FRAMES #1 TO CENTRAL MOMT OF LONGL $P_{WF_1} = (P_{tm_1}/2) \div R_{M1}$ (KIPS)										105	
CENTER DEFLECTION AS SHOWN $\delta_1 = \delta_{m1}(P_{WF_1}/.5P_{tm1})$ (IN)										3.31	
WEB FRAMES #1 DEFLECTION AS SHOWN $\delta_2 = (\delta_m - \delta_1)(L_{d_1}/L_1 - 1)$ (IN)										16.38	
LATERAL FORCE ON LONGL DUE TO MEMBRANE TENSION WF_2 $P_{tm_2} = 2T\frac{\delta_2}{L_2}$ $P_{tm_2}/2$ (KIP)											
$R_{m_2} = R_{m_1}\left(\frac{P_{tm_2}}{P_{tm_1}}\right)$											
$P_{WF_2} = \left(\frac{P_{tm_2}}{2}\right) \div R_{m_2}$										105	
$\delta_1' = \left(\frac{L_{d_1}}{2L_2}\right)\left[\frac{P_{WF_2}}{.5P_{tm_2}}\right]\delta_2 = S(L_d)\frac{P_{WF}}{T}$										9.86	
$\delta_3 = \left[\left(\frac{L_{d_1}}{2L_2}\right)\delta_2 - \delta_1'\right]\left(\frac{L_{d_2}}{L_{d_1}} - 1\right)$										9.81	

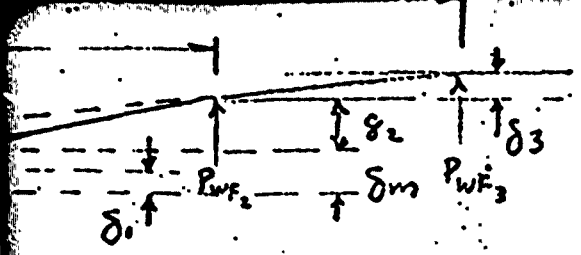

ASSUME FRAME #10 TO BE AN AVERAGE FRAME

WITH $P_{tm} = 730$

$P_{tm}/2 = 365$

$T = 2{,}300$ KIPS

3	4	5	6	7	8	9	10	11	12	13	14	15
							105					
							3.31					
							16.38					
							105					
							9.86					
							0.81					
							37.69					

SPACE DAMAGED

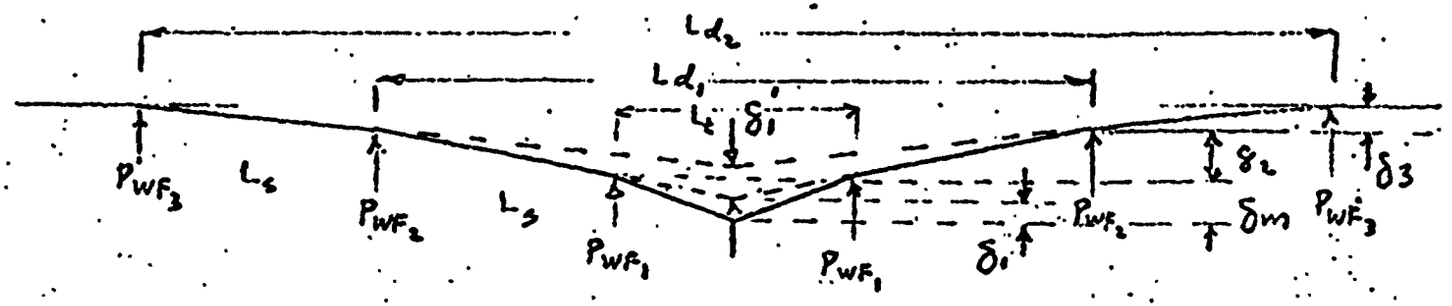

ASSUME FR
WITH P_{tm}
$P_{tm}/2$
T

SHELL LONGL NUMBER	1	2	3	4	5	6	7	8	9	10	11
RESISTANCE OF, WEB FRAMES #1 TO CENTRAL POINT OF LONGL $R_{m_1} = (P_{tm_1}/2) \div R_{m_1}$ (KIPS)										105	
CENTER DEFLECTION AS SHOWN $\delta_1 = \delta_m (P_{WF_1}/.5 P_{tm_1})$ (IN)										3.31	
WEB FRAMES #1 DEFLECTION AS SHOWN $\delta_2 = (\delta_m - \delta_1)(L_d/L_t - 1)$ (IN)										16.38	
LATERAL FORCE ON LONGL DUE TO MEMBRANE TENSION WF #2 $P_{tm_2} = 2T \frac{\delta_2}{L_s}$											
$P_{tm_2}/2$ (KIP)											
$R_{m_2} = R_{m_1} \left(\frac{P_{tm_2}}{P_{tm_1}}\right)$											
$P_{WF_2} = \left(\frac{P_{tm_2}}{2}\right) \div R_{m_2}$										105	
$\delta_1' = \left(\frac{L_{d_1}}{2L_s}\right)\left[\frac{P_{WF_2}}{.5 P_{tm_2}}\right] \delta_2 = .5\left(\frac{L_{d_1}}{L_s}\right)\frac{P_{WF}}{T}$										9.86	
$\delta_3 = \left[\left(\frac{L_{d_1}}{2L_s}\right)\delta_2 - \delta_1'\right]\left(\frac{L_{d_2}}{L_{d_1}} - 1\right)$										9.81	
$\delta = \delta_m + \delta_2 + \delta_3$											
										37.69	

No. 2087
Sheet 24

ked Reviewed

Y CALCULATION

FOR $(\delta - \delta_2 - \delta_3) \leq \delta_{tc}$
$\delta_2^2/L_s + \delta_3^2/t_s - \epsilon_c L_d$

4	5	6	7	8	9	10	11	12	13	14	15			
						1.82								
						1.85								
						.66								
						-.2								
						4.13								
						9499.								

TIC ENERGY BELOW
WIP IS NEGLECTED.

M. Rosenblatt & Son, Inc. No. 2087

DESIGN CALCULATION SHEET Sheet 24

Subject TANKER DAMAGE ANALYSIS

Ship or Project 120,000 DWT TANKER

Section 3SDD Prepared by Date Checked Reviewed

MEMBRANE TENSION PLASTIC ENERGY CALCULATION

TOTAL MEMBRANE TENSION ELONGATION FOR $(\delta - \delta_2 - \delta_3) \leq \delta_{tc}$

$$e_t = \frac{2}{L_t}\left[(\delta-\delta_2-\delta_3)^2 - \delta_{bc}^2\right] + \delta_2^2/L_s + \delta_3^2/t_s - \varepsilon_c L_d$$

SHELL LONG'L NO.	1	2	3	4	5	6	7	8	9	10	11	12
(a) $\frac{2}{L_t}\left[(\delta-\delta_2-\delta_3)^2-\delta_{bc}^2\right]$										1.82		
(b) $\left[\delta_2^2/L_s\right]^{SH_2^2}$										1.85		
(c) $\left(\delta_3^{2-\delta_{bc}^2}/L_s\right)$										.66		
(d) $-\varepsilon_c L_d$										-.2		
$e_t = (a)+(b)+(c)+(d)$										4.13		
MEMBRANE TENSION PLASTIC ENERGY, $E_t = T \times e_t$										9499.		

NOTE: VERTICAL MEMBRANE PLASTIC ENERGY BELOW FORE-FOOT OF STRIKING SHIP IS NEGLECTED.

$\delta_2/L_s + \delta_3/\mu_s - \xi_c L_d$

4	5	6	7	8	9	10	11	12	13	14	15			
						1.82								
						1.85								
						.66								
						-.2								
						4.13								
						9499.								

TIC ENERGY BELOW
DIP IS NEGLECTED.

TOTAL MEMBRANE TENSION ELONGATION FOR $(\delta - \delta_2 - \delta_3) \leq \delta_{tc}$

$e_t = \frac{2}{L_t}\left[(\delta - \delta_2 - \delta_3)^2 - \delta_{bc}^2\right] + \delta_2^2/L_s + \delta_3^2/L_s - \varepsilon_c L_d$

SHELL LONG'L NO.	1	2	3	4	5	6	7	8	9	10	11
(a) $\frac{2}{L_t}\left[(\delta-\delta_2-\delta_3)^2-\delta_{bc}^2\right]$										1.82	
(b) $\left[\delta_2^2/L_s\right]^{\delta_{bc}^2}$										1.85	
(c) $\left(\delta_3^2/L_s\right)^{\delta_{bc}^2}$										.66	
(d) $-\varepsilon_c L_d$										-.2	
e_t = (a) + (b) + (c) + (d)										4.13	
MEMBRANE TENSION PLASTIC ENERGY, $E_t = T \times e_t$										9499.	

NOTE: VERTICAL MEMBRANE PLASTIC ENERGY BELOW FOREFOOT OF STRIKING SHIP IS NEGLECTED.

THEREFORE IT IS SHOWN ABOVE THAT A TYPICAL SECTION OF PLATE WILL ABSORB

9999. KIPS-INS

COLUSION CASE 5 SHOWS A TYPICAL PLATE SECTION WILL ABSORB

5300 KIPS-INS

$\therefore$ INCREASE $= \frac{9999}{5300} \times 100 - 100 = 79.2\%$

ASSUME TOTAL ENERGY ABSORBED WITH NEW CONFIGURATION IS:

$$89,075 \frac{(100. + 79.2)}{100} = 159,622. \text{ IN-KIPS}$$

M. Rosenblatt & Son, Inc. No. 2097

DESIGN CALCULATION SHEET Sheet 45 of

Subject NON - STANDARD STRUCTURE - WIRE ROPE BARRIERS

Ship or Project TANKER COLLISION STRUCTURAL ANALYSIS

Section BSDD Prepared by JCD Date Checked Reviewed

WIRE ROPE BARRIERS

THERE ARE EXTREMELY HIGH STRENGTH STEELS AVAILABLE (ABOVE 100 KSI YIELD) WHICH ARE TOO NON-DUCTILE TO BE CONSIDERED FOR USE AS SIDE SHELL PLATING. SUCH A STEEL WOULD PRODUCE VERY LARGE FORCES ON THE WEB FRAMES DURING A COLLISION IF IT COULD BE UTILIZED AND LENGTH OF DAMAGE COULD VERY WELL BE LIMITED BY THE BULKHEADS.

IN ORDER TO AVERT THE TWO PROBLEMS MENTIONED ABOVE (1. EARLY FAILURE DUE TO NON-DUCTILITY 2. LIMITED LENGTH OF DAMAGE) AND STILL MAKE USE OF THE HIGHEST STRENGTH STEELS AND THE LARGE FORCES THEY CAN WITHSTAND, CABLES OR WIRE ROPE MADE OF THIS MATERIAL WERE CONSIDERED. THESE CABLES COULD BE LOCATED INSIDE OR OUTSIDE THE SHIP, RUNNING ALONG THE SIDE SHELL AND ANCHORED AT SUCH POINTS (LIKE STEM AND STERN) THAT ALLOW THE SMALL ELASTIC STRAINS OF THE ROPE TO GIVE DEFLECTIONS EQUAL TO THOSE OF THE DUCTILE PLATE. (IF ROPES ARE INSIDE THE SHIP THEY WOULD HAVE TO BE GUIDED THROUGH WEBS AND BULKHEADS AND ALLOWED TO SLIDE THROUGH THESE.)

M. Rosenblatt & Son, Inc. No. 2087
DESIGN CALCULATION SHEET Sheet 27 of

Subject NON-STANDARD STRUCTURE - WIRE ROPE BARRIERS
Ship or Project TANKER COLLISION STRUCTURAL ANALYSIS
Section BSLD Prepared by JCD Date Checked Reviewed

PARAMETRIC STUDY CASE 5

FROM A IT CAN BE SEEN THAT THE MEMBRANE TENSION IS APPROXIMATELY 2,400 KIPS FOR 1" (M.S.) PLATE. FOR 1 3/8" PLATE (M.S.), CASE 8 SHOWS THE TENSION IS ABOUT 3,000 KIPS. FOR 1 3/4" PLATE (M.S.) 2087-10 SHOWS THE TENSION IS ABOUT 3,700 KIPS.

∴ IT APPEARS THAT A 3/8" INCREASE IN PLATE GIVES 650 KIPS INCREASE / LONG WITH EFFECTIVE SIDE PLATE

FOR PURPOSES OF COMPARISON, BETH. STEEL'S STRONGEST WIRE ROPE: BREAKING STRENGTH = 146,000 PSI WAS USED.

A 4" DIA. ROPE WILL SUPPORT 1670 KIPS BEFORE BREAKING. FOR 0 TO MAX. DEFLECTION THE AVERAGE FORCE IS 835. KIPS, WHICH IS WHAT SHOULD BE COMPARED WITH SIDE PLATE TENSION.

∴ THEREFORE PUTTING ONE 4" ROPE BEHIND EACH LONG. WILL SLIGHTLY MORE THAN OFFSET A DECREASE IN SIDE OF 3/8". THEREFORE WIRE ROPE DOES NOT SEEM TO HAVE ANY BETTER ENERGY ABSORBING CAPABILITY OVER SOMEWHAT THICKER SIDE PLATE.

Subject NON - STANDARD STRUCTURE - DOUBLE HULL ACTING IN PARALLEL
Ship or Project TANKER COLLISION STRUCTURAL ANALYSIS
Section BSDD Prepared by JCD Date Checked Reviewed

BOTH SIDES OF DOUBLE HULL ACTING TOGETHER

CALCULATIONS OF CASE 6 SHOW THE ABSORBED ENERGY ANALYSIS FOR A DOUBLE HULL SHIP, WHEN THE TWO SIDES ACT IN SERIES.

IT WAS THOUGHT THAT THE BOTH SIDES ACTING IN PARALLEL WOULD CAUSE A CONSIDERABLE INCREASE IN ENERGY ABSORBED BECAUSE OF INCREASED WEB FRAME FORCES.

CALCULATION CASE 10 SHOWS THE ABSORBED ENERGY ANALYSIS FOR A SINGLE HULL SHIP OF 13/4" SIDE PLATE. SINCE THE MEMBRANE TENSION FORCE IS DIRECTLY PROPORTIONAL TO THE PLATE THICKNESS, FOR THE SAME BACK UP LONGITUDINALS, 1 3/4" SINGLE HULL OR 1" AND 3/4" DOUBLE HULL WILL GIVE NEARLY THE SAME MEMBRANE TENSION, SAME WEB FRAME FORCES, AND SAME MEMBRANE ENERGY.

THEREFORE THE DOUBLE SKIN WORKING TOGETHER WILL HAVE NEARLY THE SAME ENERGY ABSORPTION AS CASE 10 PLUS THE ADDED DECK DESTRUCTIVE ENERGY AND OUTER SHELL DUCTILE TEARING ENERGY. THESE WILL BE A SMALL PERCENTAGE OF THE TOTAL ENERGY ABSORBED.

THEREFORE, THE TWO HULLS ACTING IN PARALLEL WILL NOT GIVE MUCH MORE ENERGY ABSORPTION THAN A SINGLE HULL OF EQUIVALENT THICKNESS AND THE SERIES HULL OF CASE 6 DOES NOT GIVE MUCH LESS. THEREFORE THERE DOES NOT SEEM TO BE A GREAT ADVANTAGE IN PARALLEL HULL DEFORMATION.

Subject SHOCK ABSORBING SIDE

Ship or Project

Section LSDD Prepared by JCD Date Checked Reviewed

ONE SPACE DAMAGED

(A) PRESSURE TANK

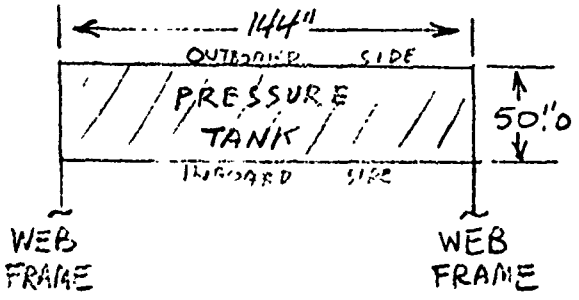

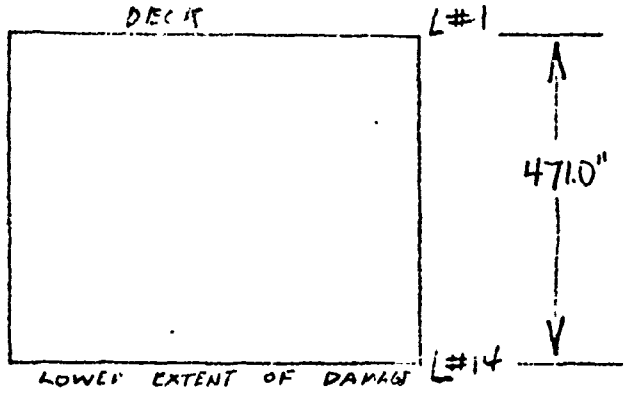

TANK VOLUME = 471.0" x 50." x 144.0"
= 3,391,200 IN^3 = V_1

AS SHIP STRIKES

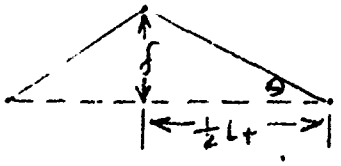

AREA OF TENT = $\frac{1}{2} \delta L_+ = 72\delta$

VOLUME = 471.0 x 72.0 δ
= 33912.0 δ IN^3 = V_{LOST}

$$\frac{V_2}{V_1} = \frac{V_1 - V_{LOST}}{V_1}$$

SHOCK ABSORBING SIDE

WEB FRAME OR SWASH BULKHEAD

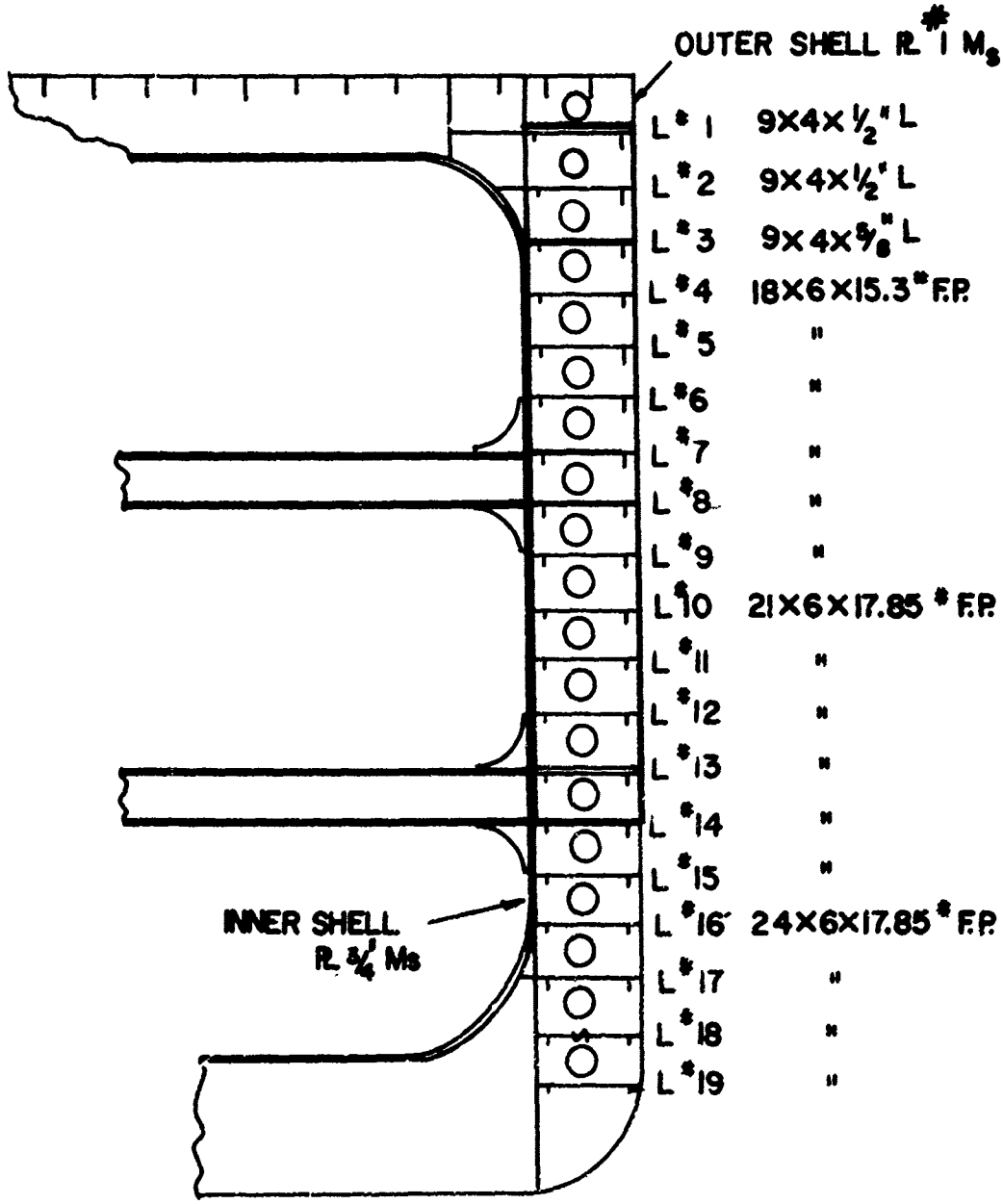

—— DENOTES PRESSURE VESSEL SHOCK ABSORBING TANK

M. Rosenblatt & Son, Inc. No. 2587

DESIGN CALCULATION SHEET Sheet 31 of

Subject NON-STANDARD STRUCTURE - SHOCK ABSORBING SIDE

Ship or Project TANKER COLLISION STRUCTURAL ANALYSIS

Section BSDD Prepared by JCD Date Checked Reviewed

V_1 IN^3	δ	$V_{LOST} = 33912.\delta$	$V_2/V_1 = \frac{V_1 - V_{LOST}}{V_1}$
3,391,200.	1.0		.99
	2.0		.98
	3.0		.97
	4.0		.96

(B) PRESSURE

MAXIMUM DEFLECTION = 11.5"
FOR ONE SPACE DAMAGED
(CASE 5)

THE DECELERATION WILL BE BASED ON THE PRESSURE HISTORY, SINCE ONLY A PRESSURE ACCEPTABLE TO A PARTICULAR PRESSURE VESSEL DESIGN WILL BE ACCEPTABLE.

COEFFICIENT OF COMPRESSIBILITY OF OIL = $70. \times 10^{-6}$
(@ 16.5°C, FROM KENT'S MECHANICAL ENGINEERS HANDBOOK)

B = COEFFICIENT OF COMPRESSIBILITY = $\frac{1}{V_1}\left[(V_1 - V_2)/(P_2 - P_1)\right]$

WHERE V_1 AND V_2 ARE VOLUMES AT SAME TEMP.
P_1 AND P_2 ARE PRESSURES (ATMOSPHERES)

1 STANDARD ATMOSPHERE $\cong$ 14.7 LB/IN^2

$$\therefore \quad B = \frac{14.7}{V_1}\left[(V_1 - V_2)/(P_2 - P_1)\right]$$

$$P_1 = 14.7$$
$$V_1 = 1.0$$

$$B = \frac{14.7}{1}\left[1 - V_2/(P_2 - 1)\right]$$

$$(P_2 - 1) = \frac{14.7}{(70. \times 10^{-6})} (1 - V_2)$$

$$V_2 = \left[-(P_2 - 14.7)(4.76 \times 10^{-6}) + 1 \right]$$

P_2 (psi)	V_2
100	~1.0
200	
300	
400	
500	~1.0
600	
700	
1000	.995
1500	
2000	
2500	.988

∴ COMPRESSIBILITY IS SMALL EFFECT AND PRESSURE IN THE TANK WILL BUILD UP VERY QUICKLY.

(C) STRUCTURE OF PRESSURE TANKS

TIMOSHENKO GIVES RESULTS FOR PLATES WITH CLAMPED EDGES AND LARGE DEFLECTIONS (BENDING (S.D.) AND MEMBRANE (L.D.)). HIS RESULTS ARE MORE CONSERVATIVE THAN THE U.S. NAVY CRITERIA WITH NO PERMANENT SET.

.5" M.S. PLATE WITH 48" WIDTH

TIMOSHENKO: $S_y = \frac{33{,}000\,(48)^2(1-(.33)^2)}{29{,}000{,}000\,(.5)^2}$

[THEORY OF PLATES AND SHELLS]

$= 9.34$

$\therefore \frac{qb^4}{Dh} \cong 100$

$D = \frac{29{,}000{,}000\,(.5)^3}{12.0\,(1-(.33)^2)} = 339{,}000$

$q = \frac{100\,(339{,}000)(.5)}{48^4} = 3.19 \text{ psi}$

$= \boxed{7.16' \text{ HEAD}}$

FOR NO PERMANENT SET (NAVY SPECS.)

$\sqrt{H} = \frac{Ct}{Fb} = \frac{350(.5)}{1.0\,(48)} = 3.65$

$\therefore \boxed{H = 13.32 \text{ FT. HEAD}}$

WITH PERMANENT SET:

$$\sqrt{H} = \frac{700(.5)}{1.0(46)} = \boxed{53.2 \text{ FT. HEAD}}$$

$$= 23.7 \text{ psi}$$

THE RESULTS FROM TIMOSHENKO ARE FOR EXACT FIXED EDGES (NO STIFFENED PLATES) AND IT IS THOUGHT THAT THIS HAS CAUSED THE DIFFERENCE WITH RESULTS FOR NO PERMANENT SET. HOWEVER SINCE WE ARE ONLY INTERESTED FOR COLLISION THE RESULTS FOR PERMANENT SET WILL BE USED

1" M.S. PLATE - 36" SPACING

$$\sqrt{H} = \frac{700(1.0)}{1.0(36.)} = 19.44$$

$$H = 377.9' \text{ HEAD} = 164.34 \text{ psi}$$

THE WEB FRAMES BETWEEN THE INSIDE AND OUTSIDE TANK WALLS MUST BE VERTICALLY STIFFENED TO TAKE THE DESIGN PRESSURE:

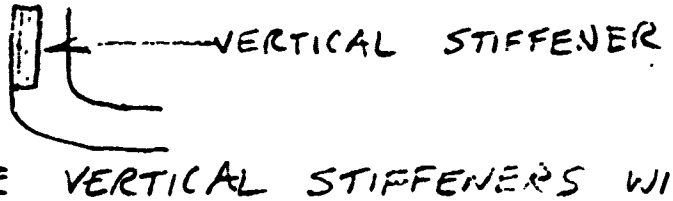

THESE VERTICAL STIFFENERS WILL BE ORIENTED SO AS TO OFFER NO RESISTANCE TO WEB FRAME FAILURE FROM COLLISION LOAD.

THE BACKUP STRUCTURE INBOARD OF THE INNER TANK WALL MUST BE SUCH THAT IT WILL NOT COLLAPSE UNDER ANY CIRCUMSTANCES.

(D) ANALYSIS OF ONE WEB AND FIVE WEB FRAME SPACES

TANK VOLUME (PAGE 3) = 3,391,200 IN^3
INCURSION INTO TANK = 11.5"

VOLUME OF OIL DISPLACED = 11.5 (33912.) = 389,988 IN^3
PRESSURE OF DISPLACED OIL = 168.
ENERGY DUE TO DISPLACED OIL = 168 $LB/IN^2 \times 389{,}988\ IN^3$
= 65,517 IN-KIPS

ESTIMATION OF COLLISION TIME = 1 SEC (WILL ACTUALLY BE LESS)

OIL TO BE MOVED = 389,988 IN^3/SEC

ASSUME 4 VALVES WITH 8" DIA. THROATS:
AREA = $4\pi(4)^2 = 201.1\ IN^2$

FLOW RATE = $\frac{389{,}988}{201.1\ IN^2} \frac{IN^3}{SEC}$ = 1939.3 IN/SEC
= 161.6 FT./SEC
OR 120 MPH

∴ NO PROBLEM

FOR NEW WEB FRAME DESIGN: [5 WEB FRAME SPACES CASE 5]

δ_m = 11.5
δ_2 = 15.34
δ_3 = 7.7

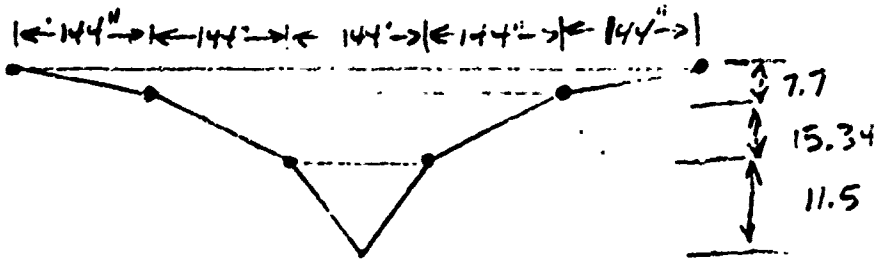

Subject NON-STANDARD STRUCTURE - SHOCK ABSORBING SIDE
Ship or Project TANKER COLLISION STRUCTURAL ANALYSIS
Section BSDD Prepared by JCD Date Checked Reviewed

TOTAL VOLUME = $5(3,391,200) = 16,956,000.\ IN^3$

VOLUME DISPLACED = $389,988 + 15.34(144)(471) + 7.7(144)(471)$
$+ 144(15.34)(471) + 7.7(144)(471)$

$= 3,515,318.\ IN^3$

ENERGY = $\Delta P = 3,515,318. \times 168. = 590573.$ IN-KIPS

$\frac{3,515,318.}{389,988.} = 9.01$ ∴ 9 TIMES AS MUCH OIL MUST BE MOVED WITH RESPECT TO ONE WEB FRAME SPACE AND ONLY 4 MORE WEB FRAME SPACES ARE AVAILABLE. THEREFORE SIZE AND NUMBER OF BOTH VALVES PER WEB FRAME SPACE MUST BE INCREASED.

TOTAL ENERGY ABSORBED = 590,573 OIL DISPL.
141,000 STRUCTURE
731,573 IN-KIPS

FOR T-2 STRIKE

$$\frac{731,573\ (12.0)^2}{512,422\ (1.64)^2} = V^2 = 71.98\ KNOT^2$$

V = 8.5 KNOTS

M. Rosenblatt & Son, Inc. No. 2087

DESIGN CALCULATION SHEET Sheet 37 of

Subject NON - STANDARD STRUCTURE - SHOCK ABSORBING SIDE

Ship or Project TANKER COLLISION STRUCTURAL ANALYSIS

Section BSDD Prepared by JCD Date Checked Reviewed

PAGES 38, 39 AND 40 HAVE BEEN DELETED.

(F) PROBLEMS ASSOCIATED WITH THE PRECEEDING ANALYSIS

VALVES: THE VALVES TO BE USED ARE PRESSURE COMPENSATED AND SET FOR WIDE OPEN @ 168 PSI.

EQUATIONS - BERNOULLI EQUATION:

$$Z_1 + \frac{144 P_1}{\rho_1} + \frac{V_1^2}{2g} = Z_2 + \frac{144 P_2}{\rho_2} + \frac{V_2^2}{2g} + h_L$$

h_L = HEAD LOSS THROUGH VALVE (FEET OF FLUID)
$Z_1 = Z_2$ = VERTICAL LOCATION OF VALVE (FEET)
P_1 = TANK PRESSURE PSI (GUAGE)
P_2 = CARGO TANK PRESSURE PSI (GUAGE)
$\rho_1 = \rho_2$ = OIL DENSITY (LBS/FT^3)
V_1 = MEAN VELOCITY OF FLOW IN TANK (FT/MIN)
V_2 = MEAN VELOCITY IN CARGO TANK (FT/MIN)
g = ACCELERATION OF GRAVITY = 32.2 FT/SEC^2

h_L - HEAD LOSS THROUGH A VALVE

$$h_L = K \frac{V^2}{2g}$$

V = MEAN FLOW - FT/SEC
K = RESISTANCE COEFFICIENT

μ = 33. CENTIPOISE

S = SPECIFIC GRAVITY @ 60°F 32.6° API CRUDE (CRANE A-1)
= .862 (53.77 LBS/FT^3)

S = .875 @ 40°F

(F) PROBLEMS ASSOCIATED WITH THE PRECEEDING ANALYSIS

VALVES: THE VALVES TO BE USED ARE PRESSURE COMPENSATED AND SET FOR WIDE OPEN @ 168 PSI.

EQUATIONS - BERNOULLI EQUATION:

$$Z_1 + \frac{144 P_1}{\rho_1} + \frac{V_1^2}{2g} = Z_2 + \frac{144 P_2}{\rho_2} + \frac{V_2^2}{2g} + h_L$$

h_L = HEAD LOSS THROUGH VALVE (FEET OF FLUID)
$Z_1 = Z_2$ = VERTICAL LOCATION OF VALVE (FEET)
P_1 = TANK PRESSURE PSI (GUAGE)
P_2 = CARGO TANK PRESSURE PSI (GUAGE)
$\rho_1 = \rho_2$ = OIL DENSITY (LBS/FT^3)
V_1 = MEAN VELOCITY OF FLOW IN TANK (FT/MIN)
V_2 = MEAN VELOCITY IN CARGO TANK (FT/MIN)
g = ACCELERATION OF GRAVITY = 32.2 FT/SEC^2

h_L - HEAD LOSS THROUGH A VALVE

$$h_L = K \frac{V^2}{2g}$$

V = MEAN FLOW - FT/SEC
K = RESISTANCE COEFFICIENT

μ = 33. CENTIPOISE

S = SPECIFIC GRAVITY @ 60°F 32.6° API CRUDE (CRANE A-1)
= .862 (53.77 LBS/FT^3)

S ≐ .875 @ 40°F

M. Rosenblatt & Son, Inc. No. 2047

DESIGN CALCULATION SHEET Sheet 42 of

Subject NON STANDARD STRUCTURE - SIDE ABSORBING SIDE

Ship or Project TANKER COLLISION STRUCTURAL ANALYSIS

Section DSDD Prepared by JCD Date Checked Reviewed

$\rho = .875 \times 62.4 = 54.6$ LBS/FT^3

VALVE DIA = 8"

VALVE LENGTH = 18"

USE SCHEDULE 40 PIPE (A-30)

$d = 7.981$

$D = .6651$

$d^3 = 508.36$

TOTAL FLOW = 3,515,318 IN^3 = 15218.0 GALLONS

ASSUME TOTAL COLLISION LASTS 1 SEC

$\therefore \frac{15218.\ \text{GAL}}{\text{SEC}} = 913070.\ \text{GPM}$

ASSUME $\frac{20}{10}$ VALVES PER WEB FRAME SPACE.

$\therefore$ 5 WEB FRAME SPACES

$\therefore \frac{100}{50}$ VALVES

$\frac{913070.\ \text{GPM}}{\frac{50}{100}\ \text{VALVES}} = 9130.\ \text{GPM/VALVE} \quad 18260.$

$R_c = \frac{50.6\,(18261.)\,54.6}{(33.)\,(7.981)} = \frac{95,778.}{191,556.}$

$L/D = 150$ [FOR IN LINE BALL] (CRANE A-30 [FULLY OPEN])

$f = .0175$ @ R_c

$.0195$ @ R_e

Subject VON STANDARD STRUCTURE - SHOCK ABSORBING SIDE
Ship or Project TANKER COLLISION STRUCTURAL ANALYSIS
Section BSDD Prepared by JCD Date Checked Reviewed

AVAILABLE PRESSURE DROP:
PRESSURE INSIDE OF TANK = 168 PSI
DEPTH OF VALVE FROM OIL SURFACE ~ 33'
~13 PSI

AVAILABLE PRESSURE FOR DROP = 155 PSI

$K = f\frac{L}{D}$ OR $\frac{L}{D} = \frac{K}{F}$

ENTRANCE LOSS - K = .04
EXIT LOSS - K = 1.0

ENTRANCE $\frac{L}{D} = \frac{.04}{.0175}$, EXIT $\frac{L}{D} = \frac{1.0}{.0175}$

$= 2.29$ $= 57.1$

TOTAL $\frac{L}{D} = 2.29 + 150 + 57.1 = 209.39$

TOTAL EQUIVALENT LENGTH OF PIPE = $\frac{L}{D} D = 209.39(.665)$

$= 139.27'$

$$\text{PRESSURE DROP} = \frac{3fLV^2}{d} = \frac{(.01294)(54.6)(.0175)(139.27)(116.97)^2}{7.981}$$

$$V = \frac{.408\,Q}{d^2} = \frac{.408\,(18{,}261.)}{7.981^2} = \frac{9130.}{58.49} = 116.97 \text{ FT/SEC}$$

82.24
295.177

∴ WITH A NUMBER OF VALVES BETWEEN 50 AND 100 THE 155 PSI PRESSURE DROP WILL BE REALIZED

M. Rosenblatt & Son, Inc. No. 2327

DESIGN CALCULATION SHEET Sheet 44 of

Subject NON STANDARD STRUCTURE - SHOCK ABSORBING SIDE

Ship or Project TANKER COLLISION STRUCTURAL ANALYSIS

Section ESDD Prepared by JCD Date Checked Reviewed

FOR VALVE :

$$\Delta P \text{ OF VALVE} = \frac{150}{209.39}(155) = 111.03$$

$$d^4 = \frac{.000017.99\,(.0195)(150.)(54.6)(9130.)^2}{111.03}$$

$$= 2157$$

$$d^2 = 46.44$$

$$d = 6.81$$

∴ 8" VALVE WILL BE O.K.

[NOTE VALVE HAS TO BE FULLY OPEN FOR PREVIOUS L/D TO HOLD]

Subject NON STANDARD STRUCTURE - SHOCK ABSORBING SIDE
Ship or Project T.A.K.E. COLLISION STRUCTURAL ANALYSIS
Section BSDD Prepared by JCD Date Checked Reviewed

ORIFICE

$$q = \text{RATE OF FLOW} = CA\sqrt{\frac{2g(144)\Delta P}{\rho}}$$

$C \sim .6$

q = FLOW RATE (FT^3/SEC)

= (FOR 100 ORIFICES) =

$$9130.\ \frac{GAL}{MIN} \times \frac{MIN}{60\ SEC} \times \frac{231\ IN^3}{GAL} \times .0005787\ \frac{FT^3}{IN^3}$$

$= 20.34\ FT^3/SEC$

$\Delta P = 168\ PSI$

$$A = \frac{20.34}{.6}\ \frac{\sqrt{54.0}}{\sqrt{2(32.2)(144)(168.)}}$$

$$= 33.9\ \frac{7.39}{1248.18} = .201\ FT^2 = 28.94\ IN^2$$

$$d = 9.22"$$

SMALLER COLLISIONS SHOULD TAKE MORE TIME TO DESTRUCT THE TOTAL δ, SO THAT THE FLOW RATES WILL NOT DECREASE SO ABRUPTLY.

SEVERITY OF COLLISION	TIME OF COLLISION	FT^3/SEC	ΔP	% MAX ENERGY $\Delta P/\Delta P_{MAX}$ $\Delta P = \frac{q^2}{q^2_{MAX}}\ \frac{\rho}{C^2 A^2 2g \cdot 144}$
MAX	ABOVE		168	100%
3/4 MAX	1.75	15.26	94.3	56%
1/2 MAX	1.5	10.17	41.9	25%
1/4 MAX	1.25	5.09	10.5	6%

Subject NON - STANDARD STRUCTURE - HONEYCOMBING WITHIN [illegible]

Ship or Project TANKER COLLISION STRUCTURAL ANALYSIS

Section BSDD Prepared by JCD Date Checked Reviewed

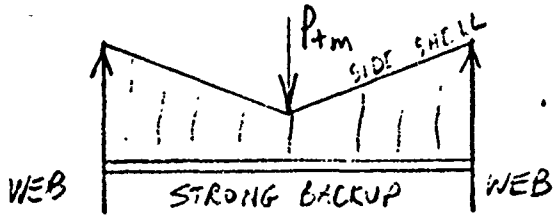

HONEYCOMB BETWEEN SIDE SHELL AND STIFF BACKUP PLATE.

THE HONEYCOMB WILL DEFORM IN COMPRESSION NEAR THE POINT OF IMPACT OF P_{+m}. AT OTHER POINTS THE RESULTANT FORCES WILL BE AT SOME ANGLE TO THE GRAIN OF THE HONEYCOMB. IF THE RESULTANT LOAD IS APPLIED AT MORE THAN 10° TO THE VERTICAL (GRAIN), THE HONEYCOMBING WILL FAIL IN SHEAR BUCKLING. THIS DOES NOT FUTURE THE PROPERTY OF CONSTANT CRUSH STRENGTH AND THEREFORE THE ENERGY ABSORBED WILL BE SMALL.

FOR THESE REASONS HONEYCOMBING WILL BE DISREGARDED IN THIS CONFIGURATION

USING SEPARATE PLATE OUTSIDE OF THE HONEYCOMB TO DISTRIBUTE THE COMPRESSIVE LOAD

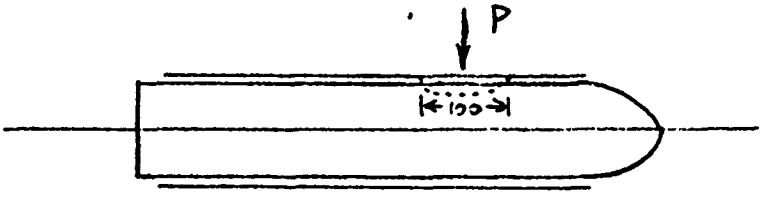

(A) BASED ON INFINITE LENGTH OF BEAM ON ELASTIC FDN.

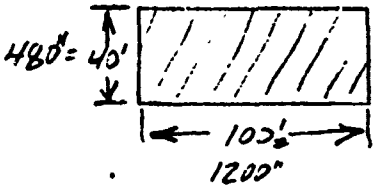

$L = 100' = 1200''$
$B = 40' = 480''$

P = STRIKING FORCE = 10,000 KIPS = 10,000,000 #
t = THICKNESS = 5"
δ = ? BASED ON INFINITE LENGTH BEAM
= USE THE CRUSHING STRENGTH OF HONEYCOMB

$$K = \frac{10,000,000}{50'' \times 100' \times 12} = \frac{10,000}{60} = 160\ \#/IN^2$$

δ AT THE LOAD

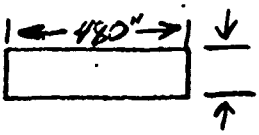

$$\delta = \frac{PB}{2K}$$

$$I = \frac{1}{12} \times 480 \times 5^3 = 5,000\ IN^4$$

$$B = \sqrt[4]{\frac{K}{4EI_z}} = \sqrt[4]{\frac{100}{4K\ 30 \times 10^6 \times 5000}}$$

$$E = 30 \times 10^6$$

$$= \sqrt[4]{\frac{160}{6000 \times 10^6}} = \frac{1}{10^2}\sqrt[4]{.0256} = \frac{1}{10^2} \times .0404 = 4.04 \times 10^{-4}$$

$$\delta = \frac{PB}{2K} = \frac{10,000,000\# \times 4.04 \times 10^{-4}}{2 \times 160} = \frac{1000 \times 4.04}{320}$$

$$= 12.6$$

FOR $t = 3''$ $\quad I = \frac{1}{12} \times 480 \times 3^3 = 1080\ IN^4$

$$B = \sqrt[4]{\frac{K}{4EI}} = \sqrt[4]{\frac{160}{4 \times 30 \times 10^6 \times 1080}} = 4.04 \times 10^{-4} \sqrt[4]{\frac{5000}{1080}}$$

$$= 4.04 \times 10^{-4} \times 1.47 = 5.93 \times 10^{-4}$$

$$\delta = 12.6 \times \frac{5.93}{4.04} = 18.5\ IN.$$

FOR $t = 1''$ $\quad I = \frac{1}{12} \times 480'' \times 1^3 = 40$

$$\sqrt[40]{\frac{5000}{40}} = \sqrt[4]{125} = 3.35$$

$$\beta = 4.04 \times 10^{-4} \times 3.35 = 13.5 \times 10^{-4}$$

$$\delta = 12.6 \times \frac{13.5}{4.04} = \underline{\underline{42.0\ IN.}}$$

Subject NON-STANDARD STRUCTURE - EXTERNAL HONEYCOMBING
Ship or Project TANKER COLLISION STRUCTURAL ANALYSIS
Section BSDD Prepared by S.T. Date Checked Reviewed

(B) BASED ON FINITE LENGTH OF BEAM ON ELASTIC FOUNDATION

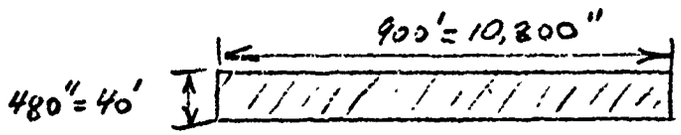

FOR 1" PLATE
$\beta = 13.5 \times 10^{-4}$ $\beta \times \ell = 13.5 \times 10^{-4} \times 10,800 = 14.6$

FOR 3" PLATE
$\beta = 5.93 \times 10^{-4}$ $\beta \times \ell = 5.93 \times 10^{-4} \times 10,800 = 6.4$

FOR 5" PLATE
$\beta = 4.04 \times 10^{-4}$ $\beta \times \ell = 4.04 \times 10^{-4} \times 10,800 = 4.36$

M. Rosenblatt & Son, Inc. No. 2087

DESIGN CALCULATION SHEET Sheet 50 of

Subject NON-STANDARD STRUCTURE - EXTERNAL HONEYCOMBING

Ship or Project TANKER COLLISION STRUCTURAL ANALYSIS

Section BSOD Prepared by S.T. Date Checked Reviewed

(1). FOR FINITE LENGTH OF BEAM WITH 5" PLATE

$\beta L = 4.36$

$\frac{\beta L}{2} = 2.18$

$k = 160\ \#/in^2$

$P = 10{,}000{,}000\ \#$

$\beta = 4.04 \times 10^{-4}$

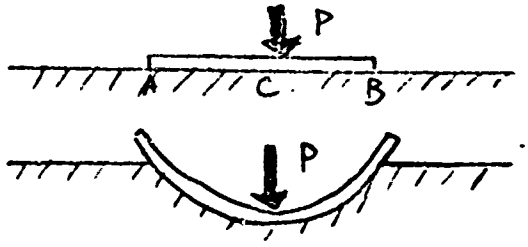

$\cos \frac{\beta l}{2} = \cos 2.18 = \cos 124.5^\circ = -.566$

$\sin \frac{\beta l}{2} = \sin 48^\circ = .824$

$\cos \beta l = \cos 4.36 = \cos 249^\circ = -.358$

$\sin \beta l = \sin 249^\circ = -.934$

$\cosh \frac{\beta l}{2} = \cosh 2.18 = 4.4797$

$\sinh \beta l = \sinh 4.36 = 39.122$

$\cosh \beta l = \cosh 4.36 = 39.135$

$$y_a = y_b = \frac{2P\beta}{K}\left(\frac{\cosh\frac{\beta l}{2}\cos\frac{\beta l}{2}}{\sinh\beta l + \sin\beta l}\right)$$

$$= \frac{2\times10\times10^2\times4.04}{167}\left[\frac{4.4797\times(-.566)}{39.122+(-.934)}\right]$$

$$= 48.3\times\left[\frac{-2.52}{38.188}\right] = \underline{\underline{-2.53"}}$$

$$y = \frac{Pf_2}{2K}\left[\frac{\cosh\beta l+\cos\beta l+2}{\sinh\beta l+\sin\beta l}\right]$$

$$= \frac{10\times10^{6}\times4.04\times10^{-4}}{2\times167}\left[\frac{39.135+(-.358)+2}{39.122+(-.934)}\right]$$

$$= 12.1\times\left[\frac{41.135}{38.188}\right] = 13.1\ IN.$$

$$M_c = \frac{P}{4\beta}\left(\frac{\cosh\beta L-\cos\beta L}{\sin\beta L+\sinh\beta L}\right) = \frac{1\times10^6}{4\times4.04\times154}\times\frac{39.135+.358}{39.122-.934} =$$

$.62\times10^{3}\times1.035 = .642\times10^{3}\ in. = .642\times10^{3}\ in.$

$$S.M. = \frac{I}{C} = \frac{5000}{2.5} = 2,000\ IN^3$$

$$\text{BENDING STRESS} = \frac{.642 \times .07}{2,000} = \frac{.642 \times 10^4}{2}$$

$$= 3,210\ KSI \quad \text{OKAY}$$

---

(2) PANEL SIZE = 100' x 40'

BASED ON FINITE LENGTH OF BEAM ON ELASTIC FOUNDATION

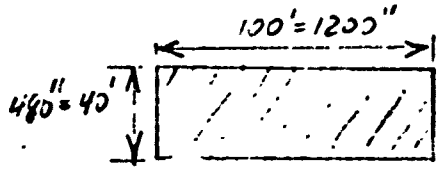

FOR 1"

$\beta = 13.5 \times 10^{-4}$ $\beta l = 13.5 \times 10^{-4} \times 1200$

$= 1.62$

MEDIUM LENGTH

$\beta l = 5.93 \times 10^{-4} \times 1200 = .712$

MEDIUM LENGTH

$\beta l = 4.04 \times 10^{-4} \times 1200 = .485$

SHORT LENGTH

FOR 5" THK. PLATE

IT CAN BE CONSIDERED AS A SHORT BEAM ON ELASTIC FDN.

$$y = \frac{P}{K l} = \frac{10,000,000}{160 \times 1200} = 50" \quad (\text{ASSUMED AT THE BEGINNING})$$

$\beta l = .465$

$\cosh \beta\ell = 1.1200$
$\sinh \beta\ell = .4992$
$\cos \beta\ell = \cos .485 = \cos 27.6° = .886$
$\sin \beta\ell = \sin 27.6° = .463$

$$M_c = \frac{10 \times 10^6}{4 \times 4.04 \times 10^{-4}} \times \frac{1.1200 - .886}{.4992 + .463}$$

$$= .62 \times 10^{10} \times \frac{.834}{.9622} = .537 \times 10^{10}$$

$$= .537 \times 10^7 \text{ in-lbs}$$

in-kips OVERSTRESSED

---

(3) PANEL SIZE = 50' x 40'

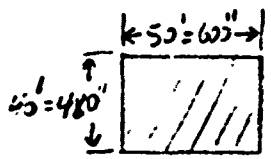

FOR 1" $\beta = 13.5 \times 10^{-4}$ $\beta\ell = 13.5 \times 10^{-4} = .62$

MEDIUM LENGTH.

FOR 3" $\beta = 5.93 \times 10^{-4}$ $\beta\ell = .356$

SHORT LENGTH

FOR 5" $\beta = 4.04 \times 10^{-4}$ $\beta\ell = .243$

SHORT LENGTH

FOR 5" PLATE

$$y = \frac{P}{K\ell} = \frac{10,000,000}{160 \times 60} = 100"$$ (½ AS DEEP AS ORIGINAL ASSUME)

$\cosh B\ell = 1.0297$
$\sinh B\ell = .2456$
$\cos B\ell = \cos 13.9° = .971$
$\sin B\ell = \sin 13.9° = .240$

$$M_c = \frac{P}{4B} \times \frac{1.0297 - .971}{.2456 + .240} = \frac{10,000,000}{4 \times 4.04 \times 10^{-4}} \times \frac{.0587}{.483}$$

$$= .62 \times 10^{10} \times .122 = .755 \times 10^{9} \text{ IN-\#} = .755 \times 10^{6} \text{ IN-KIP}$$

$$S.M. = \frac{.755 \times 10^{6}}{2000} = \frac{.755}{2} = 377 \text{ KIPS/IN}^2$$ SUFFICIENT

M. Rosenblatt & Son, Inc. No. 2287

DESIGN CALCULATION SHEET Sheet 54 of

Subject NON-STANDARD STRUCTURE - EXTERIOR LONGITUDINAL

Ship or Project TANKER COLLISION STRUCTURAL ANALYSIS

Section BSDD Prepared by G.T. Date Checked Reviewed

(4)

IF K IS DOUBLED . i.e. $K = 320$ PSI

FOR 5" PLATE 120' x 40' PANEL $I = 5000$

$$\beta = \sqrt[4]{\frac{K}{4EI_z}} = 4.04 \times 10^{-4} \sqrt[4]{2} = 4.04 \times 10^{-4} \times 1.159$$
$$= 4.8 \times 10^{-4}$$

$$\beta l = 4.8 \times 10^{-4} \times 1200 = .575 \quad \text{SHORT}$$

$$Y = \frac{10,000,000}{.320 \times 1200} = \frac{10}{.32 \times 1.2} = \frac{10}{.385} = 26"$$

$$M_c = \frac{10,000,000}{4 \times 4.2 \times 10^{-4}} \times \frac{1.170 - .839}{.6622 + .545}$$

$$= 5.2 \times 10^9 \times .274 = 1.43 \times 10^9 \text{ IN-}\#$$
$$= 1.43 \times 10^6 \text{ IN-K}$$

S.M. = 2000 IN^3 . FOR 5" PL $\frac{1}{2}$ 40' WIDE

$$S = \frac{1.43 \times 10^6}{2000} = .715 \times 10^3 = \underline{715 \text{ KSI}}$$ OK!!

SOLID ABSORBER

THIS WOULD BE LIKE THE PRESSURIZED OIL IN PRINCIPLE EXCEPT A SOLID WOULD BE USED SUCH AS "EGG CRATING" OR SOME KIND OF RUBBERIZED MATERIAL.

THE DIFFERENCE BETWEEN A SOLID AND A LIQUID IS THAT THE LIQUID WILL DISTRIBUTE PRESSURE WITH THE SPEED OF SOUND WHILE THE SOLID MUST BE PUT IN DIRECT CONTACT WITH THE FORCE.

THIS IS SIGNIFICANT BECAUSE ENERGY WILL BE ABSORBED BY SOLID AWAY FROM THE STRIKE ONLY WHEN THE NEARBY SHELL PLATE COMPRESSES IT. BECAUSE OF THE FLEXIBILITY OF THE PLATE, THIS WILL NOT HAPPEN IMMEDIATELY, BUT WILL CONTINUE THROUGHOUT THE STRIKE UNLIKE THE OIL WHICH WORKS THROUGHOUT THE DEFORMED AREA AS SOON AS RATED PRESSURE IS ATTAINED. THE SOLID SYSTEM WILL UNDOUBTEDLY REACH A MAX DEF. BEFORE ALL THE SOLID IS COMPRESSED AND WILL PROBABLY LOOK LIKE THE FOLLOWING:

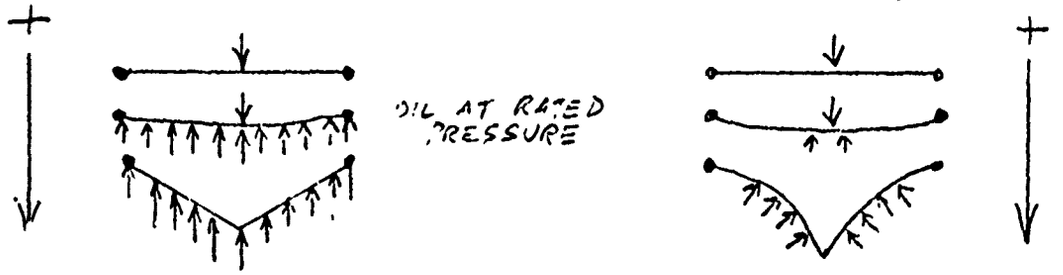

OIL SOLID

THEREFORE BECAUSE PRESSURE CANNOT BE DISTRIBUTED TO THE WHOLE WEB FRAME SPACE AT THE BEGINNING OF THE STRIKE, BUT IS DISTRIBUTED THROUGHOUT THE STRIKE (TIME INTERVAL), THE ENERGY ABSORPTION FOR THE SOLID HAS TO BE CONSIDERABLY LESS THAN THAT FOR THE OIL WHICH HAS PRESSURE DISTRIBUTION IMMEDIATELY. AGAIN IT IS ALSO EXPECTED THAT THE DEFORMATION PATTERN FOR THE TWO WILL BE DIFFERENT, THE SOLID HAVING MORE OF A CUSP AT THE STRIKE POINT, WHILE THE OIL SHOULD HAVE ABOUT THE SAME AS THE MEMBRANE ONLY DEFORMATION SHAPE.